

Volume 2, Sections 7 through 11

(NASA-CR-132575-2) ARROW-WING SUPERSONIC
CRUISE AIRCRAFT STRUCTURAL DESIGN CONCEPTS
EVALUATION. VOLUME 2: SECTIONS 7 THROUGH
11 (Lockheed-California Co.) 409 p HC
\$11.00 CSCL 0

N76-28220

Unclas
46763

by

I. F. Sakata and G. W. Davis

Prepared under Contract No. NAS1-12288

Lockheed-California Company

Burbank, California

for Langley Research Center

NATIONAL AERONAUTICS AND SPACE ADMINISTRATION



TABLE OF CONTENTS

Section

Page

Volume 1

	Summary	iii
	Introduction	v
	Acknowledgement	xi
1	Structural Design Concepts	1-1
2	Baseline Configuration	2-1
3	Aerodynamics	3-1
4	Structural Design Criteria	4-1
5	Structural Design Loads	5-1
6	Structural Temperatures	6-1

Volume 2

7	Materials and Producibility	7-1
8	Basic Design Parameters	8-1
9	Structural Analysis Models	9-1
10	Vibration and Flutter	10-1
11	Point Design Environment	11-1

Volume 3

12	Structural Concept Analysis	12-1
13	Fatigue and Fail-Safe Analysis	13-1
14	Acoustics	14-1

Volume 4

15	Mass Analysis	15-1
16	Production Costs	16-1
17	Concept Evaluation and Selection	17-1
18	Design	18-1
19	Propulsion-Airframe Integration	19-1
20	Advanced Technology Assessment	20-1
21	Design Methodology	21-1



SUMMARY

An analytical study was performed to determine the structural approach best suited for the design of a Mach 2.7 arrow-wing supersonic cruise aircraft.

Results, procedures, and principal justification of results are presented in Reference 1. Detailed substantiation data are given herein. In general, each major analysis is presented sequentially in separate sections to provide continuity in the flow of the design concepts analysis effort. In addition to the design concepts evaluation and the detailed engineering design analyses, supporting tasks encompassing: (1) the controls system development (2) the propulsion-airframe integration study, and (3) the advanced technology assessment are presented.

- Reference 1 Sakata, I. F. and Davis, G. W.: Evaluation of Structural Design Concepts for an Arrow-Wing Supersonic Cruise Aircraft NASA CR- 1976

INTRODUCTION

The design of an economically viable supersonic cruise aircraft requires reduced structural mass fractions attainable through application of new materials, advanced concepts and design tools. Configurations, such as the arrow-wing, show promise from the aerodynamic standpoint; however, detailed structural design studies are needed to determine the feasibility of constructing this type of aircraft with sufficiently low structural mass fraction.

For the past several years, the NASA Langley Research Center has been pursuing a supersonic cruise aircraft research program (1) to provide an expanded technology base for future supersonic aircraft, (2) to provide the data needed to assess the environmental and economic impacts on the United States of present and especially future foreign supersonic cruise aircraft, and (3) to provide a sound technical basis for any future consideration that may be given by the United States to the development of an environmentally acceptable and economically viable commercial supersonic cruise aircraft.

The analytical study, reported herein, was performed to provide data to support the selection of the best structural concept for the design of a supersonic cruise aircraft wing and fuselage primary structure considering near-term start-of-design technology. A spectrum of structural approaches for primary structure design that has found application or had been proposed for supersonic aircraft design; such as the Anglo-French Concorde supersonic transport, the Mach 3.0-plus Lockheed F-12 and the proposed Lockheed L-2000 and Boeing B-2707 supersonic transports were systematically evaluated for the given configuration and environmental criteria.

The study objectives were achieved through a systematic program involving the interactions between the various disciplines as shown in Figures A through C. These figures present an overview of the study effort and provides a summary statement of work, as follows:

- (1) Task I - Analytical Design Studies (Figure A).- This initial task involved a study wherein a large number of candidate structure

concepts were investigated and subjected to a systematic evaluation process to determine the most promising concepts. An airplane configuration refinement investigation, including propulsion-airframe integration study were concurrently performed.

- (2) Task II - Engineering Design/Analyses (Figure B).-- The most promising concepts were analyzed assuming near-term start-of-design technology, critical design conditions and requirements identified, and construction details and mass estimates determined for the Final Design airplane. Concurrently, the impact of advanced technology on supersonic cruise aircraft design was explored.
- (3) Task III - Mass Sensitivity Studies (Figure C).-- Starting with the Final Design airplane numerous sensitivity studies were performed. The results of these investigations and the design studies (Task I and Task II) identified opportunities for structural mass reduction and needed research and technology to achieve the objectives of reduced structural mass.

Displayed on the figures are the time-sequence and flow of data between disciplines and the reason for the make-up of the series of sections presented in this report. The various sections are independent of each other, except as specifically noted. Results of this structural evaluation are reported in Reference 1. This reference also includes the procedures and principal justification of results, whereas this report gives detailed substantiation of the results in Reference 1. This report is bound as four separate volumes.

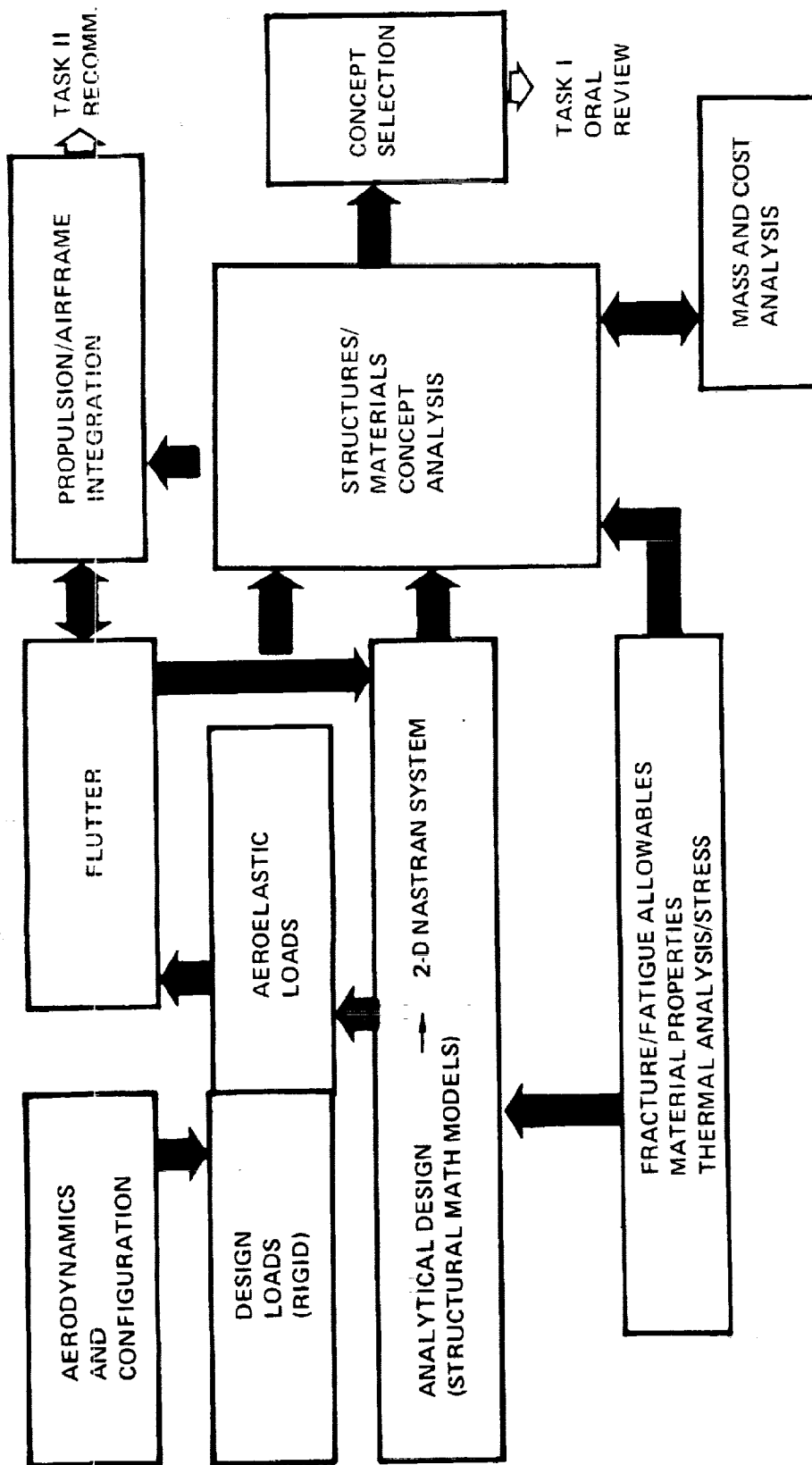


Figure A. Analytical Design Studies - Task I

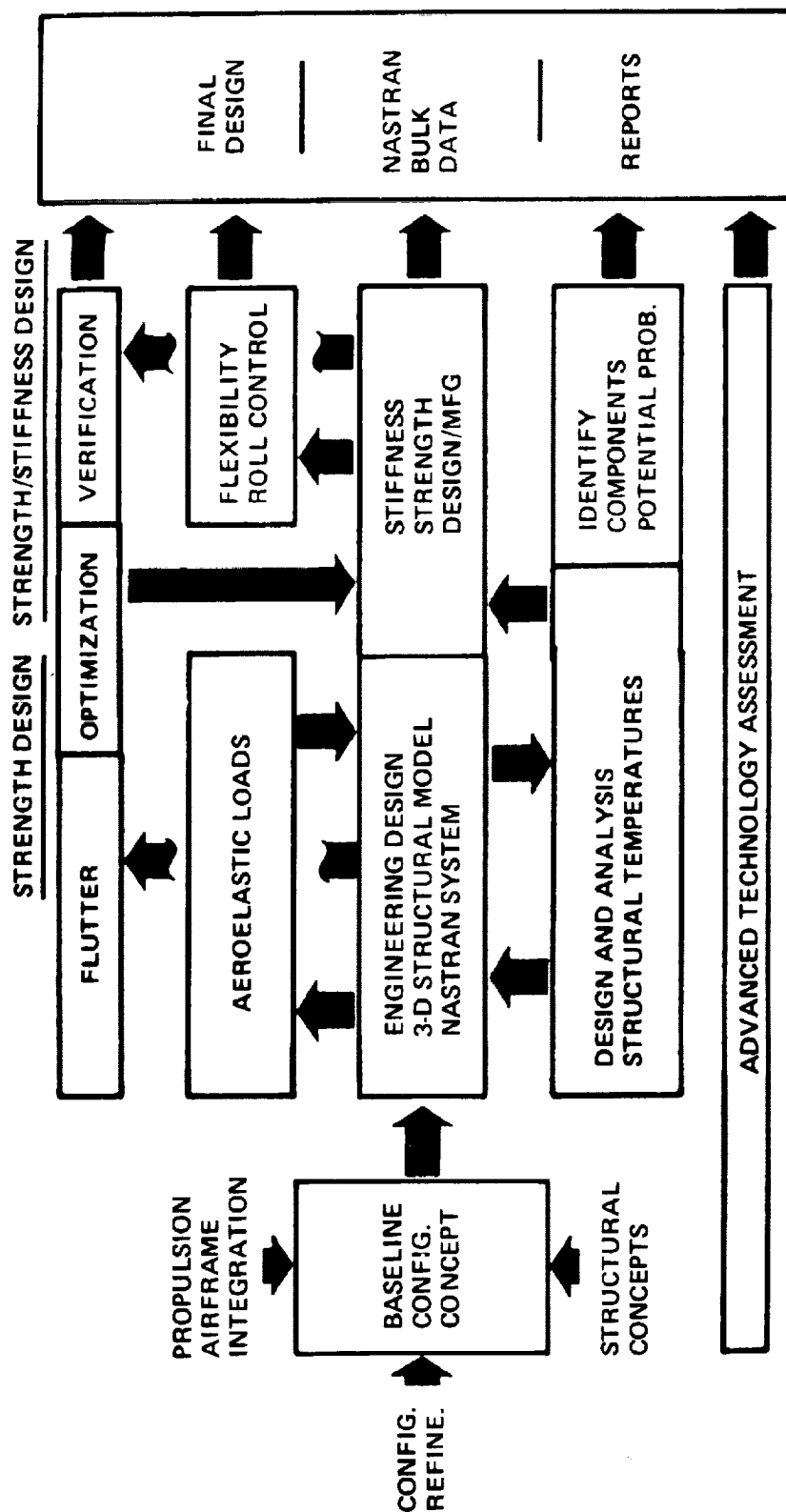


Figure B. Engineering Design and Analyses

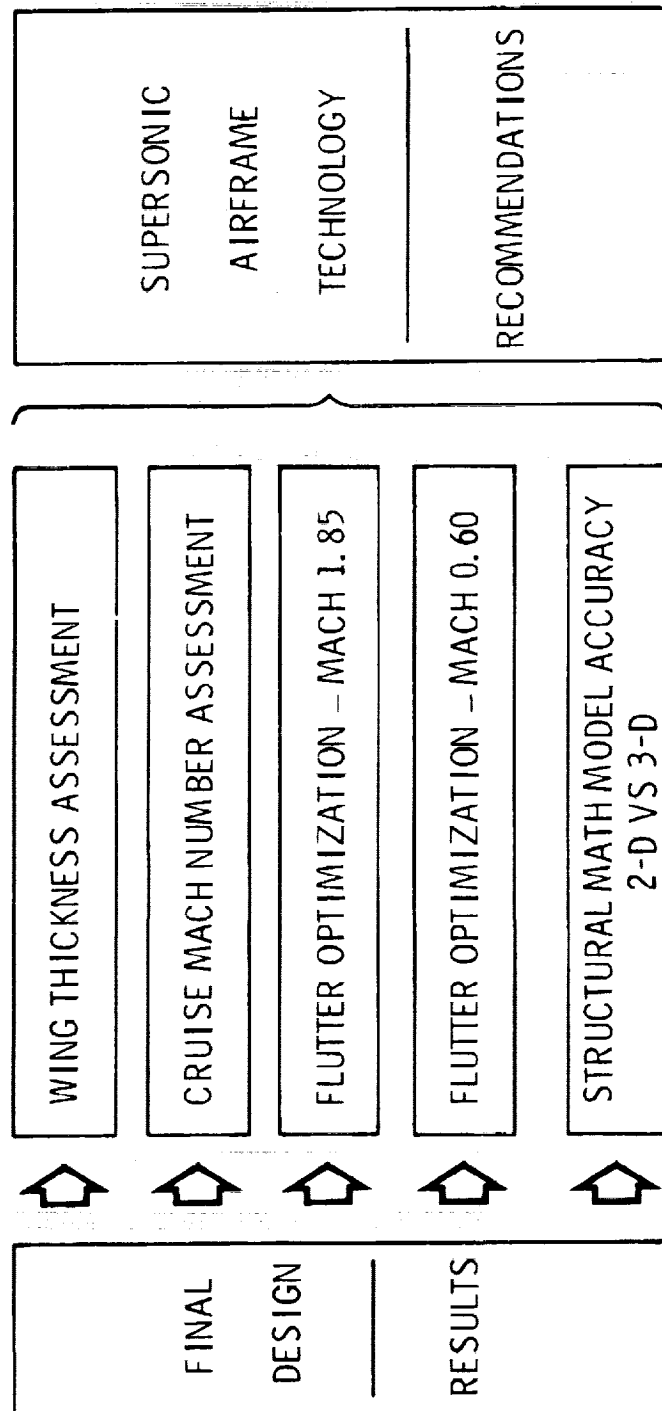


Figure C. Mass Sensitivity Studies



ACKNOWLEDGEMENT

This investigation was conducted under NASA Contract No. NAS1-12288, Study of Structural Design Concepts for an Arrow-Wing Supersonic Transport Configuration. The study was performed within the Science and Engineering Branch of the Lockheed-California Company, Burbank, California, with the participation of the Lockheed-Georgia Company in a composite design subcontract effort. I. F. Sakata was the Project Engineer, and G.W. Davis was the Lead Engineer. The other contributors to the program are acknowledged at each section.

Mr. J. C. Robinson of the Design Concepts Section, Thermal Structures Branch, and Dr. E. C. Yates, Jr., Computer Aided Methods Branch, Structures and Dynamics Division, NASA Langley Research Center, Hampton, Virginia, were the Technical Representative of the Contracting Officer (TRCO), and Alternate TRCO, respectively for the project.

PRECEDING PAGE BLANK NOT FILMED

—

—

—

SECTION 7

MATERIALS AND PRODUCIBILITY

BY

I. F. SAKATA, M. TIKTINSKY, L. D. FOGG AND J. VAN HAMERSVELD



CONTENTS

<u>Section</u>	<u>Page</u>
INTRODUCTION	7-1
MATERIALS	7-1
Metallic Materials	7-1
Composite Materials	7-10
PRODUCIBILITY	7-16
Fabrication Technologies	7-22
Manufacturing Guidelines	7-23
Fabrication Limits and Constraints	7-25
Materials and Processes Compatibility	7-26
Fabrication and Assembly Schedule	7-26
POTENTIAL MANUFACTURING PROBLEM AREAS	7-41
REFERENCES	7-51

LIST OF FIGURES

<u>Figure</u>		<u>Page</u>
7-1	Titanium Alloy Material Efficiency Comparison	7-6
7-2	Aging Response of Beta Alloys	7-9
7-3	Tensile Strength of Boron-Polyimide Reinforced with Titanium	7-13
7-4	Compressive Strength of Boron-Polyimide with Reinforced Titanium	7-14
7-5	Compressive Stress-Strain for Titanium Reinforced with Graphite-Polyimide	7-15
7-6	Tensile Strength of Titanium Reinforced with Boron-Aluminum	7-17
7-7	Compressive Strength of Titanium Reinforced with Boron-Aluminum	7-18
7-8	Strength, Stiffness and Density of Titanium Reinforced with Boron-Aluminum	7-19
7-9	Long Term Aging-Polyimide Adhesives	7-20
7-10	Boron-Polyimide Reinforced Tank Wall Caps - Autoclave Curing Method.	7-35
7-11	Boron-Polyimide Reinforced Truss Spar Caps - Autoclave Curing Method	7-35
7-12	Borsic-Aluminum Reinforced Tank Wall Caps - Aluminum Brazing Method	7-36
7-13	Borsic-Aluminum Reinforced Truss Spar Caps - Autoclave Curing Method	7-36
7-14	Boron-Aluminum Reinforced Tank Wall Caps - Diffusion Bond Method	7-38
7-15	Boron-Aluminum Reinforced Truss Spar Caps - Diffusion Bond Method	7-38
7-16	Facility Set-up Diagram	7-39
7-17	Boron-Polyimide Reinforced Spar-Heat Expanding Rubber Curing Method	7-40
7-18	Boron-Polyimide Reinforced Spar-Heat Expanding Rubber Curing Method	7-40



LIST OF TABLES

<u>Table</u>		<u>Page</u>
7-1	Materials and Fabrication Selection	7-2
7-2	Preliminary Design Properties for Titanium Alloy Sheet	7-4
7-3	Preliminary Design Composite Properties for Linear and Non-Linear Computer Programs	7-12
7-4	Polyimide Adhesives	7-21
7-5	Vendor Contacts Made for Arrow-Wing Structures Study	7-24
7-6	Materials and Processes Compatibility	7-27
7-7	Process Fabrication Schedule - Beaded Skin Panels	7-30
7-8	Fatigue Properties of Weld Bonded Beta Titanium Alloy	7-33
7-9	Potential Manufacturing Problems - Wing Surface Panel Concept - Convex Beaded Skins	7-43
7-10	Potential Manufacturing Problems - Wing Surface Panel Concept - Honeycomb Sandwich Skins	7-45
7-11	Potential Manufacturing Problems - Joining Structural Assemblies	7-47
7-12	Potential Manufacturing Problems - Tank Sealing Concepts	7-48
7-13	Potential Manufacturing Problems - Fuselage Shell Concept - Skin/Stringer Panels	7-49

PRECEDING PAGE BLANK NOT FILMED



SYMBOLS AND NOTATIONS

D	Diameter
e	Elongation in percent; the minimum distance from a hole center line to the edge of the sheet
E	Modulus of elasticity in tension
E_c	Modulus of elasticity in compression
F_{bru}	Ultimate bearing stress
F_{bry}	Bearing yield stress
F_{cy}	Compressive yield stress at which permanent strain equals 0.002
F_{ty}	Tensile yield stress at which permanent strain equals 0.002
F_{tu}	Ultimate tensile stress
F_{su}	Ultimate stress in pure shear (represents the average shearing stress over the cross section)
G	Modulus of rigidity
K_{Ic}	Plane strain fracture toughness index
K_{Iscc}	Minimum threshold value of the stress intensity for cracked specimens subjected to sustained load for extended period of time in a specified environment
L	Longitudinal grain direction
LT	Long-transverse grain direction

μ Poisson's ratio

ρ Density

SECTION "

MATERIALS AND PRODUCTIBILITY

INTRODUCTION

The materials and advanced producibility methods that offer potential structural mass savings in the design of the primary structure for a supersonic cruise aircraft are identified and reported in this section. A summary of the materials and fabrication techniques selected for this analytical effort is presented in Table 7-1. Both metallic and composite material systems were selected for application to a near-term start-of-design technology aircraft. As indicated on the summary table, selective reinforcement of the basic metallic structure was considered as the appropriate level of composite application for the near-term design.

The materials eventually selected for a supersonic cruise aircraft will be those with the best combination of properties required for a specific design. These properties include (1) mechanical and physical properties, (2) ease of manufacture, (3) cost effectiveness and (4) minimum mass. Thus, material selection requires thorough knowledge and evaluation of materials, processing, properties and cost, considering the design environment for the specific design.

MATERIALS

Metallic Materials

Titanium alloys were considered for supersonic transport application in the 1960 time-period. The leading titanium alloy for sheet metal construction under consideration during the mid-sixties was Ti-8Al-1Mo-1V alloy. At that time results of environmental tests, using a precracked fracture specimen, demonstrated that Ti-8Al-1Mo-1V was susceptible to stress corrosion cracking in salt water and other aqueous environments.

As the result of the problems encountered with the Ti-8Al-1Mo-1V alloy, all candidates were reevaluated with the emphasis on stress corrosion cracking. The

TABLE 7-1. MATERIALS AND FABRICATION SELECTION

SELECTION	JUSTIFICATION
<p>TI-6AL-4V COND. D3A OR RA FOR ALL BRAZEMENTS AND WELDMENTS.</p> <p>BETA C FOR COMPLEX CONTOURED PARTS JOINED BY MECHANICAL FASTENERS OR ADHESIVE BONDING.</p> <p>HERCULES HT-5 GRAPHITE AND MONSANTO SKYBOND 703 FOR COMPOSITE REINFORCED STRUCTURE. BORON FIBERS MAY BE USED WITH THE NOTED RESINS WHERE REQUIRED FOR CRITICAL COMPRESSION APPLICATION.</p> <p>POLYIMIDE/ADHESIVES</p> <p>BORSIC-6061 ALUMINIUM</p> <p>BRAZING (ALUMINIUM BRAZE FILLER METAL)</p> <p>FIXTURE BRAZING</p> <p>RIVET-BOND</p> <p>SEALANT - DOW CORNING'S 77-028 FLUOROSILICONES</p>	<p>TI-6AL-4V WITH CONTROLLED BETA AND ALPHA-BETA WORKING AND THERMAL CYCLING EXHIBITS EXCELLENT FRACTURE TOUGHNESS CHARACTERISTICS, STRESS CORROSION RESISTANCE, HIGH MODULUS, AND FATIGUE CHARACTERISTICS COMPETITIVE WITH OTHER ALLOYS. BRAZE CYCLES ARE COMPATIBLE WITH THE ALPHA-BETA TRANSUS TEMPERATURES FOR DUPLEX ANNEALING. ALUMINIUM AND OTHER MODERATE TEMPERATURE BRAZING ALLOYS ARE COMPATIBLE WITH THE LOW TEMPERATURE THERMAL ANNEALING CYCLE. WELDING CAN BE CONTROLLED TO PROVIDE MINIMUM DEGRADATION OF FATIGUE PROPERTIES.</p> <p>BETA C HAS ONE OF THE HIGHEST STRENGTH-WEIGHT RATIO OF THE ADVANCED TITANIUM ALLOYS WITH HIGH STRESS CORROSION RESISTANCE AND FRACTURE TOUGHNESS. BETA C HAS GOOD ROOM TEMPERATURE FORMABILITY AND WELDABILITY IN THE SOLUTION ANNEALED CONDITION. THE ROOM TEMPERATURE FORMING CAPABILITY MAY RESULT IN REDUCING THE COST OF FABRICATING TITANIUM PARTS FROM APPROXIMATELY 4 TIMES THAT OF ALUMINIUM TO 1.5-2 TIMES OF ALUMINIUM.</p> <p>CONDENSATION POLYIMIDES SUCH AS MONSANTO SKYBOND 703 HAVE A MORE STABLE CHEMICAL STRUCTURE, A MORE EXTENSIVE DATA BASE AND MANUFACTURING HISTORY. BY 198X LONG TERM AGING OF BORON/POLYIMIDE AND GRAPHITE/POLYIMIDE AT 450°F WITH COMBINED STRESS LOADING AND ENVIRONMENTAL CONDITIONS WILL BE ACCOMPLISHED.</p> <p>POLYIMIDE ADHESIVES HAVE BEEN EVALUATED AFTER LONG-TERM ELEVATED TEMPERATURE AGING AT TEMPERATURES UP TO 600°F WITH TITANIUM AND COMPOSITE ADHERENTS.</p> <p>BRAZEMENTS TO ITSELF OR TO TITANIUM WILL BE USED WHERE MINIMUM DEGRADATION OF BORON IS REQUIRED AND ADVANTAGE TAKEN OF HIGH PEEL STRENGTH CAPABILITY. STAINLESS STEEL MESH (APPROXIMATELY 5% BY WEIGHT) WILL BE INCORPORATED IN THE BRAZED BORSIC ALUMINIUM WHERE REQUIRED TO OFFSET DIFFERENCES IN TRANSVERSE COEFFICIENTS OF EXPANSION BETWEEN TITANIUM AND THE B/AL.</p> <p>MODERATE SIZE HONEYCOMB SANDWICH PANELS (3' X 25') HAVE BEEN PRODUCED AND MATCHING PART TOLERANCE REQUIREMENTS DO NOT INVOLVE COSTLY FABRICATION PRACTICES. THIS PROCESS CAN BE EXPANDED TO FABRICATE LARGE PANEL STRUCTURE CONFORMING TO COMPLEX CONTOURS AND WITH LOAD CARRYING CAP MEMBERS INTEGRAL WITH THE PANEL, THEREBY MINIMIZING THE NUMBER OF COMPONENT PARTS AND ELIMINATING MECHANIZED FASTENERS.</p> <p>PANEL STRUCTURES OF THE SKIN/STRINGER, OR DOUBLE BEADED SKIN CONCEPT CAN BE PRODUCED UTILIZING AN ISOTHERMAL BRAZING PROCESS WITH PRIOR RESISTANCE WELDING TO MAINTAIN COMPONENT ALIGNMENT. THIS PROCESS WILL APPLY HEAT LOCALLY TO ACCOMPLISH THE BRAZE WITH REDUCED TOOLING COST AND SHORTER PROCESSING CYCLES.</p> <p>USE SPRING LOADED CLAMPS IN PREDRILLED HOLES TO APPLY REQUIRED CONTACT PRESSURE AND HEAT (STRIP HEATING, HEATING BLANKETS, ETC.) IN TOOL TO CURE THE ADHESIVE. AFTER POST CURE, FASTENERS CAN BE INSTALLED IN PREDRILLED HOLES.</p> <p>THE AST FUEL TANKS WILL BE DESIGNED TO MINIMIZE THE REQUIREMENT FOR SEALING. EXTENSIVE USE WILL BE MADE OF SEAM WELDING, WELD-BONDING AND BRAZING. DATA HAS BEEN GENERATED ON DOW-CORNING'S SEALANT WHICH INDICATES LONG TERM RESISTANCE TO 500°F (450°F) EXPOSURE.</p>

ORIGINAL PAGE IS
OF POOR QUALITY

Boeing Company under FAA sponsorship, conducted an investigation on Ti-6Al-4V and Ti-4Al-3Mo-1V which demonstrated superior properties as the result of the reevaluation effort. The results of these studies, as well as others conducted by industry - including work by Lockheed on the Beta alloys-were reviewed and titanium alloy 6Al-4V (annealed) was selected as the primary structural material for the near-term supersonic transport design. To identify the importance of higher strength properties on design, however, the titanium alloy Beta C was also selected. Beta C is representative of the more recently developed Beta titanium alloys which exhibit high strength properties obtained by solution treating and aging and also has high formability characteristics of the unalloyed titanium.

Mechanical Properties - The preliminary design properties for the selected titanium alloys used for supersonic cruise aircraft primary wing and fuselage structure design are presented in Table 7-2. The data for Ti-6Al-4V are from Reference 1. Data are presented for the mechanical properties established under both the MIL-T-9047 Specifications and the Aerospace Materials Specification (AMS) 4906. Limited formability and marginal fracture toughness for the solution treated and aged (STA) condition precludes its general use and the data is presented for comparison purpose only.

Beta C (Ti-3Al-8V-6Cr-4Mo-4Zr), Beta III (Ti-11Mo-6.5Zr-4.5Sn) and Ti-8Mo-8V-2Al-3Fe data are from Reference 1 and 2. They are heat treatable beta-titanium alloys offering outstanding cold formability and simple heat treatment to high strengths. Sheet and foil can be produced by cold rolling in coil form. Sheet can be cold formed to complex configurations. Formed parts can be subsequently aged to high strength with very little distortion. The high strength condition has the additional characteristics of being tough, thermally stable, and relatively insensitive to accelerated crack growth in aqueous environment and good resistance to hot-salt stress corrosion. These alloys offer cost reduction potential, however, in certain applications their use is handicapped by their high density. The data presented for these alloys, however, show marked improvement over the titanium alloy Ti-13V-11Cr-3Al (B120VCA).

Material Efficiency Parameters - The room temperature properties of current alpha-beta and beta titanium alloys are summarized and used to develop the various alloy efficiency parameters to aid in the material selection process. These parameters include:

TABLE 7-2. PRELIMINARY DESIGN PROPERTIES FOR TITANIUM ALLOY SHEET

ALLOY	Ti 6Al 4V							BETA C	BETA III	8-8-2-3	B120VCA
Specification	MIL-T-9047			AMS 4906				PRODUCER'S			MIL-T-9046
Form	SHEET, STRIP, AND PLATE			CONTINUOUSLY ROLLED SHEET & STRIP				SHEET & STRIP			
Condition	ANNEALED		STA	ANNEALED				SOLUTION TREATED & AGED			
Thickness, in.	≤ 0.1875			> 0.008 - > 0.025		> 0.025 - ≤ 0.060		≤ 0.187			< 4.0
Basis	A	B	S	A	B	A	B	S ^f	S ^f	S	B
Mechanical Properties											
F _{TU} , ksi											
L	134	139	160	140 ^c	149	140 ^d	145	180	180	174	175
LT	134	139	160	140 ^c	148	140 ^d	147	180	180
F _{TY} , ksi											
L	126	131	145	122	130	122 ^e	128	170	175	158	165
LT	126	131	145	126 ^c	140	126 ^d	135	170	175
F _{CY} , ksi											
L	132	138	154	125	134	125	132	170	175	177	167
LT	132	138	162	129	144	129	139	170	175
F _{SU} , ksi	79	81	100	90	95	90	93	108
F _{BRU} , ksi											
(e/D) = 1.5	197	204	236	216	228	216	224	255
(e/D) = 2.0	252	261	286	280	295	280	290	323
F _{HR} , ksi											
(e/D) = 1.5	171	178	210	166	176	166	174	224
(e/D) = 2.0	208	216	232	203	216	203	214	255
e, percent	8 ^g	...	5 ^b	7	...	8 ^c	...	6	6	...	4
E, 10 ³ ksi	16.0							15.4	15.0	14.0	15.5
E _c , 10 ³ ksi	16.4							14.8	16.0	15.9	16.0
G, 10 ³ ksi	6.2							5.8	5.9
μ	0.31							0.33	0.33
ρ, lb/in ³	0.160							0.174	0.183	0.175	0.174

- a. 8 - 0.025 to 0.062 in.; 10 - 0.063 in. and above
b. 5 - 0.050 in. and above; 4 - 0.033 to 0.048 in.; 3 - 0.032 in. and below
c. The A-values are higher than specification values as follows:
F_{TU}(L) = 145 ksi, F_{TU}(LT) = 144 ksi, F_{TY}(LT) = 134 ksi
d. The A-values are higher than specification values as follows:
F_{TU}(L) = 141 ksi, F_{TU}(LT) = 143 ksi, F_{TY}(LT) = 131 ksi
e. Estimated value based on limited test data
f. Properties reflect producer's guaranteed minimum
g. 5.4 (68 - 900F)
h. Thickness 0.025 in. and above

ORIGINAL PAGE IS
OF POOR QUALITY

- Specific tensile strength (F_{tu}/ρ) to indicate those alloys capable of providing minimum mass components where tensile loadings are critical at room and elevated temperature.
- Specific elastic modulus (E/ρ) to indicate those alloys that are capable of providing minimum mass structures where column stiffness or plate buckling are critical structural conditions.
- Damage tolerance capability ($(K_{Ic}/F_{ty})^2$) to aid in selecting alloys and/or conditions that offer the potential of minimum risk of premature failure.
- Room temperature stress corrosion susceptibility as measured by K_{Isc}/ρ .
- Room temperature formability as indicated by the ratio of bend radius to thickness (r/t).
- Maximum tension-tension fatigue strength at 10^6 cycles with $R = 0.1$ and $K_t = 1$ and $K_c = 3$ divided by density to indicate the susceptibility of the titanium alloys to crack initiation and fatigue failure.

Modulus-Density Critical Elements: A review of Figure 7-1 indicates that for modulus-density critical elements, such as wing skins which are critical in buckling or stiffness load conditions:

- The high aluminum alpha-beta alloys have the highest modulus-density ratios of any of the current and recently developed titanium alloys. Obviously, alloys such as Ti-8-1-1 used in the previous SST studies would be extremely attractive because of its low density (0.158 lbs/cu in.) and relatively high modulus ($17-18 \times 10^6$ psi). However, the known "water-susceptibility" of this alloy has prejudiced its consideration in this program.
- Ti-6Al-6V-2Sn, the current alpha-beta alloy with high modulus-density ratio is not available as cold rolled sheet or strip, is susceptible to alloy segregation, and is not outstanding in its fracture toughness nor stress corrosion resistance.
- Ti-6Al-2Sn-2Mo-2Cr-2Zr-0.25 Si (Ti-6-22-22) also has been reported to exhibit high modulus-density ratios and has been rolled into sheet products. The properties shown in Figure 7-1 are for annealed sheet. If the modulus values

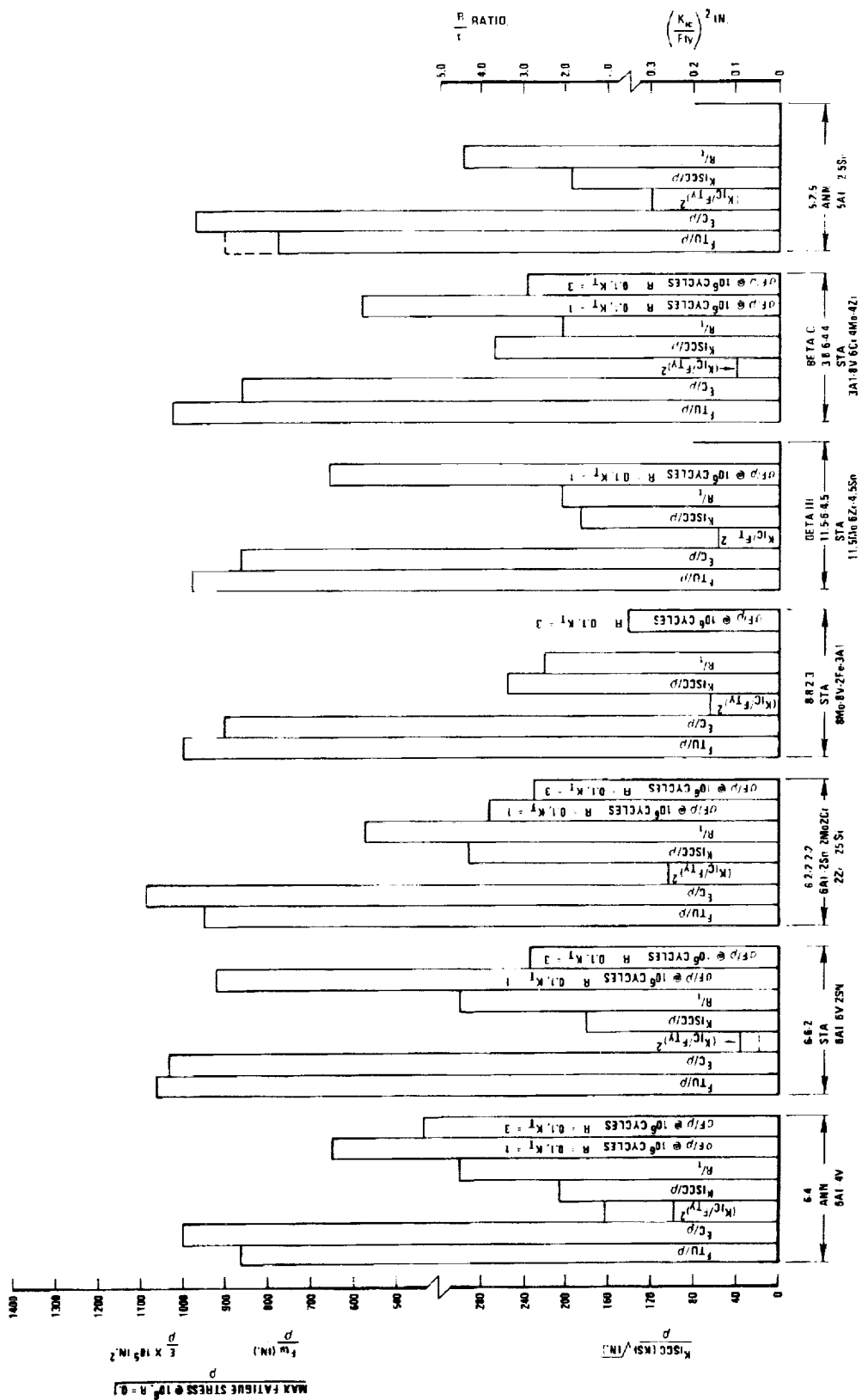


Figure 7-1. Titanium Alloy Material Efficiency Comparison

can be reproduced in sheet form, and the silicon addition (for high temperature properties) does not affect the stability of the alloy at moderate temperatures (i.e., 400-600 F), this alloy warrants consideration as an alternate to Ti-6Al-4V.

- Ti-6Al-4V is available as cold rolled sheet and strip, can be processed to provide high fracture toughness and stress corrosion resistance characteristics, and is considered the most promising material for modulus-density critical applications.
- An alternate material with modulus-density ratios approaching that of Ti-6Al-4V is Ti-5Al-2.5Sn. It can be used where its lower tensile strength or restricted hot formability (due to cold working) does not impose a weight penalty.
- Attempts to obtain improved modulus-density ratios in titanium alloys by such techniques as texturing are only partially successful. The resulting directionality is a problem both in fabrication and design and the improvement is subject to degradation upon hot working to obtain complex contours.
- A review of data on the super-alpha alloys (those alloys developed for 900 F creep applications such as Ti-11 or Ti-5621S) has not revealed any advantage for the use of these alloys in the moderate temperature region of 400 F-600 F, and such as required for supersonic cruise aircraft design.
- The metallic matrix composites, such as boron-borsic/aluminum, boron/titanium, etc., have very high modulus-density ratios and are not plotted on the chart with the titanium alloys.

Tensile-Strength Critical Elements: The most efficient material for these applications are the solution treated and aged beta titanium alloys, such as Ti-8-8-2-3. In addition, these alloys, besides being available as cold rolled sheet-strip-extrusion, do provide the capability of room temperature forming to relatively complex contours. The aging process is relatively simple, not requiring rapid quenching from special protective atmospheres, and can be combined with cold work to obtain even higher strength levels.

Unfortunately, as with other titanium alloys, the aging cycles used to date result in lower fracture toughness properties, i.e., K_{IC} values, of approximately 50 ksi $\sqrt{\text{in.}}$.

and notch tensile ratios for 0.040 sheet material of approximately 0.8. Similar data have been reported for stress corrosion resistance.

The fatigue "cut-off" on beta alloys must be higher than the alpha-beta cut-off by at least the density-ratio (i.e., 0.160/0.174) to avoid any weight penalties. Unfortunately, fatigue data for beta titanium is extremely limited. Meager data indicates properties directly comparable to and in certain instances 25-percent greater than the alpha-beta alloys.

Application of beta-alloys, such as Ti-8-8-2-3, therefore will require:

1. The development of fatigue data as a function of alloy and production and assembly methods that will confirm the capability of realizing the tensile-strength weight advantages, and
2. The establishment of aging cycles which can minimize the noted reductions in fracture toughness and stress corrosion resistance. The need to develop such aging cycles is important since it has been determined that welded or weld bonded components with this alloy offer promise for minimum weight structures.

Aging Response. - Typical of many heat treatable metals the beta titanium alloys exhibit both a response to cold working plus a combination of cold working and aging as well as overaging. The results of various cold working and aging tests, performed at Lockheed, are summarized in Figure 7-2.

Cleaning. - The normal cleaning and/or pickling solutions for alpha-beta titanium alloys proved inadequate for cleaning of aged beta titanium alloys such as Beta C and Ti-8-8-2-3. Standard shop nitric-hydrofluoric acid concentrations left a dark smut on the surface of the aged titanium alloy products. The smut film was not identified but only abrasive cleaning or extremely concentrated solutions of nitric-hydrofluoric acid could provide a clean, bright surface for subsequent welding and/or weld bonding work.

Fusion Welding. - TIG and EB welds in solution treated and solution treated and aged beta titanium alloys were made utilizing techniques and procedures typical of standard alpha-beta titanium alloys.

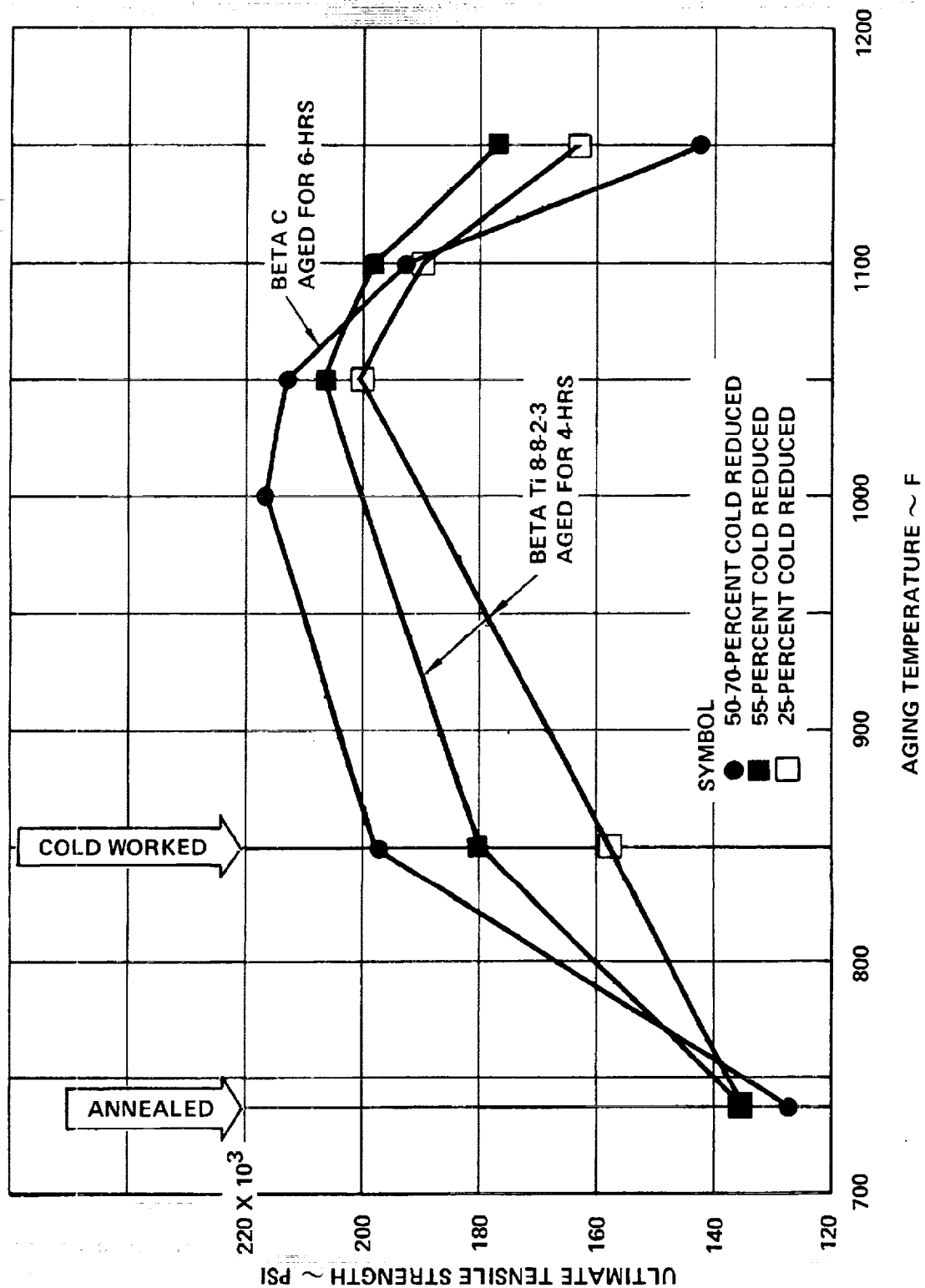


Figure 7-2. Aging Response of Beta Alloys

Weld Bonding. - Beta titanium alloy (Ti-8-8-2-3) cold rolled strip was aged to approximately 160 ksi and resistance (spot) weld schedules developed to provide a consistent interfacial gap of 0.002 to 0.005 in. After welding, half of the specimens were infiltrated with an epoxy resin (B. F. Goodrich, Type A, 1396B) in the initial interfacial gap by resin capillary flow during the cure cycle.

Test on the weld bonded specimens compared to the as-welded specimens, showed the following results:

- Shear strength of weld bonded specimens 2-1/2 times that of as welded specimens.
- Tensile strength of weld bonded specimens equal to as welded specimens.
- Fatigue strengths and lives of weld bonded specimens improved greatly over the fatigue strength of as welded specimens.

Composite Materials

The application of composites to the primary structure for the near-term supersonic cruise aircraft design was limited to selective reinforcement of the basic titanium structure. Furthermore, based on the principles of maximum return for minimum cost and risk, the application was primarily unidirectional reinforcing of members carrying axial loads, such as spar caps and stringers. Other guidelines included: (1) All exposed surfaces were titanium; (2) All load transfer at joints were made through titanium structure; and (3) At least minimum gage titanium was maintained on all design concepts.

Material Properties. - The composite materials used for reinforcement purposes were MODMOR II/Skybond 703 graphite polyimide (Gr/PI), Boron/Skybond 703 (B/PI) and 5.6 Boron/1100 Aluminum with titanium interleaves (B/Al).

For composites the static material properties are based on currently published (1970-1972 technology) data which have minimal statistical basis (average or B-basis properties). It is implicitly assumed that material development will continue and that these properties are representative of minimum allowables available at start-of-design. Reduction of properties due to environmental aging, etc., is undetermined at this time and the evaluation of this effect is not included.

The polyimide matrix composites can sustain service temperatures in the range of 500 F to 600 F. However, aging degradation is evident above 500 F. Graphite/polyimide composites have considerable potential for reducing thermal deformations and stresses because of their low coefficient of thermal expansion. Boron/polyimide has the highest compressive efficiency.

Boron/aluminum composites have a high compressive structural efficiency, and can sustain temperatures to 800 F. Stress-to-rupture tests to 600 F for long periods of time have shown no evidence of aging degradation. However, constant amplitude fatigue properties are degraded in the 400 F temperature range after 10^6 cycles. Its compressive efficiency makes it suitable for use as a stiffening element in concert with titanium structural elements.

Table 7-3 summarizes the preliminary design composite properties for linear and non-linear computer programs used in the composite design. The stability analysis requires linear properties while the material property characterization program uses non-linear data. The polyimide (PI) data is from Reference 3. The boron/aluminum (B/Al) properties are for 5.6 mil boron using 1100 aluminum alloy for the matrix in combination with interleaved titanium foils. Published test results show significant improvements in transverse ductility and overall performance over the 6061 aluminum matrix system. To characterize composite reinforced titanium, Ti-6Al-4V properties were obtained from Reference 1 with the Ramberg Osgood properties for the non-linear programs from Reference 4.

Composite Reinforced Titanium.— To explore the benefits to be derived from selective composite reinforcement of titanium structure, various arrangements of materials and plies were evaluated. The strength and stiffness properties of various laminates were determined using the data of Table 7-3 in conjunction with the Lockheed developed computer programs.

Figures 7-3 and 7-4 show the tensile and compressive strengths (loaded in the filament direction) of titanium selectively reinforced with various proportions (by cross-sectional area) of unidirectional boron-polyimide. The material properties are from Table 7-3, and the thermal differential due to curing was assumed to be -300°F . A value of 90,000 psi was selected as the fatigue cutoff strength of titanium alloy-Ti-6Al-4V. The tensile strength of the compound composite at which the octahedral stress in the titanium is 90,000 psi is shown on Figure 7-3.

TABLE 7-3. PRELIMINARY DESIGN COMPOSITE PROPERTIES FOR
LINEAR AND NON-LINEAR COMPUTER PROGRAMS

MATERIAL		MODMOR II/SKYBOND 703, Gr/Pl $t = 0.007 \text{ in/play}; V_f = 0.6; \rho = 0.051; 0.56 \text{ lb/in}^3$		BORON/SKYBOND 703, B/Pl $t = 0.0055 \text{ in/play}; V_f = 0.5; \rho = 0.068; 0.072 \text{ lb/in}^3$		5.6 BORON/ 1100 ALUMINUM, B/Al $t = 0.0075 \text{ in/play}; V_f = 0.42; \rho = 0.098; 0.098 \text{ lb/in}^3$		TITANIUM 6Al-4V $\rho = 0.160 \text{ lb/in}^3$	
		RT	550 F	RT	550 F	RT	550 F	RT	550 F
PROPERTY DATA NOTATION(d)	ALT. SYMBOLS	UNITS		UNITS		UNITS		UNITS	
		LINEAR	NON-LINEAR	LINEAR	NON-LINEAR	LINEAR	NON-LINEAR	LINEAR	NON-LINEAR
ELASTIC STIFFNESS	E1	22.8	22.8	20.35	20.35	32.2	32.2	33.3	33.3
	E2	1.98	1.98	0.822	0.822	2.44	2.44	4.6	4.6
	G	0.71	0.71	0.436	0.436	0.894	0.894	1.25	1.25
EXPAN COEFF.	α	0.33	0.33	0.2	0.2	0.31	0.31	0.25	0.25
	ν	0	0	0	0	0	0	0	0
	ν_{12}	-0.17	-0.17	0	0	2.8	2.8	3.2	3.2
LONGITUDINAL TENSION	Alpha (1)	9.45	9.45	15.0(a)	15.0(a)	10.5	10.5	5.7	5.7
	Alpha (2)	7.5	7.5	4.0	4.0	5.0	5.0	3.0	3.0
	Intermediate Strain	170.0	170.0	81.4	81.4	161.0	161.0	94.0	94.0
LONGITUDINAL COMPR.	Intermediate Stress	8.5	8.5	7.11	7.11	6.34	6.34	6.5	6.5
	Ult. Strain, Eps U (1, 1)	193.8	193.8	144.7	144.7	204.0	204.0	160.0	160.0
	Ult. Stress	145.0	145.0	38.9	38.9	226.2	226.2	343.0	343.0
TRANSVERSE TENSION	Intermediate Strain	4.1	4.1	3.9	3.9	1.4	1.4	1.15	1.15
	Intermediate Stress	8.0	8.0	3.2	3.2	3.1	3.1	10.0	10.0
	Ult. Strain, Eps U (2, 1)	4.32	4.32	4.9	4.9	2.56	2.56	5.0	5.0
TRANSVERSE COMPR.	Ult. Stress	8.6	8.6	4.0	4.0	4.884	4.884	23.0(b)	23.0(b)
	Intermediate Strain	6.8	6.8	8.0	8.0	4.0	4.0	1.15	1.15
	Intermediate Stress	13.0	13.0	6.5	6.5	9.3	9.3	10.0	10.0
SHEAR	Ult. Strain, Eps U (2, 2)	-8.525	-8.525	12.0	12.0	4.7	4.7	-8.53	-8.53
	Ult. Stress	16.9	16.9	8.7	8.7	10.28	10.28	37.5(b)	37.5(b)
	Intermediate Strain	12.0	12.0	12.0	12.0	10.7	10.7	3.4	3.4
SHEAR	Intermediate Stress	6.0	6.0	3.0	3.0	6.0	6.0	5.0	5.0
	Ult. Strain, Eps U (3, 1)	11.0	11.0	26.0	26.0	35.0	35.0	13.05/8.42(c)	13.05/8.42(c)
	Ult. Stress	7.8	7.8	4.91	4.91	9.34	9.34	10.0	10.0

NOTES: (a) Estimated from Boron/Epoxy
(b) Transverse stress/strain values valid only when minimum of 20-percent titanium foils are interfused with B/Al
(c) Fatigue cutoff
(d) Symbols and notation for computer program code input

ORIGINAL PAGE IS
OF POOR QUALITY

Figure 7-5 presents the stress-strain relationship of graphite-polyimide (Gr/PI) unidirectional reinforcement (0-degree plies) of Ti-6Al-4V annealed. The influence of various percentages (of cross sectional area) of Gr/PI reinforcing is displayed. Stiffness increased between 10 to 30 percent over the basic titanium alloy are noted.

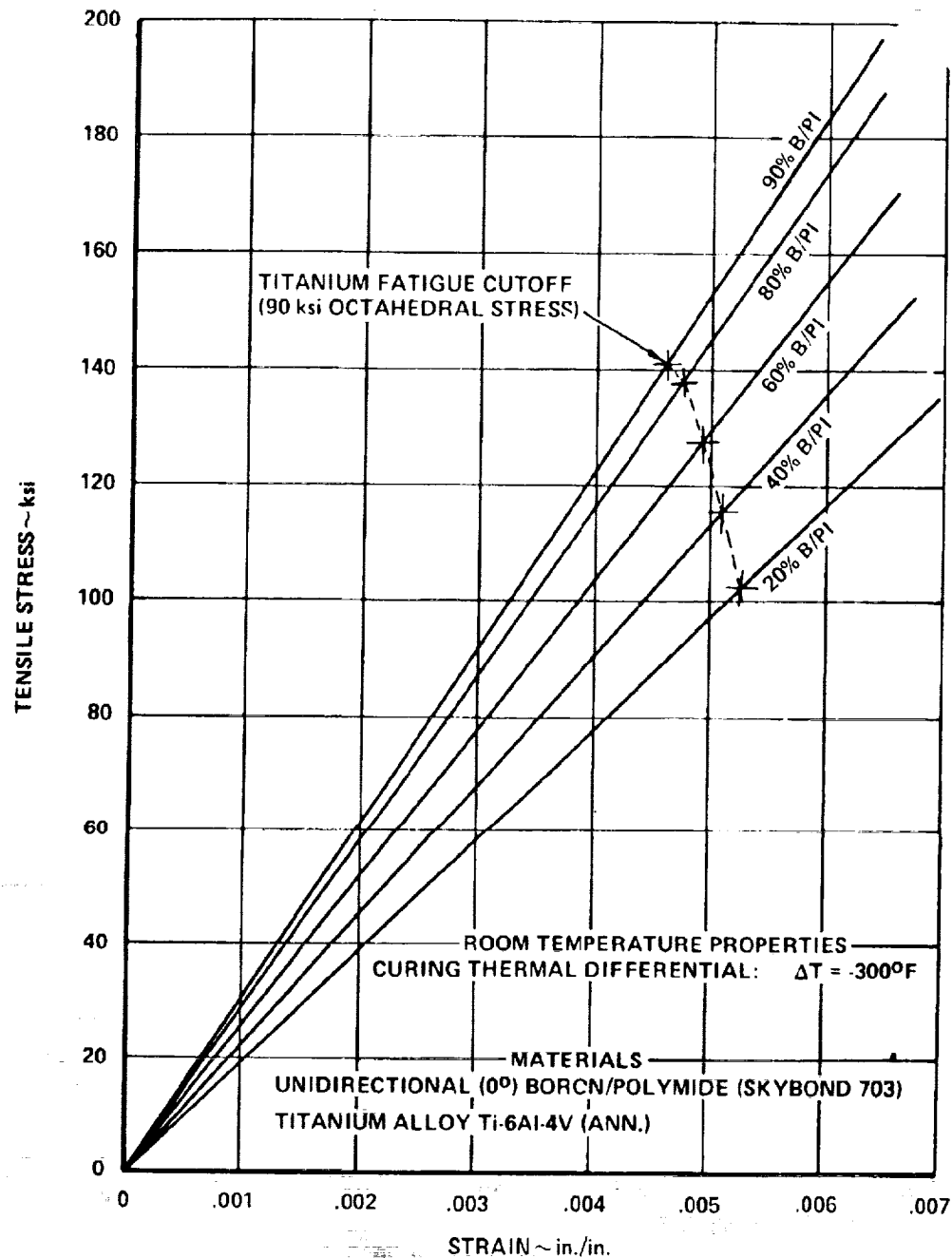


Figure 7-3. Tensile Strength of E/PI Reinforced Titanium

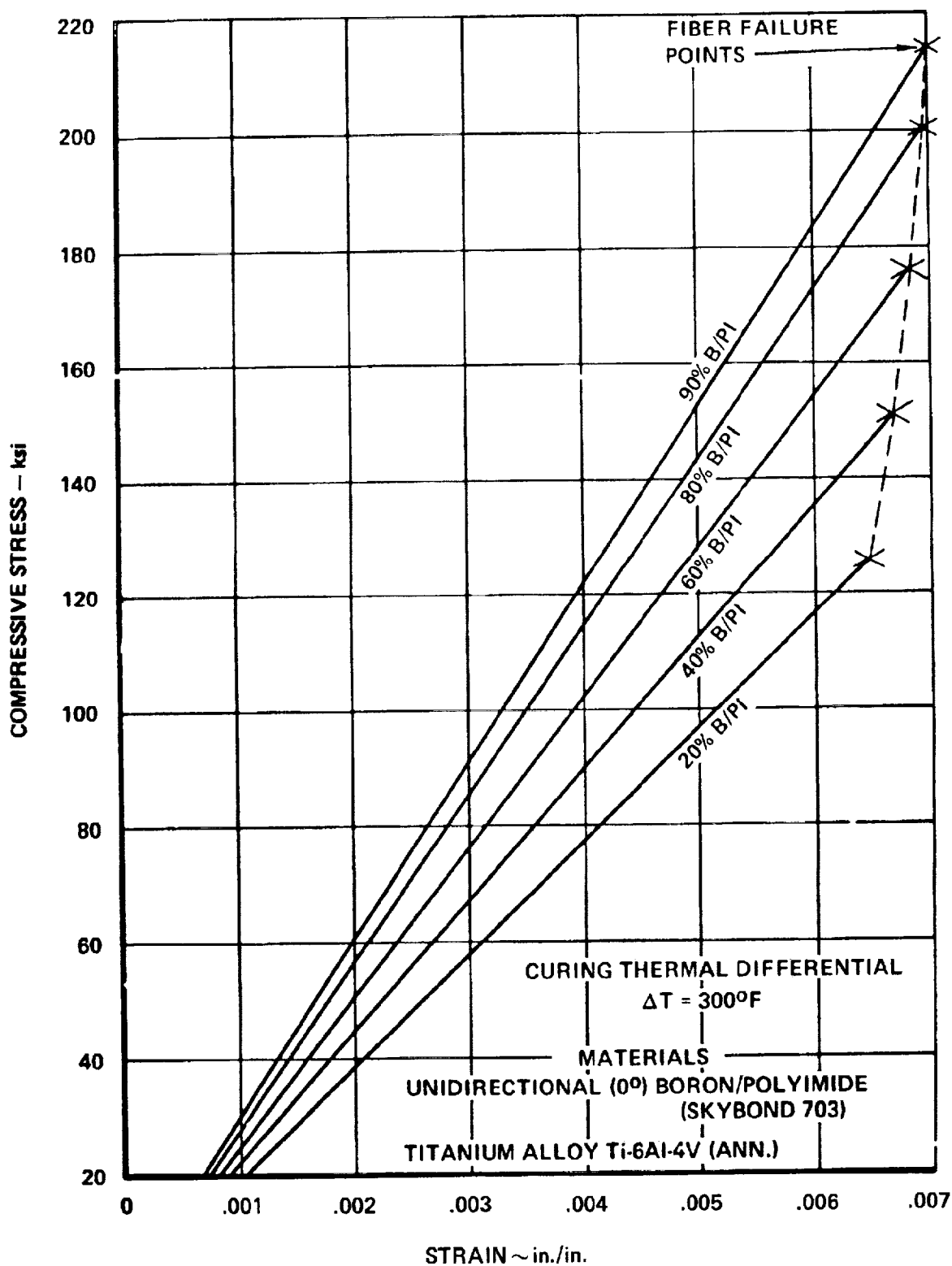


Figure 7-4. Compressive Strength of B/PI Reinforced Titanium

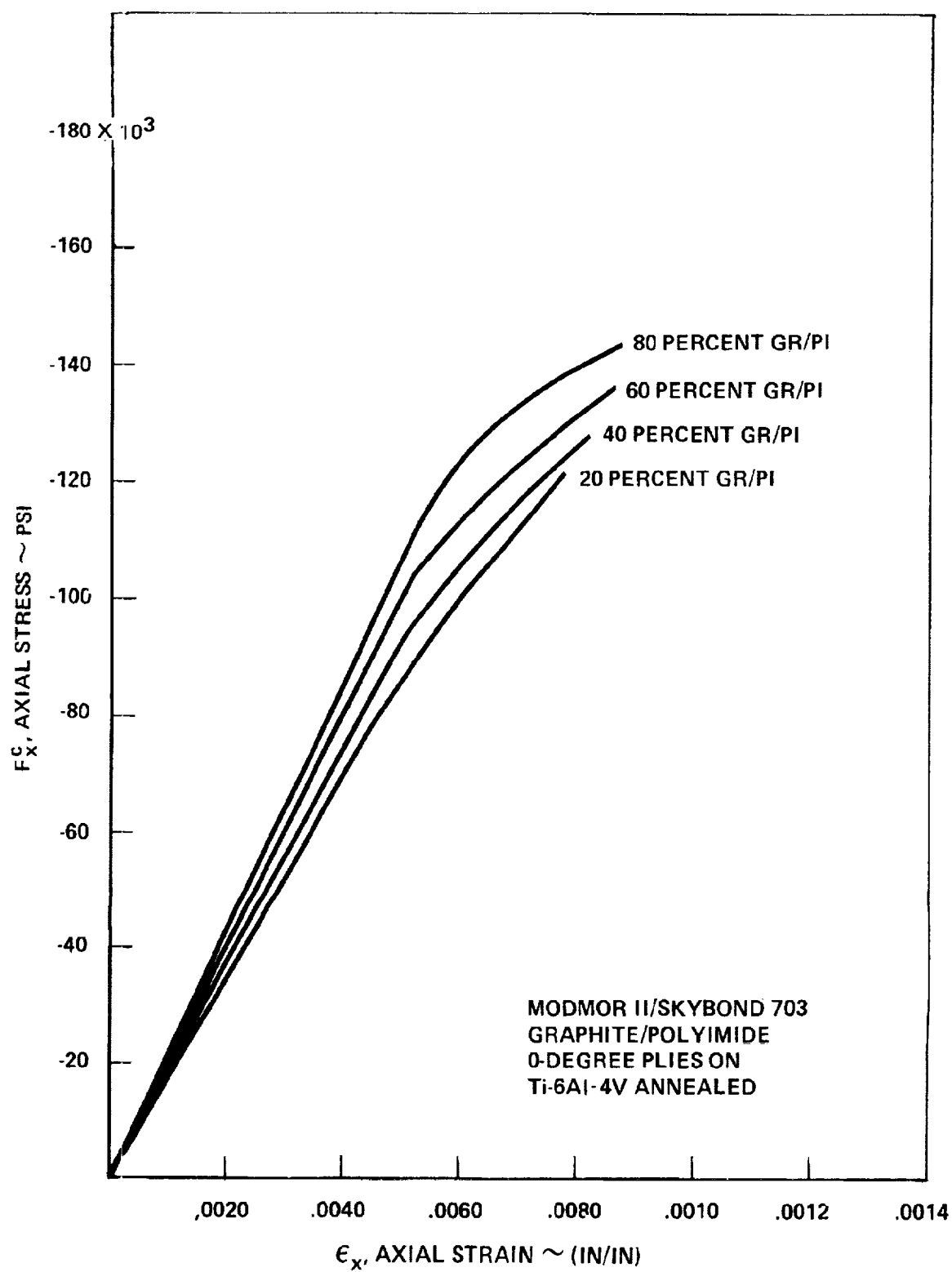


Figure 7-5. Compressive Stress-Strain for Titanium Reinforced with Graphite-Polyimide

Figures 7-6, 7-7, and 7-8 summarize data computed for studies related to boron/aluminum (B/Al) reinforced titanium. The tensile stress-strain data of Figure 7-6 displays the changes in material property characteristics with the percentage increase in unidirectional B/Al. A change in elastic modulus from 23×10^6 psi for 40-percent B/Al to 29.9×10^6 psi for 80-percent B/Al is noted with a corresponding decrease in material density.

The fatigue cutoff for B/Al was estimated by observing limited data for boron/6061 aluminum reported in Reference 5 for various fiber volume fractions. The strains corresponding to the fatigue limit for 42-percent fiber volume were taken as design cutoff values for B/Al/Ti. The fatigue cutoff stress for titanium (90,000 psi) is indicated on the figure for reference.

The strength, modulus, and density of B/Al/Ti is summarized in Figure 7-8 with the corresponding usage of boron aluminum as a fraction of the total area.

Polyimide adhesive data are presented in Figure 7-9 and Table 7-4. FM-34, a condensation-polyimide adhesive film manufactured by American Cyanamid, has been aged 20,000 hours at 500 F with virtually no reduction in bond strength on titanium. This is a strong indication that the condensation-polyimides as matrix materials would have long-term 450 F - 500 F property retention. Addition-polyimides have recently been evaluated as structural adhesives, and look reasonably good after 1000 hours at 600 F. There is not enough aging data, however, for a comparison with the condensation-polyimide adhesives.

PRODUCIBILITY

Producibility technology studies were performed as an integral part of the analytical design effort to focus upon the practical requirements of manufacture. The studies were conducted to establish feasibility for the application of advanced manufacturing techniques to large scale production. Specific studies encompassed:

- Improved fatigue quality through minimizing fasteners by use of welding, bonding, and brazing
- Large scale fabrication to minimize the number of joints
- Minimizing or eliminating tank sealing by use of large scale application of welding, bonding and brazing

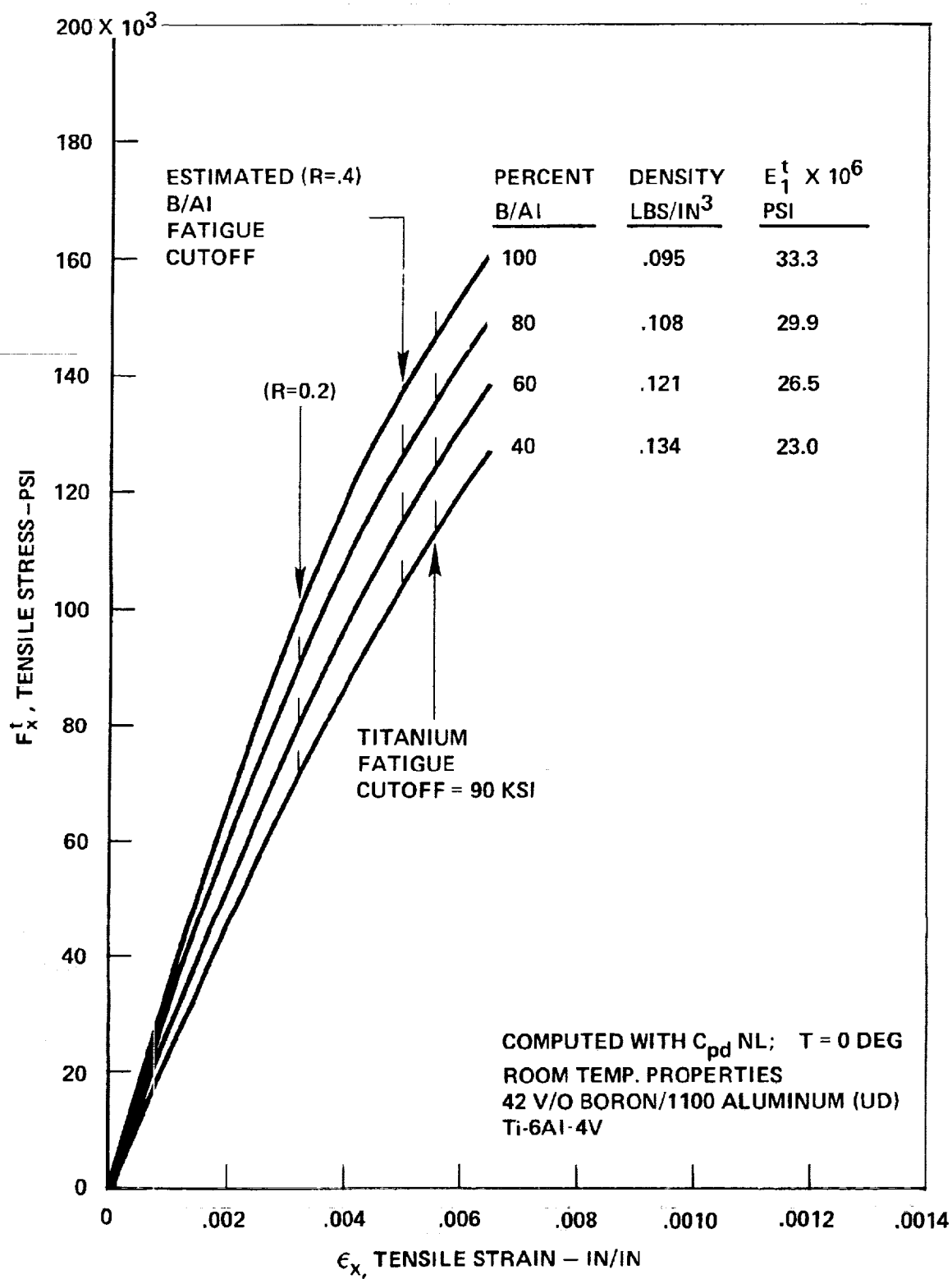


Figure 7-6. Tensile Strength of Titanium Reinforced with Boron-Aluminum

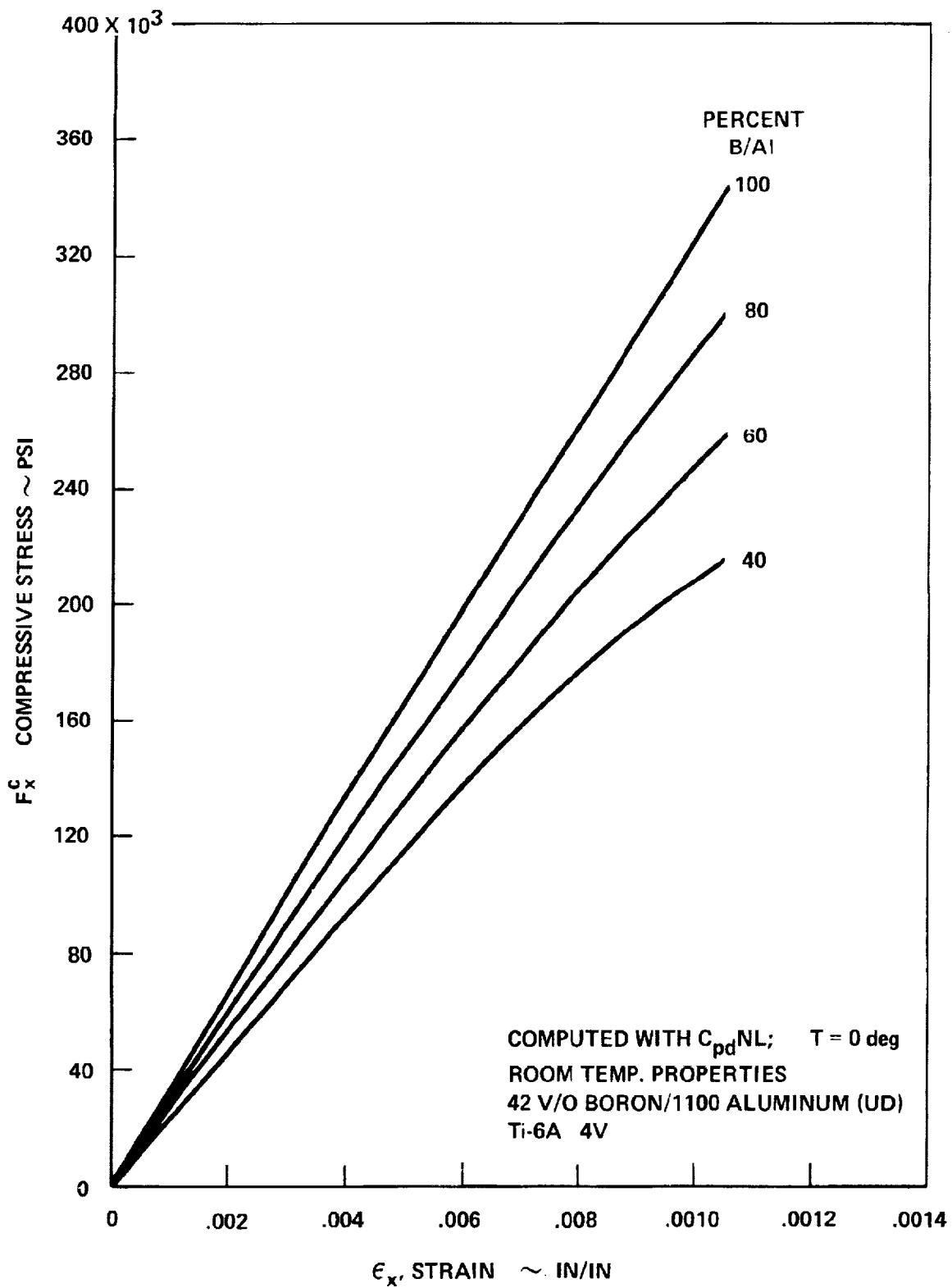


Figure 7-7. Compressive Strength of Titanium Reinforced with Boron-Aluminum

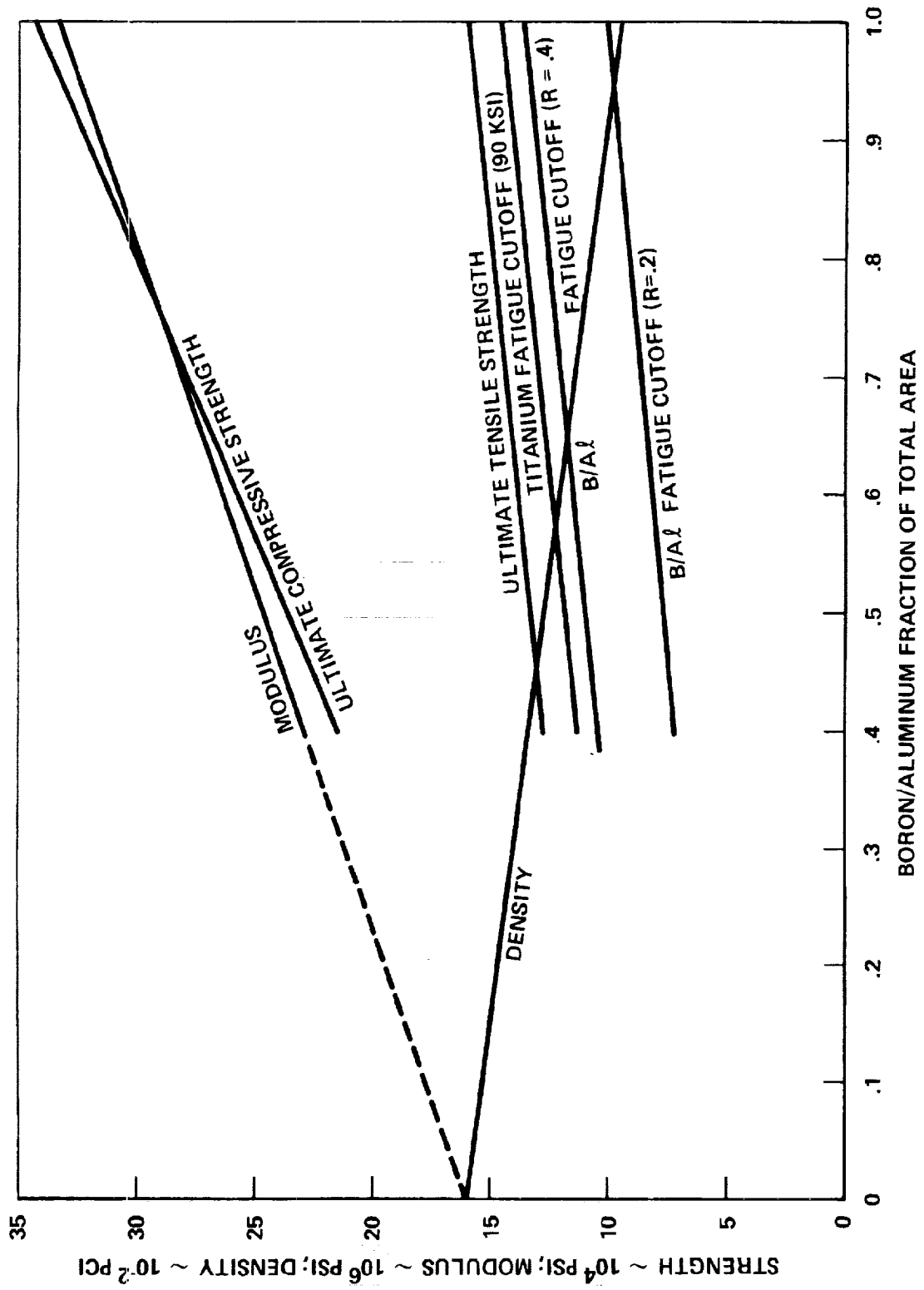


Figure 7-8. Strength, Stiffness and Density of Titanium Reinforced with Boron-Aluminum

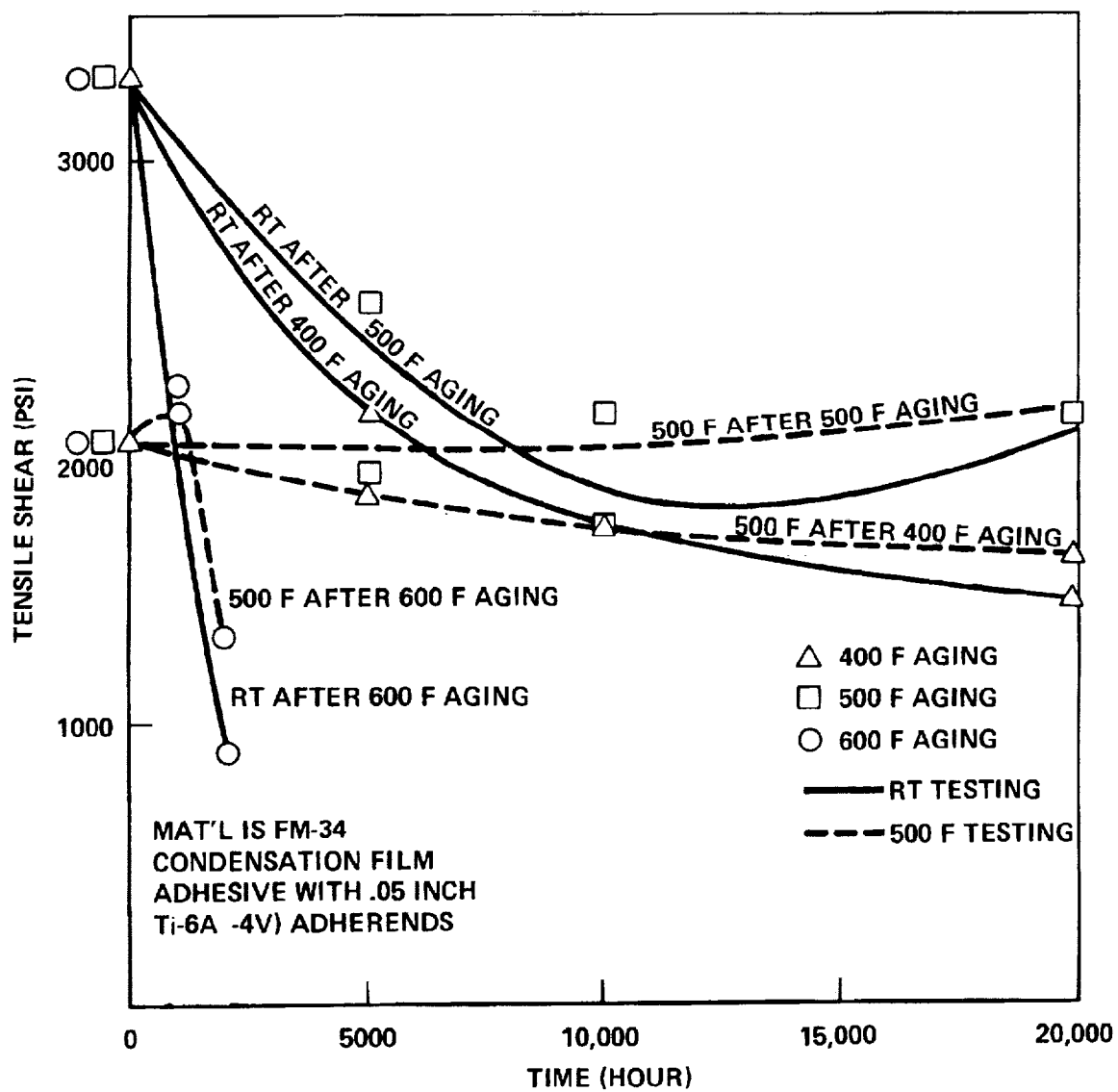


Figure 7-9. Long Term Aging-Polyimide Adhesives

TABLE 7-4. POLYIMIDE ADHESIVES

ADHESIVE DESCRIPTION	ADHERENDS	TEST TEMPERATURE	AGING CONDITIONS	MECHANICAL PROPERTIES		FABRICATION PROCEDURES	REMARKS	DATA SOURCE
				TENSILE SHEAR (psi)	SHORT BEAM SHEAR (ksi)			
FM 34 polyimide adhesive - supported with style 112 glass cloth carrier - fr. wt. 135 gsf ± 0.10 - condensate type P1 - 14% max. vol. Used with BR 34 primer.	6-4 titanium .090 inch thick	75 ± 5°F	-	3300 avg.		Titanium cleaning - solvent wipe (MEK) "spray" clean 15 min. at 180°F. Rinse - hot (150°F) then cold water pickle at RT 5 min in sol'n 15% HNO ₃ 3% HF. Rinse. Apply "Pass-Jet 107" by brush. Dry 20 min. Rinse. Air dry below 150°F. Bond within 16 hrs. BR 34 applied by brush, roller, or spray. Procedure used not indicated. Applied to dry film thickness 1 - 2 mils. Cured by 30 min. air dry 30 min. at 220°F. 45 min. at 410°F. Primer applied to both surfaces by roller 05 - 10 psi each side. Adhesive bond cycle - 30 min. to 550°F. 90 min. at 550°F. and 90 psi. Sandwich cure - 30 min. to 350°F. 60 - 120 min. hold. 25 psi and vacuum. Cool to RT under pressure. Post cure place in 350°F oven. Raise to 550°F in 60 min. Hold 2 hrs.	All tests per MMM A-132 except peels. The peel methods given are described in LCP 86-1228. Sandwich tests per MIL A-25463 values are defined as averages. Aging data taken from charts to nearest hundred. Sandwich values given as range. Note: use of perforated core recommended for sandwich bonding.	American Cyanamid Co. Bloomington, Ind. Data sheet
			30 days salt water spray	2475 avg.				
			7 days imm. in JP-4 fuel (MIL J-5624)	3350 avg.				
			30 days imm. in tap water	2100 avg.				
			5000 hrs. at 600°F	2500 avg.				
			10,000 hrs. at 500°F	1700 avg.				
			20,000 hrs. at 500°F	2100 avg.				
		500°F	-	2000 avg.				
			5000 hrs. at 400°F	1800 avg.				
			10,000 hrs. at 400°F	1700 avg.				
			20,000 hrs. at 400°F	1600 avg.				
			5000 hrs. at 500°F	1900 avg.				
			10,000 hrs. at 500°F	2100 avg.				
			20,000 hrs. at 500°F	2100 avg.				
TRW adhesive film AEF - addition type polyimide. Supported on style 104 glass scrim bondline thickness .009 inch.	6-4 titanium .090 inch thick	70°F	-	3400 avg. σ = 200	16.2 (avg. of 8) σ = 1.4	Titanium alloy cleaned by paraffin method (similar to method described for FM 34. Adhesive cured in oven for 15 min. at 275°F plus 5 min. at 350°F. Then placed in autoclave under 100 psig N ₂ . Heated to 575°F at 30°F/min. Cured 1 hr. Cooled to RT. under vacuum. Post-cured 16 hr. at 550°F. This cure cycle used for primary bonded graphite/titanium bonds also. P13N composite adherend cured in mold open for 2 hr. at 400°F. Then mold placed in 600°F press. Cured 1 hr. under pressure.	* Exceed yield strength of titanium - 17 ksi. ** Shear failure with in the composite short beam shear. Test specimens 650 x .250 in. x .1 tested in flexure using single point loading. The two supports were 10 calib 41 apart. Loading rate .05 inch/min. tensile shear per MMM A-132.	NASA CR 112003. "The development of autoclave or pressureable thermally stable adhesives for titanium alloy and graphite composite structures" Vaughan and Jones TRW Dec 1971
		600°F	-		10.9 σ = 0.3			
		70°F	200 hr. at 600°F		18.0 (avg. of 5) σ = 1.5			
			500 hr. at 600°F		21.5 (avg. of 5) σ = 1.2			
			1000 hr. at 600°F		21.1 (avg. of 5) σ = 1.4			
		-66°F	-		30.2 (avg. of 5) σ = 2.9			
		70°F	200 hr. at -65°F		24.5 (avg. of 5) σ = 1.3			
			500 hr. at -65°F		24.1 (avg. of 5) σ = 1.5			
			1000 hr. at -65°F		22.4 (avg. of 5) σ = 1.0			

ORIGINAL PAGE IS
OF POOR QUALITY

Emphasis was placed on an integrated design/manufacturing approach to develop low cost producible structural design concepts utilizing advanced materials and fabrication processes consistent with technology levels associated with near-term start of design. The design and manufacturing data available from the Lockheed L-2000 supersonic transport, the Lockheed YF-12 supersonic aircraft, and numerous industry contacts, were utilized in developing solutions to design problems encountered in the study.

An important facet of the producibility technology study was the establishment of manufacturing guidelines to assist in the design concepts development. Fabrication limits and constraints were developed for forming, joining, metal removal and assembly technologies (Section 8, Basic Design Parameters). Tentative fabrication and assembly schedules were developed for the major components, and finally, manufacturing - materials - process problems were identified for the various structural design concepts for wing and fuselage primary structure design.

Fabrication Technology

Fabrication Technology for titanium materials were based upon an assessment of the industry state-of-the-art. It was assumed that certain technological levels required for the early 1980 time period would have been developed. The technologies utilized in the design concept development included:

- Weld bond and rivet bond - high temperature resins - either polyimide (PI), PPQ or others.
- Metal-to-metal or metal-to-core bonding - high temperature resins
- Electron beam (EB), tungsten inert gas (TIG), plasma-arc welding.
- Brazing - weldbrazing of large complex shaped panels
- Chemical cleaning - preweld bond and braze of Beta alloys - post aging cleaning
- Complex structural shapes - extrusions - welding - diffusion bonding, etc.
- Hot die-vacuum forming or large panel sizes (15 ft. x 35 ft)

- Composites - high temperature either PI or PPQ or other matrix - aluminum metal matrix
- Complex tooling methods - large size components - welded truss spars, 80 ft. length - skin panels, 15 ft. x 30 ft. - EB welding of major assembly joints.
- Titanium fasteners
- Fuel tank sealing - high temperature sealant materials

Current research and development being explored by government and industry were evaluated to determine design applicability and need for additional work to obtain a viable fabrication process that meet the supersonic cruise aircraft performance and life requirements. The high temperature resin weld bond process was considered as the primary candidate to join the skin panels (i.e., convex beaded) to produce high fatigue life joints; weld brazing was selected as the alternate system.

Manufacturing Guidelines

Realistic manufacturing guidelines for the structural design of a supersonic cruise aircraft were established. The ground rules included policy guidelines for fabrication, tooling, facilities and subcontractor requirements. In addition, supplier conferences were held with industry representatives (Table 7-5) to review specific design approaches to establish equipment capabilities and availability, and fabrication process limitations and constraints.

A transportation study was conducted for the potential subcontract of fuselage sections, trailing edges, leading edges, pylons, empennage, etc. The structural sizes were limited to maximum railroad shipping package envelope requirements. For cross country shipping, the maximum available envelope was 10 feet 6 inches x 19 feet 6 inches x 89 feet.

The guidelines are summarized as follows:

1. Potential production quantity is based on 300 to 350 aircraft at a rate of 4 aircraft per month.
2. Complete aircraft assembled by the Lockheed-California Company (Calac)
3. Wing structure segments to be fabricated and assembled by Calac - skin panel details and spars may be subcontracted.

TABLE 7-5. VENDOR CONTACTS MADE FOR ARROW WING STRUCTURES STUDY

<u>VENDOR</u>	<u>SUBJECT DISCUSSED</u>
Aeronca Mfg.	Aluminum Brazed Honeycomb Sandwich
Rohr Aircraft	Liquid Interface Diffusion (LID) Diffusion Braze Process
Northrop Aircraft	Nor-Ti-Bond Diffusion Braze Process
TRW Systems	Weld Bond
Advanced Structures and Technology Co.	STRESSKIN
Sciaky Brothers, Inc.	Welding
Avco	Metal Matrix Composites
Holosonics	NDT Inspection Methods

4. Titanium fabrication capability would be available at Calac for the potential large size detail components. Specific equipment are hot presses - hot vacuum forming - hot stretch press forming - welding (T.I.G., resistance, plasma and E.B.) - autoclaves for high temperature and pressure curing resins - high temperature post curing adhesive ovens - aluminum brazing furnaces.
5. TIG/EB portable/stationary welding equipment for assembly of major structural components - wing segments - fuselage sections.
6. Large size components - minimum mechanical joints.
7. Fabrication size limitations are:
 - Forming skin panels 15 ft. x 35 ft. (maximum)
 - Brazed skin panels 68 inches x 40 ft. (maximum)
 - Bonded and weld bond panels 15 ft. x 50 ft. (maximum)
 - Fuselage panels 12 ft. x 50 ft. (maximum)
8. Automatic welding - all but welded joints
 - Skin panel welds planned
 - Formed skin panel welds stress relieved
 - Welds shaved on all surfaces - except inside of tubular
 - Welding schedules - sequenced to minimize residual stresses
 - Manual welding limited to absolute minimum

9. Assembly parameters - surface panels to substructure

- Spar spacing - 21 in. minimum for personnel accessibility
- Minimum cross section access 12 in. x 19 in.
- Beyond (minimum cross section) arm hole access doors (5 in. x 8 in.)
- spanwise pitch 54 in. each spar bay
- Blind fasteners - minimum usage
- Composite reinforced spars - no riveting allowed

10. Mechanical Fasteners

- Titanium rivets (Beta alloys or others); size limit 0.156 diameter
- Hi-tigue 6Al-4V STA
- Shear type low profile head - acceptable for outer skin
- Single row fastener - unacceptable for fuel tank joint splices
- Blind fasteners not permissible in fuel tank area

11. Access Doors

- Clamped type - avoid fastener holes
- Manufacturing access - prefer blind fasteners over access doors
- Two access doors per tank for assembly and inspection (13. x 18 in.)

Fabrication Limits and Constraints

The fabrication limits were identified for the all metal (titanium) skin stiffened and monocoque design concepts and reported in Section 8, Basic Design Parameters. These fabrication limits are realistic estimations of the state-of-the-art for fabrication of titanium hardware components for the 1980 time period. Data was derived from titanium mill product producers, fabrication equipment suppliers, Lockheed fabrication experience, industry and government reports (i.e., SST Technology Follow-On Program-Phase I, Federal Aviation Administration)

Fabrication limits were established for material sizes and gates for the Alpha-Beta and Beta titanium alloys and the process technologies to convert the material into structural components.

Detailed fabrication limits were established for:

Forming - room and elevated temperatures - minimum bend radius at temperatures - panel sizes - equipment and facility constraints.

Joining - welded, brazed, weld bonded and mechanical fastened assemblies such as:

- Spars, ribs, spar and rib joint interface
- Skin panel attachment to substructure
- Assembly limits for production segments - minimum spar spacing requirements and inspection accessibility
- Metal removal - minimum thicknesses for chemical and machining detail components

Materials and Processes Compatibility

The effects of titanium alloy (Alpha-Beta and Beta) compatibility on standard aircraft fabrication processing methods were reviewed; and the materials and processes compatibility data of Table 7-6 were developed. A rating system from 1 to 10 was developed to indicate process feasibility, deleterious effects of processing on the end-product and other data required for decision making process. Ratings 5 and above require process development programs to determine application feasibility. Typical development areas for the (6Al-4V and Beta titanium alloys) are:

- | | |
|-----------------------|-----------------------------------|
| ● Isothermal forging | ● Weld braze |
| ● Progressive rolling | ● Rivet bond (polyimide resin) |
| ● Stretch forming | ● Adhesive bond (polyimide resin) |
| ● Peen forming | ● Weld bond (polyimide resin) |
| ● Laser welding | |

Fabrication and Assembly Schedule

Producibility studies were conducted during the design phase to establish tentative fabrication and assembly schedules for construction of major structural components with several schedules highlighted below.



Chordwise Stiffened Beaded Skin Panels. - A process fabrication schedule developed for the beaded skin panels is presented in Table 7-7. The data presents a step-by-step processing sequence for both the Alpha-Beta and Beta titanium alloy materials. A brief summary of this proposed process is described below:

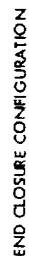
1. Formed outer skins - cold preform using a Verson Wheelon rubber form press. Maximum standard sheet size for .015 inch thick skins is 48-inches by 144 inches. TIG butt weld cold preformed sheet details to final size panel configuration - stress relieve weld joints. Hot size to final contour using hot ceramic die forming method.
2. Formed inner skins - cold preform corrugation beads (3 to 4 bead width) by brake or Yoder roll form. Preform the end closures and then hot size (platen press). Hot roll size to final corrugation bead widths. Butt weld details to produce the final size panel. Hot vacuum form to size in ceramic die to achieve mating compound formed contour.

The development of crack free surface, compound contoured, resistance heated ceramic dies (15 ft. x 35 ft.) with constant surface temperature controls is one of the major manufacturing problems to be resolved.

Weld Bond of Beaded Panels. - To reduce the number of mechanical fasteners and improve fatigue life, weld bonding of the beaded outer skin to inner skin is proposed to assemble the wing surface panels.

Polyimide resins are required to meet the 460^oF surface temperature of the Mach 2.7 cruise conditions. An industry search indicated that weld bonding with the standard condensation-polyimides was not considered feasible because of the problem of excessive volatiles. The addition-polyimides can be pre-staged to remove volatiles prior to assembly and cure. However, studies exploring this approach identified disadvantages for fabrication of large compound contoured skin panels and precluded its use. The development of a polyimide system suitable for capillary flow weld bonding indicates that the addition-type resin systems could be modified so that a low viscosity phase occurs well below the gel temperature. It appears that a capillary flow-addition type polyimide resin could be developed. This approach provides the most promising system for widespread applicability.

ORIGINAL PAGE IS
OF POOR QUALITY



7-30

ORIGINAL PAGE IS
OF POOR QUALITY

7-31

SKIN PANELS WITH GAGE THICKNESS COMBINATIONS OF (.015 AND .010) WILL RESULT IN FEATHER EDGES IN COUNTER SUNK HOLES.

To obtain more confidence in the capillary flow weld bond process, a feasibility study was conducted utilizing an epoxy resin system (until a qualified polyimide is established). The preliminary results of this study are noted below:

- Cleaning method for both spotwelding and adhesive bond - chemical cleaning per Spec LCP-7610198 plus mechanical abrasion with scotch bright produced a 50 micro ohms resistance surface good for 48 hours with no contamination or increase in resistivity.
- Gap spacing of .003-in. to .005-in. were held and repeatable by controlling the forging cycle during the weld schedule sequence.
- A Goodrich Type A 1396B epoxy 250 F curing resin was used.
- Excellent capillary flow was achieved through a 1-inch width weld joint.
- Lap shear tests indicated a 2-1/2 times load increase over standard spot welds.
- Fatigue tests of Ti-8-8-2-3 weld bonded specimens showed marked improvement over as-welded specimens (Table 7-8).

The encouraging results noted above indicate that weld bonding is a promising joining process.

To join the outer and inner beaded wing skin panel requires a blind capillary flow system. The proposed fabrication limits were established for the typical joint geometry. The proposed process steps are described as follows:

- Clean outer and inner interface skin surfaces.
- By automatic tape dispensing machine, place the P.I. resin tape (.004-in. to .005-in.) down the outer edges of the joint surfaces of the inner skin panel.
- Locate the outer skin on the inner skin
- Spot weld down the center in between the resin tapes
- Oven cure assembly at 350 F
- Post oven cure assembly at 600 F
- Ultrasonic inspect bond areas for voids

A development program is required to establish a viable process procedure to produce a quality PI resin weldbond joint for large beaded panel wing skins. In addition, development of an automatic tape dispensing machine and a 5-axis spot welder is required for fabrication of these large panel sizes.

TABLE 7-8. FATIGUE PROPERTIES OF WELD BONDED BETA TITANIUM ALLOY

MATERIALS	CONDITION	LOAD	NO. OF CYCLES TO FAILURE	REMARKS
Ti-8-8-2-3 (Aged to 160 ksi- F_{tu} approx.)	As welded	270 lbs	0.120×10^6	Failed
	As welded	400 lbs	0.043×10^6	Failed
Ti-8-8-2-3 (Aged to 160 ksi- F_{tu}) plus B. F. Goodrich Epoxy Resin Type A-1396B	As welded plus resin infiltrated and cured	270 lbs	3.4×10^6	No failure. Test stopped.
		400 lbs	5.0×10^6	No failure (increased load to 600 lbs)
		600 lbs	1.4×10^6	Failed
		700 lbs	0.5×10^6	Failed

Composite Reinforced Spar Caps - Significant structural mass reduction was achieved by the application of organic and metal matrix composites to reinforce the titanium alloy spar caps (Reference Section 12, Structural Concept Analysis). The fabrication and assembly schedule considering (1) the autoclave curing method for the boron-polyimide reinforcement, (2) the aluminum brazed method for the borsic-aluminum reinforcement and, (3) the diffusion bond method for the boron-aluminum reinforcement are highlighted below:

(1) Autoclave Curing Method - Boron/Polyimide Reinforced Spar Cap (Figures 7-10 and 7-11):

- Boron/PI reinforcements procured to contour in separate tool.
- Clean titanium spar cap (Chem-etch)
- Place PI adhesive film on spar cap flanges.
- Boron/PI reinforcements bonded to spar cap as shown in the figure.
- Vacuum bag autoclave process (350 F @ 150 psi).
- Post cure 600 F; 4-6 hours (after removed for tools)

(2) Aluminum Braze Method - Borsic/Aluminum Reinforced Spar Caps: Figures 7-12 and 7-13).

- Interface surfaces of stainless steel vacuum bag pressure pads, spacers etc. coated with stopoff (microbrazed).
- Clean titanium spar cap (Chem-etch)
- Coat titanium filler blocks for insertion in titanium spar cap.
- Preform Borsic/Aluminum (B/Al) laminate reinforcement strips to contour by diffusion bond process.
- Place coated filler blocks in titanium spar cap
- Place 719 braze alloy on titanium spar cap flanges (tack-spot in place)
- Place on preformed B/Al reinforcement strip laminate and locating pressure pads.
- Encapsulate assembly with preformed stainless steel vacuum bag; seam-weld closing edges.
- Purge with argon gas; draw vacuum.
- Place assembly in hydroclave.
- Heat up to 1030 F @ 250 psi.
- Cool to R.T.; remove from hydroclave.
- Remove stainless steel vacuum bag.
- Remove spar from tools.
- Check contour and warpage

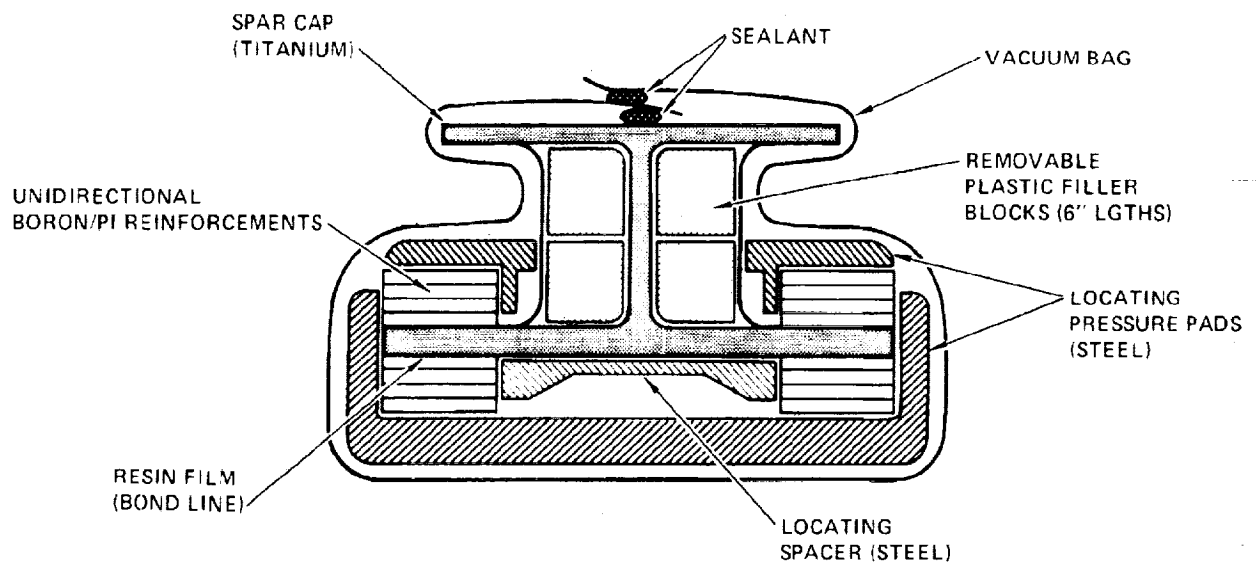


Figure 7-10. Boron-Polyimide Reinforced Tank Wall Caps - Autoclave Curing Method

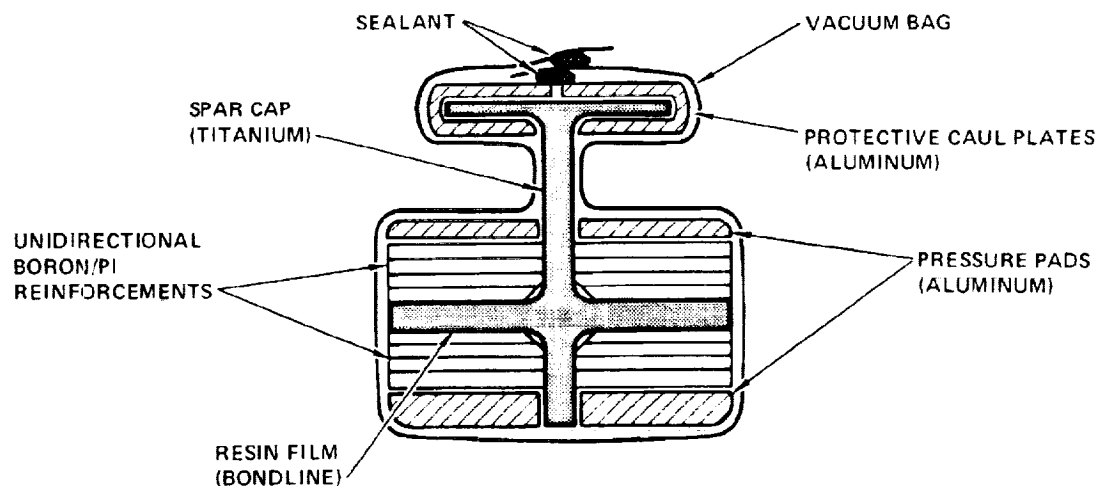


Figure 7-11. Boron-Polyimide Reinforced Truss Spar Caps - Autoclave Curing Method

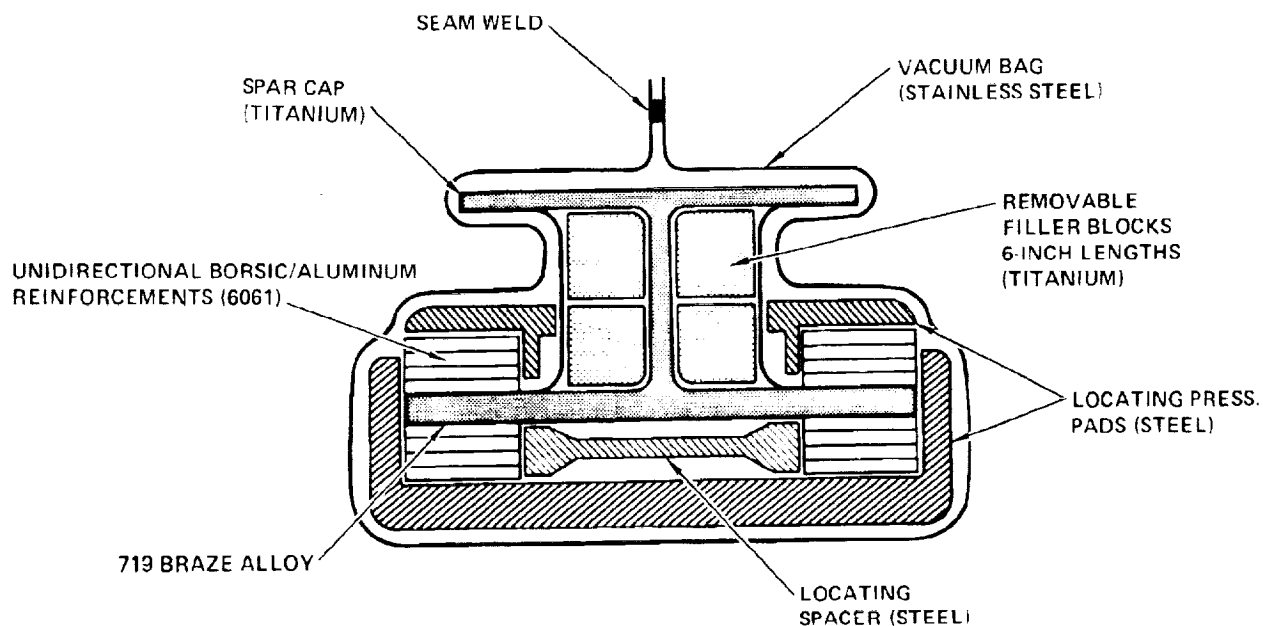


Figure 7-12. Borsic-Aluminum Reinforced Tank Wall Caps - Aluminum Brazing Method

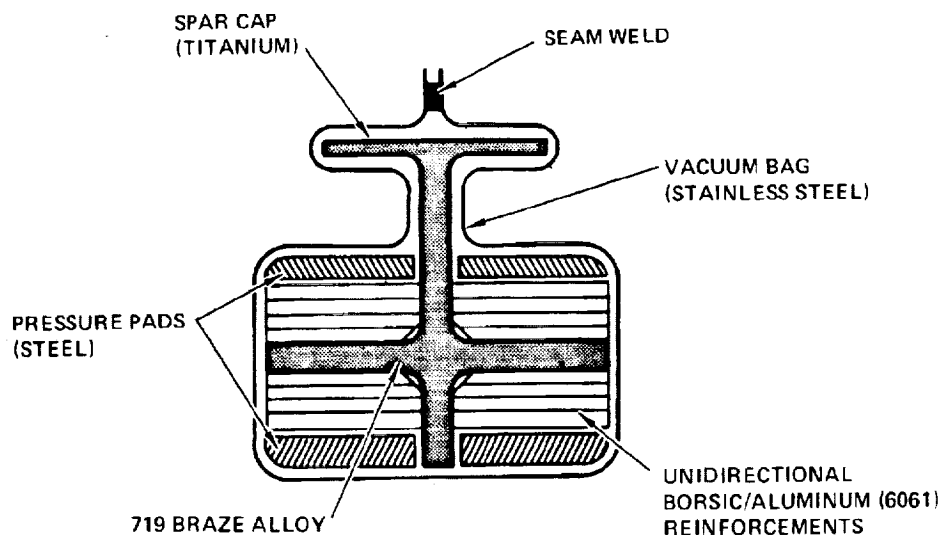


Figure 7-13. Borsic-Aluminum Reinforced Truss Spar Caps - Autoclave Curing Method

(3) Diffusion Bond Method - Boron/Aluminum Reinforce Spar Cap (Figures 7-14 and 7-15):

- Die interface surfaces coated with stopoff (microbrazo)
- Clean titanium spar cap (chem-etch).
- Lay up green tape (boron/aluminum) to specified layers in lower die cavity.
- Place in titanium spar cap
- Place in spacer blocks
- Lay up green tape (boron/aluminum) to specified layers on titanium cap surface.
- Locate and assembly upper die blocks.
- Encapsulate die block assembly with preformed stainless steel vacuum bag; seam weld closing edges.
- Purge with argon gas; draw vacuum.
- Place die assembly in furnace - heat up to 950 F (Figure 7-16)
- Move die assembly by mechanical means to adjoining press for progressive step by step diffusion bonding cycle and into an adjacent staging cooling furnace (Figure 7-16)
- Cool in furnace to R.T. (Figure 7-16)
- Remove stainless steel vacuum bag
- Remove spar from tools
- Check for contour warpage

(4) Heat expanding rubber oven curing method - Boron polyimide reinforced spar (Figure 7-17 and Figure 7-18).

- Boron/PI reinforcements prepreg - lay up to spar cap contour in tool
- Mold heat expanding rubber (silastic "E") to prescribed shapes in aluminum molds
- Clean titanium spar cap (chem-etch)
- Place PI adhesive film on spar cap flanges.
- Place boron/PI laminate on spar cap
- Place in heat expanding rubber shapes - caul plates - pressure pads
- Assembly clamp plates
- Remove all tooling
- Place assembly in oven
- Post cure spar caps 600 F; 4 to 6 hours
- Heat up to 350 F - cure 2 hours

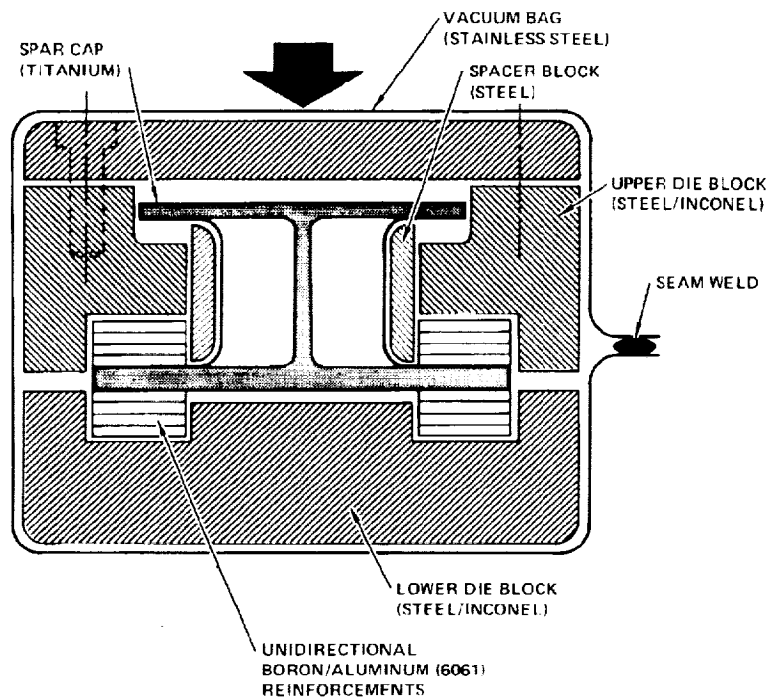


Figure 7-14. Boron-Aluminum Reinforced Tank Wall Caps - Diffusion Bond Method

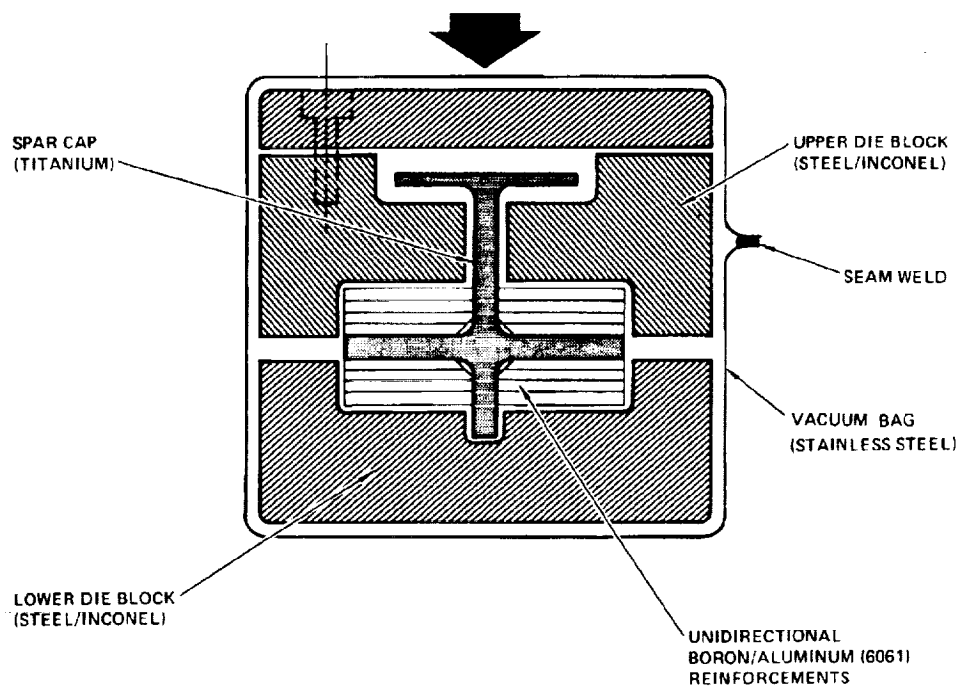


Figure 7-15. Boron-Aluminum Reinforced Truss Spar Caps - Diffusion Bond Method

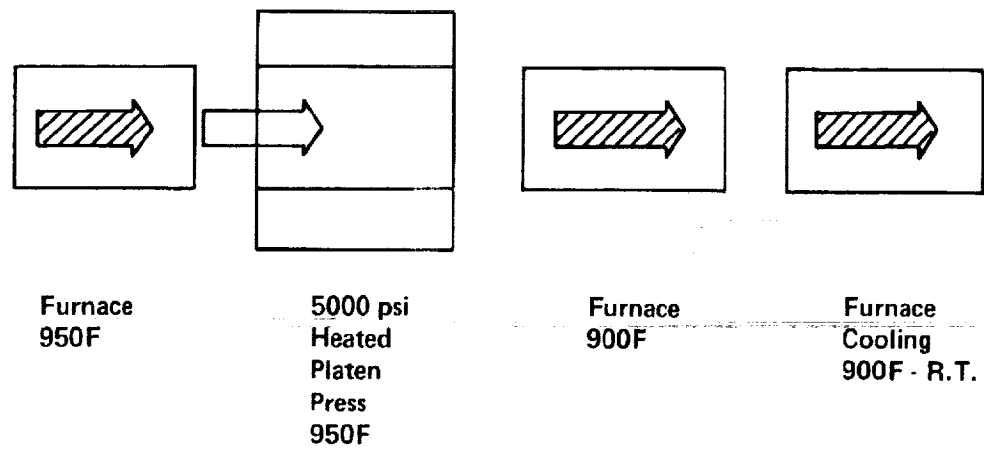


Figure 7-16. Facility Set-up Diagram

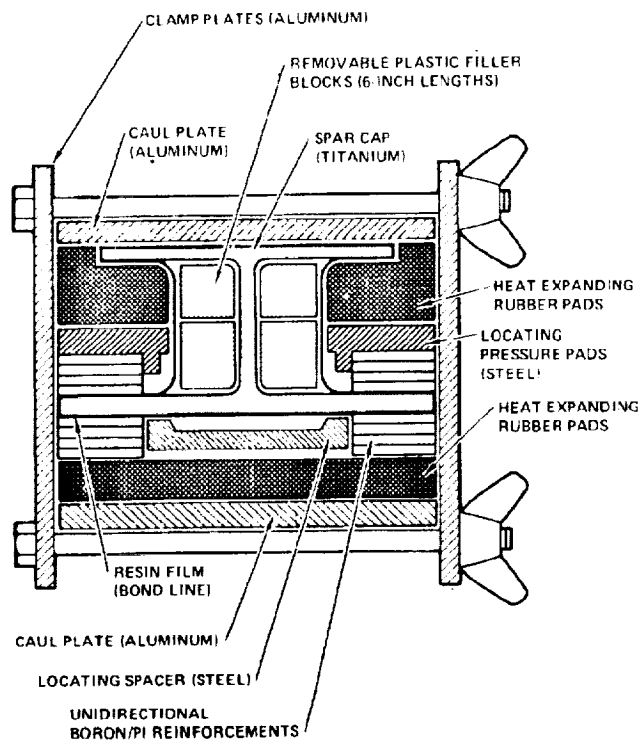


Figure 7-17. Boron-Polyimide Reinforced Spar-Heat Expanding Rubber Oven Curing Method

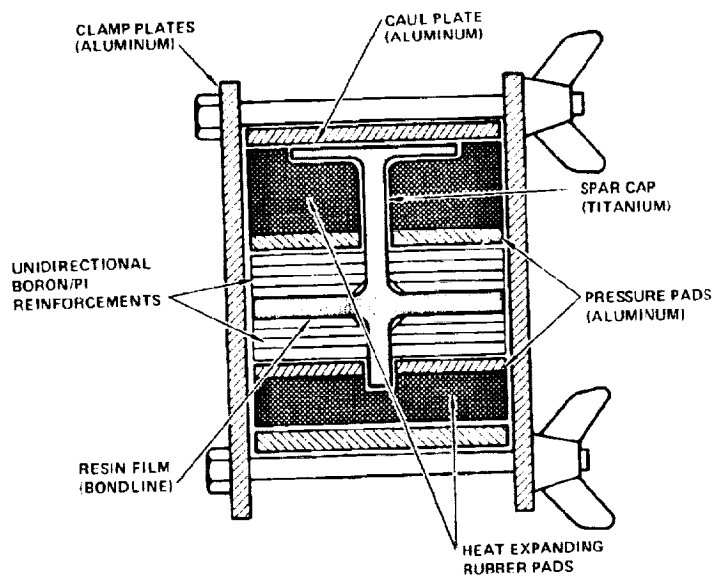


Figure 7-18. Boron-Polyimide Reinforced Spare-Heat Expanding Rubber Oven Curing Method

POTENTIAL MANUFACTURING PROBLEMS

The critical problems identified in the fabrication technology discipline are joining, forming, sealing and related fabrication equipment requirements. These technology disciplines were further affected by the material constraints. Some industry research and development programs have been initiated in these technologies, however, the specific application of the technologies to the Mach 2.7 arrow-wing design configurations presented many new problems to be resolved.

Tables 7-9 through 7-13 summarize the manufacturing technology problem areas identified for the beaded skin and monocoque surface panel designs. The technology problem areas were defined in a format describing the structural component design, critical manufacturing parameters, development programs required, potential problem areas and related technical comments.

Specific technology problem areas summarized on the tables are outlined in more detail below:

1. Chordwise Stiffened Wing Design - Convex Beaded Surface Panels

- Panel size: 15 feet by 35 feet
- Material: Titanium alloy Ti-6Al-4V annealed and Beta alloy
- Welding thin gage sheet (.010-.030 in.) - equipment - tooling - welding schedules
- Vacuum forming (1450 F) - beaded panels - tooling - temperature zone control techniques.
- Continuous roll forming (cold - 1450 F) - beaded inner skin shapes - 35 ft. lengths
- Weld bonding - capillary flow - P.I. resin systems - application techniques.
- Weld bonding - surface treatments - spot welds - P.I. resins.
- Riveting - weld bond panels to substructure - rivet materials - methods.
- Isothermal brazing - beaded panels - spar cap clips - brazing alloy selections.
- F.B. welding spar - mating wing assembly - equipment - weld schedules.
- Weld brazing - capillary flow - brazing alloy selection - tooling techniques - process methods
- Tank sealing - faying surfaces - interstices between structural members - corner caps - overlapping surfaces - coating fasteners.

2. Fuselage Design - Hat Stiffened Skin/Stringer Shell

- Panel size; 15 feet by 50 feet
- Material: Titanium alloy Ti-6Al-4V annealed and Beta alloy
- Weld bond assemblies - curing ovens - temperature zone control - P.I. resins.
- Rivet Bond - longitudinal plus circumferential final assembly splices - localized curing equipment - temperature zone controls - curing schedules - P.I. resins
- Welding - longitudinal plus circumferential final assembly splices - equipment design - weld schedules - NDI.
- Tapered section stringer - rolling equipment - uniform thickness control - spring back - repeatability - Beta alloys - 50 ft. lengths.

3. Monocoque Wing Design - Honeycomb Sandwich Surface Panels

- Panel size: 68 inch by 40 feet
- Material: Titanium alloy Ti-6Al-4V annealed and Beta alloy.
- Brazing facilities - tooling - uniform heat up and cooling rates - warpage and shrinkage - compound contours - NDI methods.
- Doublers - fail-safe straps - faying surface porosity - surface concepts (holes, grooves, shim strips, etc.,) - surface area size limits - NDI.
- Brazing stopoff - prevent vertical core cell wall braze flow - reduce conductivity - reduce weight.
- Repair methods - materials - process application techniques - equipment.

The key parameter in these selected problem areas were the size effect of the structural components upon the fabrication technologies and facility requirements. The state-of-the-art process methods, tooling concepts and related equipment would need to be scaled-up to produce on a production basis repeatable quality large unit hardware components.

The information developed above and in Tables 7-9 through 7-13 does provide sufficient data to serve as a basis for the planning of R&D programs for the development of a viable supersonic cruise aircraft.

TABLE 7-9. POTENTIAL MANUFACTURING PROBLEMS-WING SURFACE PANEL CONCEPT-
CONVEX BEADED SKINS

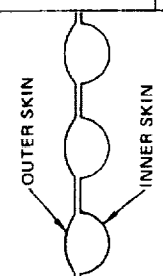

STRUCTURAL COMPONENT	CRITICAL MANUFACTURING PARAMETER	DEVELOPMENT PROGRAMS REQUIRED	POTENTIAL PROBLEM AREAS	COMMENTS
1. <u>BASIC PANEL</u> 	<ul style="list-style-type: none"> WING SURFACES - Welding of thin gage sheet (.010 to 0.30") to fabricate panels Panel sheet sizes (15' x 35') TIG/Plasma Arc Welding Systems Butt Welds 	<ul style="list-style-type: none"> Tooling & automatic welding equipment Weld schedules Post weld treatment, i.e. planishing, etc. NDI techniques 	<ul style="list-style-type: none"> Minimize mismatch, warpage and shrinkage Determine weld treatment to maintain good fatigue & fracture toughness characteristics Inspection to insure full penetration, no voids, porosities or other flaws 	<ul style="list-style-type: none"> Weld quality critical to permit subsequent forming and assembly and minimize need for fuel tank sealants Provide slow crack growth structures without resorting to excessive redundancy
	<ul style="list-style-type: none"> WING SURFACES - Vacuum forming (1450°F) of outer and inner skin panels Skins are preformed prior to vacuum forming to final configuration 6Al 4V and aged Beta Ti alloys skins require hot forming to compound contour Panel size (15' x 35') 	<ul style="list-style-type: none"> Tooling - compound contoured resistance heated ceramic dies Large die surfaces - constant surface temperature control system required for heat up and cooling cycles Inert gas cooling system to reduce process forming time 	<ul style="list-style-type: none"> Size effect (15' x 35') in fabricating a crack free surface Selection of heating elements arrangements to produce constant surface temperatures Electrical controls to feed heating elements to maintain constant temperatures for heat up and cooling rates within 1,250°F Techniques to flow cooling gas over surface of part to maintain constant surface cooling rate 	<ul style="list-style-type: none"> Thermal expansion of Ti preform beaded skin panels must be interfaced with the heated ceramic die surface configurations (Compound contour and beaded surface) Forming process cycle should be less than 8 hrs (Heat up and cool down) Constant surface temperature control required to prevent warpage and to make the part match the die surface contour and configurations
2. <u>INNER SKIN</u> 	<ul style="list-style-type: none"> WING SURFACES - Continuous roll forming - cold and hot (1450°F) beaded inner skin (3 to 4 beads/panel) 35' lengths 	<ul style="list-style-type: none"> Progressive rolling equipment cold for solution treated Beta alloys and hot (1450°F) for 6Al 4V alloy 	<ul style="list-style-type: none"> Design equipment to minimize metal thickness reduction in producing beaded configurations Equipment required to roll continuously 3 or 4 bead width configurations in one pass 	<ul style="list-style-type: none"> Cold rolling method must be designed to compensate for spring back of material to obtain net dimensions Hot rolling method must produce straight length sections with minimum warpage and distortion

TABLE 7-9. POTENTIAL MANUFACTURING PROBLEMS-WING SURFACE PANEL CONCEPT-
CONVEX BEADED SKINS (CONTINUED)

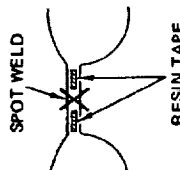
STRUCTURAL COMPONENT	CRITICAL MANUFACTURING PARAMETER	DEVELOPMENT PROGRAMS REQUIRED	POTENTIAL PROBLEM AREAS	COMMENTS
3. JOINING OF SKINS 	<ul style="list-style-type: none"> Weld Bonding - Capillary flow resin method - P.I. Surface treatment for spot weld - bonding Placing of resin tape to prevent spot weld contamination Curing and post curing ovens for 15' x 35' skin panels 	<ul style="list-style-type: none"> Design applicator to automatically prelay resin system at beaded interface joints prior to spot welding Resin material developed to function with applicator equipment Welding schedules to provide 3 to 4 mil surface gap NDI techniques to indicate porosity - disbond areas 	<ul style="list-style-type: none"> Resin tape thickness to be held to a maximum of 4 to 5 mil thickness TAPE type resin system is required, it must not flow and/or contaminate weld area during welding cycle Resin system to have a long out time life during application and spot welding operation for large size panels 15' x 35' 	<ul style="list-style-type: none"> Applicator system and equipment should be designed to laydown resin tape on panel sizes 15' x 35' utilizing N/C tape Compound contoured panel surfaces Resin system must be void free and low viscosity during cure cycle to achieve maximum flow and compatible with oxide film formed on clear skins by atmospheric exposure
	<ul style="list-style-type: none"> Weld Bonding - Spot welding equipment Materials - 6 Al-4V annealed - Beta alloys annealed and heat treated 	<ul style="list-style-type: none"> Design 5 axis N/C automatic spot welding machine to weld 15' x 35' beaded stiffened compound contoured skin panels 	<ul style="list-style-type: none"> Spot weld schedules to maintain a uniform laying surface gap 3 to 4 mils for capillary flow requirements Welding schedules for 3 layer enclosure joints (outer and inner skins and double interface surfaces) Minimum joint thickness .025" (.010 + .015 gage materials) 	<ul style="list-style-type: none"> Spot weld quality is critical since spot welds are considered to transmit the primary load in a weld bond joint The resin system provides the fatigue improvement in the joint
	<ul style="list-style-type: none"> Weld Bonding - Surface treatments for spot welding and P.I. resins Materials 6Al-4V annealed and heat treated 	<ul style="list-style-type: none"> Surface treatments to provide minimum ohm resistance for spot welding and be compatible with P.I. resin system. Also, to provide minimum pick up of oxide film during lengthy out time processing of large panel sizes 	<ul style="list-style-type: none"> Surface treatment materials should not cause any degradation to the mechanical properties of 6Al-4V and Beta alloys (O₂, H₂) Process repeatability a major requirement 	<ul style="list-style-type: none"> Surface treatments should be easy to apply and repeatable consistent with maximum values of surface cleanliness and minimum oxide film pick up

TABLE 7-10. POTENTIAL MANUFACTURING PROBLEMS-WING SURFACE PANEL CONCEPT-HONEYCOMB SANDWICH SKINS

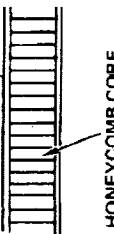
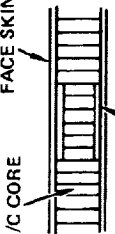
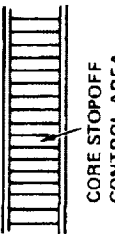
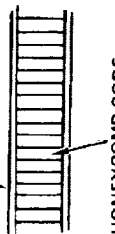
STRUCTURAL COMPONENT	CRITICAL MANUFACTURING PARAMETERS	DEVELOPMENT PROGRAMS REQUIRED	POTENTIAL PROBLEM AREAS	COMMENTS
1. BASIC PANEL 	Brazing - Honeycomb sandwich panels <ul style="list-style-type: none"> Face skins Titanium alloy 6Al-4V Core Ti-3Al-2.5V Panel size 68" x 40" Face skin gages min. 10 mil to .187" max. Brazing alloy 3003 aluminum 	<ul style="list-style-type: none"> Tooling and equipment to provide - pressure - temperature - inert gas to braze compound contoured panels 68" x 40" size Heating techniques to provide uniform heating and cooling over large surface panels during brazing cycle Improve and/or develop new methods of poke welding core to core and core to inserts/edge closures 	<ul style="list-style-type: none"> Braze alloy run off during brazing of large compound contoured skin panels Control brazing temp. and time to prevent formation of brittle intermetallic or excessive alum. diffusion into Ti surfaces Prevent panel growth and warpage during brazing cycle Fatigue life (50,000 hrs) at operational cycled temperatures - Crack propagation of face skins - brazed in fail safe straps 	<ul style="list-style-type: none"> Brazing cycle time of 6 to 8 hrs should be reduced 25 to 40% to improve production rates Tooling and equipment should be developed to have common heating units that can take a series of similar contour panel configurations
2. DOUBLERS/FAIL SAFE STRAPS 	Brazing - Doublers/fail safe straps <ul style="list-style-type: none"> Interface surface concepts Surface area size limits Faying surface porosity 	<ul style="list-style-type: none"> Determine surface area size limits to minimize interface porosity of smooth faced doublers/fail safe straps Determine surface area size limits for surface concepts of doublers/fail safe straps utilizing (perforated holes, grooves, shim strips, etc.) Develop NDI techniques to pickup interface porosity 	<ul style="list-style-type: none"> Interface porosity during the brazing of doublers/fail safe straps Control interface gap thickness - by surface concepts - eliminate gas bubbles to prevent porosity from occurring Refining NDI methods to pickup porosity interface layer 	<ul style="list-style-type: none"> If interface porosity cannot be eliminated, relate porosity to loss in properties
3. CORE STOPOFF 	Brazing - Core stopoff materials and processes <ul style="list-style-type: none"> Prevent vertical cell wall braze flow during brazing cycle Stopoff applied to 1/2 cell core strips prior to core assembly 	<ul style="list-style-type: none"> Stopoff materials that prevent capillary flow of braze alloy in the vertical cell wall Processes to apply stopoff material to core 1/2 segments Spot welding techniques to weld through stopoff material in assembly of the core NODES 	<ul style="list-style-type: none"> Stopoff materials must not contaminate brazing alloy during the brazing cycle Stopoff material must not cause corrosion to occur in the core Stopoff materials must not contaminate spot welds during core assembly 	<ul style="list-style-type: none"> If stopoff materials can be developed and applied economically to prevent vertical core cell capillary flow, the results will reduce panel conductivity and panel weight
4. BETA ALLOY 	Brazing - Beta titanium alloys <ul style="list-style-type: none"> Beta "C" Beta B-8-2-3 Brazing plus aging Beta alloy face skins Alum. brazing alloys 	<ul style="list-style-type: none"> Vacuum hot forming Beta face skins to compound contour prior to brazing cycle Brazing alloy and brazing schedule for Beta alloys Aging heat treatment cycle after completion of brazing cycle to achieve predicted mechanical properties 	<ul style="list-style-type: none"> Effects on predicted mechanical properties by hot forming face skins prior to brazing cycle forming requires (1000° to 1400°F range) Brazing alloy and brazing schedule must be compatible with aging heat treatment cycle Control brazing temp. and time plus aging temp. and time of Beta alloys to prevent intermetallic or excessive aluminum diffusion into Ti surfaces 	<ul style="list-style-type: none"> Brazing plus aging of Beta alloy face skin is a complex metallurgical problem to obtain the benefits of higher strength properties of Beta alloys Selection of brazing alloys and Beta aging parameters are the key areas of investigation and process development

TABLE 7-10. POTENTIAL MANUFACTURING PROBLEMS-WING SURFACE PANEL CONCEPT-HONEYCOMB SANDWICH SKINS (CONTINUED)

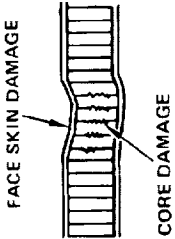
STRUCTURAL COMPONENT	CRITICAL MANUFACTURING PARAMETERS	DEVELOPMENT PROGRAMS REQUIRED	POTENTIAL PROBLEM AREAS	COMMENTS
<p>5. REPAIR METHODS</p>  <p>FACE SKIN DAMAGE</p> <p>CORE DAMAGE</p>	<ul style="list-style-type: none"> • Brazed Panels - Structural repair methods • Repair method temperature less than 1200°F • Organic resin matrix bonding - foam in place • Potting compounds - organic plus ceramic materials • Mechanical fastening patch plates • Low temperature braze alloy and/or solder 	<ul style="list-style-type: none"> • Process methods for bonding surface patch plates plus foam reinforcement of damaged core areas utilizing H.T. organic resin systems • Tooling - heating pad equipment to cure and post cure resin systems • Design equipment to be portable and easily installed for curing process • Portable NDI techniques to assure reliability and quality of repair • Potting compounds (organic + ceramic mixtures) application techniques and curing methods • Installation techniques for attaching patch plates utilizing Delron and/or blind fasteners. Also, a fastener plus H.T. resin bond method 	<ul style="list-style-type: none"> • No repair method should cause damage to the brazed joints • Temperature constrained to less than 1200°F • Heating control systems for H.T. resin systems to maintain required heat up and cooling rates within $\pm 25^\circ\text{F}$ • Mechanical fastener repair methods must meet long life fatigue requirements - minimum effects on causing crack propagation from patch repair area • NDI portable equipment to pick up porosity and disbond areas of repair area 	<ul style="list-style-type: none"> • All repair methods should require the minimum of repair time to keep the aircraft in service • Repair technique should be simple and easy to apply by field service personnel • Repair methods must be inspectable - operate effectively in the temperature environment and meet the fatigue life, etc. of the structural parameters

TABLE 7-11. POTENTIAL MANUFACTURING PROBLEMS--JOINING STRUCTURAL ASSEMBLIES

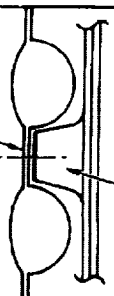
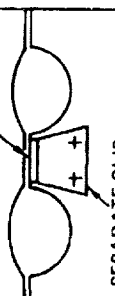
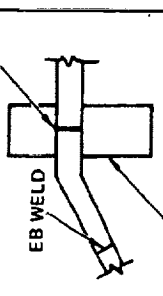
STRUCTURAL COMPONENT	CRITICAL MANUFACTURING PARAMETER	DEVELOPMENT PROGRAMS REQUIRED	POTENTIAL PROBLEM AREAS	COMMENTS
<p>1. <u>SURFACE PANEL TO SUBSTRUCTURE--RIVETING</u></p>  <p>RIVET JOINT</p> <p>INTEGRAL CLIP</p>	<ul style="list-style-type: none"> Riveting -- Minimum gage weld bonded panels to substructure Titanium alloy rivets (3/32 -- 5/32D) preferred -- other materials may be required 	<ul style="list-style-type: none"> Rivet materials -- Low upset forces Riveting equipment Riveting procedures to minimize deformation of thin skin panels and/or degradation of P.I. resin 	<ul style="list-style-type: none"> Pillowing of skins after riveting Joint deformation due to low creep strength Cracking of P.I. resin film Dissimilar metal corrosion of rivets not a Ti alloy Thermal stresses due to differential coefficient of expansion of rivet if not a Ti alloy Fretting -- faying surfaces 	<ul style="list-style-type: none"> Riveting equipment designed to be able to attach 15 ft x 35 ft skin panel to substructure. Min. clearance opening 1.3 inches Rivet materials -- low upset pressure -- high strength and low creep requirements
<p>2. <u>SURFACE PANEL TO SUBSTRUCTURE--BRAZING</u></p>  <p>BRAZE JOINT</p> <p>SEPARATE CLIP</p>	<ul style="list-style-type: none"> Isothermal brazing -- Panel to spar cap clips Aluminum type brazing alloys Titanium alloys 6Al-4V Beta alloys annealed and STA. Brazing and aging of Beta alloys -- one operation 	<ul style="list-style-type: none"> Tooling and equipment to provide -- pressure -- temperature Inert gas -- clip alignment to braze localized areas Techniques to apply foil tapes to faying joint surfaces by automatic equipment 	<ul style="list-style-type: none"> Run off of braze alloy during brazing of large compound contoured skin surfaces Control brazing temp. and time to prevent formation of brittle intermetallic or excessive aluminum diffusion in Ti surfaces Minimize oxide from forming by using a braze alloy compatible with surface oxide film formed on cleaned skins prior to brazing 	<ul style="list-style-type: none"> Tooling and equipment must be versatile to rapidly apply the brazing method for localized joints on a production basis
<p>3. <u>WING TIP TO AFT BOX--WELDING</u></p>  <p>EB WELD</p> <p>EB WELD</p> <p>PORTABLE EB WELDER (ENVELOPE)</p>	<ul style="list-style-type: none"> EB Welding Spars -- at mating wing assembly joint (i.e. BL470) Spar spacing 21 inches 6 Spars at joint 	<ul style="list-style-type: none"> Portable EB welding equipment -- clamp on type; preferably miniaturization of EB equipment in view of available space Portable NDI equipment to inspect joints on assembled structure Techniques to thermal/mechanical work to stress relieve including families of time-temperature -- residual stress curves Weld schedules for "Double-T" spar caps 	<ul style="list-style-type: none"> Spar joint alignment and fit up tolerance critical Dimensional control, increase susceptibility to stress corrosion Reduced fatigue and fracture toughness properties NDI to detect lack of fusion porosity, and other weld defects and determining the three dimensional location of defects in weldments 	<ul style="list-style-type: none"> Spar weld joints are highly loaded Joint interface tolerances for EB welding to be held to 5 mil Portable milling machining tooling required to mill weld surfaces smooth after welding

TABLE 7-12. POTENTIAL MANUFACTURING PROBLEMS-TANK SEALING CONCEPTS


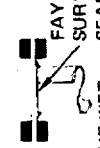
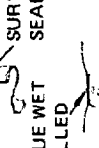
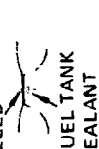
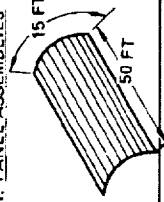
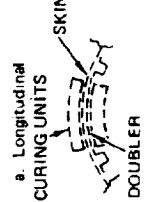
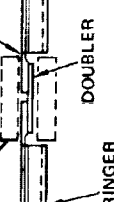
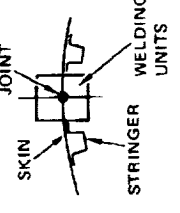

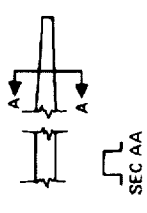
STRUCTURAL COMPONENT	CRITICAL MANUFACTURING PARAMETER	DEVELOPMENT PROGRAMS REQUIRED	POTENTIAL PROBLEM AREAS	COMMENTS
<p>1. FAYING SURFACE, SEAM AND FASTENER</p>  <p>HI-TIGUE WET INSTALLED</p>  <p>FAYING SURFACE SEALANT</p>  <p>HI-TIGUE WET INSTALLED</p>  <p>FUEL TANK SEALANT</p>	<ul style="list-style-type: none"> • Interstices between structural members: <ul style="list-style-type: none"> • Corner caps • Overlapping surfaces • Coating fasteners, welds and pin hole openings • Beaded skin panel joined by weld bonding 	<ul style="list-style-type: none"> • Sealing materials to withstand fuel tank thermal environment - fuel 170°F - fuel vapor 400°F - 3 PSIA pressure • Application techniques - and/or elevated - humidity effects • Surface treatments and primer systems compatible with sealing materials 	<ul style="list-style-type: none"> • Peel strengths, pressure blow out, weight loss lap shear, low temperature flexibility, groove reversion and shrinkage • P.I. resins exposed to hot fuel for long time may result in resin degradation - protective coatings may need to be developed 	<ul style="list-style-type: none"> • Service life 50,000 Hrs in environment • Materials to retain - 65°F flexibility, be blowout proof and have minimum shrinkage at joint interfaces • Rely on P.I. resin bond to prevent fuel from getting into corrugation bead • "O" Rings may be used around surface fasteners to assist in joint sealing • Fluorosilicones and fluorocarbon sealants require improvements in service life and for high temperature operations

TABLE 7-13. POTENTIAL MANUFACTURING PROBLEMS-FUSELAGE SHELL CONCEPT-SKIN/STRINGER PANELS

STRUCTURAL COMPONENT	CRITICAL MANUFACTURING PARAMETER	DEVELOPMENT PROGRAMS REQUIRED	POTENTIAL PROBLEM AREAS	COMMENT
1. PANEL ASSEMBLIES 	<ul style="list-style-type: none"> Weld bond assemblies (15 ft x 50 ft) P.I. resin systems Surface treatment for spot weld bonding Maintain critical spot weld gap 3 to 4 mils for resin capillary flow requirement 	<ul style="list-style-type: none"> Ovens capable of curing and post curing P.I. resin system for fuselage panels (15 ft x 50 ft) Automatic resin tape applicator equipment Resin system developed to function with applicator equipment 	<ul style="list-style-type: none"> Maintain constant temperature control zones in large size ovens for the heat up and cool down cycle rates for P.I. resin systems Resin system to have a long out time capability for application - spot welding large size panels 	<ul style="list-style-type: none"> Inert atmosphere may be required to prevent oxidation during post curing cycle of certain types of P.I. resin systems
2. PANEL SECTION SPLICE a. Longitudinal CURING UNITS 	<ul style="list-style-type: none"> Longitudinal skin splice - rivet bond Skin splice 50 Ft (length) Rivet bond joint to be cured and post cured after riveting during final assembly of fuselage sections P.I. resin systems 	<ul style="list-style-type: none"> Heating pad equipment to cure and post cure P.I. resin system Processing techniques to assure reliable and quality joints of selected P.I. resins and thermal resistant support carriers Design of portable equipment. Must be installed for curing process 	<ul style="list-style-type: none"> Heating system to provide constant surface temperature in the joint area Heating system required to maintain heat up and cooling rates within $\pm 25^\circ\text{F}$ Dimensional control of thermal resistant P.I. resin carrier to maintain uniform rivet grip length 	<ul style="list-style-type: none"> Heating equipment must not interfere with other assembly and installation tasks within the fuselage section Equipment must fit into available space and interface clearances
b. Circumferential CURING UNITS 	<ul style="list-style-type: none"> Circumferential skin splice - rivet bond Skin splice 204 inches (Length) Rivet bond joint to be cured and post cured after riveting during final assembly of fuselage sections P.I. resin systems 	(Same as above rivet bond requirements)	(Same as above rivet bond requirements)	(Same as above rivet bond requirements)

ORIGINAL PAGE IS
OF POOR QUALITY

TABLE 7-13. POTENTIAL MANUFACTURING PROBLEMS-FUSELAGE SHELL CONCEPT-
SKIN/STRINGER PANELS (CONTINUED)

STRUCTURAL COMPONENT	CRITICAL MANUFACTURING PARAMETER	DEVELOPMENT PROGRAMS REQUIRED	POTENTIAL PROBLEM AREAS	COMMENTS
<p>1. <u>PANEL SECTION</u> <u>SPLICE</u></p> <p>a. Longitudinal WELD JOINT</p>  <p>SKIN STRINGER WELDING UNITS</p>	<ul style="list-style-type: none"> Longitudinal skin splice - welding Skin splice 50Ft (length) Welding to be performed during final assembly of fuselage sections Fit up and joint alignment critical 	<ul style="list-style-type: none"> TIG/Plasma welding equipment for skin splice and frame splice joints Design equipment to be portable and easily installed for splice joint assembly Processing techniques and weld schedules to assure quality Thermal stress relieving equipment may also be required - portable Methods of controlling heat flow i.e., chill rates 	<ul style="list-style-type: none"> Determine pre and/or post weld thermal mechanical treatments to maintain good fatigue and fracture toughness characteristics NDI inspection to insure full penetration, no voids or porosity or other flaws Warpage and distortion control techniques Heat flow control required to avoid excessive temperatures in adjacent bonded/brazed components 	<ul style="list-style-type: none"> Welding equipment must not interfere with other assembly and installation tasks within the fuselage section Gas shielding of upper and lower joint surface critical to prevent oxide contamination N/C and T.V. monitoring of weld joint required Equipment must fit into available space and interface clearances
<p>b. Circumferential WELD JOINT</p>  <p>STRINGER WELDING UNITS</p>	<ul style="list-style-type: none"> Circumferential skin splice - welding Skin splice 204 inches (length) Welding to be performed during final assembly of fuselage sections 	<p>(Same as above weld joint requirements)</p>	<p>(Same as above weld joint requirements)</p>	<p>(Same as above weld joint requirements)</p>
<p>2. <u>TAPERED STRINGERS</u></p>  <p>SEC AA</p>	<ul style="list-style-type: none"> Tapered section stringers Beta Alloys - gages .020 in to .060 in. Stringer length, 50Ft. 	<ul style="list-style-type: none"> Rolling equipment to product tapered thickness and cross section configuration Hat section stringers Contouring equipment to form tapered stringers 	<ul style="list-style-type: none"> Uniform thickness and section shape Minimum bend radius required Spring back must be compensated in rolling method and controlled during subsequent thermal treatments Correlation of cold reduction and thermal cycle for consistent mechanical properties 	<ul style="list-style-type: none"> Process repeatability a requirement Feasibility experimentally proven Preliminary data on the effects of cold rolling on aged properties must be substantiated to provide both process limitations and minimum design properties

REFERENCES

- 1 MIL-HDBK5B, "Metallic Materials and Elements for Aerospace Vehicle Structures," 1 September 1971
- 2 Wood, R.A., Favor, R.J., "Titanium Alloys Handbook" MCIC-HB-02 Metals and Ceramics Information Center, Battelle - Columbus Laboratories, Columbus, Ohio, December 1972
- 3 Birchfield, E.B., and Kollmansberger, F., "Develop Fabrication/Processing Techniques for High Temperature Advanced Composites for Use in Aircraft Structures." AFML-TR-91, McDonnell Aircraft, July 1972
- 4 Lockheed Stress Memo Manual, Lockheed - California Company
- 5 Hancock, J.R., "Fatigue of Boron-Aluminum Composites", November 1972.



SECTION 8

BASIC DESIGN PARAMETERS

BY

J. E. RHODES, J. VAN HAMERSVELD, C. W. LINDBLOM

1

2

3

CONTENTS

<u>Section</u>	<u>Page</u>
INTRODUCTION	8-1
FABRICATION LIMITS	8-2
Chordwise Stiffened Wing Design	8-2
Spanwise Stiffened Wing Design	8-13
Monocque Wing Design	8-17

1

2

3

LIST OF FIGURES

<u>Figure</u>		<u>Page</u>
8-1	Structural Details - Chordwise Stiffened Wing Design	8-3
8-2	Fabrication Limits - Chordwise Stiffened Surface Panel Concepts	8-4
8-3	Fabrication Limits - Intermediate Spar and Skin Attachment - Chordwise Stiffened Wing Design	8-6
8-4	Fabrication Limits - Intermediate Rib and Skin Attachment - Chordwise Stiffened Wing Design	8-7
8-5	Fabrication Limits - Intermediate Spar and Rib Intersection - Chordwise Stiffened Wing Design	8-8
8-6	Fabrication Limits - Tank Rib and Closure Intersection - Chordwise Stiffened Wing Design	8-9
8-7	Fabrication Limits - Surface Panel End Closures - Chordwise Stiffened Wing Design	8-10
8-8	Surface Panel Mechanical Attachments	8-11
8-9	Installation Space Requirements for Various Fasteners	8-12
8-10	Fabrication Limits - Rib and Spar Webs	8-14
8-11	Fabrication Limits - Spanwise Stiffened Surface Panel Concepts	8-15
8-12	Fabrication Limits - Intermediate Rib and Spar Intersection - Spanwise Stiffened Wing Design	8-16
8-13	Fabrication Limits - Intermediate Rib and Skin Attachment - Spanwise Stiffened Wing Design	8-18
8-14	Fabrication Limits - Monocoque Surface Panel Concepts	8-19
8-15	Fabrication Limits - Inserts and Closures - Monocoque Wing Design	8-20
8-16	Fabrication Limits - Inserts and Closures - Monocoque Wing Design	8-21

PRECEDING PAGE BLANK NOT FILMED

C

.

C

C

LIST OF TABLES

<u>Table</u>		<u>Page</u>
8-1	Vendor Contacts Made for Arrow-Wing Structure Study	8-1

PRECEDING PAGE BLANK NOT FILMED



SECTION 8

BASIC DESIGN PARAMETERS

INTRODUCTION

The basic design parameters established for each structural arrangement and concept are presented in this section. These parameters specify realistic fabrication limits and constraints considering the available state-of-the-art of manufacturing titanium hardware for the near-term start-of-design supersonic cruise aircraft.

The parameters were defined after numerous consultations with vendors and other contractors (Table 8-1), extensive literature surveys and fabrication experience, and close collaboration between design, producibility, materials and structure specialists. Titanium mill product producers defined material sheet sizes that would be available. Fabrication equipment supplier data and transportation limits defined the maximum panel size that could be successfully manufactured. Foreign object damage (FOD) considerations defined skin gage thickness limits for the exposed surfaces of the wing.

TABLE 8-1. VENDOR CONTACTS MADE FOR ARROW WING STRUCTURES STUDY

<u>Vendor</u>	<u>Subject Discussed</u>
Aeronca Mfg.	Aluminum Brazed Honeycomb Sandwich
Rohr Aircraft	Liquid Interface Diffusion (LID) Diffusion Braze Process
Northrop Aircraft	Nor-Ti-Bond Diffusion Braze Process
TRW Systems	Weld Bond
Advanced Structures and Technology Co.	STRESSKIN
Sciaky Brothers, Inc.	Welding
Avco	Metal Matrix Composites
Holosonics	NDT Inspection Methods

The application of these data to the concept design and analysis effort ensured consistency between the structural arrangements defined for the various design approaches and the analytical results reported in Section 12, Structural Concept Analysis.

FABRICATION LIMITS

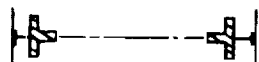
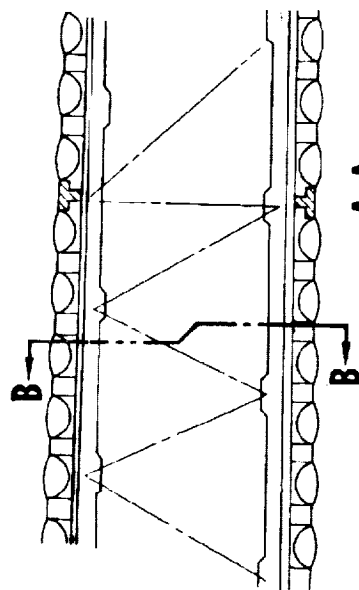
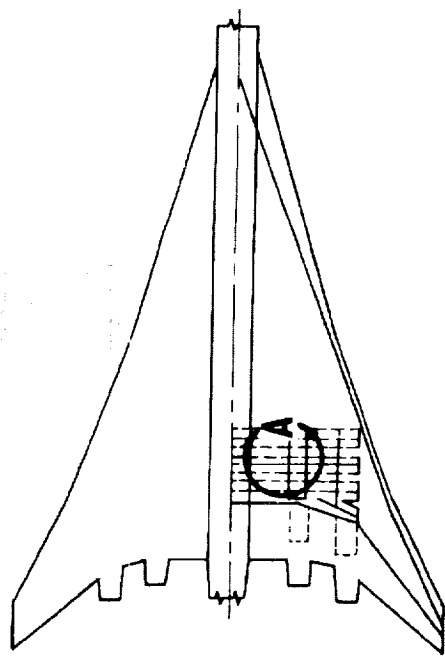
Fabrication limits and design constraints for the chordwise stiffened wing design are defined in the following paragraphs for various locations of the wing aft box structure depicted on Figure 8-1. These structural details are applicable to the entire wing planform with the mechanical attachment and shear web details applicable to all three design approaches.

Chordwise Stiffened Wing Design

Surface Panel Concepts. - The chordwise stiffened wing design utilizes surface panels which have stiffening elements oriented in the chord direction. Structurally efficient beaded skin designs as shown in Figure 8-2 are employed. The shallow depressions or protrusions of the outer skin provide smooth displacements under thermally induced strains and operational loads. Panel spanwise thermal stresses are minimized by allowing thermal deformations in the spanwise direction.

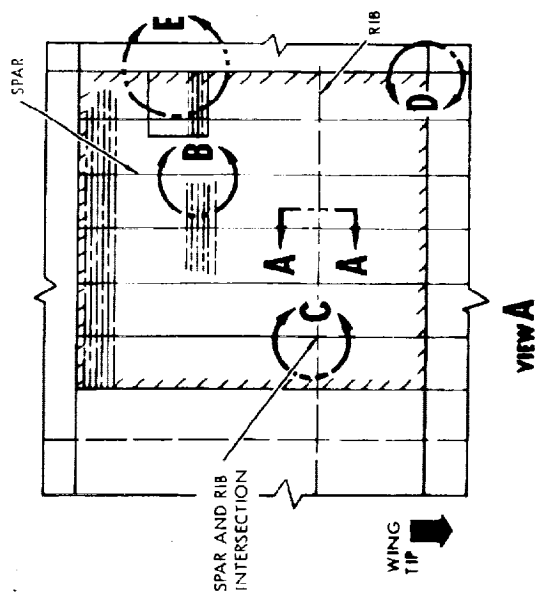
Figure 8-2 presents the fabrication limits for the surface panel concepts. The shallow protrusions or depressions of the outer skin permit cold preforming of large panel sizes followed by vacuum hot forming at 1450F. For the inner skin, the use of Ti-6Al-4V requires hot forming of a three bead width to avoid excessive thinning. The end closures are then welded to the corrugated panel followed by vacuum hot forming of the full width panel. The use of Beta alloy permits cold forming three bead width, however, solution treating and aging of 1100F is required after a hot-forming operation. Weld bonding is considered as the principle method of attaching the inner skin to the outer skin, as indicated on the figure.

Intermediate Spar and Skin Attachment. - The wing bending and shear loads for the chordwise stiffened wing design are transmitted by submerged spar caps and truss



SECTION B-B

SECTION A-A



REFERENCE FOR DETAILS

AREA	REFERENCE	FIGURE
BASIC PANEL	SECTION A-A	8-2
INTERMEDIATE SPAR AND SKIN ATTACHMENTS	SECTION A-A	8-3
INTERMEDIATE RIB AND SKIN ATTACHMENTS	VIEW 6	8-4
INTERMEDIATE SPAR AND RIB INTERSECTION	VIEW C	8-5
TANK CLOSURE RIB AND SPAR INTERSECTION	VIEW D	8-6
PANEL END CLOSURE AND ACCESS PANEL	VIEW E	8-7
PANEL MECHANICAL ATTACHMENT DETAILS		8-8
SHEAR WEB DETAIL	VIEW D	8-9

Figure 8-1. Structural Details - Chordwise Stiffened Wing Design

CONCEPT	FACE MATL.	INNER STIFF MATL.	SKIN GAUGES	SHEET SIZE (INS)	OUTER PANEL SIZE (FT)	INNER PANEL SIZE	FORMING LIMITS				FOREIGN OBJECT DAMAGE LIMITS	METHOD OF ATTACH IN-TO OUTER SURFACE	CONTOUR LIMITS	COMMENT
							METHOD	OUTER SKIN $\frac{D}{W}$ (MAX.)	INNER SKIN MIN. BEND RADI	H/W				
	Ti-6Al-4V	Ti-6Al-4V	MIN .010	36 x 144	15' x 35'	THREE BEAD WIDTH FORMING LIMITATION, WELD FROM SMALLER SIZE SHEETS	PERFORM COLD PLUS				.010	WELD BOND CAPTARY ACTION FOR MIN. WT.	NO PRACTICAL LIMIT	SKINS WILL BE INDUCED BY VELD QUALITY INDEX $K_2 = 4$ ASSUMED
	AN-NEALED	AN-NEALED	MAX .125	60 x 200		WELD FROM SMALLER SIZE SHEETS	VACUUM HOT FORM FULL WIDTH PANEL 1450°F	.10	.48 MAX		MIN. .6			
	Ti-6Al-4V	BETA ALLOY STA	MIN .010	24 x 144	15' x 35'	WELD FROM SMALLER SIZE SHEETS			.40 MAX					
	AN-NEALED		MAX .125	60 x 200		AS ABOVE								
	Ti-6Al-4V	Ti-6Al-4V	MIN .010	36 x 144	15' x 35'	THREE STIFFENER WIDTH FORMING LIMITATION, WELD FROM SMALLER SIZE SHEETS							AS ABOVE	
	AN-NEALED	AN-NEALED	MAX .125	60 x 200		WELD FROM SMALLER SIZE SHEETS		AS ABOVE						
	Ti-6Al-4V	BETA ALLOY STA	MIN .010	24 x 144	15' x 35'	WELD FROM SMALLER SIZE SHEETS								
	AN-NEALED		MAX .125	60 x 200		AS ABOVE								

Figure 8-2. Fabrication Limits - Chordwise Stiffened Surface Panel Concepts

ORIGINAL PAGE 13
OF POOR QUALITY

webs as shown in Figure 8-3. The structure is fabricated by welding (E.B. and T.I.G.) of machined extrusions, forgings and tubes of Ti-6Al-4V annealed or Beta alloy. The various parameters used for design of these spars and the integral skin attachment clips are identified on the figure.

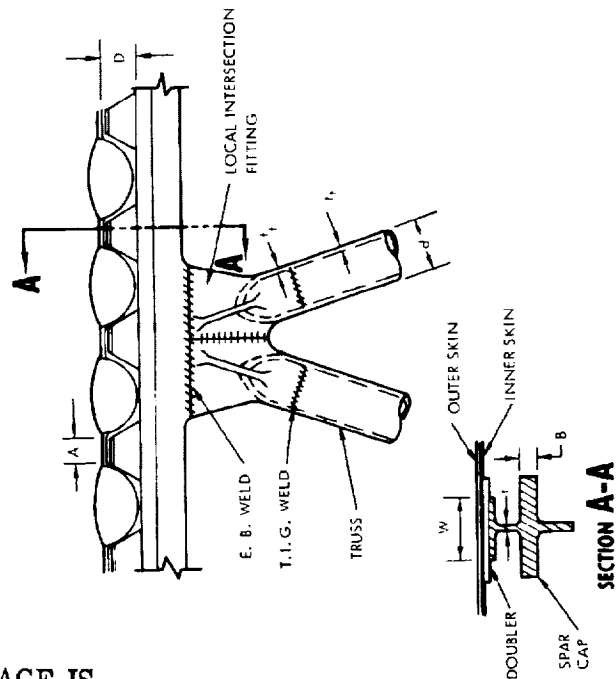
Intermediate Rib and Skin Attachment. - Widely spaced ribs of both tee-section and I-section caps are used in conjunction with the surface panels to transmit the chordwise wing loads. The rib assemblies shown in Figure 8-4 are fabricated by welding of machined extrusions, forgings and tubes of titanium alloy. The various design parameters are shown on the figure, including specific constraints for attaching the surface panels to the rib structure.

Intermediate Spar and Rib Intersection. - Figure 8-5 presents the basic and alternate design for the submerged spar cap and rib cap intersection. Both designs incorporate an intersection fitting welded (integral) to the spar cap and truss web. The rib trusses are mechanically fastened to the intersection fitting as shown. The alternate design indicates the local modifications essential to accommodate the I-section rib cap.

Tank Rib and Closure Intersection. - At all fuel tank closures (rib and spar direction), circular-arc (sine wave) corrugated webs are used. An intersection fitting machined from Ti-6Al-4V or Beta alloy forging is E.B. welded to the spar cap and T.I.G. welded to the spar web as shown in Figure 8-6. The chordwise continuity is provided by mechanical attachments through the rib cap and the intersection fitting using Hi-Tigue fasteners.

Surface Panel End Closures. - Although large panel sizes are postulated, the practical limits defined in Figure 8-2 necessitates the use of end closures to provide chordwise continuity of the structure. Figure 8-7 shows the minimum limits for the end closure design. Although the final design will require experimental validation, local thickening of the panel at the attachments is provided by a tapered finger doubler that is weld bonded to the skin. The local thickening permits the fastener shear force to act on the panel neutral axis and to avoid local instability between and beyond the ends of the beads.

ORIGINAL PAGE IS
OF POOR QUALITY

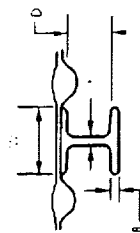
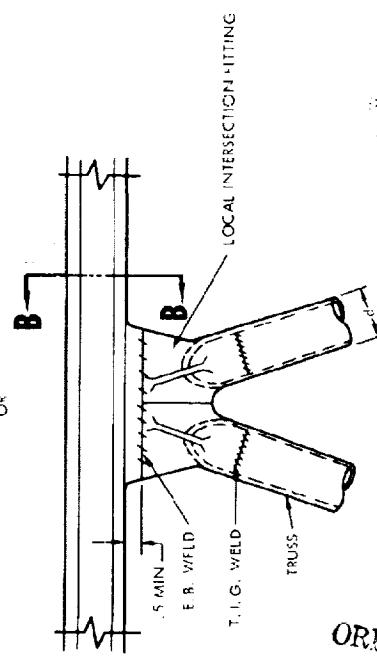
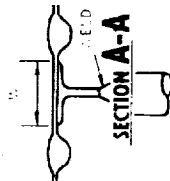
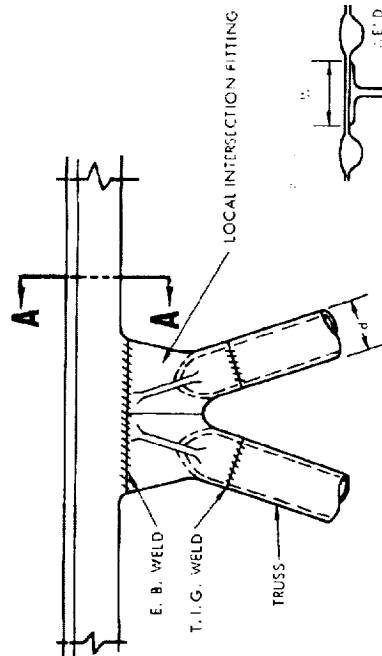


SPAR CAP (SECTION A-A)	
MATERIAL	TI-6AL-4V ANNEALED OR BETA ALLOY
FORM	MACHINED FROM ROUGH EXTRUSION
EXTRUSION LIMIT	ENCLOSURE WITHIN 20 INCH DIA.; MINIMUM THICKNESS .196 IN.; PROJECTED THICKNESS .060 IN.
ROUGH EXTRUSION DIMENSION RATIO	$\frac{A}{B} > .15$
FINAL MACHINE MIN. THICKNESS	.040 IN. OVER LONG LENGTH .020 IN. LOCALLY
MAXIMUM LENGTH OF EXTRUSION	240 INS. PLASMA ARC 'E.B.' WELD FOR ADDED LENGTH

TRUSS (MINIMUM DIMENSIONS - INCHES)	
LOCAL INTERSECTION FITTING	MACHINED FORGING E.B. WELDED TO CAP LEG
LOCAL THICKNESS FINAL MACHINE	.020 IN.
O. D. TRUSS TUBE	.50 IN.
I. D. TRUSS TUBE	.020 IN.

CLIP TO SKIN (MINIMUM DIMENSIONS - INCHES)	
A, SKIN FLANGE	.45 IN.
B, FLANGE WIDTH	.75 IN.
C, DOUBLER PAD	H = .010; H = FLUSH FASTENER HEIGHT
D, CLIP HEIGHT	DEPENDENT ON ATTACHMENT; RIVETS 1.3 IN.; HI TIGHT 1 INCH; BLIND BOLTS .50 IN.

Figure 8-3. Fabrication Limits - Intermediate Spar and Skin Attachment -
Chordwise Stiffened Wing Design



SECTION B-B

RIB CAP - SECTION A-A AND B-B			
MATERIAL	Ti-6Al-4V ANNEALED OR BETA ALLOY STA		
FORM	MACHINED FROM ROUGH EXTRUSION		
EXTRUSION LIMIT	ENCLOSURE WITHIN 20 INCH DIAMETER	MIN THICKNESS .138 IN.	PROJECTED THICKNESS .060 IN.
ROUGH EXTRUSION DIMENSIONAL RATIO	1.25 : 1		
FINAL MACHINE MIN THICKNESS	.040 IN. OVER LONG LENGTH	.020 IN. LOCALLY	
MAXIMUM LENGTH OF EXTRUSION	240 IN. PLASMA ARC E. B. WELD FOR ADDED LENGTH		

TRUSS MINIMUM DIMENSIONS - INCHES	
LOCAL INTERSECTION FITTING	MACHINED FORGING E. B. WELD TO CAP LEG
LOCAL THICKNESS FINAL MACHINE	.000 IN.
O. D. TRUSS TUBE	.30 IN.
I. D. TRUSS TUBE	.020 IN.

RIB CAP TO SKIN	
W. T. CAP	1/2 INCH MAXIMUM
D. CLEARANCE MIN	DEPENDENT ON ATTACHMENT: E. B. WELD, 1.3 IN. MIN. TIG WELD, 1.0 IN. MIN. BOND BOLT, .50 IN.

Figure 8-4. Fabrication Limits - Intermediate Rib and Skin Attachment - Chordwise Stiffened Wing Design

ORIGINAL PAGE IS
OF POOR QUALITY

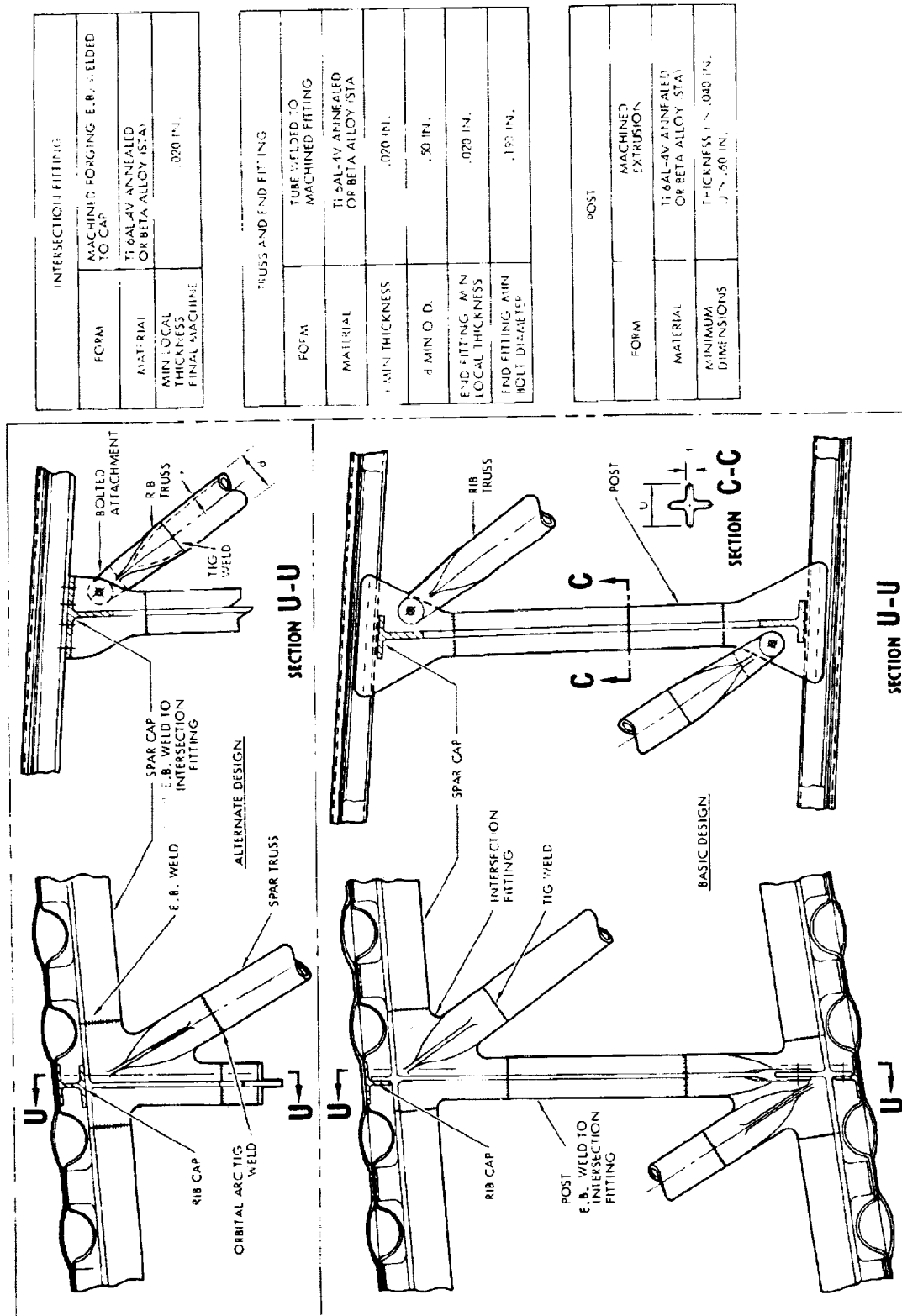
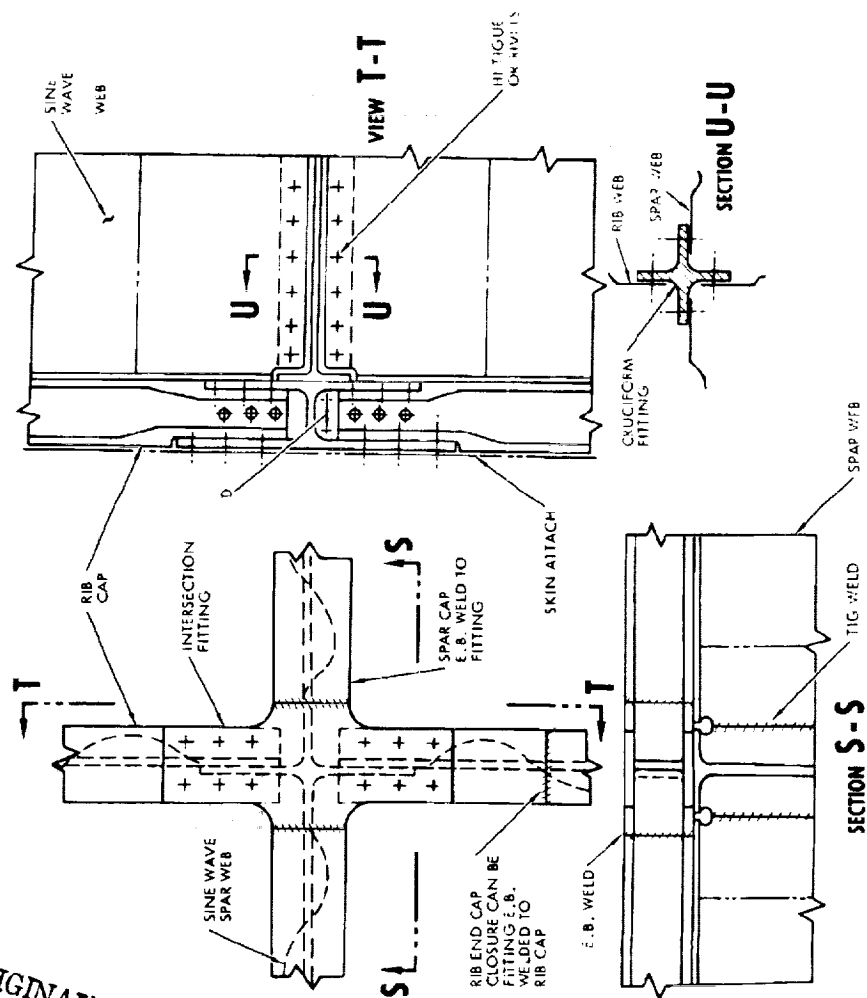


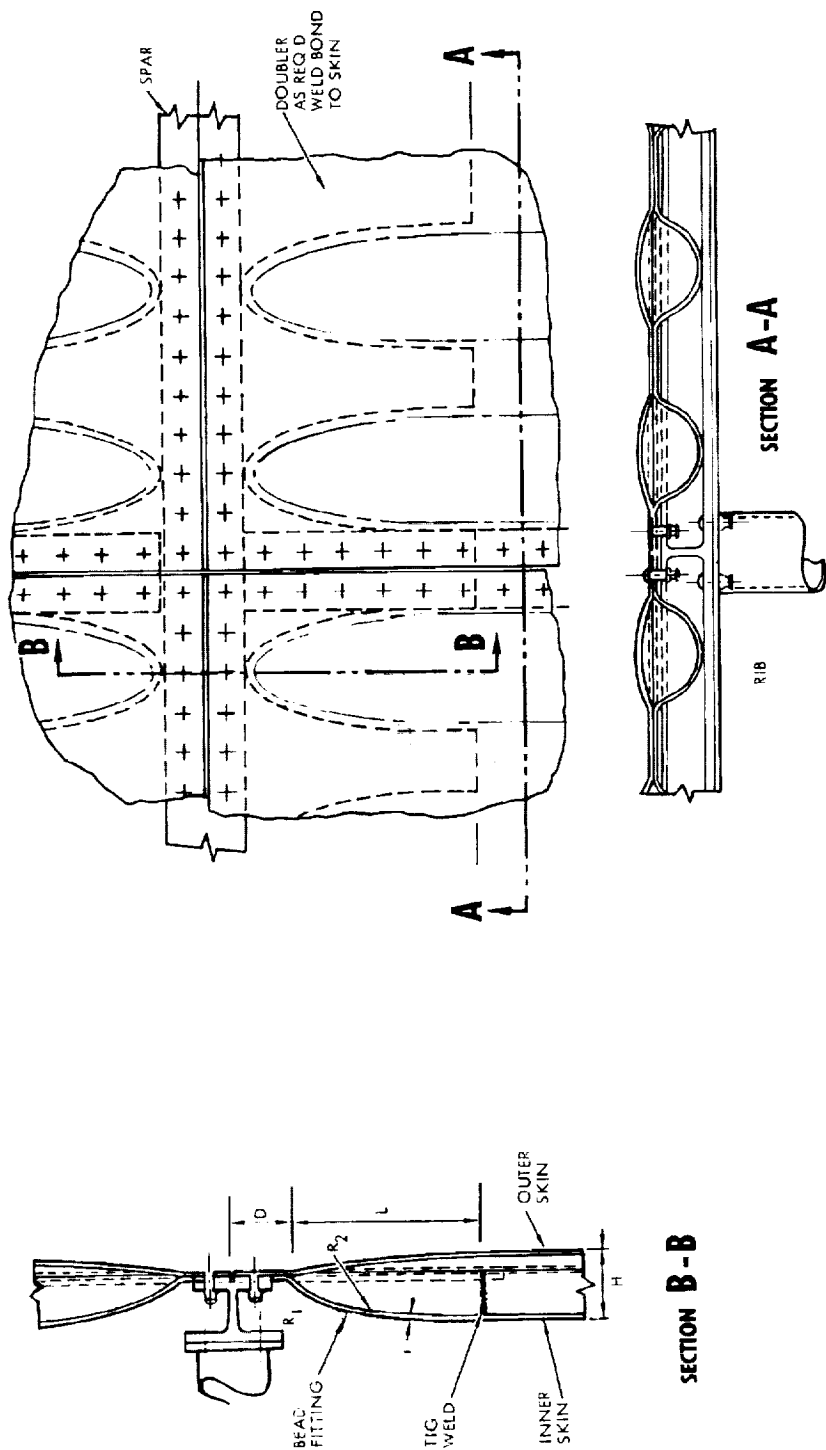
Figure 8-5. Fabrication Limits - Intermediate Spar and Rib Intersection - Chordwise Stiffened Wing Design

ORIGINAL PAGE 13
OF POOR QUALITY



INTERSECTION FITTING			
MATERIAL	T1 & A1-4V CP BETA ALLOY FORGING MACHINED MIN. AFTER FORGING .003 IN.		
ATTACHMENT TO SPAR	E.B. WELD FITTING TO SPAR CAP TO MAKE AN INTEGRAL STRUCTURE		
ATTACHMENT TO RIB CAP	MECHANICALLY ATTACH RIB CAP TO FITTING WITH HI TIGUE OR BLIND BOLTS		
ATTACHMENT ACCESS DIMENSION D	HI TIGUE RIVETS 1.0 IN. 1.3 IN. .5 IN.		

Figure 8-6. Fabrication Limits - Tank Rib and Closure Intersection - Chordwise Stiffened Wing Design



BEAD END CLOSURE LIMITS

MATERIAL	T ₃ 6Al-4V ANNEALED OR BETA ALLOY STA			
FORMING	DIE FORMED; T ₃ 6Al-4V-HOT BETA ALLOY-COLD THEN AGED			
MINIMUM GAGE	.010 IN.			
FORMING LIMITS	MIN L 2H	MIN R ₁ AND R ₂ .05 IN.	MIN. D 2H	

Figure 8-7. Fabrication Limits - Surface Panel End Closures -
Chordwise Stiffened Wing Design

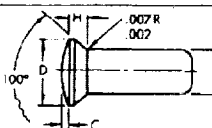
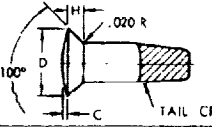
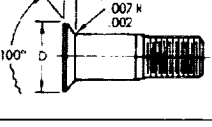
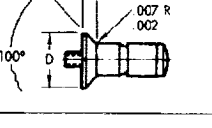
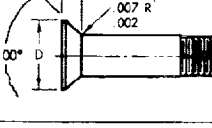
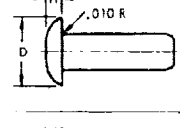
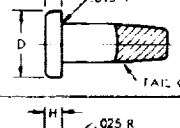
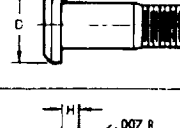
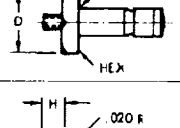

CANDIDATE FASTENERS																				
TYPE FASTENER		DIMENSIONS	MATERIAL	COMMENTS																
FLUSH HEAD	RIVETS (UPSET)	 <p>LS 10052</p> <table><tr><th>B (DIA)</th><th>H</th><th>C</th><th>D (MIN)</th></tr><tr><td>.096</td><td>.021</td><td>.004</td><td>.126</td></tr><tr><td>.127</td><td>.028</td><td>.005</td><td>.174</td></tr><tr><td>.153</td><td>.036</td><td>.007</td><td>.225</td></tr></table>	B (DIA)	H	C	D (MIN)	.096	.021	.004	.126	.127	.028	.005	.174	.153	.036	.007	.225	<ul style="list-style-type: none">A 286 CRESCP TiMONEL	<ul style="list-style-type: none">UPSET RIVETS NOT ACCEPTABLE IN WELD BONDED AREAS BECAUSE OF PROBABLE DAMAGE TO BONDMILLING OF INSTALLED HEADS FOR MAXIMUM FLUSHNESS NOT FEASIBLE FOR A286 AND TITANIUM RIVETS
	B (DIA)	H	C	D (MIN)																
	.096	.021	.004	.126																
	.127	.028	.005	.174																
	.153	.036	.007	.225																
RIVETS (UPSET)	 <p>CHEFFY BUCKS CSR 924 (NAS 1397)</p> <table><tr><th>DIA</th><th>H</th><th>C</th><th>D (MIN)</th></tr><tr><td>.096</td><td>-</td><td>-</td><td>-</td></tr><tr><td>.127</td><td>-</td><td>-</td><td>-</td></tr><tr><td>.164</td><td>.034</td><td>.005</td><td>.230</td></tr></table>	DIA	H	C	D (MIN)	.096	-	-	-	.127	-	-	-	.164	.034	.005	.230	<ul style="list-style-type: none">6 Al-4V (95 KSI) SHEAR	<ul style="list-style-type: none">UPSET RIVETS NOT ACCEPTABLE IN WELD BONDED AREAS BECAUSE OF PROBABLE DAMAGE TO BONDCREEP OF UPSET TAIL WILL RESTRICT USAGE IN TENSION APPLICATIONSMAY REQUIRE ANTI-FRETTING COATINGS IN TITANIUM STRUCTURES	
DIA	H	C	D (MIN)																	
.096	-	-	-																	
.127	-	-	-																	
.164	.034	.005	.230																	
HI-TIGUE	 <p>MOD. HEAD - ALT 315-5-</p> <table><tr><th>DIA</th><th>H</th><th>D</th></tr><tr><td>.127</td><td>.028</td><td>.174</td></tr><tr><td>.163</td><td>.036</td><td>.225</td></tr></table>	DIA	H	D	.127	.028	.174	.163	.036	.225	<ul style="list-style-type: none">A 286 CRES6 Al-4V	<ul style="list-style-type: none">SELECTED FOR ALL AREAS WITH BONDING OR CRITICAL IN FATIGUEINTERFERENCE FIT REQUIRED FOR MINIMUM INSTALLATION ACCESS SPACE REQUIREMENT								
DIA	H	D																		
.127	.028	.174																		
.163	.036	.225																		
BLIND	 <p>MOD. HEAD - NAS 167C</p> <table><tr><th>DIA</th><th>H</th><th>D</th></tr><tr><td>.127</td><td>.028</td><td>.174</td></tr><tr><td>.164</td><td>.036</td><td>.225</td></tr></table>	DIA	H	D	.127	.028	.174	.164	.036	.225	<ul style="list-style-type: none">A 286 CRES6 Al-4V	<ul style="list-style-type: none">NOT ACCEPTABLE IN AREAS REQUIRING SEALINGPROTRUDING BROKEN STEM MAY PRESENT FLUSHNESS PROBLEMSANTI-FRETTING COATING OR BRUSHING REQUIRED IN TITANIUM STRUCTURES								
DIA	H	D																		
.127	.028	.174																		
.164	.036	.225																		
SCREWS	 <p>MOD. HEAD - NAS 440C-4500</p> <table><tr><th>DIA</th><th>H</th><th>D</th></tr><tr><td>.111</td><td>.021</td><td>.126</td></tr><tr><td>.137</td><td>.028</td><td>.174</td></tr><tr><td>.163</td><td>.036</td><td>.225</td></tr></table>	DIA	H	D	.111	.021	.126	.137	.028	.174	.163	.036	.225	<ul style="list-style-type: none">A 286 CRES6 Al-4V	<ul style="list-style-type: none">USABLE IN AREAS WITH BONDING AND WHERE REMOVAL IS REQUIREDANTI-FRETTING COATING OR BRUSHING REQUIRED IN TITANIUM STRUCTURES					
DIA	H	D																		
.111	.021	.126																		
.137	.028	.174																		
.163	.036	.225																		
PROTRUDING HEAD	RIVETS (UPSET)	 <p>LS 13971</p> <table><tr><th>DIA</th><th>H</th><th>D</th></tr><tr><td>.096</td><td>-</td><td>.196</td></tr><tr><td>.128</td><td>.030</td><td>.262</td></tr><tr><td>.160</td><td>.044</td><td>.328</td></tr></table>	DIA	H	D	.096	-	.196	.128	.030	.262	.160	.044	.328	<ul style="list-style-type: none">A 286 CRESCP TiMONEL	<ul style="list-style-type: none">UPSET RIVETS NOT ACCEPTABLE IN WELD BOND AREAS BECAUSE OF PROBABLE DAMAGE TO BONDMILLING OF INSTALLED HEADS FOR MAXIMUM FLUSHNESS - NOT FEASIBLE FOR A286, AND TITANIUM RIVETS				
	DIA	H	D																	
	.096	-	.196																	
	.128	.030	.262																	
	.160	.044	.328																	
RIVETS (UPSET)	 <p>CHEFFY BUCKS CSR 924</p> <table><tr><th>DIA</th><th>H</th><th>D</th></tr><tr><td>.096</td><td>-</td><td>-</td></tr><tr><td>.127</td><td>-</td><td>-</td></tr><tr><td>.164</td><td>.055</td><td>.235</td></tr></table>	DIA	H	D	.096	-	-	.127	-	-	.164	.055	.235	<ul style="list-style-type: none">6 Al-4V (95 KSI) SHEAR	<ul style="list-style-type: none">UPSET RIVETS NOT ACCEPTABLE IN WELD BONDED AREAS BECAUSE OF PROBABLE DAMAGE TO BONDCREEP OF UPSET TAIL WILL RESTRICT USAGE IN TENSION APPLICATIONSMAY REQUIRE ANTI-FRETTING COATINGS IN TITANIUM STRUCTURES					
DIA	H	D																		
.096	-	-																		
.127	-	-																		
.164	.055	.235																		
HI-TIGUE	 <p>ALT 315-5-</p> <table><tr><th>DIA</th><th>H</th><th>D</th></tr><tr><td>.096</td><td>-</td><td>-</td></tr><tr><td>.127</td><td>-</td><td>-</td></tr><tr><td>.165</td><td>.047</td><td>.263</td></tr></table>	DIA	H	D	.096	-	-	.127	-	-	.165	.047	.263	<ul style="list-style-type: none">A 286 CRES6 Al-4V	<ul style="list-style-type: none">SELECTED FOR ALL AREAS WITH BONDING OR CRITICAL IN FATIGUEINTERFERENCE FIT REQUIRED FOR MINIMUM INSTALLATION ACCESS SPACE REQUIREMENT					
DIA	H	D																		
.096	-	-																		
.127	-	-																		
.165	.047	.263																		
BLIND	 <p>NAS 1669</p> <table><tr><th>DIA</th><th>H</th><th>D</th></tr><tr><td>.096</td><td>-</td><td>-</td></tr><tr><td>.127</td><td>-</td><td>-</td></tr><tr><td>.164</td><td>.096</td><td>.25</td></tr></table>	DIA	H	D	.096	-	-	.127	-	-	.164	.096	.25	<ul style="list-style-type: none">A 286 CRES6 Al-4V	<ul style="list-style-type: none">NOT ACCEPTABLE IN AREAS REQUIRING SEALINGANTI-FRETTING COATING OR BRUSHING REQUIRED IN TITANIUM STRUCTURES					
DIA	H	D																		
.096	-	-																		
.127	-	-																		
.164	.096	.25																		
SCREWS	 <p>NAS 5702-5102</p> <table><tr><th>DIA</th><th>H</th><th>D</th></tr><tr><td>.096</td><td>-</td><td>-</td></tr><tr><td>.127</td><td>-</td><td>-</td></tr><tr><td>.164</td><td>.102</td><td>.322</td></tr></table>	DIA	H	D	.096	-	-	.127	-	-	.164	.102	.322	<ul style="list-style-type: none">A 286 CRES6 Al-4V	<ul style="list-style-type: none">USABLE IN AREAS WITH BONDING AND WHERE REMOVAL IS REQUIRED					
DIA	H	D																		
.096	-	-																		
.127	-	-																		
.164	.102	.322																		

Figure 8-8. Surface Panel Mechanical Attachments

Surface Panel Mechanical Attachments. - A fastener study was made to select the types of fastener that could be used to attach the wing surface panels to the substructure. Figure 8-8 presents the flush and protruding head fasteners selected with low profile head configurations. In addition, minimum fastener installation clearances shown in Figure 8-9 were established. As shown, blind fasteners require the minimum space for installation. The space requirement for Hi-Tigue fasteners is based on the use of a special tool.

Blind - Jo-bolts, V-bolts, and Huck-bolts (A286, Ti-6Al-4V materials) are candidate blind fasteners. Blind bolts are not considered as good as a rivet or bolt type fastener for structural applications because of the reduced clamping action and tension allowables. However, they do provide the minimum installation clearance requirement and may be required in critical internal clearance areas of the wing structure. The use of blind fasteners are avoided in tank areas.

Rivets - CP Titanium, A286, Monel, and Cherrybucks (Ti-6Al-4V) are potential candidates. Rivets do require the maximum installation space since the materials are difficult to upset and require heavy bucking bars. Cracking the weld bond resin is a concern and will require experimental evaluation to determine if degradation of the polyimide resin occurs during the riveting operation.

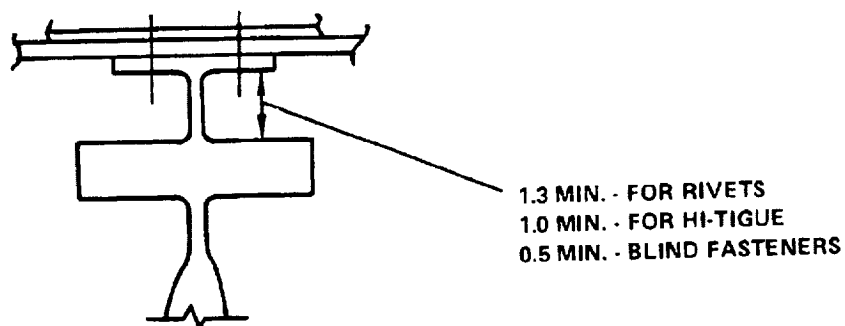


Figure 8-9. Installation Space Requirements for Various Fasteners

Hi-Tigue - A286, Ti-6Al-4V (STA) are the most acceptable fastener for skin to substructure attachment. The installation clearance was established by the use of a special installation tool developed by the Hi-Shear Corporation. A special tool (No. HLA1034) slides in between the spar base and the underside of the spar clip to torque the Hi-Tigue nut. All studs are driven with an interference fit to prevent the stud from turning during the nut torquing process.

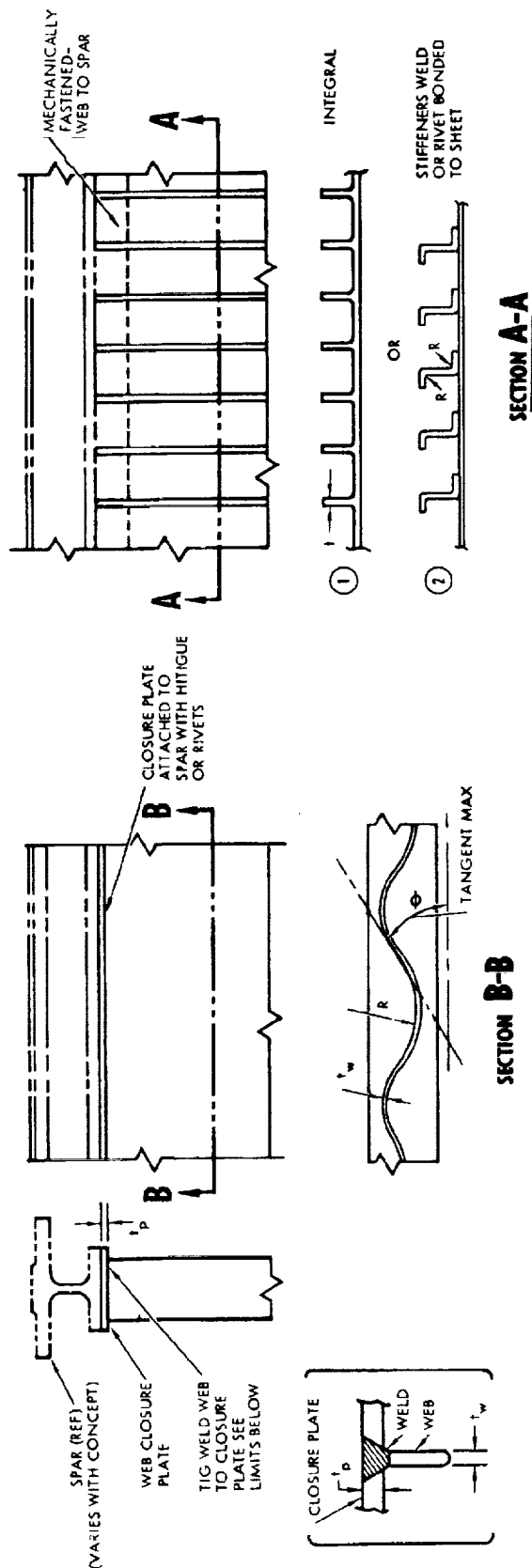
Rib and Spar Webs. - At fuel tank closures or in dry bays where the wing box depth precludes the use of truss webs, circular-arc (sine wave) corrugated webs are used. Cold forming of corrugations is accomplished to a $24t$ radius as shown in Figure 8-10. The thickness relationship between the closure plate and the corrugated web is 4 to 1.

An alternate approach to the closed web design is also shown on the figure. Both the integrally stiffened and sheet stiffened design are presented with their applicable design parameters.

Spanwise Stiffened Wing Design

Surface Panel Concepts. - The spanwise stiffened wing design utilizes surface panels which have stiffening elements oriented in the spar direction. Figure 8-11 presents the fabrication limits and constraints for the panel configurations considered. Smooth skins are required for aerodynamic performance, thus the skin panels must accommodate the chordwise thermal strains without buckling. For the zee-stiffened and the hat-stiffened designs, weld bonding is considered as the primary method of attaching the stiffeners to the skin. For the integrally stiffened designs, the parts are shot peened subsequent to the chemical milling operation. A fatigue quality index of 4 is assumed for establishing design allowables.

Intermediate Rib and Spar Intersection. - The wing bending and shear loads for the spanwise stiffened wing design are transmitted by the surface panels and spars. Figure 8-12 presents the fabrication limits for a typical welded spar assembly consisting of the spar cap and truss structure. Submerged rib caps are employed and provide stability to the surface panels. Continuity of the rib structure is provided by the forged intersection fitting and its attachment to the rib cap as indicated on the figure.



1 INTEGRAL STIFFENED WEB	
MATERIAL	Ti 6Al-4V OR BETA ALLOY PLATE OR EXTRUSION
MIN THICKNESS, t (IN.)	.040 AFTER MACHINING .020 AFTER CHEM-MILLING
EXTRUSION LIMITS	(SEE TABLE FOR INTEGRAL STIFFENED SURFACE PANEL)

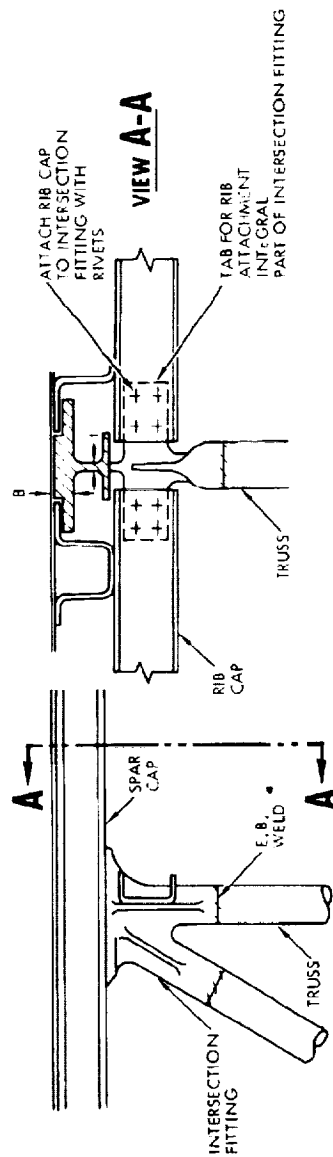
2 SHEET STIFFENED WEB	
MATERIAL	Ti 6Al-4V ANNEALED OR BETA ALLOY (STA) SHEET
MIN BEND RADIUS FOR STIFFENERS, R	3t

SINE WAVE SHEAR WEB	
MATERIAL CLOSURE PLATE AND WEB	Ti 6Al-4V SHEET (ANNEALED) OR BETA ALLOY (STA)
MIN GAUGE	.010 IN.
MIN RADIUS R SINE WEB	COLD FORMING 24 t _w
WELD JOINT LIMIT MELT THRU	$\frac{t_p}{t_w} < 4:1$
TANGENT ANGLE, θ	60° TO 89°

Figure 8-10. Fabrication Limits - Rib and Spar Webs

CONCEPT	FACE MATERIAL	INNER STIFF MATERIAL	SKIN GAUGES	SHEET SIZE	OUTER PANEL SIZE	FORMING LIMITS FOR STIFFENERS TI 6AL-4V HOT FORMED BETA C COLD FORMED AND AGED					FOREIGN OBJECT DAMAGE LIMITS	METHOD OF ATTACH TO OUTER SURFACE	CONTOUR LIMITS	COMMENT
						R AND T	P ₁ AND T	H ₁ AND b ₂	H	I				
	TI 6AL-4V ANNEALED OR BETA ALLOY STA	TI 6AL-4V ANNEALED OR BETA ALLOY STA	MIN .010 MAX .125	36 x 144 60 x 200	15' x 30' WELD FROM SMALLER SIZE SHEETS	MIN .015 MAX .025	P ₁ .75 MIN .015 MAX .025	P ₁ .40 MIN SET TO GIVE BOND AND OR BRAZE AREA b ₂ .25	.50 IN. MIN PRACTICAL DIMENSION	.15 MIN	P ₁ OUTER SKIN WING UPPER SURFACE .015 WING LOWER SURFACE .020	WELD BOND CAPILLARY ACTION OR WELD BRAZE	INNER STIFFENER STRETCHED FORMED	SKINS WILL HAVE K _T INDUCED BY WELD QUALITY INDEX K _Q = 4 ASSUMED
	AS ABOVE	AS ABOVE	MIN .010 MAX .125	24 x 144 60 x 200	AS ABOVE	MIN .010 MAX .125	MIN .40 MAX .45 FOR INDIVIDUAL HATS .40 FOR CONTINUOUS HATS AS ABOVE	MIN .40 MAX .45 FOR INDIVIDUAL HATS .40 FOR CONTINUOUS HATS AS ABOVE	MIN .40 MAX .45 FOR INDIVIDUAL HATS .40 FOR CONTINUOUS HATS AS ABOVE	N/A	AS ABOVE	AS ABOVE	AS ABOVE	
	TI 6AL-4V ANNEALED OR BETA ALLOY STA	TI 6AL-4V ANNEALED OR BETA ALLOY STA	MIN .010 MAX .125	36 x 144 60 x 200	15' x 30' WELD FROM SMALLER SIZE SHEETS	MIN .015 MAX .025	P ₁ .75 MIN .015 MAX .025	P ₁ .40 MIN SET TO GIVE BOND AND OR BRAZE AREA b ₂ .25	.50 IN. MIN PRACTICAL DIMENSION	.15 MIN	P ₁ OUTER SKIN WING UPPER SURFACE .015 WING LOWER SURFACE .020	WELD BOND CAPILLARY ACTION OR WELD BRAZE	INNER STIFFENER STRETCHED FORMED	SKINS WILL HAVE K _T INDUCED BY WELD QUALITY INDEX K _Q = 4 ASSUMED
	AS ABOVE	AS ABOVE	MIN .010 MAX .125	24 x 144 60 x 200	AS ABOVE	MIN .010 MAX .125	MIN .40 MAX .45 FOR INDIVIDUAL HATS .40 FOR CONTINUOUS HATS AS ABOVE	MIN .40 MAX .45 FOR INDIVIDUAL HATS .40 FOR CONTINUOUS HATS AS ABOVE	MIN .40 MAX .45 FOR INDIVIDUAL HATS .40 FOR CONTINUOUS HATS AS ABOVE	N/A	AS ABOVE	AS ABOVE	AS ABOVE	

Figure 8-11. Fabrication Limits - Spanwise Stiffened Surface Panel Concepts



SPAR (SECTION A-A)	
MATERIAL	Ti 6 AL-4V ANNEALED; RETA ALLOY (STA)
FORM	MACHINED FROM ROUGH EXTRUSION
EXTRUSION CROSS SECTION LIMIT	ENCLOSURE WITHIN .20 IN. DIA. MIN THICKNESS, .188 IN., PROJECTED THICKNESS .060 IN.
ROUGH EXTRUSION DIMENSION RATIO	$\frac{t}{B} \geq .15$
FINAL MACHINING MINIMUM THICKNESS	.040 IN. OVER LONG LENGTH .020 IN. LOCALLY
MAXIMUM LENGTH OF EXTRUSION	240 IN.; PLASMA ARC/E.B. WELD FOR ADDED LENGTH

TRUSS	
LOCAL INTERSECTION FITTING	MACHINE FORGING/E.B. WELDED TO CAP LEG
MINIMUM LOCAL THICKNESS FINAL MACHINE	.020 IN.
TRUSS TUBE MINIMUM O.D.	.50 IN.
TRUSS TUBE MINIMUM T	.020 IN.

Figure 8-12. Fabrication Limits - Intermediate Rib and Spar Intersection - Spanwise Stiffened Wing Design

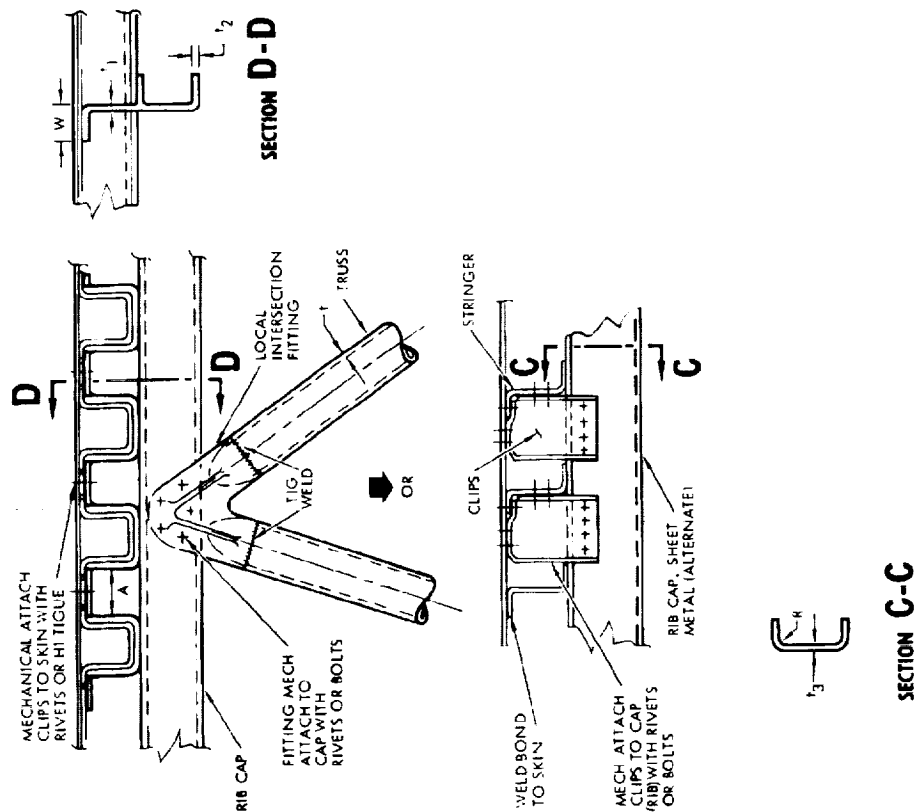
Intermediate Rib and Skin Attachment. - The submerged rib cap design with and without the integral clips for surface panel attachment are shown in Figure 8-13. For both design approaches, the intersection fitting of the truss structure is mechanically fastened to the rib cap. The minimum design parameters are specified with the maximum dictated by the loading requirements.

Monocoque Wing Design

Surface Panel Concepts. - The monocoque wing design consists of biaxially stiffened surface panels which support inplane loads both in the span and chord direction. The monocoque construction has a smooth skins that results in minimum aerodynamic drag.

The biaxially stiffened panels for which design parameters were established are shown in Figure 8-14 and include the brazed honeycomb sandwich, the diffusion bonded Stressskin sandwich and the corrugated sandwich. The various constraints imposed to the Stressskin and corrugated sandwich designs identifies the brazed honeycomb sandwich panel as the candidate monocoque design.

Inserts and Closures. - Figures 8-15 and 8-16 presents the design parameters for the inserts and closures for the surface panels discussed above. The term "inserts" refers to hard points for intermediate support; "closures" refer to the panel end support as dictated by panel size constraints of Figure 8-14. The lack of shear continuity is noted for both the Stressskin and corrugated sandwich designs.







RIB CAP SECTION D-D	
MATERIAL	T1 6 AL-4V ANNEALED OR BETA ALLOY STA
FORM	MACHINED FROM ROUGH EXTRUSION
EXTRUSION LIMIT	ENCLOSURE WITHIN 20 IN. DIAMETER
ROUGH EXTRUSION DIMENSION RATIO	$\frac{r_1}{r_2} > .15$
ROUGH EXTRUSION MINIMUM THICKNESS	.19 INCH
FINAL MACHINE MINIMUM THICKNESS	.040 IN. OVER LONG LENGTH .020 IN. LOCALLY

TRUSS	
LOCAL INTERSECTION FITTING	FORGED MACHINE WELDED FITTING
MINIMUM LOCAL THICKNESS FINAL MACHINE	.020 INCH
TRUSS TUBE MINIMUM O.D.	.50 INCH
TRUSS TUBE MIN + O.D.	.020 INCH

RIB CLIP TO SKIN	
MINIMUM T	.50 INCH
MINIMUM A	.65 INCH

RIB CAP SECTION C-C	
MATERIAL	T1 6 AL-4V ANNEALED OR BETA ALLOY STA
MINIMUM r_2	.015
MINIMUM RADIUS RAG P	R_3

Figure 8-13. Fabrication Limits - Intermediate Rib and Skin Attachment -
Spanwise Stiffened Wing Design

CONCEPT	FACE MATERIAL	CORE MATERIAL	FACE SKIN GAGE (IN.)	SHEET SIZE (IN.)	PANEL SIZE (IN.)	MATERIAL CONDITION		CELL		DEPTH	BRAZE ALLOY	FORM		FACE SHEET THICKNESS		COMMENTS	CONCLUSION	
						BEFORE BRAZE	BRAZE ALLOY	CL. GAGE (IN.)	CELL (IN.)			TYPE	MIN. SHEET	MAX. SHEET				
	Ti-6Al-4V ANNEALED	Ti-3Al-2.5V	MIN	46 x 144	63 IN. X 40 FT			002	1.8 TO 1.2	0 TO 4.12 IN.	3003 A	NO PRACTICAL LIMIT	0.010 MIN	1.000 MAX	NO PRACTICAL LIMIT	BRAZE ALLOY AND ANNEALED CONDITION. CELL STRENGTH 17,400 PSI. BRAZE 1740 F.	LIMITED TO Ti-6Al-4V APPEARED FACTS	
				24 x 144														
			MAX	60 x 200	WELD SHEETS			002	1.8 TO 1.2									
				96 x 200														
	Ti-6Al-4V ANNEALED	Ti-3Al-2.5V	MIN	24 x 144	68 IN. X 40 FT. WELD SHEETS			002	1.8 TO 1.2							INITIAL COLD FORMING ADVANTAGE	CONDITION OF BETA ALLOY AFTER AGING NOT RESOLVED.	
				60 x 200														
			MAX	96 x 340														BRAZE ALLOY TO AVOID DIFFUSION NOT RESOLVED.
	Ti-6Al-4V ANNEALED	Ti-3Al-2.5V	MIN	AS ABOVE	4 FT. X 13 FT. PRESENT			002	1.4 CELL 1.2 THICK	0.50 IN.		CAN VARY INDIVIDUAL RIBBON THICKNESS	0.010 MIN	NOT FEASIBLE	NOT VACUUM AND CREEP FORMING	SHEAR HE BONDING MUST BE EXTERNAL AFTER DIFFUSION. BOND SURFACE HAS BUILT UP IN INITIAL TACK WELD	LIMITED TO Ti-6Al-4V FACTS	
			MAX		80 IN. X 24 FT. PRESENT			003 PRESENT 175 IPRC - REJECTED			2.0 IN. THICK		CONSTANT THICKNESS OVER FULL LENGTH OF RIBBON					CONDITION OF BETA ALLOY AFTER DIFFUSION UNKNOWN
	Ti-6Al-4V ANNEALED	Ti-6Al-4V ANNEALED	MIN	AS ABOVE	APPROX 80 IN. X 24 FT			008								FORMING DIFFICULT	LIMITED TO Ti-6Al-4V / BRAZED	
			MAX		DEPENDS ON WELD PROCESS												BETA ALLOY BONDING OF DIFF. BONDED	

1/3-1/4 CELL UNDER DEVELOPMENT

Figure 8-14. Fabrication Limits - Monocoque Surface Panel Concepts

INSERTS			CLOSURES	
CANDIDATE	LIMITS	CONCLUSIONS	CANDIDATE	LIMITS
<p>ALUM-BRAZE HONEYCOMB WELDED ASSEMBLY</p>	<ul style="list-style-type: none"> BRAZE STARVATION ON $w > 1.3$ INCH MIN WALL THICKNESS 1 OF CAP WALLS .040 AFTER MACHINING .020 AFTER CHEM. MILLING 	<ul style="list-style-type: none"> STRENGTH LIMIT SET BY BRAZE JOINT SHEAR STRENGTH 		<ul style="list-style-type: none"> w AND t SAME LIMITS AS INSERT $f > .55$ TO AVOID DAMAGE TO BRAZE DURING E.B. WELDING OF PANEL ASSEMBLIES
<p>ALUM-BRAZE HONEYCOMB MECHANICAL ATTACH</p>	<ul style="list-style-type: none"> BRAZE STARVATION MAY REQUIRE VENT. HOLES IN DOUBLER OR DOUBLER SPLIT UP DOUBLER MUST BE THICK ENOUGH TO PREVENT FEATHER EDGES DUE TO CSK ATTACHMENT 	<ul style="list-style-type: none"> SPACER CAN BE USED IN LIEU OF HIGH DENSITY CORE FOR LOW LOADINGS 		<ul style="list-style-type: none"> MIN GAUGE FOR WELDED FITTING AFTER CHEM. MILL .020 WITH ADEQUATE LOWER DOUBLER STRENGTH LIMITED ONLY BY E.B. WELD 90° FFF
<p>BONDED HONEYCOMB MECHANICAL ATTACH</p>	<ul style="list-style-type: none"> DOUBLER MUST BE THICK ENOUGH TO PREVENT FEATHER EDGES DUE TO CSK ATTACHMENT 	<ul style="list-style-type: none"> AS ABOVE EXCEPT DOUBLERS WILL BE WIDER TO GIVE SAME ALLOWABLE SHEAR LOAD 		<ul style="list-style-type: none"> CAN BE USED FOR MEDIUM AND LOW INTENSITY LOADINGS
<p>DOUBLER</p>	<ul style="list-style-type: none"> DOUBLER MUST BE THICK ENOUGH TO PREVENT FEATHER EDGES DUE TO CSK ATTACHMENT 	<ul style="list-style-type: none"> AS ABOVE EXCEPT DOUBLERS WILL BE WIDER 		<ul style="list-style-type: none"> AS ABOVE EXCEPT DOUBLERS WILL BE WIDER

Figure 8-15. Fabrication Limits - Inserts and Closures - Monocoque Wing Design.


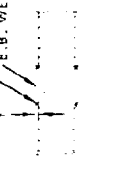
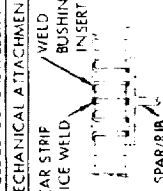




INSERTS			CLOSURES		
CANDIDATE	LIMITS	CONCLUSIONS	CANDIDATE	LIMITS	CONCLUSIONS
WELDED CORE (STRESS IN) WELDED ATTACHMENT  SPAR/RIB	<ul style="list-style-type: none"> MIN THICKNESS A" WELD 1 .015 INCH LOW ALLOWABLE IN WELD AREA UNLESS LOCAL AREA INCREASED LACK OF SHEAR ATTACHMENT TO CORE 	<ul style="list-style-type: none"> LACK OF SHEAR ATTACHMENT TO CORE WILL ESTABLISH STRENGTH LIMIT DUE TO NORMAL LOADING 	TIG WELD E.B. WELD 	SAME AS INSERT	<ul style="list-style-type: none"> LACK OF SHEAR ATTACHMENT WILL RESULTS IN LOCAL BENDING AND TENSION IN CORE
WELDED CORE (STRESS IN) MECHANICAL ATTACHMENT SHEAR STRIP WELD SPURCE WELD BUSHING INSERT  SPAR/RIB	AS ABOVE	<ul style="list-style-type: none"> LACK OF SHEAR ATTACHMENT TO CORE STRENGTH LIMITED BY CROSS SECTION THRU BUSHING AND WELD 	SPURCE PLATE  TIG OR PLASMA WELD	<ul style="list-style-type: none"> 1 MTN .015 INCH LACK OF SHEAR ATTACHMENT TO CORE WELD STRENGTH LIMITS END LOAD CAPABILITY 	AS ABOVE
CORRUGATED SANDWICH TRUSS CORE WELDED ATTACHMENT  TIG WELD	<ul style="list-style-type: none"> 1 MIN = 0.15 INCH STRENGTH LIMITED BY WELD AND LOCAL BENDING 	<ul style="list-style-type: none"> LACK OF GOOD SHEAR CONTINUITY LIMITS NORMAL LOADING 	E.B. WELD  TIG WELD	SAME AS INSERT	
CORRUGATED SANDWICH MECHANICAL ATTACHMENT DETAILS AND COMMENTS SAME AS CLOSURE	DETAILS AND COMMENTS SAME AS CLOSURE	DETAILS AND COMMENTS SAME AS CLOSURE	WELDED SPACERS 	SAME AS ABOVE	

Figure 8-16. Fabrication Limits - Inserts and Closures - Monocoque Wing Design

ORIGINAL PAGE IS
OF POOR QUALITY

1

2

3

SECTION 9

STRUCTURAL ANALYSIS MODELS

by

G. W. DAVIS, G. A. GALINS, G. J. LENGUEL

1

2

3

CONTENTS

<u>Section</u>	<u>Page</u>
INTRODUCTION	9-1
MODELING TECHNIQUE	9-2
2-D Structural Model	9-3
3-D Structural Model	9-5
STRUCTURAL MODELS - TASK I	9-11
Structural Arrangement - Task I	9-13
Model Flexibilities - Task I	9-14
Temperature Input - Task I	9-18
External Loads Input - Task I	9-18
STRUCTURAL MODEL - TASK IIA	9-23
Structural Arrangement - Task IIA	9-23
Model Flexibilities - Task IIA	9-23
Temperature Input - Task IIA	9-24
External Loads Input - Task IIA	9-24
STRUCTURAL MODEL - TASK IIB	9-24
Structural Arrangement - Task IIB	9-24
Model Flexibilities - Task IIB	9-25
Temperature Input - Task IIB	9-25
External Loads Input - Task IIB	9-31
RESULTS	9-35
Displacements	9-35
Running Loads	9-51
REFERENCES	9-63

1

2

3

LIST OF FIGURES

<u>Figure</u>		<u>Page</u>
9-1	Structural Model Usage	9-2
9-2	Finite Element Structural Model, 2-D NASTRAN	9-2
9-3	Finite Element Structural Model, 3-D NASTRAN	9-6
9-4	Inner Wing Planform, Task IIB Structural Model (3-D)	9-7
9-5	Outer Wing Planform, Task IIB Structural Model (3-D)	9-9
9-6	Fuselage Frame (FS2565), Task IIB Structural Model (3-D)	9-12
9-7	Wing Surface Panel Candidates	9-12
9-8	Summary of Structural Arrangements	9-15
9-9	Structural Temperatures, Mid-Cruise Condition, Task I	9-21
9-10	Fuselage Equivalent Extensional and Shear Thicknesses, Task IIB Models	9-27
9-11	Wing Panel Equivalent Extensional and Shear Thicknesses, Task IIB Final Design Model	9-29
9-12	Structural Temperatures, Transonic Descent Condition, Task IIB Final Design Model	9-33
9-13	Comparison of Wing Rear Beam Displacements, Task I Models	9-36
9-14	Comparison of Wing Rear Beam Displacements, Task IIB Models	9-36
9-15	Comparison of Wing Rear Beam Displacements, Task I, IIA, and IIB Models	9-37
9-16	Comparison of Fuselage Displacements, Task I, IIA, and IIB Models	9-37
9-17	Wing Upper Surface Maximum Tension Loads, Task IIB Final Design Model	9-39
9-18	Wing Upper Surface Maximum Compression Loads, Task IIB Final Design Model	9-41
9-19	Wing Upper Surface Maximum Spanwise Tension and Compression Loads, Task IIB Final Design Model	9-43

LIST OF FIGURES (Continued)

<u>Figure</u>		<u>Page</u>
9-20	Wing Lower Surface Maximum Chordwise Tension Loads, Task IIB Final Design Model	9-45
9-21	Wing Lower Surface Maximum Chordwise Compression Loads, Task IIB Final Design Model	9-47
9-22	Wing Lower Surface Maximum Spanwise Tension and Compression Loads, Task IIB Final Design Model	9-49
9-23	Fuselage Panels Maximum Tension Loads, Task IIB Final Design Model	9-57
9-24	Fuselage Panels Maximum Compression Loads, Task IIB Final Design Model	9-59

LIST OF TABLES

<u>Table</u>		<u>Page</u>
9-1	Wing Panel Equivalent Extensional and Shear Thicknesses, Task I Chordwise Model	9-16
9-2	Wing Panel Equivalent Extensional and Shear Thicknesses, Task I Spanwise Model	9-16
9-3	Wing Panel Equivalent Extensional and Shear Thicknesses, Task I Monocoque Model	9-17
9-4	Fuselage Section Properties, Task I Models	9-17
9-5	Summary of Temperature Conditions, Task I, IIA, and IIB	9-19
9-6	Summary of Load Conditions, Task I, IIA and IIB	9-19
9-7	Wing Panel Equivalent Extensional and Shear Thickness, Task IIB Strength Design - Hybrid Model	9-26
9-8	Wing Panel Equivalent Extensional and Shear Thickness, Task IIB Strength/Stiffness - Hybrid Model	9-26
9-9	Comparison of Wing Surface Load Intensities - All Models, Mach .90 Load Condition	9-52
9-10	Effect of Jig-Shape on Wing Upper Surface Load Intensities, Task IIB Hybrid Model	9-52
9-11	Comparison of Wing Upper Surface Load Intensities - Task I and Task IIB Models, Mach 1.25 Load Condition	9-56
9-12	Comparison of Wing Lower Surface Load Intensities - Task I and Task IIB Models, Mach 1.25 Load Condition	9-56
9-13	Comparison of Fuselage Panel Load Intensities - Task IIB Strength and Strength/Stiffness Models, Mach 1.25 Load Condition	9-61

1

2

3

LIST OF SYMBOLS

BL	Butt line
FS	Fuselage station
f_x	Extensional stress in the x-axis
g	Gravitational acceleration
I_y, I_z	Area moment of inertia of the fuselage cross section associated with the y- and z-axes
J	Polar moment of inertia of the fuselage cross section
M	Moment; Mach number
M_x, M_y, M_z	Moments about the x-, y-, and z-axes
N_x, N_y, N_{xy}	Inplane running loads (lb./in.) acting in the x-and y-axes and the x-y plane
n_z	Load factor in the z-direction
P_x, P_y, P_z	Forces in x-, y-, and z-directions
t_f	Face sheet thickness
t_x, t_y, t_{xy}	Effective extensional and shear thicknesses in x-y coordinate system
V_A, V_C, V_D, V_S	Design maneuvering speed, design cruise speed, design dive speed, and design stall speed
v_e	Equivalent airspeed (knots)
x, y, z	Cartesian coordinates
X_{cg}	Location of the center of gravity along the x-axis
$\theta_x, \theta_y, \theta_z$	Rotation about the x-, y-, and z-axes

PRECEDING PAGE BLANK NOT FILMED



SECTION 9

STRUCTURAL ANALYSIS MODELS

INTRODUCTION

A series of finite element structural analysis models were used for the evaluation of structural design concepts for the arrow-wing supersonic cruise aircraft. These models were coded in NASTRAN, and Lockheed-California Company's NASTRAN-FAMAS structural analysis system was used to provide internal loads and displacements for stress analyses, to calculate structural deflection influence coefficients for aeroelastic load analyses, and to determine reduced stiffness and mass matrices, and compute vibration modes for flutter analyses.

The finite element structural models used for the structural study effort are summarized on the flow schematic in Figure 9-1. The models were characterized by the applicable wing primary load-carrying structural arrangements described in Section 1, Structural Design Concepts. Three general types of structure and a combination thereof were evaluated:

- (1) Semimonocoque, Chordwise - uniaxially stiffened surface panels with the stiffeners oriented to support chordwise loads.
- (2) Semimonocoque, Spanwise - uniaxially stiffened surface panels with the stiffeners oriented to support spanwise loads
- (3) Monocoque - Biaxially stiffened surface panels which support both spanwise and chordwise loads.
- (4) Hybrid - wing surfaces which utilize a combination of semimonocoque and monocoque structural concepts.

Simplified two-dimensional (2-D) models were used for the initial studies for rapid, cost effective evaluation studies of the effects of the primary wing loads. For detail structural design and verification of the final design configuration a three-dimensional (3-D) model was formulated.

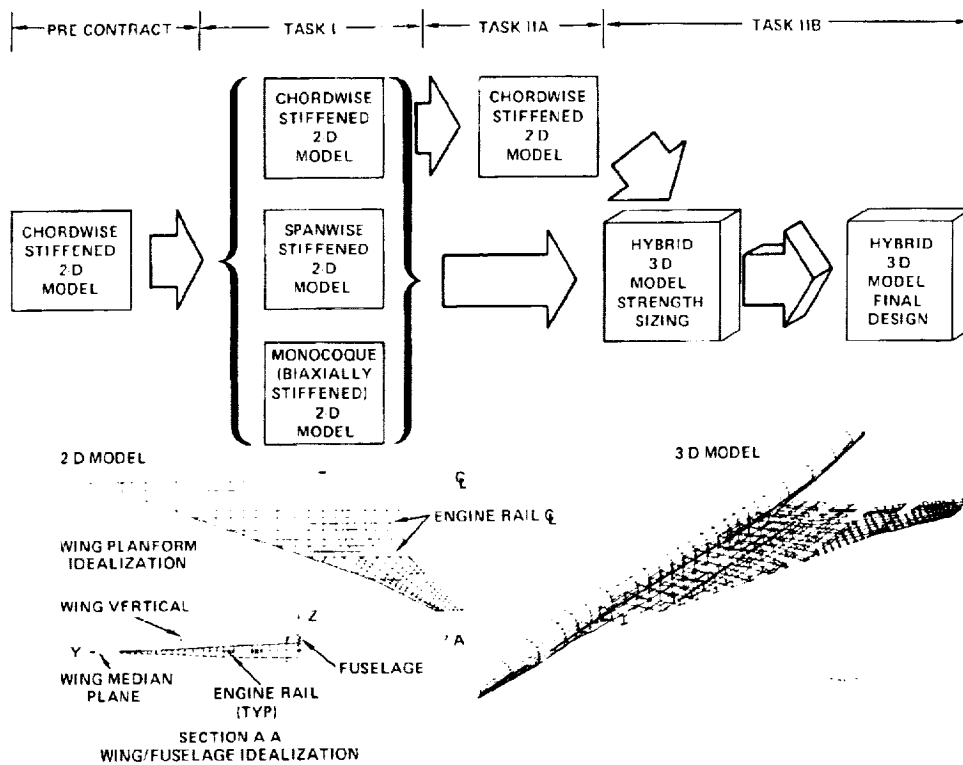


Figure 9-1. Structural Model Usage

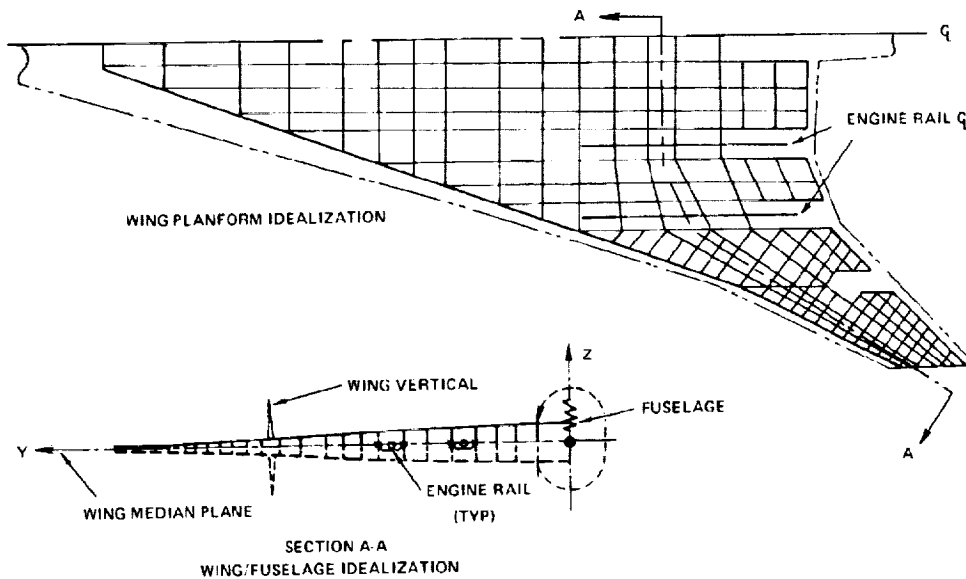


Figure 9-2. Finite Element Structural Model, 2-D NASTRAN

The following paragraphs describe the basic modeling techniques and their application to the Task I and Task II analyses, the model input data, and the results of the analysis.

MODELING TECHNIQUE

Two different modeling techniques were used in the finite element structural models, they were:

- A simplified pseudo 3-D model was formulated to evaluate the effects of primary wing loads, i.e., out-of-plane (P_z , M_x , M_y) loads. This modeling technique, hereafter referred to as the 2-D model, represents a wing that is symmetrical about an X-Y midplane with a beam representation of the fuselage to provide fuselage interface effects on the wing structure. Applications of the 2-D modeling technique included the three Task I structural arrangement models and the Task IIA configuration refinement investigation model.
- A detailed 3-D model was formulated in Task IIB for the structural design and verification of the final design configuration. This model incorporates a full wing model with camber and twist, with the capability to transmit inplane (P_x , P_y , M_z) as well as out-of-plane (P_z , M_x , M_y) loads, and a fuselage shell model composed of skin, stringers and frames.

The size parameters for these models (2-D and 3-D) are compared below:

<u>MODEL</u>	<u>GRID POINTS</u>	<u>ELEMENTS</u>	<u>D.O.F.</u>
2-D	530	1300	1050
3-D	715	2450	2200

2-D Structural Model

A total of four structural models were developed employing the two-dimensional modeling technique; these were: the three structural models used for the Analytical Design Studies of Task I and the Task IIA configuration refinement investigation model.

A representative description of the modeling technique used on the 2-D models is shown in Figure 9-2. This model represents the actual wing upper surface planform with a simplified wing cross-section and the fuselage is idealized as a simple beam. For the wing, a horizontal midplane (X-Y plane) of structural symmetry is assumed, which permits the size of the model to be substantially smaller since only the upper

half of the wing needs to be specified in the model. The wing cross-section of the model is symmetrical about the X-Y plane, the Z coordinates (measured from the X-Y plane) defining the upper wing surface are equal to one half the total wing depth and the model section properties are equal to the average stiffness of the wing upper and lower surfaces.

The wing midplane of symmetry is constrained to prevent all inplane (X, Y, θ_z) displacements. Therefore the 2-D models are used primarily for analysis of the primary wing loads: vertical shear force (P_z), wing bending (M_x) and wing torsion (M_y), and their corresponding displacements.

The model network is identical for all 2-D structural models with the exception of the Task IIA model which incorporated a fuselage forebody and wing tip revision for the configuration change investigation. Each model is unique in terms of the section property sizing and the elements used to represent the wing primary load carrying structure. For the semimonocoque arrangements the wing surfaces were modeled using NASTRAN rod and shear-panel elements. Wing surface representation for the monocoque arrangement was made using NASTRAN rod and quadrilateral membrane elements.

The wing vertical fin model consists of a two-dimensional (X-Z plane) grid of NASTRAN bar and shear panel elements representing the equivalent bending and torsion stiffness of the fin. Fin loads are introduced into the wing by means of NASTRAN multipoint constraint (MPC) equations which are applied at the interface of the fin with the wing box.

The engine support rails are represented in the model by NASTRAN bar elements with the capability to transmit axial, torsional, vertical and lateral bending loads from the engines into the wing box. The rails are located at the constrained wing midplane and are connected by MPC equations to the X-Y rigid body motions of the wing for the vibration analyses.

The 2-D models represent the fuselage as a simple beam and use NASTRAN bar elements with torsional, vertical and lateral bending stiffness. The fuselage beam is connected to the wing model by MPC equations and scalar springs (NASTRAN CELAS elements) representing an approximation of the fuselage frame flexibility.

A network of unit loads is applied to the model grid points and is used to calculate structural deflection influence coefficients (S.I.C.). In addition, this network is used as the load points to introduce design loads into the model structure. For the 2-D models, the SIC point loads are concentrated unit loads applied to the model grid points as summarized below:

Wing - P_z unit loads are applied to all surface grid points except the intermediate control surface spar and wing tip secondary ribs. M_x and M_y unit loads are applied at the leading edge spar and wing main rib intersections.

Wing vertical fin - P_y unit loads are applied at all grid points.

Engines - P_y , P_z , M_x , M_y and M_z unit loads are applied at two points for each engine.

Fuselage - P_z and P_y unit loads are applied at all fuselage node points.

Main landing gear - P_x , P_y , P_z , M_x , and M_y unit loads are applied to the main landing gear load point which in turn is connected to the wing structure by MPC equations.

Nose landing gear - M_x and M_y unit loads are applied directly to the fuselage node point representing the nose landing gear location.

The effect of temperature differences between the upper and lower wing surfaces on wing bending was investigated for two typical design conditions, start-of-cruise and mid-cruise. Temperature loads were applied to the wing, vertical fin, engine rails and fuselage using NASTRAN's TEMP and TEMPRB temperature inputs. The wing temperatures specified in the model inputs represent the antisymmetric temperature component, i.e., the temperature difference between the upper and lower surfaces. Thus the thermal load analysis on the 2-D models is consistent with the limitations of the wing X-Y midplane boundary condition which requires that applied loads on the wing upper surface are antisymmetric with respect to the lower surface.

3-D Structural Model

For the Task IIB analyses, a more detailed, three-dimensional (3-D) model was used. An isometric view of this model is shown in Figure 9-3.

The inner and outer wing planform grid for the 3-D structural model are shown in Figures 9-4 and 9-5, and include the NASTRAN grid point and panel identification numbers. In addition, Figure 9-4 contains the model identification for both the inboard and outboard engine rails.

The wing planform grid in the 3-D model is identical to the 2-D model grid used in Task IIA; however, for the 3-D model both upper and lower wing surfaces are represented, including camber and twist of the actual airfoil. Flexible control

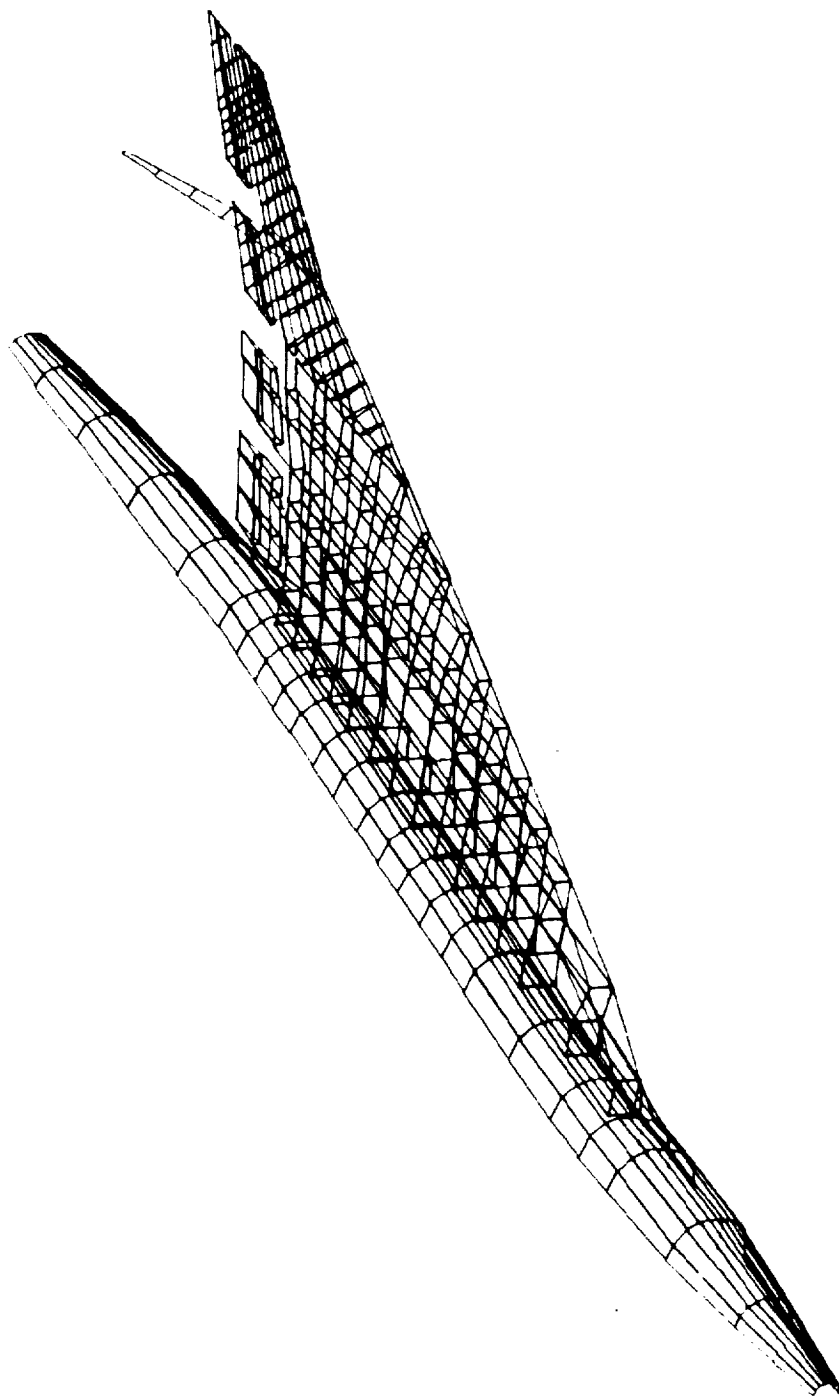


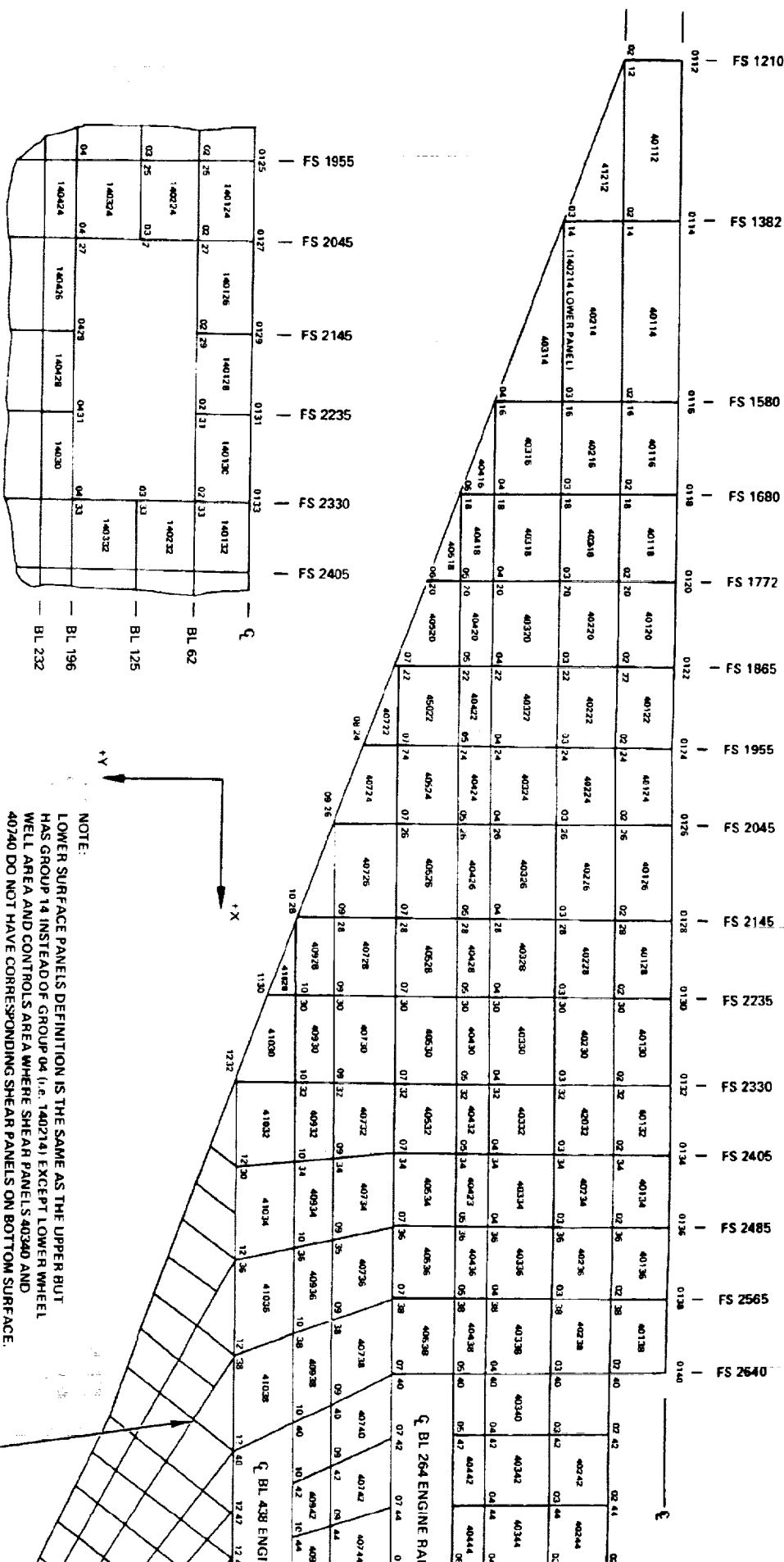
Figure 9-3. Finite Element Structural Model, 3-D NASTRAN

WING LOWER SURFACE
MAIN LANDING GEAR WHEEL WELL

EXHIBIT FRAME 2

NOTE:
LOWER SURFACE PANELS DEFINITION IS THE SAME AS THE LOWER BUT HAS GROUP 14 INSTEAD OF GROUP 04 (i.e. 140214) EXCEPT LOWER WHEEL WELL AREA AND CONTROLS AREA WHERE SHEAR PANELS 40340 AND 40740 DO NOT HAVE CORRESPONDING SHEAR PANELS ON BOTTOM SURFACE.

OUTER WING
PLATFORM,
FIGURE 9-5



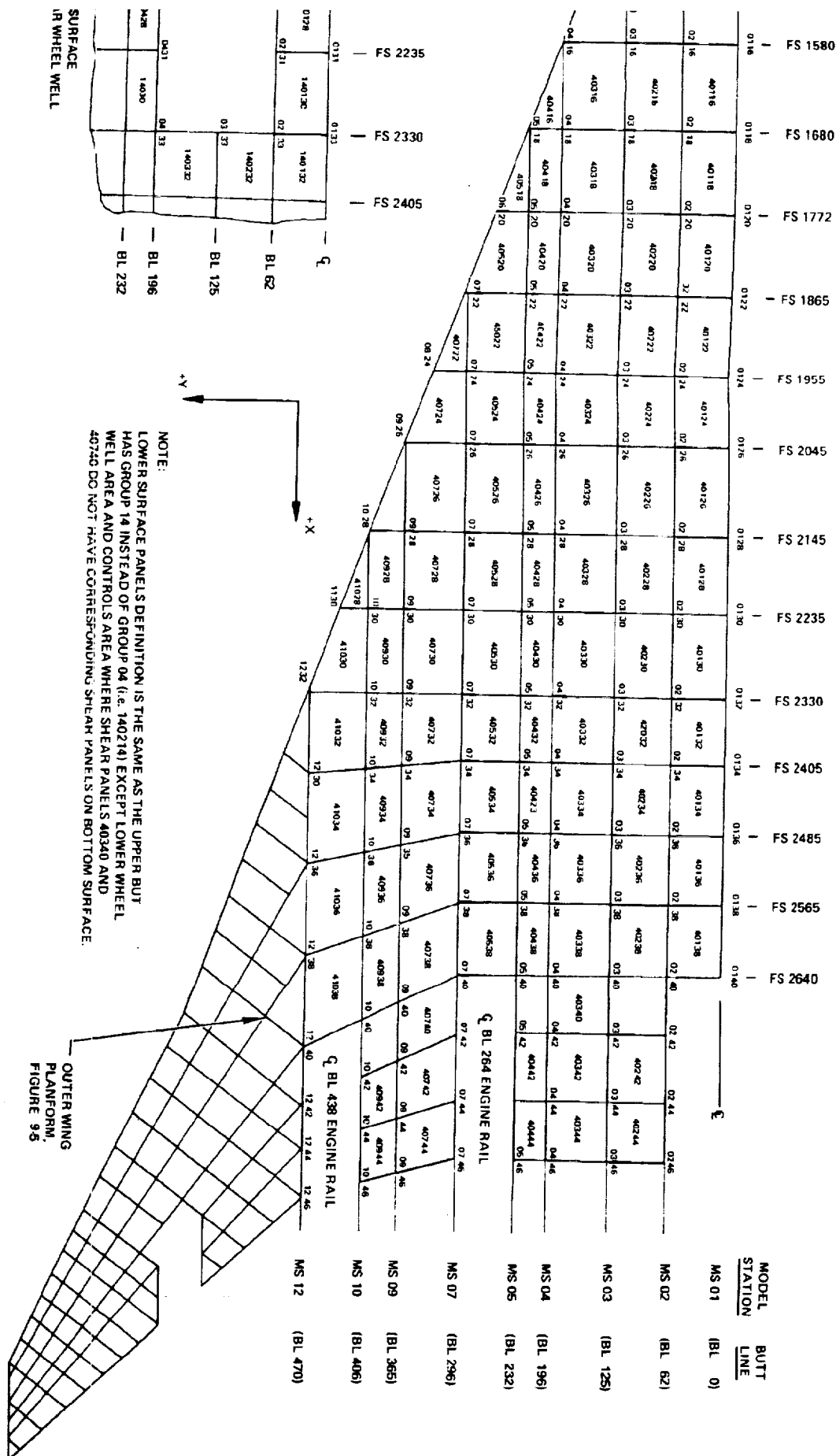
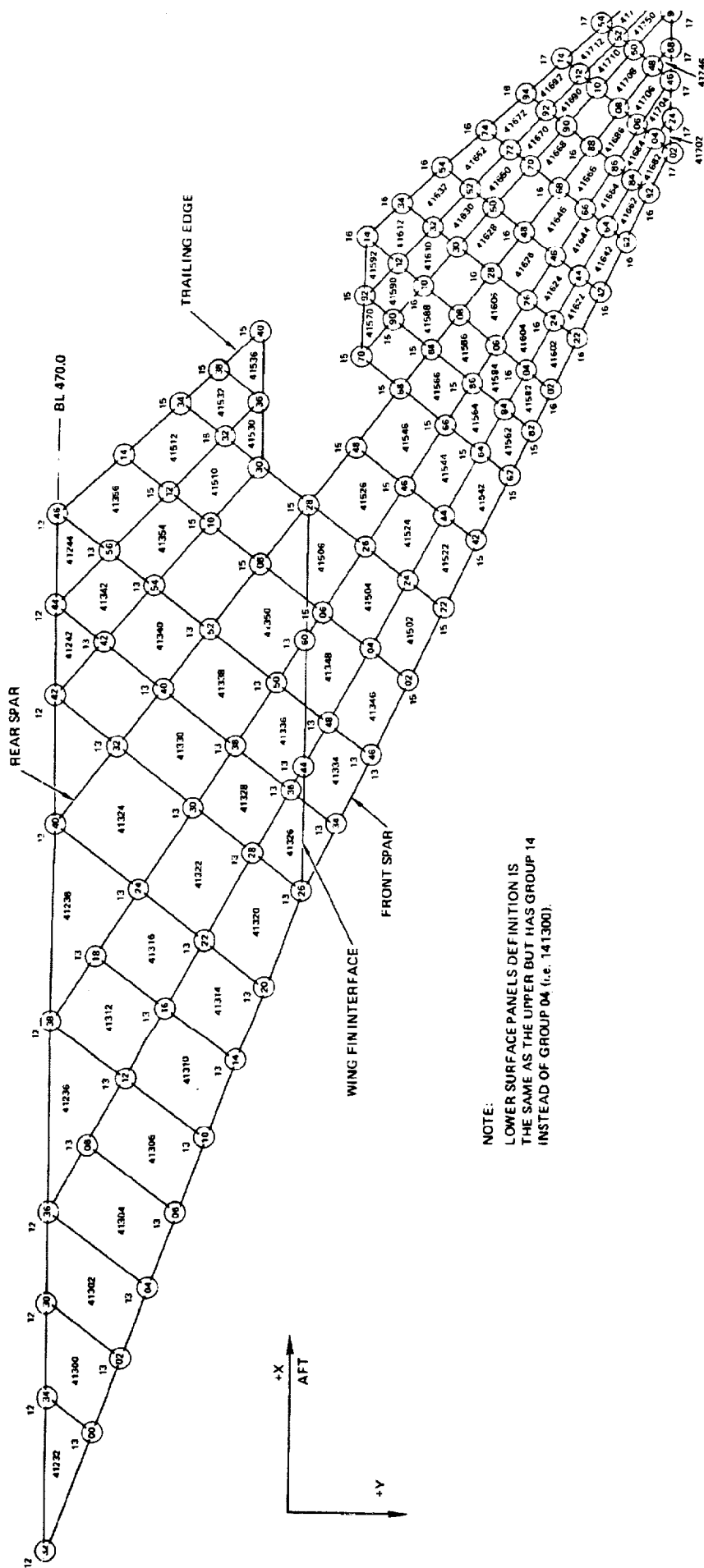


Figure 9-1. Inner Wing Platform,
Task IFR Structural Model (3-D)



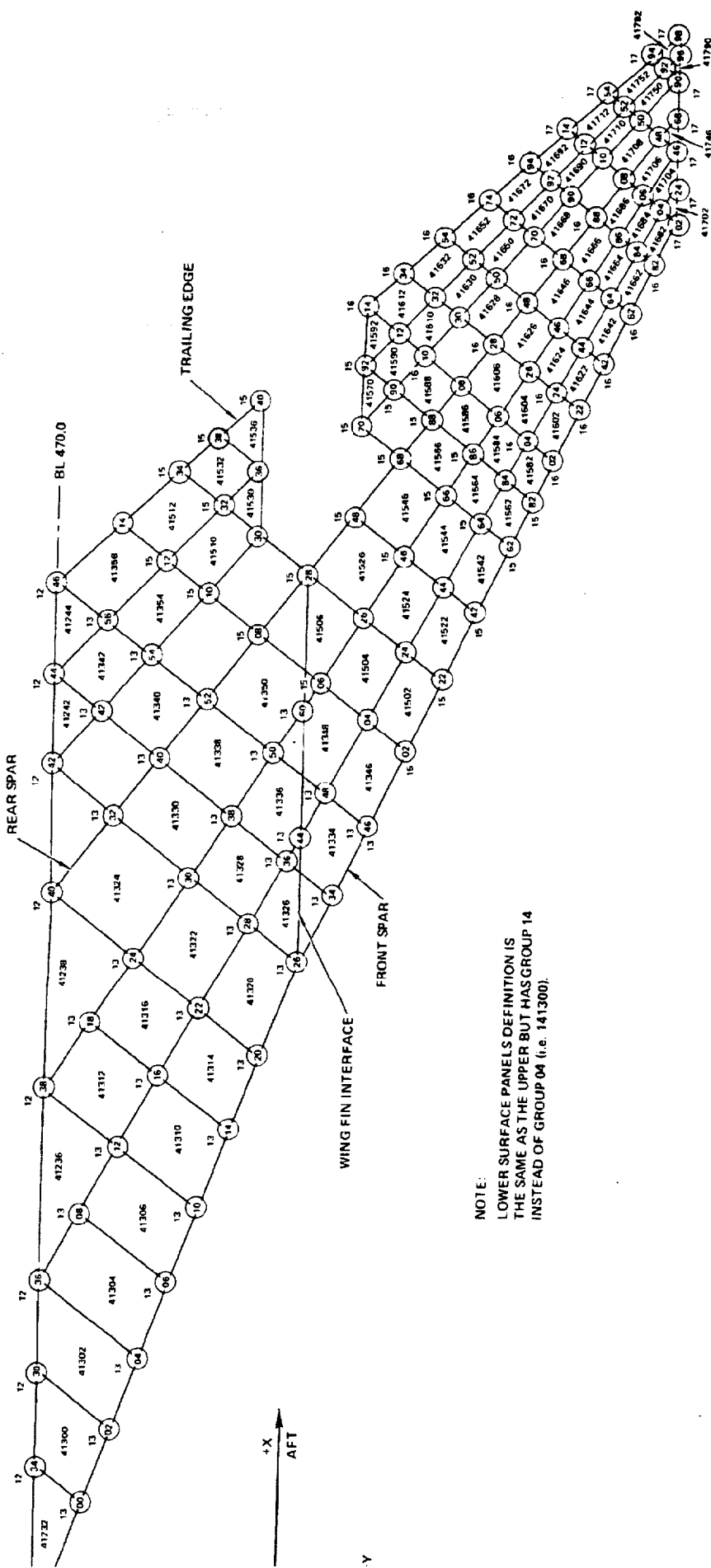
PRECEDING PAGE BLANK NOT FILMED

FOLDOUT FRAME /

FOLDOUT FRAME :

Figure 10.1. Wing Foldout Frame, Back View (Structural Model)





NOTE:
 LOWER SURFACE PANELS DEFINITION IS
 THE SAME AS THE UPPER BUT HAS GROUP 14
 INSTEAD OF GROUP 04 (i.e. 141300).

Figure 9-5. Outer Wing Element, Tank IIS Structural model (3-D)

1

2

3

surface actuators are represented using NASTRAN CELAS elements and MPC equations. The elimination of the X-Y wing midplane of structural symmetry (and load antisymmetry) used on the 2-D models required a redefinition of the location for the wing interfaces with the vertical fin, main landing gear and engines.

The 3-D model fuselage is idealized using 25 frame stations with approximately 10 nodes describing the fuselage half-circumference. NASTRAN bar elements are used to represent fuselage frames with rod elements and quadrilateral shear panels used to represent the fuselage shell. A typical frame model drawing, FS 256b, is shown in Figure 9-6 and includes the grid point and element identification. In addition, the wing interface with the frame is indicated by dashed lines.

A network of unit loads, as described for the 2-D models, was used on the 3-D models to calculate SIC's and to introduce design loads into the model structure. Effective unit load locations are in general identical to those used for the 2-D models. Exceptions are unit loads for the main landing gear and wing engines where a refined location was required on the more detailed 3-D models.

The unit loads applied to the 3-D model fuselage differ from those used on the 2-D models in their application as distributed loads at each frame station. The corresponding structural influence coefficients on the 3-D fuselage model represent an average deflection of the frame node points to which the unit load was distributed. For the 3-D model the temperature distributions were applied to the structural model at both upper and lower wing surfaces, the vertical fin and fuselage. Actual temperatures (instead of the temperature differences used on the 2-D model) were input using NASTRAN TEMP and TEMPRB specifications.

STRUCTURAL MODELS - TASK I

The three structural models used for Task I analytical studies employed the 2-D modeling technique, and represented each of the three general types of wing load carrying structure:

- Chordwise stiffened wing surfaces
- Spanwise stiffened wing surfaces
- Monocoque (biaxially stiffened) wing surfaces.

PRECEDING PAGE BLANK NOT FILMED

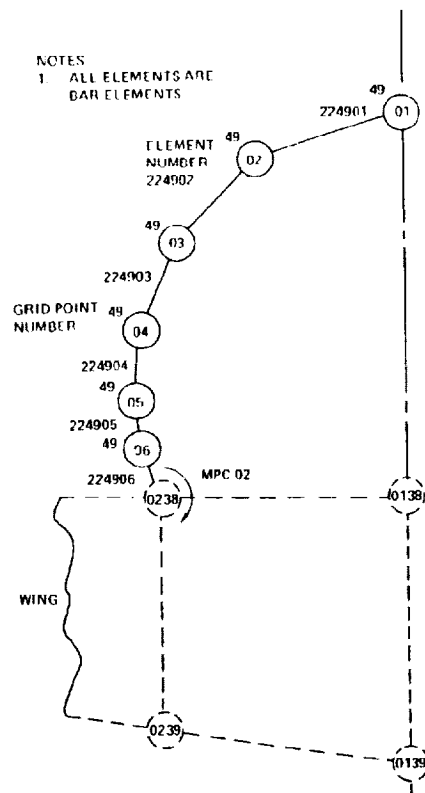


Figure 9-6. Fuselage Frame (FS 2565), Task IIB Structural Model (3-D)

WING CANDIDATES	
MONOCOQUE 	MONOCOQUE (BIAXIALLY STIFFENED) HONEYCOMB SANDWICH TRUSS CORE
SEMIMONOCOQUE -SPANWISE 	SPANWISE STIFFENED ZEE STIFFENED INTEGRAL ZEE HAT SECTION STIFFENED INTEGRALLY STIFFENED
SEMIMONOCOQUE -CHORDWISE 	CHORDWISE STIFFENED CIRCULAR ARC - CONVEX BEADED CIRCULAR ARC - CONCAVE BEADED CORRUGATION - CONCAVE BEADED HAT STIFFENED - CONCAVE BEADED

Figure 9-7. Wing Surface Panel Candidates

The model network is identical for all the structural arrangements; however, the model is unique for each of the three arrangements in terms of the section property sizing and the elements used to represent the surfaces. For the spanwise and chordwise stiffened arrangements the wing surfaces were modeled using NASTRAN rod and shear panel elements. Wing surface representation for the monocoque arrangement was made using NASTRAN rod and quadrilateral membrane elements.

The finite element input data included defining the structure flexibilities and the load/temperature environment. This required:

- (1) Representing the structural arrangement under consideration by the corresponding idealized bending, extensional, and shear flexibilities.
- (2) Identifying the critical "hot" conditions from the structural temperature analysis of Section 6, and inputting the effective temperatures for calculations of the thermal stresses.
- (3) Defining the external loads (aeroelastic) for the critical flight and landing conditions and inputting these loads for the NASTRAN deflection and internal loads analysis.

These data are described in the following sections under the headings of Structural Arrangement, Model Flexibilities, Temperature Input, and External Loads Input.

Structural Arrangement - Task I

A representative wing panel concept was selected from each general type of wing structure (i.e., spanwise, chordwise, and monocoque). Figure 9-7 contains the candidate wing concepts considered in Task I; those concepts selected for input into the models were:

- Chordwise - hat-stiffened concave-beaded skin panel
- Spanwise - hat-section stiffened panel
- Monocoque - honeycomb sandwich panel.

As the representative fuselage concept the Zee-stiffened panel design was selected for all Task I models. Selection of this concept and its associated stiffness (I_x , I_y , J) were based on the results of prior investigations conducted on the M 2.7 Fixed Wing SST by the Lockheed and Boeing Companies, references 1 and 2.

A detail description of the wing and fuselage primary structural-material arrangement, surface panels and substructure, incorporated into the Task I models is contained in Figure 9-8.

Model Flexibilities - Task I

The bending, extensional, and shear stiffness corresponding to each of the three Task I structural arrangements were input into their respective models.

As previously stated, the chordwise and spanwise models utilized axial and shear panel elements for representing the wing surface panels. The equivalent flat plate extensional (t_x and t_y) and shear (t_{xy}) thicknesses were calculated for each wing panel concept and input into the appropriate model element; e.g., for the spanwise and chordwise surface panels, the equivalent extensional stiffnesses attributed to the surface panels are simulated in the model rod elements by the product of the extensional thicknesses times the effective widths.

As an indicator of the chordwise model wing stiffness, the calculated extensional and shear thicknesses are shown in Table 9-1. For this arrangement (chordwise) the equivalent extensional thickness in the x-direction (t_x) reflects the panel and rib cap areas, and t_y is the equivalent extensional thickness of the spars. The rib and spar spacing are also indicated for each of the point design regions. The corresponding extensional and shear thicknesses for the spanwise arrangement are shown in Table 9-2 and reflect the hat-section stiffened panel concept. For this arrangement, the extensional thicknesses in the x- and y-directions reflect the rib caps, and panel and spar caps, respectively. The monocoque model uses the NASTRAN quadrilateral membrane element (PQDMEM) for defining the section properties of the wing surface panels and axial elements (CONRODS) for the spar and rib caps. The honeycomb sandwich panel concept is utilized for the monocoque structural model. For this concept the wing surface extensional and shear thicknesses are equal and this thickness is specified directly for the membrane elements. The monocoque wing surface extensional and shear thicknesses are shown in Table 9-3; for comparison with the spanwise and chordwise concept extensional thicknesses (t_x and t_y), the actual rib and spar caps have been converted to an equivalent panel thickness (i.e., area divided by effective width) and are included in the thicknesses given in Table 9-3.

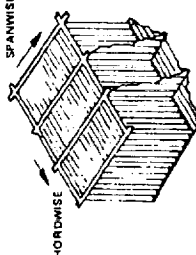


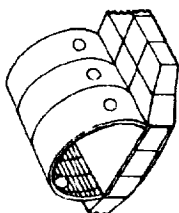
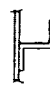

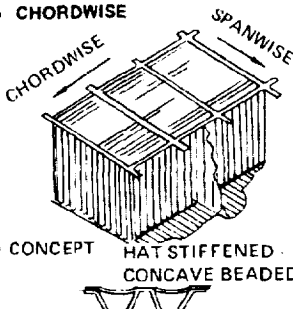
STRUCTURAL APPROACH	STRUCTURAL ARRANGEMENTS		
	TASK I	TASK IIA	TASK IIB
WING 	WING (BASIC AND TIP) <ul style="list-style-type: none"> • SURFACE PANELS CHORDWISE MODEL -- • SPANWISE MODEL -- • MONOCOQUE MODEL -- MAT'L -- T16A1-4V ANN. • SUBSTRUCTURE METALLIC SPAR AND RIB CAPS -- SUBMERGED CAPS FOR SPANWISE AND CHORDWISE CONCEPTS TRUSS AND CIRCULAR-ARC WEBS MAT'L -- T1A1-4V ANN. 	WING (BASIC AND TIP) <ul style="list-style-type: none"> • SURFACE PANELS SAME AS TASK I DESIGN, CHORDWISE MODEL. MAT'L -- • SUBSTRUCTURE SAME AS TASK I DESIGN, CHORDWISE MODEL. MAT'L -- 	WING <ul style="list-style-type: none"> • BASIC WING SURFACE PANELS CHORDWISE STIFFENED -- • WING TIP PANELS MONOCOQUE ALUM. BRAZED HONEYCOMB • SUBSTRUCTURE METALLIC RIB CAPS SUBMERGED SPAR CAPS -- BPI REINFORCED (AFT BOX REGION) TRUSS AND CIRCULAR-ARC WEBS MAT'L -- T16A1-4V ANN. 
FUSELAGE 	FUSELAGE <ul style="list-style-type: none"> • ZEE -- STIFFENED CONCEPT MAT'L -- T16A1-4V ANN. 	FUSELAGE <ul style="list-style-type: none"> • SAME STRUCTURAL CONCEPTS AS TASK I 	FUSELAGE <ul style="list-style-type: none"> • SHELL (SKIN/STRINGER) HAT STIFFENED CONCEPT (MIDBODY AND AFT BODY) • ZEE STIFFENED CONCEPT ((FOREBODY) MAT'L -- T16A1-4V ANN. • FRAMES FLOATING FRAMES T16A1-4V ANN. 

Figure 9-8. Summary of Structural Arrangements

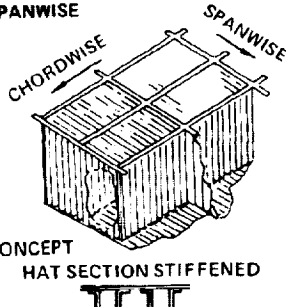
TABLE 9-1. WING PANEL EQUIVALENT EXTENSIONAL AND SHEAR THICKNESSES, TASK I CHORDWISE MODEL

ARRANGEMENT/CONCEPT	POINT DESIGN REGION	LOCATION	SPACING (IN)		EXTENSIONAL AND (1)(2) SHEAR THICKNESS (IN.)		
			SPAR	RIB	t_x	t_y	t_{xy}
<ul style="list-style-type: none"> • CHORDWISE  <ul style="list-style-type: none"> • CONCEPT HAT STIFFENED CONCAVE BEADED 	40322	FORWARD WING BOX	30.0	65.0	.068	.023	.046
	40236	AFT WING BOX	20.0	65.0	.068	.167	.030
	40536		20.0	60.0	.122	.134	.048
	41036		20.0	60.0	.126	.080	.049
	41316	WING TIP	20.0	65.0	.200	.119	.100
	41348		30.0	60.0	.169	.142	.080

NOTES:

- (1) THICKNESSES REPRESENT AVERAGE VALUE OF WING UPPER AND LOWER SURFACES.
(2) INCLUDES THICKNESSES OF CAPS AND/OR PANELS WHERE APPLICABLE.

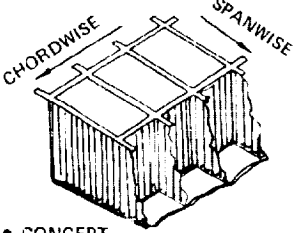
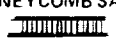
TABLE 9-2. WING PANEL EQUIVALENT EXTENSIONAL AND SHEAR THICKNESSES, TASK I SPANWISE MODEL

ARRANGEMENT/CONCEPT	POINT DESIGN REGION	LOCATION	SPACING (IN)		EXTENSIONAL AND (1)(2) SHEAR THICKNESS (IN.)		
			SPAR	RIB	t_x	t_y	t_{xy}
<ul style="list-style-type: none"> • SPANWISE  <ul style="list-style-type: none"> • CONCEPT HAT SECTION STIFFENED 	40322	FORWARD WING BOX	50.0	30.0	.014	.065	.028
	40236	AFT WING BOX	50.0	30.0	.016	.169	.078
	40536		50.0	30.0	.018	.181	.084
	41036		50.0	30.0	.022	.135	.062
	41316	WING TIP	47.6	30.0	.012	.181	.083
	41348		33.4	30.0	.011	.125	.052

NOTES:

- (1) THICKNESSES REPRESENT AVERAGE VALUE OF WING UPPER AND LOWER SURFACES.
(2) INCLUDES THICKNESSES OF CAPS AND/OR PANEL WHERE APPLICABLE.

TABLE 9-3. WING PANEL EQUIVALENT EXTENSIONAL AND SHEAR THICKNESSES, TASK I MONOCOQUE MODEL.

ARRANGEMENT/CONCEPT	POINT DESIGN REGION	LOCATION	SPACING (IN)		EXTENSIONAL AND (1)(2) SHEAR THK. (IN)		
			SPAR	RIB	t_x	t_y	t_{xy}
<ul style="list-style-type: none"> MONOCOQUE 	40322	FORWARD WING BOX	40	80.0	.047	.082	.030
	40236	AFT WING BOX	40.0	80.0	.115	.147	.097
	40536		40.0	80.0	.150	.180	.130
	41036		40.0	80.0	.107	.131	.095
<ul style="list-style-type: none"> CONCEPT 	41316	WING TIP	30.0	40.0	.145	.190	.132
	41348		20.0	40.0	.131	.181	.117

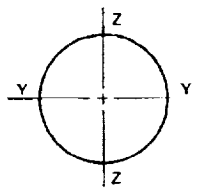
NOTES:

- (1) THICKNESSES REPRESENT AVERAGE VALUE OF WING UPPER AND LOWER SURFACES.
- (2) INCLUDES THICKNESSES OF CAPS AND/OR PANELS WHERE APPLICABLE.

TABLE 9-4. FUSELAGE SECTION PROPERTIES, TASK I MODELS

FUSELAGE STATION	NASTRAN ELEMENT ID.	SECTION PROPERTIES			FUSELAGE STATION	NASTRAN ELEMENT ID.	SECTION PROPERTIES		
		$I_y \times 10^{-3}$ (IN. ⁴)	$I_z \times 10^{-3}$ (IN. ⁴)	$J \times 10^{-3}$ (IN. ⁴)			$I_y \times 10^{-3}$ (IN. ⁴)	$I_z \times 10^{-3}$ (IN. ⁴)	$J \times 10^{-3}$ (IN. ⁴)
200	70102	14.2	13.2	21.9	2045	70126	125.0	66.5	112.5
400		20.5	20.8	31.2	2145	128	133.0		117.5
600		28.2	32.0	46.9	2235	130	143.5		121.0
800		42.0	48.5	65.6	2330	132	150.5		123.5
1000		62.5	66.5	86.0	2405	134	147.5		125.0
1210		84.5		101.6	2485	136	131.0		125.0
1382		99.0		100.0	2585	138	110.0	66.5	123.5
1580		106.5		90.9	2640	140	99.5	56.0	117.2
1680		111.0		88.0	2800	143	87.5	56.0	96.9
1772		114.5		90.5	3000	145	58.5	46.8	62.5
1885	70124	117.5		96.5	3200	146	29.5	28.8	32.9
1955		120.5	66.5	105.0	3360	70147	19.0	16.2	22.0
2045					3470				

SIGN CONVENTION:



NOMENCLATURE:

I_{yy} = AREA MOMENT OF INERTIA ABOUT y-AXIS.

I_{zz} = AREA MOMENT OF INERTIA ABOUT z-AXIS.

J = POLAR MOMENT OF INERTIA

As previously noted, all Task I models idealize the fuselage as a simple beam. The beam properties (torsional, and vertical and lateral bending inertia) input into the model were based on the results contained in References 9-1 and 9-2, and are shown in Table 9-4.

Temperature Input - Task I

The critical temperature conditions selected for input to the Task I structural models are shown in Table 9-5. The conditions selected were the start-of-cruise and midcruise conditions which represent the maximum positive temperature gradient (i.e., exposed surface hotter than the interior surface) and maximum temperature conditions, respectively.

Structural temperatures were defined for each structural model; a display of the structural temperatures are shown in Figure 9-9. These temperatures are used to calculate the thermal gradients through the wing which are specified in the structural models. The corresponding temperatures for the spanwise and monocoque models are contained in Section 6, Structural Temperatures.

External Load Input - Task I

A summary of the load conditions used for analysis of the Task I structural model is shown in Table 9-6. The flight parameters associated with these design conditions are defined in Section 5, Structural Design Loads.

The initial NASTRAN internal loads run was conducted on the chordwise structural model and included a comprehensive investigation of 47 load conditions. After reviewing the chordwise internal loads, the non-critical conditions were removed and an amended load matrix was used for the spanwise and monocoque structural models. A total of 28 load conditions were input to these models, see Table 9-6.

The chordwise load matrix included:

- Twenty (20) ascent conditions covering the Mach 0.33, Mach 0.40, Mach 0.90, Mach 1.25, and Mach 1.90 symmetric maneuver conditions;
- Eight (8) cruise conditions encompassing both cruise (Mach 2.7) and dive (Mach 2.9) speed conditions;

TABLE 9-5. SUMMARY OF TEMPERATURE CONDITIONS,
TASK I, IIA, AND IIB

TASK/MODEL	FLIGHT CONDITIONS		
	START-OF CRUISE M2.7	MID-CRUISE M2.7	DESCENT M1.25
TASK I (2 D MODEL)			
• CHORDWISE	✓	✓	—
• SPANWISE	✓	✓	—
• MONOCOQUE	✓	✓	—
TASK IIA (2 D MODEL)			
• CHORDWISE	—	—	—
TASK IIB (3 D MODEL)			
• HYBRID (STRENGTH)	✓	✓	✓
• HYBRID (STRENGTH/STIFFNESS)	✓	✓	✓

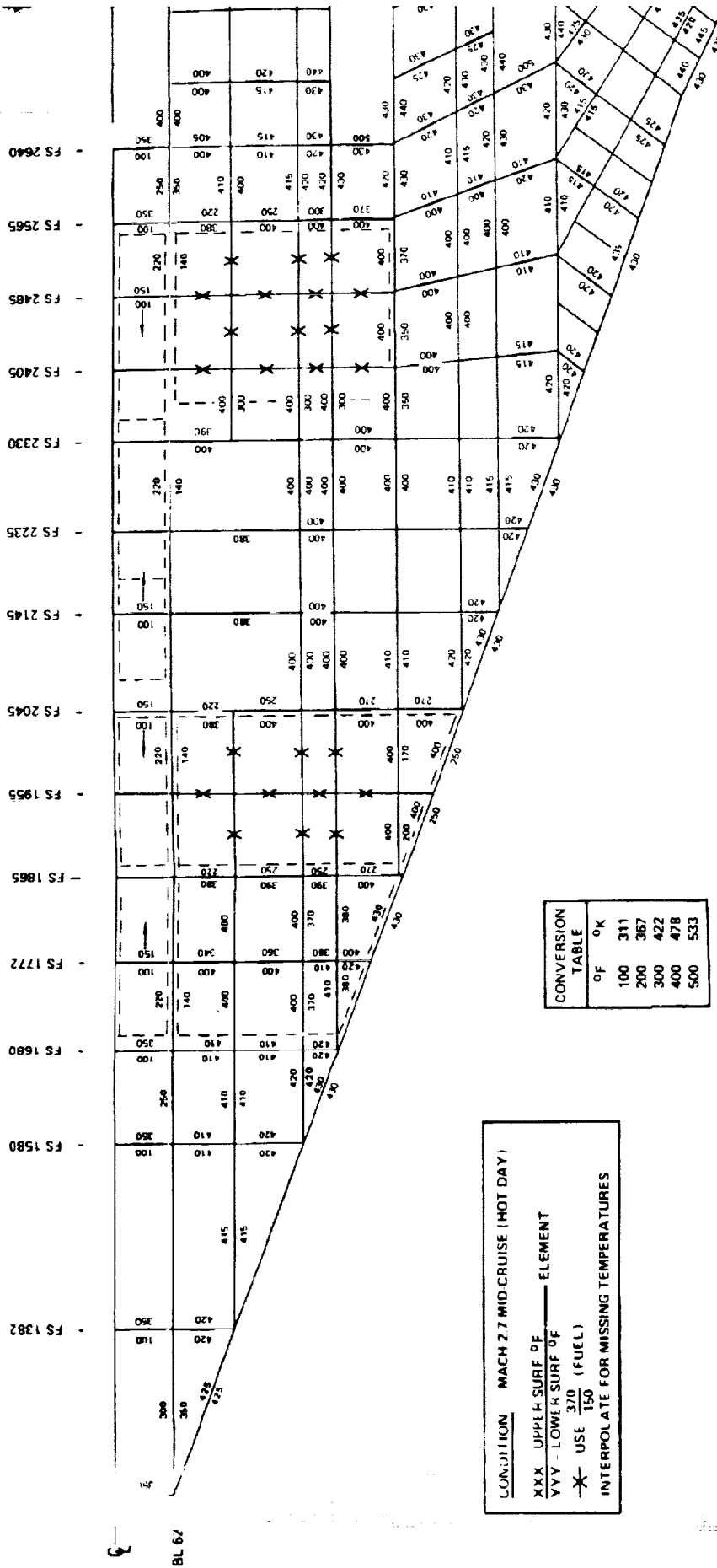
TABLE 9-6. SUMMARY OF LOAD CONDITIONS, TASK I, IIA AND IIB

TASK/MODEL	NUMBER/TYPE CONDITIONS					
	SYMM. FLT. COND.			GUST CONDS.	ROLL CONDS.	LANDING CONDS.
	ASCENT TO CRUISE	CRUISE CONDS.	DESCENT FROM CRUISE			
TASK I (2 D MODEL)						
• CHORDWISE	20	8	—	—	16	3
• SPANWISE	17	8	—	—	—	3
• MONOCOQUE	17	8	—	—	—	3
TASK IIA (2 D MODEL)						
• CHORDWISE	8	—	—	—	—	—
TASK IIB (3 D MODEL)						
• HYBRID (STRENGTH)	13	4	2	—	—	—
• HYBRID (STRENGTH/STIFF.)	13	4	2	2	—	4

1

2

3



ORIGINAL PAGE IS
OF POOR QUALITY

PRECEDING PAGE BLANK NOT FILMED

FOLLOUT FRAME

FOLLOUT FRAME

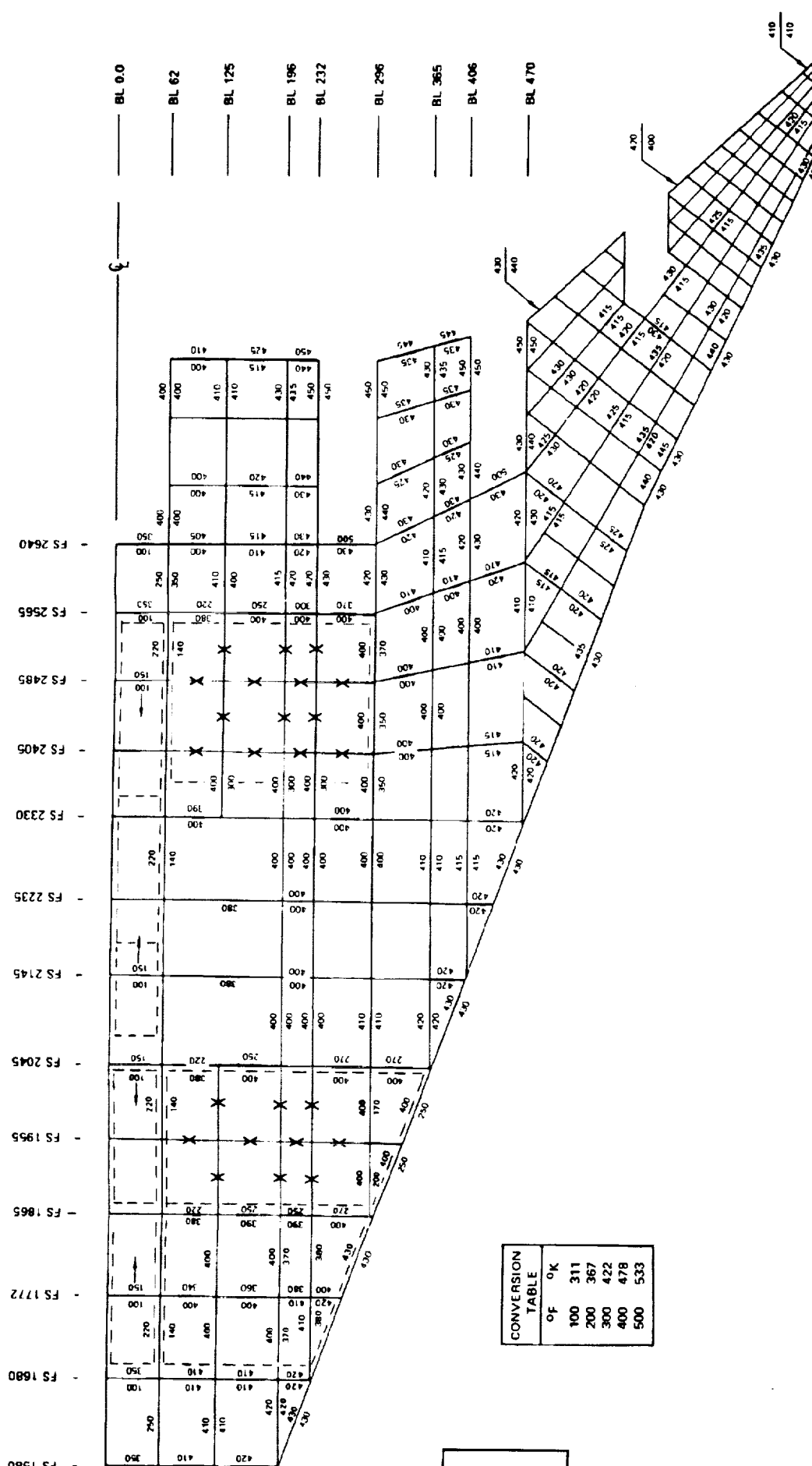


Figure 9-9. Structural Temperatures, Mid-Cruise Condition, Tank I

- Sixteen (16) asymmetric conditions which include both steady and accelerated roll conditions; and,
- Three (3) preliminary tail-down landing conditions.

The load conditions input to the spanwise and monocoque models were identical to the chordwise model except for the removal of the non-critical negative one "g" symmetric maneuver conditions and the roll conditions.

STRUCTURAL MODEL - TASK IIA

In support of the Task IIA Configuration Change Investigation an additional 2-D structural model was established. This model was obtained by revising the coordinates of the Task I Chordwise Model to reflect the airplane configuration changes, i.e., shortened fuselage forebody and revised wingtip sweep angle. In addition, the mass distribution was adjusted to correspond to the new center of gravity travel diagram incorporated for this investigation. An abbreviated design cycle was conducted using this 2-D structural model. The input data for this model is described in the following sections.

Structural Arrangement - Task IIA

The structural arrangement incorporated into this structural model reflects the identical arrangement used for the Task I Chordwise Model, i.e., chordwise stiffened wing surfaces with a conventional fuselage. Refer to Figure 9-8 for a more detailed description.

Model Flexibilities - Task IIA

The element property data are identical to those used for the Task I chordwise models; therefore, the wing surface thicknesses and fuselage section properties shown in Tables 9-1 and 9-4 are also appropriate for this model.

PRECEDING PAGE BLANK NOT FILMED

Temperature Input - Task IIA

As indicated in Table 9-5, no temperature conditions were considered for the Task IIA internal load runs.

External Loads Input - Task IIA

New Aerodynamic Influence Coefficients (AIC's), steady and unsteady, were calculated for the Mach 0.9 subsonic flight condition. This required updating the AIC model to reflect the configuration changes. The grid transforms (AIC to SIC) were revised and the net loads were calculated for the Mach 0.9 symmetric maneuver condition and formatted for NASTRAN input. This condition included four load factors for each velocity (V_C and V_A) investigated. The load factors used were: positive 1.0-g, a positive 2.5-g steady-state maneuver and a 2.5-g transient maneuver, and a negative 1.0-g flight attitude.

STRUCTURAL MODEL - TASK IIB

The structural modeling effort associated with the Task IIB Detail Engineering Studies was conducted by exercising the design cycle twice; first, for a baseline strength design airplane and then performing an iteration on that design to incorporate the stiffness requirements dictated by the flutter optimization study. Each of these runs employed a 3-D structural model with the flexibilities associated with the cycle under consideration (i.e., strength or strength/stiffness design).

Structural Arrangement - Task IIB

As a result of the screening effort conducted during the Task I Analytical Design Studies, the most promising structural-material approach was selected for application to the Task IIB studies. This structural approach was a hybridization of the chord-wise and monocoque wing designs utilizing both metallic and composite materials. This hybrid arrangement consists of the following structural approaches:

Fuselage-shell: Conventional skin/stringer/frame design utilizing Ti-6Al-4V (ann.) material.

- Wing-forward and aft box: Metallic chordwise stiffened wing panels (convex-beaded concept), submerged metallic spar caps with composite reinforcement (B/PI-Bonded) and appropriate substructure.
- Wing tip: Monocoque wing panels (6Al-4V titanium honeycomb sandwich panel with aluminum brazed core), metallic (6Al-4V) substructure with rib/spar caps embedded in the basic panel.

For comparison with the Task I and IIA arrangements a general description of the Task IIB hybrid arrangement is included in Figure 9-8. This hybrid arrangement is used for both the strength and strength/stiffness designed models with only the flexibilities (element properties) altered to reflect the specific stage of the design.

Model Flexibilities - Task IIB

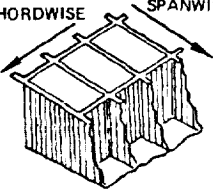
The flexibilities used for the strength designed hybrid model are shown in Table 9-7. The equivalent extensional and shear thicknesses for the appropriate wing rib and spar spacing are presented for selective wing planform locations.

The corresponding data for the strength/stiffness designed hybrid model is contained in Table 9-8. For both designs, the extensional stiffness (EA) of the composite reinforced spar caps was converted to an equivalent metallic stiffness and included in the t_y values at the applicable point design regions. The fuselage-shell extensional and shear thicknesses for the strength and strength/stiffness designs were invariant and a comprehensive listing is displayed in Figure 9-10. The corresponding listing of wing thicknesses used for the strength/stiffness hybrid model is shown in Figure 9-11.

Temperature Input - Task IIB

The thermal strains/stresses for three critical temperature conditions were investigated for the Task IIB effort. In addition to the maximum positive temperature gradient (Start-of-Cruise) and maximum temperature (Mid-Cruise) conditions, the temperatures for a maximum negative temperature gradient condition (exposed surface cooler than the interior surface) were included for input to the structural models. The latter condition represents a Mach 1.25 descent at V_D . A comparison of the temperature conditions used for all the Task I, IIA, and IIB structural models is

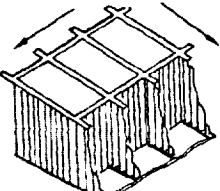
TABLE 9-7. WING PANEL EQUIVALENT EXTENSIONAL AND SHEAR THICKNESS, TASK IIB STRENGTH DESIGN - HYBRID MODEL

ARRANGEMENT/CONCEPT	POINT DESIGN REGION	LOCATION	SPACING (IN.)		WING SURFACE	EXTENSIONAL AND SHEAR THICKNESS (IN.) (1)		
			SPAR	RIB		t_x	t_y	t_{xy}
<ul style="list-style-type: none"> HYBRID ARRANGEMENT PANEL CONCEPTS  <ul style="list-style-type: none"> CIRCULAR ARC CONVEX BEADED WING TIP HONEYCOMB SANDWICH 	40322	FORWARD WING BOX	20.0	60.0	UPPER LOWER	.038 .043	.012 .016	.028 .032
	40236	AFT WING BOX	20.0	60.0	UPPER LOWER	.048 .058	.151 .229	.035 .043
	40536		20.0	60.0	UPPER LOWER	.074 .061	.135 .197	.055 .045
	41036		40.0	60.0	UPPER LOWER	.076 .093	.143 .188	.066 .083
	41316	WING TIP	30.0	60.0	UPPER LOWER	.119 .143	.121 .144	.110 .132
	41348		20.0	60.0	UPPER LOWER	.082 .101	.089 .108	.073 .091

NOTES:

(1) THICKNESS INCLUDE CAP AND/OR PANEL THICKNESSES AS APPLICABLE

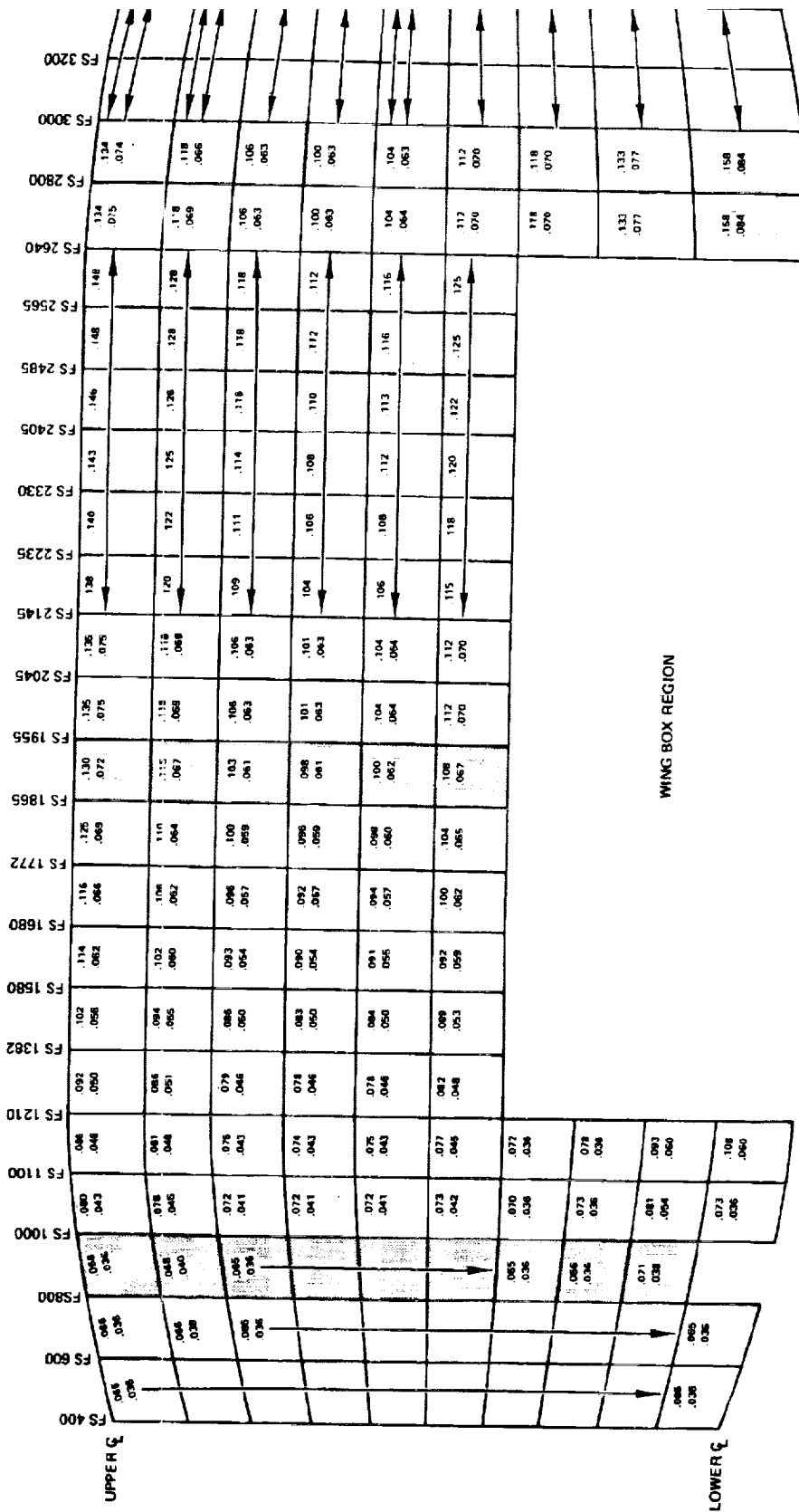
TABLE 9-8. WING PANEL EQUIVALENT EXTENSIONAL AND SHEAR THICKNESS, TASK IIB STRENGTH/STIFFNESS - HYBRID MODEL

ARRANGEMENT/CONCEPT	POINT DESIGN REGION	LOCATION	SPACING (IN.)		WING SURFACE	EXTENSIONAL & SHEAR THICKNESS (IN.) (1)		
			SPAR	RIB		t_x	t_y	t_{xy}
<ul style="list-style-type: none"> HYBRID ARRANGEMENT PANEL CONCEPT  <ul style="list-style-type: none"> CIRCULAR ARC CONVEX BEADED WING TIP HONEYCOMB SANDWICH 	40322	FORWARD WING BOX	22.7	60.0	UPPER LOWER	.037 .047	.012 .016	.028 .032
	40236	AFT WING BOX	21.2	60.0	UPPER LOWER	.058 .061	.148 .225	.039 .043
	40536		21.2	60.0	UPPER LOWER	.079 .066	.146 .209	.052 .043
	41036		21.2	60.0	UPPER LOWER	.077 .093	.120 .154	.066 .082
	41316	WING TIP	40.0	40.0	UPPER LOWER	.130 .157	.153 .174	.124 .150
	41348		30.0	40.0	UPPER LOWER	.145 .145	.165 .168	.135 .135

NOTES

(1) THICKNESSES INCLUDE CAP AND/OR PANEL THICKNESS AS APPLICABLE.

ORIGINAL PAGE IS
OF POOR QUALITY



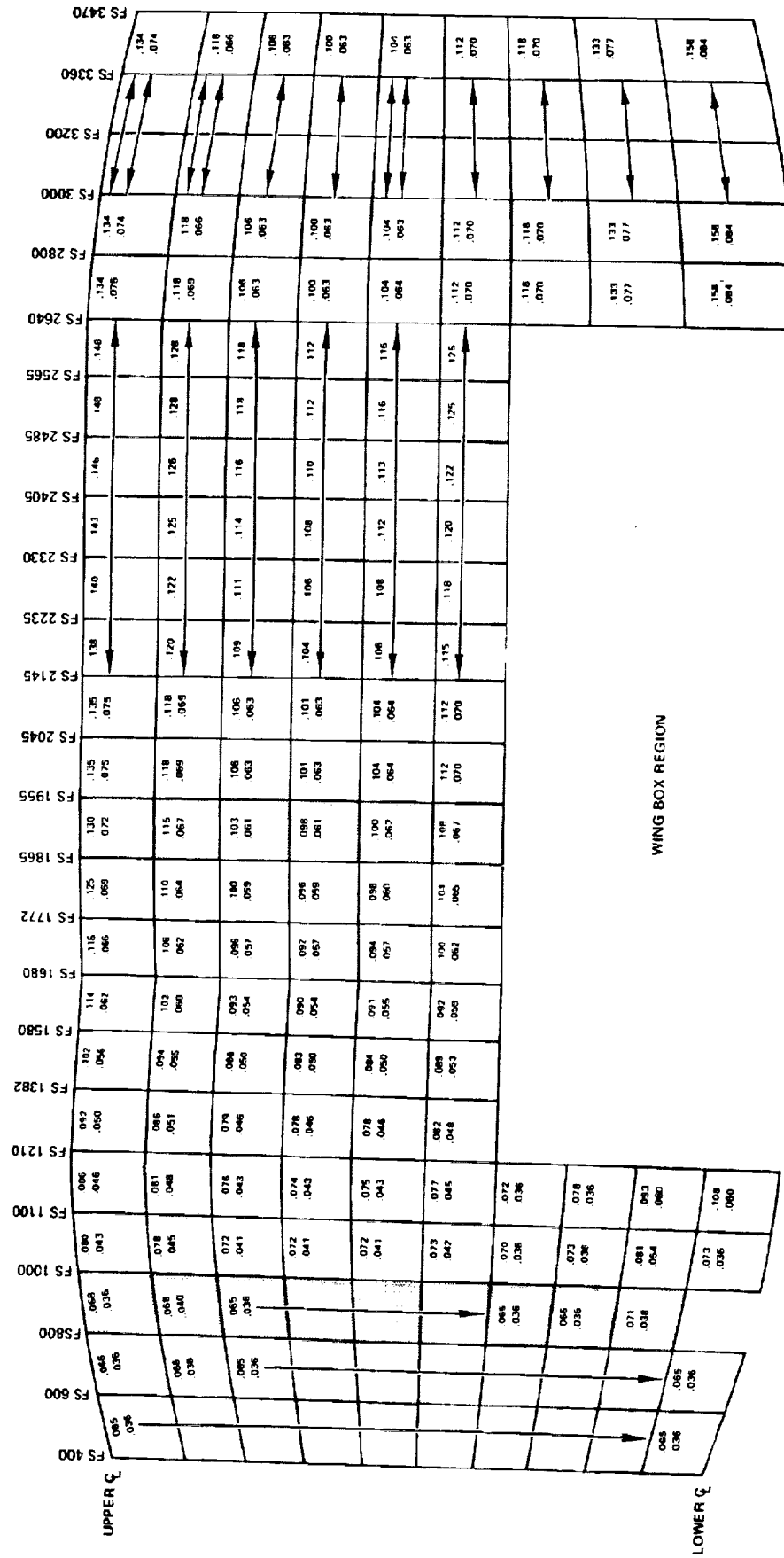
NOTES:
(1) THICKNESS LEGEND

.XXX t_x EXTENSIONAL THICKNESS
.XXX t_{xy} SHEAR THICKNESS

Figure 2-10. Surlage Equivalent Extensional Shear Thicknesses, Tusk IIb Models

FOLDOUT FRAME

FOLDOUT FRAME



NOTES:
 (1) THICKNESS LEGEND
 .XXX t_{xx} EXTENSIONAL THICKNESS
 .XXX t_{xy} SHEAR THICKNESS

Figure 9-10. Fuselage Equivalent Extensional and Shear Thicknesses, Task 11B Models

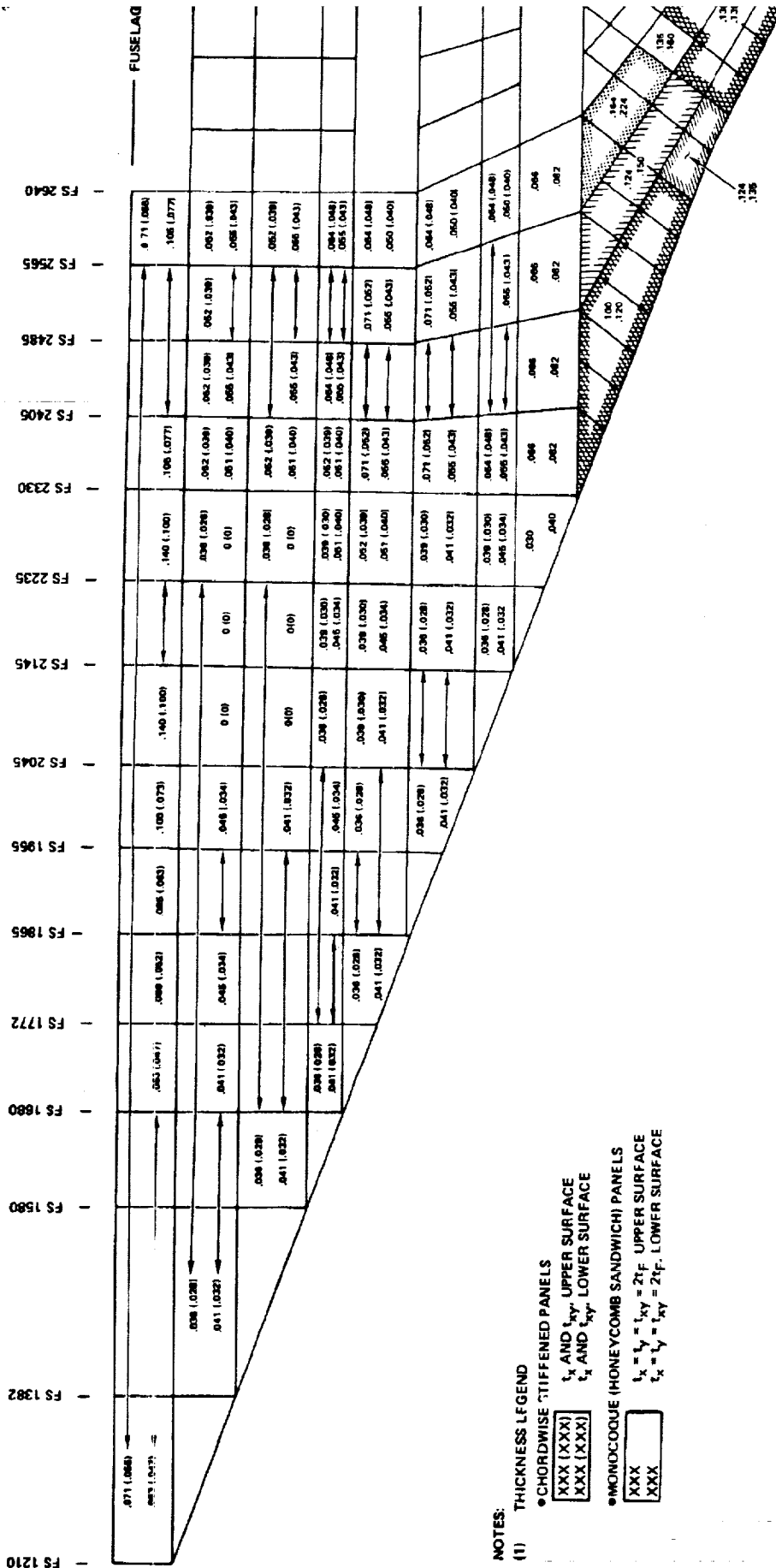
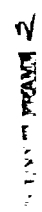


Figure 9-11.
Thick

PRECEDING PAGE BLANK NOT FILMED

FOOTOUT FRAMES



b6-20

shown in Table 9-5. The structural temperatures for the Mach 1.25 descent condition are displayed in Figure 9-12, the Start-of-Cruise and Mid-Cruise temperatures are included in Section 6, Structural Temperatures.

External Loads Input - Task IIB

A summary of the number and type of load conditions used on the strength and strength/stiffness models are shown in Table 9-6. The initial NASTRAN internal loads run was based on the aeroelastic loads of the strength designed model and included a total of nineteen (19) conditions; specifically:

- Thirteen (13) ascent conditions covering the Mach 0.4, Mach 0.9, and Mach 1.25 symmetric flight conditions;
- Four (4) Mach 2.7 flight conditions covering the Start-of-Cruise and Mid-Cruise conditions; and
- Two (2) descent conditions at Mach 1.25 for the steady state and transient maneuvers.

The static aeroelastic loads applied to the strength/stiffness structural model included the above 19 conditions and an additional 6 load conditions, which were:

- Positive and negative gust conditions at Mach 0.9 (V_0); and
- Four (4) dynamic landing conditions for fuselage design.

A preliminary assessment of the effect of airframe flexibility on loads was conducted using the flexibilities of the strength designed model. Aeroelastic loads were calculated considering the manufactured aircraft shape (jig shape) to be that which deforms to the mid-cruise shape under mid-cruise loading. Aeroelastic loads were calculated using the jig shape as the initial shape (as compared to mid-cruise shape) and these loads used in a NASTRAN internal loads run. The resulting internal load intensities indicated an appreciable effect in the more flexible regions of the airplane, e.g., approximately a 7- to 9-percent increase in the wing upper surface spanwise load intensities in the aft box region. Considering these results, the jig shape required to produce the mid-cruise shape under mid-cruise loads was defined for the strength/stiffness structural model and included in the static aeroelastic load calculations for all Mach numbers considered.

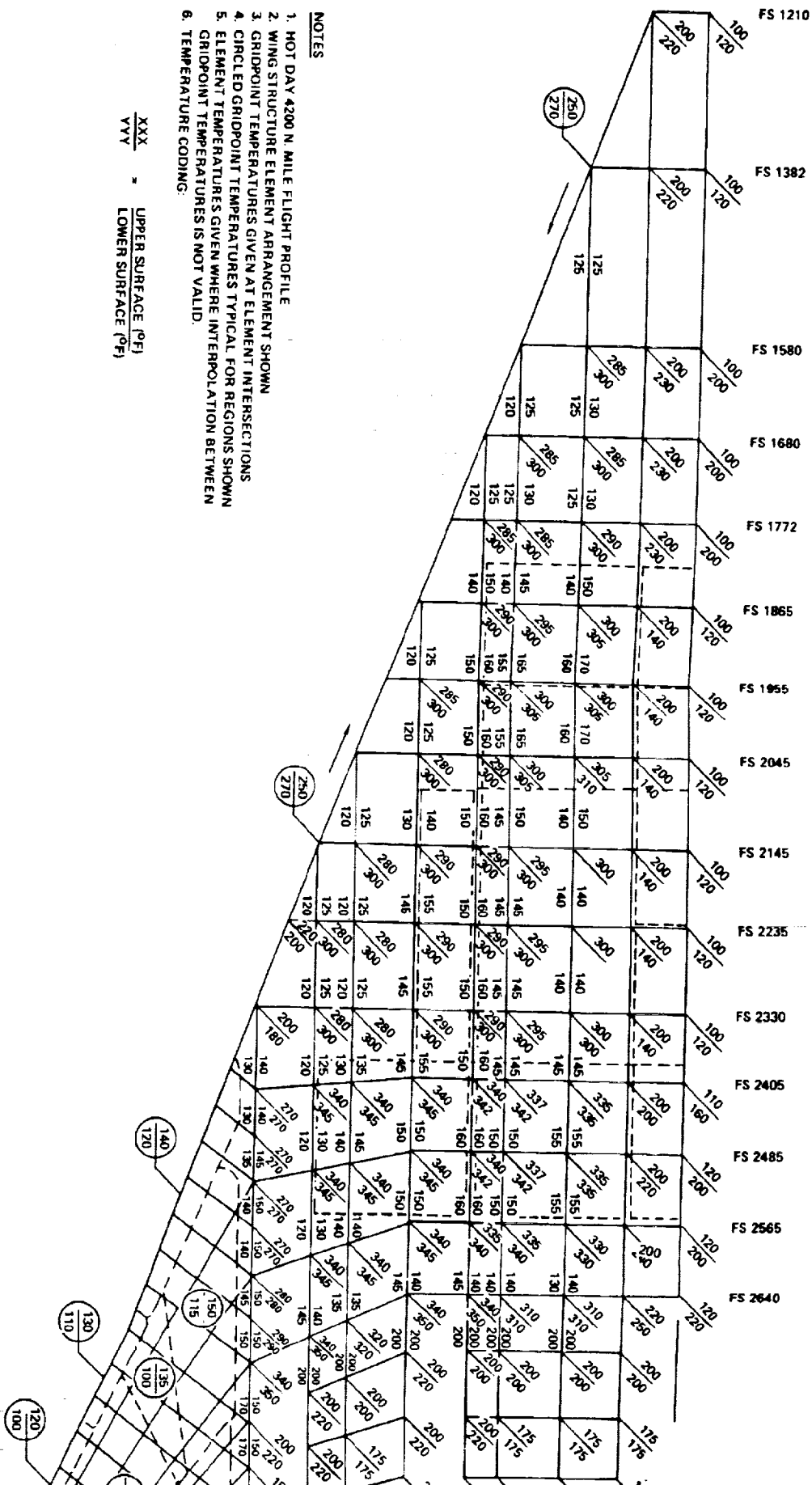


PRECEDING PAGE BLANK NOT FILMED

FOLDOUT FRAME

- NOTES
1. HOT DAY 4200 N. MILE FLIGHT PROFILE
 2. WING STRUCTURE ELEMENT ARRANGEMENT SHOWN
 3. GRIDPOINT TEMPERATURES GIVEN AT ELEMENT INTERSECTIONS
 4. CIRCLED GRIDPOINT TEMPERATURES TYPICAL FOR REGIONS SHOWN
 5. ELEMENT TEMPERATURES GIVEN WHERE INTERPOLATION BETWEEN GRIDPOINT TEMPERATURES IS NOT VALID
 6. TEMPERATURE CODING:

$$\frac{XXX}{YYY} = \frac{\text{UPPER SURFACE (°F)}}{\text{LOWER SURFACE (°F)}}$$



FOLDOUT FRAME

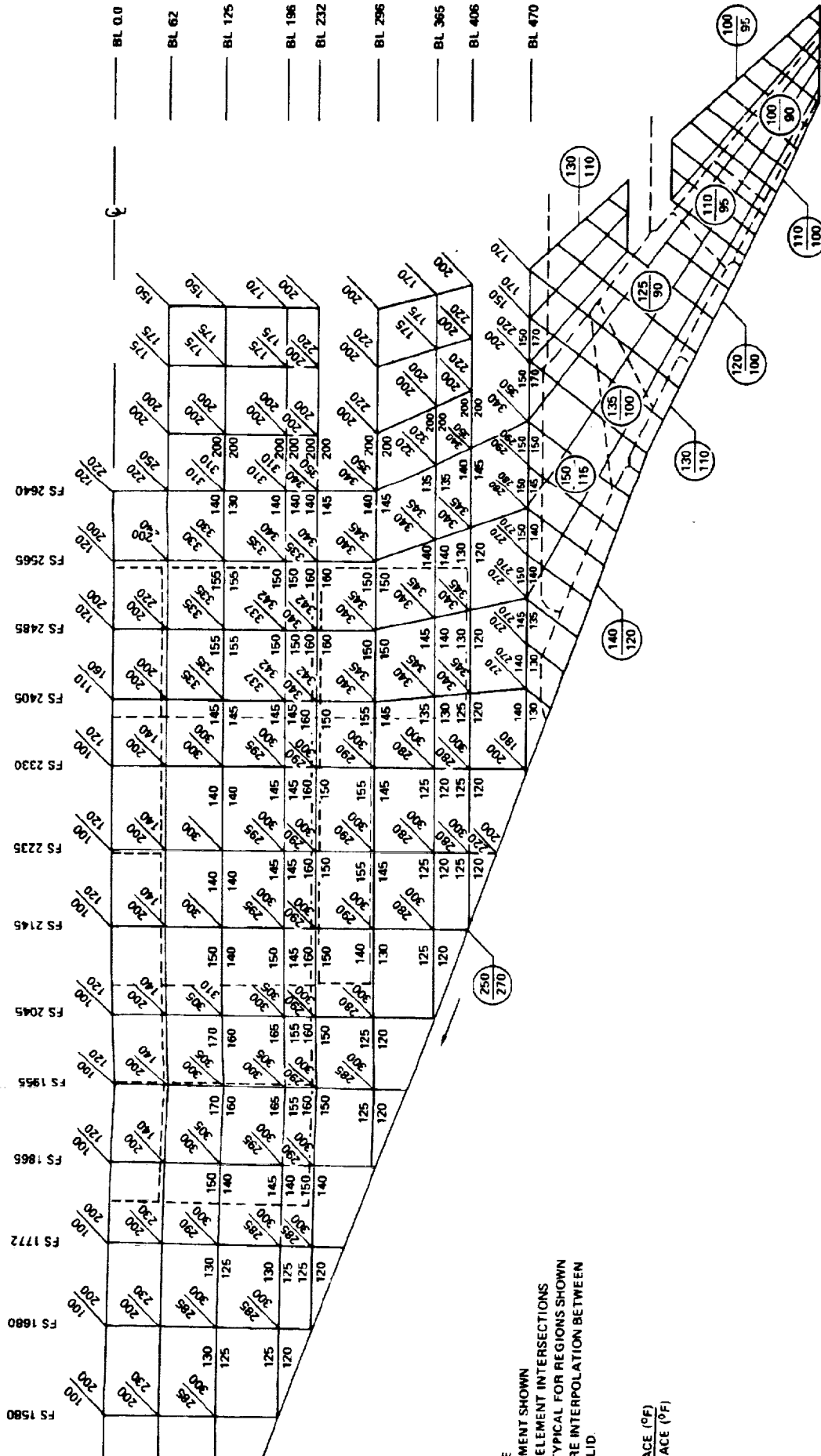


Figure 9-12. Structural Temperatures, Transonic Descent Condition, Task IIB Final Design Model

RESULTS

The results of the Task I, Task IIA, and Task IIB structural modeling efforts are discussed in this section. The results of the NASTRAN static solution (displacements, internal forces and stresses) and the auxiliary program for calculating running load are presented.

Displacements

A comparison of the Task I wing rear beam displacements for a symmetric maneuver at Mach 1.25 are shown in Figure 9-13. These vertical displacements (z-direction) are plotted along the rear beam and indicate the relative wing stiffness of the three Task I models. A review of this data indicates the spanwise-and chordwise-stiffened structural models are more flexible than the monocoque model, i.e., chordwise and spanwise model wing tip displacements are approximately 35-percent greater than the monocoque tip displacement.

The comparable wing rear beam displacements for both the hybrid strength designed and final strength/stiffness designed 3-D structural models are displayed in Figure 9-14. The final design model (strength/stiffness) shows a maximum wing tip displacement of 200 inches for the 2.5-g symmetric flight condition at Mach 1.25, approximately 20.0 inches less than the strength designed model. A wing rear beam displacement comparison of the Task I Chordwise, Task IIA Chordwise, and the Task IIB Final Design models is shown in Figure 9-15. The load condition used for this comparison was a 2.5-g symmetric flight condition at Mach 0.90. The Task IIA and IIB models reflect the baseline configuration and flight attitude changes associated with the redefinition of the airplane concept after the Task I analysis. Figure 9-15 indicates a wing tip displacement of 156 inches (13 feet) for the final Task IIB Hybrid Design; the corresponding displacements for the Task I and Task IIA chordwise models are 180 and 195 inches, respectively.

A comparison of the Task I, Task IIA, and Task IIB fuselage displacements is shown in Figure 9-16. These displacements are for a 2.5-g symmetric maneuver condition at Mach 0.9. A maximum nose displacement of 20.0 inches (negative) is shown for the Task I chordwise model; whereas, the nose displacements for the Task II models, which reflect the shortened forebody, are negligible. The Task IIA chordwise model has the maximum positive tail displacement (approximately 30.0 inches) and the

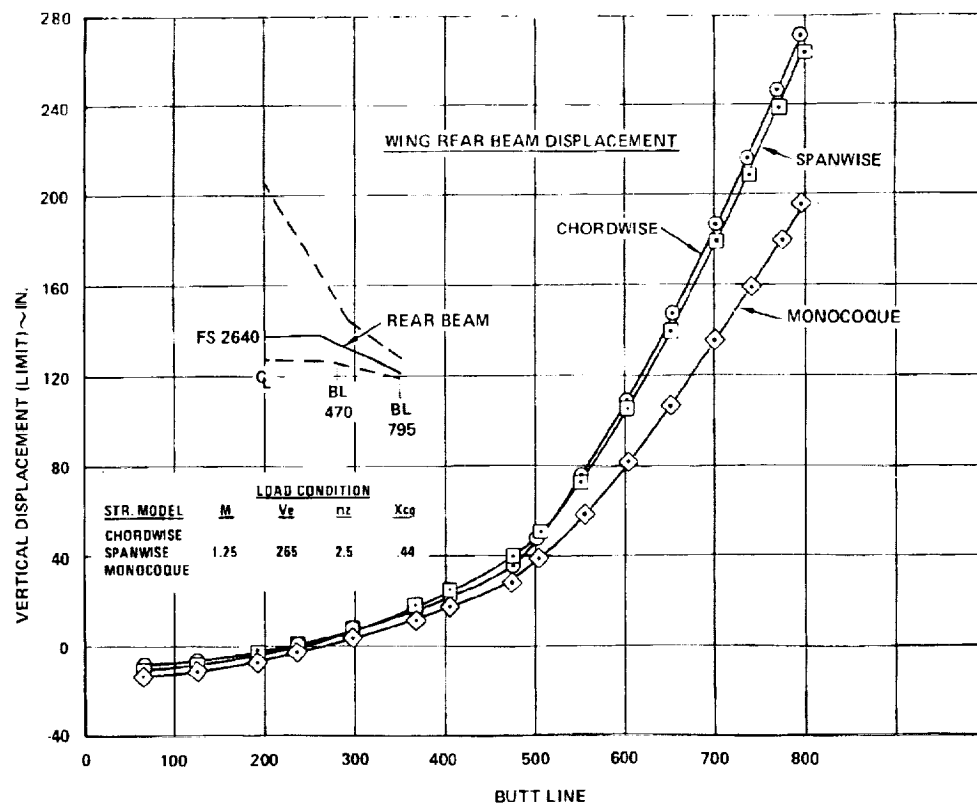


Figure 9-13. Comparison of Wing Rear Beam Displacements, Task I Models

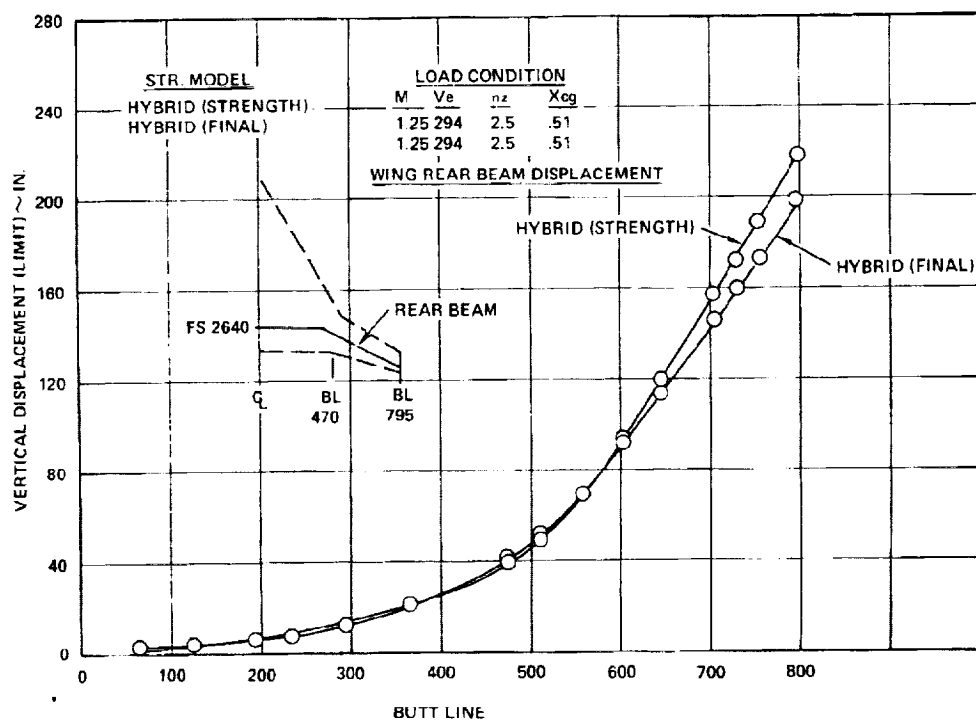


Figure 9-14. Comparison of Wing Rear Beam Displacements, Task IIB Models

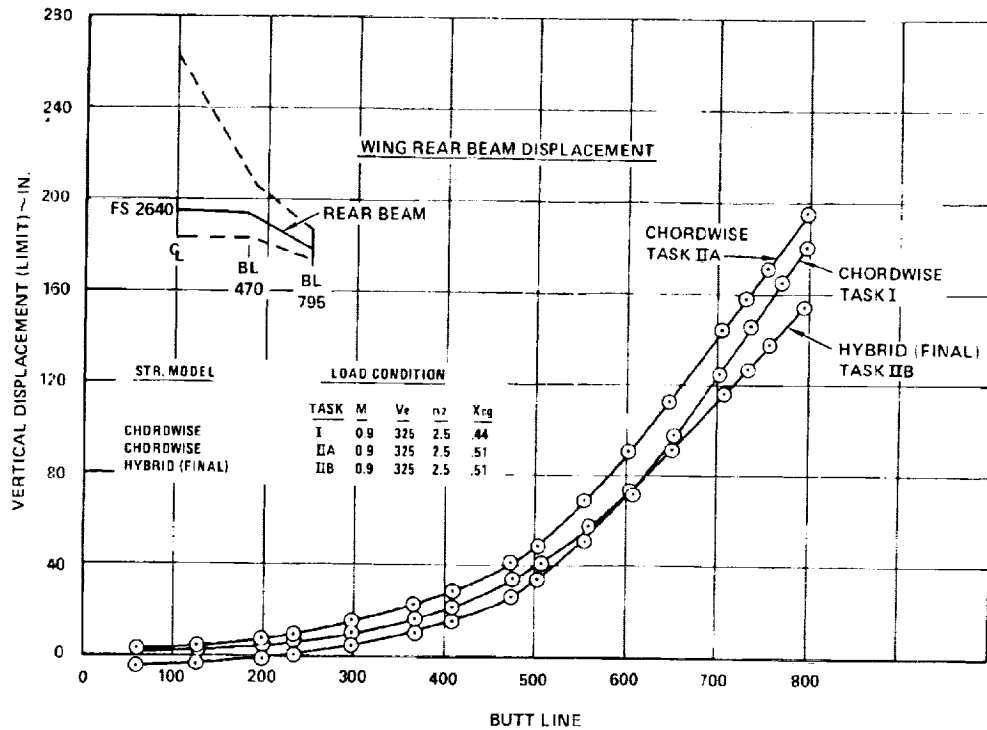


Figure 9-15. Comparison of Wing Rear Beam Displacements, Task I, IIA, and IIB Models

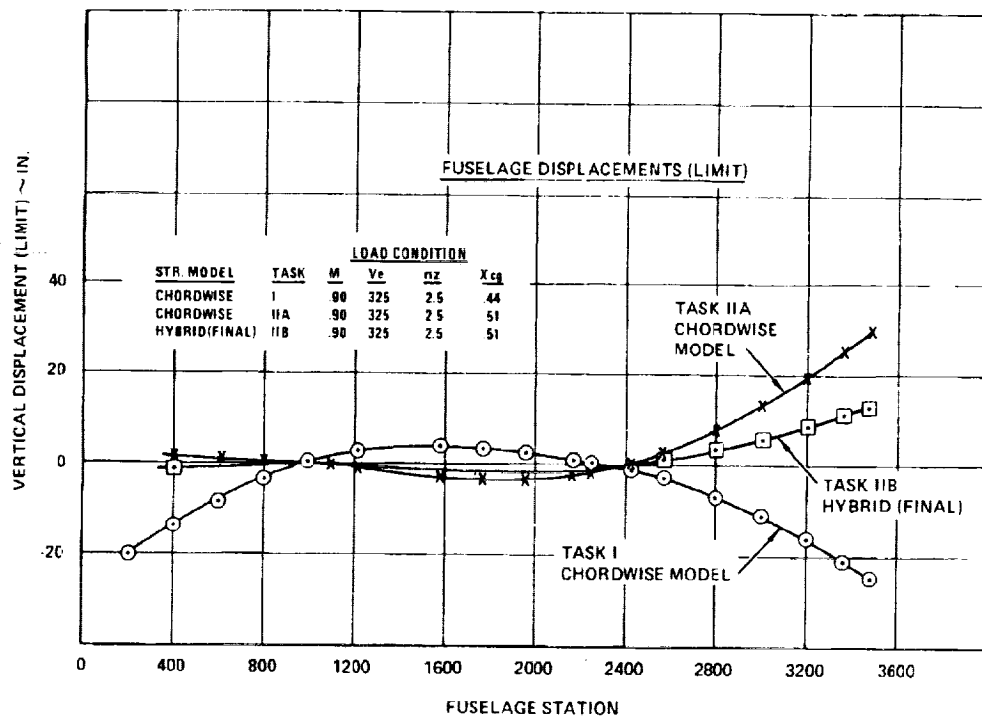
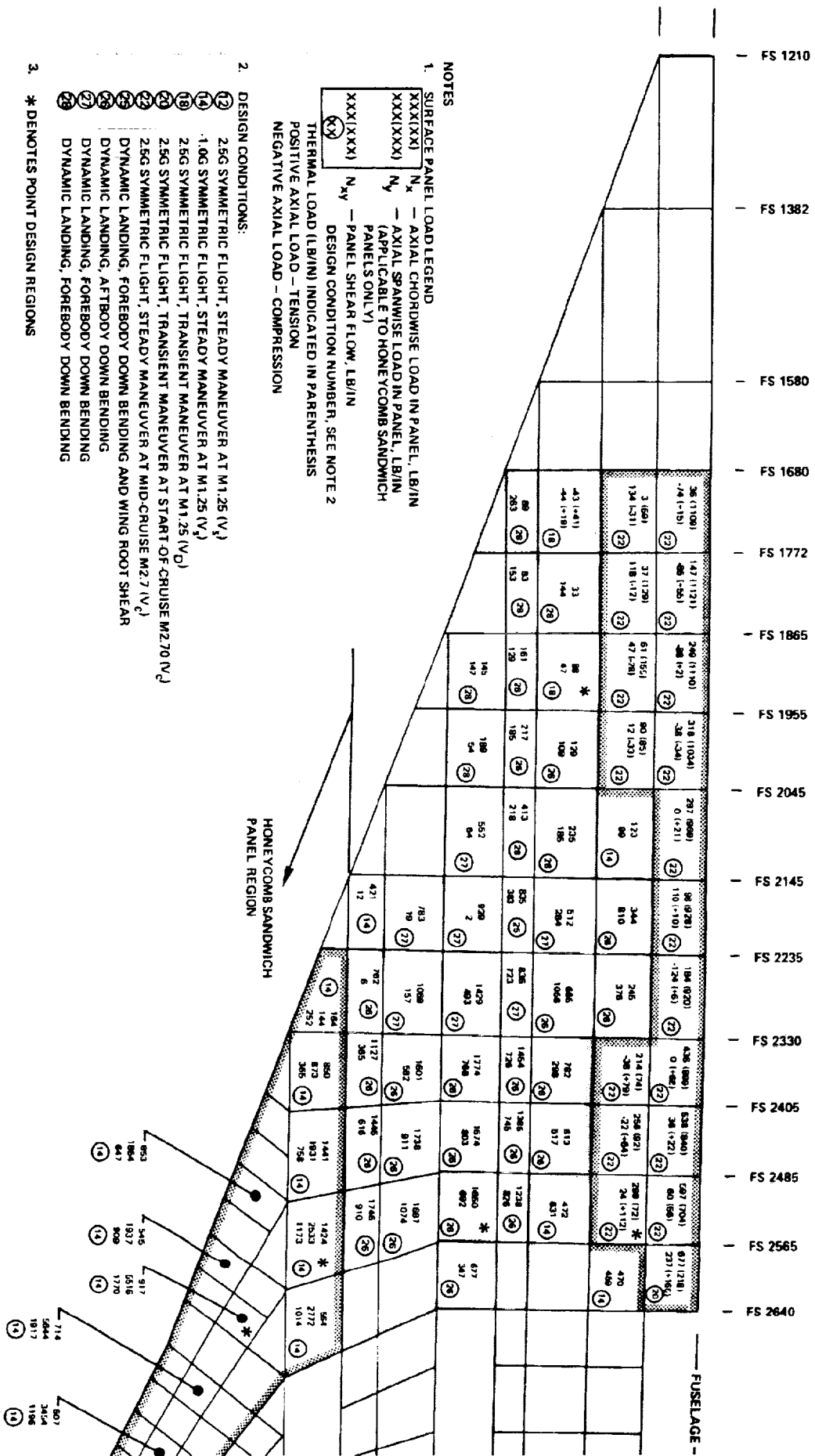


Figure 9-16. Comparison of Fuselage Displacements, Task I, IIA, and IIB Models



1. SURFACE PANEL LOAD LEGEND
- XXX(XX) N_x - AXIAL CHORDWISE LOAD IN PANEL, LB/IN
 XXX(XXX) N_y - AXIAL SPANWISE LOAD IN PANEL, LB/IN
 (APPLICABLE TO HONEYCOMB SANDWICH PANELS ONLY)
 XXX(XXX) N_{xy} - PANEL SHEAR FLOW, LB/IN
- DESIGN CONDITION NUMBER, SEE NOTE 2
- THE THERMAL LOAD (LB/IN) INDICATED IN PARENTHESIS
- POSITIVE AXIAL LOAD - TENSION
- NEGATIVE AXIAL LOAD - COMPRESSION
2. DESIGN CONDITIONS:
- (12) 2.5G SYMMETRIC FLIGHT, STEADY MANEUVER AT M1.25 (V_1)
 - (14) 1.0G SYMMETRIC FLIGHT, STEADY MANEUVER AT M1.25 (V_1)
 - (18) 2.5G SYMMETRIC FLIGHT, TRANSIENT MANEUVER AT M1.25 (V_1)
 - (20) 2.5G SYMMETRIC FLIGHT, TRANSIENT MANEUVER AT START OF CRUISE M2.70 (V_2)
 - (22) 2.5G SYMMETRIC FLIGHT, STEADY MANEUVER AT MID-CRUISE M2.70 (V_2)
 - (26) DYNAMIC LANDING, FOREBODY DOWN BENDING AND WING ROOT SHEAR
 - (28) DYNAMIC LANDING, AFTBODY DOWN BENDING
 - (27) DYNAMIC LANDING, FOREBODY DOWN BENDING
 - (29) DYNAMIC LANDING, FOREBODY DOWN BENDING
3. * DENOTES POINT DESIGN REGIONS



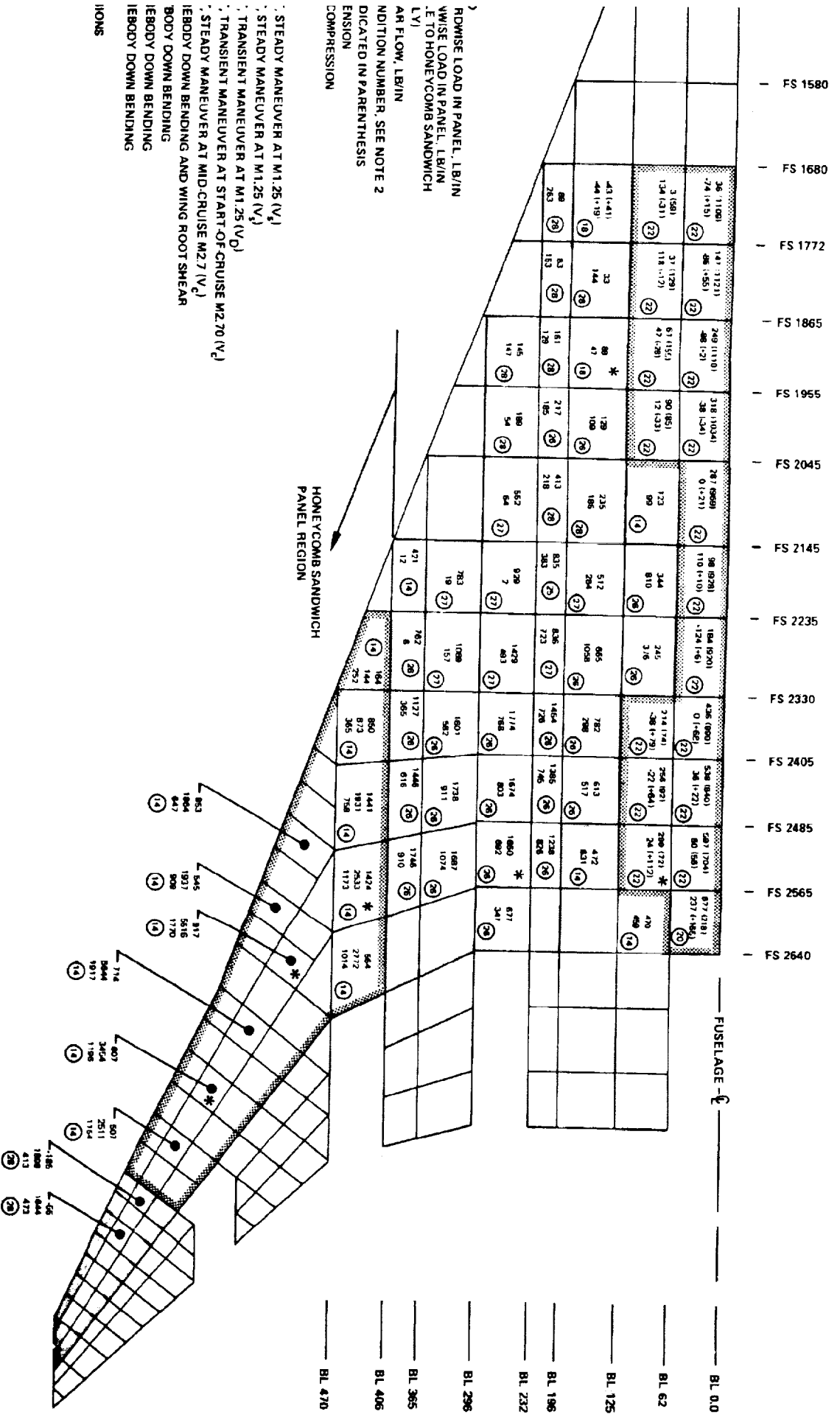


Figure 9-17. Wing Upper Surface Maximum Tension Loads, Tank IIB Final Design Model

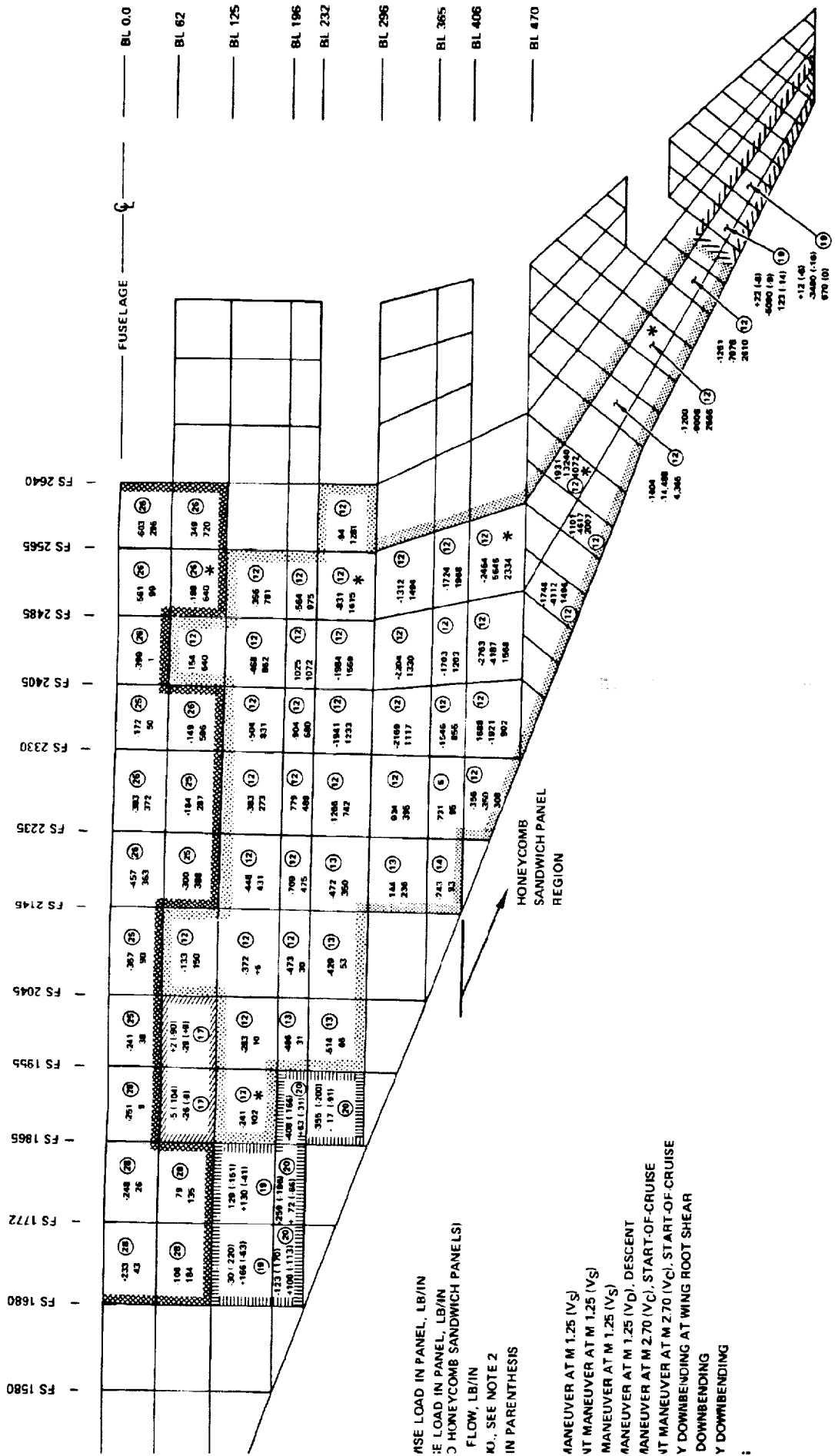
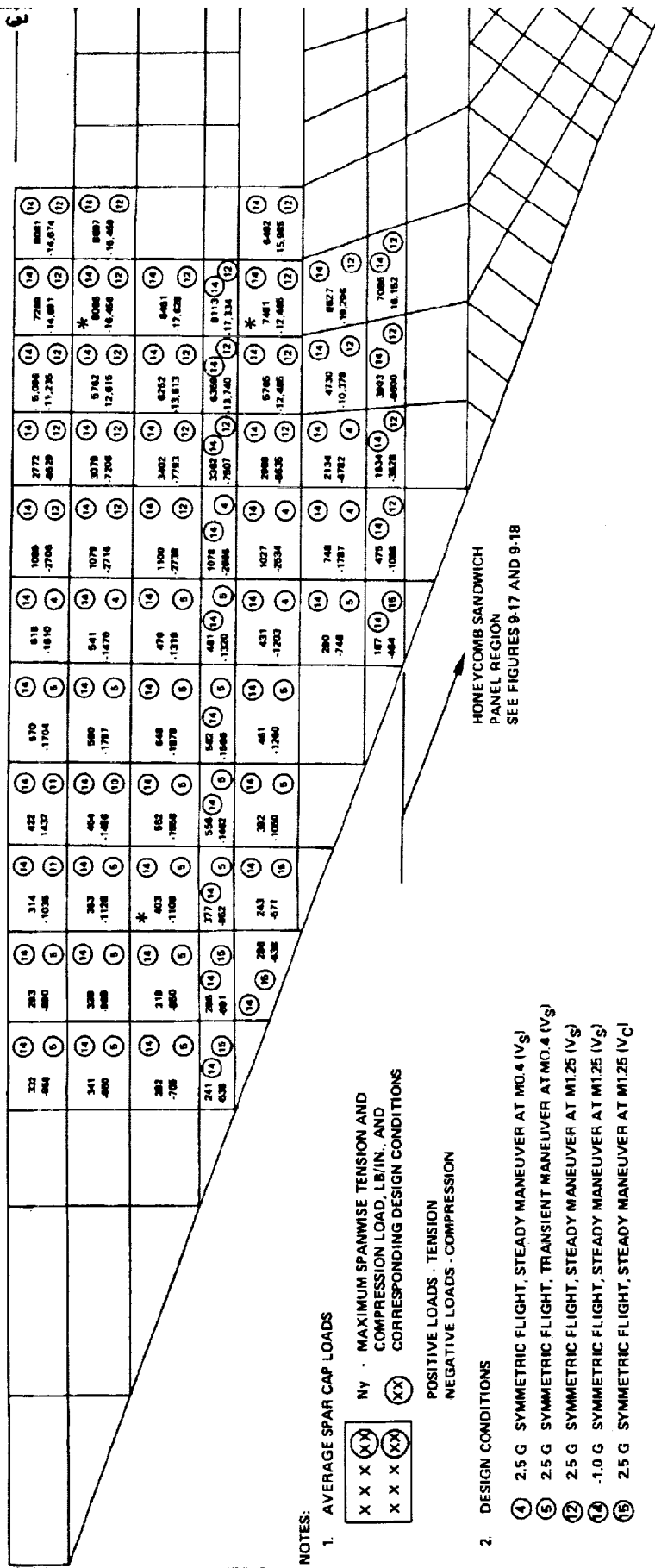


Figure 9-18. Wing Upper Surface Maximum Compression Loads, Task IIB Final Design Model

WINGMAN FRANCIS

FUSELAGE STATION

FS 1210 FS 1382 FS 1580 FS 1580 FS 1680 FS 1772 FS 1865 FS 1955 FS 2045 FS 2145 FS 2235 FS 2330 FS 2405 FS 2485 FS 2565 FS 2640



NOTES:

1. AVERAGE SPAR CAP LOADS

Ny - MAXIMUM SPANWISE TENSION AND COMPRESSION LOAD, LB/IN., AND CORRESPONDING DESIGN CONDITIONS

XX - TENSION
XX - COMPRESSION

POSITIVE LOADS - TENSION
NEGATIVE LOADS - COMPRESSION

2. DESIGN CONDITIONS

- ④ 2.5 G SYMMETRIC FLIGHT, STEADY MANEUVER AT MO.4 (V_S)
- ⑤ 2.5 G SYMMETRIC FLIGHT, TRANSIENT MANEUVER AT MO.4 (V_S)
- ⑫ 2.5 G SYMMETRIC FLIGHT, STEADY MANEUVER AT M1.25 (V_S)
- ⑭ -1.0 G SYMMETRIC FLIGHT, STEADY MANEUVER AT M1.25 (V_S)
- ⑮ 2.5 G SYMMETRIC FLIGHT, STEADY MANEUVER AT M1.25 (V_C)

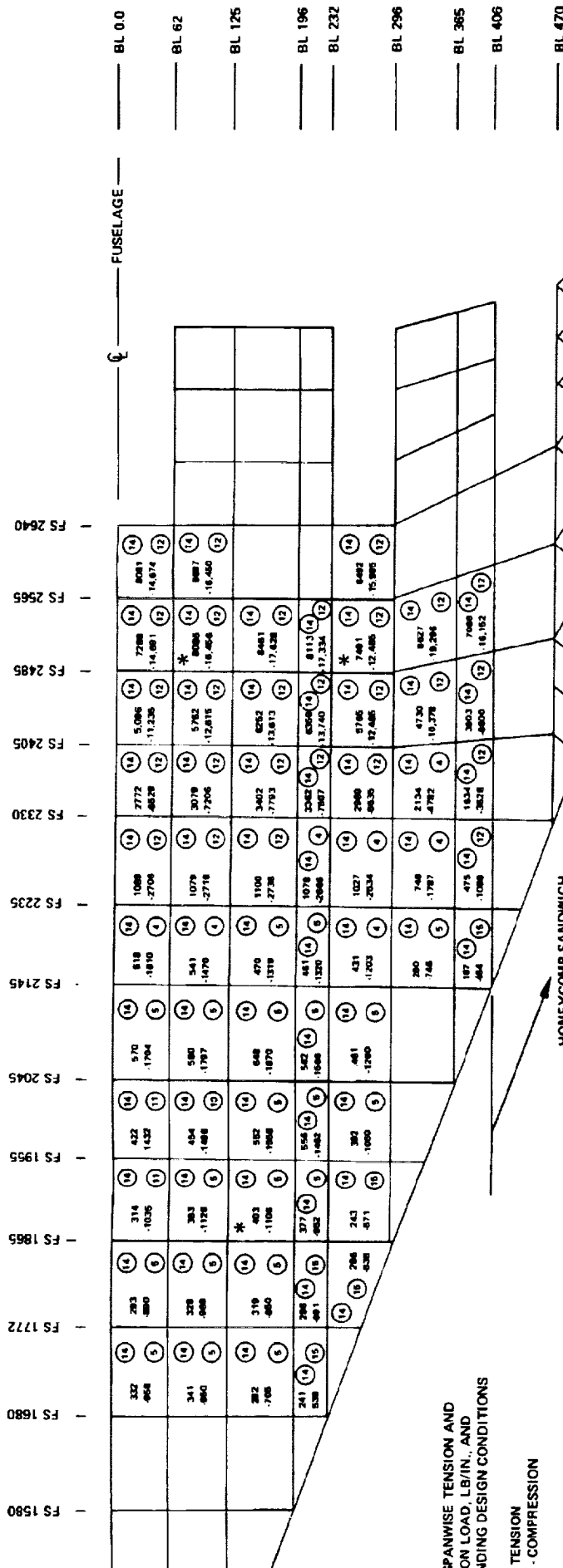
3. * DENOTES POINT DESIGN REGIONS

PRECEDING PAGE BLANK NOT FILLED

FOLDOUT FRAME /

FOLDOUT FRAME

FUSELAGE STATION



SPANWISE TENSION AND
ON LOAD, LB/IN., AND
WING DESIGN CONDITIONS

TENSION
- COMPRESSION

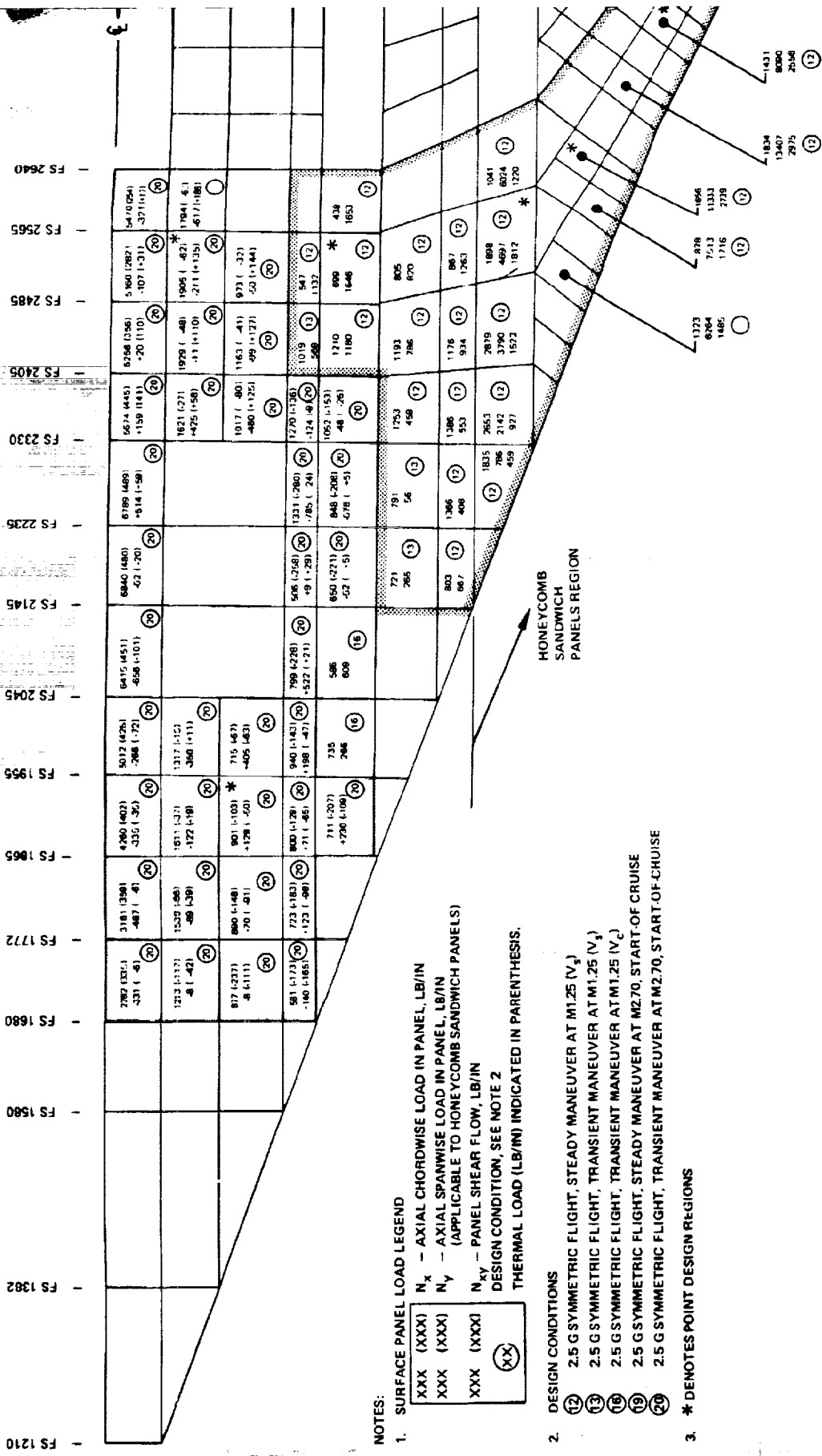
HONEYCOMB SANDWICH
PANEL REGION
SEE FIGURES 9.17 AND 9.18

- STEADY MANEUVER AT MO.4 (V_S)
- TRANSIENT MANEUVER AT MO.4 (V_S)
- STEADY MANEUVER AT M1.25 (V_S)
- STEADY MANEUVER AT M1.25 (V_S)
- STEADY MANEUVER AT M1.25 (V_C)

MS

Figure 9-17. Wing Upper Surface Maximum Spanwise Tension and Compression Loads, Task IIB Final Design Model

FOLDOUT FRAMES 3-9-4



NOTES:

1. SURFACE PANEL LOAD LEGEND
 - XXX (XXX) N_x - AXIAL CHORDWISE LOAD IN PANEL, LB/IN
 - XXX (XXX) N_y - AXIAL SPANWISE LOAD IN PANEL, LB/IN (APPLICABLE TO HONEYCOMB SANDWICH PANELS)
 - XXX (XXX) N_{xy} - PANEL SHEAR FLOW, LB/IN
 - XX (XX) - DESIGN CONDITION, SEE NOTE 2
 - Thermal Load (LB/IN) INDICATED IN PARENTHESIS.

2. DESIGN CONDITIONS
 - 12 2.5 G SYMMETRIC FLIGHT, STEADY MANEUVER AT M1.25 (V_d)
 - 13 2.5 G SYMMETRIC FLIGHT, TRANSIENT MANEUVER AT M1.25 (V_d)
 - 16 2.5 G SYMMETRIC FLIGHT, TRANSIENT MANEUVER AT M1.25 (V_d)
 - 19 2.5 G SYMMETRIC FLIGHT, STEADY MANEUVER AT M2.70, START-OF-CRUISE
 - 20 2.5 G SYMMETRIC FLIGHT, TRANSIENT MANEUVER AT M2.70, START-OF-CRUISE
3. * DENOTES POINT DESIGN REGIONS

PROCEEDING PAGE BLANK NOT FILMED

ROLL-OUT FRAME

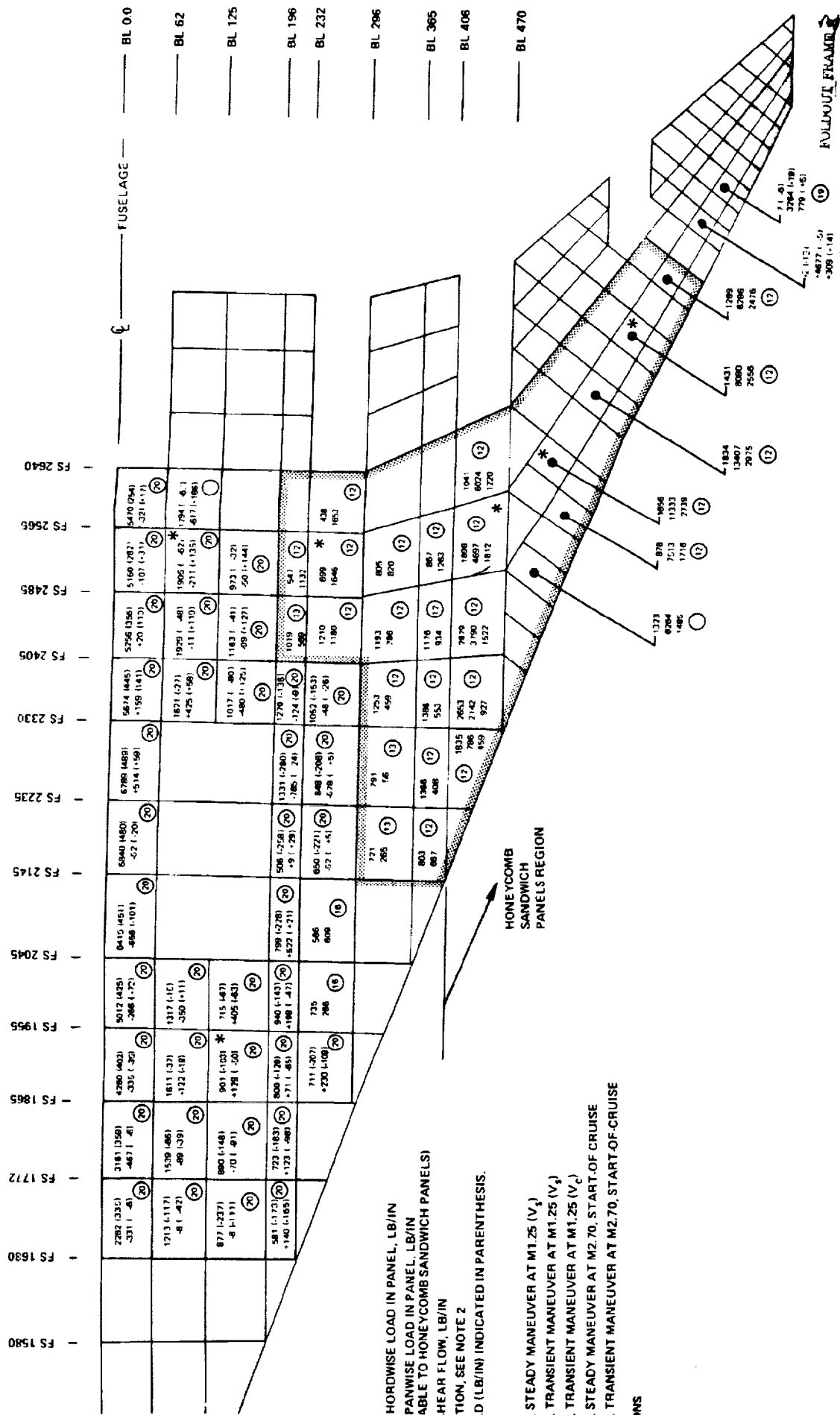
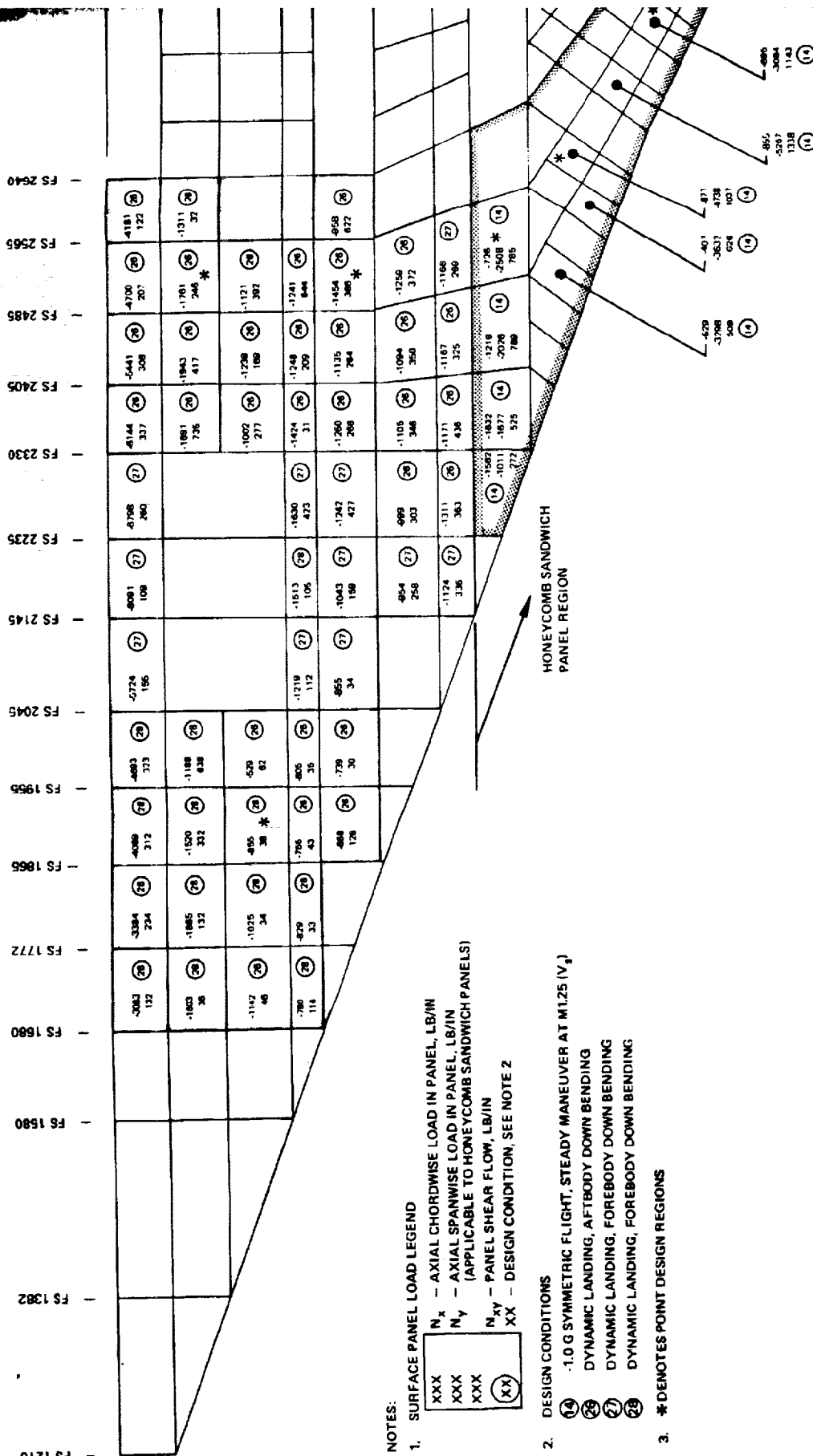


Figure 9-10. Wing Lower Surface Maximum Chordwise Tension Loads, Track IIB Final Design Model

FUSELAGE STATION



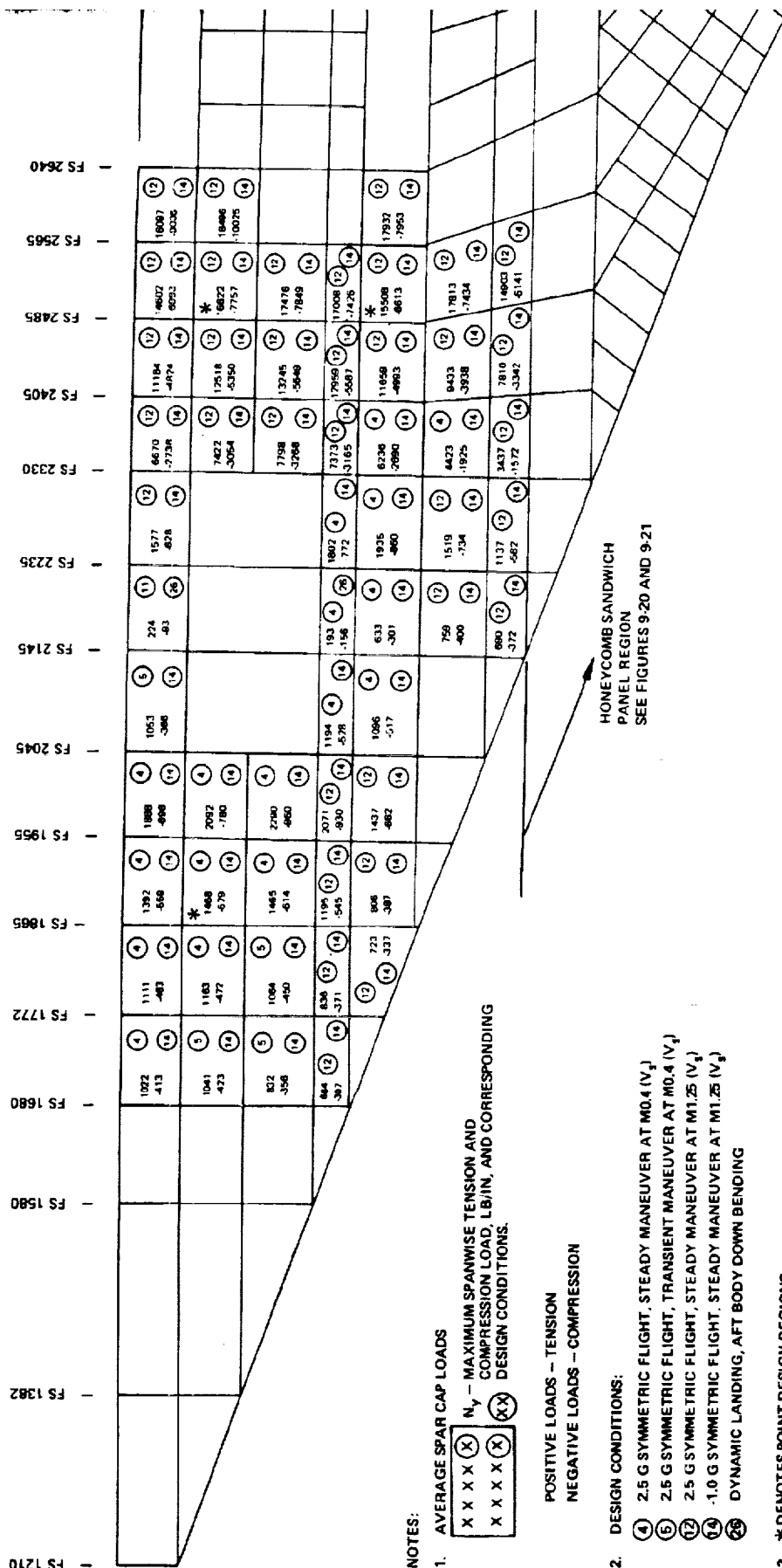
NOTES:

1. SURFACE PANEL LOAD LEGEND
 N_x - AXIAL CHORDWISE LOAD IN PANEL, LB/IN
 N_y - AXIAL SPANWISE LOAD IN PANEL, LB/IN
 (APPLICABLE TO HONEYCOMB SANDWICH PANELS)
 N_{xy} - PANEL SHEAR FLOW, LB/IN
 XX - DESIGN CONDITION, SEE NOTE 2
2. DESIGN CONDITIONS
 14 - 1.0 G SYMMETRIC FLIGHT, STEADY MANEUVER AT M1.25 (V_0)
 15 - DYNAMIC LANDING, AFTBODY DOWN BENDING
 16 - DYNAMIC LANDING, FOREBODY DOWN BENDING
 17 - DYNAMIC LANDING, FOREBODY DOWN BENDING
 18 - DYNAMIC LANDING, FOREBODY DOWN BENDING
 19 - DYNAMIC LANDING, FOREBODY DOWN BENDING
 20 - DYNAMIC LANDING, FOREBODY DOWN BENDING
 21 - DYNAMIC LANDING, FOREBODY DOWN BENDING
 22 - DYNAMIC LANDING, FOREBODY DOWN BENDING
 23 - DYNAMIC LANDING, FOREBODY DOWN BENDING
 24 - DYNAMIC LANDING, FOREBODY DOWN BENDING
 25 - DYNAMIC LANDING, FOREBODY DOWN BENDING
 26 - DYNAMIC LANDING, FOREBODY DOWN BENDING
 27 - DYNAMIC LANDING, FOREBODY DOWN BENDING
 28 - DYNAMIC LANDING, FOREBODY DOWN BENDING
 29 - DYNAMIC LANDING, FOREBODY DOWN BENDING
 30 - DYNAMIC LANDING, FOREBODY DOWN BENDING
 31 - DYNAMIC LANDING, FOREBODY DOWN BENDING
 32 - DYNAMIC LANDING, FOREBODY DOWN BENDING
 33 - DYNAMIC LANDING, FOREBODY DOWN BENDING
 34 - DYNAMIC LANDING, FOREBODY DOWN BENDING
 35 - DYNAMIC LANDING, FOREBODY DOWN BENDING
 36 - DYNAMIC LANDING, FOREBODY DOWN BENDING
 37 - DYNAMIC LANDING, FOREBODY DOWN BENDING
 38 - DYNAMIC LANDING, FOREBODY DOWN BENDING
 39 - DYNAMIC LANDING, FOREBODY DOWN BENDING
 40 - DYNAMIC LANDING, FOREBODY DOWN BENDING
 41 - DYNAMIC LANDING, FOREBODY DOWN BENDING
 42 - DYNAMIC LANDING, FOREBODY DOWN BENDING
 43 - DYNAMIC LANDING, FOREBODY DOWN BENDING
 44 - DYNAMIC LANDING, FOREBODY DOWN BENDING
 45 - DYNAMIC LANDING, FOREBODY DOWN BENDING
 46 - DYNAMIC LANDING, FOREBODY DOWN BENDING
 47 - DYNAMIC LANDING, FOREBODY DOWN BENDING
 48 - DYNAMIC LANDING, FOREBODY DOWN BENDING
 49 - DYNAMIC LANDING, FOREBODY DOWN BENDING
 50 - DYNAMIC LANDING, FOREBODY DOWN BENDING
 51 - DYNAMIC LANDING, FOREBODY DOWN BENDING
 52 - DYNAMIC LANDING, FOREBODY DOWN BENDING
 53 - DYNAMIC LANDING, FOREBODY DOWN BENDING
 54 - DYNAMIC LANDING, FOREBODY DOWN BENDING
 55 - DYNAMIC LANDING, FOREBODY DOWN BENDING
 56 - DYNAMIC LANDING, FOREBODY DOWN BENDING
 57 - DYNAMIC LANDING, FOREBODY DOWN BENDING
 58 - DYNAMIC LANDING, FOREBODY DOWN BENDING
 59 - DYNAMIC LANDING, FOREBODY DOWN BENDING
 60 - DYNAMIC LANDING, FOREBODY DOWN BENDING
 61 - DYNAMIC LANDING, FOREBODY DOWN BENDING
 62 - DYNAMIC LANDING, FOREBODY DOWN BENDING
 63 - DYNAMIC LANDING, FOREBODY DOWN BENDING
 64 - DYNAMIC LANDING, FOREBODY DOWN BENDING
 65 - DYNAMIC LANDING, FOREBODY DOWN BENDING
 66 - DYNAMIC LANDING, FOREBODY DOWN BENDING
 67 - DYNAMIC LANDING, FOREBODY DOWN BENDING
 68 - DYNAMIC LANDING, FOREBODY DOWN BENDING
 69 - DYNAMIC LANDING, FOREBODY DOWN BENDING
 70 - DYNAMIC LANDING, FOREBODY DOWN BENDING
 71 - DYNAMIC LANDING, FOREBODY DOWN BENDING
 72 - DYNAMIC LANDING, FOREBODY DOWN BENDING
 73 - DYNAMIC LANDING, FOREBODY DOWN BENDING
 74 - DYNAMIC LANDING, FOREBODY DOWN BENDING
 75 - DYNAMIC LANDING, FOREBODY DOWN BENDING
 76 - DYNAMIC LANDING, FOREBODY DOWN BENDING
 77 - DYNAMIC LANDING, FOREBODY DOWN BENDING
 78 - DYNAMIC LANDING, FOREBODY DOWN BENDING
 79 - DYNAMIC LANDING, FOREBODY DOWN BENDING
 80 - DYNAMIC LANDING, FOREBODY DOWN BENDING
 81 - DYNAMIC LANDING, FOREBODY DOWN BENDING
 82 - DYNAMIC LANDING, FOREBODY DOWN BENDING
 83 - DYNAMIC LANDING, FOREBODY DOWN BENDING
 84 - DYNAMIC LANDING, FOREBODY DOWN BENDING
 85 - DYNAMIC LANDING, FOREBODY DOWN BENDING
 86 - DYNAMIC LANDING, FOREBODY DOWN BENDING
 87 - DYNAMIC LANDING, FOREBODY DOWN BENDING
 88 - DYNAMIC LANDING, FOREBODY DOWN BENDING
 89 - DYNAMIC LANDING, FOREBODY DOWN BENDING
 90 - DYNAMIC LANDING, FOREBODY DOWN BENDING
 91 - DYNAMIC LANDING, FOREBODY DOWN BENDING
 92 - DYNAMIC LANDING, FOREBODY DOWN BENDING
 93 - DYNAMIC LANDING, FOREBODY DOWN BENDING
 94 - DYNAMIC LANDING, FOREBODY DOWN BENDING
 95 - DYNAMIC LANDING, FOREBODY DOWN BENDING
 96 - DYNAMIC LANDING, FOREBODY DOWN BENDING
 97 - DYNAMIC LANDING, FOREBODY DOWN BENDING
 98 - DYNAMIC LANDING, FOREBODY DOWN BENDING
 99 - DYNAMIC LANDING, FOREBODY DOWN BENDING
 100 - DYNAMIC LANDING, FOREBODY DOWN BENDING
3. * DENOTES POINT DESIGN REGIONS

PRECEDING PAGE BLANK NOT FILM!

WOLDOUR FR-1441

FUSELAGE STATION



NOTES:

1. AVERAGE SPAR CAP LOADS
 X X X X (X) N_y - MAXIMUM SPANWISE TENSION AND COMPRESSION LOAD, LB/IN, AND CORRESPONDING DESIGN CONDITIONS.
 X X X X (X) XX

POSITIVE LOADS - TENSION
 NEGATIVE LOADS - COMPRESSION

2. DESIGN CONDITIONS:

- (4) 2.5 G SYMMETRIC FLIGHT, STEADY MANEUVER AT M0.4 (V₁)
- (5) 2.5 G SYMMETRIC FLIGHT, TRANSIENT MANEUVER AT M0.4 (V₁)
- (7) 2.5 G SYMMETRIC FLIGHT, STEADY MANEUVER AT M1.25 (V₁)
- (14) -1.0 G SYMMETRIC FLIGHT, STEADY MANEUVER AT M1.25 (V₁)
- (25) DYNAMIC LANDING, AFT BODY DOWN BENDING

3. * DENOTES POINT DESIGN REGIONS

PRECEDING PAGE BLANK NOT FILMT.

OUTDOOR FRAME /

Figure 9-22. Wing Compressive

FUSELAGE STATION

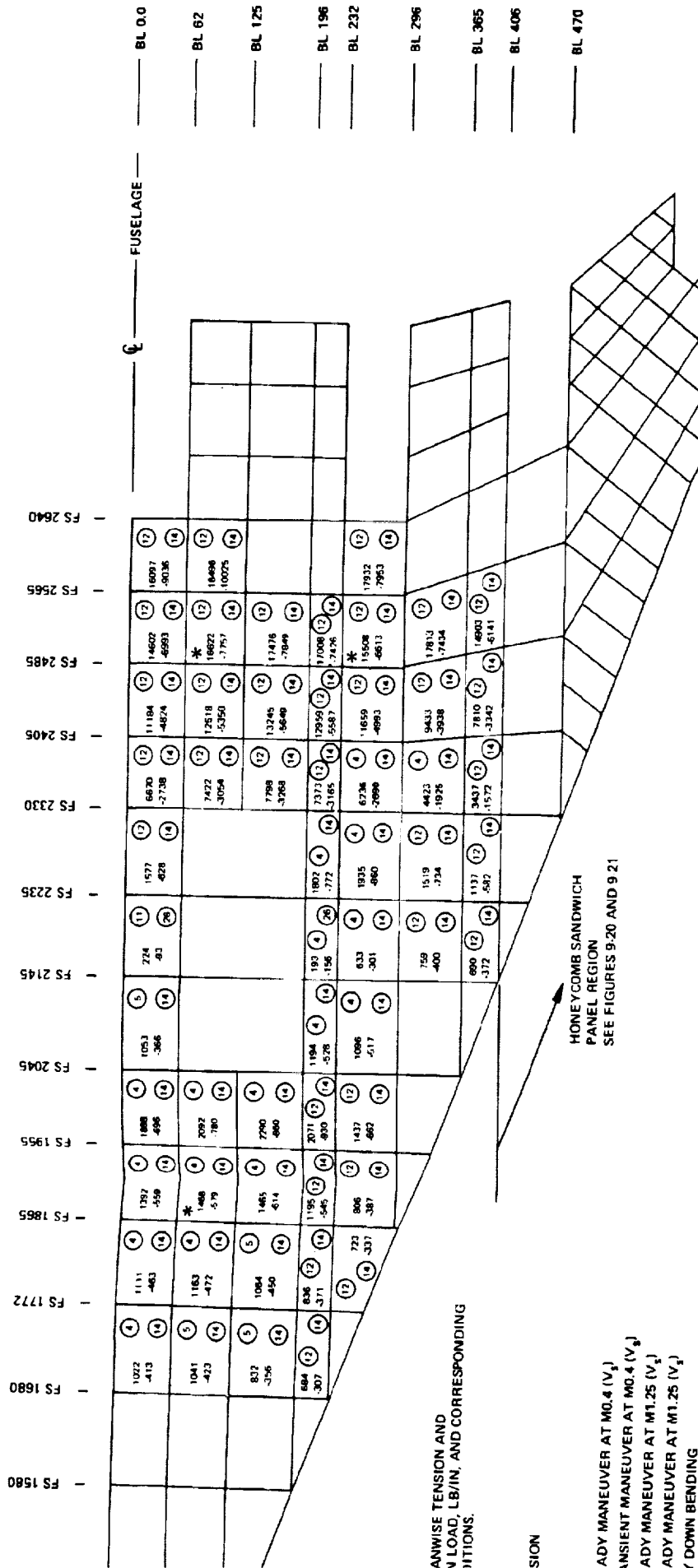


Figure 9-22. Wing Lower Surface Maximum Spanwise Tension and Compression Loads, Task IIB Final Design Model

Task I model the maximum negative displacement (approximately 25.0 inches). An intermediate value of 13.0 inches is noted for the Task IIB Hybrid Model. This variation in tail deflection (magnitude and direction) is directly related to the load rebalancing required to maintain the rearward shift in center of gravity incorporated on the Task II models (i.e., wing pitch-up moment for the Task II models requires a positive tail force).

Running Loads

The results of the NASTRAN static solution (internal forces/stresses) were used as the basis for Task I, Task IIA, and Task IIB stress analysis. These forces/stresses were converted into running loads (N_x , N_y , and N_{xy}) for combination with the local loading and/or manufacturing effect accounted for in the detail stress analysis. Only running loads are presented, no stresses or internal forces (pound) are displayed to alleviate any possible misinterpretation of these results as the total internal stress/load state.

The running loads were calculated by performing a series of simple matrix operations on specific stress and thickness matrices, e.g., chordwise wing surface load (N_x) is equal to the product of the average stress (f_x) of adjacent rod elements and the extensional thickness (t_x).

Running loads were calculated for all Task I and Task II models. Comparisons of load intensities at the point design regions are shown for all these models. In addition, a comprehensive listing of the running loads for the final Task IIB structural model are displayed on wing and fuselage planforms.

A planform containing the wing upper surface maximum chordwise (N_x) tension loads and corresponding shear flows is shown in Figure 9-17. The maximum compressive loads are shown in Figure 9-18. The maximum tension and compression loads for the upper spar caps are shown on Figure 9-19. The corresponding wing lower surface running loads are shown in Figures 9-20, 9-21, and 9-22. These figures indicate the wing critical design conditions and the corresponding surface load intensities for these conditions. Furthermore, the identification of common design regions are noted by shading and the six wing point-design regions are indicated by asterisks.

A comparison of the wing upper surface load intensities (lb/in.) are shown in Table 9-9 for all structural models. These loads are based on the results of the

PRECEDING PAGE BLANK NOT FILLED

TABLE 9-9. COMPARISON OF WING SURFACE LOAD INTENSITIES - ALL MODELS, MACH 0.90 LOAD CONDITION

PANEL IDENTIFICATION		*LOAD INTENSITY (ULTIMATE), LBS/IN.						
		DIRECTION	TASK I			IIA	TASK IIB	
REGION	NUMBER		CHORDWISE	SPANWISE	MONOCOQUE		HYBRID (STRENGTH)	HYBRID (FINAL)
WING FORWARD	40322	Nx	10	148	199	819	122	219
		Ny	1145	1155	595	1120	1109	1049
		Nxy	201	275	211	143	112	75
WING AFT BOX	40236	Nx	188	122	925	377	179	15
		Ny	10846	12181	8102	11474	12779	14311
		Nxy	418	1181	858	436	271	272
	40536	Nx	85	132	1483	471	458	315
		Ny	10680	12318	8763	11207	12680	14410
		Nxy	1118	2288	2521	1409	1068	1159
	41036	Nx	274	36	1094	567	1052	1562
		Ny	6570	6876	4544	7040	3522	4725
		Nxy	1369	2027	1949	1581	1583	1773
WING TIP	41316	Nx	701	298	932	592	1226	1478
		Ny	11655	12546	8268	12145	9504	10106
		Nxy	3492	3240	2528	3773	3686	3730
	41348	Nx	719	574	605	1068	877	856
		Ny	6293	5886	4731	6402	5148	6598
		Nxy	1535	1797	2132	1990	2290	2608

*LOAD CONDITIONS:

TASK I CONDITION 12: MACH 0.90, $n_z = 2.5$, $W = 700,000$ LB, $V_e = 325$ KEAS

TASK IIA CONDITION 9: MACH 0.90, $n_z = 2.5$, $W = 700,000$ LB, $V_e = 325$ KEAS

TASK IIB CONDITION 8: MACH 0.90, $n_z = 2.5$, $W = 700,000$ LB, $V_e = 325$ KEAS

TABLE 9-10. EFFECT OF JIG-SHAPE ON WING UPPER SURFACE LOAD INTENSITIES, TASK IIB HYBRID MODEL

PANEL IDENTIFICATION		* LOAD INTENSITY (ULTIMATE), LBS/IN.			PERCENTAGE DIFFERENCE (%)	
		DIRECTION	ASSUMED JIG SHAPE			
			MID-CRUISE	ZERO LOAD		
WING – FORWARD	40322	NX NY NXY	- 151 - 1106 130	- 166 - 1083 124	+10 - 2 - 5	
WING – AFT BOX	40236	NX NY NXY	67 14650 453	- 133 - 15596 499	+98 +7 +10	
		40536	NX NY NXY	- 1073 14303 1495	1182 - 15315 1750	+10 +7 +17
			41036	NX NY NXY	- 1812 - 4220 2106	- 2096 - 4612 2471
	41316			NX NY NXY	- 1638 - 12407 4009	- 1700 - 14280 4262
		41348		NX NY NXY	- 1207 - 6897 2284	1187 - 8192 2560

* LOAD CONDITIONS:

TASK IIB CONDITION 12: MACH 1.25, $n_z = 2.5$, $W = 690,000$ LB, $V_e = 294$ KEAS

ORIGINAL PAGE IS
OF POOR QUALITY

NASTRAN static solution and are defined at the six point-design regions used for the structural analysis.

The direction of the inplane loads corresponds to the basic airplane axes with the exception of the wing tip regions (panels 41316 and 41318). For these panels the y-direction (spanwise) is parallel to the rear beam of the wingtip structure and the x-direction (chordwise) perpendicular to the rear beam. Conventional sign notation is used; positive signs denote tensile forces and conversely, negative signs denote compression.

From a review of Table 9-9, the following general comments concerning the Task I loads are noted:

- (1) In general, the spanwise arrangement which has the greatest spanwise stiffness also has the highest spanwise load intensities (N_y). The chordwise arrangement has slightly smaller values and the monocoque arrangement the lowest values.
- (2) From a comparison of the chordwise load intensities (N_x) of the chordwise and spanwise arrangements, the chordwise arrangement, which has higher chordwise stiffness, also exhibits higher chordwise load intensities. The monocoque arrangement has the highest chordwise load intensities of all the arrangements, which is indicative of the Poisson's effect of the biaxial concept (honeycomb sandwich) used in modeling this arrangement.
- (3) In general, the highest inplane shear (N_{xy}) values are indicated for the spanwise and monocoque arrangements with the chordwise arrangement having the lowest values. This is probably related to the chordwise arrangement being the most flexible arrangement and exhibiting the largest aeroelastic effect, i.e., the wing tip airloads shift inboard with the associated reduction in wing net shear, spanwise bending and torsion.

Again with reference to Table 9-9, comments concerning a comparison between the Task I and Task IIA chordwise arrangements are noted. The configuration and mass distribution changes incorporated in the Task IIA model should be recalled.

- (1) The spanwise load intensities (N_y) were almost identical for the two arrangements, with the Task IIA arrangement exhibiting slightly higher values.

- (2) In general, the Task IIA chordwise load intensities for the wing aft box region were higher than those of the Task I, which is indicative of the aftward shift in center of gravity incorporated in the Task IIA model.
- (3) The inplane shear (N_{xy}) values indicated the same trend as the spanwise loads, i.e., slightly higher values for the Task IIA arrangement.

The differences in load intensities between the Task IIB strength and final (strength/stiffness) designs are related to the following changes:

- (1) The strength model reflects the stiffness resulting from the strength analysis with no added stiffness for flutter suppression, whereas, the final design incorporates the results of additional strength analyses and the stiffness requirements of the flutter optimization study.
- (2) The applied aeroelastic loads reflect the mass distribution (i.e., variation in inertia loads) and stiffness characteristics of each model. In addition, the aeroelastic loads for the final design include the effects of the jig-shape.

A study of the effect of the assumed unloaded shape of the aircraft was conducted using the Task IIB strength sized model. Structural deflections, determined for a one-g condition during mid-cruise flight, were applied negatively to the mid-cruise configuration to define the jig-shape (i.e., shape of aircraft for manufacture and assembly in a jig). Aeroelastic loads were then calculated for the 2.5-g symmetric maneuver condition at Mach 1.25 using both the jig-shape and the mid-cruise shape as the unloaded shape. A summary of the variation of the point design load intensities using the two shapes is shown in Table 9-10 with the percentage differences indicated. Additional commentary concerning this jig-shape study was previously presented in the External Loads Input - Task IIB Subsection.

All loads intensities increased when the jig-shape was used in the aeroelastic loads calculations; the exception being the spanwise (N_y) and shear loads (N_{xy}) at point design region 40322 which were reduced by 2 percent and 5 percent respectively. As expected, the largest load intensity variations occurred on the more flexible regions of the wing (e.g., a 19 percent increase in spanwise load intensity for point design region 41348 - approximately center span of the wing tip. Because of the large variation in load intensity attributed to the jig-shape effect,

the results of this study were incorporated into the structural sizing of the element properties for the Final Design Task IIB model. In addition, the final aeroelastic loads included the jig-shape effect.

For the sake of completeness, the load intensities for a 2.5-g symmetric flight condition at Mach 1.25 are presented in Tables 9-11 and 9-12 for the upper and lower wing surfaces respectively. These loads are ultimate values and represent a more critical flight condition (stress analysis) than the load intensities for the Mach 0.90 condition displayed in Table 9-9. The loads for the Task IIA structural model are not included in Tables 9-11 and 9-12, since only the critical flutter condition (Mach 0.90) was investigated for that study.

The fuselage ultimate running loads for the Task IIB structural model are shown on Figures 9-23 and 9-24. These figures contain the maximum tension and compression loads and their corresponding shear flows. The thermal components are indicated for the applicable design conditions. A running load comparison at the fuselage point design regions is contained in Table 9-13. This table compared only the resultant loads of the two Task IIB structural model runs since the 2-D structural models of Task I and Task IIA did not include detail fuselage modeling.

TABLE 9-11. COMPARISON OF WING UPPER SURFACE LOAD INTENSITIES -
TASK I AND TASK IIB MODELS, MACH 1.25 LOAD CONDITION

PANEL IDENTIFICATION		*LOAD INTENSITY (ULTIMATE), LBS/IN.					
		DIRECTION	TASK I			TASK IIB	
REGION	NUMBER		CHORDWISE	SPANWISE	MONOCOQUE	HYBRID (STRENGTH)	HYBRID (FINAL)
WING- FORWARD	40322	Nx	455	11	51	151	242
		Ny	1063	1185	529	1106	1032
		Nxy	120	290	191	130	102
WING AFT BOX	40236	Nx	658	306	1193	67	183
		Ny	16338	16986	11638	14650	16456
		Nxy	1316	2541	2099	453	491
	40536	Nx	1305	518	3171	1073	831
		Ny	14325	16409	11424	14303	16372
		Nxy	2354	4173	4647	1495	1615
WING TIP	41036	Nx	1435	450	2219	1812	2464
		Ny	9156	9499	6423	4220	5645
		Nxy	2237	3227	3209	2106	1915
	41316	Nx	571	162	1587	1638	1931
		Ny	16982	17948	12183	12407	13240
		Nxy	4807	4292	3310	4009	4072
	41348	Nx	1433	1028	1190	1207	1200
		Ny	10800	9412	7263	6897	9006
		Nxy	2483	2750	3285	2284	2666

*LOAD CONDITIONS:

TASK I CONDITION 31: MACH 1.25, nz = 2.5, W = 690,000 LB, Ve = 265 KEAS.
TASK IIB CONDITION 12: MACH 1.25, nz = 2.5, W = 690,000 LB, Ve = 294 KEAS

TABLE 9-12. COMPARISON OF WING LOWER SURFACE LOAD INTENSITIES -
TASK I AND TASK IIB MODELS, MACH 1.25 LOAD CONDITION

PANEL IDENTIFICATION		*LOAD INTENSITY (ULTIMATE), LBS/IN.					
		DIRECTION	TASK I STRUCTURAL ARRANGEMENTS			TASK IIB	
REGION	NUMBER		CHORDWISE	SPANWISE	MONOCOQUE	HYBRID (STRENGTH)	HYBRID (FINAL)
WING- FORWARD	140322	Nx	455	11	51	597	434
		Ny	1063	1185	529	1400	1425
		Nxy	120	290	191	215	166
WING- AFT BOX	140236	Nx	658	306	1193	246	62
		Ny	16338	16986	11638	15196	16622
		Nxy	1316	2541	2099	367	781
	140536	Nx	1305	518	3171	1099	699
		Ny	14325	16409	11424	14014	15508
		Nxy	2354	4173	4647	1599	1646
WING- TIP	141036	Nx	1435	450	2219	1297	1898
		Ny	9156	9499	6423	3588	4697
		Nxy	2237	3227	3209	1909	1812
	141316	Nx	571	162	1587	1405	1656
		Ny	16982	17948	12183	11188	11333
		Nxy	4807	4292	3310	2990	2739
	141348	Nx	1433	1028	1190	1379	1431
		Ny	10800	9412	7263	6657	8090
		Nxy	2483	2750	3285	2281	2556

*LOAD CONDITIONS:

TASK I CONDITION 31: MACH 1.25, nz = 2.5, W = 690,000 LB, Ve = 265 KEAS.
TASK IIB CONDITION 12: MACH 1.25, nz = 2.5, W = 690,000 LB, Ve = 294 KEAS.

ORIGINAL FRAME
OF POOR QUALITY

Figure 9-23. Fuselage Panels Maximum Tension Loads, Mask IIB Final Design Model

NOTES:

(1) PANEL LOAD LEGEND

XXX(XXX)
XXX(XXX)
XXX(XXX)
NXX, PANEL AXIAL LOAD, LB/IN.
NXX, PANEL SHEAR FLOW, LB/IN.



(2) DESIGN CONDITIONS

- | | |
|----|---|
| 20 | 2.5G SYMM. FLIGHT, TRANS. MANEUVER @ START OF CRUISE M2.7 |
| 22 | 2.5G SYMM. FLIGHT, STEADY MANEUVER @ MID-CRUISE M2.7 |
| 24 | STATIC GUST (NEGATIVE), M0.90 (Vc) CLIMB |
| 25 | DYNAMIC LANDING, FOREBODY DOWN BENDING & WING ROOT SHEAR |
| 26 | DYNAMIC LANDING, AFTBODY DOWN BENDING |
| 27 | DYNAMIC LANDING, FOREBODY DOWN BENDING |
| 28 | DYNAMIC LANDING, FOREBODY DOWN BENDING |

FOLDOUT FRAME 9-30



TABLE 9-13. COMPARISON OF FUSELAGE PANEL LOAD INTENSITIES - TASK IIB
STRENGTH AND STRENGTH/STIFFNESS MODELS, MACH 1.25 LOAD CONDITION

LOCATION	(1) FUSELAGE PANEL LOAD INTENSITIES (ULT.), LB/IN.								
	DIRECTION	STRENGTH DESIGN				STRENGTH/STIFFNESS			
		FS 900	FS 1910	FS 2525	FS 2900	FS 900	FS 1910	FS 2900	FS 2900
UPPER PANEL	N _x	473	3867	-1002	-635	497	-3078	772	909
	N _{xy}	33	158	166	67	29	103	178	81
SIDE PANEL	N _x	-121	270	61	82	-156	-4	-107	-257
	N _{xy}	158	594	1127	257	169	452	1218	394
LOWER PANEL	N _x	LDG GEAR WELL	WING	WING	1070 8	LDG GEAR WELL	WING	WING	-728 75
	N _{xy}								

(1) LOAD CONDITION—CONDITION 12 : MACH 1.25, N_z = 2.5, W = 690,000 LB., V₀ = 294 KEAS

PRECEDING PAGE BLANK NOT FILMED

1

2

3

REFERENCES

1. Lockheed-California Company. Supersonic Transport Development Program, Phase III Proposal, Volume II-C Airframe Design, FA-SS-66-7, September 1966
2. The Boeing Company. Mach 2.7 Fixed Wing SST Model 969-336C (SCAT-15F), D6A11666-1, 1969

PRECEDING PAGE BLANK NOT FILMED

1

2

3

SECTION 10

VIBRATION AND FLUTTER

BY

A.F. MESSINA, R.S. PETERSON, E.A. GOFORTH,
N.A. RADOVICICH, R. GLORIA



CONTENTS

<u>Section</u>	<u>Page</u>
INTRODUCTION	10-1
ANALYTICAL METHODS	10-3
Structural Model	10-3
Vibration Analysis	10-10
Aerodynamic Formulation	10-13
Flutter Analysis	10-20
Flutter Optimization	10-23
ANALYTICAL DESIGN STUDIES - TASK I	10-28
Chordwise Stiffened Design	10-29
Spanwise Stiffened and Monocoque Design	10-50
Flutter Optimization	10-50
ENGINEERING DESIGN STUDIES - TASK II	10-57
Configuration Change Investigation - Task IIA	10-57
Engineering Design - Task IIB	10-64
Final Design Verification	10-78
SENSITIVITY STUDIES	10-99
Stability Mode Flutter Investigation	10-99
Engine Placement Investigation	10-103
Engine Support Stiffness Investigation	10-105
Mach 0.60 and Mach 1.85 Flutter Investigation	10-107
REFERENCES	10-117

1

2

3

LIST OF FIGURES

<u>Figure</u>		<u>Page</u>
10-1	Design Flutter Boundary	10-2
10-2	Symmetric Degrees of Freedom for Vibration Analysis	10-10
10-3	Theoretical Aerodynamic Distribution	10-14
10-4	Subsonic Aerodynamic Grid	10-15
10-5	Supersonic Aerodynamic Grid	10-17
10-6	Normalized $C_{L\alpha}$ Versus Reduced Frequency	10-19
10-7	The Effects of Number of Modes on the Flutter Solution	10-21
10-8	Flutter Speed Variation With Number of Modes	10-24
10-9	Types of Design Variables	10-27
10-10	Symmetric Vibration Mode 1	10-32
10-11	Symmetric Vibration Mode 2	10-32
10-12	Symmetric Vibration Mode 3	10-33
10-13	Symmetric Vibration Mode 4	10-33
10-14	Symmetric Vibration Mode 5	10-34
10-15	Symmetric Vibration Mode 6	10-34
10-16	Symmetric Vibration Mode 7	10-35
10-17	Symmetric Vibration Mode 8	10-35
10-18	Symmetric Flutter Analysis - Mach 0.6 - OWE	10-37
10-19	Symmetric Flutter Analysis - Mach 0.9 - FFFP	10-37
10-20	Flutter Speeds for Symmetric Bending and Torsion Mode	10-38
10-21	Flutter Speeds for Symmetric Hump Mode	10-38
10-22	Flutter Speeds for Symmetric Stability Mode	10-39
10-23	Participation Coefficients - Mach 0.9 - FFFP - Mode 8	10-39

LIST OF FIGURES (Cont.)

<u>Figure</u>		<u>Page</u>
10-24	Participation Coefficients - Mach 0.9 - OWE - Mode 8	10-40
10-25	Participation Coefficients - Mach 0.9 - OWE - Mode 7	10-40
10-26	Participation Coefficients - Mach 0.9 - OWE - Mode 3	10-43
10-27	Symmetric Flutter Analysis - Mach 0.9 - FFFP - Rigidized Wing	10-43
10-28	Antisymmetric Vibration Mode 1	10-45
10-29	Antisymmetric Vibration Mode 2	10-45
10-30	Antisymmetric Vibration Mode 3	10-46
10-31	Antisymmetric Vibration Mode 4	10-46
10-32	Antisymmetric Vibration Mode 5	10-47
10-33	Antisymmetric Vibration Mode 6	10-47
10-34	Antisymmetric Vibration Mode 7	10-48
10-35	Antisymmetric Vibration Mode 8	10-48
10-36	Antisymmetric Flutter Analysis - Mach 0.9 - OWE	10-49
10-37	Antisymmetric Flutter Analysis - Mach 0.9 - FFFP	10-49
10-38	Symmetric Flutter Analysis - Spanwise Stiffened Arrangement	10-52
10-39	Symmetric Flutter Analysis - Monocoque Arrangement	10-52
10-40	Flutter Speeds for the Structural Arrangements	10-53
10-41	Design Regions for Flutter Optimization	10-53
10-42	Flutter Optimization - Chordwise Stiffened Arrangement	10-56
10-43	Flutter Optimization - Monocoque Arrangement	10-56
10-44	Configuration Comparison - Task I and Task IIA	10-58
10-45	Symmetric Vibration Mode 1	10-58
10-46	Symmetric Vibration Mode 2	10-60

LIST OF FIGURES (Cont.)

<u>Figure</u>		<u>Page</u>
10-47	Symmetric Vibration Mode 3	10-60
10-48	Symmetric Vibration Mode 4	10-61
10-49	Symmetric Vibration Mode 5	10-61
10-50	Symmetric Vibration Mode 6	10-62
10-51	Symmetric Vibration Mode 7	10-62
10-52	Symmetric Vibration Mode 8	10-63
10-53	Symmetric Flutter Analysis - Task IIA	10-63
10-54	Design Cycle - Strength	10-65
10-55	Symmetric Flutter Analysis - Mach 0.9 - OWE	10-68
10-56	Symmetric Flutter Analysis - Mach 0.9 - FFFP	10-68
10-57	Flutter Speeds for Symmetric Bending and Torsion Mode	10-69
10-58	Flutter Optimization Design Regions	10-69
10-59	Surface Panel Thickness - Strength Design	10-71
10-60	Surface Panel Thickness - Stiffness Requirements	10-71
10-61	Design Cycle - Strength/Stiffness	10-82
10-62	Symmetric Vibration Mode 1 - FFFP	10-83
10-63	Symmetric Vibration Mode 2 - FFFP	10-83
10-64	Symmetric Vibration Mode 3 - FFFP	10-84
10-65	Symmetric Vibration Mode 4 - FFFP	10-84
10-66	Symmetric Vibration Mode 5 - FFFP	10-85
10-67	Symmetric Vibration Mode 6 - FFFP	10-85
10-68	Symmetric Vibration Mode 7 - FFFP	10-86
10-69	Symmetric Vibration Mode 8 - FFFP	10-86

LIST OF FIGURES (Cont.)

<u>Figure</u>		<u>Page</u>
10-70	Symmetric Vibration Mode 9 - FFFP	10-87
10-71	Symmetric Vibration Mode 1 - OWE	10-87
10-72	Symmetric Vibration Mode 2 - OWE	10-88
10-73	Symmetric Vibration Mode 3 - OWE	10-88
10-74	Symmetric Vibration Mode 4 - OWE	10-89
10-75	Symmetric Vibration Mode 5 - OWE	10-89
10-76	Symmetric Vibration Mode 6 - OWE	10-90
10-77	Symmetric Vibration Mode 7 - OWE	10-90
10-78	Symmetric Vibration Mode 8 - OWE	10-91
10-79	Symmetric Vibration Mode 9 - OWE	10-91
10-80	Symmetric Flutter Analysis - Mach 0.9 - OWE	10-93
10-81	Symmetric Flutter Analysis - Mach 0.9 - FFFP	10-93
10-82	Symmetric Flutter Analysis - Mach 0.60 - OWE	10-94
10-83	Symmetric Flutter Analysis - Mach 1.85 - OWE	10-94
10-84	Flutter Speeds for Symmetric Bending and Torsion Mode	10-96
10-85	Flutter Speeds for Symmetric Stability Mode	10-96
10-86	Participation Coefficients - Stability Mode	10-100
10-87	Symmetric Vibration Mode 3	10-102
10-88	Symmetric Vibration Mode 4	10-102
10-89	Symmetric Vibration Mode 5	10-103
10-90	Flutter Speed Variation with Engine Placement	10-104
10-91	Engine Support Stiffness Sensitivity	10-106

ORIGINAL PAGE IS
OF POOR QUALITY

LIST OF FIGURES (Cont.)

<u>Figure</u>		<u>Page</u>
10-92	Flutter Speeds for the Final Design Airplane	10-109
10-93	Symmetric Flutter Analysis - Final Design Airplane	10-109
10-94	Design Regions and Variables for Mach 1.85 Flutter Optimization	10-111
10-95	Surface Panel and Web Thickness - Mach 1.85 Flutter Optimization	10-111
10-96	Mach 1.85 Flutter Optimization Results - Bending and Torsion Mode	10-112
10-97	Symmetric Flutter Analysis - Mach 0.60 - OWE	10-112
10-98	Additional Beam Element Stiffness for the Fuselage	10-113
10-99	Design Variables for Mach 0.60 Flutter Optimization	10-113

LIST OF TABLES

<u>Table</u>		<u>Page</u>
10-1	Vibration Degrees of Freedom	10-5
10-2	Analytical Methods for Vibration Analysis	10-11
10-3	Vibration and Flutter Analysis - Task I	10-30
10-4	Lower Frequency Symmetric Vibration Modes - Chordwise Stiffened	10-31
10-5	Lower Frequency Antisymmetric Vibration Modes - Chordwise Stiffened	10-42
10-6	Lower Frequency Symmetric Vibration Modes for the Structural Arrangements	10-51
10-7	Lower Frequency Symmetric Vibration Modes - Task IIA	10-59
10-8	Lower Frequency Symmetric Vibration Modes - Strength Design	10-67
10-9	Summary of Flutter Speeds - Strength Design	10-70
10-10	Flutter Optimization Results	10-73
10-11	Center Panel Thickness - Modified Base Case	10-75
10-12	Lower Frequency Symmetric Vibration Modes - Final Design	10-81
10-13	Lower Frequency Antisymmetric Vibration Modes - Final Design	10-92
10-14	Summary of Flutter Speeds - Task II	10-97
10-15	Structural Mode Frequency Sensitivities	10-101
10-16	Vibration Results - Mach 1.85 Optimization	10-110
10-17	Vibration Analysis Results - 50th Order	10-114

LIST OF SYMBOLS

$[A(k)]$	Aerodynamic Influence Coefficient Matrix
$[A(k,M)]$	Aerodynamic Influence Coefficient Matrix expressed as a function of k and M
A_n	Amplitude of successive cycles
b_o	Reference length
C	Local chord
C_l	Local lift curve slope
$C_{l,\alpha}$	Lift curve slope
\bar{C}	Area/span
$CC_l/\bar{CC}_{l,\alpha}$	Normalized lift distribution
f	Frequency in cycles/second
g	Structural damping factor
g_o	Gravitational constant
$[K]$	Stiffness matrix
$[K_o]$	Base stiffness matrix
k	Reduced frequency, $\omega b_o/V$
M	Mach number
$[M]$	Inertia matrix
N_D	Number of design variables
N_1	Number of $[\Delta K]$ matrices for the design variable 1
p	Non-dimensional time derivative operator, $\left(\frac{b_o}{V}\right)\left(\frac{d}{dt}\right)$
$\{Q\}$	Matrix of aerodynamic forces
$\{q\}$	Column of displacements and rotations of structural nodes
$\{\ddot{q}\}$	Column of translational and rotational accelerations at structural nodes

LIST OF SYMBOLS (Cont.)

$[T]$	Eigenvector matrix used for modalization matrix of modal columns
$[T]^T$	Transpose of the Eigenvector matrix $[T]$
V	True airspeed
$[W_0]$	Base weight matrix
$\{X\}$	Column of modal coordinates
α_μ	La Grange coefficients used in matrix interpolation $\prod_{\substack{n=1 \\ n \neq \mu}}^N \frac{\beta_\ell - \tilde{\beta}_\ell^n}{\tilde{\beta}_\ell^\mu - \tilde{\beta}_\ell^n}$
β_ℓ	ℓ^{th} design variable, $\left(\bar{\beta}_\ell + \hat{\beta}_\ell \right)$, expressed in weight units
$\bar{\beta}_\ell$	Increment in ℓ^{th} design variable due to updating of base structure
$\hat{\beta}_\ell$	Increment in ℓ^{th} design variable necessary to satisfy flutter constraint (in addition to $\bar{\beta}_\ell$)
β_ℓ^*	$\begin{cases} 0 & \text{for Type I design variable} \\ \tilde{\beta}_\ell^1 & \text{for Type II design variable} \end{cases}$
$\tilde{\beta}_\ell^\mu$	Values of β_ℓ for which $[\Delta K]$ matrices are calculated
δ	Real part of the complex variable p
$[\Delta W]^{(\ell)}$	Initial weight matrix due to "step" increase for Type II design variable
$[\Delta \tilde{x}_\mu]^{(\ell)}$	Increment in stiffness matrix, over $[K_0]$, calculated for $\tilde{\beta}_\ell^\mu$
ρ	Air density
ρ_0	Air density at sea level
σ	Air density ratio, $\left(\frac{\rho}{\rho_0} \right)$
ω	Angular frequency in radians/second
$\left[\frac{\partial W}{\partial \beta_\ell} \right]^{(\ell)}$	Increment in weight matrix due to β_ℓ

SECTION 10

VIBRATION AND FLUTTER

INTRODUCTION

The significant results of the vibration and flutter analyses of the arrow-wing supersonic cruise aircraft are presented in this section. These results include the structural dynamic characteristics of the aircraft employing the various structural arrangements and concepts which have been investigated to establish the best approaches for a Mach 2.7 cruise aircraft design.

To obtain realistic structural mass trends and to identify the importance of flutter on the design of supersonic cruise aircraft, compliance with the intent of FAR 25 was established as a design objective. FAR 25.692 defines that the airplane must be designed to be free from flutter and divergence at speeds up to $1.2V_D$. In accordance with Reference 1 this margin is applied to equivalent speeds both at constant altitude and constant Mach number, Figure 10-1. The flutter margin requirement in the below-sea level regime of the equivalent airspeed versus altitude envelope is based on a 44-percent static pressure margin as indicated on the figure.

The vibration analyses were performed with NASTRAN using the Givens Method. The flutter analyses were performed within the Lockheed Computer System named FAMAS using the p-k Method. The p-k Method permits a flutter analysis to be performed which yields a solution of matched Mach number, altitude and velocity.

Starting from the strength-designed structure, the required flutter margin was achieved by use of a method of flutter optimization employing computer graphics. In optimizing for flutter, stiffness and corresponding mass increments were investigated as a means of satisfying the flutter constraint and the minimum mass combination identified.

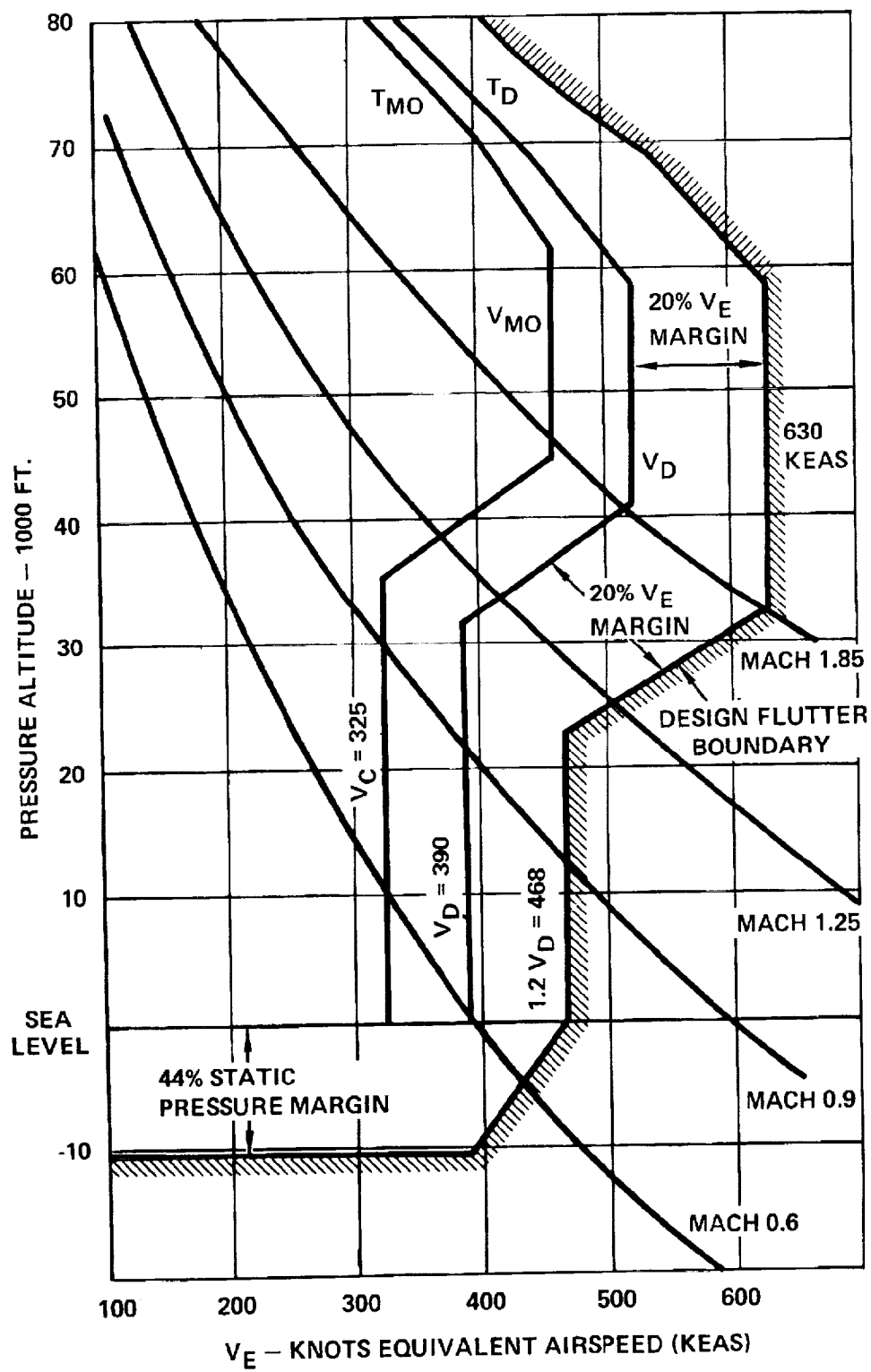


Figure 10-1. Design Flutter Boundary

ANALYTICAL METHODS

The analytical methods which were applied to flutter analysis and in the flutter optimization of the baseline configurations of the arrow-wing supersonic cruise aircraft are described in the following paragraphs. These analytical methods are presented under the heading of

- Structural Model
- Vibration Analysis
- Aerodynamic Formulation
- Flutter Analysis
- Flutter Optimization

Structural Model

A series of finite element structural analysis models was used for the study. These models were constructed in the NASTRAN System and are described in Section 9.

Two-Dimensional Structural Model. - The Task I and Task IIA structural models are two-dimensional (2-D) models which represent a wing that is symmetrical about an X-Y mid-plane. A beam representation of the fuselage is included to provide fuselage interface effects on the wing structure.

Three structural arrangements as characterized by the wind surface panels were modeled for Task I, namely:

- Chordwise-stiffened wing
- Spanwise-stiffened wing
- Monocoque (biaxially stiffened) wing

The model network is identical for all the three structural arrangements; however, the model is unique for each of the three arrangements in terms of the section property data and the elements used to represent the wing.

The Task IIA structural model was the Task I chordwise-stiffened structural arrangement modified to reflect the configuration refinements and center of gravity travel recommended in Section 2.

Three-Dimensional Structural Model. -- For the Task IIB analyses, a more detailed, three-dimensional (3-D) model was used. The wing planform grid for the 3-D model was identical to the 2-D model grid used in Task IIA; however, for the 3-D model both upper and lower wing surfaces are represented including the camber and the twist of the airfoil. The model incorporated a wing representation with the capability to transmit inplane as well as out-of plane loads, and a fuselage shell model composed of skin, stringers, and frames elements. The 3-D model wing surface represented a hybrid structural arrangement. The inboard wing has chordwise-stiffened wing panels; whereas the wingtip, outboard of B.L. 406, is monocoque (biaxially stiffened). Model analyses during Task IIB were performed for two sets of structural sizes -- the first represented strength requirements only and the second incorporated strength requirements plus stiffness requirements.

The control surfaces for the Task IIB structural model satisfied the irreversibility criteria of Reference 1. No requirements for mass balance or for irreversibility were specified for the Task I and the Task IIA structural models.

The engine rail stiffnesses were designed by a rotation consideration of one-degree of engine rotation per-g. A strength designed engine rail would give approximately four degrees of engine rotation per-g which was unsatisfactory. This engine rail rotation requirement was established to minimize the nacelle rotation relative to the wing and minimizing the misalignment between the engine inlet and the engine.

The structural model data used in the vibration analyses consisted of stiffness matrices and associated mass matrices. These matrices are of 188th order symmetrically and 178th order antisymmetrically. The degrees of freedom and the coordinate system associated with these matrices are given in Table 10-1. These degrees of freedom are shown on the airplane planform of Figure 10-2.

TABLE 10-1. VIBRATION DEGREES OF FREEDOM

COMPONENT	DEGREE OF FREEDOM NO.		DEGREE OF FREEDOM		GEOMETRIC LOCATION		SIC NO.	GRID NO.
	SYM	A/S	SYM	A/S	FUSELAGE STATION	BUTT LINE		
FUSELAGE	1	1	Z	Y	400.	0.0	1	3150
	2	2			600.		2	3250
	3	3			800.		3	3350
	4	4			1000.		4	3450
	5	5			1100.		5	3550
	6	6			1210.		6	0112
	7	17B			1382.		7	0114
	8				1580.		8	0116
	9				1680.		9	0118
	10				1772.		10	0120
	11				1865.		11	0122
	12				1955.		12	0124
	13				2045.		13	0126
	14				2145.		14	0128
	15				2235.		15	0130
	16				2330.		16	0132
	17				2405.		17	0134
	18				2485.		18	0136
	19				2565.		19	0138
	20	7		Y	2640.		20	0140
	21	8			2800.		21	5150
	22	9			3000.		22	5250
	23	10			3200.		23	5350
	24	11			3360.		24	5450
	25	12			3470.		25	5550
WING	26	13		Z	1210.	62.	26	212
	27	14			1382.		27	214
	28	15			1580.		28	216
	29	16			1680.		29	218
	30	17			1772.		30	220
	31	18			1865.		31	222
	32	19			1955.		32	224
	33	20			2045.		33	226
	34	21			2145.		34	228
	35	22			2235.		35	230
	36	23			2330.		36	232
	37	24			2405.		37	234
	38	25			2485.		38	236
	39	26			2565.		39	238
	40	27			2640.		40	240
	41	28			2710.		41	242
	42	29			2855.		42	246
	43	30			1382.	125.	43	314
	44	31			1580.		44	316
	45	32			1680.		45	318
	46	33			1772.		46	320
	47	34			1865.		47	322
	48	35			1955.		48	324
	49	36	Z	Z	2045.		49	326

ORIGINAL PAGE IS
OF POOR QUALITY

TABLE 10-1. VIBRATION DEGREES OF FREEDOM (CONT'D)

COMPONENT	DEGREE OF FREEDOM NO.		DEGREE OF FREEDOM		GEOMETRIC LOCATION		SIC NO.	GRID NO.
	SYM	A/S	SYM	A/S	FUSELAGE STATION	BUTT LINE		
WING	50	37	Z		2145.	125.	50	328
	51	38			2235.		51	330
	52	39			2330.		52	332
	53	40			2405.		53	334
	54	41			2485.		54	336
	55	42			2565.		55	338
	56	43			2640.		56	340
	57	44			2710.		57	342
	58	45			2855.		58	346
	59	46			1580.	196.	59	416
	60	47			1680.		60	418
	61	48			1772.		61	420
	62	49			1865.		62	422
	63	50			1955.		63	424
	64	51			2045.		64	426
	65	52			2145.		65	428
	66	53			2235.		66	430
	67	54			2330.		67	432
	68	55			2405.		68	434
	69	56			2485.	196.00	69	436
	70	57			2565.		70	438
	71	58			2640.		71	440
	72	59			2710.		72	442
	73	60			2855.		73	446
	74	61			1865.	299.50	89	722
	75	62			1955.	296.00	90	724
	76	63			2045.		91	726
	77	64			2145.		92	728
	78	65			2235.		93	730
	79	66			2330.		94	732
	80	67			2405.		95	734
	81	68			2485.		96	736
	82	69			2565.		97	738
	83	70			2640.		98	740
	84	71			2713.		99	742
	85	72			2855.		100	746
	86	73			2045.	365.	102	926
	87	74			2145.		103	928
	88	75			2235.		104	930
	89	76			2330.		105	932
	90	77			2410.		106	934
	91	78			2500.		107	936
	92	79			2590.		108	938
	93	80			2678.		109	940
	94	81			2743.		110	942
	95	82			2868.		111	946
	96	83			2145.	402.00	112	1028

TABLE 10-1. VIBRATION DEGREES OF FREEDOM (CONT'D)

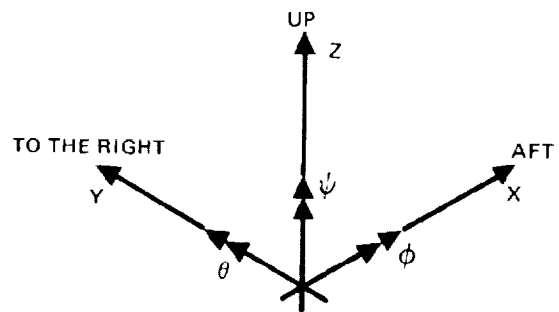
COMPONENT	DEGREE OF FREEDOM NO.		DEGREE OF FREEDOM		GEOMETRIC LOCATION		SIC NO.	GRID NO.
	SYM	A/S	SYM	A/S	FUSELAGE STATION	BUTT LINE		
WING	97	84	Z		2235.	406.00	113	1030
	98	85			2330.		114	1032
	99	86			2415.		115	1034
	100	87			2508.		116	1036
	101	88			2603.		117	1038
	102	89			2700.		118	1040
	103	90			2763.	406.	119	1042
	104	91			2880.	406.	120	1046
	105	92			2330.	470.	122	1232
	106	93			2420.		123	1234
	107	94			2520.		124	1236
	108	95			2625.		125	1238
	109	96			2730.		126	1240
	110	97			2798.		127	1242
	111	98			2900.		128	1246
	112	99			2475.5	523.	130	1304
	113	100			2555.5	552.	131	1310
	114	101			2636.5	581.3	132	1320
	115	102			2589.5	511.7	133	1312
	116	103			2659.2	554.3	134	1322
	117	104			2691.	516.8	135	1324
	118	105			2686.8	600.	136	1326
	119	106			2703.	581.	137	1328
	120	107			2732.8	546.5	138	1330
	121	108			2769.	503.3	139	1332
	122	109			2755.7	639.5	140	1346
	123	110			2770.	622.	141	1348
	124	111			2796.	592.	142	1350
	125	112			2828.5	554.	143	1352
	126	113			2854.	524.	144	1354
	127	114			2818.	676.	145	1522
	128	115			2831.5	660.	146	1524
	129	116			2854.	633.	147	1526
	130	117			2382.	600.	148	1528
	131	118			2905.5	573.	149	1530
	132	119			2949.	521.5	150	1534
	133	120			2998.	573.	151	1540
	134	121			2882.	712.	152	1562
	135	122			2894.	698.	153	1564
	136	123			2914.	675.3	154	1566
	137	124			2937.7	647.	155	1568
	138	125			2958.5	623.	156	1570
	139	126			3046.	628.	157	1614
	140	127			3007.	668.	158	1610
	141	128			2961.	758	159	1622
	142	129			2971.8	745.2	160	1624
	143	130			2987.	727.2	161	1626

ORIGINAL PAGE IS
OF POOR QUALITY

TABLE 10-1. VIBRATION DEGREES OF FREEDOM (CONT'D)

COMPONENT	DEGREE OF FREEDOM NO.		DEGREE OF FREEDOM		GEOMETRIC LOCATION		SIC NO.	GRID NO.
	SYM	A/S	SYM	A/S	FUSELAGE STATION	BUTT LINE		
WING	144	131	Z		3005.5	705.5	162	1628
	145	132			3023.8	684.	163	1630
	146	133			3062.	639.	164	1634
	147	134			2993	777.	165	1662
	148	135			3003.	764.2	166	1664
	149	136			3017.	748.3	167	1666
	150	137			3033.5	729.	168	1668
	151	138			3050.3	709.	169	1670
	152	139			3087.5	665.5	170	1674
	153	140			3025.1	795.	171	1702
	154	141			3035.	783.	172	1704
	155	142			3046.5	769.	173	1706
	156	143			3061.	752.	174	1708
	157	144			3077.	734.	175	1710
	158	145			3113.	691.5	176	1714
	159	146			3054.1	795.	177	1724
	160	147			3082.9	795.	178	1746
	161	148			3111.3	795.	179	1768
	162	149			3141.3	795.	180	1790
	163	150			3211.	795.	181	1798
	164	151			3174.5	756.	182	1794
VERTICAL WING	165	152	Y		2734.	600.	189	1344
	166	153			2807.		190	1360
	167	154			2790.		191	1458
	168	155			2847.		192	1460
	169	156			2913.5		193	1462
	170	157			2981.3		194	1464
	171	158			3049.		195	1466
	172	159			3116.5		196	1468
	173	160			2882.		197	1528
	174	161			2949.		198	1472
	175	162			3002.		199	1474
	176	163			3062.5		200	1476
	177	164			3123.5		201	1478
	178	165			3136.5		202	1480
ENGINE	OUTBOARD	179	166	Y	2660.	264.	203	660
		180	167	Z	2660.	264.	183	660
		181	168	ϕ	2660.	264.	235	660
		182	169	Y	2800.	264.	204	662
		183	170	Z	2800.	264.	184	662
		184	171	Y	2720.	438.	205	1160
		185	172	Z	2720.	438.	185	1160
		186	173	ϕ	2720.	438.	237	1160
		187	174	Y	2855.	438.	206	1162
		188	175	Z	2855.	438.	186	1162
FUSELAGE		176	ϕ		3360.	0.0	211	5450
		177	ϕ		3470	0.0	212	5550

TABLE 10-1. VIBRATION DEGREES OF FREEDOM (CONT'D)



RIGHT HAND RULE FOR THE RIGHT SIDE
OF THE AIRPLANE

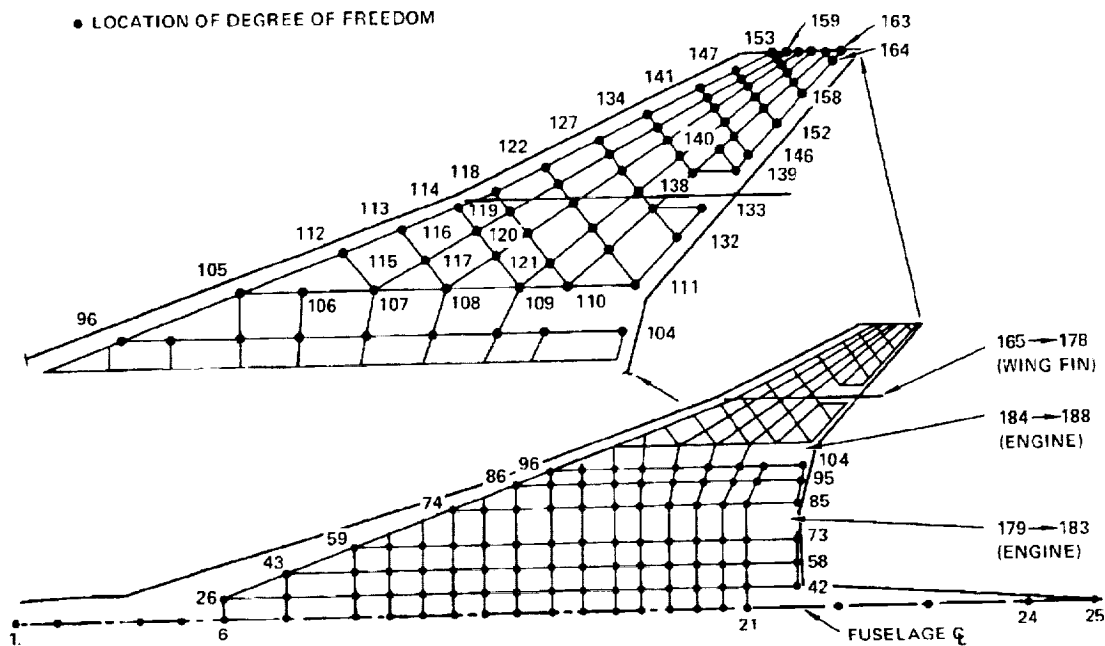


Figure 10-2. Symmetric Degrees of Freedom for Vibration Analysis

Table 10-1 also correlates the degrees of freedom to the structural influence coefficient (SIC) and to the NASTRAN grid. The SIC and NASTRAN grid relate directly to the structural model.

The choice of the number of symmetric degrees of freedom was based on the constraint that a 188th order vibration problem was the maximum size that could be run in the Lockheed FAMAS computer system. It is felt that a 188th order problem retains adequate structural definition and still gives good visibility for model trouble shooting and verification.

Vibration Analysis

Vibration cases were run using several different approaches and results compared to select the analytical method for application to the design concepts study (Table 10-2). The three methods investigated were: Inverse Power (INV) and Givens (GIV) method available in NASTRAN and the FAMAS QR method.

The first eigenvalue routine executed was the Inverse Power (INV). The approach was to take advantage of the sparseness of the stiffness and inertia matrices in the F-set (858th order) and solve for a limited number of modes. Computer time for the INV method was 80.5 seconds of CPU time per mode.

Because of the very high computer times, the problem was reduced to the A-set coordinates (188th order). This matrix reduction required 89 seconds. The INV method was again executed and resulted in 60.5 seconds of CPU time per mode; whereas, the Givens method for the same reduced order problem resulted in 2.3 seconds of CPU time per mode.

The reduction to 188th order eliminated only a few inertial degrees of freedom and resulted in a problem size small enough so that the FAMAS QR method could also be exercised. The QR method resulted in 3.6 seconds of CPU time per mode.

The Givens and QR methods not only result in a marked reduction in computer time but also solve for all 188 roots, a definite advantage over the INV

TABLE 10-2. ANALYTICAL METHODS FOR VIBRATION ANALYSIS

METHOD	MATRIX SIZE	NUMBER ROOTS	CPU TIME (SEC)		FREQUENCY (2) (HZ)	
			TOTAL	PER MODE (1)	MODE 1	MODE 2
INVERSE POWER	858	20	1610	80.5	1.470223	2.049600
INVERSE POWER	188	2	121	60.5	1.471204	2.055224
GIVENS	188	188 (40 VECTORS)	83	2.1	1.471203	2.055210
GIVENS	188	188 (40 VECTORS)	93	2.3	0.9275528	1.007738
QR	188	188 (40 VECTORS)	145	3.6	0.9275518	1.007738
(1) BASED ON NUMBER OF EIGEN VECTORS FOUND (2) FREQUENCIES 1 AND 2 ARE NOT NECESSARILY THE LOWEST FREQUENCIES. ALSO THE LAST TWO CASES (GIVEN AND QR) USED A DIFFERENT MASS MATRIX THAN THE FIRST THREE CASES.						

Method where it is possible to miss a mode. No significant differences in accuracy were noted between the three methods as shown in Table 10-2.

Based on the results presented the Givens Method was superior to the other methods and was selected as the vibration analysis method for the study.

The stiffness matrices of each structural arrangement (Section 9) were combined with the appropriate inertia matrices (reference Section 15 - Mass Analysis) to compute the symmetric and antisymmetric eigenvectors and eigenvalues of the free-free airplane. The inertia matrices were formed for two airplane weight conditions namely:

- Operating weight empty (OWE)
- Full fuel and full payload (FFFP).

These weight conditions represent the extremes of minimum and maximum weight. No intermediate weight conditions were examined.

The structural and inertial representations lead to the following matrix vibration equation:

$$[M] \{\ddot{q}\} + [K] \{q\} = \{0\} \quad (10-1)$$

where: $[M]$ is the inertia matrix

$[K]$ is the stiffness matrix

$\{q\}$ column of displacements and rotations at structural nodes

$\{\ddot{q}\}$ column of translational and rotational accelerations at structural nodes

In general 50 vibration modes were extracted from each vibration solution for use in the flutter analysis and flutter optimization. These vibration modes are expressed in equation (10-2)

$$\{q\} = [T] \{X\} \quad (10-2)$$

where $[T]$ = eigenvector matrix used for modalization matrix of modal columns

$\{X\}$ = column of modal coordinates.

Aerodynamic Formulation

The steady and unsteady aerodynamic influence coefficients (AIC) were computed for Mach 0.60, 0.90, and 1.25 for the Task I configuration and Mach 0.60, 0.90 and 1.85 for the Task II configuration. The Mach 0.60 and 0.90 AIC were computed by the Doublet-Lattice method of Reference 2. The Mach 1.25 and 1.85 AIC were computed by the Mach Box method of Reference 5. The AIC were computed for the wing, the wing fin and the empennage surfaces. These AIC were adjusted, when required, to reflect measured steady state lift coefficients and aerodynamic centers. The Mach 0.60 and 0.90 AIC account for the interference between the wing and the wing fin. The Mach 1.25 and 1.85 AIC do not account for the interference between the wing and the wing fin. Fuselage aerodynamics were not included in either Mach number ranges investigated.

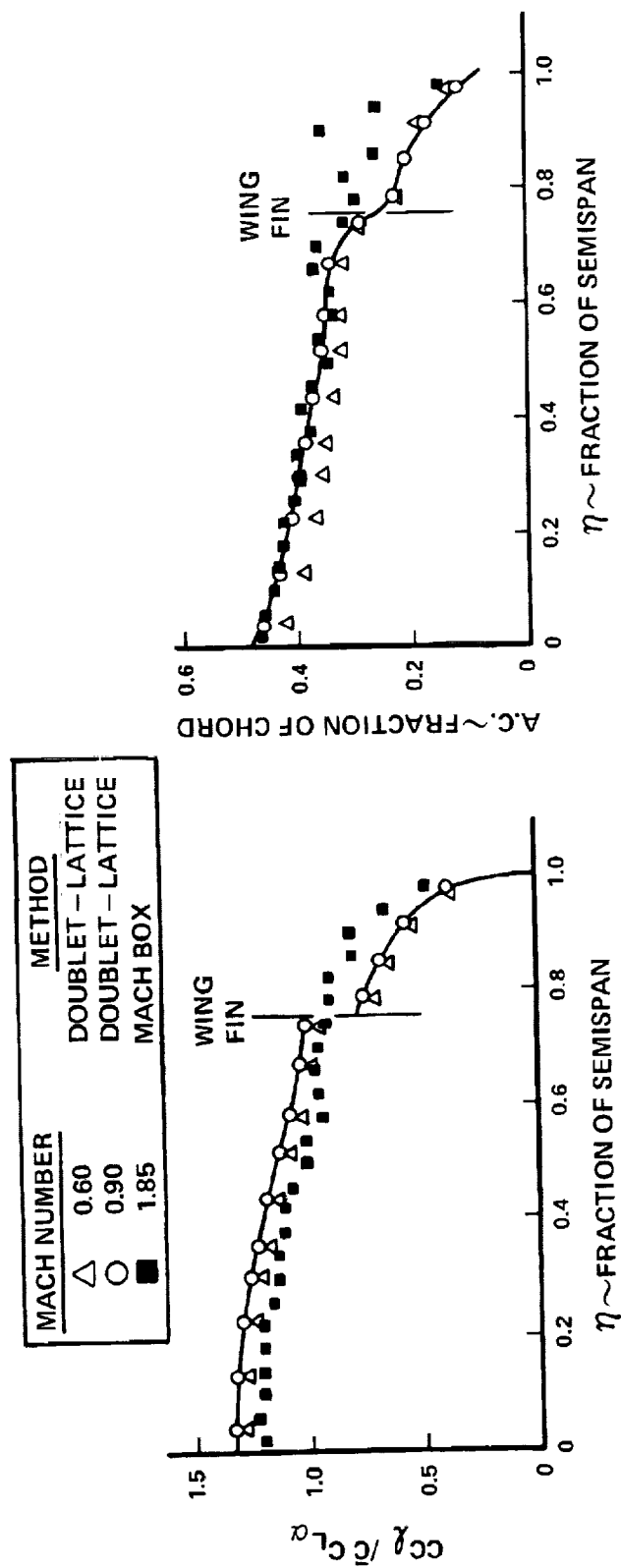
The significance of the aerodynamic interference between the wing and wing fin is shown by Figure 10-3, which presents $CC_l / C_{L\alpha}$ and aerodynamic center versus fraction of the semispan. The data visually relates the wing fin interference effect on the distribution for the applicable Mach numbers. The interference effect results in an increase in the $CC_l / C_{L\alpha}$ distribution inboard of the wing fin and a decrease in the $CC_l / C_{L\alpha}$ distribution outboard of the wing fin.

A typical aerodynamic grid used for the Doublet-Lattice aerodynamics is presented in Figure 10-4. The downwashes are applied at the $3/4$ chord of the boxes and the lift forces are defined at the $1/4$ chord of the boxes.

The Mach 1.85 aerodynamic grid is presented in Figure 10-5. The downwashes are applied at the $1/2$ chord of the boxes and the lift forces are defined at the $1/2$ chord of the boxes.

The normalized $C_{L\alpha}$ versus reduced frequency is presented in Figure 10-6. The normalized $C_{L\alpha}$ is $C_{L\alpha}$ at a finite reduced frequency divided by $C_{L\alpha}$ for a reduced frequency of zero. The figure presents the real and imaginary parts

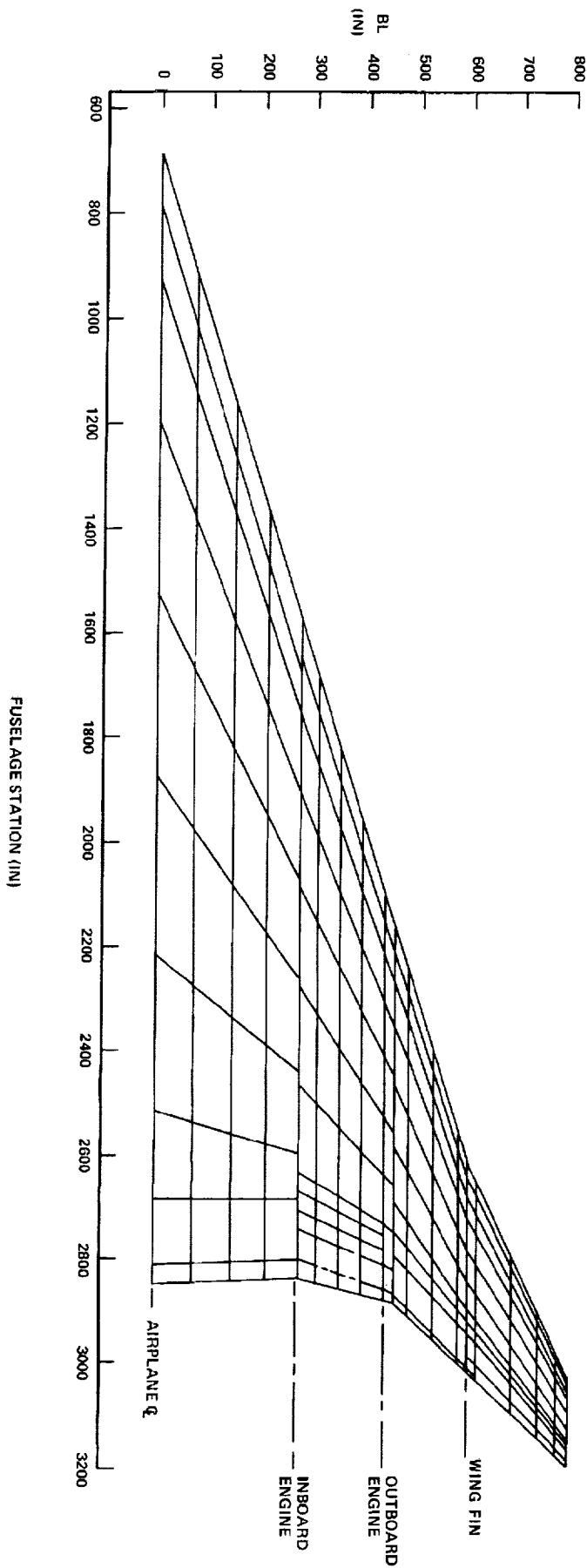
REDUCED FREQUENCY = 0, α = UNIT DOWNWASH



NOTE: THE WING/WING FIN AERODYNAMIC INTERFERENCE EFFECT:
 • INCLUDED IN THE MACH 0.60 AND 0.90 AERODYNAMICS
 • NOT INCLUDED IN THE MACH 1.85 AERODYNAMICS

Figure 10-3. Theoretical Aerodynamic Distribution

DOUBLET LATTICE
220 BOX SCHEME (INCLUDING FIN)



FOLDOUT FRAME

Figure 10-4. Supersonic Aerodynamic FOLDOUT FRAME
10-15

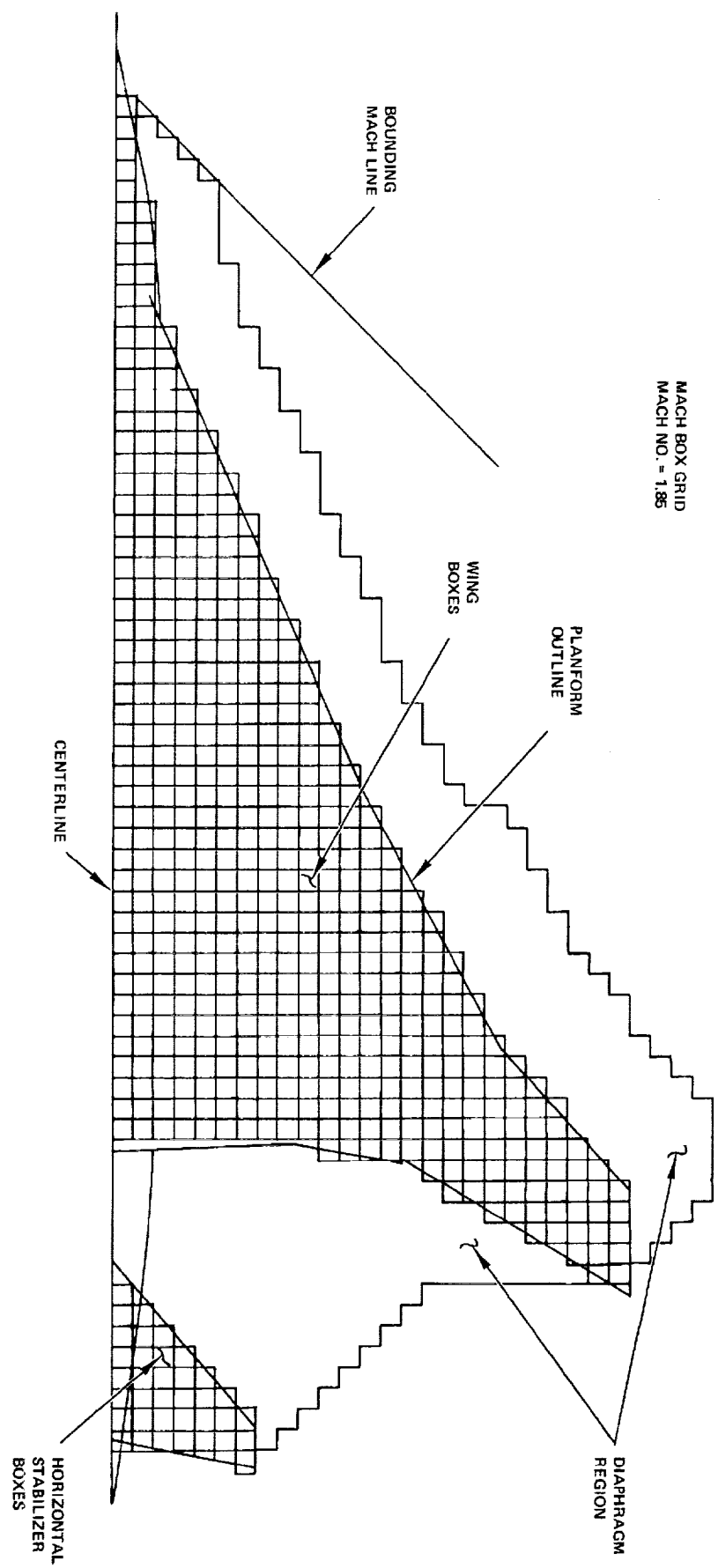
1

2

3

PRECEDING PAGE BLANK NOT FILMED

FOOTNOTES



MACH BOX GRID
MACH NO. = 1.85

Figure 10-5. Supersonic Aerodynamic Grid

1

2

3

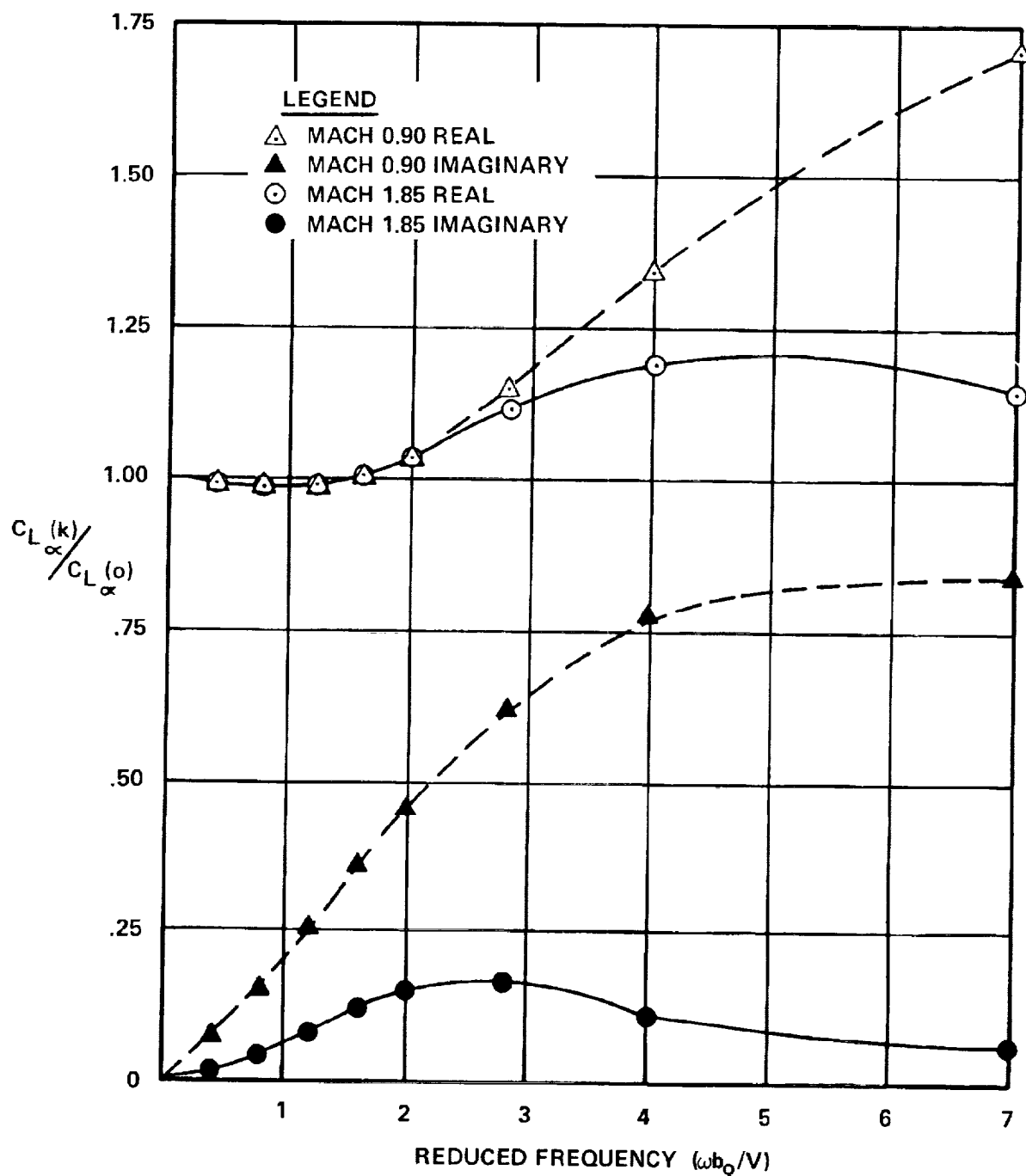


Figure 10-6. Normalized $C_{L\alpha}$ Versus Reduced Frequency

PRECEDING PAGE BLANK NOT FILMED

of the normalized $C_{l\alpha}$ for Mach 0.90 and 1.85 and thus shows the variation in amplitude/phase as a function of Mach number and reduced frequency. As can be seen the Mach 1.85 aerodynamics is composed primarily of the real part. This differs from the Mach 0.90 aerodynamics which exhibits a mix of the real and the imaginary parts.

Flutter Analysis

The following development of the flutter equation is presented primarily because it reflects a departure from the more familiar k method. The principal features provided by this formulation are that the frequency and damping solutions are obtained directly for matched altitude and Mach number and the damping solutions correspond to logarithmic decay.

The aerodynamic forces $\{Q\}$ resulting from oscillatory motion about a position of equilibrium can be expressed as follows

$$\{Q\} = 1/2 \rho V^2 [A(k,M)] \{q\} \quad (10-3)$$

where ρ = air density

V = true airspeed

$[A(k,M)]$ = aerodynamic influence coefficient matrix which is a function of k and M

$k = \omega \frac{b_o}{V}$, reduced frequency

M = Mach number

ω = frequency

b_o = reference length

$\{q\}$ = column of displacements and rotations

Inserting the aerodynamic forcing function (10-3) on the right hand side of the equation of motion (10-1) and introducing a structural damping factor, g , yields equation (10-4)

$$[M] \{\ddot{q}\} + (1 + ig) [K] \{q\} - 1/2 \rho V^2 [A(k, M)] \{q\} = \{0\} \quad (10-4)$$

All analyses assume a structural damping (g) of 2-percent for each mode.

Let a non-dimensional operator be defined as $p = \frac{b_o}{V} \frac{d}{dt}$ (10-5)

where $\frac{d}{dt}$ = time derivative.

Substituting equation (10-2) and (10-5) into equation (10-4) and rearranging the terms gives the basic flutter equation

$$[T]^T \left[[M] \frac{V^2}{b_o^2} p^2 + (1 + ig) [K] - \sigma V^2 1/2 \rho_o [A(k, M)] \right] [T] \{X\} = [T]^T [D(p, k)] [T] \{X\} = \{0\} \quad (10-6)$$

where ρ_o = air density at sea level

σ = air density ratio, ρ/ρ_o

$[T]^T$ = transpose of $[T]$

The method of solution to equation (10-6) is referred to as the p-k Method. The p-k Method is described in Reference 3. The solution to equation (10-6) defines rate of decay and frequency for preselected values of speed and gives matched altitude, Mach number, and reduced frequency for each mode at each preselected velocity.

All matrices in equation (10-6) are real and uniquely defined, except $[A(k, M)]$, which is complex and must be given for a sufficient number of k values. Equation (10-6) is solved at several values of V and σ , or combinations thereof, for complex roots p associated with the modes of interest. Modes of interest are determined from vibration analysis or from previous flutter analysis.

The process of determinant iteration is completed mode by mode for one speed and then at successive preselected speeds. For one mode at one particular speed, the process is started by initial trials for p:

$$p_1 = \delta_1 + ik_1 \quad p_2 = \delta_2 + ik_2 \quad (10-7)$$

$[A(k_1)]$ and $[A(k_2)]$ are computed by interpolation. Using equation (10-6) the values

$$D_1 = |[D(p_1, k_1)]| \quad D_2 = |[D(p_2, k_2)]| \quad (10-8)$$

are determined. The method gives a first iterated value for p:

$$p_3 = (p_2 D_1 - p_1 D_2) / (D_1 - D_2) \quad (10-9)$$

The process is repeated according to the recurrence formula

$$p_{i+2} = (p_{i+1} D_i - p_i D_{i+1}) / (D_i - D_{i+1}) \quad (10-10)$$

until a specified degree of convergence is attained. From the converged root $p_c = \delta_c + ik_c$, the frequency and damping are computed

$$f = \frac{V k_c}{2\pi c} ; 2\gamma = \frac{1}{\pi} \ln \frac{a_n + 1}{a_n} = 2 \frac{\delta_c}{k_c} \quad (10-11)$$

The above procedure is known as the one-dimensional Regula Falsi Method which is valid where equation 10-6 is analytic in p.

Two fundamental questions arose when applying equation (10-6) to the flutter analysis, namely:

- How many vibration modes are required to arrive at the converged flutter solution?
- How many AIC matrices, as a function of reduced frequency (k), are required to arrive at a converged flutter solution?

Both of these questions were investigated during the course of the flutter studies.

Velocity versus damping for the 10, 15, and 20 vibration mode flutter analyses are shown in Figure 10-7. It can be seen that the character of the flutter modes can be significantly changed by going from 20 to 10 vibration modes but the minimum flutter speed did not change appreciably. Figure 10-8 shows the flutter velocity of the bending and torsion flutter mode as a function of the number of vibration modes used in the flutter analysis. This figure shows that the flutter velocity changes only 1 percent when the number of vibration modes varies from 20 to 50. As a consequence of this study, 20 or more vibration modes were used for all flutter analyses.

The number of AIC matrices required to arrive at a converged flutter solution was investigated by running a flutter analysis with AIC matrices corresponding to 17 k values and then repeating this analysis with every other AIC matrix eliminated. Within the reading accuracy of the flutter plots the results from these analyses were identical. As a consequence of this study AIC matrices corresponding to 9 or more k values were used for the flutter analyses.

Flutter Optimization

An interactive computer graphics program was utilized in the optimization of the arrow-wing supersonic transport configuration. An abbreviated description of the equations, method of solution, and optimization procedure are presented in the following paragraphs.

The flutter equation is written as follows:

$$[T]^T [D(k, \hat{\beta}_\ell)] [T] \{q\} = 0 \quad (10-12)$$

with

$$[D(k, \hat{\beta}_\ell)] = \frac{V^2}{g_o b_o^2} \left[[W_o] + \sum_{\ell=1}^{N_D} \left([\Delta W]^{(\ell)} + \left[\frac{\partial W}{\partial \beta_\ell} \right]^{(\ell)} (\bar{\beta}_\ell + \hat{\beta}_\ell - \beta_\ell^*) \right) \right] p^2$$

$$+ (1 + i g_s) \left[[K_o] + \sum_{\ell=1}^{N_D} \left(\sum_{\mu=1}^{N_\ell} \alpha_\mu [\Delta \tilde{K}_\mu]^{(\ell)} \right) \right] - 1/2 \rho V^2 [A(k)]$$

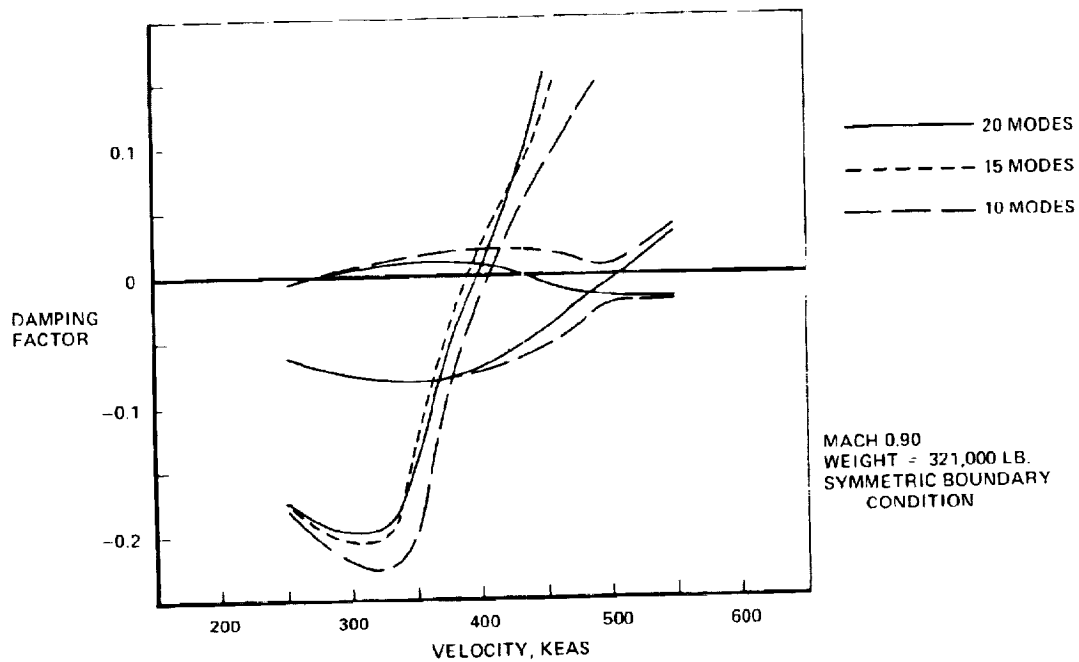


Figure 10-7. The Effects of Number of Modes on the Flutter Solution

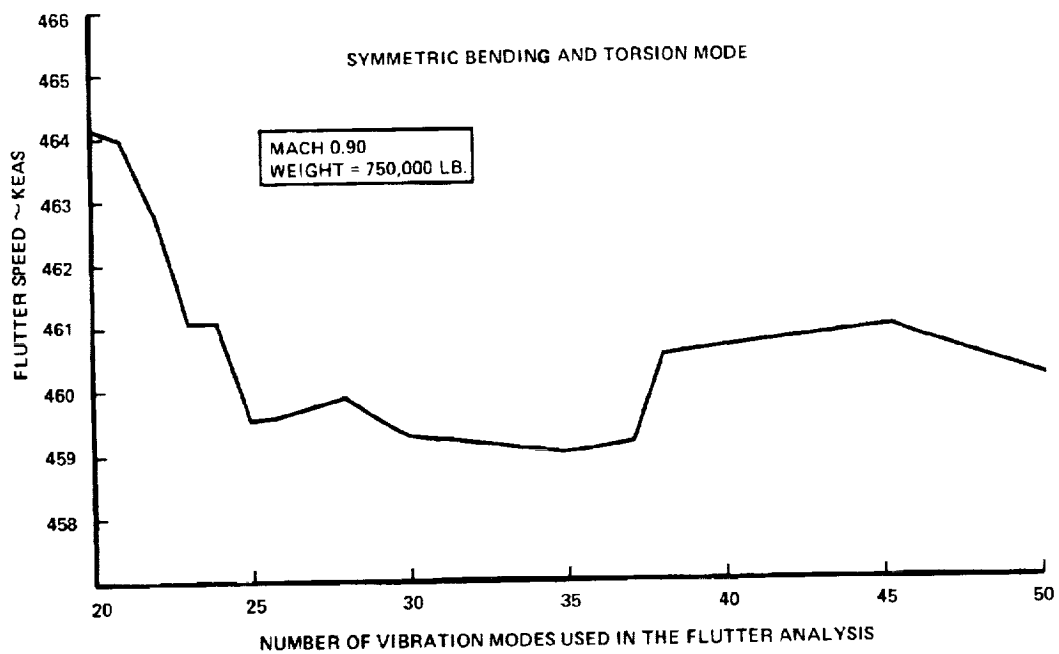


Figure 10-8. Flutter Speed Variation With Number of Modes

where $\begin{bmatrix} W_o \end{bmatrix}$ = base weight matrix

$\begin{bmatrix} K_o \end{bmatrix}$ = base stiffness matrix

$[A(k)]$ = aerodynamic influence coefficient matrix

$[T]$ = matrix of modal columns

g_o = gravitational constant

b_o = reference length

V = true airspeed

k = reduced frequency $\left(= \frac{\omega b_o}{V} \right)$

p = non-dimensional operator $\left(= \frac{b_o}{V} \frac{d}{dt} \right)$

g = structural damping

ρ = air density

β_l = l^{th} design variable $-(\bar{\beta}_l + \hat{\beta}_l)$, expressed in weight units

$\bar{\beta}_l$ = increment in l^{th} design variable due to updating of base structure

$\hat{\beta}_l$ = increment in l^{th} design variable necessary to satisfy flutter constraint (in addition to $\bar{\beta}_l$)

α_μ = La Grange coefficients used in matrix interpolation $= \prod_{\substack{n=1 \\ n \neq \mu}}^{N_l} \frac{\beta_l - \tilde{\beta}_l^n}{\tilde{\beta}_l^\mu - \tilde{\beta}_l^n}$

β_l^* = $\begin{cases} 0 & \text{for Type I design variable} \\ \tilde{\beta}_l^1 & \text{for Type II design variable} \end{cases}$

$\tilde{\beta}_l^\mu$ = values of β_l for which $[\Delta K]$ matrices are calculated

$[\Delta W]^{(l)}$ = initial weight matrix due to "step" increase for Type II design variable

$$\left[\frac{\partial W}{\partial \beta_\ell} \right]^{(\ell)} = \text{increment in weight matrix due to } \beta_\ell$$

$$\left[\Delta \tilde{K}_\mu \right]^{(\ell)} = \text{increment in stiffness matrix (over } [K_\mu]), \text{ calculated for } \tilde{\beta}_\ell^\mu$$

N_D = number of design variables

N_ℓ = number of $[\Delta K]$ matrices for design variable ℓ

This formulation allows for definition of design variables in two different ways. The Type II design variable assumes an initial stiffness/weight "step" increase. This was used in the Task I optimization; the front and rear beam shear webs were first increased in thickness in order to create a more uniform "torsion box." Type I design variables do not have this initial step. Consequently, one of the matrices used for interpolation to form the stiffness matrix is a null matrix. This then requires one less $[\Delta K]$ matrix to be calculated. The Type I design variables were used for the bending variables in Task I and for all variables in Task II. Plots of a typical element in the stiffness matrix versus β_ℓ make the distinction between Types I and II clearer, and are shown in Figure 10-9.

Design variables were defined by dividing the wing planform into sections known as "design regions." Within a design region, more than one design variable may be defined. This is true for the Task I optimization, where bending and torsion design variables exist for each region in the outer wing area. Because all the Task II design regions are for the monocoque outer wing, there exists only one design variable per region. Both bending and torsional stiffness may be varied with these design variables. Task I and Task II design regions used in the optimization process are shown in the appropriate results subsection.

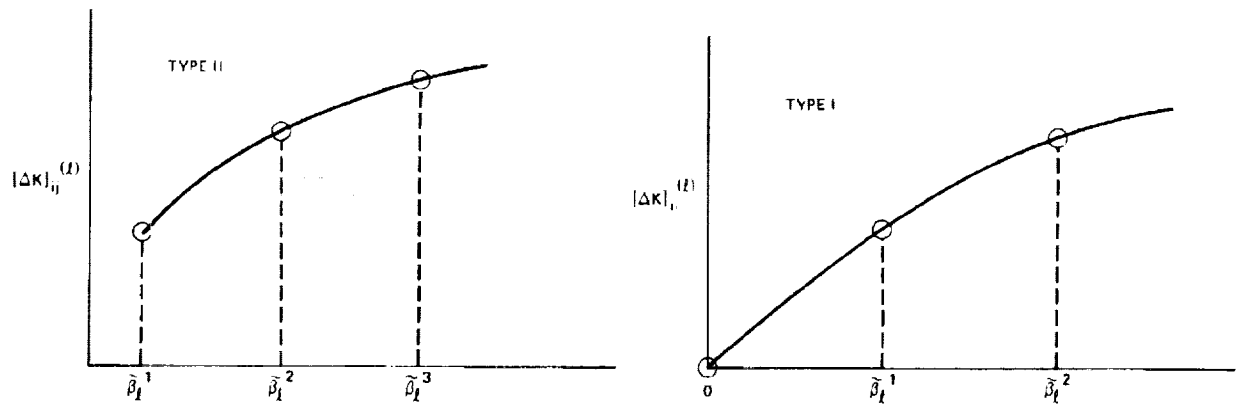


Figure 10-9. Types of Design Variables

In producing the necessary matrices for the optimization program, the sizing data for the NASTRAN structural model were changed; this produced matrices $[\Delta W]^{(l)}$, $\left[\frac{\partial W}{\partial \beta_l}\right]^{(l)}$, and $[\Delta K_\mu]^{(l)}$ corresponding to the $\tilde{\beta}_l^\mu$ values of each design variable. These matrices were then stored on a disc and used in the optimization procedure.

The optimization program forms the total flutter matrix and solves for k and $\hat{\beta}_l$ using the Two-Dimensional Regula Falsi Procedure. This is an iterative method of solving two equations (the real and imaginary parts of the flutter equation) with two unknowns (k and $\hat{\beta}_l$). It is used when the equations are not amenable to explicit solutions. The equation

$$\left| [T]^T \begin{bmatrix} D(k, \hat{\beta}_l) \end{bmatrix} [T] \right| = 0 \quad (10-13)$$

is solved by projecting planes which approximate the real and imaginary surfaces of the above determinant as a function of $\hat{\beta}_l$ and k . Iteration continues

until a satisfactory convergence criterion is achieved. A more detailed discussion of this method can be obtained in Reference 6.

The optimization procedure consists of solving for $\hat{\beta}_i$, the "amount" of the i^{th} design variable (in weight units) necessary to achieve the required flutter speed, V_f , which is input to the program. Thus the design variable with the minimum $\hat{\beta}_i$ is the most effective in achieving the flutter requirement. More structure is added to the effective design variables (by increasing $\bar{\beta}_i$ for each one), and $\hat{\beta}_i$ is again calculated for each. This updating procedure is followed until the $\hat{\beta}_i$ solutions become uniform, indicating that an optimum solution has been achieved.

In practice, it was found that the solution was highly dependent on the eigenvector matrix, $[T]$, used for modalization. Therefore, when a solution strayed too far from the base stiffness and mass matrices which produced these mode shapes, it was necessary to calculate new eigenvalues and eigenvectors and remodelize the problem. The procedure described above was then initiated again, continuing in this manner until convergence upon an optimum solution was obtained.

ANALYTICAL DESIGN - TASK I

The analytical design effort examined the structural dynamic characteristics of the baseline aircraft employing the various structural arrangements and concepts discussed in Section 1, Structural Design Concepts. The initial effort was performed to identify the importance of the flutter requirements on the overall design of an arrow-wing supersonic cruise aircraft.

The specific objectives included (1) identifying of the flutter conditions that influence the design of the primary wing and fuselage structure of the baseline aircraft, (2) defining the most critical conditions for flutter (i.e., airplane

mass, Mach number) for flutter analysis, (3) performing the required analyses to determine the flutter speeds for the structural arrangements, and (4) defining the appropriate stiffness and/or mass through a flutter optimization procedure to achieve the required flutter speed.

The scope of the Task I vibration and flutter analyses effort is presented in Table 10-3.

The chordwise stiffened structural model was the first of the three models to be operational and the anticipated flutter results were that the symmetric boundary condition would be more critical than the antisymmetric boundary condition. Thus, the chordwise stiffened model was analyzed in detail with emphasis on the symmetric boundary condition. The spanwise stiffened and monocoque models were analyzed for only the most critical of the chordwise stiffened arrangement conditions, i.e., a particular weight, boundary condition and Mach number.

Chordwise Stiffened Design

Symmetric Vibration. - Symmetric vibration analyses were performed for the operating weight empty (OWE) and for the full fuel and full payload (FFFP) conditions. These conditions represent an aircraft weight of 321,000 pounds and 750,000 pounds, respectively. The symmetric vibration analysis solves a 188th order system in NASTRAN using the Givens Method. The analysis solves for all the eigenvalues and for 50 eigenvectors. These 50 vectors are associated with the lowest frequency modes.

A summary of the lower frequency symmetric vibration modes for the chordwise stiffened arrangement is presented in Table 10-4. Mode frequency comparisons (Hertz) for the operating weight empty (OWE) and the full fuel and full payload (FFFP) weight conditions are shown for the strength-designed chordwise stiffened arrangement. The associated vector plots for the OWE condition are also shown for the first eight modes in Figures 10-10 through 10-17.

TABLE 10-3. VIBRATION AND FLUTTER ANALYSIS - TASK I

BASELINE ARRANGE- MENT	VIBRATION ANALYSES				FLUTTER ANALYSES						
	SYMMETRIC AIRCRAFT WEIGHT-LBS.		ANTISYMMETRIC AIRCRAFT WEIGHT-LBS.		MACH NO.	AIRCRAFT WEIGHT-LBS.					
	321000	750000	321000	750000		321000	750000	321000	750000		
CHORDWISE	✓	✓	✓	✓	0.60	✓	✓				
					0.90	✓	✓	✓			✓
					1.25	✓	✓				
SPANWISE		✓			0.60						
					0.90		✓				
					1.25						
MONOCOQUE		✓			0.60						
					0.90		✓				
					1.25						

OWE = 321,000-LB
FFFP = 750,000-LB

TABLE 10-4. LOWER FREQUENCY SYMMETRIC VIBRATION MODES - CHORDWISE STIFFENED

MODE NUMBER	MODE DESCRIPTION	MODE FREQUENCY ~ HERTZ	
		OWE	FFFP
1	RIGID BODY	0.000	0.000
2	RIGID BODY	0.001	0.001
3	WING 1ST BENDING	1.009	0.933
4	FUSELAGE 1ST BENDING	1.381	1.206
5	ENGINE PITCH IN PHASE	1.641	1.627
6	ENGINE PITCH OUT OF PHASE	1.817	1.815
7	FUSELAGE 2ND BENDING	2.784	2.261
8	WING 1ST TORSION	3.288	3.104

OWE ~ WEIGHT = 321,000 LBS
 FFFP ~ WEIGHT = 750,000 LBS

SYMMETRIC VIBRATION MODES OWE - CHORDWISE STIFFENED

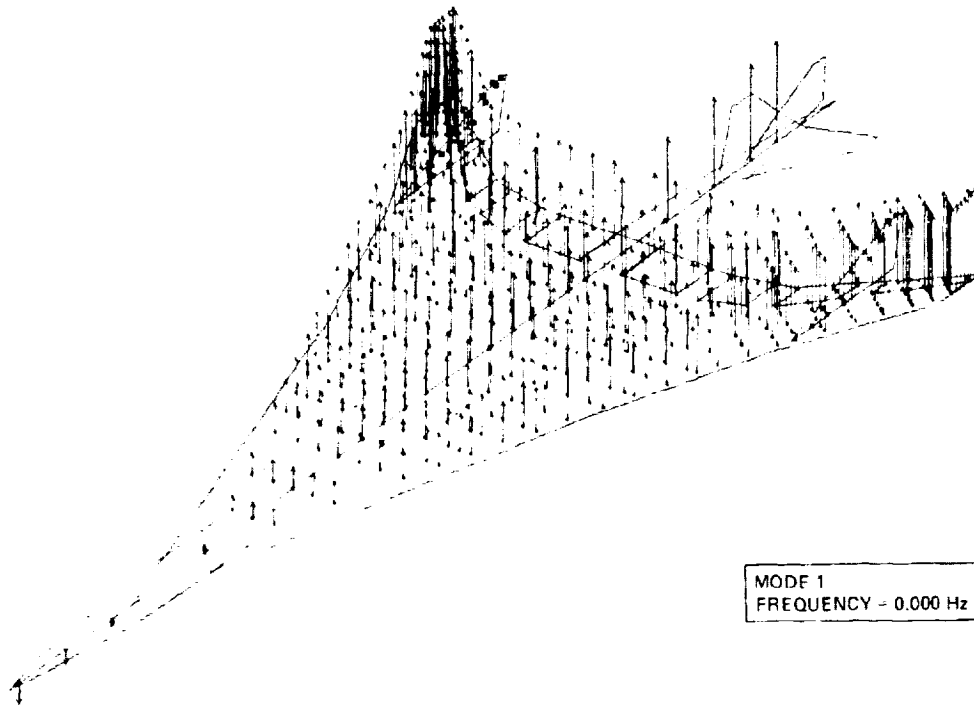


Figure 10-10. Symmetric Vibration Mode 1

SYMMETRIC VIBRATION MODES OWE - CHORDWISE STIFFENED

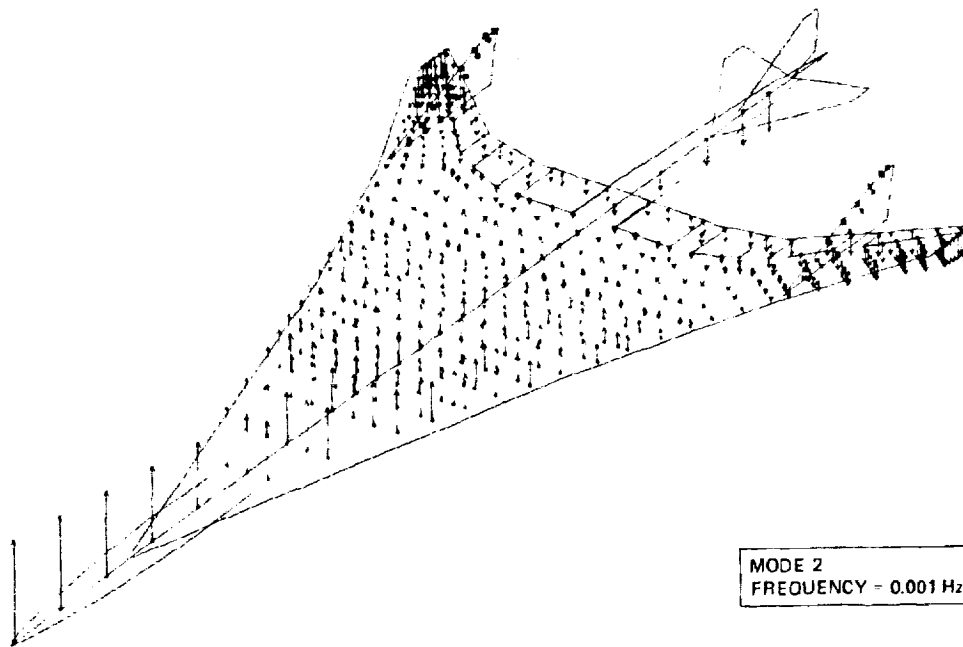


Figure 10-11. Symmetric Vibration Mode 2

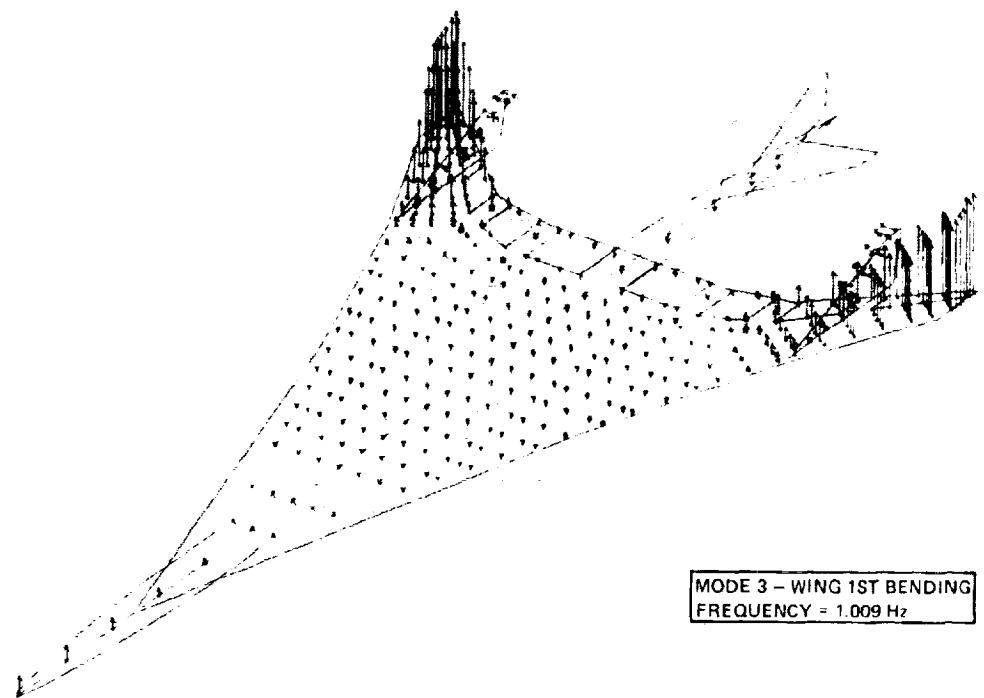


Figure 10-12. Symmetric Vibration Mode 3

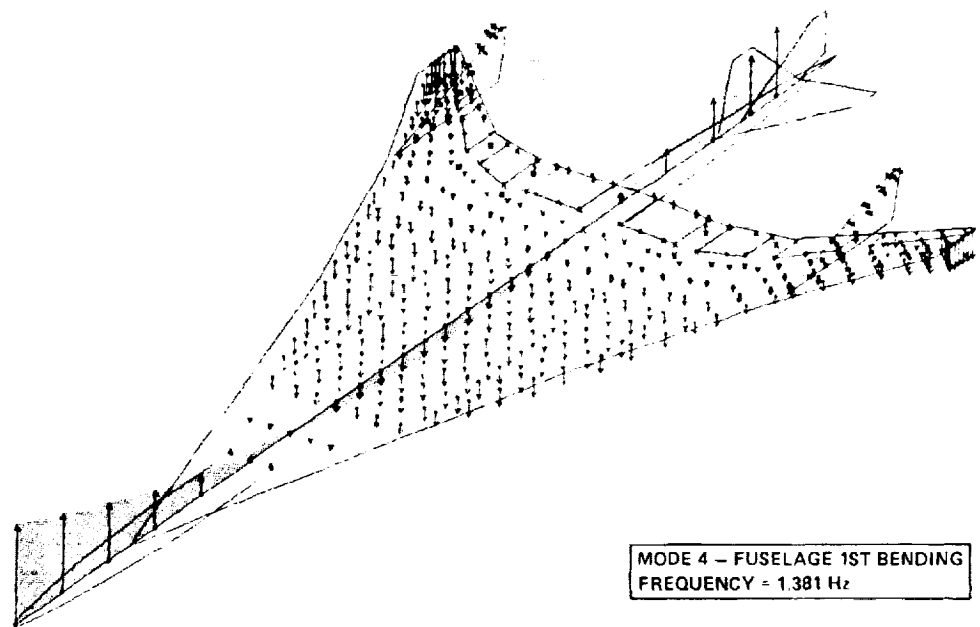


Figure 10-13. Symmetric Vibration Mode 4

SYMMETRIC VIBRATION MODES OWE - CHORDWISE STIFFENED

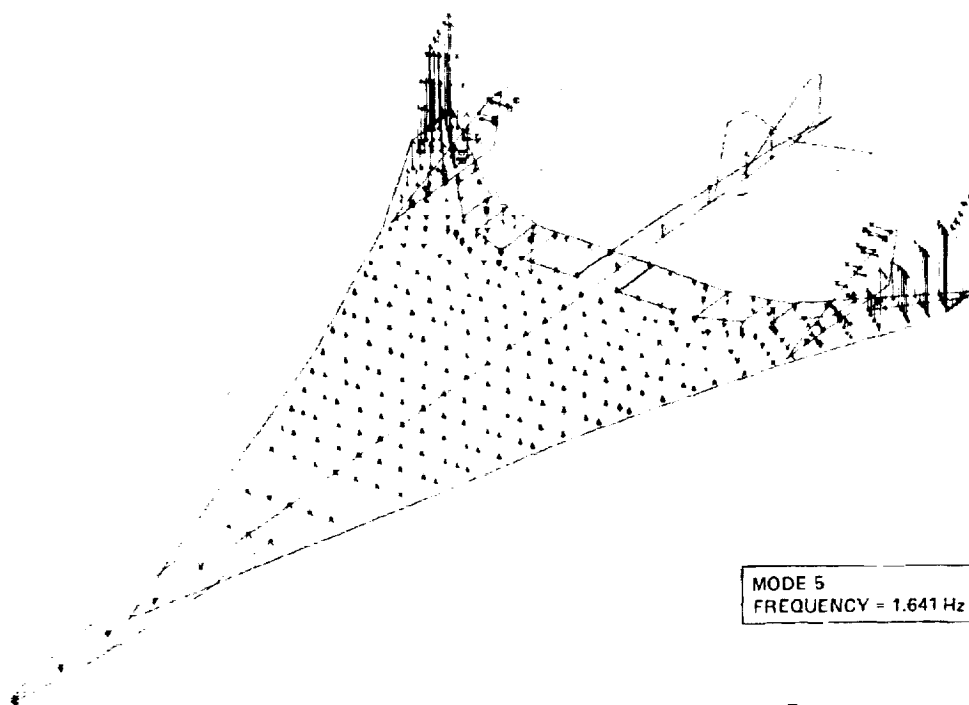


Figure 10-14. Symmetric Vibration Mode 5

SYMMETRIC VIBRATION MODES OWE - CHORDWISE STIFFENED

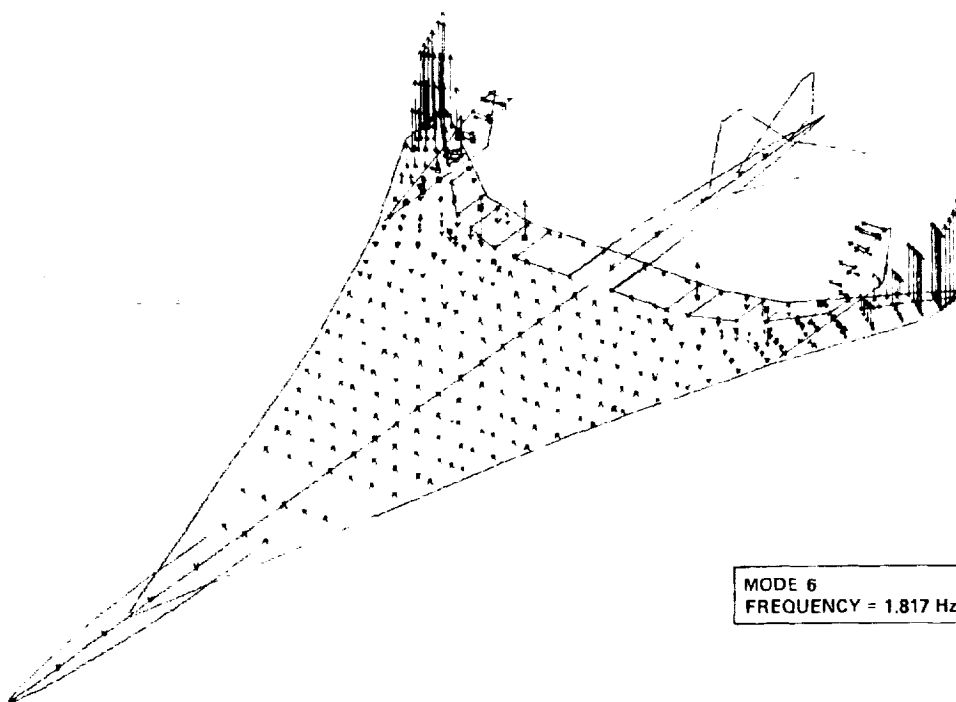


Figure 10-15. Symmetric Vibration 6

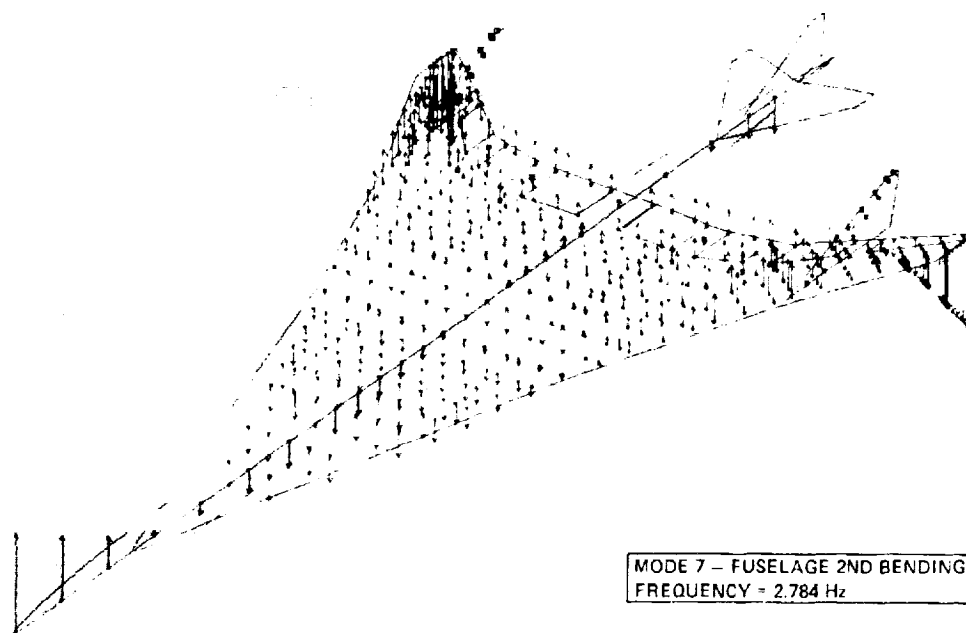


Figure 10-16. Symmetric Vibration Mode 7

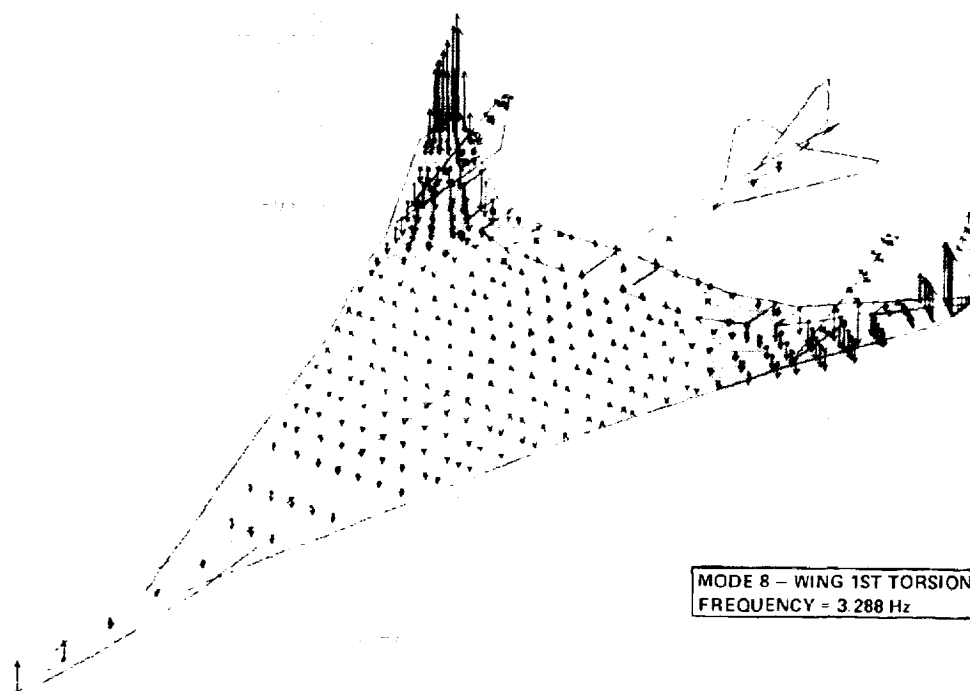


Figure 10-17. Symmetric Vibration Mode 8

Symmetric Flutter. - Symmetric flutter solutions for the 321,000 pound aircraft at Mach 0.60 are shown in Figure 10-18. The mode identification numbers of 3 through 8 correspond to the mode number identification presented for the lower frequency symmetric vibration modes of Table 10-4. Three distinct flutter mechanisms are noted: The bending and torsion mode, the hump mode, and the stability mode. The flutter speed for the bending and torsion mode is 460 KEAS; the stability and hump modes have identical flutter speeds of 400 KEAS.

Symmetric flutter solutions for the 750,000 pound aircraft at Mach 0.90 are shown as Figure 10-19. The bending and torsion mode is the only distinct mode noted with a flutter speed of 379 KEAS.

A summary of the flutter speeds for the chordwise stiffened arrangement is presented in Figure 10-20 through 10-22 for the symmetric bending and torsion mode, the symmetric hump mode, and the symmetric stability mode. These figures show the V_D and $1.2 V_D$ envelope as a function of pressure altitude versus knots equivalent airspeed overlaid with the analysis Mach number lines of 0.60, 0.90, and 1.25. Flutter boundaries for the various modes are indicated by a cross-hatched line. The lowest flutter speed (379 KEAS) occurs for the symmetric bending and torsion mode at Mach 0.90.

Participation Coefficients - Participation coefficients are the complex eigenvectors associated with the roots of a flutter equation. These participation coefficients give insight into the structural modes involved in a flutter mechanism.

The participation coefficients for the bending and torsion mode flutter (Mode 3 of Figure 10-19) reveal that at flutter, this mode is principally composed of the zero airspeed Modes 3 and 8 (Table 10-4). Participation coefficients resulting from symmetric flutter analyses at Mach 0.90 for both the full fuel and full payload (FFFP) and the operating weight empty (OWE) conditions are shown in Figure 10-23 and 10-24, respectively. As indicated on these figures, the zero airspeed wing 1st bending mode rapidly transitions through the adjacent higher frequency modes and couples at flutter with the

SYMMETRIC FLUTTER ANALYSIS - CHORDWISE STIFFENED ARRANGEMENT
MACH NO. = 0.6
WEIGHT = 321,000 LBS

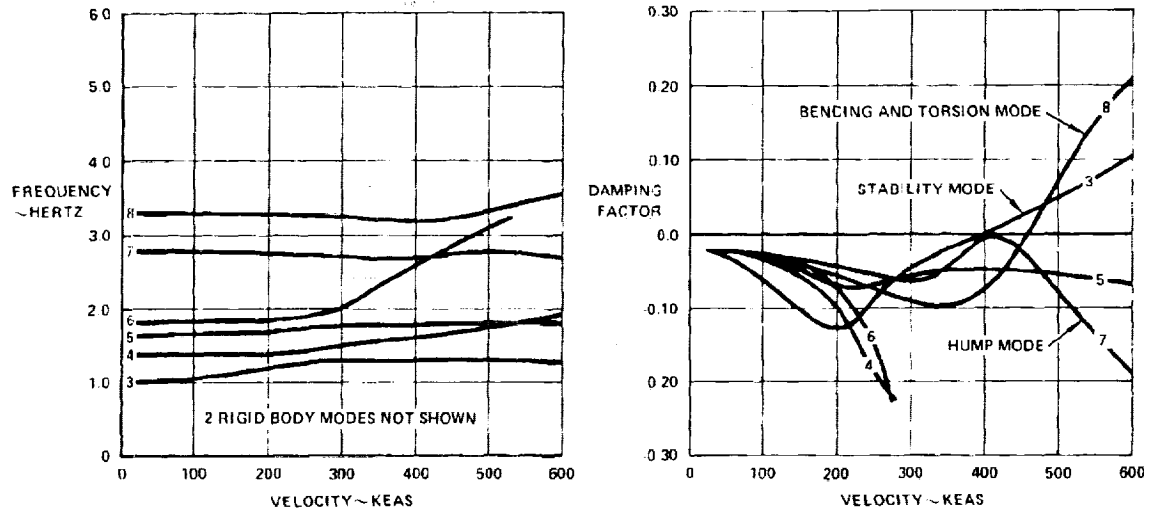


Figure 10-18. Symmetric Flutter Analysis - Mach 0.6 - OWE

SYMMETRIC FLUTTER ANALYSIS - CHORDWISE STIFFENED ARRANGEMENT
MACH NO. = 0.9
WEIGHT = 750,000 LBS

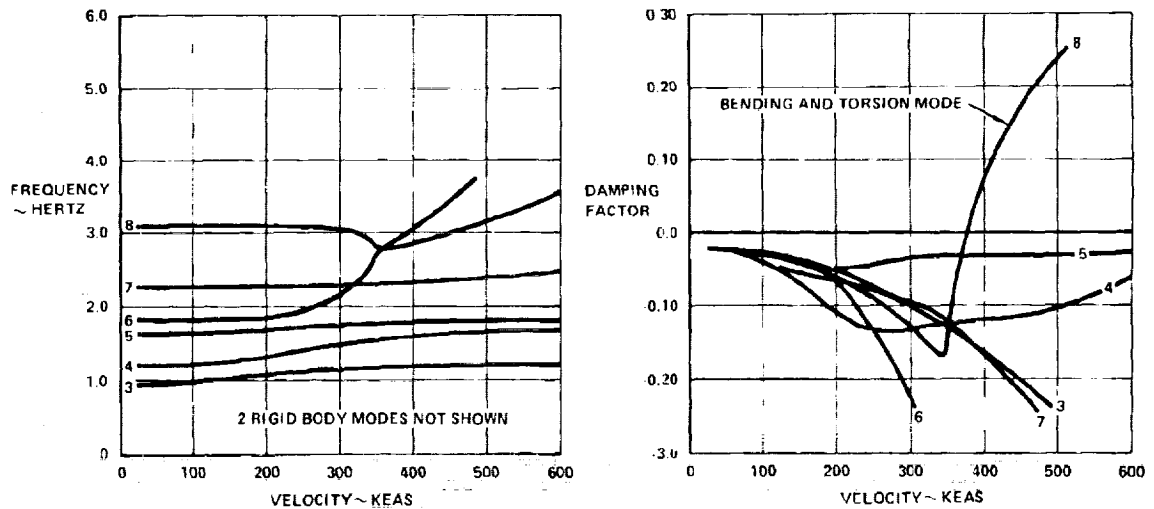


Figure 10-19. Symmetric Flutter Analysis - Mach 0.9 - FFFP

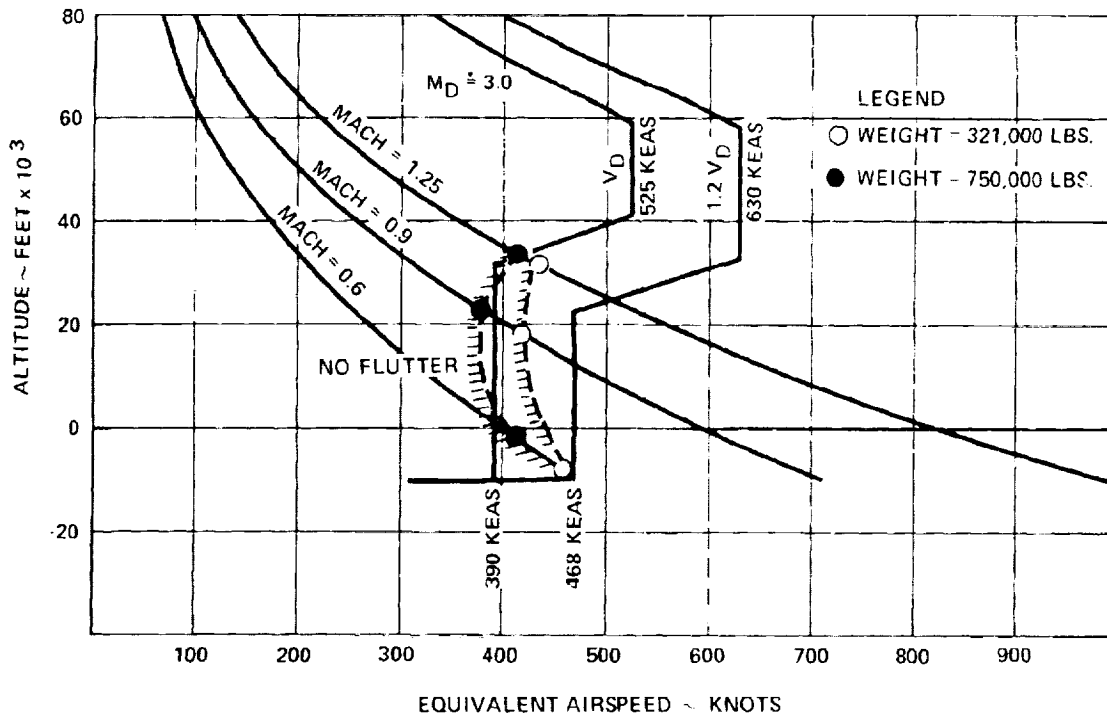


Figure 10-20. Flutter Speeds for Symmetric Bending and Torsion Mode

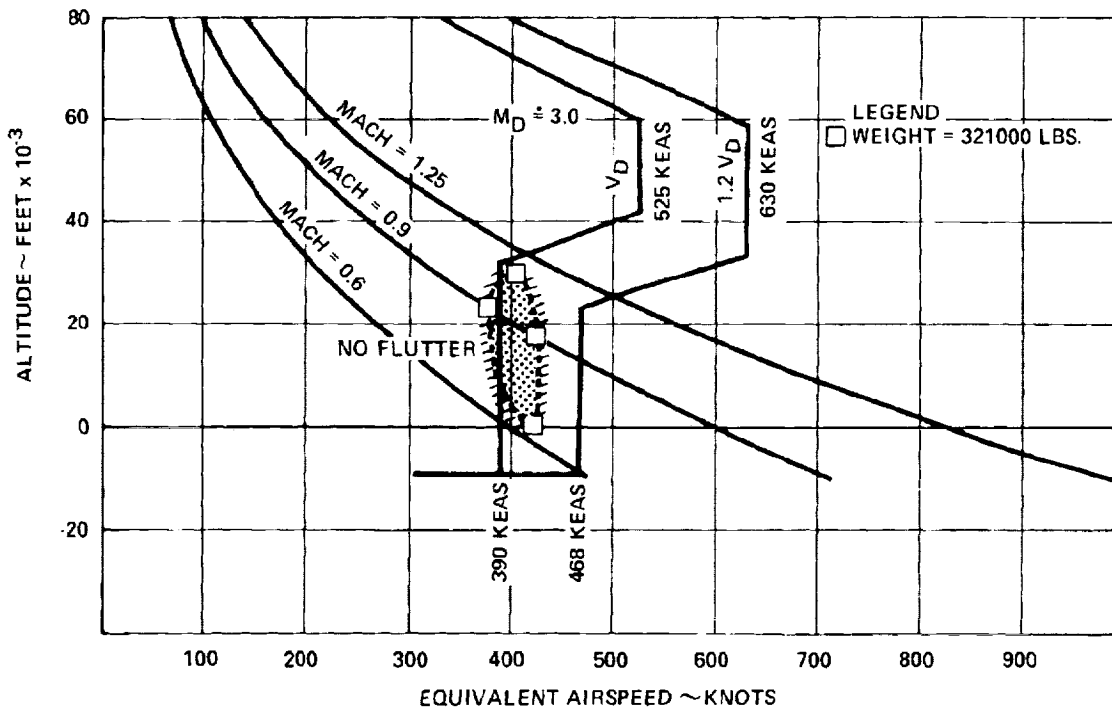


Figure 10-21. Flutter Speeds for Symmetric Hump Mode

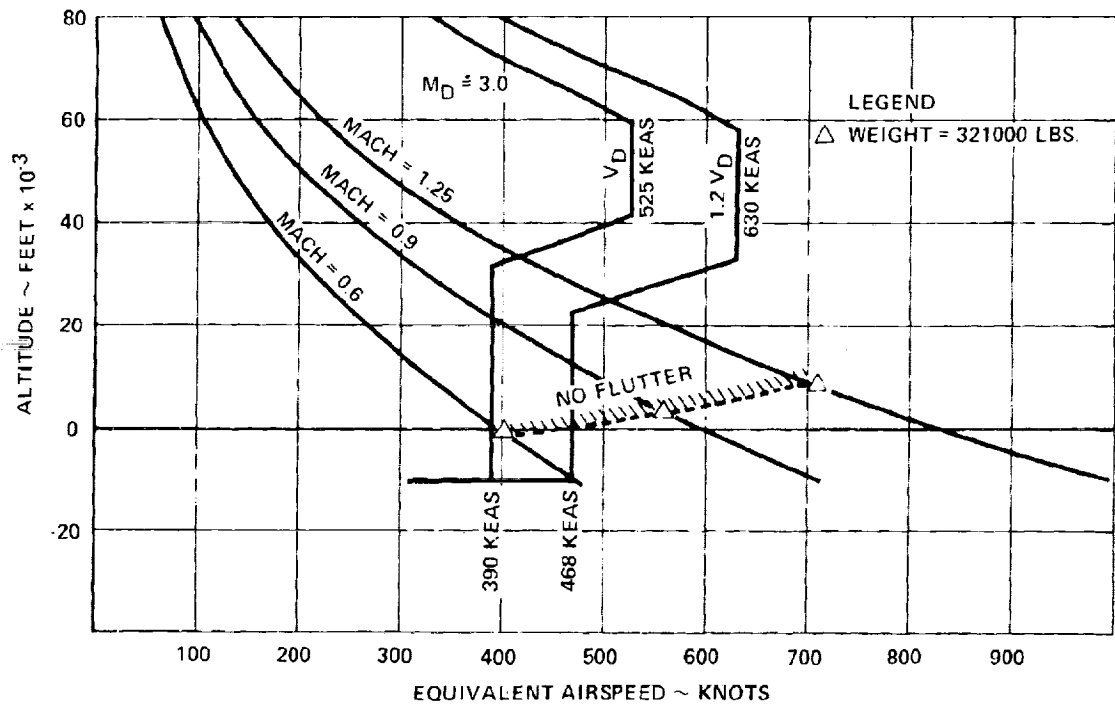


Figure 10-22. Flutter Speeds for Symmetric Stability Mode

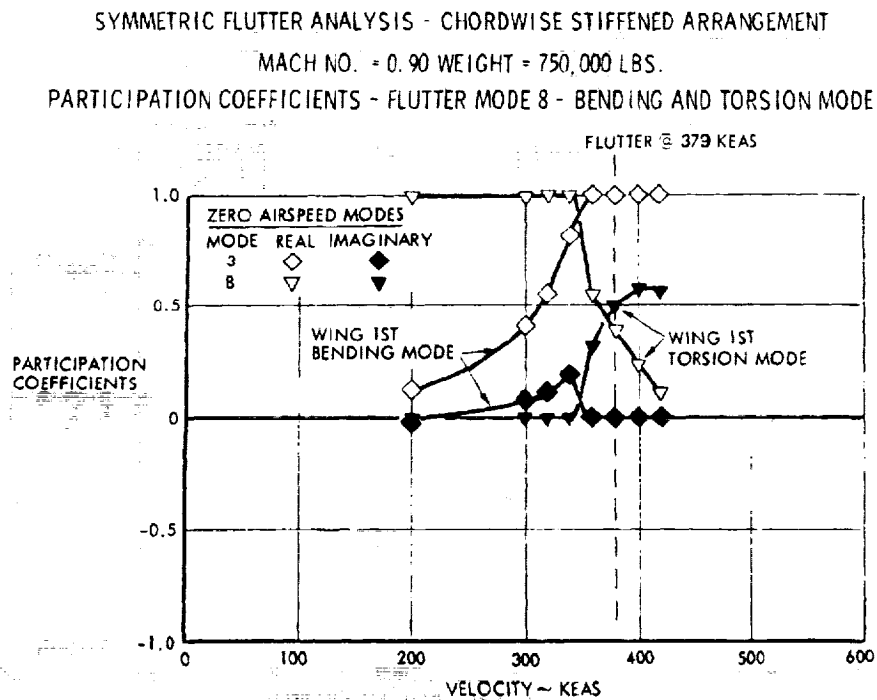


Figure 10-23. Participation Coefficients - Mach 0.9 - FFP-Mode 8

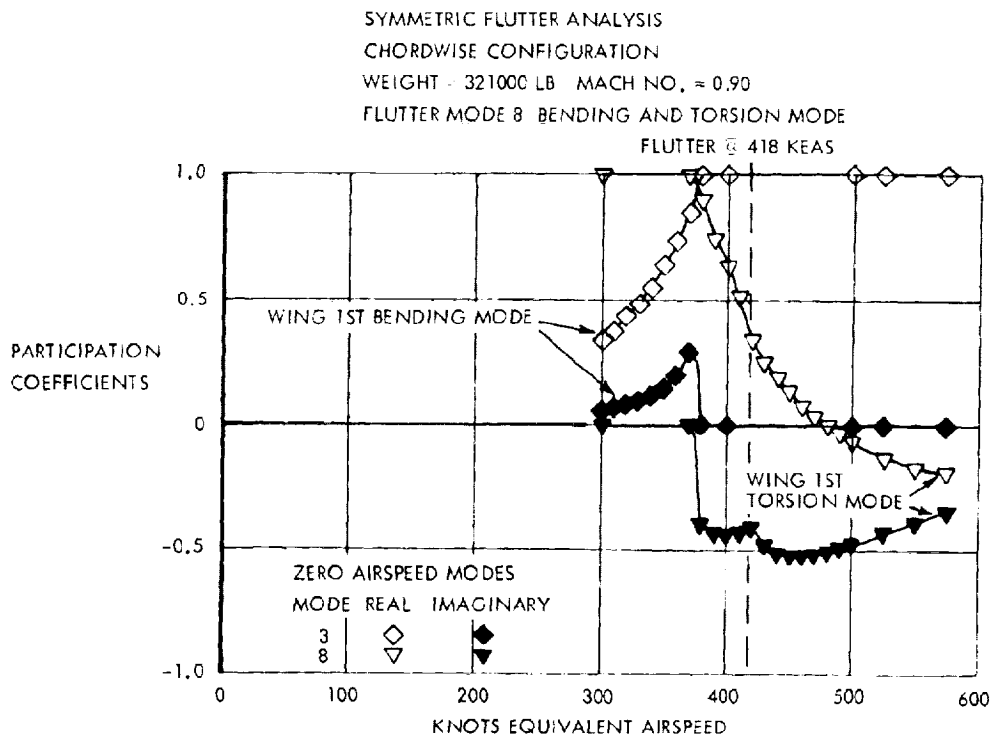


Figure 10-24. Participation Coefficients - Mach 0.9 - OWE - Mode 8

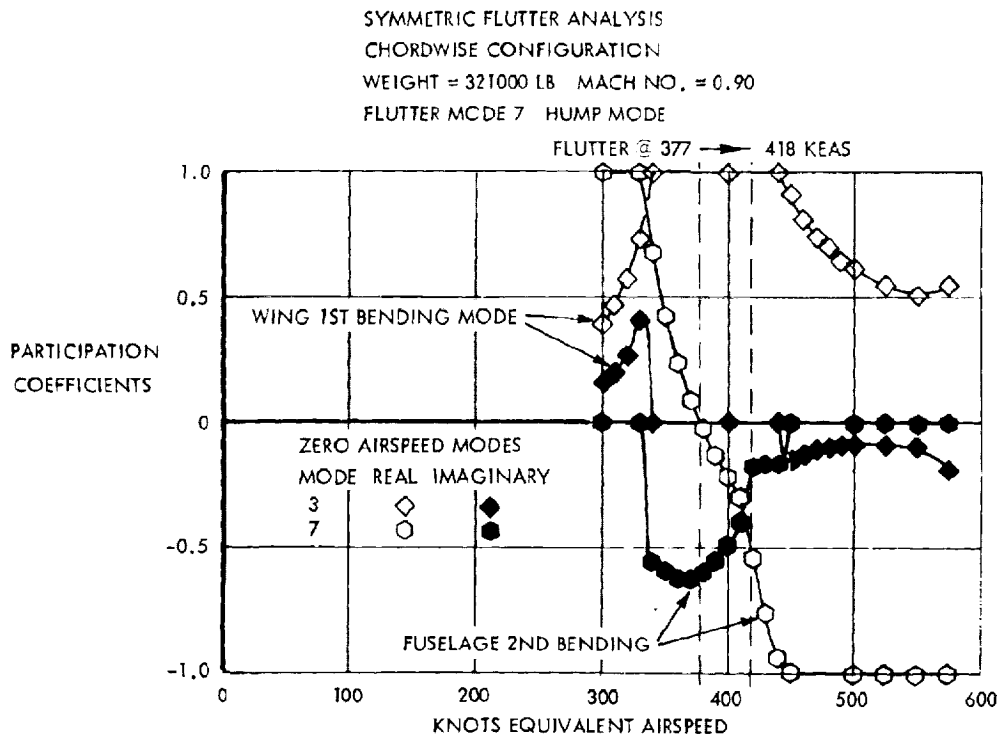


Figure 10-25. Participation Coefficients - Mach 0.9 - OWE - Mode 7

zero airspeed wing 1st torsion mode. This conclusion is not obvious by reference to the frequency velocity diagram of Figure 10-19.

The participation coefficients for the hump mode flutter (Mode 7 of Figure 10-18) reveal that at flutter, this mode is principally composed of the zero airspeed Modes 3 and 7 (Table 10-4). As shown in Figure 10-25, the zero airspeed wing 1st bending mode couples at flutter with the zero airspeed fuselage 2nd bending mode. It is worth noting that the fuselage 2nd bending mode and the wing 1st torsion mode are very similar in wing mode shape for the 321,000 pound aircraft. This similarity is probably due to the frequency proximity of these two modes. The vibration analysis for the 750,000 pound aircraft shows that the fuselage 2nd bending mode and the wing 1st torsion mode are more separated in frequency. The 750,000 pound aircraft fuselage 2nd bending mode vectors show negligible characteristics of the wing 1st torsion mode and therefore the hump mode flutter does not result.

The participation coefficients for the stability mode flutter (Mode 3 of Figure 10-18) reveal that at flutter, this mode is principally composed of the zero airspeed Modes 1 and 4 (Table 10-4). It can be seen in Figure 10-26 that the zero airspeed rigid body mode couples at flutter with the zero airspeed fuselage 1st bending mode. It was further demonstrated that the fuselage 1st bending mode is involved in the flutter mechanism by mathematically eliminating the fuselage 1st bending mode from the flutter analysis. As a result of this operation, the stability mode flutter was eliminated.

Antisymmetric Vibration. - The antisymmetric vibration analysis solves a 177th order system with NASTRAN. A summary of the lower frequency vibration modes for the chordwise stiffened arrangement is presented in Table 10-5. This summary compares the mode frequencies of the 321,000 and 750,000 pound aircraft. These antisymmetric mode characteristics are similar to the symmetric modes, with the exception that the antisymmetric fuselage bending mode frequencies are significantly greater than the corresponding symmetric fuselage bending mode frequencies. This difference in fuselage bending mode frequencies is understandable since the fuselage centerbody was structurally represented to be flexible symmetrically and to be rigid antisymmetrically.

TABLE 10-5. LOWER FREQUENCY ANTISYMMETRIC VIBRATION MODES - CHORDWISE STIFFENED

CHORDWISE STIFFENED ARRANGEMENT

MODE NUMBER	MODE DESCRIPTION	MODE FREQUENCY ~ HERTZ	
		OWE	FFFP
1	RIGID BODY	0.000	0.000
2	RIGID BODY	0.000	0.000
3	RIGID BODY	0.000	0.000
4	WING 1ST BENDING	1.228	0.908
5	ENGINE PITCH IN PHASE	1.514	1.457
6	ENGINE PITCH OUT OF PHASE	1.821	1.805
7	FUSELAGE 1ST BENDING	1.998	1.949
8	WING 1ST TORSION	3.034	2.319
9	FUSELAGE 2ND BENDING	3.370	3.056

OWE ~ WEIGHT = 321,000 LBS.

FFFP ~ WEIGHT = 750,000 LBS.

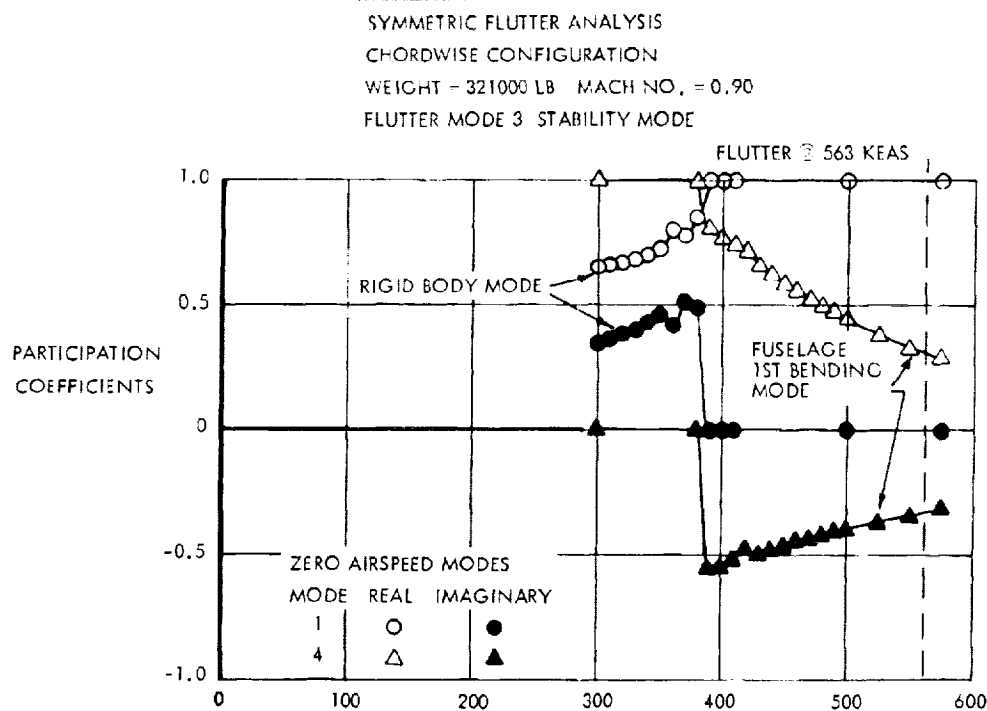


Figure 10-26. Participation Coefficients - Mach 0.9 - OWE - Mode 3

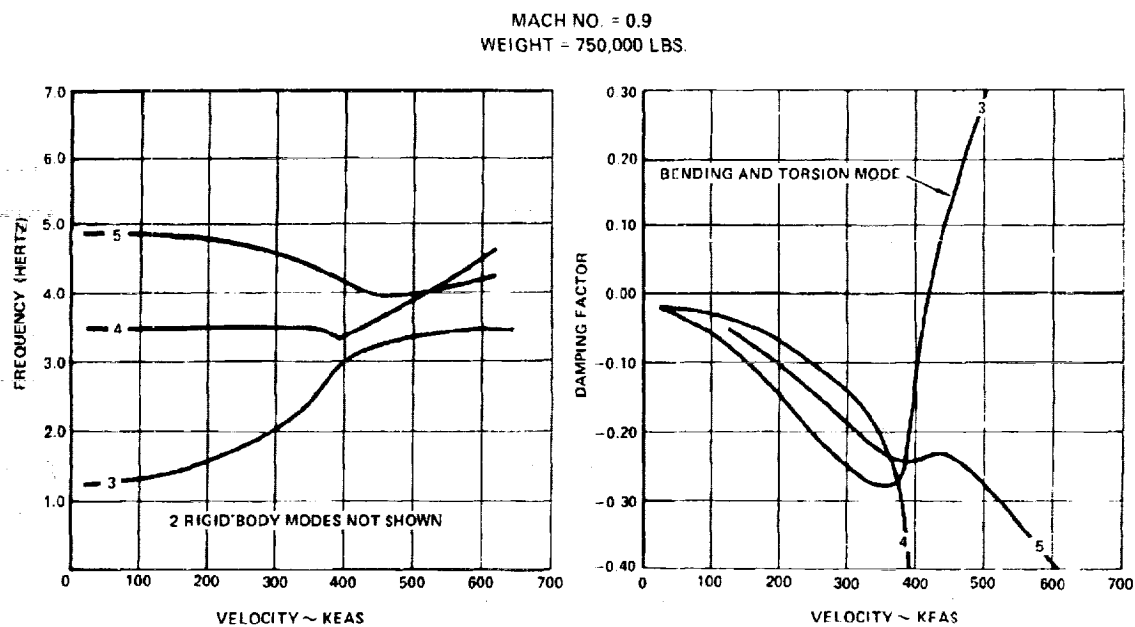


Figure 10-27. Symmetric Flutter Analysis - Mach 0.9 - FFFP - Rigidized Wing

The mode shapes for the 750,000 pound aircraft are shown in Figures 10-28 through 10-35 for the first eight modes for the chordwise stiffened arrangement.

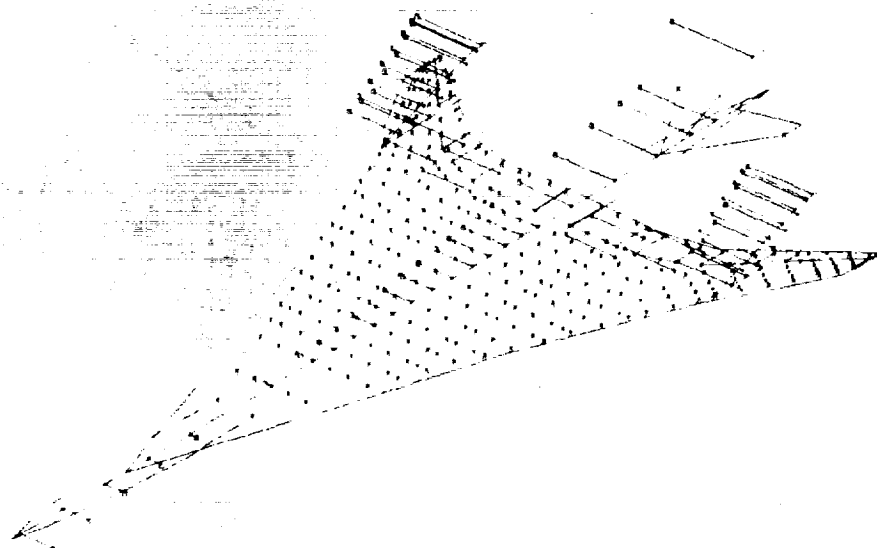
Antisymmetric Flutter. - The antisymmetric flutter analysis (Figures 10-36 and 10-37) examined the chordwise stiffened arrangement for the 321,000 and the 750,000 pound aircraft at Mach 0.90. The mode identification numbers correspond to the lower frequency antisymmetric vibration modes presented in Table 10-5. The results of this analysis show that the antisymmetric flutter mechanisms are exactly similar in name to the symmetric flutter mechanisms. The antisymmetric bending and torsion mode flutter velocities are greater than the corresponding symmetric bending and torsion mode flutter velocities (i.e., 500 KEAS for the 750,000 pound aircraft). The hump mode resulted in the lowest flutter speed of 300 KEAS, but was not evaluated further at this time. It was anticipated that stiffening the wing tip would eliminate or increase the hump mode flutter speed beyond the design boundary.

Rigidized Wing Inboard of BL 470. - The chordwise stiffened arrangement for the 750,000 pound aircraft was analyzed for the aircraft rigidized except for a flexible wing outboard of Buttline 470. The flutter analysis of this configuration shows (Figure 10-27) that for Mach 0.90, the wing 1st bending mode rapidly increases in frequency with increasing velocity and coalesces with the wing 1st torsion mode to flutter at 418 KEAS. This flutter mechanism is identical to the flutter mechanism for the unrigidized aircraft. For the unrigidized or flexible aircraft the bending and torsion mode flutter velocity is 379 KEAS.

Conclusions - Based on the results presented in this section for the chordwise-stiffened design, the most critical symmetric flutter condition occurs at a Mach number of 0.90 for the 750,000 pound aircraft. This most critical condition is therefore selected as the candidate for the vibration and flutter analysis of the spanwise and monocoque wing designs. It was also revealed by the preceding analysis of rigidizing the wing inboard of BL 470 that the wing tip structure (outer wing) controls the bending and torsion mode flutter mechanism.

ORIGINAL PAGE IS
OF POOR QUALITY

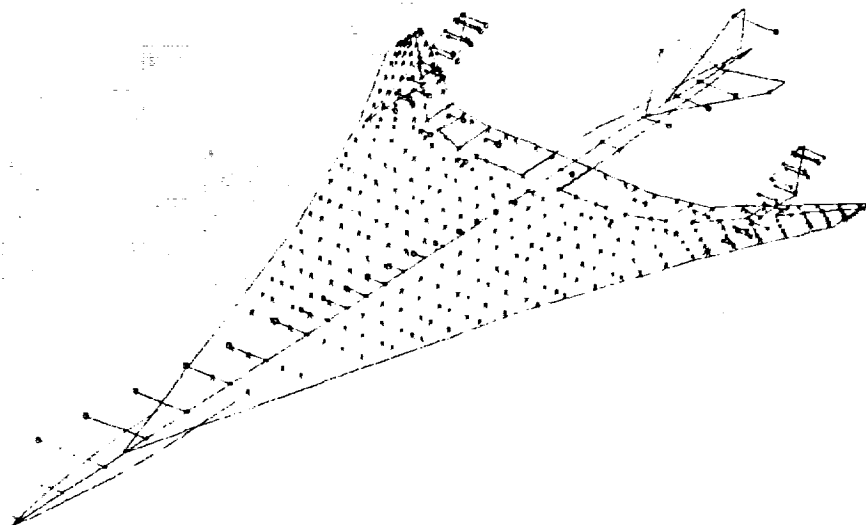
ANTISYMMETRIC VIBRATION MODES FFFP - CHORDWISE STIFFENED
MODE 1 - RIGID BODY



FREQUENCY = 0.000 Hz

Figure 10-28. Antisymmetric Vibration Mode 1

ANTISYMMETRIC VIBRATION MODES FFFP - CHORDWISE STIFFENED
MODE 2 - RIGID BODY



FREQUENCY = 0.000 Hz

Figure 10-29. Antisymmetric Vibration Mode 2

ANTISYMMETRIC VIBRATION MODES FFFP - CHORDWISE STIFFENED
MODE 3 - RIGID BODY

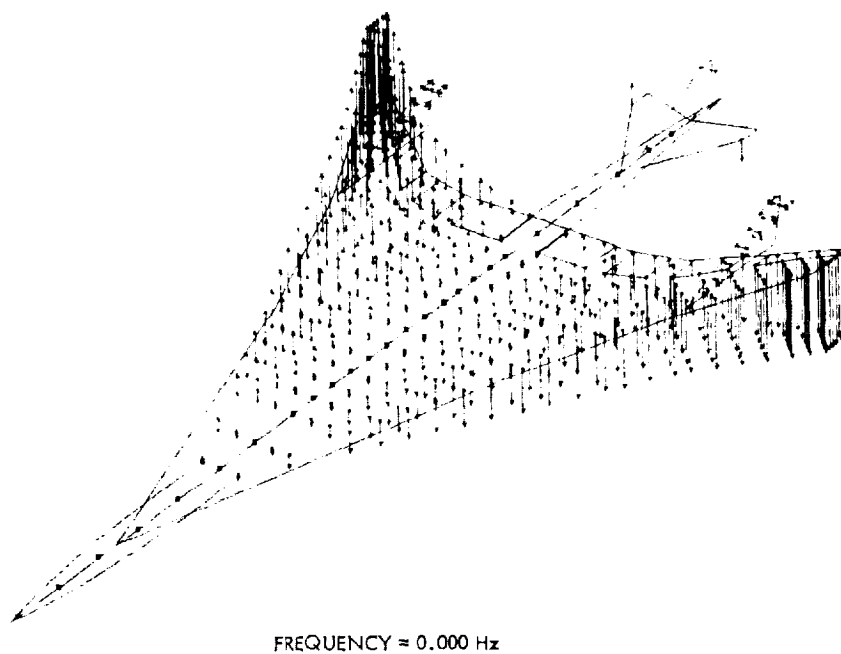


Figure 10-30. Antisymmetric Vibration Mode 3

ANTISYMMETRIC VIBRATION MODES FFFP - CHORDWISE STIFFENED
MODE 4 - WING 1ST BENDING

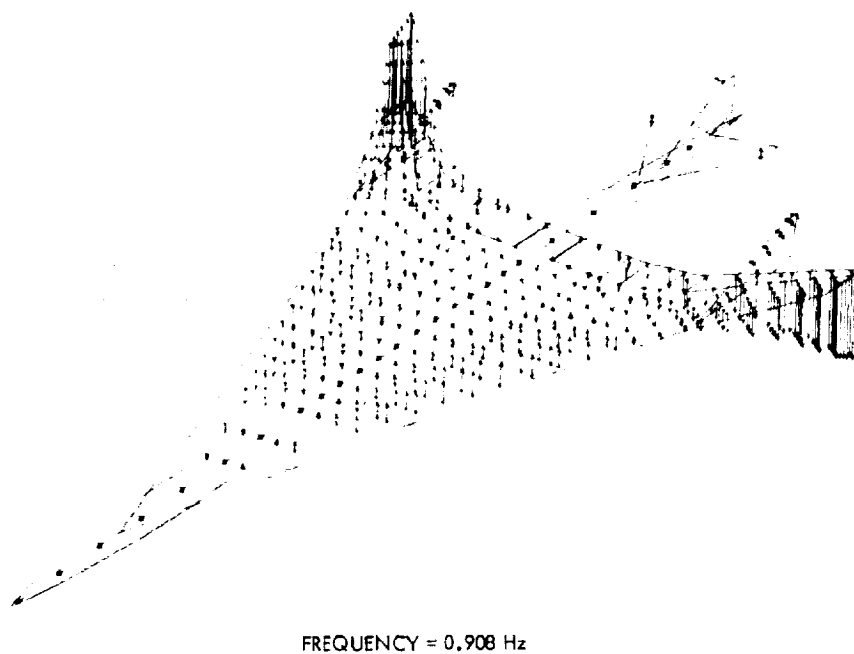


Figure 10-31. Antisymmetric Vibration Mode 4

ANTISYMMETRIC VIBRATION MODES FFFP - CHORDWISE STIFFENED
MODE 5 - ENGINE PITCH IN PHASE

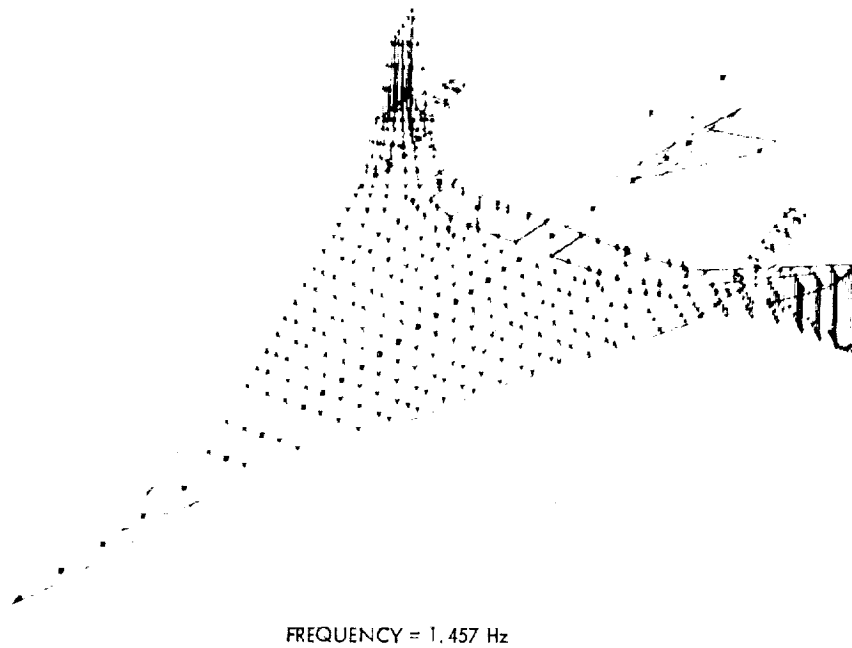


Figure 10-32. Antisymmetric Vibration Mode 5

ANTISYMMETRIC VIBRATION MODES FFFP - CHORDWISE STIFFENED
MODE 6 - ENGINE PITCH OUT OF PHASE

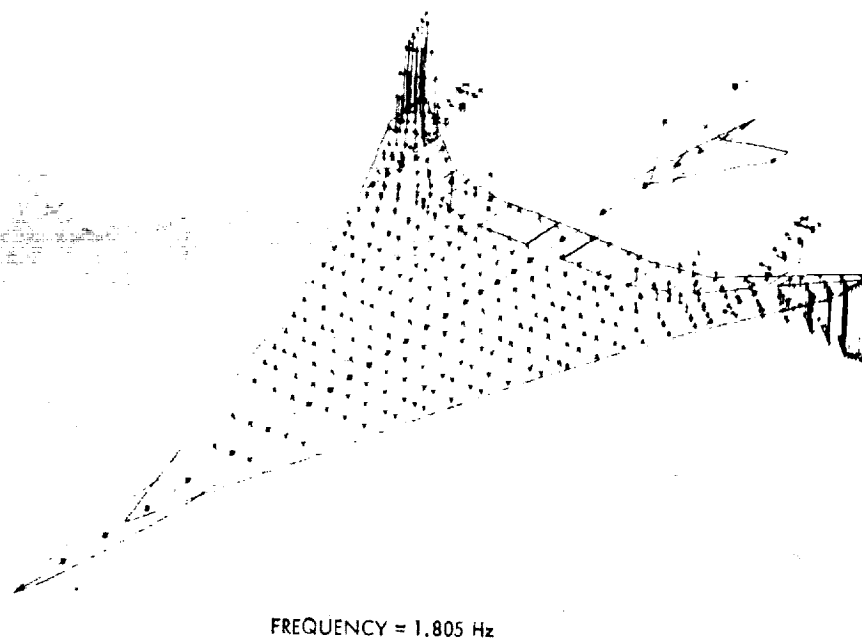
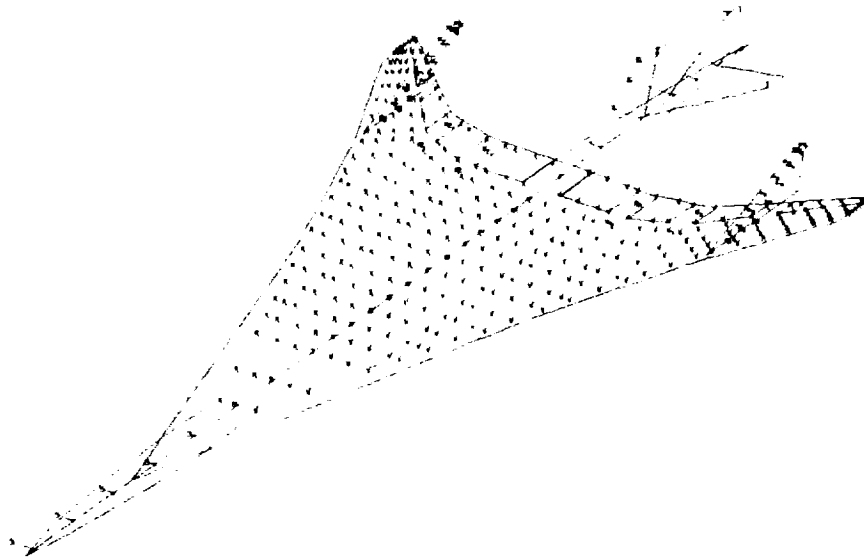


Figure 10-33. Antisymmetric Vibration Mode 6

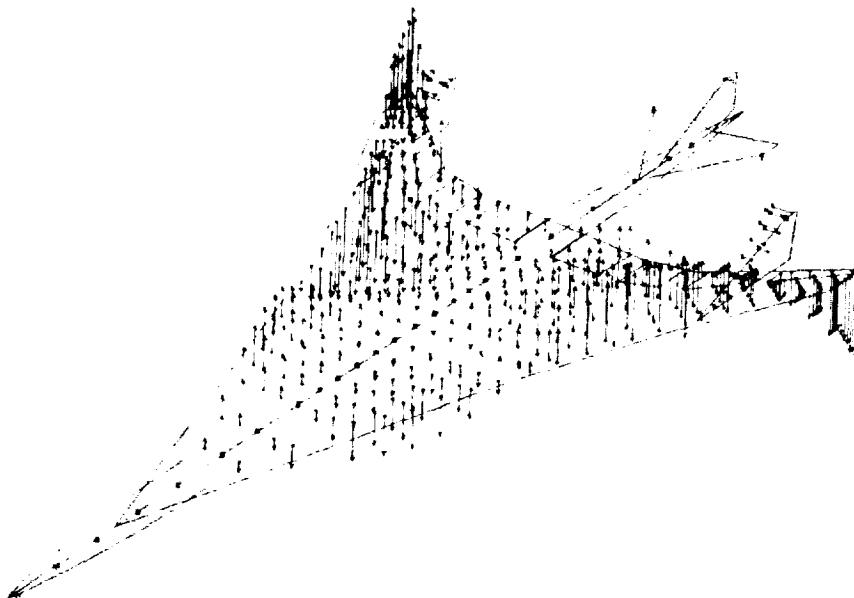
ANTISYMMETRIC VIBRATION MODES FFFP - CHORDWISE STIFFENED
MODE 7 - FUSELAGE 1ST BENDING



FREQUENCY = 1.949 Hz

Figure 10-34. Antisymmetric Vibration Mode 7

ANTISYMMETRIC VIBRATION MODES FFFP - CHORDWISE STIFFENED
MODE 8 - WING 1ST TORSION



FREQUENCY = 2.319 Hz

Figure 10-35. Antisymmetric Vibration Mode 8

ANTISYMMETRIC FLUTTER ANALYSIS - CHORDWISE STIFFENED ARRANGEMENT
MACH NO. = 0.9
WEIGHT = 321,000 LBS

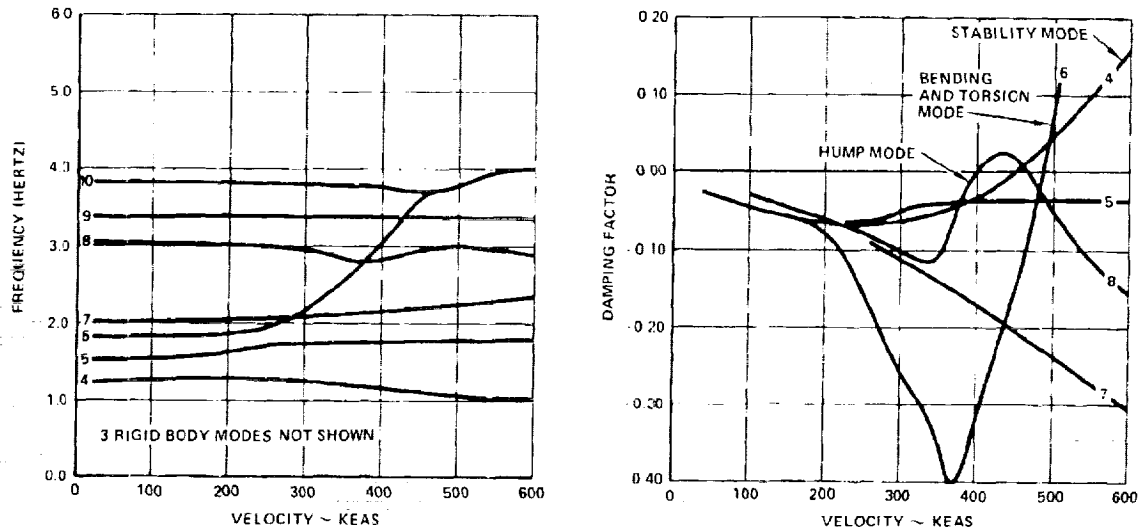


Figure 10-36. Antisymmetric Flutter Analysis - Mach 0.9 - OWE

ANTISYMMETRIC FLUTTER ANALYSIS - CHORDWISE STIFFENED ARRANGEMENT
MACH NO. = 0.9
WEIGHT = 750,000 LBS.

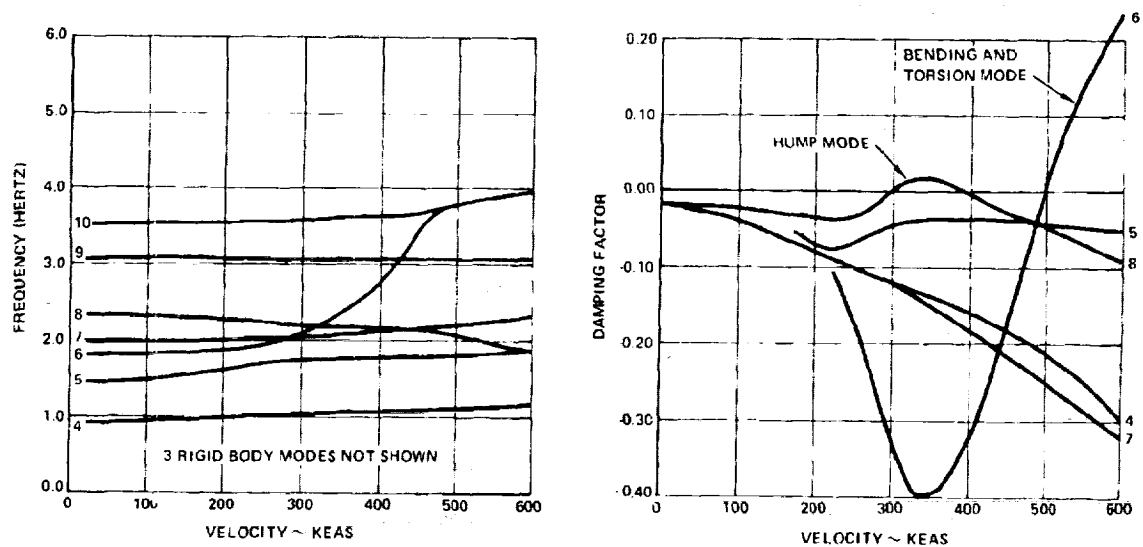


Figure 10-37. Antisymmetric Flutter Analysis - Mach 0.9 - FFFP

Sparwise Stiffened and Monocoque Designs

Symmetric Vibration. - A summary of the lower frequency symmetric vibration modes for the spanwise-stiffened and the monocoque arrangements is presented in Table 10-6 for the full fuel and full payload (FFFP) weight condition. The chordwise stiffened design results of Table 10-4 are shown for reference. The mode frequency comparison indicates that the monocoque design has the greatest stiffness and that the spanwise stiffened design is the most flexible. The mode shapes (not presented) for these three structural arrangements are virtually identical.

Symmetric Flutter. - Symmetric flutter solutions for the 750,000 pound aircraft at Mach 0.90 are shown for the spanwise stiffened and the monocoque arrangements on Figures 10-38 and 10-39, respectively. The analysis of the spanwise design shows two distinct flutter mechanisms: the bending and torsion mode and the stability mode. The bending and torsion mode is the only distinct mechanism noted for the monocoque design. The flutter speeds for the spanwise stiffened and the monocoque arrangements are 364 KEAS and 423 KEAS respectively for the symmetric bending and torsion mode for the 750,000 pound aircraft at Mach 0.90. The flutter speeds for the three structural arrangements investigated are summarized on Figure 10-40.

Flutter Optimization

The vibration and flutter analyses conducted on the chordwise-stiffened, the spanwise-stiffened and the monocoque structural arrangements indicated that the symmetric bending and torsion mode for the full fuel and full payload (FFFP) condition at Mach 0.90 resulted in the lowest symmetric flutter speed. The evidence of the stability mode flutter mechanism for the operating weight empty (OWE) condition at Mach 0.60 as well as the hump mode for the anti-symmetric boundary condition were also noted. A review of the results of the foregoing analyses suggests that stiffening the wing tip structure will eliminate the hump mode flutter and will permit the bending and torsion mode flutter speeds to be pushed beyond the $1.2 V_D$ envelope. Elimination of

ORIGINAL PAGE IS
OF POOR QUALITY

TABLE 10-6. LOWER FREQUENCY SYMMETRIC VIBRATION MODES FOR THE STRUCTURAL ARRANGEMENTS

AIRCRAFT WEIGHT = 750,000 POUNDS

MODE NUMBER	MODE DESCRIPTION	MODE FREQUENCY - HERTZ		
		SPANWISE ARRANGEMENT	CHORDWISE ARRANGEMENT	MONOCOQUE ARRANGEMENT
1	RIGID BODY	0.000	0.000	0.000
2	RIGID BODY	0.000	0.001	0.000
3	WING 1ST BENDING	0.905	0.933	1.010
4	FUSELAGE 1ST BENDING	1.174	1.206	1.267
5	ENGINE PITCH IN PHASE	1.635	1.627	1.714
6	ENGINE PITCH OUT OF PHASE	1.825	1.815	1.955
7	FUSELAGE 2ND BENDING	2.129	2.261	2.236
8	WING 1ST TORSION	3.032	3.104	3.371

SYMMETRIC FLUTTER ANALYSIS - SPANWISE STIFFENED ARRANGEMENT
MACH NO. - 0.9
WEIGHT = 750,000 LBS.

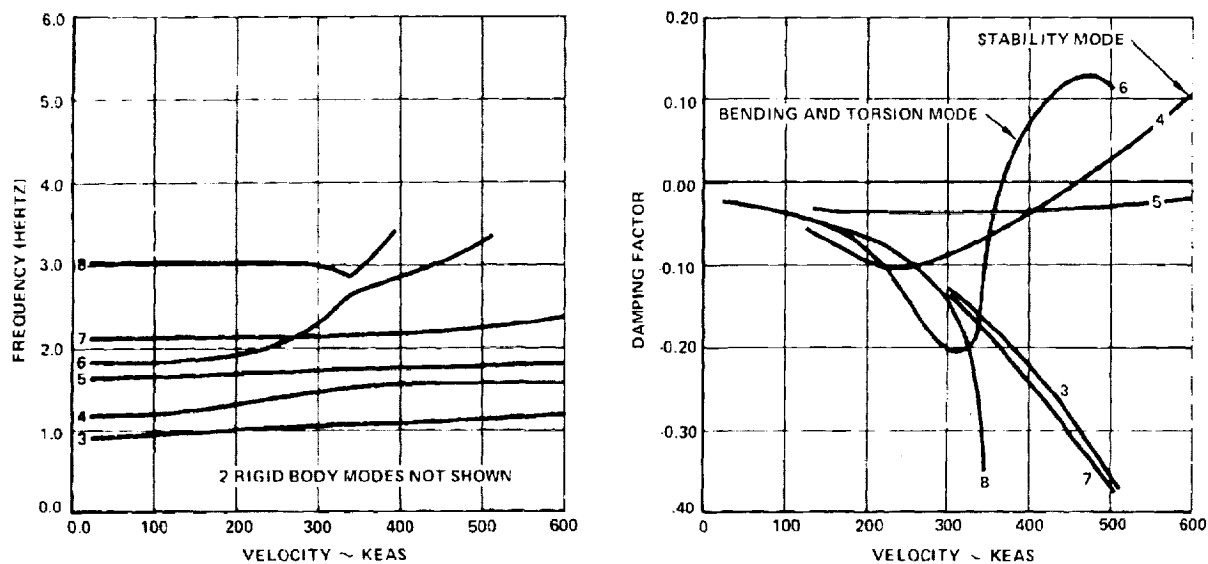


Figure 10-38. Symmetric Flutter Analysis - Spanwise Stiffened Arrangement

SYMMETRIC FLUTTER ANALYSIS - MONOCOQUE ARRANGEMENT
MACH NO. - 0.9
WEIGHT = 750,000 LBS

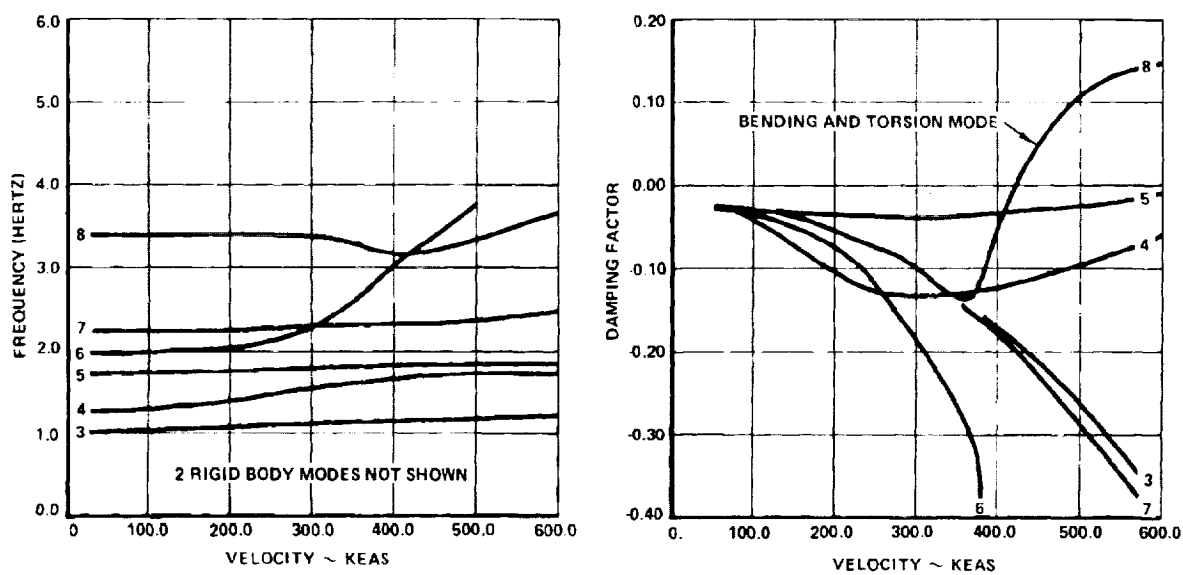


Figure 10-39. Symmetric Flutter Analysis - Monocoque - Arrangement

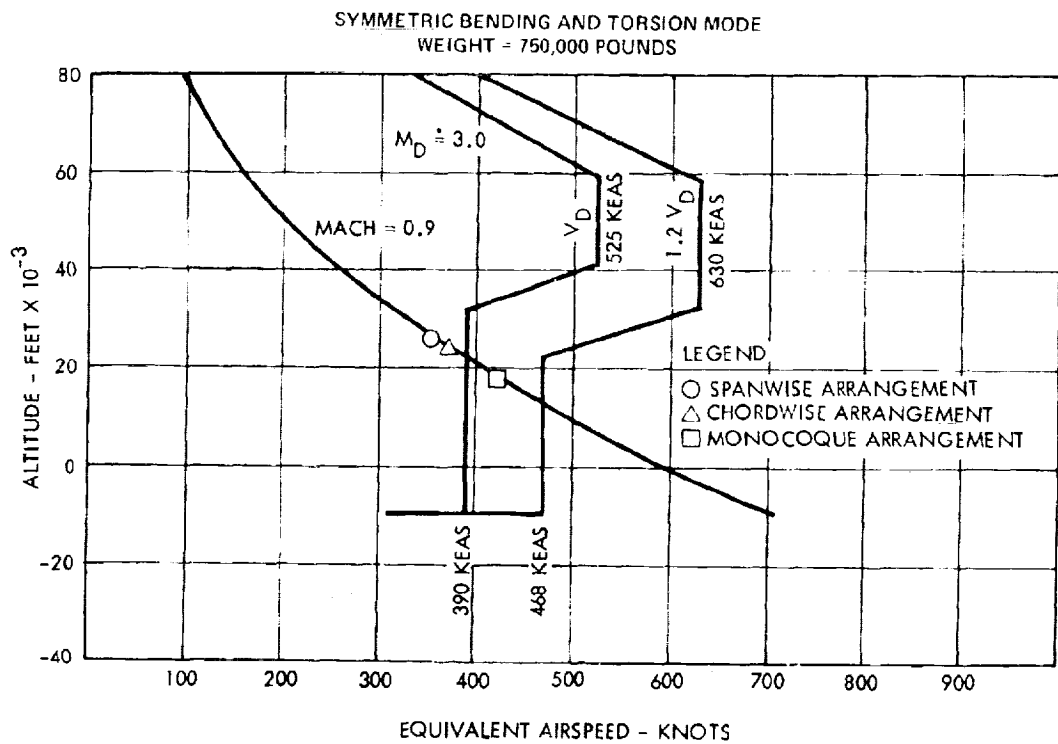


Figure 10-40. Flutter Speeds for the Structural Arrangements

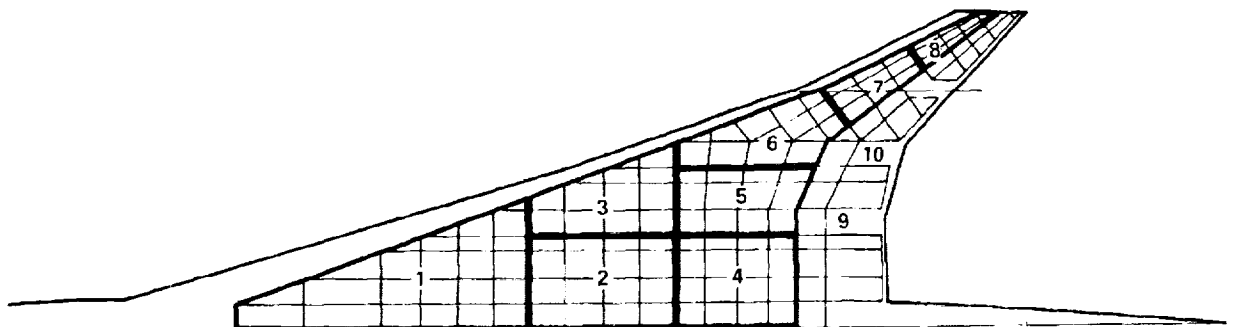


Figure 10-41. Design Regions for Flutter Optimization

the stability mode flutter can most probably be accomplished by stiffening the fuselage. It is recognized that all modes of flutter must be eliminated in the final design of the arrow-wing configuration supersonic cruise transport. This, however, would require further analysis of both the wing and fuselage of the aircraft. A review of Section 2, Baseline Configuration Concept, indicates that configuration changes are planned. The planned changes with regard to the center of gravity location, the pitch moment of inertia, the aerodynamic static margin, fuselage geometry changes and structural model representation, will impact the stability mode flutter speed in a manner yet unknown. As a consequence flutter optimization was not performed on the stability mode.

The evaluation of the various wing structural arrangements can best be accomplished by addressing the symmetric bending and torsion flutter mechanism for the Mach 0.90 FFFP condition. Incremental stiffness requirements and resulting mass additions to push the flutter speed beyond the $1.2 V_D$ envelope or 468 KEAS are determined for these structural arrangements.

To determine the effectiveness and the optimum distribution of material within a particular region of the airplane, the wing planform was divided into 8 regions plus 2 additional regions for each engine rail. Figure 10-41 displays the location of the 10 regions on the wing planform:

1. Forward apex
2. Center box, including landing gear well
3. Center box, outboard of landing gear well
4. Aft box, inboard of the inboard engine rib
5. Aft box, between the engine ribs
6. Transition, aft box to outer wing
7. Outer wing, straddling the wing fin
8. Wing tip
9. Inboard engine rail
10. Outboard engine rail

Natural boundaries were utilized to establish the 10 design regions as indicated by their location with respect to the landing gear well, major chordwise ribs, wing vertical, etc.

The interactive computer graphics program, described earlier, was exercised in determining the most effective region and mass additions required to achieve the desired flutter speed for the structural arrangements. This optimization was conducted using 20 "fixed" eigenvectors for modalization. No updating of mode shapes due to stiffness and mass changes arrived at during the optimization process was attempted in the Task I effort. The results below should therefore be viewed only as trend indicators when comparing one design concept to another.

Chordwise-Stiffened Design. - The chordwise-stiffened arrangement was optimized by increasing spar cap areas and the skin and web thicknesses to provide increases in span bending stiffness and torsional stiffness, respectively. For the chordwise stiffened arrangement 2210 pounds of additional structural material was required in Region 8 to increase the bending and torsion flutter speed from 379 KEAS to 468 KEAS. The optimum stiffness/mass distribution is 425 pounds in the spar caps and 680 pounds in the webs and skin (per side) as shown in Figure 10-42.

Monocoque Design. - The flutter optimization of the monocoque arrangement evaluated the effectiveness of the design regions to achieve the required flutter speed. The structural mass resulting from the addition of skin thickness in the appropriate design regions to provide a simultaneous increase in bending and torsional stiffness to the wing tip structure is shown in Figure 10-43. Region 8 was the most effective region requiring 1240 pounds (620 pounds per side) of additional structural material to increase the bending and torsion flutter velocity from 423 KEAS to 468 KEAS.

Spanwise-Stiffened Design. - The spanwise-stiffened design was not optimized for flutter but the flutter weight penalty was estimated using the data of the foregoing analyses. Estimates for the penalties associated with the spanwise design are presented in Section 12, Structural Concept Analysis. It is anticipated that since the spanwise-stiffened design has the greatest

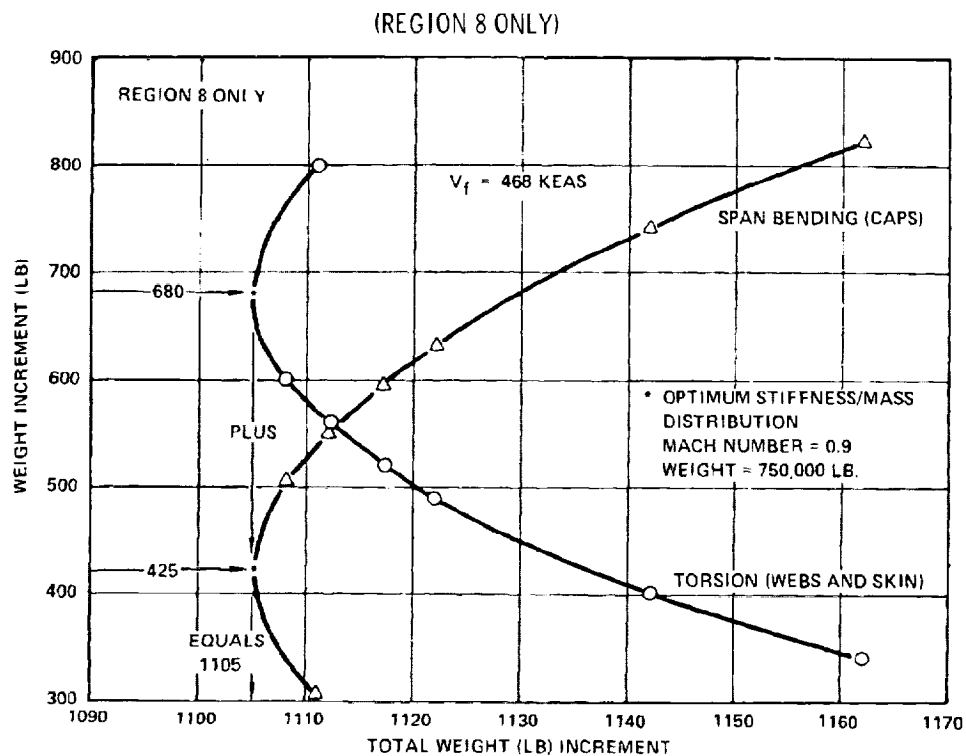


Figure 10-42. Flutter Optimization - Chordwise Stiffened Arrangement

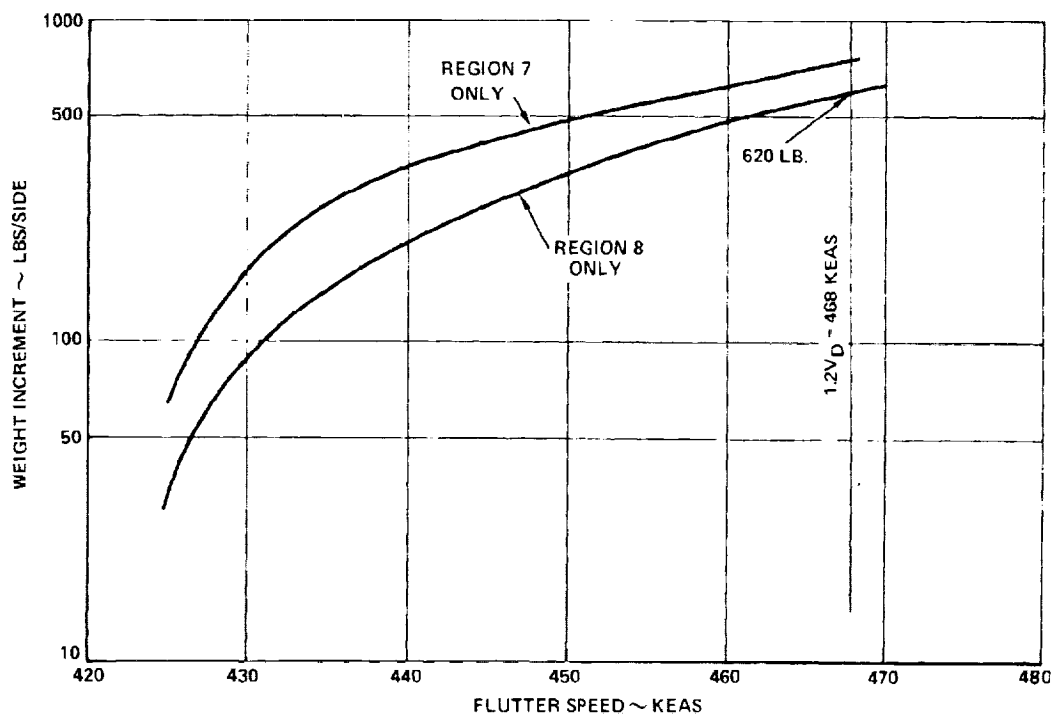


Figure 10-43. Flutter Optimization - Monocoque Arrangements

flexibility, the flutter weight penalties associated with this design will be the greatest.

ENGINEERING DESIGN STUDIES - TASK II

The Engineering Design Studies of Task II are directed toward the detail design and analyses of the structural approach selected as a result of the Task I Analytical Design effort. It is planned in three parts:

1. Configuration Change Investigation - Task IIA
2. Engineering Design Studies - Task IIB
3. Final Design Verification - Task IIC

Configuration Change Investigation - Task IIA

An abbreviated study was conducted using the 2-D NASTRAN structural model which incorporated the airplane configuration changes identified in Section 2, Baseline Configuration Concept. These configuration changes are identified in Figure 10-44; and include the shortened fuselage, the decrease in tip sweep, the increase in aileron area and the associated changes in the wing tip structural box. The fuel tank arrangement and fuel management were also changed to meet the specified center of gravity travel requirements. The element property specifications were identical to the chordwise stiffened arrangement of Task I, however, appropriate mass changes were included.

Symmetric Vibration. - A summary of the lower frequency symmetric vibration modes for the chordwise-stiffened arrangement is presented in Table 10-7 for the aircraft weight of 750,000 pounds. Mode frequency comparisons (Hertz) are presented for the Task IIA and Task I chordwise stiffened designs. Since both designs are represented by identical element flexibilities, the slight decrease in mode frequencies for the Task IIA design is primarily attributed to the increase in tip mass and the distribution of that mass.

The associated vector plots for the full fuel and full payload (FFFP) weight condition are shown for the first eight modes in Figures 10-45 through 10-52.

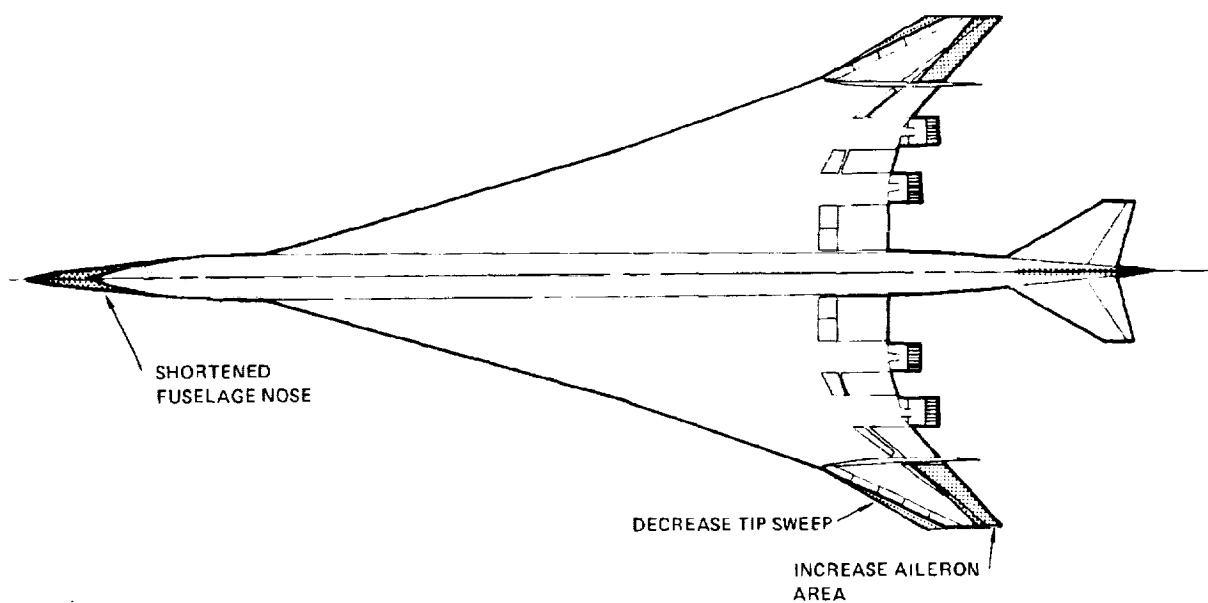


Figure 10-44. Configuration Comparison - Task I and Task IIA

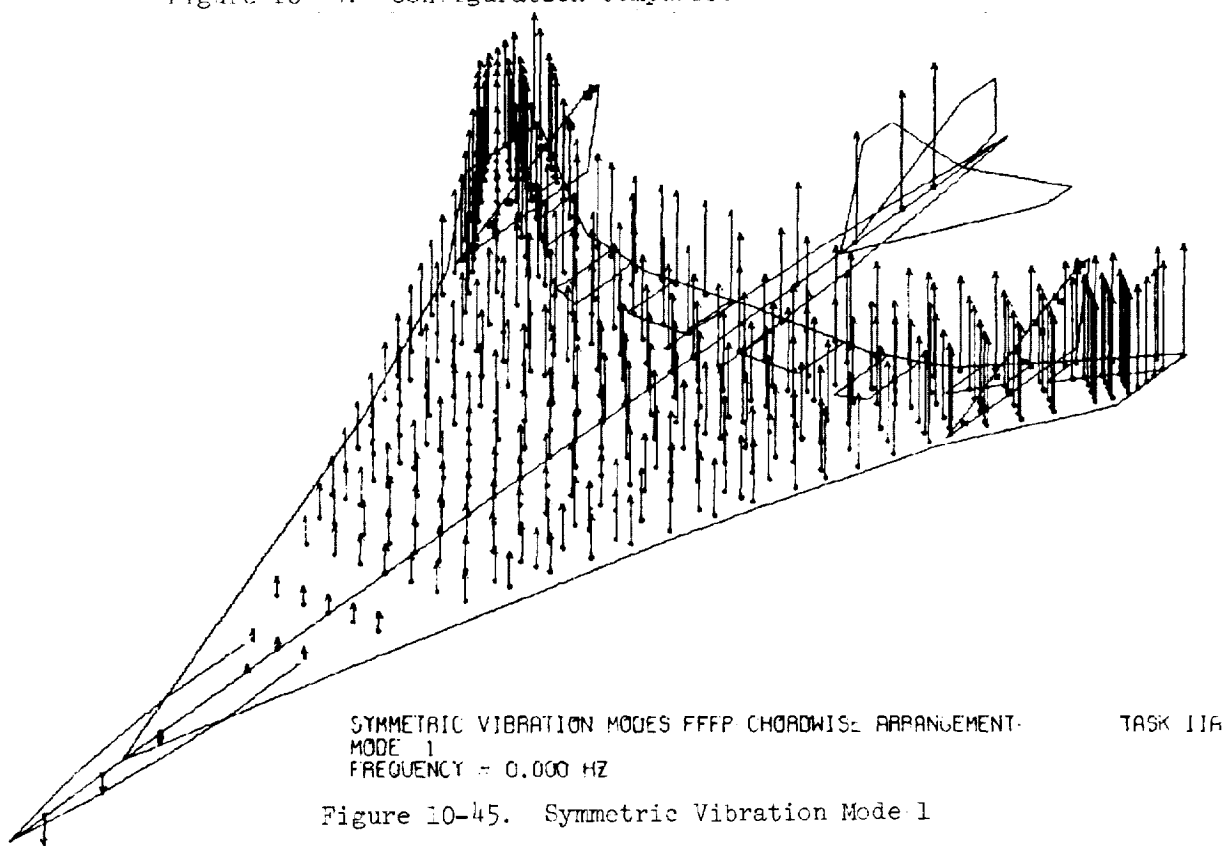


Figure 10-45. Symmetric Vibration Mode 1

TABLE 10-7. LOWER FREQUENCY SYMMETRIC VIBRATION MODES - TASK 11A

AIRCRAFT WEIGHT = 750,000 LBS

MODE NUMBER		MODE FREQUENCY ~ HERTZ	
		TASK II-A	TASK I
1	RIGID BODY	0.000	0.000
2	RIGID BODY	0.000	0.001
3	WING 1ST BENDING	0.868	0.933
4	FUSELAGE 1ST BENDING	1.192	1.206
5	ENGINE PITCH IN PHASE	1.410	1.627
6	ENGINE PITCH OUT OF PHASE	1.544	1.815
7	FUSELAGE 2ND BENDING	2.313	2.261
8	WING 1ST TORSION	2.862	3.104

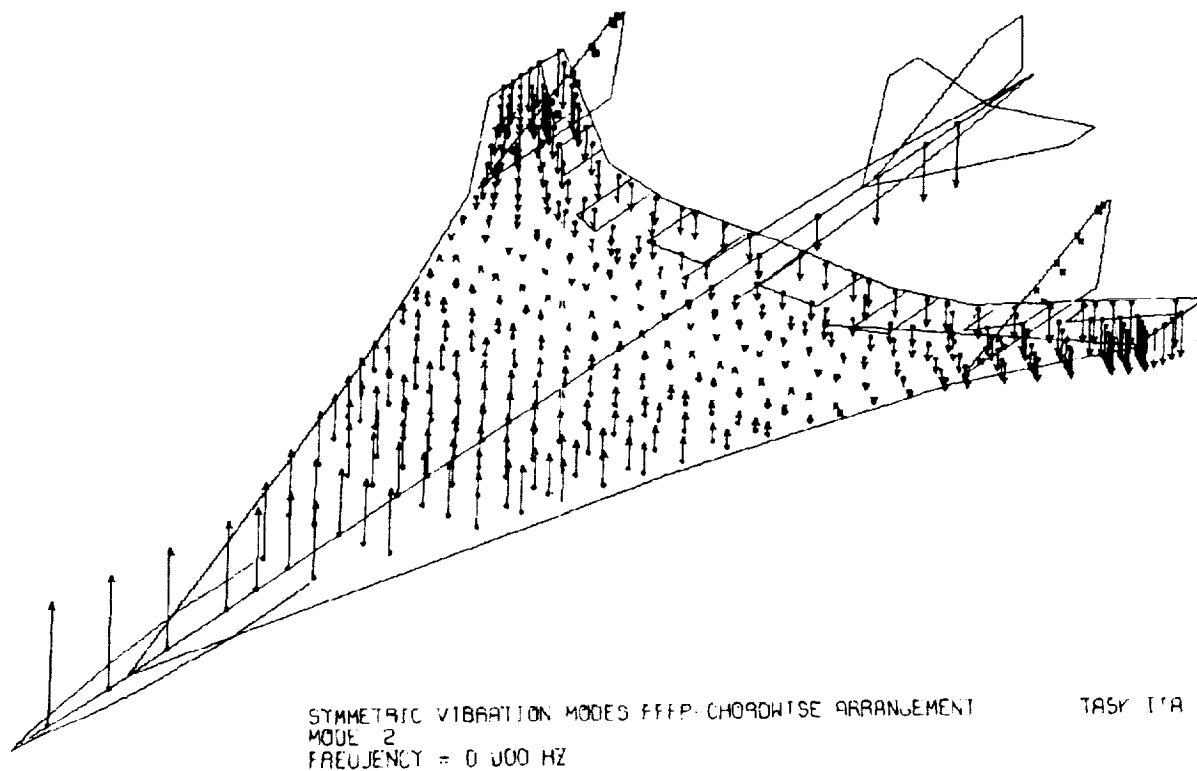


Figure 10-46. Symmetric Vibration Mode 2

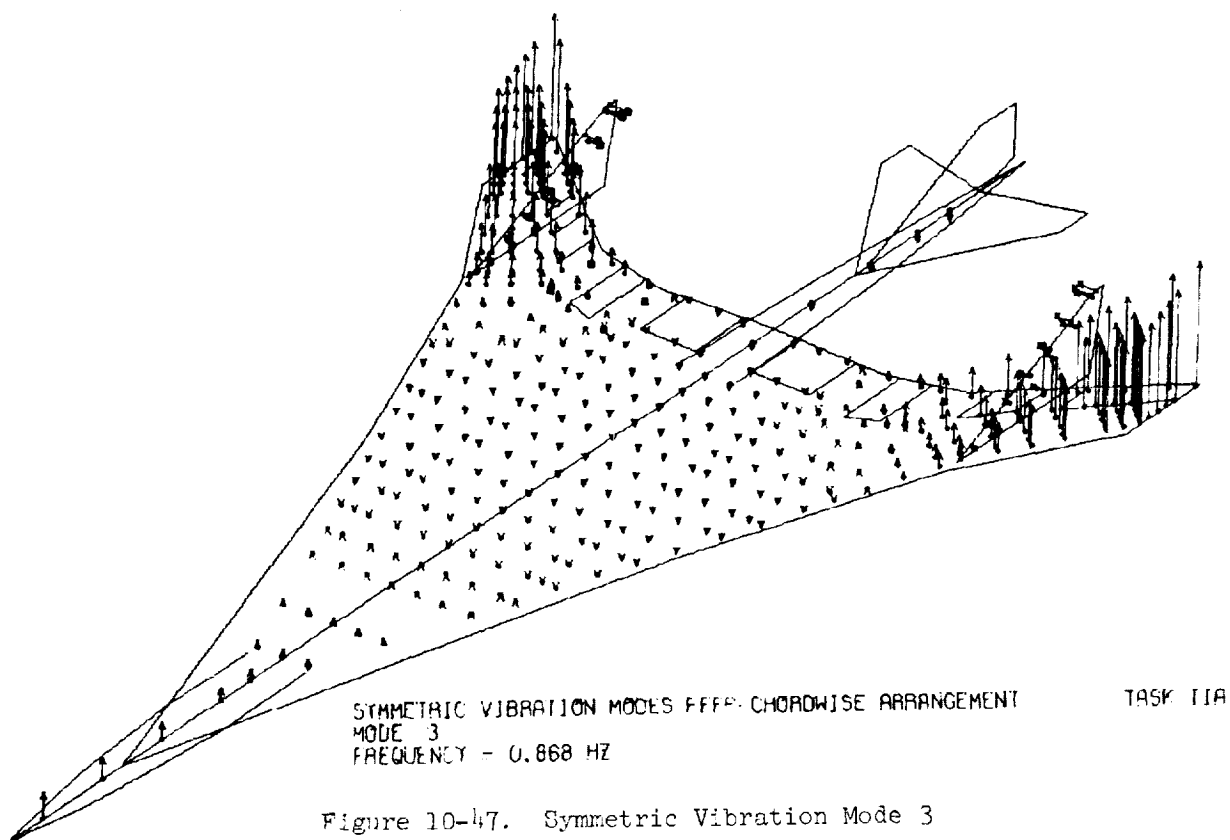


Figure 10-47. Symmetric Vibration Mode 3

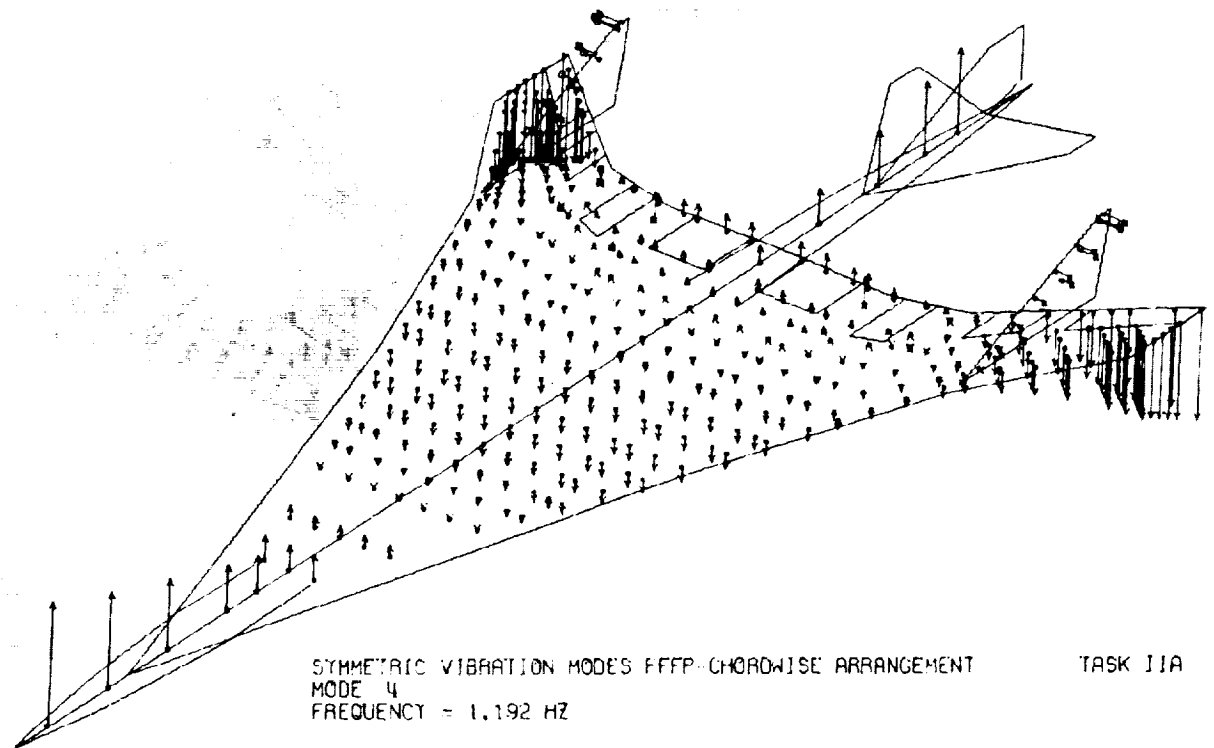


Figure 10-48. Symmetric Vibration Mode 4

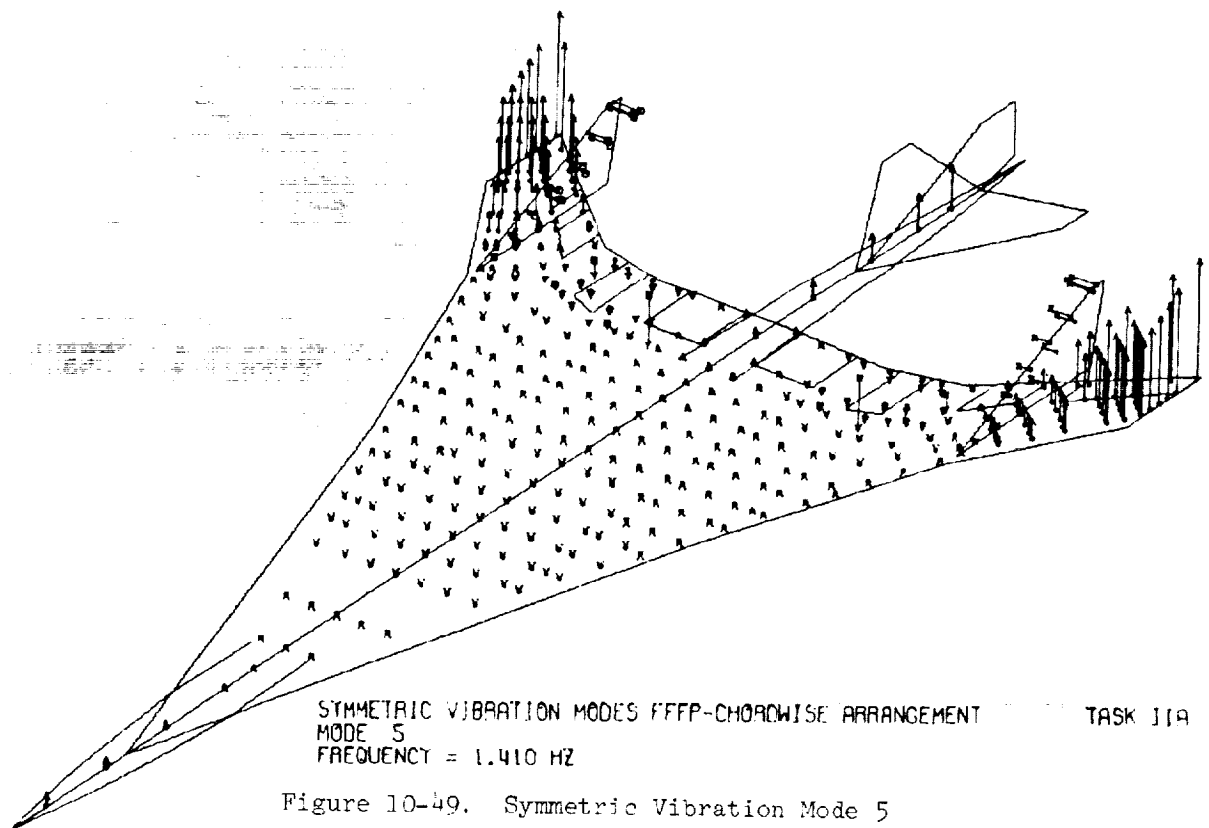


Figure 10-49. Symmetric Vibration Mode 5

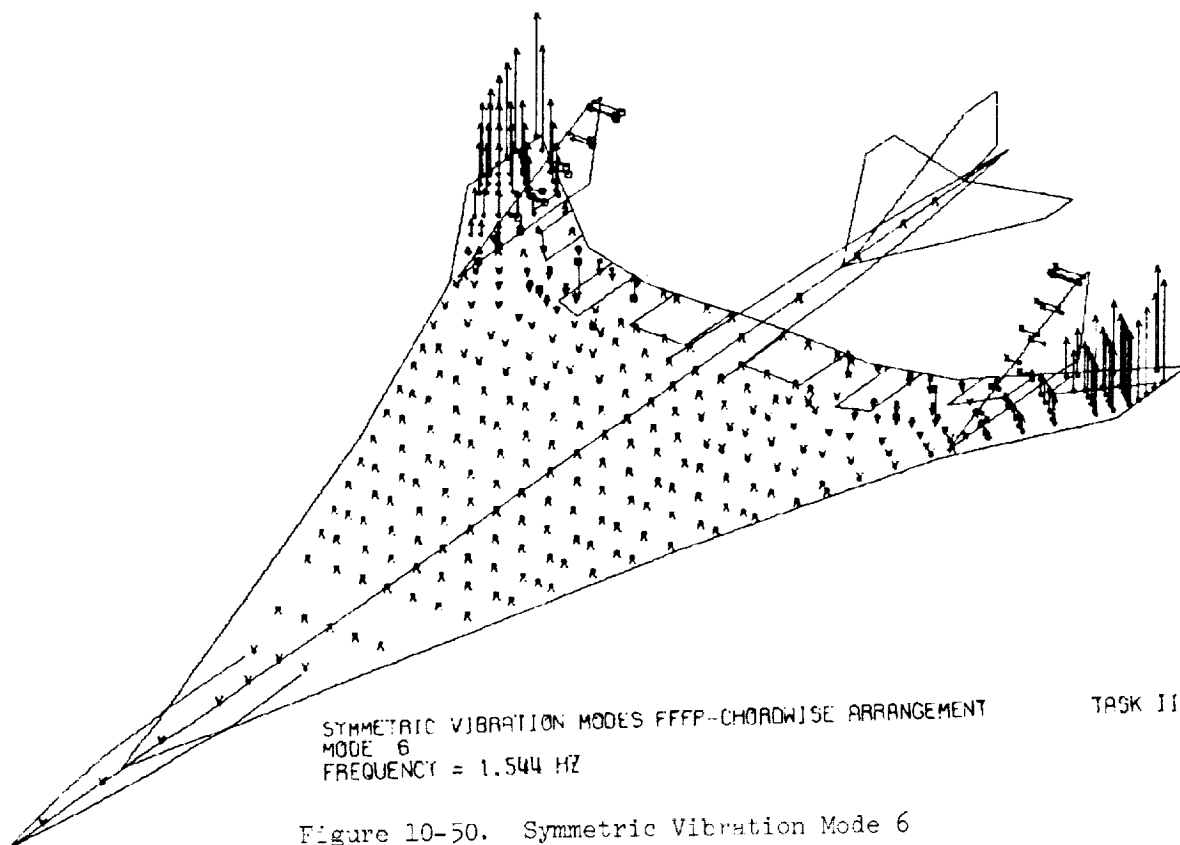


Figure 10-50. Symmetric Vibration Mode 6

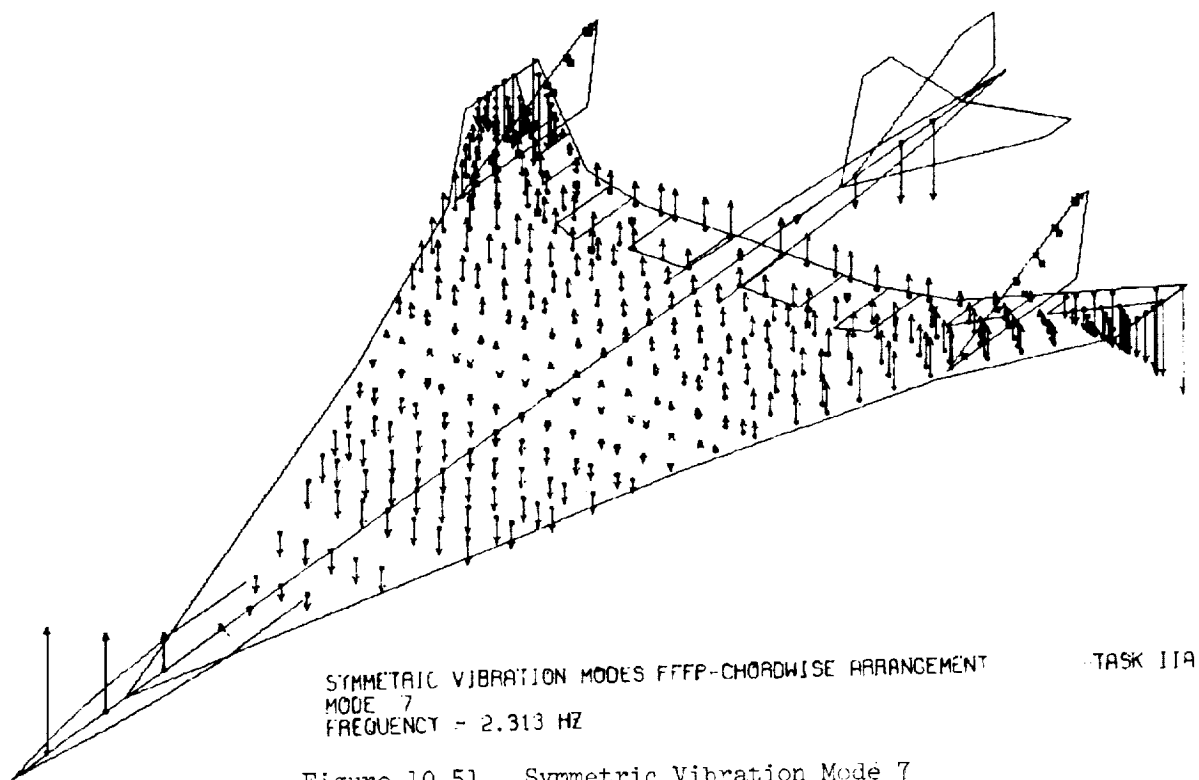
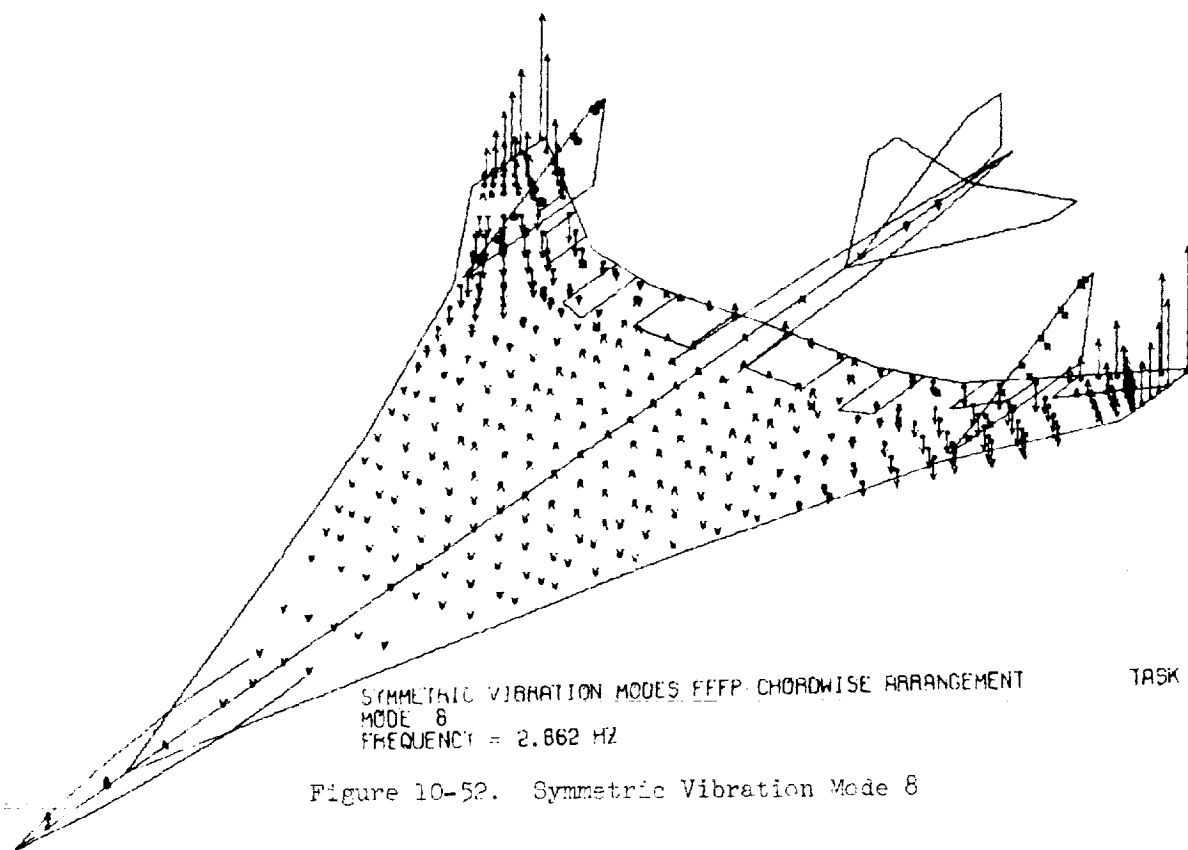


Figure 10-51. Symmetric Vibration Mode 7



TASK IIA

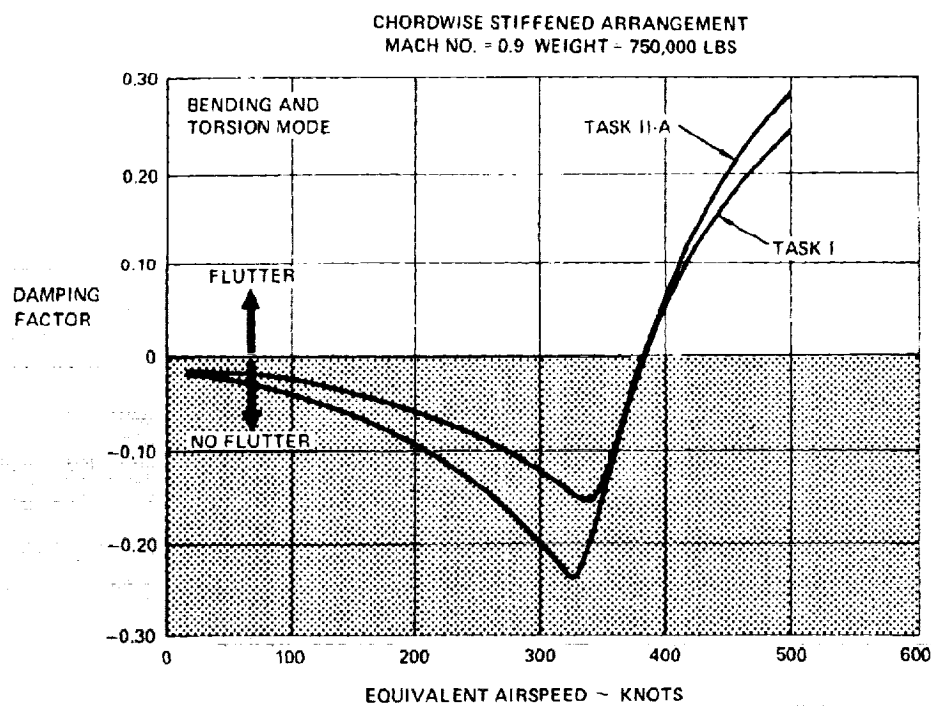


Figure 10-53. Symmetric Flutter Analysis - Task IIA

Symmetric Flutter. - The results of the symmetric flutter analysis for Task IIA are compared in Figure 10-53 with the Task I findings. These data are based on an aircraft weight of 750,000 pounds at Mach 0.90 for the chordwise stiffened design. The flutter speeds and flutter mechanism (bending and torsion mode) as displayed in the figure are virtually identical.

Results. - The findings of this investigation as to the effect of the configuration and mass changes on flutter were significant. The fact that the resulting flutter speed and mechanism were virtually identical for comparable condition, enables one to interpret the Task I results into the Task IIB domain with confidence. Thus, continuity between the initial analytical task and the detail design studies is provided.

Engineering Design Studies - Task IIB

The configuration refinements identified in Section 2, Baseline Configuration, were adopted for the Task II detail design study effort. The structural approach selected for further analysis was a hybrid structural arrangement consisting of the chordwise-stiffened design for the wing structure inboard of BL 406 and the monocoque design for the stiffness critical wing tip structure. A three-dimensional (3-D) structural model, described in the Analytical Methods section, was used with strength-designed element flexibilities.

The vibration and flutter analyses for the strength-design cycle is presented in Figure 10-54. The interrelationship with the other disciplines directly involved in the design cycle is indicated on the figure. The analyses were performed (1) to identify the critical airplane weight condition, (2) to determine the flutter speeds for the OWE and the FFFP weight conditions, and (3) to perform flutter optimization of the wing tip structure to establish the optimum placement of the incremental stiffness over the strength-design to achieve the required flutter speed.

Symmetric Vibration. - Symmetric vibration analyses were performed for the operating weight empty (OWE, 311,000 pound) and the full fuel and full

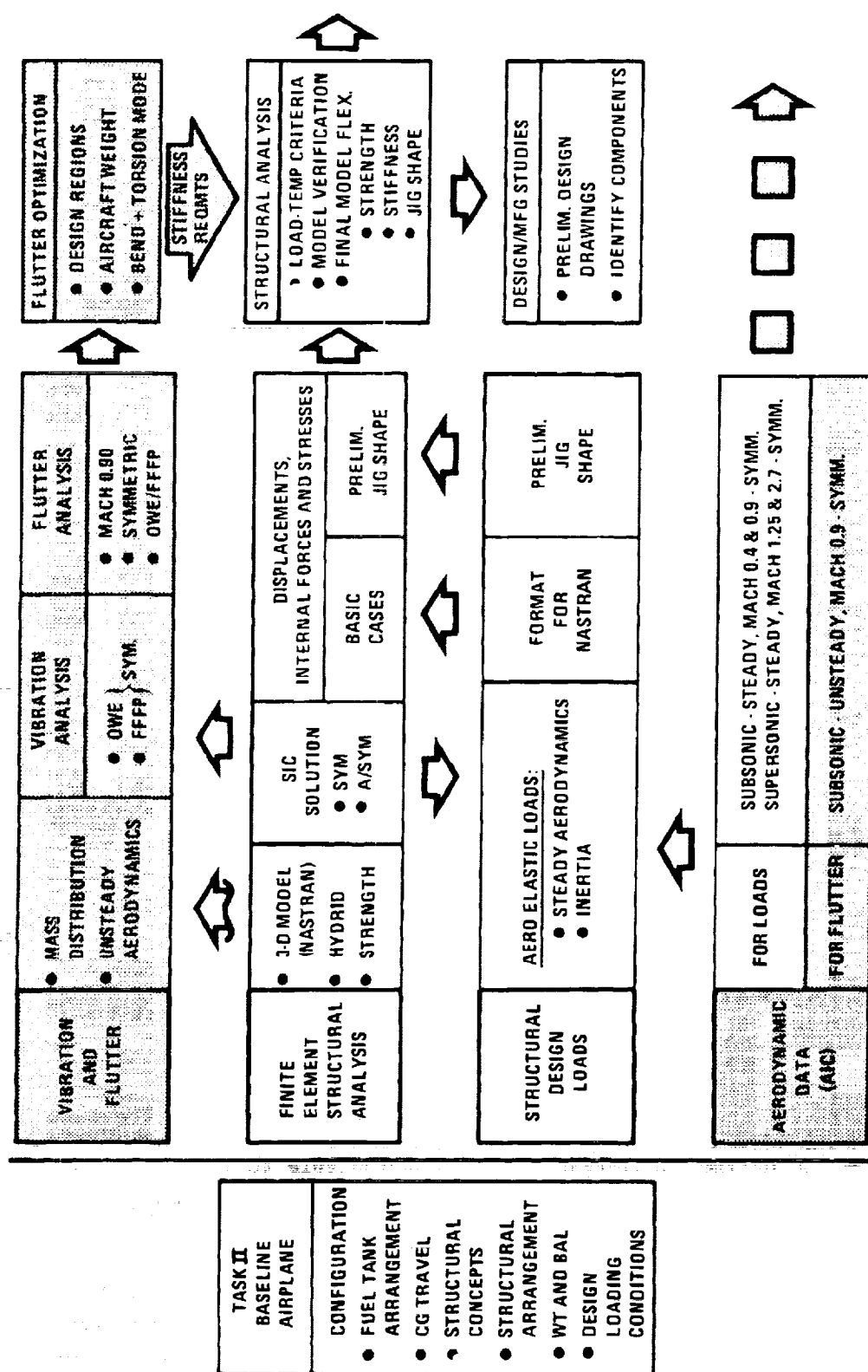


Figure 10-54. Design Cycle - Strength

payload (FFFP, 750,000 pound) weight conditions. The model analyses were conducted for an aircraft with strength-designed flexibilities and mass distribution reflecting the configuration changes adopted (i.e., shortened fuselage, revised fuel tank arrangement (over Task I), increased low speed aileron area, increased engine size and mass).

A summary of the lower frequency symmetric vibration modes and frequencies is presented in Table 10-8. Since the Task IIB airplane structural arrangement is a hybrid consisting of the chordwise-stiffened and monocoque designs, a direct comparison with the Task I mode frequencies (Table 10-6) cannot be made. In general, however, the mode frequencies for the FFFP weight condition for Task IIB exhibit slightly reduced engine pitch - in phase, engine pitch - out of phase, and wing first torsion mode frequencies. These reduced frequencies can be attributed to the greater engine mass and aft center of gravity for the wing tip structural mass resulting from the increased low speed aileron area incorporated in the Baseline Configuration for Task II.

Symmetric Flutter. - Symmetric flutter solutions for the 311,000 pound and the 750,000 pound aircraft are shown in Figures 10-55 and 10-56, respectively. These results for Mach 0.90 indicate two distinct flutter mechanisms: the bending and torsion mode and the stability mode. As noted on Table 10-9, the flutter speed for both weight conditions is 310 KEAS for the bending and torsion mode. The flutter speed for the stability mode is 504 KEAS and 584 KEAS for the OWE and the FFFP conditions, respectively. These results when compared with the Task I findings indicate that the flutter speed for the strength-designed hybrid aircraft is lower than the monocoque and the chordwise-stiffened designs of Task I.

Flutter Optimization. - The optimization of the strength-designed aircraft was performed to define the weight penalty attributable to flutter on an arrow-wing configuration supersonic cruise aircraft (taxi weight of 750,000 pounds). The symmetric bending and torsion mode flutter mechanism for the Mach 0.90 FFFP condition was addressed. Figure 10-57 shows the V_D and $1.2 V_D$ envelope as a function of pressure altitude versus knots equivalent airspeed overlayed with the analysis Mach number line of 0.90. The flutter speed of 310 KEAS

TABLE 10-8. LOWER FREQUENCY SYMMETRIC VIBRATION MODES - STRENGTH DESIGN

TASK II - STRENGTH

MODE NUMBER	MODE DESCRIPTION	MODE FREQUENCY ~ HERTZ	
		OWE	FFFP
1	RIGID BODY	0.000	0.000
2	RIGID BODY	0.000	0.000
3	WING 1ST BENDING	0.960	0.888
4	FUSELAGE 1ST BENDING	1.520	1.233
5	ENGINE PITCH IN PHASE	1.445	1.417
6	ENGINE PITCH OUT OF PHASE	1.607	1.590
7	FUSELAGE 2ND BENDING	3.297	2.392
8	WING 1ST TORSION	2.715	2.793

OWE ~ WEIGHT = 311,000 LBS.

FFFP ~ WEIGHT = 750,000 LBS.

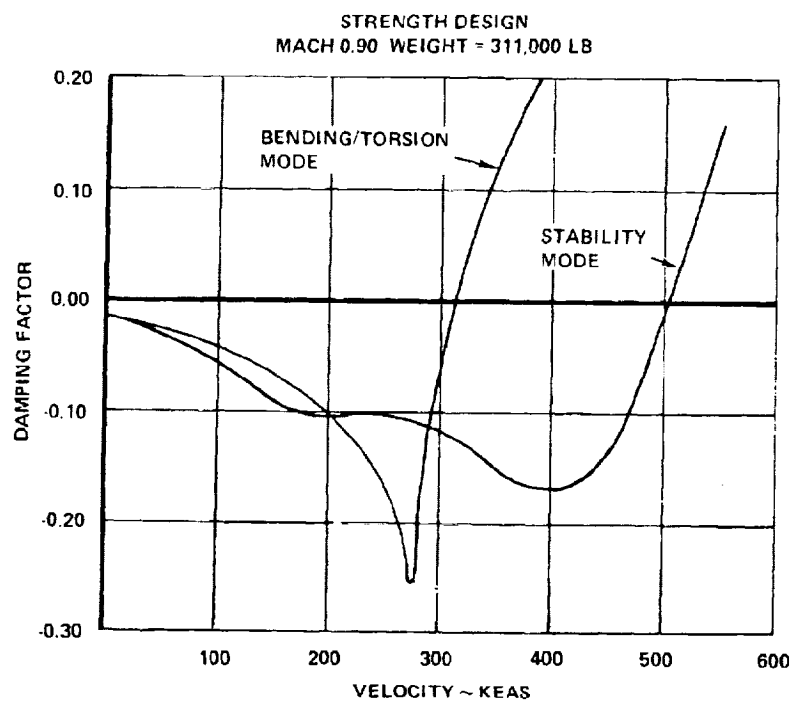


Figure 10-55. Symmetric Flutter Analysis - Mach 0.9 - OWE

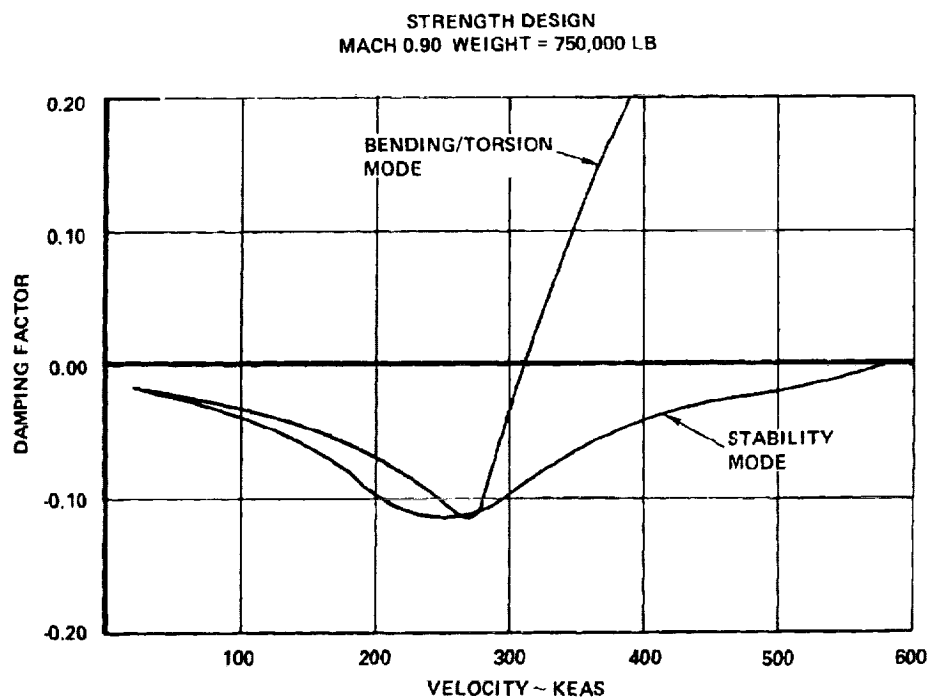


Figure 10-56. Symmetric Flutter Analysis - Mach 0.9 - FFFP

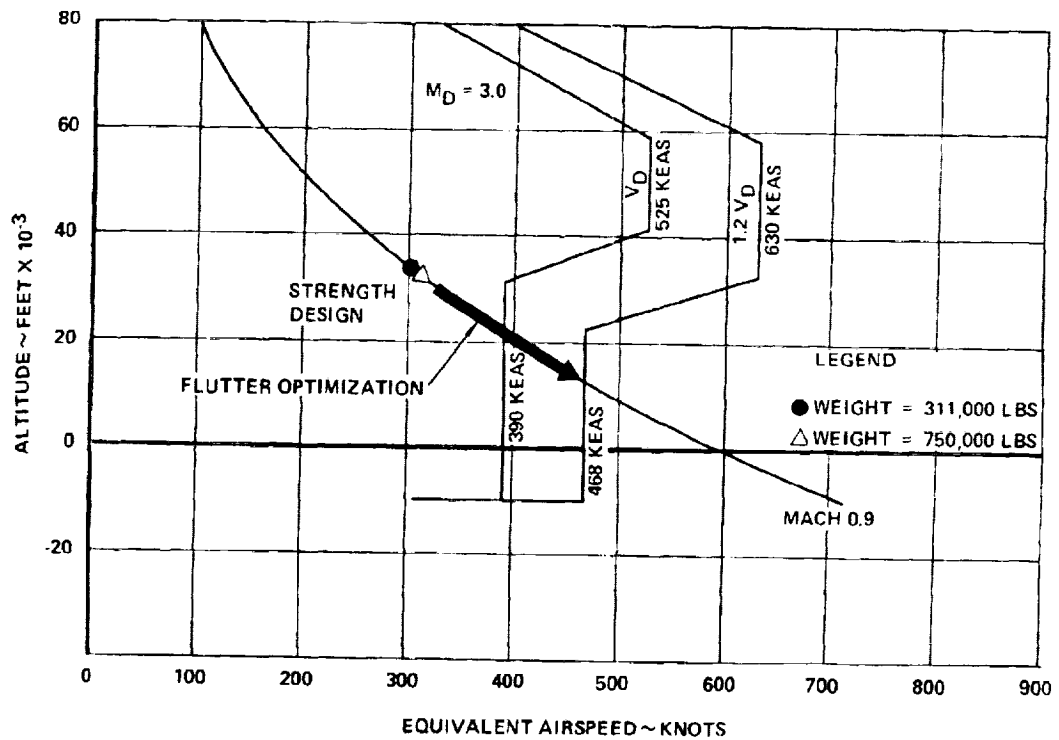


Figure 10-57. Flutter Speeds for Symmetric Bending and Torsion Mode

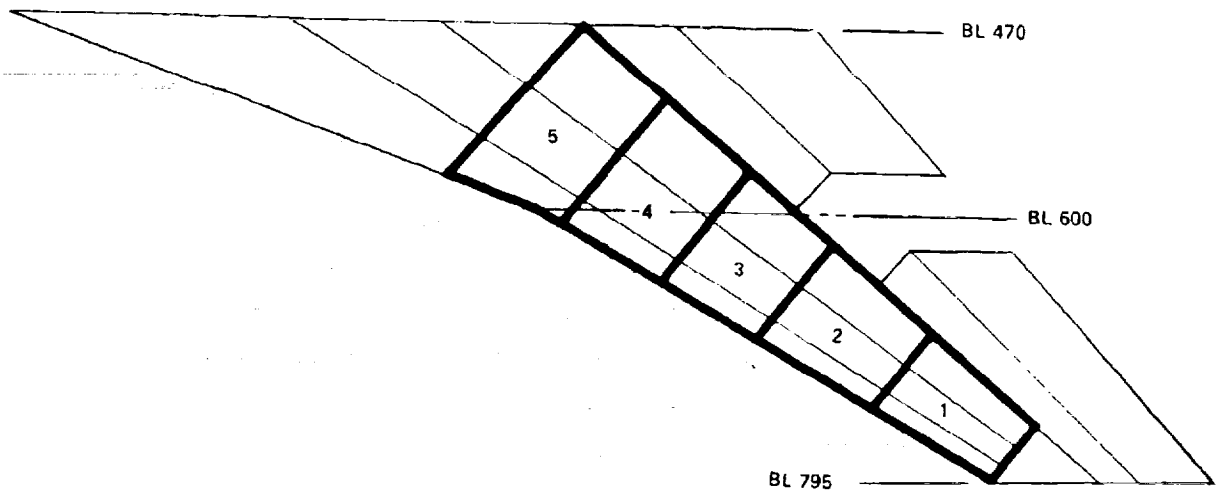


Figure 10-58. Flutter Optimization Design Regions

TABLE 10-9. SUMMARY OF FLUTTER SPEEDS - STRENGTH DESIGN

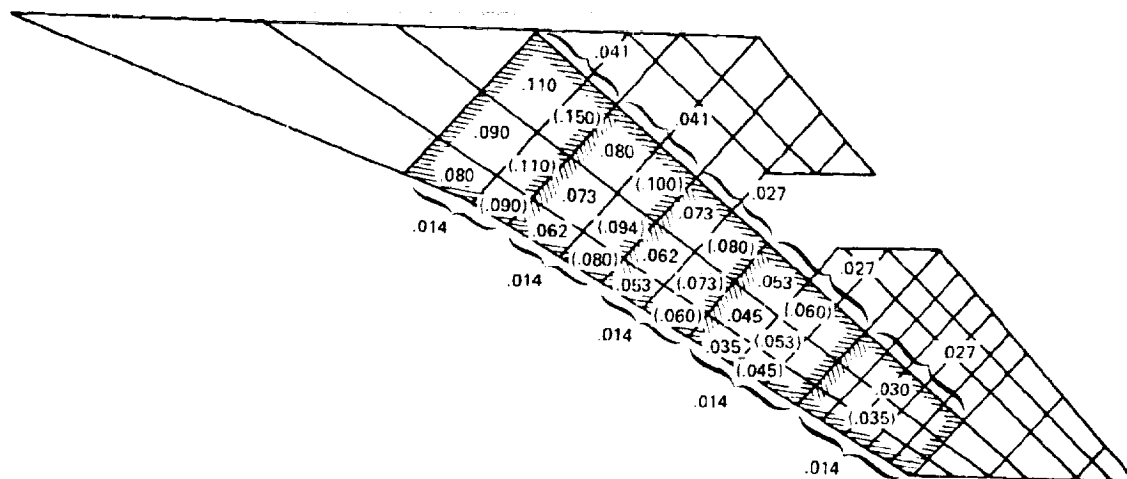
STRENGTH DESIGN:		MACH 0.9, SYMMETRIC BOUNDARY CONDITION
V_f (OWE AND FFFP)	= 310 KEAS	(BENDING AND TORSION MODE)
V_f (OWE)	= 504 KEAS	(STABILITY MODE)
V_f (FFFP)	= 584 KEAS	(STABILITY MODE)

for the strength-designed aircraft is also shown. Through the flutter optimization process (discussed in the Analytical Methods section) the flutter speed was increased beyond the $1.2 V_D$ boundary to 470 KEAS.

The previous solution for the monocoque design (Task I) showed the effectiveness of stiffness and mass additions to the wing tip structure to achieve the desire flutter speed. It was also shown that the bending and torsion mode flutter mechanism was controlled by the wing inertial and flexibility characteristics outboard of BL 470. Thus, to establish the stiffness requirements for flutter suppression the optimization effort focused on the wing tip structure.

Five design regions were defined for the wing tip structure planform (in lieu of 2 for Task I) as indicated on Figure 10-58. The selection of these design regions was based on (1) a review of the Task I results highlighted above, (2) the anticipated structural arrangement for the honeycomb sandwich surface panel design (i.e., panel size, joints, substructure) and (3) the structural behavior (deformations) of the strength-designed wing tip structure. The establishment of the design region boundaries considered the location of the wing vertical and appropriate ribs and spars as may be required. However, the primary influence in the selection was the natural boundaries defined by the structural model, as shown in Figure 10-59.

The flutter optimization was completed and incremental stiffness additions to the wing tip structure identified to achieve 470 KEAS. The optimization



NOTE:

XXX = UPPER SURFACE EFFECTIVE THICKNESS (IN)
 (XXX) = LOWER SURFACE EFFECTIVE THICKNESS (IN)

Figure 10-59. Surface Panel Thickness - Strength Design

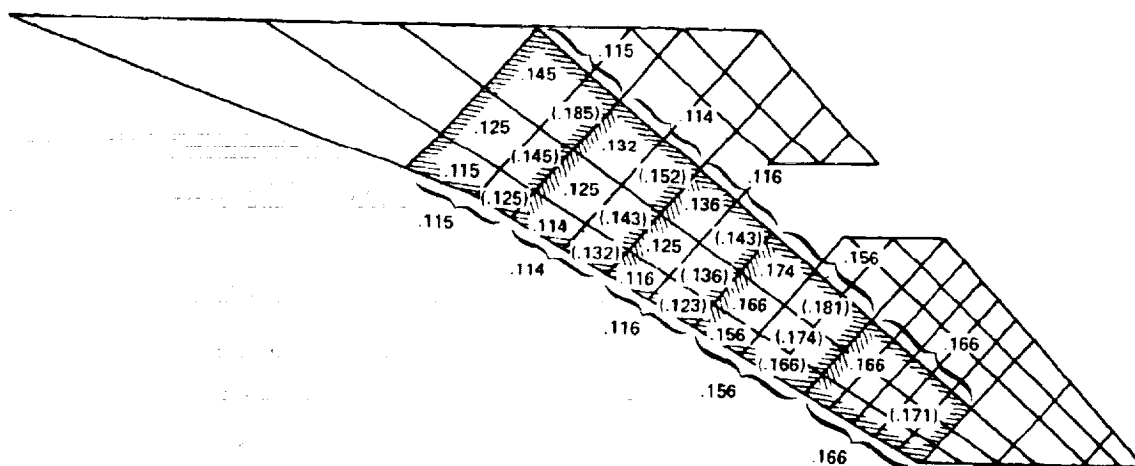


Figure 10-60. Surface Panel Thickness - Stiffness Requirements

process included constraints imposed by design and manufacturing considerations. Fifty modes were used for modalization in the Task II optimization. Four 188th order vibration analyses were conducted during the optimization process. These cases assured that proper mode shapes were being used as the optimization process continued. Each vibration case reflected the stiffness and mass changes called for by the graphics program at that point in the process. The steps taken in the optimization process are detailed below. Tabulation of the step by step data is shown in Table 10-10.

- (1) An examination of the strength requirements of Task IIB and the stiffness requirements of Task I reveals that an increment of approximately 700 percent is necessary to approach the anticipated thickness requirement. This requires the calculation of a sufficient number of $[\Delta K]$'s to provide valid results. It was determined in Task I that if there was a large increase in thickness required in one region, nonlinearities introduced inaccuracies. This problem could be avoided if structure were added to the analysis model to bring it closer to the expected solution. Again, Task I experience indicated that up to an increase of 100 percent, the design variables were very close to being linear.
- (2) A modified base structure was established by making appropriate changes to the NASTRAN elements for the upper panels (CQDMEM), the lower panels (CQDMEM), and the front and rear spar webs (CSHEAR).

The modifications (Δt) were made consistent with the increments shown on Table 10-11. The center panel thicknesses for the modified base case are shown; modifications to the fore and aft panels were similarly made. The estimated weights for these modifications were 715 pounds and 42 pounds (per side) for the panels and spar webs, respectively.

A computer run was made using NASTRAN to generate a new base stiffness matrix for the changes described above. This modified

DESIGN REGION	$\Delta t/\Delta W$ (in/lb)	MODIFIED BASE			OPT-1			OPT-2			OPT-2'			OPT-2''			OPT-3		
		$t(A)$ (in)	$W(B)$ (lb)	W (lb)	Δt (in)	t (in)	W (lb)	Δt (in)	t (in)	W (lb)	Δt (in)	t (in)	W (lb)	Δt (in)	t (in)	W (lb)	Δt (in)	t (in)	
1	0.4333×10^{-3}	0.150	346.16	-100	-0.0433	0.1067	-100	-0.0433	0.1067	-276.93	-0.12	0.03	-276.93	-0.120	0.030	-276.93	-0.12	0.030	-20.0
2	0.32739×10^{-3}	0.135	412.35	534	0.1702	0.3052	400	0.1310	0.2660	-274.9	-0.09	0.045	-274.90	-0.090	0.045	-274.90	-0.09	0.045	322.7
3	0.3808×10^{-3}	0.124	325.64	-200*	-0.0762*	0.0478*	-115	-0.0438	0.0802	-112.9	-0.043	0.081	40.00	0.015	0.139	148.50	0.057	0.181	-115.0
4	0.2962×10^{-3}	0.073	246.44	-10*	-0.0030*	0.0700*	0	0	0.0730	765.0	0.2266	0.2996	467.10	0.138	0.211	246.40	0.073	0.145	75.0
5	0.2604×10^{-3}	0.090	345.65	45	0.0117	0.1017	45	0.0117	0.1017	35.0	0.009	0.099	200.00	0.052	0.142	345.60	0.090	0.180	125.0
$\Sigma(C)$				269			230			135.36			155.3			188.67			367.7

DESIGN REGION	$\Delta t/\Delta W$ (in/lb)	MODIFIED BASE			OPT-5			OPT-5'			OPT-5''			OPT-6			OPT-6'			OPT-6''		
		$t(A)$ (in)	$W(B)$ (lb)	W (lb)	Δt (in)	t (in)	W (lb)	Δt (in)	t (in)	W (lb)	Δt (in)	t (in)	W (lb)	Δt (in)	t (in)	W (lb)	Δt (in)	t (in)	W (lb)	Δt (in)	t (in)	
1	0.4333×10^{-3}	0.015	346.16	10.7	0.005	0.155	-276.93	-0.120	0.030	-70.0	-0.030	0.120	25.1	0.011	0.161	36.4	0.016	0.166	49.3	0.021	0.171	
2	0.32739×10^{-3}	0.135	412.35	60.0	0.020	0.155	293.00	0.096	0.231	125.0	0.041	0.176	79.0	0.026	0.161	94.0	0.031	0.166	111.0	0.036	0.071	
3	0.3808×10^{-3}	0.124	162.82	2.6	0.001	0.125	2.60	0.001	0.125	2.6	0.001	0.125	2.6	0.001	0.125	2.6	0.001	0.125	2.6	0.001	0.125	
4	0.2962×10^{-3}	0.073	246.44	177.0	0.052	0.125	177.00	0.052	0.125	177.0	0.052	0.125	177.0	0.052	0.125	177.0	0.052	0.125	177.0	0.052	0.125	
5	0.2604×10^{-3}	0.090	345.65	134.4	0.035	0.125	134.40	0.035	0.125	134.4	0.035	0.125	134.4	0.035	0.125	134.4	0.035	0.125	134.4	0.035	0.125	
$\Sigma(C)$				384.7			330.07			369.0			418.1			444.4			474.3			

NOTES:

(A) CENTER PANEL THICKNESS (UPPER SURFACE)

(B) TOTAL MASS OF PANELS INCLUDING STRENGTH-DESIGN REQUIREMENTS

(C) WEIGHT INCREMENT OVER MODIFIED BASE (PER SIDE)

* THIS EXCEEDS MAXIMUM ALLOWABLE DECREASE IN WT FROM MODIFIED BASE CASE
(AND PUTS REGION BELOW STRENGTH - DESIGN)

FOLDOUT FRAMES /

FOLDOUT FRAMES 2

TABLE: 10-10. FLUTTER OPTIMIZATION RESULTS

OPT-1'			OPT-2'			OPT-2''			OPT-3			OPT-4			OPT-4'			
t (in)	W (lb)	Δt (in)	t (in)	W (lb)	Δt (in)	t (in)	W (lb)	Δt (in)	t (in)	W (lb)	Δt (in)	t (in)	W (lb)	Δt (in)	t (in)	W (lb)	Δt (in)	
0.1067	-100	-0.0433	0.1067	-276.93	-0.12	0.03	-276.93	-0.120	0.030	-276.93	-0.12	0.030	-20.0	-0.009	0.141	-65.0	-0.028	0.122
0.3052	400	0.1310	0.2660	-274.9	-0.09	0.045	-274.90	-0.090	0.045	-274.90	-0.09	0.045	322.7	0.106	0.241	322.7	0.106	0.241
0.0478*	-115	-0.0438	0.0802	-112.9	-0.043	0.081	40.00	0.015	0.139	148.50	0.057	0.181	-115.0	-0.044	0.080	-115.0	-0.044	0.080
0.0700*	0	0	0.0730	765.0	0.2266	0.2996	467.10	0.138	0.211	246.40	0.073	0.146	75.0	0.022	0.095	147.4	0.044	0.117
0.1017	45	0.0117	0.1017	35.0	0.009	0.099	200.00	0.052	0.142	345.60	0.090	0.180	125.0	0.033	0.123	85.0	0.022	0.112
	230			135.36			155.3			188.67			387.7			375.1		365.3

OPT-5'			OPT-5''			OPT-6			OPT-6'			OPT-6''		
t (in)	W (lb)	Δt (in)	t (in)	W (lb)	Δt (in)	t (in)	W (lb)	Δt (in)	t (in)	W (lb)	Δt (in)	t (in)	W (lb)	Δt (in)
0.155	-276.93	-0.120	0.030	-70.0	-0.030	0.120	25.1	0.011	0.161	36.4	0.016	0.166	49.3	0.021
0.155	293.00	0.096	0.231	125.0	0.041	0.176	79.0	0.026	0.161	94.0	0.031	0.166	111.0	0.036
0.125	2.60	0.001	0.125	2.6	0.001	0.125	2.6	0.001	0.125	2.6	0.001	0.125	2.6	0.001
0.125	177.00	0.052	0.125	177.0	0.052	0.125	177.0	0.052	0.125	177.0	0.052	0.125	177.0	0.052
0.125	134.40	0.035	0.125	134.4	0.035	0.125	134.4	0.035	0.125	134.4	0.035	0.125	134.4	0.035
	330.07			369.0			418.1			444.4			474.3	

IN REQUIREMENTS

WT FROM MODIFIED BASE CASE

FOLDOUT FRAME:

FOLDOUT FRAME 2

10-73

TABLE 10-11. CENTER PANEL THICKNESS - MODIFIED BASE CASE

Design Region	Strength t (in.)	Modification Δt (in.)	Percent Modification (Δ -%)	Anticipated Solution (in.)	Modified Base	
					t_u (in.)	t_l (in.)
1	0.030 (u)	0.120	400	0.260	0.150	0.155
	0.035 (l)					
2	0.045 (u)	0.090	200	0.260	0.135	0.143
	0.053 (l)					
3	0.062 (u)	0.062	100	0.120	0.124	0.135
	0.073 (l)					
4	0.073 (u)	0	0	0.073	0.073	0.091
	0.091 (l)					
5	0.090 (u)	0	0	0.090	0.090	0.110
	0.110 (l)					

NOTE: (u), upper surface thickness
(l), lower surface thickness

PRECEDING PAGE BLANK NOT FILMED

base, shown in Table 10-10, is the basis for the subsequent flutter optimization effort.

- (3) Fifty mode shapes from the strength-sized vibration case were used to modalize $[\Delta K]$ and $[\Delta M]$ matrices for use in the optimization process. The first cycle in this process yielded the OPT-1' structure. The mathematical model was updated to correspond to this structure and another vibration case was run.
- (4) These modes were used to update (remodalize) the $[\Delta K]$ and $[\Delta M]$ matrices, and the graphics program was used for optimization — yielding the OPT-2' structural solution.
- (5) The OPT-2' structure was used in a 188th order vibration case and the resulting modes used to update $[\Delta K]$'s and $[\Delta M]$'s. By moving the structure from regions 1 and 2 to 4 and 5, the flutter speed decreased from 455 KEAS for the OPT-1' structure to 416 KEAS for the OPT-2' structure. It was observed that this movement increased the frequency of mode 1 and decreased mode 8, the two modes which interact to cause flutter.
- (6) With the decrease in the flutter speed noted, it was then decided to go back to the OPT-1' structure and make only a 25-percent change in the existing structural distribution. With this limitation, the OPT-3 structure was calculated. A 50th order vibration analysis was conducted on the graphics scope and the results showed very little frequency shift (or change in eigenvectors) for this structural distribution.
- (7) Remodalization with 50 modes from the OPT-3 structure was performed and through graphics flutter analysis it was determined that a flutter speed of 468 KEAS was achieved. The flutter weight penalty was 1145 pounds (per side).
- (8) Continuing to optimize with the above modes, the OPT-4' structure was established. The resulting weight penalty for flutter was 1122 pounds (per side), thus indicating that the

distribution of stiffness was approaching an optimum. A review of the panel thicknesses, however, indicated that the distribution was not favorable from the design and manufacturing viewpoint.

- (9) A review of the center panel thicknesses for regions 3, 4, and 5 for the OPT-3 and the OPT-4' structure indicated thickness variations from 0.080 to 0.123 inch and 0.080 to 0.125 inch for the respective structure. Furthermore, review of the structural arrangement drawings revealed that the wing fin is diagonally located in these regions. Practically, it would be highly desirable if the thickness of the three regions were identical. Therefore, 0.125 inch was selected for center panel thickness for regions 3, 4, and 5.
- (10) To determine the approximate weight penalty over a flutter optimum case, further analyses on the graphics scope were performed. Two cases for further analysis were identified:

Case A Regions 3, 4, and 5 = 0.125 inch

Regions 1 and 2 optimized

Case B Regions 3, 4, and 5 = 0.125 inch

Region 1 = Region 2

Case A resulted in the OPT-5" structure and a total flutter weight penalty of 1126 pounds (per side). The thickness requirements for regions 1 and 2 were 0.120 and 0.176 inch, respectively.

Case B resulted in the OPT-5 structure and a total flutter weight penalty of 1142 pounds (per side). The best solution previously (with good mode shapes) was the OPT-4' structure which resulted in a total flutter penalty of 1122 pounds (per side). Thus it appears that the weight penalty for (B) is approximately 20 pounds per side or 40 pounds per aircraft. A continued optimization/remodalization process could possibly result in less penalty than 1122 pounds (per side) for the OPT-4' structure, however, it is unlikely that it would be substantially less.

Thus, it appears that the above manufacturing constraints do not add a significant amount to the flutter weight penalty.

- (11) A 188th order modal update was performed with the OPT-5 structure producing the QV15 mode shapes. $[\Delta K]$'s and $[\Delta M]$'s were remodalized with these results. With these new mode shapes the flutter speed for the OPT-5 structure was 465.6 KEAS, 2.4 KEAS from 1.2 V_D .
- (12) For the final structure, the Case B approach was adopted from the standpoint of overall practicability and near minimum weight. It was further decided to require a flutter speed of 470 KEAS, allowing the additional 2 KEAS, to account for the assumption of linear $[\Delta K]$'s and for the fact that the 188th order remodalization does not reflect a true sizing change.

The final solution was the OPT-6' structure, which resulted in a 1201 pound (per side) increase over the strength-design. Thus the flutter weight penalty, considering design and manufacturing constraints, for the Baseline Configuration for Task II is 2402 pounds. The center panel thickness for Regions 1 and 2 is 0.166 inch and for Regions 3, 4, and 5 is 0.125 inch as shown in Table 10-10. The corresponding panel thicknesses for the lower surface and the fore and aft panels are presented in Figure 10-60.

Final Design Verification Studies

The element specifications of the strength/stiffness design reflect the changes to the airframe resulting from the strength analysis (including jig shape assessment), stiffness requirements and the associated structural weight distribution defined by the flutter optimization results, and design and manufacturing considerations. The latter includes further consideration of uniform thickness of material over a complete design region (reference Section 12, Structural Concepts Analysis).

The vibration and flutter analyses for the strength/stiffness design cycle are presented in Figure 10-61. The interrelationships with the structural model and unsteady aerodynamic data requirements for the flutter analysis at Mach 0.60, Mach 0.90 and Mach 1.85 are indicated on the figure.

The results of the modal and flutter analyses verify the capability of the final design airplane to meet or exceed the specified requirements. Furthermore, if deficiencies are identified, further recommendations for research and development studies are delineated.

Symmetric Vibration. - Symmetric vibration analyses were conducted for the operating weight empty (OWE) and the full fuel and full payload (FFFP) weight conditions. These extreme weight conditions represent an airplane weight of 314,000 pounds and 750,000 pounds, respectively. The 3000 pound increase in the OWE is the collective result of structural penalties for flutter and additional strength requirements.

A summary of the lower frequency symmetric vibration modes and frequencies is presented in Table 10-12. The mode frequency (Hertz) comparison with the strength-design (Table 10-8) indicates that for both weight conditions all modes, with the exception of the fuselage second bending mode for the OWE condition, exhibit an increase in frequency. The associated vector plots for the full fuel and full payload (FFFP) are presented in Figures 10-62 through 10-70 for the first nine modes. The vector plots for the operating weight empty (OWE) condition are presented in Figures 10-71 through 10-79 for the same nine modes.

Antisymmetric Vibration. - A summary of the lower frequency vibration modes for the final design is presented in Table 10-13. The summary compares the mode frequencies for the final design and the chordwise stiffened design of Task I for the full fuel and full payload weight condition. All frequencies are approximately the same with exception of the fuselage second bending mode which is less for the final design.

Symmetric and Antisymmetric Flutter. - Symmetric and antisymmetric flutter analyses were performed at Mach 0.90. The significant symmetric flutter

modes are shown in Figures 10-80 and 10-81. Note that the symmetric bending and torsion flutter speed for the 314,000 pound and the 750,000 pound airplane are almost identical. This was also true for the strength-designed airplane analyzed in Task IIB (Table 10-9). These results imply that the flutter speed is insensitive to fuel and payload scheduling. The anti-symmetric flutter speeds for the 750,000 airplane were well in excess of 600 KEAS.

The difference between the 514 KEAS flutter speed and the desired 470 KEAS for an optimum design can be explained by the changes due to design and manufacturing considerations which were made to the structure after a "flutter optimum" design (OPT-6') had been computed (reference Section 12, Structural Concepts Analysis). This was proven by resizing the NASTRAN model to correspond exactly to the OPT-6' structure and conducting a vibration and flutter analysis on this structure. The result was a flutter speed of 475 KEAS; the 5 KEAS difference being explained by the assumption of linear stiffness variation for design variables in Task II. Thus the validity of the optimization method was demonstrated.

The 314,000 pound airplane for the symmetric boundary condition exhibited the lowest flutter speed, thus this condition was selected for the flutter investigation at Mach 0.60 and Mach 1.85.

Figure 10-82 presents the results of the symmetric flutter solution at Mach 0.60. The damping factor versus flutter speed variation for Mach 0.60 displays three distinct flutter mechanisms: the bending and torsion mode, the stability mode and the hump mode. The flutter speed for the stability mode is 410 KEAS and the bending and torsion mode flutter speed is 639 KEAS. These mode shapes and the resulting flutter speeds are very similar to the Task I chordwise stiffened design shown earlier on Figure 10-18. It is noted that the stability mode characteristics remain essentially unchanged by the stiffening of the wing tip structure.

The symmetric flutter analysis results at Mach 1.85 are presented in Figure 10-83. The flutter mechanisms observed for this Mach number are the

TABLE 10-12. LOWER FREQUENCY SYMMETRIC VIBRATION MODES - FINAL DESIGN

HYBRID STRUCTURAL ARRANGEMENT

MODE DESCRIPTION	MODE FREQUENCY ~ HERTZ	
	OWE	FFFP
RIGID BODY	0.000	0.000
RIGID BODY	0.000	0.000
WING 1ST BENDING	0.996	0.915
FUSELAGE 1ST BENDING	1.645	1.345
ENGINE PITCH IN PHASE	1.499	1.494
ENGINE PITCH OUT OF PHASE	1.752	1.735
FUSELAGE 2ND BENDING	3.025	2.478
WING 1ST TORSION	3.694	3.174

OWE ~ WEIGHT = 314,000 LBS
 FFFP ~ WEIGHT = 750,000 LBS

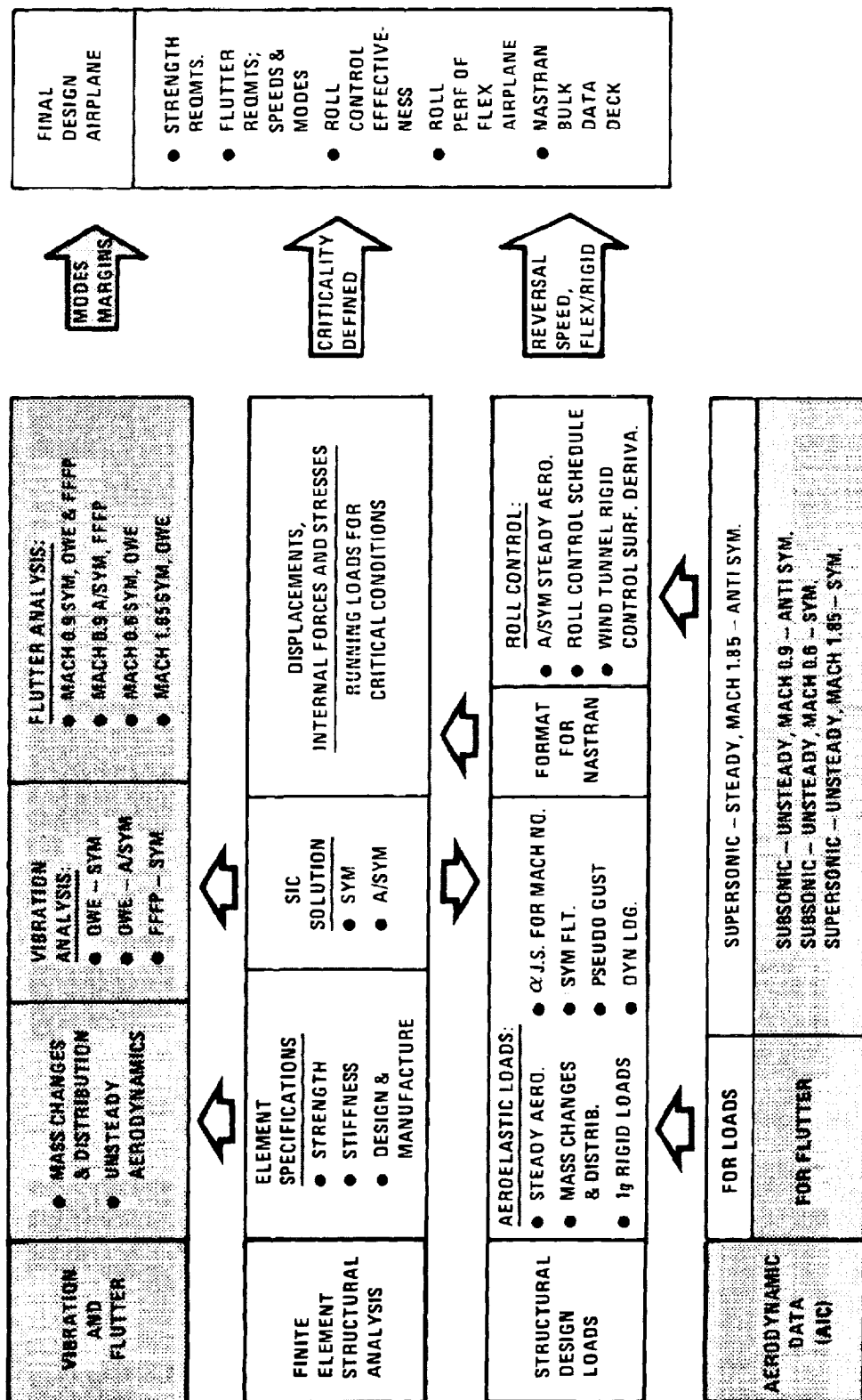


Figure 10-61. Design Cycle - Strength/Stiffness

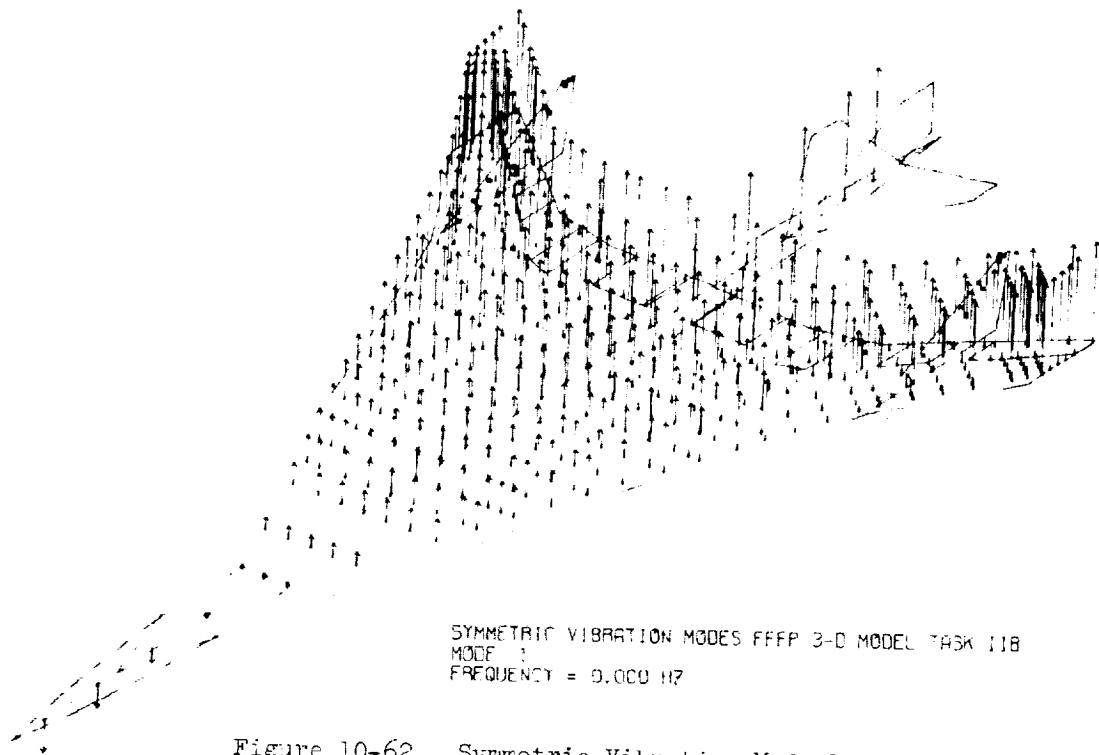


Figure 10-62. Symmetric Vibration Mode 1 - FFPP

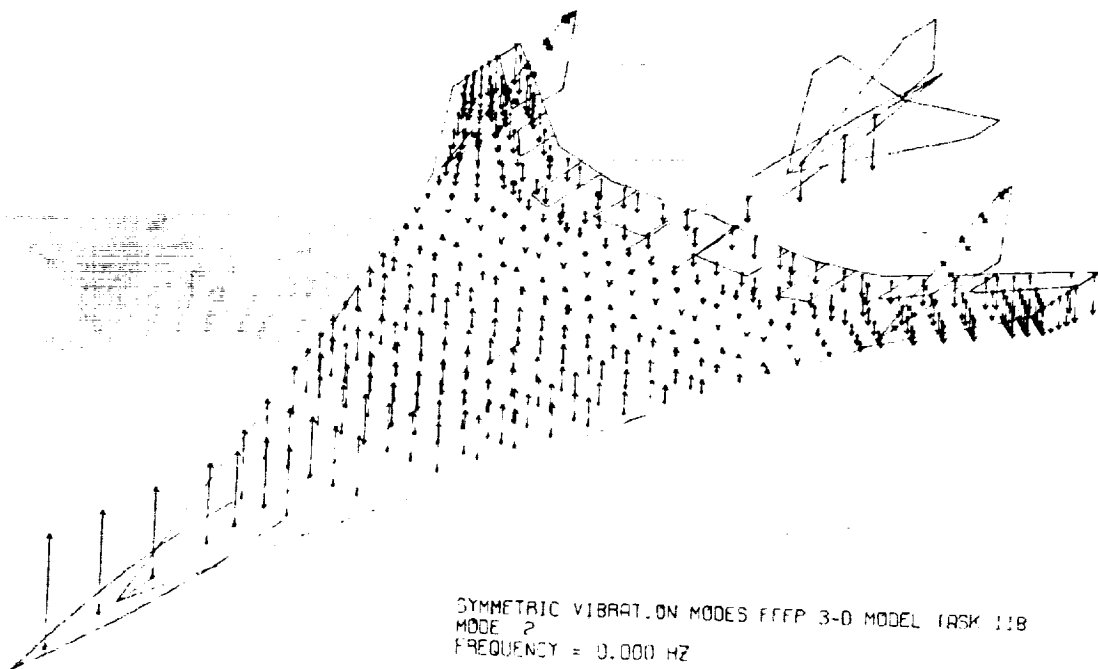


Figure 10-63. Symmetric Vibration Mode 2 - FFPP

ORIGINAL PAGE IS
OF POOR QUALITY

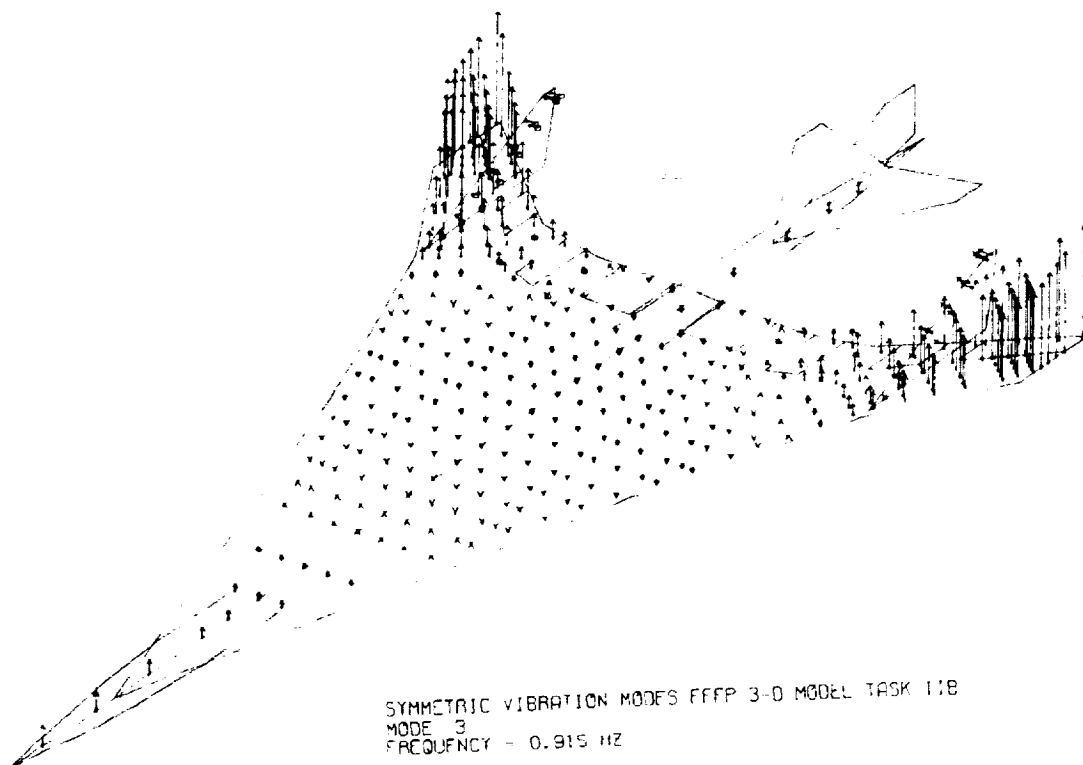


Figure 10-64. Symmetric Vibration Mode 3 - FFFP

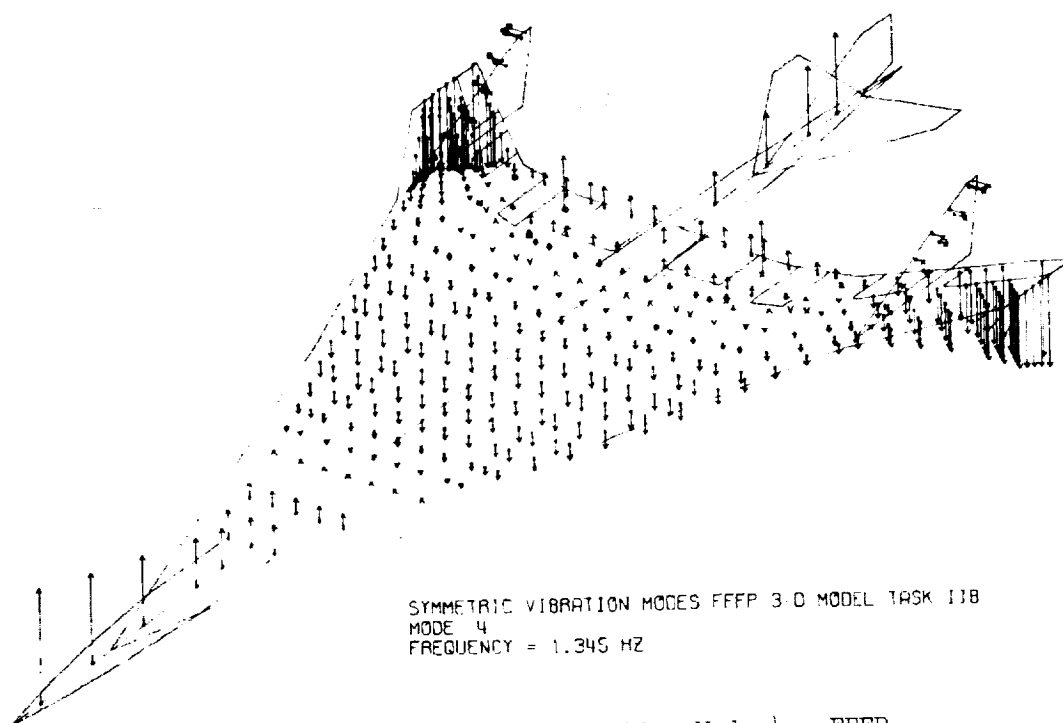


Figure 10-65. Symmetric Vibration Mode 4 - FFFP

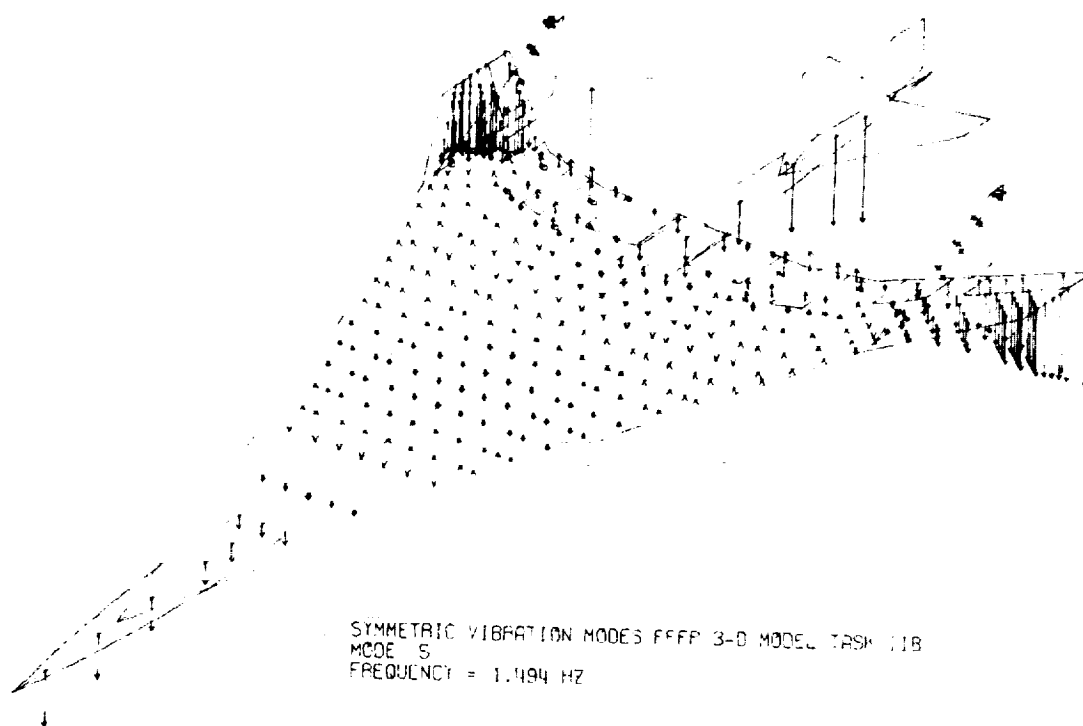


Figure 10-66. Symmetric Vibration Mode 5 - FFFP

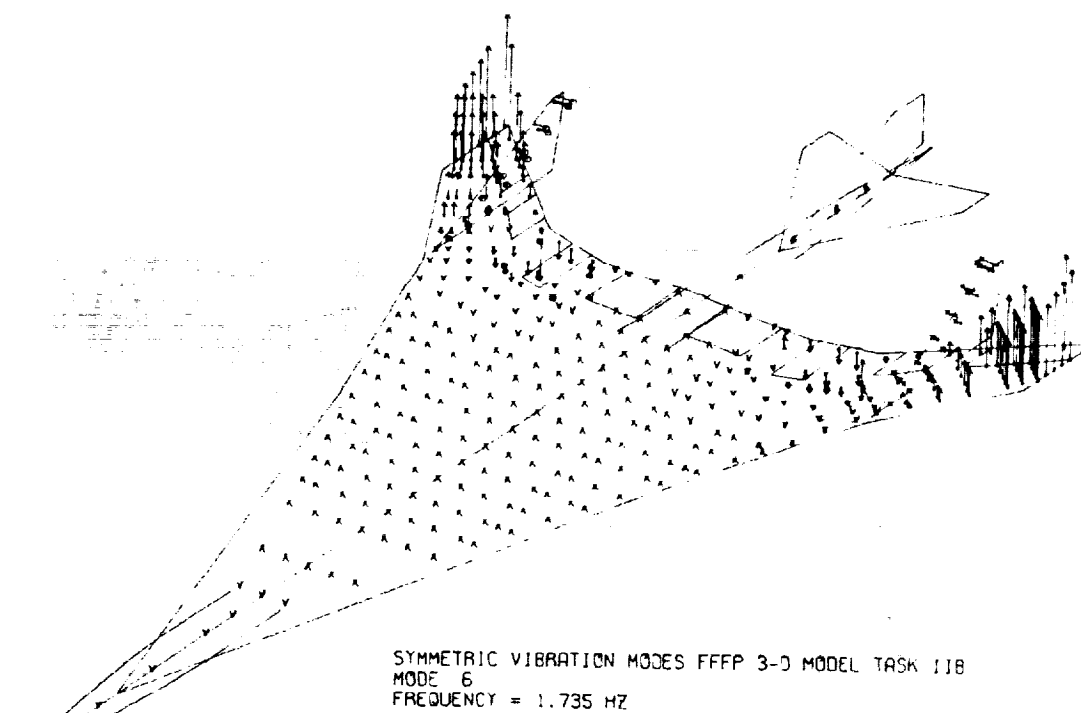


Figure 10-67. Symmetric Vibration Mode 6 - FFFP

ORIGINAL PAGE IS
OF POOR QUALITY

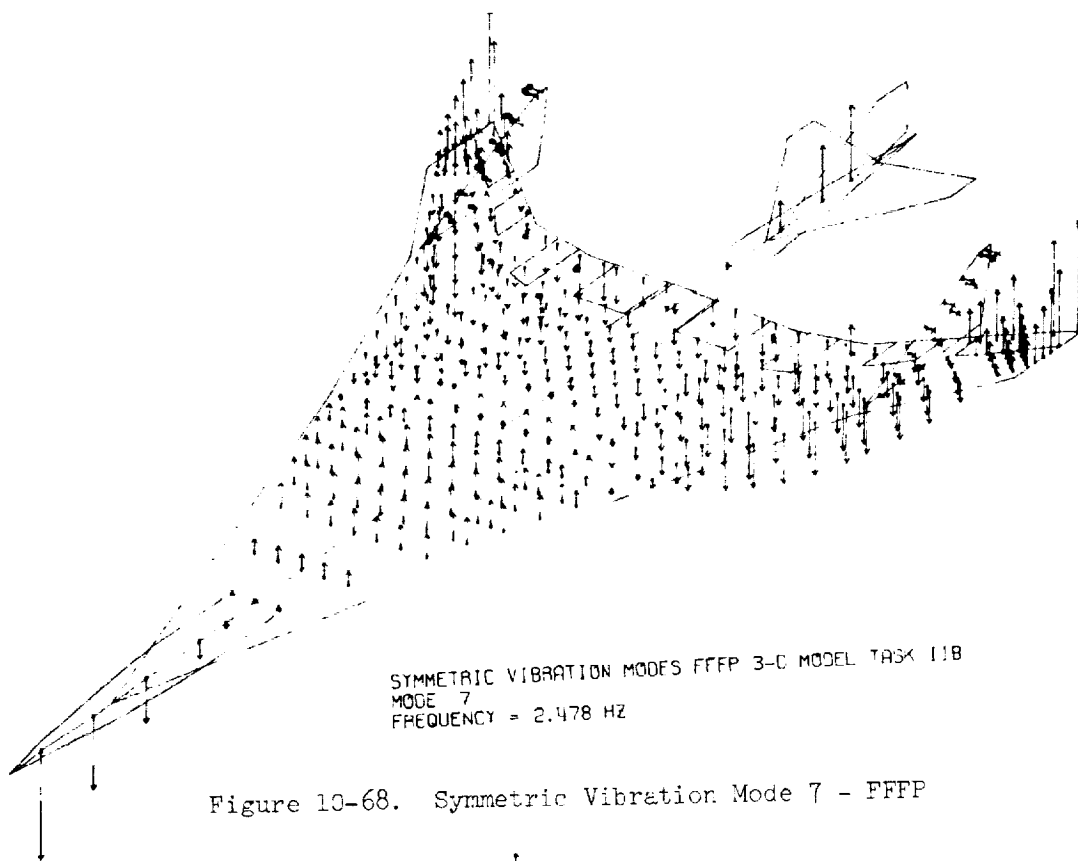


Figure 10-68. Symmetric Vibration Mode 7 - FFFP

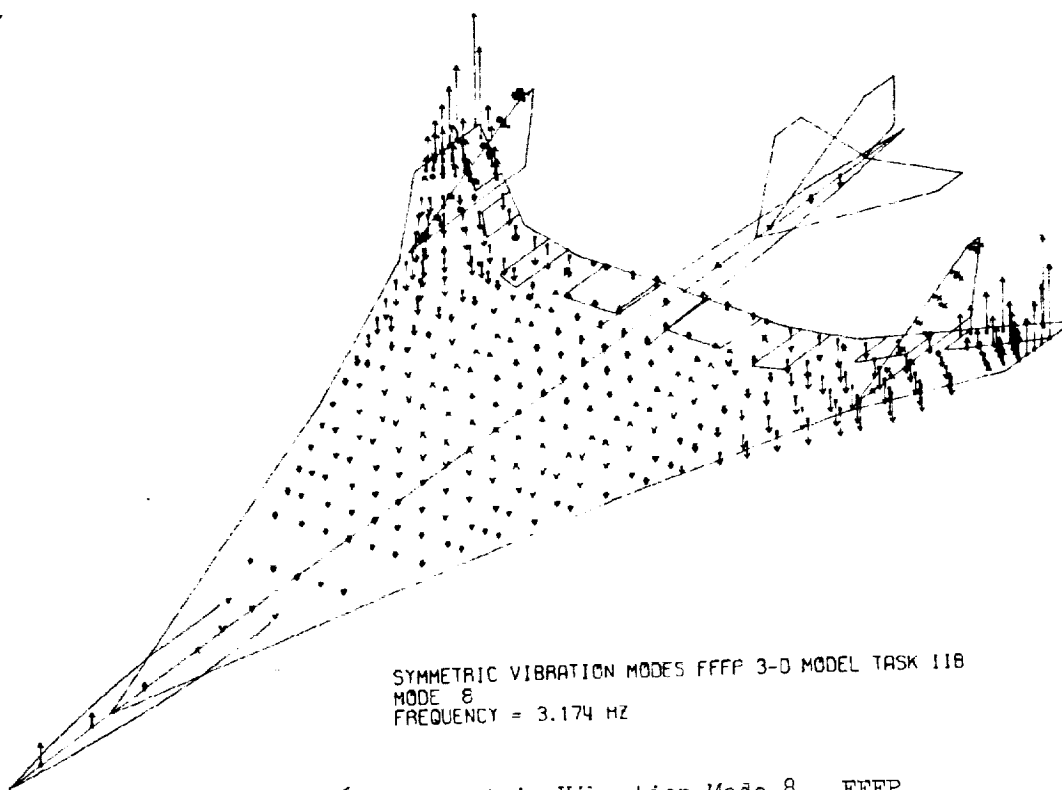


Figure 10-69. Symmetric Vibration Mode 8 - FFFP

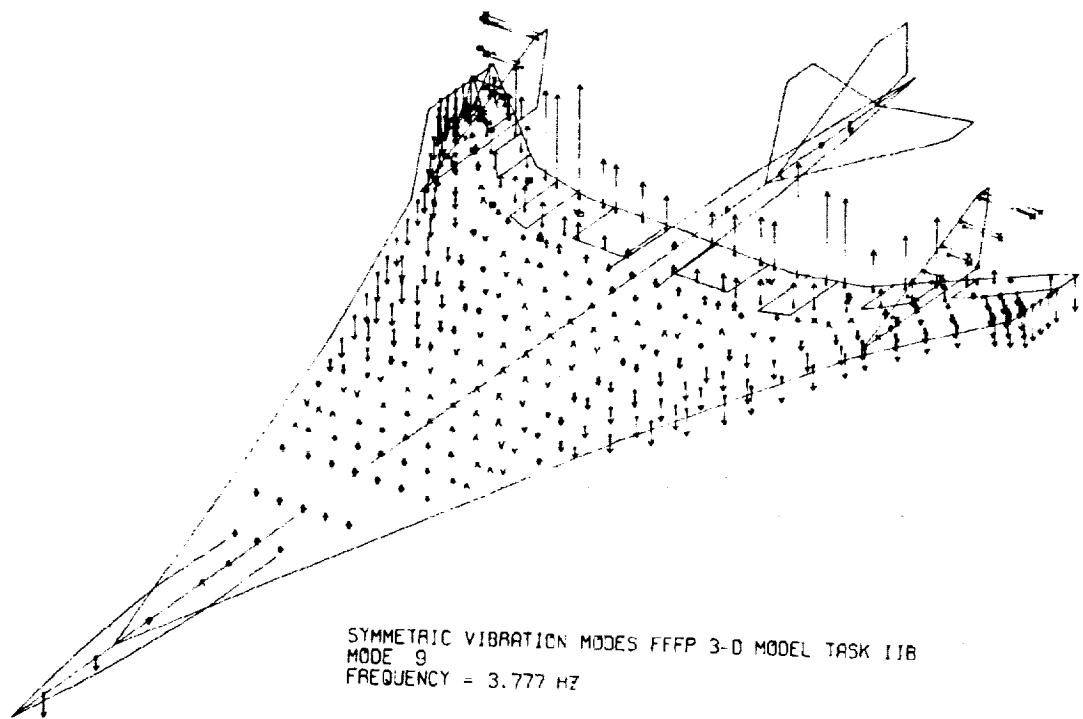


Figure 10-70. Symmetric Vibration Mode 9 - FFFP

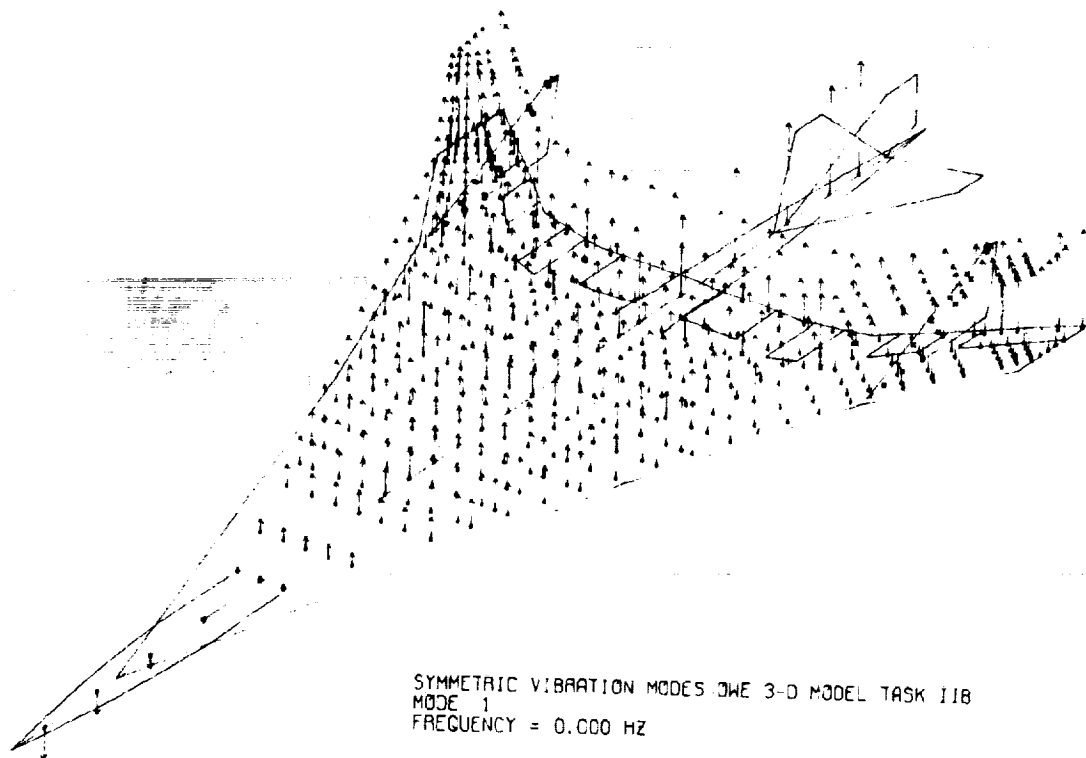


Figure 10-71. Symmetric Vibration Mode 1 - OWE

ORIGINAL PAGE IS
OF POOR QUALITY

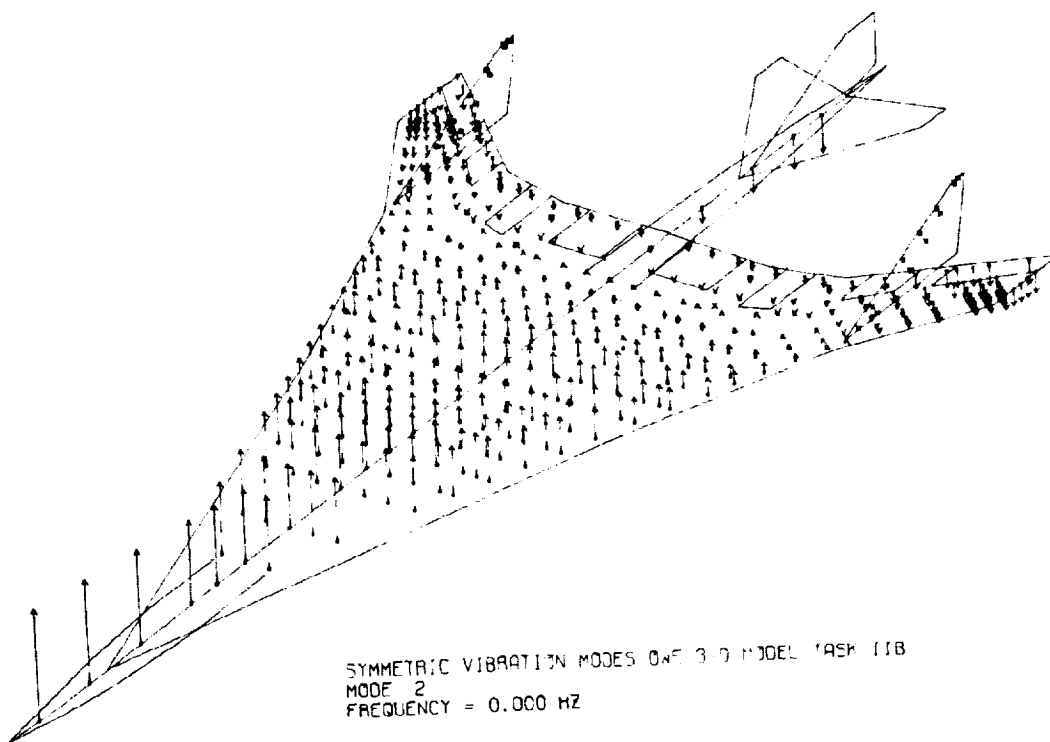


Figure 10-72. Symmetric Vibration Mode 2 - OWE

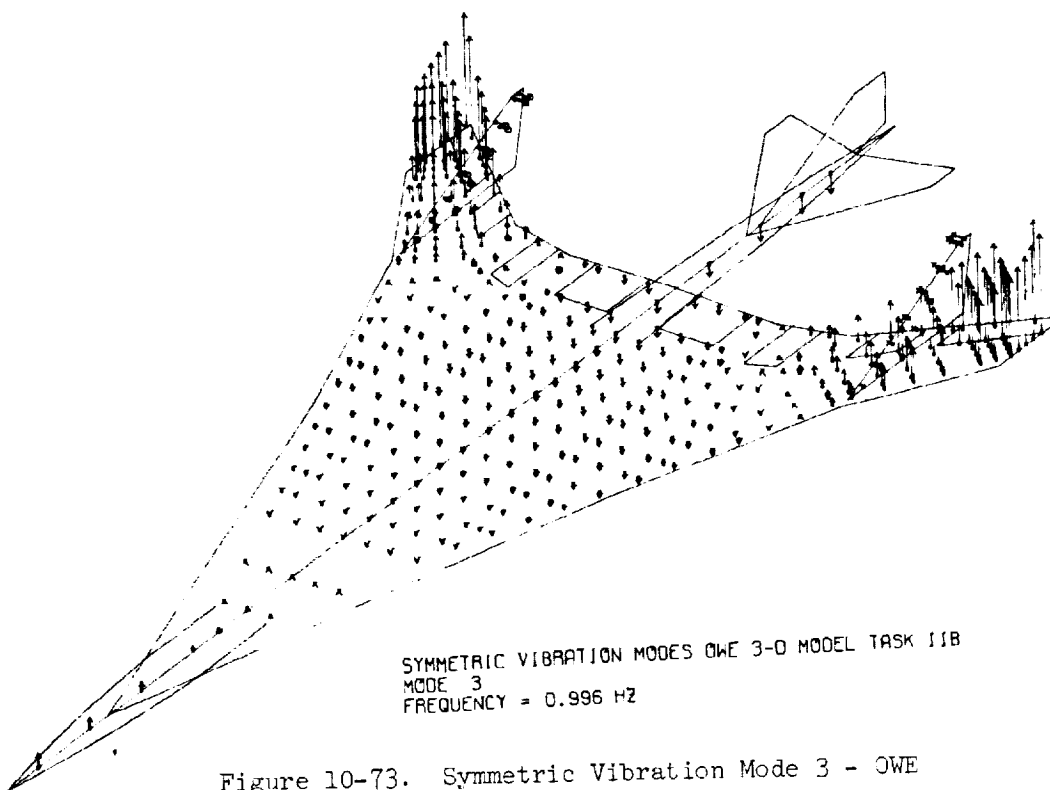


Figure 10-73. Symmetric Vibration Mode 3 - OWE

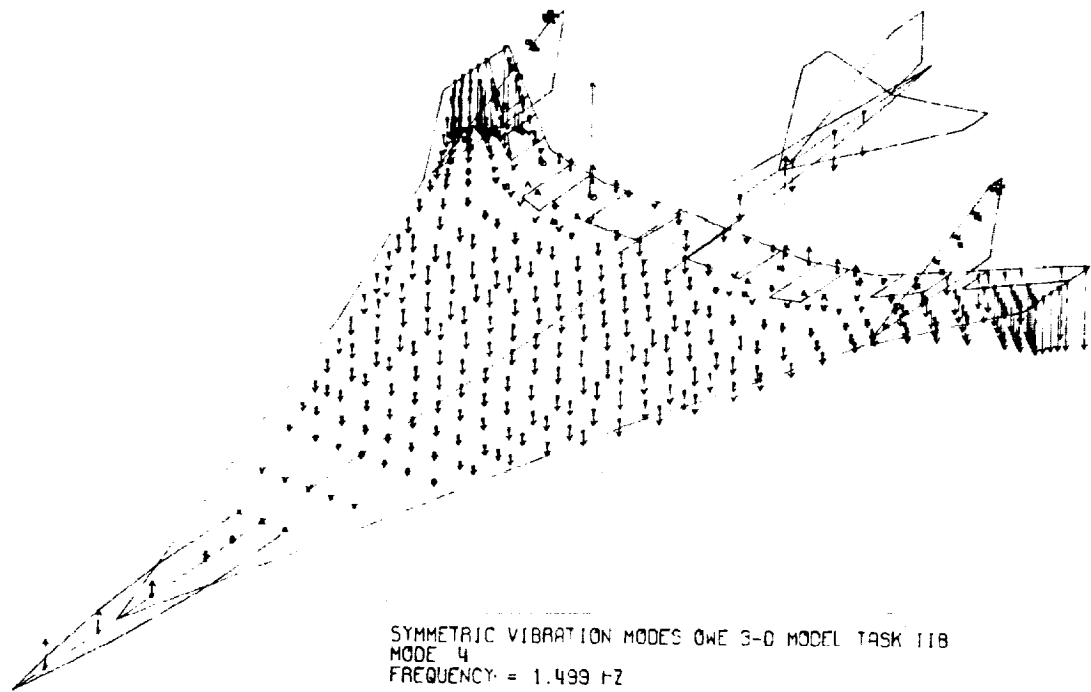


Figure 10-74. Symmetric Vibration Mode 4 - OWE

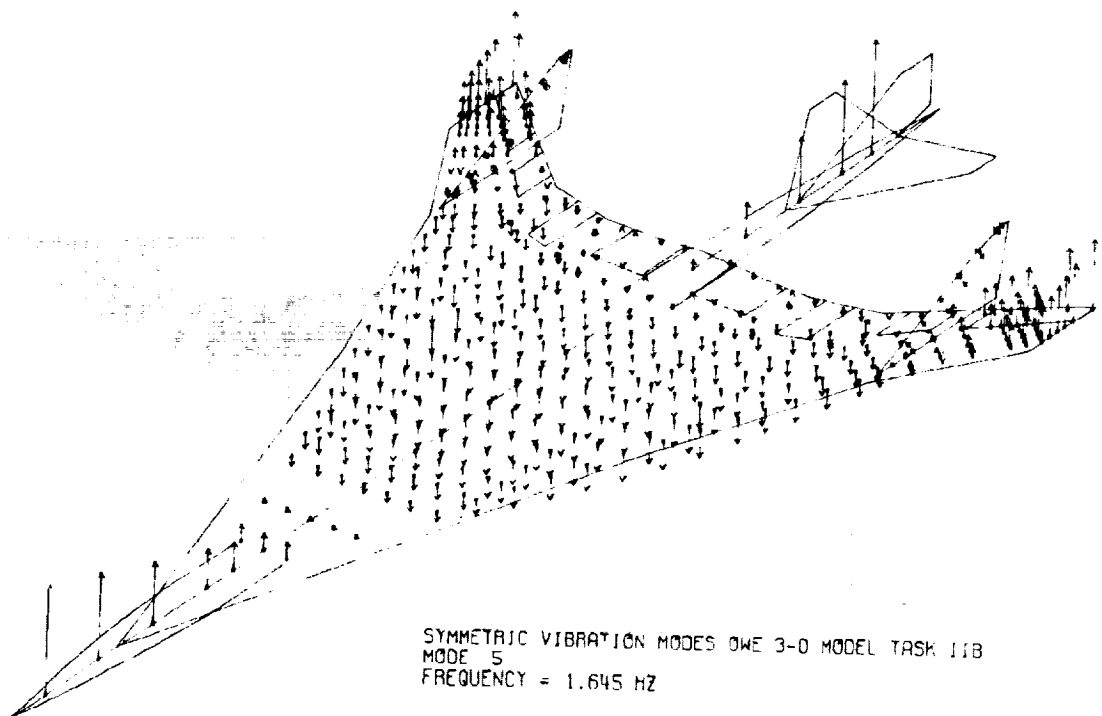


Figure 10-75. Symmetric Vibration Mode 5 - OWE

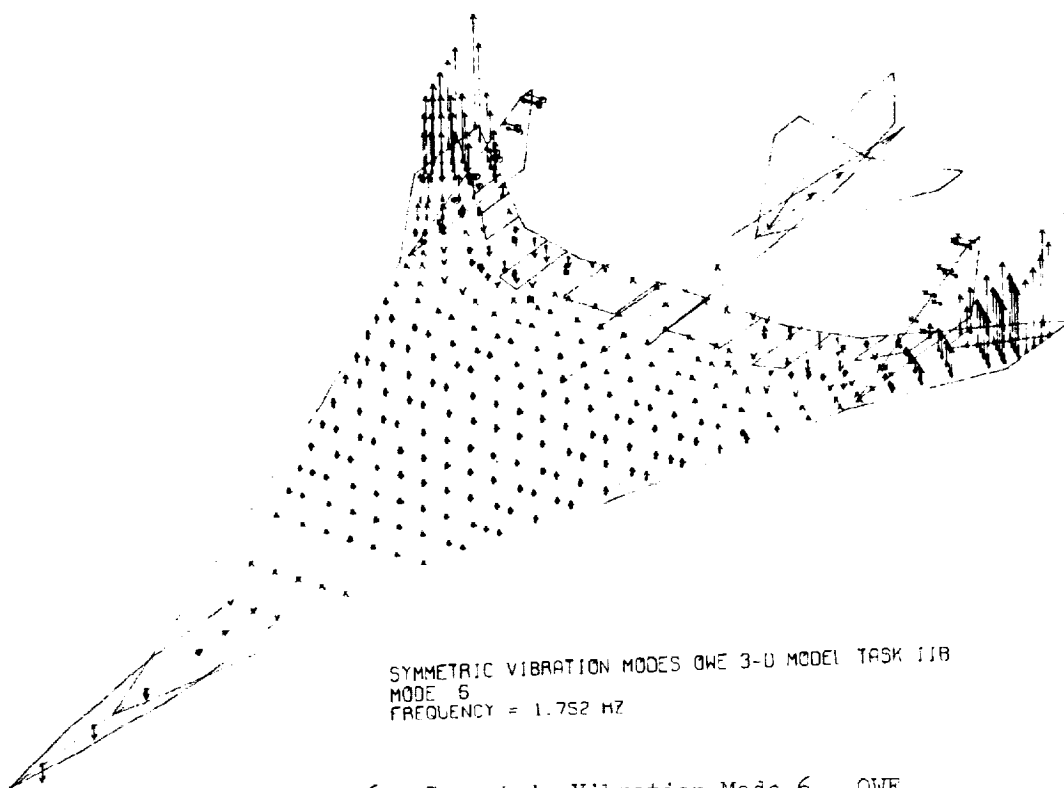


Figure 10-76. Symmetric Vibration Mode 6 - OWE

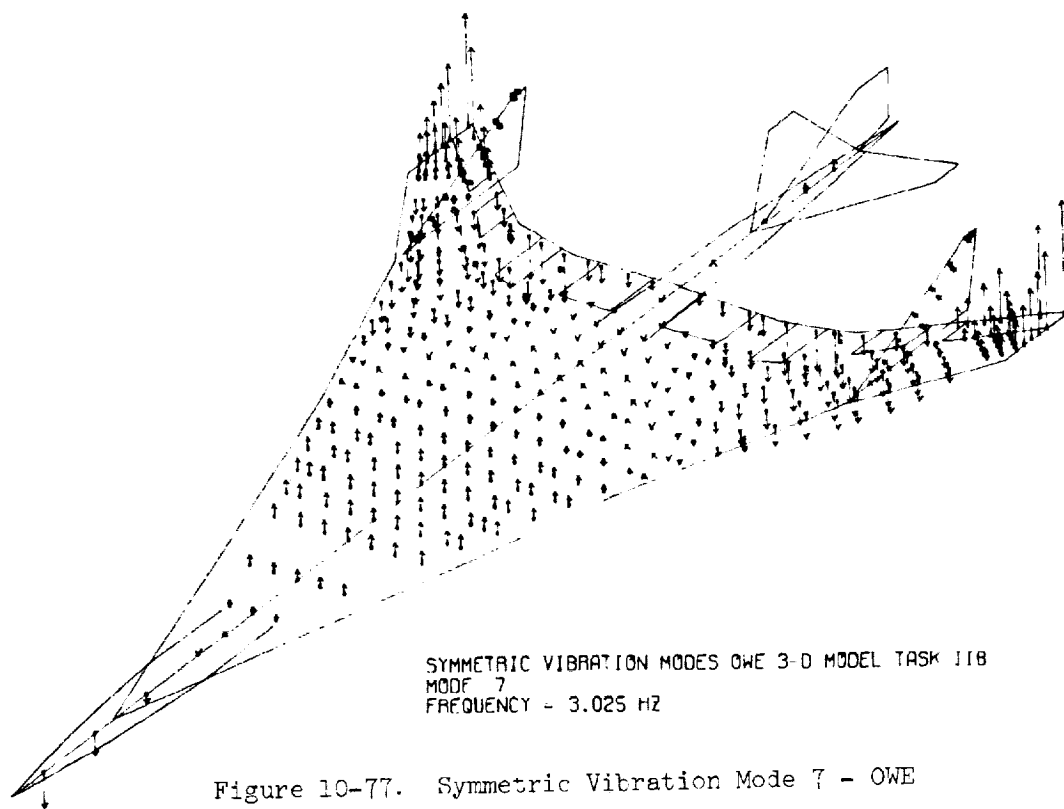


Figure 10-77. Symmetric Vibration Mode 7 - OWE

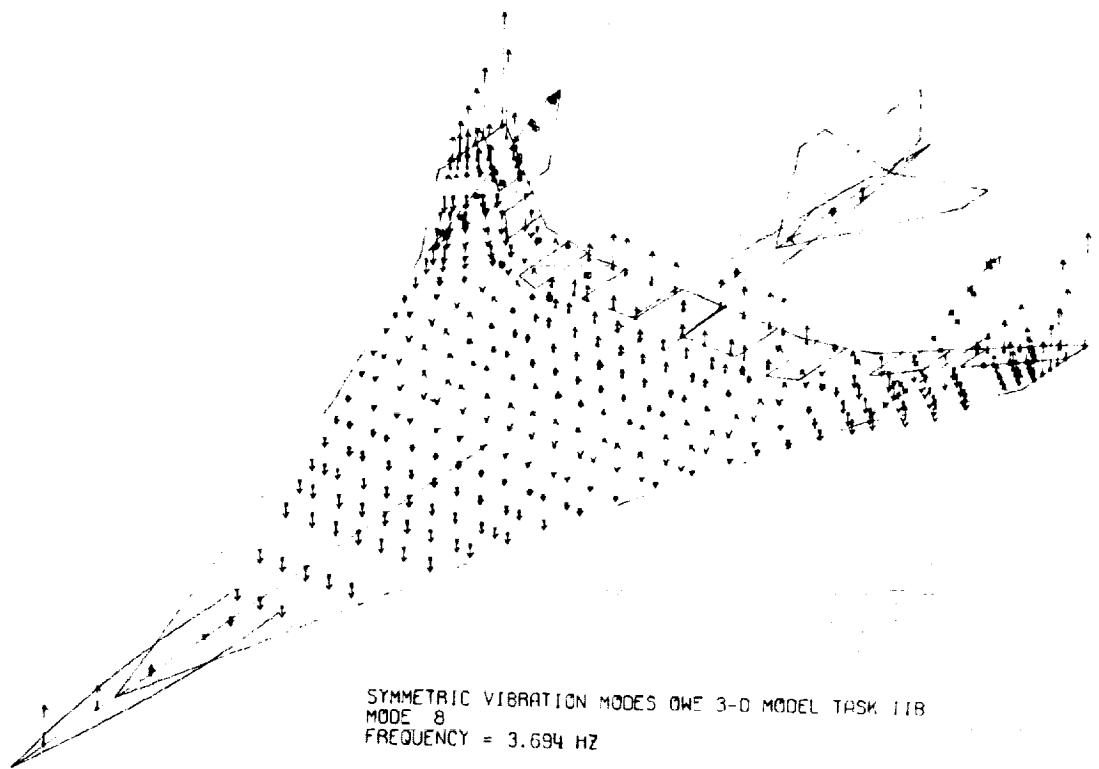


Figure 10-78. Symmetric Vibration Mode 8 - OWE

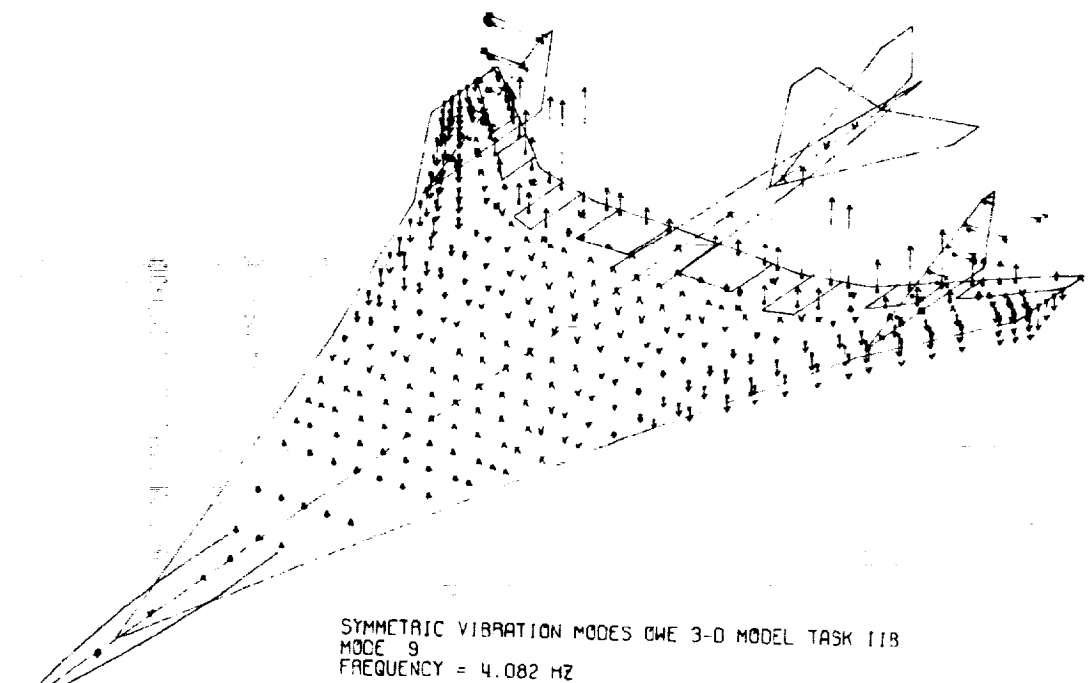


Figure 10-79. Symmetric Vibration Mode 9 - OWE

TABLE 10-13. LOWER FREQUENCY ANTISYMMETRIC VIBRATION MODES - FINAL DESIGN

MODE NUMBER	MODE DESCRIPTION	MODE FREQUENCY ~ HERTZ	
		HYBRID FINAL DESIGN TASK IIC	CHORDWISE STIFFENED TASK I
1	RIGID BODY	0.000	0.000
2	RIGID BODY	0.000	0.000
3	RIGID BODY	0.000	0.000
4	WING 1ST BENDING	1.017	0.908
5	ENGINE PITCH IN PHASE	1.405	1.457
6	ENGINE PITCH OUT OF PHASE	1.717	1.805
7	FUSELAGE 1ST BENDING	1.802	1.949
8	WING 1ST TORSION	2.575	2.319
9	FUSELAGE 2ND BENDING	2.226	3.056

FFFFP ~ AIRPLANE MASS = 750,000 LB. (340,000 kg)

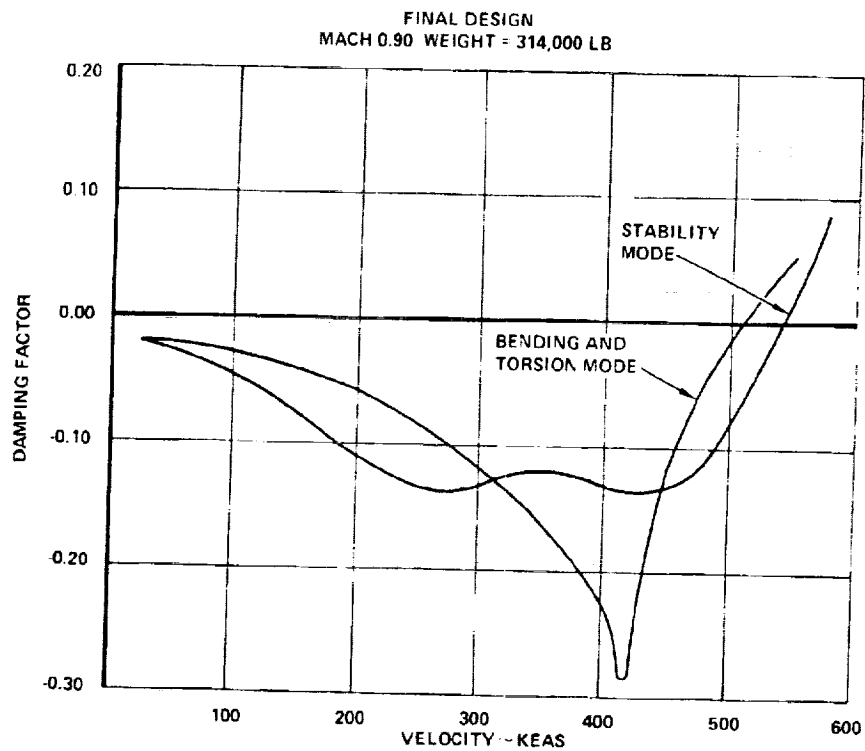


Figure 10-80. Symmetric Flutter Analysis - Mach 0.9 - OWE

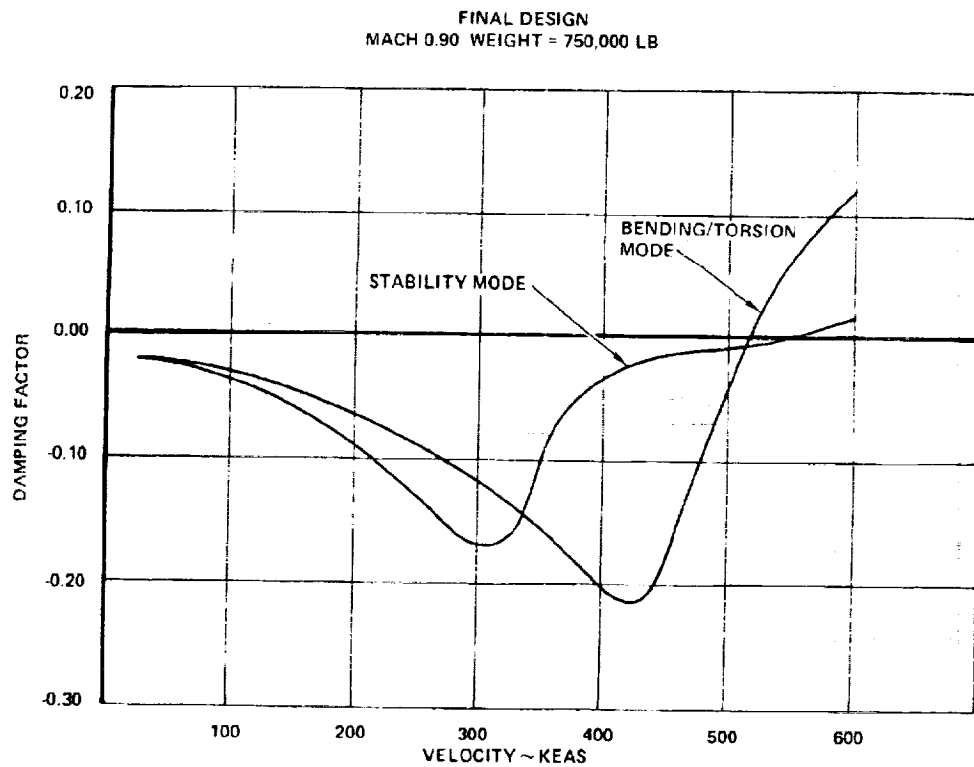


Figure 10-81. Symmetric Flutter Analysis - Mach 0.9 - FFFP

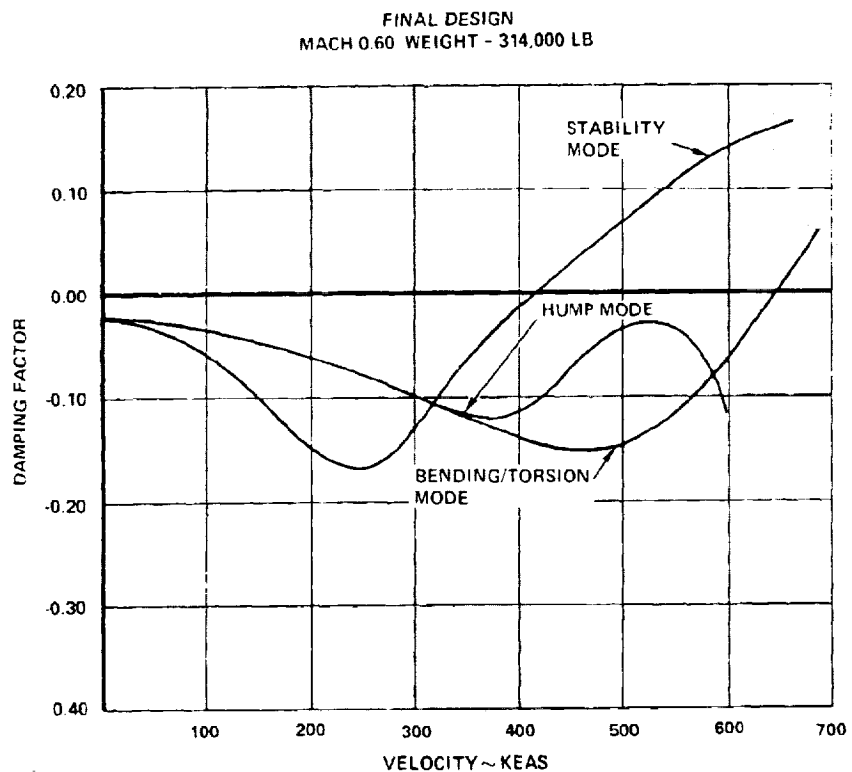


Figure 10-82. Symmetric Flutter Analysis - Mach 0.60 - OWE

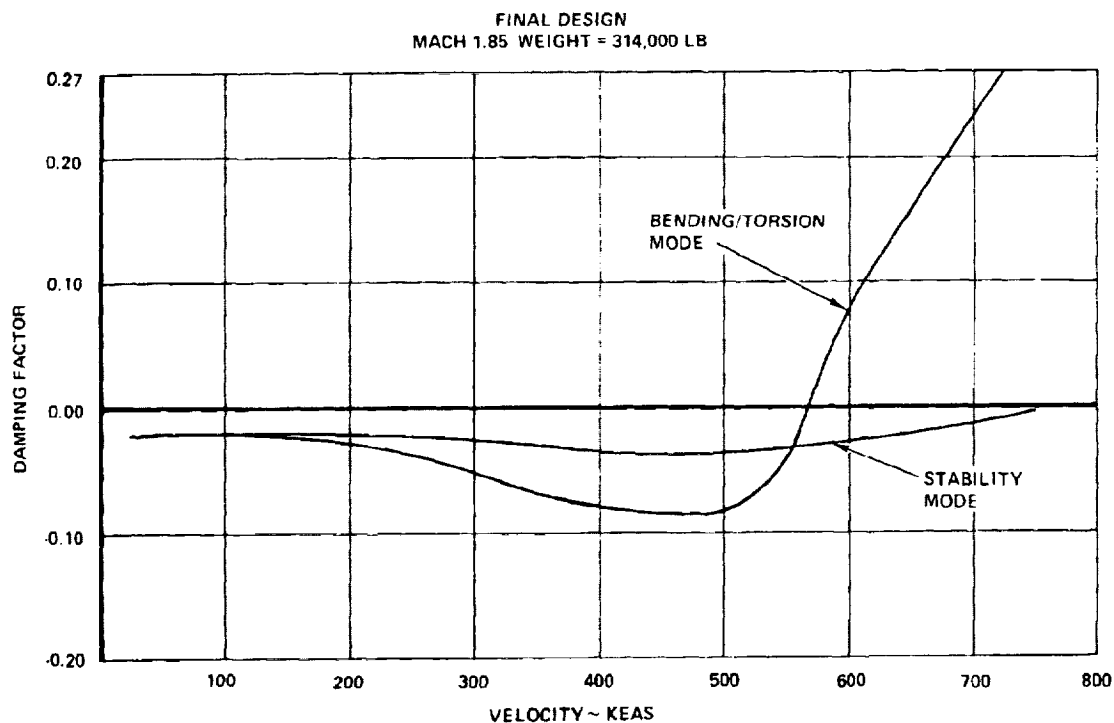


Figure 10-83. Symmetric Flutter Analysis - Mach 1.85 - OWE

bending and torsion mode and the stability mode. The resulting flutter speeds are 563 KEAS and 770 KEAS for the respective modes noted above.

Figure 10-84 presents the symmetrical flutter speeds for the bending and torsion mode. Although the $1.2 V_D$ boundary is cleared at Mach 0.60 and Mach 0.90, only $1.07 V_D$ is achieved at Mach 1.85.

The symmetric stability mode flutter speeds are shown in Figure 10-85. The flutter boundary defined by the cross-hatched line indicates that the flutter speeds are very sensitive to Mach number, unlike the bending and torsion mode. For the stability mode, the flutter boundary is cleared at the higher Mach numbers, however, the results indicate $1.05 V_D$ at Mach 0.60.

A summary of flutter speeds as the result of the Task II strength-design and final design analysis is presented in Table 10-14. Relative to the flutter speed requirements defined by the design flutter boundary, all Mach numbers investigated have adequate flutter margins of safety with the exception of the following:

- (1) At Mach 0.60, a flutter speed deficiency of 20 KEAS for the stability mode
- (2) At Mach 1.85, a flutter speed deficiency of 67 KEAS for the bending and torsion mode.

The deficiencies indicated above were corrected and appropriate weight penalties determined. The results are reported in the Sensitivity Studies subsection. A valid preliminary design definition of the arrow-wing configuration supersonic cruise aircraft was established.

It is speculated that the Mach 1.85 aerodynamics might yield a conservative flutter speed. This is based on the fact that:

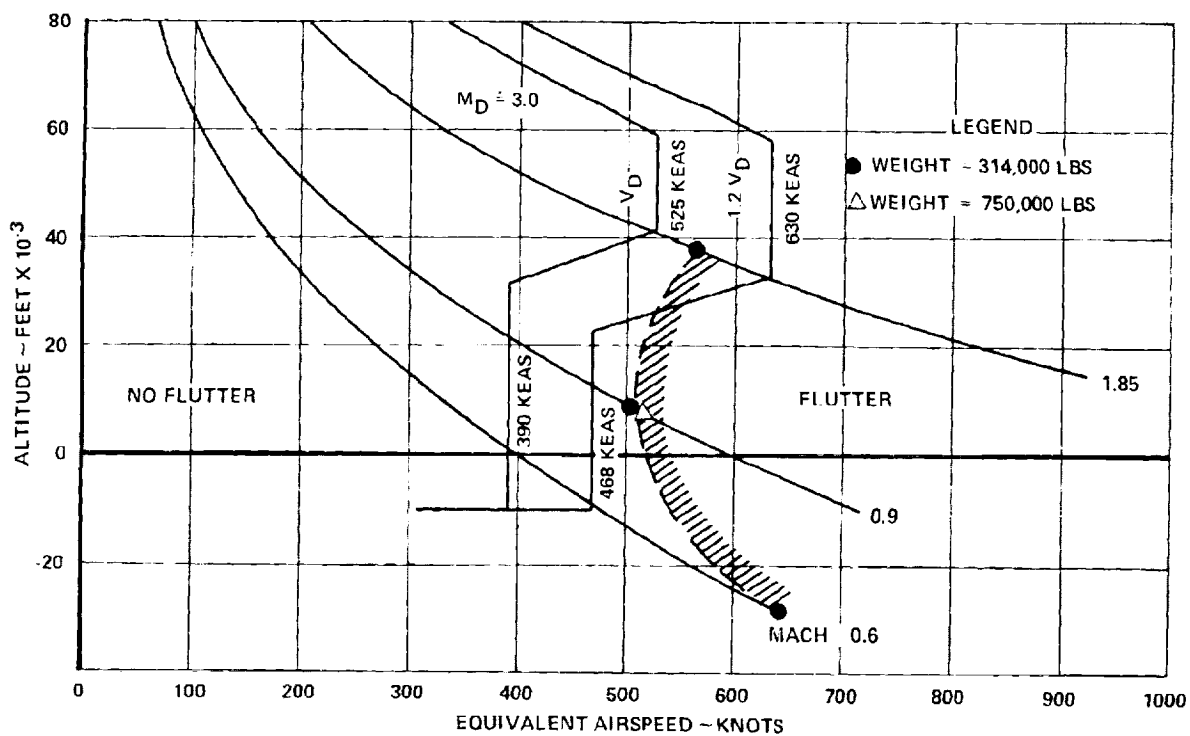


Figure 10-84. Flutter Speeds for Symmetric Bending and Torsion Mode

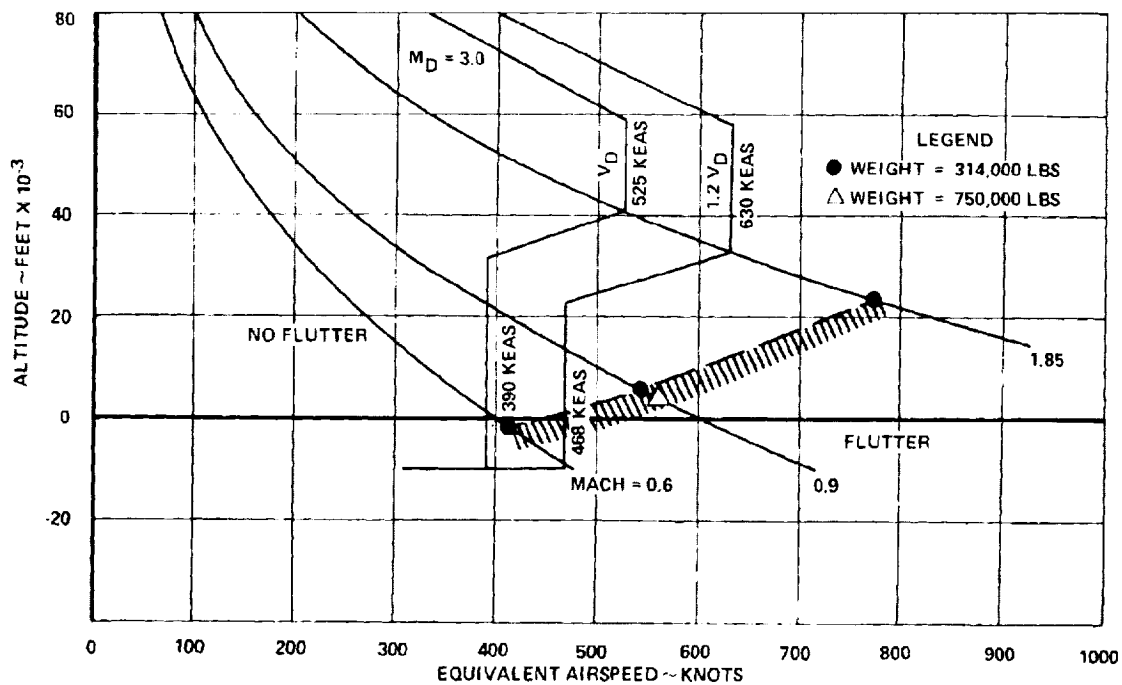


Figure 10-85. Flutter Speeds for Symmetric Stability Mode

TABLE 10-14. SUMMARY OF FLUTTER SPEEDS - TASK II

STRENGTH DESIGN: MACH 0.9, SYMMETRIC BOUNDARY CONDITION

V_f (OWE AND FFFP) = 310 KEAS (BENDING AND TORSION MODE)
 V_f (OWE) = 504 KEAS (STABILITY MODE)
 V_f (FFFP) = 584 KEAS (STABILITY MODE)

FINAL DESIGN: (V_D = 390 KEAS FOR M0.60 & M0.90; V_D = 525 KEAS FOR M1.85)

MACH NO.	BOUNDARY CONDITION	WEIGHT CONDITION (A)	V_f ~ FLUTTER SPEED (KEAS)		
			BENDING & TORSION	HUMP	STABILITY
0.60	SYMM.	OWE	639	(HUMP MODE IS EVIDENT)	410
0.90	SYMM.	OWE FFFP	505 514	> 600 > 600	539 555
0.90	ANTISYMM.	FFFP	> 600	> 600	> 600
1.85	SYMM.	OWE	563	—	770

(A) OWE = 313,842 LB.; FFFP = 750,000 LB.

- (1) The wing-to-wing fin aerodynamic interference is not included in the Mach Box aerodynamics. The significance of this effect is displayed in Figure 10-3 and discussed in the Aerodynamic Formulation section. For the Mach 1.85 aerodynamics where this effect is not included, the $\overline{CC}_1/\overline{CC}_{L\alpha}$ is relatively greater outboard of the wing fin than for the aerodynamics where this effect is included. This is significant since it was also shown (Figure 10-27) that the wing tip region characteristics impact the bending and torsion mode flutter.
- (2) The locus of the aerodynamic centers is not a continuous function on the wing tip as shown on Figure 10-3. This effect could also affect the flutter speed and suggests that a finer Mach Box grid be considered for the wing tip or the wing tip aerodynamic center be adjusted to reflect measured values.

Flutter Recommendations

The following sensitivity studies are recommended to be conducted to support the current studies relative to defining the Final Design of an arrow-wing configuration supersonic cruise aircraft that fully meets the flutter requirements of the design envelope. These studies, when completed will be documented under the Sensitivity Study section.

- (1) Mach 1.85 Convergence Study - Establish two Mach Box grids, one corresponding to that used in the study and one finer, with a plane of symmetry at the BL 470. Calculate the aerodynamics and determine the flutter speeds.
- (2) Mach 1.85 Flutter Optimization - Determine the stiffness and mass increments required to clear the 1.2 V_D envelope using the graphics flutter analysis system (refer to the Sensitivity Studies subsection).
- (3) Mach 0.60 Stability Mode Flutter Study - Use a bending beam analogy for fuselage stiffening in order to determine the weight penalty required to suppress the stability mode flutter (refer to the Sensitivity Studies subsection).

SENSITIVITY STUDIES - TASK III

Stability Mode Flutter Investigation

The final design verification study (Task IIC) resulted in a Stability Mode flutter speed of 410 KEAS at Mach 0.60. In order to gain further understanding of the flutter mechanism involved, the participation coefficients were examined. In addition, a structural mode frequency sensitivity study was performed using the graphics flutter analysis system.

Participation Coefficients. - The participation coefficients for the Stability Mode are shown in Figure 10-86. These participation coefficients are shown for the airspeeds of 250, 300, 340, 380, 420 and 460 KEAS. Only the participation coefficients with significant amplitude are displayed. Certain observations can be made on the participation coefficients of Figure 10-86, namely:

- At the lower airspeeds, the Wing First Bending Mode (zero airspeed Mode No. 3) is the principal contributor. But as the airspeed increases, the Wing First Bending Mode exits as a contributor.
- As airspeed increases a Rigid Body Mode (zero airspeed Mode No. 1) becomes the principal contributor.
- At the flutter speed a Rigid Body Mode (zero airspeed Mode No. 1), an Engine Pitch Mode (zero airspeed Mode No. 4) and the Fuselage First Bending Mode (zero airspeed Mode No. 5) are the prime contributors.

The participation coefficients thus show that the most likely way to increase the flutter speed of the Stability Mode is to change the character of the Fuselage First Bending Mode and/or the character of the Engine Pitch Mode.

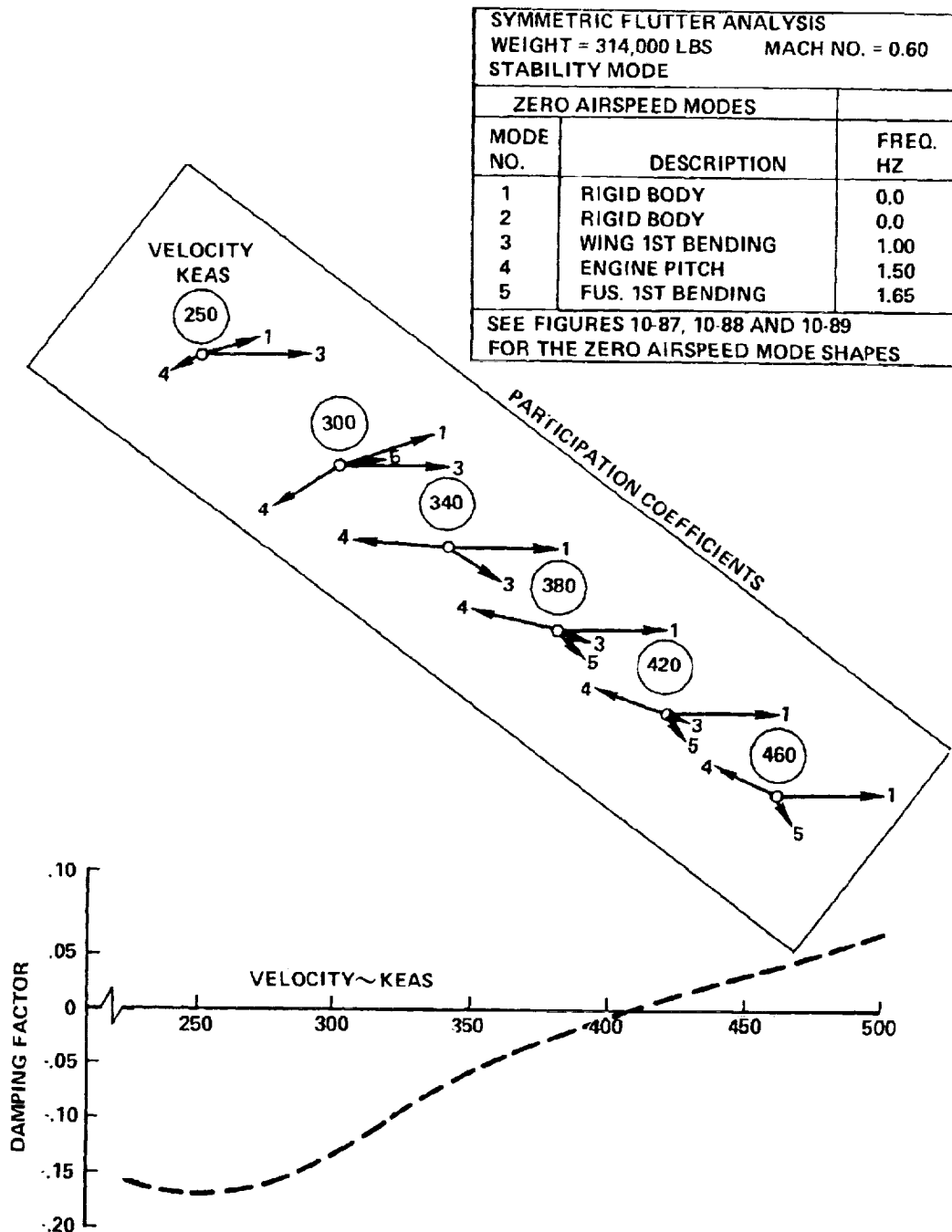


Figure 10-86. Participation Coefficients - Stability Mode

Structural Mode Frequency Perturbations. — An abbreviated study was made using the graphics system to perturb the frequencies of the first three structural modes to determine the effect on the Stability Mode flutter speed. The investigation was approached from the standpoint of a sensitivity study in that the percent change in frequency required to raise the flutter speed by a given amount was determined.

The results obtained for the first three structural modes are presented in Table 10-15.

The vibration mode shapes associated with these modes are presented in Figures 10-87, 10-88, and 10-89. These modes were selected for the study based on the magnitude of their participation coefficients as determined from the flutter analysis. The results indicate that all three modes require an increase in frequency to obtain an increase in flutter speed, however, Mode 4 is the most effective. Figure 10-83 shows the motions associated with Mode 4. In addition to wing tip bending, the inboard engine pitch and fuselage motions are also predominant. These results indicate that a relatively small percentage change (1.07 percent) in Mode 4 is required to raise the flutter speed 5 KEAS.

TABLE 10-15. STRUCTURAL MODE FREQUENCY SENSITIVITIES

Mode No.	Vibration Frequency (Hz)	Flutter Speed (KEAS)	Required Increase in Frequency (Percent)
-	-	410	Base Case
3	0.996	415 420	27.8 41.1
4	1.499	415 420	1.07 2.11
5	1.645	415 425	6.84 16.85

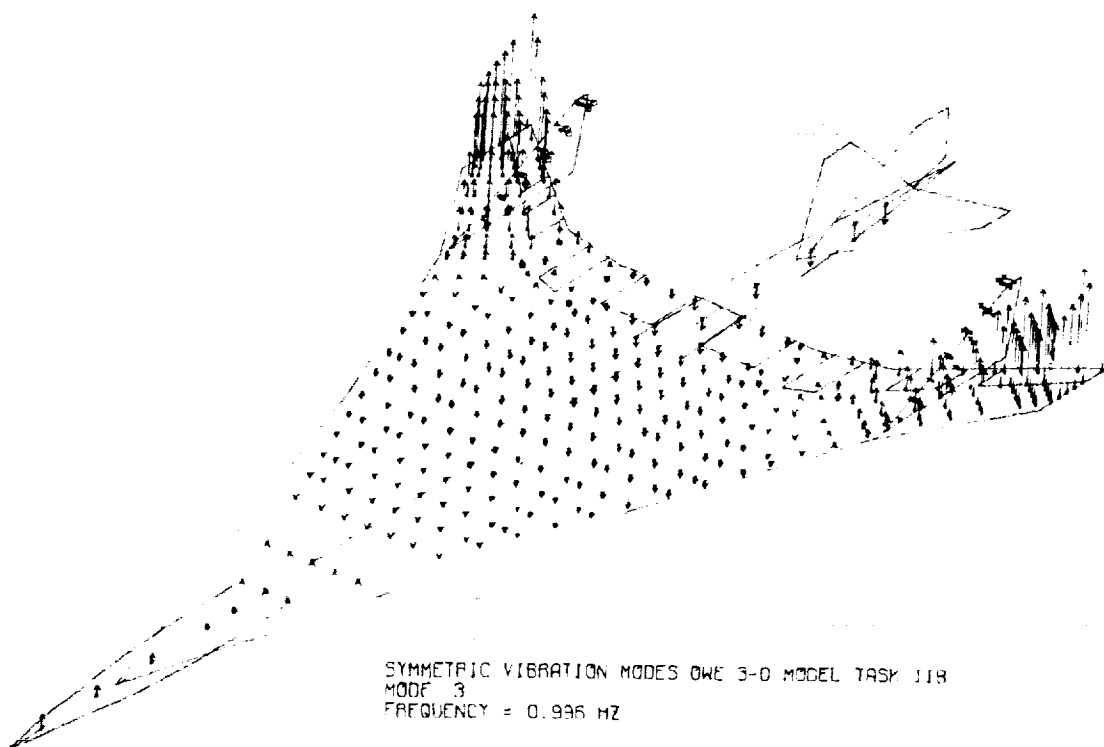


Figure 10-87. Symmetric Vibration Mode 3

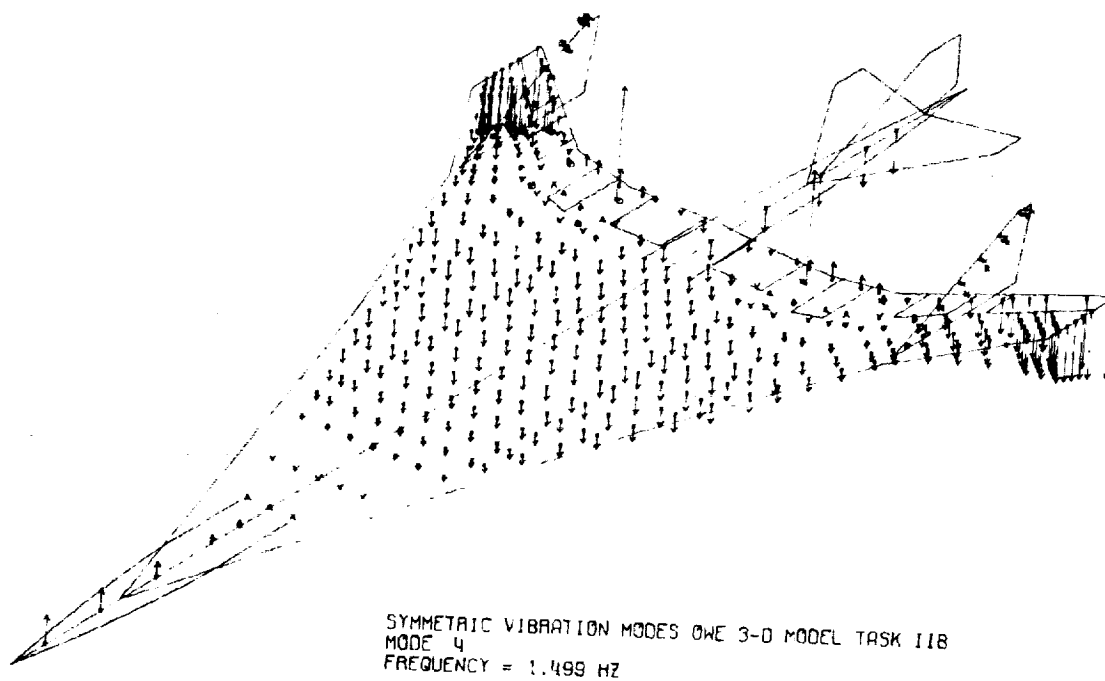


Figure 10-88. Symmetric Vibration Mode 4

ORIGINAL PAGE IS
 OF POOR QUALITY

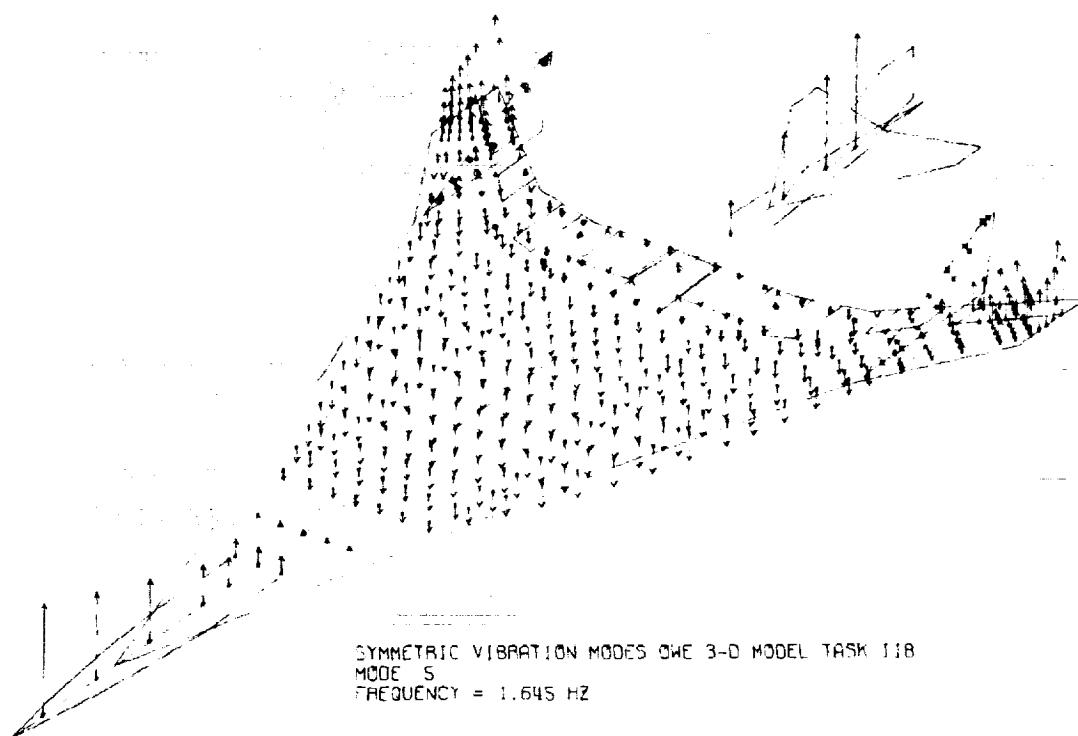


Figure 10-89. Symmetric Vibration Mode 5

The results of this abbreviated study show significant trends but do not provide meaningful design information as to what physical characteristics of the airplane need to be changed and by what amount, to most effectively obtain the desired increase in frequency in Mode 4. The mode shape in Figure 10-88 indicates that the inboard engine and fuselage are prime candidates. The wing tip is not a candidate as indicated by the ineffectiveness of Mode 3, which is primarily wing tip bending.

Engine Placement Investigation

The engine placement investigation was conducted to provide design data to support the Propulsion-Airframe Investigation Study (Section 19) to establish the best aft mounted installation for the propulsion package. This study was performed at the conclusion of Task I and made use of the chordwise stiffened design analysis model (2-D NASTRAN). The model reflected an airplane with a gross taxi mass of 750,000 pounds and addressed the Mach 0.90 bending and torsion mode

flutter mechanism. The flutter speeds were determined for the various engine locations identified below and displayed on Figure 10-90:

- (A) Baseline engine location
- (B) Inboard engine forward - the center of gravity of the inboard engine was moved to the forward engine mount (approximately 100 inches)
- (C) Outboard engine over the inboard engine - the outboard engine mass was zeroed and the inboard engine mass doubled
- (D) Outboard engine forward - the center of gravity of the outboard engine was moved to the forward engine mount (approximately 100 inches)
- (E) Both engines forward - the center of gravity of both engines were moved to the forward engine mount (approximately 100 inches)

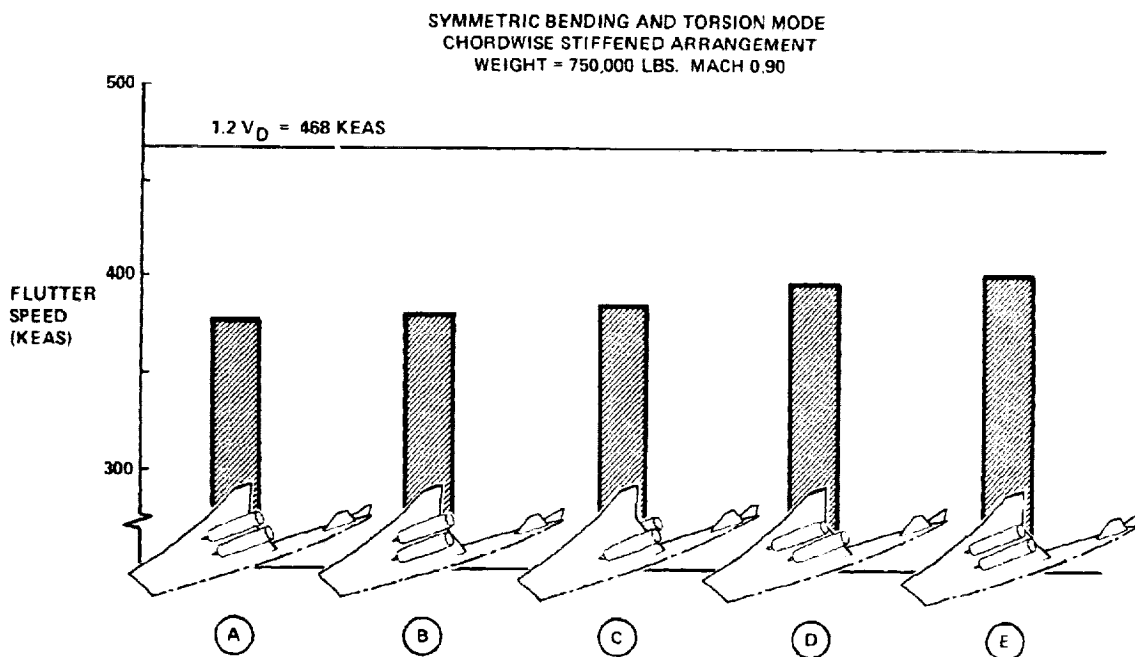


Figure 10-90. Flutter Speed Variation with Engine Placement

All of the engine placement variations from the baseline resulted in an increase in the bending and torsion mode flutter speed.

This investigation did not address the stability mode. This mode may be more sensitive to the engine placement than the bending and torsion mode.

Engine Support Stiffness Investigation

The engine support stiffness investigation was performed by investigating the bending and torsion mode flutter to establish design trends that might be applied to the Propulsion-Airframe Integration Study reported in Section 19. This abbreviated study provided structural mass trends as the stiffness of the outboard engine support structure (rail) was varied from the baseline design (i.e., deflection design of 1-degree/unit vertical load factor). Only 20 eigenvectors were used for modalization, and no updating of mode shapes was done during the rail stiffness variations. The following analysis should be viewed, therefore, as a trend study and not a detailed, complete analysis.

The study was conducted using the graphics flutter analysis system, making use of the flutter optimized chordwise stiffened design. The Mach 0.90 symmetric bending and torsion mode flutter mechanism was addressed for the full fuel and full payload weight condition.

The "softening" of the engine rail was reflected by the removal of mass corresponding to a prescribed stiffness. Through the optimization process, the bending stiffness and the torsional stiffness of region 8 was altered from the baseline design to achieve the required flutter speed of $1.2 V_D$ (468 KEAS). Figure 10-91 shows the potential structural mass saving by decreasing the engine support stiffness to a value somewhat less than the 1-degree/g used for the design. As indicated on the figure, the deflection design criteria requires 1105 pounds in region 8. This corresponds to the 425 pounds of spanwise bending material and 680 pounds of material for torsion displayed on Figure 10-42. As mass is removed from the engine rail, additional bending material and a decreasing amount of torsion material was

required to achieve 468 KEAS. The net effect was the decrease in the flutter weight increment (i.e., mass increment to region 8 less the delta-rail weight) as the engine rail stiffness/mass was reduced.

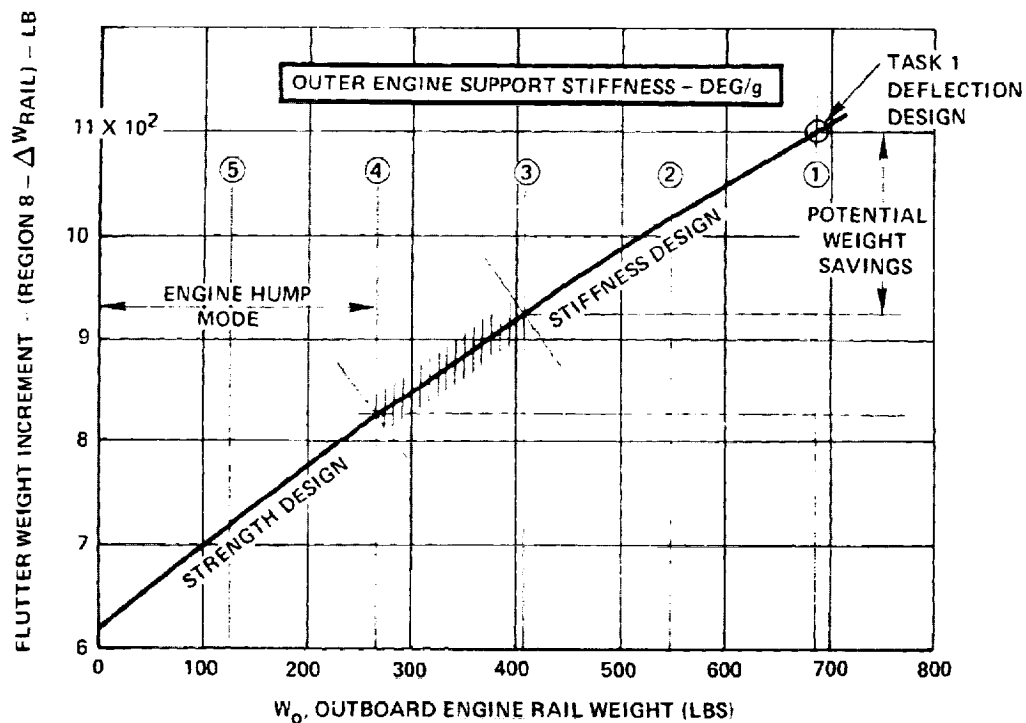


Figure 10-91. Engine Support Stiffness Sensitivity

Mach 0.60 and Mach 1.85 Flutter Investigations

Investigations were conducted to determine the stiffness required and structural mass trends on the wing tip and engine support structure of the Final Design airplane. The graphics flutter analysis system was employed to establish the most effective regions and amount of stiffness/mass required.

Background. - The vibration and flutter analyses performed on the chordwise-stiffened, the spanwise-stiffened, and the monocoque structural arrangements (Task I), indicated that the symmetric bending and torsion mode for the full-fuel and full-payload (FFFP) condition at Mach 0.90 resulted in the lowest flutter speed. The evidence of the stability mode flutter mechanism for the operating weight empty (OWE) condition at Mach 0.60 was also noted. The results of the analyses suggested that stiffening the wing tip structure would eliminate the hump mode flutter and would permit the bending and torsion mode flutter speeds to be increased beyond the $1.2 V_D$ envelope. Elimination of the stability mode flutter would most probably be accomplished by stiffening the fuselage or the engine support structure. It was recognized early in the program that all modes of flutter must be eliminated in the final design of the arrow-wing configuration supersonic transport. The planned changes with regard to the fuselage geometry and structural representation, the aerodynamic static margin, the center-of-gravity location and the pitch-moment of inertia for the Detailed Engineering Design Studies (Task II) would impact the stability mode flutter speed in a manner yet unknown. As a consequence flutter optimization was not performed for the stability mode at that time.

Thus, evaluation of the various wing structural arrangements was accomplished by addressing the symmetric bending and torsion mode flutter mechanism at Mach 0.90. Incremental stiffness requirements and resulting mass additions to increase the flutter speed beyond the $1.2 V_D$ envelope of 468-KEAS (867-km/h) were established. For the Final Design airplane, a verification study was performed to determine the flutter speeds at the study Mach number (Mach 0.90), a critical supersonic Mach number (Mach 1.85) and a reduced subsonic Mach number (Mach 0.60). Flutter speed deficiencies were noted for both the supersonic and reduced subsonic conditions (Figure 10-92), thus, the following investigations were performed.

Flutter Optimization - Mach 1.85. - The flutter analysis performed for the Final Design airplane showed a flutter deficiency of 67-KEAS (124-km/h) at Mach 1.85. To determine the required structural changes to correct this deficiency, flutter optimization studies were conducted to establish the incremental-stiffness and mass required using the graphic flutter analysis system.

Results of the flutter analysis for the Final Design airplane are shown in Figure 10-93, and indicate a flutter speed of 563-KEAS (1043-km/h) for the bending and torsion mode. The deficiency in flutter speed is also displayed in Figure 10-92 by the flutter boundary indicated by the cross-hatched lines.

Surface panels of 0.08-inch (0.002-m) and 0.04-inch (0.001-m) thickness were used to form $[\Delta K]$ and $[\Delta M]$ matrices for Regions 1 and 2 (Figure 10-94). In addition, $[\Delta M]$'s were formed to investigate the effect of adding mass ballast alone along the leading edge (Design Variables 3 through 10).

Two remodelizations were conducted, each reflecting an increase only in Design Variable 2, since it remained the most effective throughout the analysis. The base vibration case and two updates are identified as NV24, QV16, and QV17. Frequencies from these vibration cases are tabulated in Table 10-16. The flutter speed for the structure which produced the new modes was also calculated after each update. The final solution to reach $1.2 V_D$ was 599-lb (272-kg) of structure added to Design Variable 2. This incremental mass (per side) must be added to the Final Design airplane. The final thickness for the wing tip box surface panels and spar webs are shown in Figure 10-95.

The final structural solution from the Mach 1.85 optimization was used in the flutter analyses for the other two Mach numbers which were investigated. The final flutter speeds for the bending and torsion mode are given below:

<u>Mach No.</u>	<u>V_f</u>
0.60	695-KEAS (1287-km/h)
0.90	615-KEAS (1139-km/h)
1.85	630-KEAS (1167-km/h)

The points are displayed on the design envelope of Figure 10-96. No appreciable change in flutter speeds for the stability mode resulted from this addition.

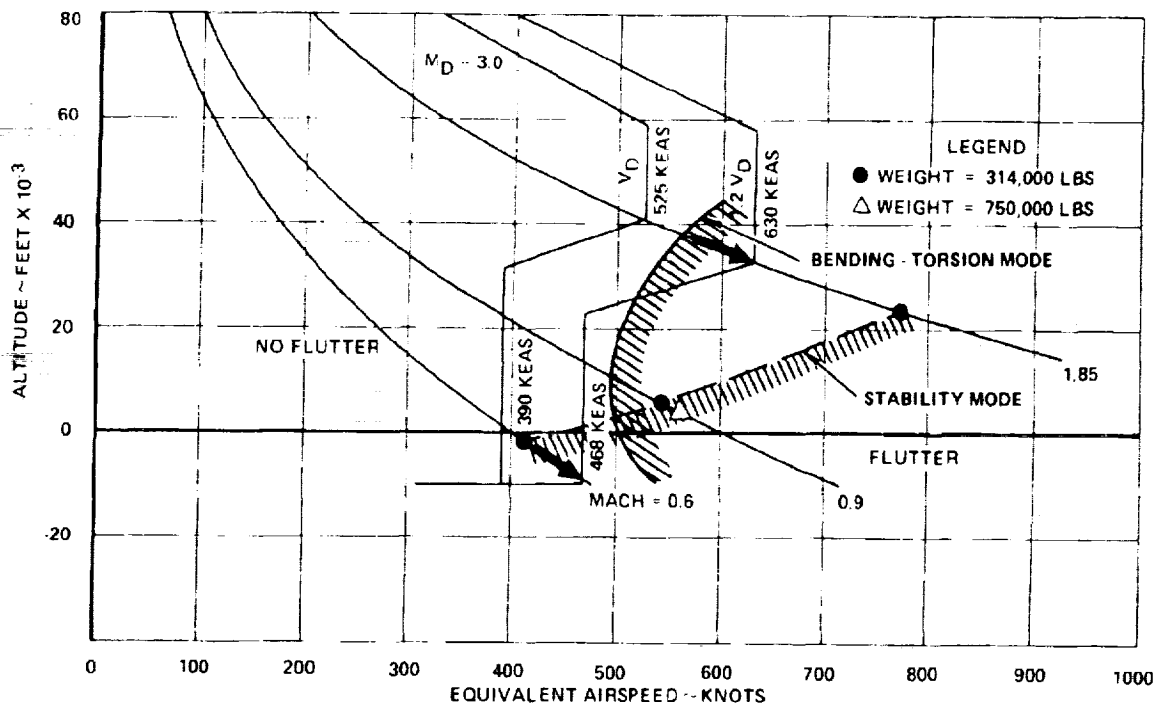


Figure 10-92. Flutter Speeds for the Final Design Airplane

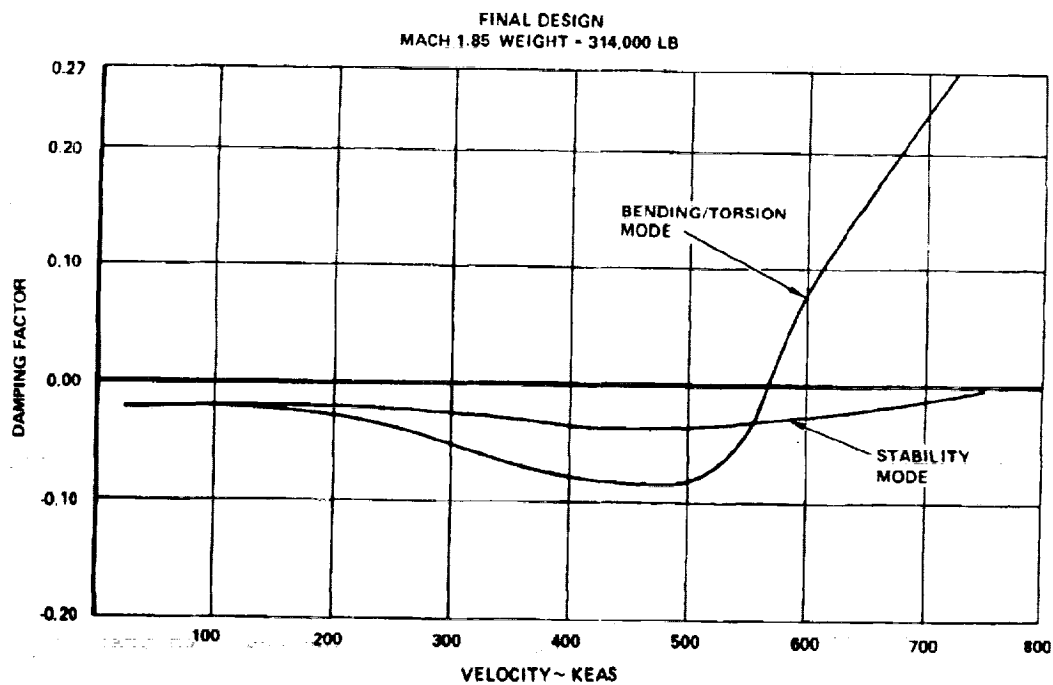


Figure 10-93. Symmetric Flutter Analysis - Final Design Airplane

TABLE 10-16. VIBRATION RESULTS - MACH 1.85 OPTIMIZATION

MODE NO.	MODE DESCRIPTION	NV24 (Base)	QV16	QV17
3	Wing 1st Bending	0.996	1.006	1.012
4	Engine Pitch In Phase	1.499	1.501	1.501
5	Fuselage 1st Bending	1.645	1.647	1.647
6	Engine Pitch Out of Phase	1.752	1.783	1.802
7	Fuselage 2nd Bending	3.025	3.043	3.053
8	Wing Torsion	3.694	3.718	3.729
Structural Mass lb. (Added to D.V.2) (kg)		0 (0)	351.56 (159.46)	593.29 (269.11)
V _F Flutter Speed KEAS (km/h)		557.5 (1032)	599 (1109)	629 (1165)

Flutter Optimization - Mach 0.60. - The Final Design airplane showed a stability mode flutter speed of 410-KEAS (759-km/hr) for Mach 0.60. This flutter analysis, shown in Figure 10-97, gave a flutter speed 58-KEAS (107-km/h) less than required by the 1.2 V_D envelope shown in Figure 10-92.

Sensitivity Studies (described earlier) of participation coefficients for this case and perturbations of the frequencies of the first three structural modes indicated that adding structure to the fuselage and inboard engine support beam may increase the flutter speed. As a more physically meaningful investigation, bending beams were attached to the fuselage and support beams.

Five beams, having one bending element between each of the 25 fuselage grid points, were modeled using the bending stiffness data of Figure 10-98. The two beams at the extreme ends of the fuselage were given a tapered distribution as indicated. Because pitching rotations for the fuselage were not available in the 188th order system, it was necessary to overlap the beams to transfer bending moments from one beam element to the next. These beams, as shown in Figure 10-99, were the first five design variables used in the graphics flutter optimization

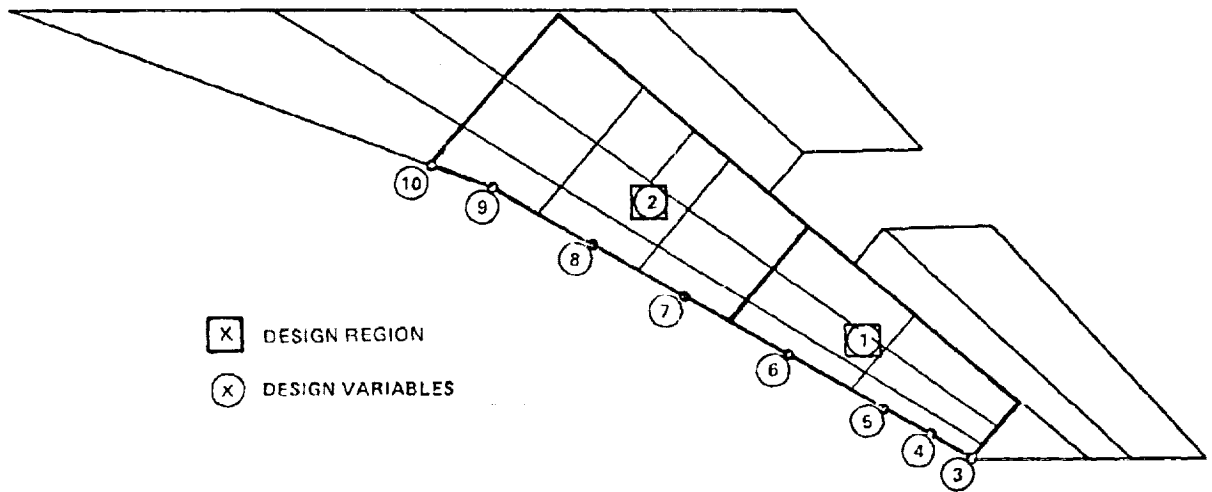


Figure 10-94. Design Regions and Variables for Mach 1.85 Flutter Optimization

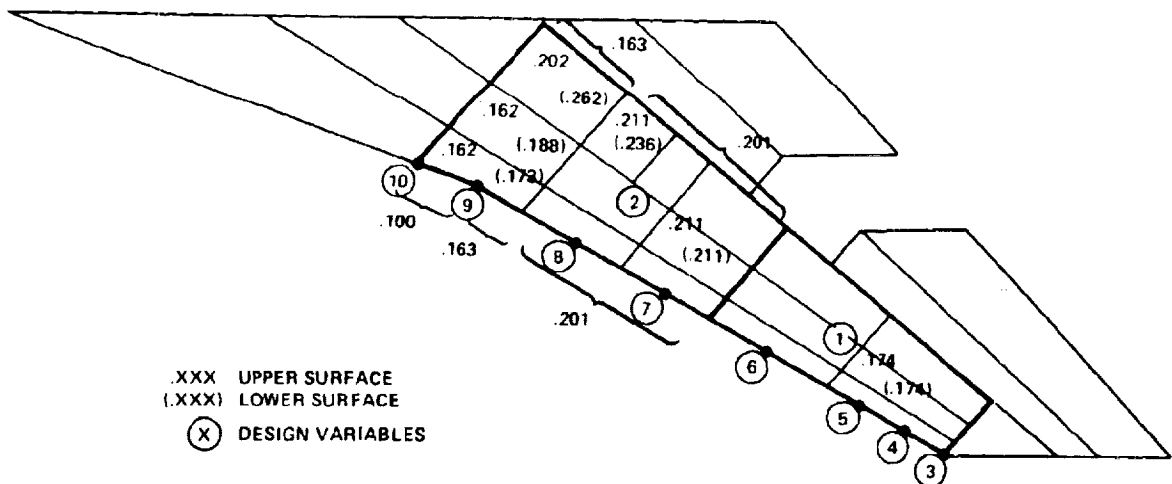


Figure 10-95. Surface Panel and Web Thickness - Mach 1.85 Flutter Optimization

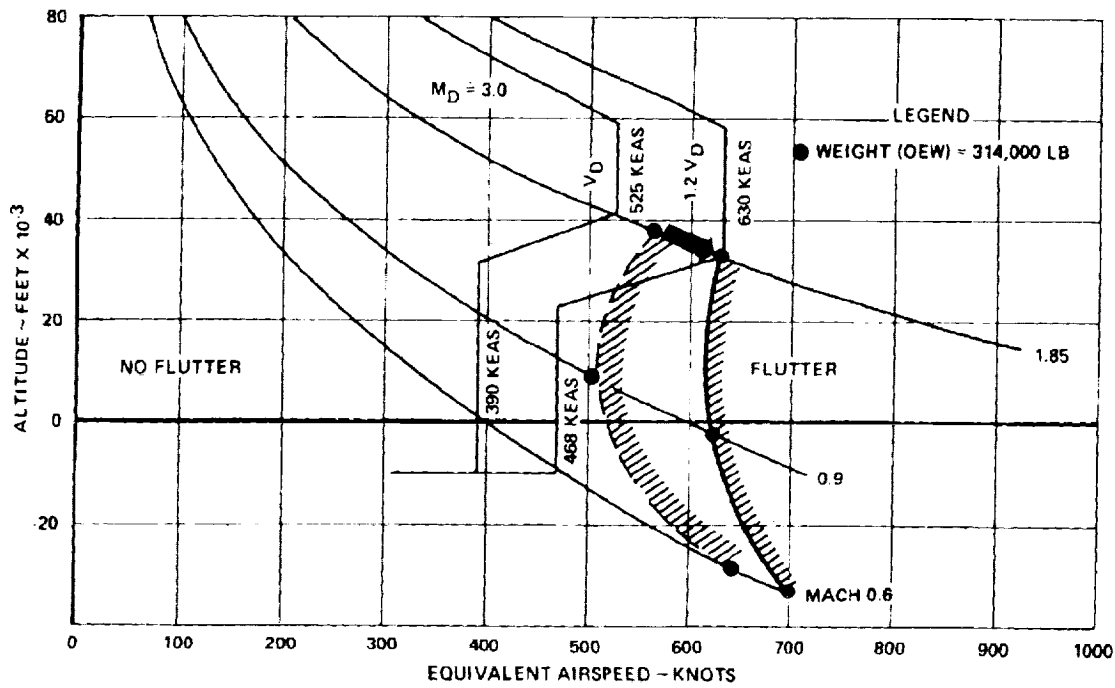


Figure 10-96. Mach 1.85 Flutter Optimization Results - Bending and Torsion Mode

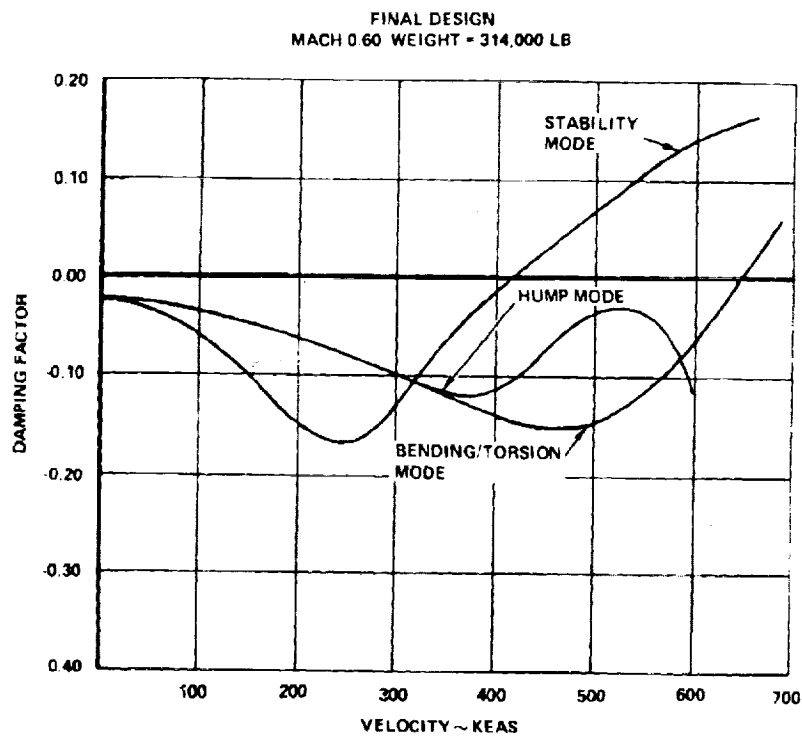


Figure 10-97. Symmetric Flutter Analysis - Mach 0.60 - OWE

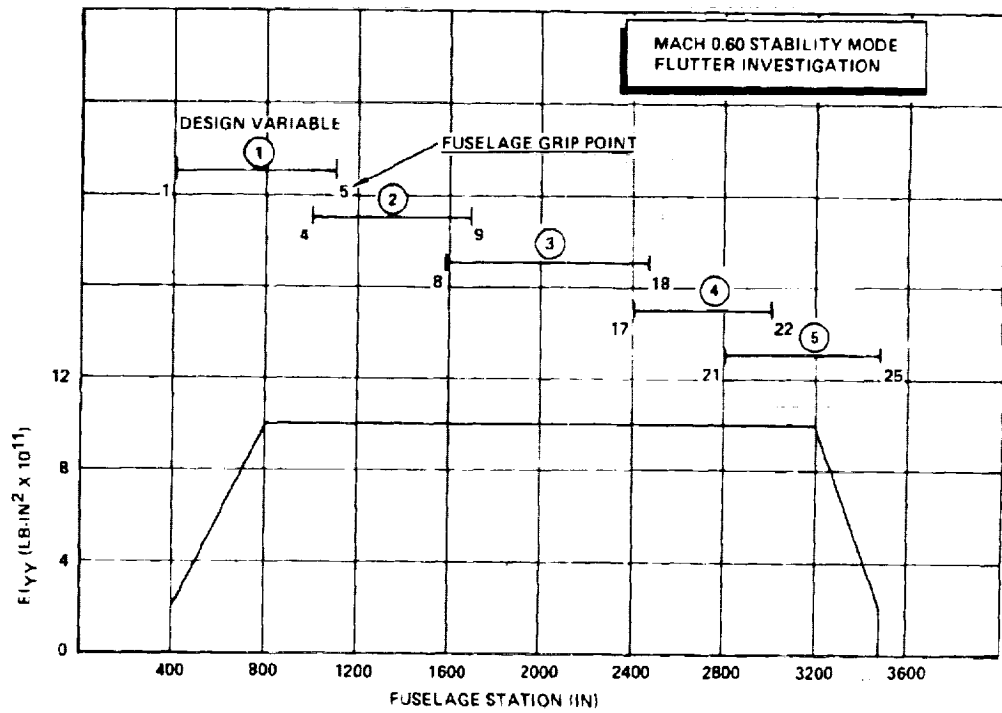


Figure 10-98. Additional Beam Element Stiffness for the Fuselage

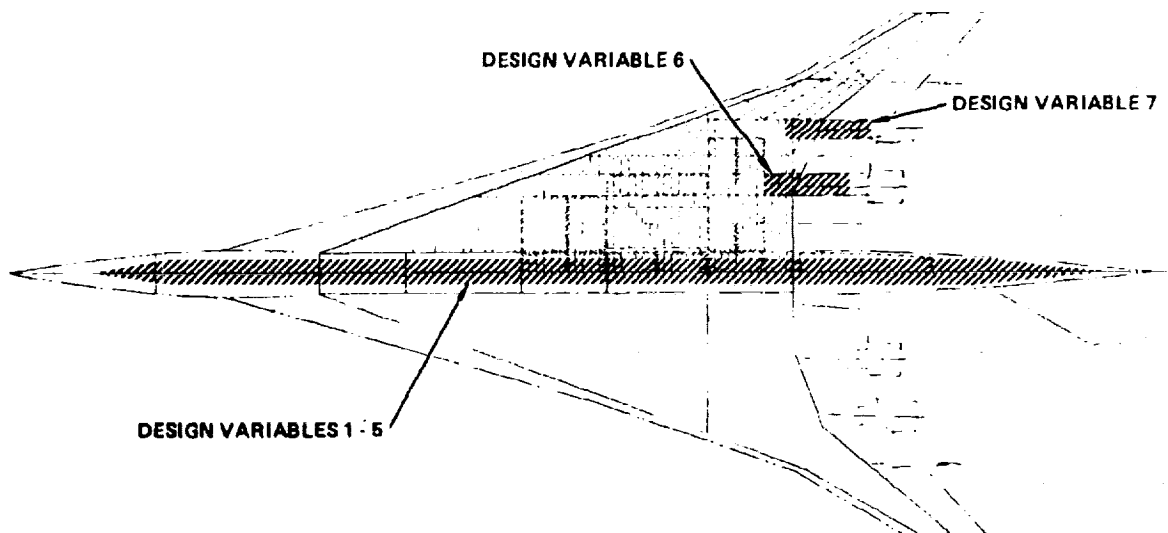


Figure 10-99. Design Variables for Mach 0.6 Flutter Optimization

program. Design Variable 6 consisted of a uniform beam added to the inboard engine support beam from F.S. 2565 to F.S. 2800. Design Variable 7 was a uniform beam added to the outboard engine support beam from F.S. 2614 to F.S. 2855. Both engine support beam $[\Delta K]$'s were calculated using a constant EI_{yy} of 10^{10} (2870 TN-m²). All of the design variables consisted of $[\Delta K]$ matrices only; no change in mass was included since the application of boron-aluminum composite reinforcement would yield increased stiffness at potentially less mass.

An initial investigation of frequency shift due to several of the Design Variables (DV3, DV6, and DV7) was conducted using computer graphics. The $[\Delta K]$ matrices, modalized with 50 eigenvectors from case NV24, were scaled by a factor and then added to the base modalized stiffness matrix. Vibration analyses were then performed on these 50th order matrices; the results are shown in Table 10-17. The previous sensitivity study indicated that it was desirable to increase the frequency of the 1.499 Hz mode; increasing the inboard engine support beam accomplished this objective.

TABLE 10-17. VIBRATION ANALYSIS RESULTS-50TH ORDER

MODE DESCRIPTION	FREQUENCY (Hz)					
	BASE (NV24)	DV3 $\beta=-0.4$	DV3 $\beta=0.2$	DV3 $\beta=0.4$	DV6 $\beta=0.4$	DV7 $\beta=0.4$
Wing 1st Bending	0.996	0.990	0.997	0.998	0.996	1.000
Engine Pitch in Phase	1.499	1.480	1.500	1.501	1.689	1.499
Fuselage 1st Bending	1.645	1.524	1.687	1.713	1.641	1.647
Engine Pitch Out of Phase	1.752	1.746	1.759	1.773	1.821	1.875
Fuselage 2nd Bending	3.025	2.990	3.037	3.046	3.056	3.178
Wing Torsion	3.694	3.296	3.710	3.720	3.711	3.716

The graphics flutter optimization program was used to calculate sensitivities and to find an optimum solution. The structure was optimized, constraining V_f to be 468-KEAS (867-km/h), and a 188th order remodalization was conducted. The solution, using these modal shapes as generalized coordinates to represent the structure, resulted in stiffening the aft part of the inboard

engine support beam to increase EI_{yy} by 0.4685×10^{10} lb-in² (1345TN-m²). Stiffening of the fuselage, as suggested by the frequency perturbation approximation, was relatively inefficient when the necessary mass increase was also included.

The above solution should be viewed as approximate, inasmuch as several shortcuts were employed. These were the following:

- (1) Simple beams were strapped to existing structure - this avoided resizing the NASTRAN model. However, because rotation degrees of freedom were not explicitly retained, some error was introduced when the scaled $[K]$ matrices and the base stiffness matrix, all of which are reduced, were added together in the optimization process. Implied to this is the assumptions that design variables are linear.
- (2) The mode shapes were updated by scaling the 188th order $[K]$ matrices and adding these to the base stiffness matrix. The resulting vibration case does not correspond exactly to a model sizing change.

In spite of the approximate nature of the final solution, it is felt that the study pointed out the proper structural parameters which should be changed in order to clear the envelope. In addition, an approximate idea of the magnitude of these changes was obtained.

1

2

3

REFERENCES

1. MIL-A-8870(ASG): "Military Specification, Airplane Strength and Rigidity, Vibration, Flutter, and Divergence," dated 18 May 1960.
2. Albano, E. and Rodden, W. P., "A Doublet-Lattice Method for Calculating Lift Distributions on Oscillating Surfaces in Subsonic Flows," AIAA Journal, Volume 7, February 1969, pp 279-285, Errata AIAA Journal, Volume 7, November 1969, p 2192.
3. Hassig, H. J., "An Approximate True Damping Solution of the Flutter Equation by Determinate Iteration," Journal of Aircraft, Volume 8, November 1971, pp 885-889.
4. Radovcich, N. A., "Structural Optimization with Flutter Speed and Minimum Gage Constraints," Lockheed-California Company Report LR 26405, April 15, 1974.
5. Pines, S., Dugundji, J., and Neuringer, J., "Aerodynamic Flutter Derivatives for a Flexible Wing with Supersonic and Subsonic Edges, J. Aeronaut. Sci. 22, pp 693-700 (1955).
6. Korn, G. A. and Korn, T. M., Mathematical Handbook for Scientists and Engineers, Second Edition, pp 719-721.

PRECEDING PAGE BLANK NOT FILMED



SECTION 11
POINT DESIGN ENVIRONMENT

BY
G. W. DAVIS

1

2

3

CONTENTS

<u>Section</u>	<u>Page</u>
INTRODUCTION	11-1
AIRPLANE DESIGN ENVIRONMENT - TASK I	11-1
Point Design Regions	11-2
Wing Design Load Conditions	11-5
Wing Aerodynamic Pressures	11-5
Wing Fuel Tank Pressures	11-7
Wing Internal Loads	11-12
Wing Point Design Environment	11-29
General Fuselage Environment	11-50
Fuselage Cabin Pressure	11-50
Fuselage Internal Loads	11-51
Fuselage Point Design Environment	11-56
AIRPLANE DESIGN ENVIRONMENT - TASK IIA	11-56
AIRPLANE DESIGN ENVIRONMENT - TASK IIB	11-58
Design Load Conditions	11-62
Wing Aerodynamic Pressures	11-62
Fuel Tank Pressures	11-62
Wing Internal Loads	11-70
Wing Point Design Environment	11-78
Fuselage Cabin Pressure	11-90
Fuselage Internal Loads	11-90
Fuselage Point Design Environment	11-100
REFERENCES	11-113



LIST OF FIGURES

<u>Figure</u>		<u>Page</u>
11-1	Definition of Wing Point Design Regions	11-4
11-2	Definition of Fuselage Point Design Regions - Task I	11-4
11-3	Aerodynamic Pressure Grid	11-6
11-4	Fuel Tank Locations - Task I	11-10
11-5	Wing Upper Surface Load Intensities, Chordwise Arrangement	11-15
11-6	Wing Upper Surface Load Intensities, Spanwise Arrangement	11-17
11-7	Wing Upper Surface Load Intensities, Monocoque Arrangement	11-19
11-8	Wing Thermally Induced Load Intensities, Chordwise Arrangement	11-23
11-9	Wing Thermally Induced Load Intensities, Spanwise Arrangement	11-25
11-10	Wing Thermally Induced Load Intensities, Monocoque Arrangement	11-27
11-11	Fuselage Shear Diagram - Task I	11-52
11-12	Fuselage Bending Moment Diagram - Task I	11-52
11-13	Definition of Fuselage Point Design Regions - Task IIB	11-61
11-14	Structural Arrangement - Task IIB	11-61
11-15	Fuel Tank Locations - Task IIB	11-67
11-16	Wing Upper Surface Maximum Chordwise Compression Loads, Final Design - Task IIB	11-71
11-17	Wing Lower Surface Maximum Chordwise Tension Loads, Final Design - Task IIB	11-73
11-18	Cabin Pressure Structural Design Envelope	11-91
11-19	Fuselage Panel Maximum Compression Loads, Task IIB Final Design Model	11-95
11-20	Fuselage Panel Maximum Tension Loads, Task IIB Final Design	11-97
11-21	Fuselage Panel Identification System, Task IIB	11-101

—

—

—

LIST OF TABLES

<u>Table</u>		<u>Page</u>
11-1	Critical Load Conditions - Task I	11-6
11-2	Wing Pressure Loadings - Task I	11-8
11-3	Wing Aerodynamic Pressure Loadings, Point Design Regions - Task I	11-9
11-4	Summary of Fuel Heights - Task I	11-11
11-5	Summary of Load Factors - Task I	11-11
11-6	Fuel Tank Pressures - Task I .	11-13
11-7	Wing Upper Surface Load Intensities - All Models, Mach 1.25 Load Condition	11-21
11-8	Summary of Wing Thermal Stresses and Strains - Task I	11-30
11-9	Wing Surface Panel Temperatures, Chordwise Arrangement - Task I	11-31
11-10	Wing Point Design Environment, Chordwise Arrangement - Task I, Mach 0.40 Load Condition	11-32
11-11	Wing Point Design Environment, Chordwise Arrangement - Task I, Mach 0.90 Load Condition	11-33
11-12	Wing Point Design Environment, Chordwise Arrangement - Task I, Mach 1.25 Load Condition	11-34
11-13	Wing Point Design Environment, Chordwise Arrangement - Task I, Start-of-Cruise Condition	11-35
11-14	Wing Point Design Environment, Chordwise Arrangement - Task I, Mid-Cruise Condition	11-36
11-15	Wing Point Design Environment, Chordwise Arrangement - Task I, Mach 1.25 (V_g) Load Condition	11-37
11-16	Wing Point Design Environment, Spanwise Arrangement - Task I, Mach 0.40 Load Condition	11-38
11-17	Wing Point Design Environment, Spanwise Arrangement - Task I, Mach 0.90 Load Condition	11-39
11-18	Wing Point Design Environment, Spanwise Arrangement - Task I, Mach 1.25 Load Condition	11-40

PRECEDING PAGE BLANK NOT FILMED

LIST OF TABLES (Cont)

<u>Table</u>		<u>Page</u>
11-19	Wing Point Design Environment, Spanwise Arrangement - Task I, Start-of-Cruise Condition	11-41
11-20	Wing Point Design Environment, Spanwise Arrangement - Task I, Mid-Cruise Condition	11-42
11-21	Wing Point Design Environment, Spanwise Arrangement - Task I, Mach 1.25 (V_S) Condition	11-43
11-22	Wing Point Design Environment, Monocoque Arrangement - Task I, Mach 0.40 Load Condition	11-44
11-23	Wing Point Design Environment, Monocoque Arrangement - Task I, Mach 0.90 Load Condition	11-45
11-24	Wing Point Design Environment, Monocoque Arrangement - Task I, Mach 1.25 Load Condition	11-46
11-25	Wing Point Design Environment, Monocoque Arrangement - Task I, Start-of-Cruise Condition	11-47
11-26	Wing Point Design Environment, Monocoque Arrangement - Task I, Mid-Cruise Condition	11-48
11-27	Wing Point Design Environment, Monocoque Arrangement - Task I, Mach 1.25 (V_S) Condition	11-49
11-28	Fuselage Cabin Pressure - Task I	11-53
11-29	Fuselage Panel Load Intensities, Parametric Frame Spacing Study - Task I	11-53
11-30	Fuselage Panel Load Intensities, Concept Screening Study - Task I	11-54
11-31	Fuselage Panel Load Intensities, Detailed Concept Analysis - Task I	11-54
11-32	Temperature and Gradients for Fuselage Skin Panels - Task I	11-55
11-33	Fuselage Point Design Environment, Detailed Concept Analysis - Task I, Start-of-Cruise Condition	11-57
11-34	Wing Surface Load Intensities - Task IIA, Mach 0.90 Load Condition	11-59

LIST OF TABLES (Cont)

<u>Table</u>		<u>Page</u>
11-35	Wing Point Design Environment, Chordwise Arrangement - Task IIA, Mach 0.90 Load Condition	11-60
11-36	Summary of Load Conditions - Task IIB	11-63
11-37	Critical Load Conditions, Strength Design - Task IIB	11-64
11-38	Critical Load Conditions, Strength/Stiffness Design - Task IIB	11-65
11-39	Wing Pressure Loadings, Point Design Regions - Task IIB	11-66
11-40	Summary of Fuel Heights - Task IIB	11-68
11-41	Summary of Load Factors - Task IIB	11-68
11-42	Fuel Tank Pressures - Task IIB	11-69
11-43	Comparison of Wing Surface Load Intensities - Task IIB, Mach 1.25 Load Condition	11-75
11-44	Summary of Wing Upper Surface Thermal Stresses and Strains, Task IIB	11-76
11-45	Summary of Wing Lower Surface Thermal Stresses and Strains, Task IIB	11-77
11-46	Temperatures and Gradients for Wing Structure - Task IIB	11-79
11-47	Wing Point Design Environment, Strength Design - Task IIB, Mach 0.50 and 0.90 (V_S) Load Conditions	11-80
11-48	Wing Point Design Environment, Strength Design - Task IIB, Mach 0.90 (V_C) and 1.25 (V_S) Load Conditions	11-81
11-49	Wing Point Design Environment, Strength Design - Task IIB, Mach 1.25 (V_S), $n_z = -1.0$ -g and Mach 1.25 (V_C) Load Conditions	11-82
11-50	Wing Point Design Environment, Strength Design - Task IIB, Mach 1.25 (V_D) Descent and Mach 2.7 (Start-of-Cruise) Load Conditions	11-83
11-51	Wing Point Design Environment, Strength Design - Task IIB, Mach 2.7 (Mid-Cruise) Load Condition	11-84

LIST OF TABLES (Cont)

<u>Table</u>		<u>Page</u>
11-52	Wing Point Design Environment, Final Design - Task IIB, Mach 0.40 and 0.90 (V_S) Load Conditions	11-85
11-53	Wing Point Design Environment, Final Design - Task IIB, Mach 0.90 (V_C) and 1.25 (V_S) Load Conditions	11-86
11-54	Wing Point Design Environment, Final Design - Task IIB, Mach 1.25 (V_S), $n_z = -1.0$ -g and Mach 1.25 (V_C) Load Conditions	11-87
11-55	Wing Point Design Environment, Final Design - Task IIB, Mach 1.25 (V_T) Descent and Mach 2.7 Start-of-Cruise Load Conditions	11-88
11-56	Wing Point Design Environment, Final Design - Task IIB, Mach 2.7 Mid-Cruise Load Conditions	11-89
11-57	Fuselage Cabin Pressure - Task IIB	11-92
11-58	Comparison of Fuselage Panel Load Intensities - Task IIB, Mach 1.25 Load Condition	11-92
11-59	Fuselage Skin Panels Maximum Thermal Gradients and Temperatures, Task IIB	11-99
11-60	Fuselage Point Design Environment, Strength Design - Task IIB, Mach 0.90 (V_S) Load Condition	11-102
11-61	Fuselage Point Design Environment, Strength Design - Task IIB, Mach 1.25 (V_S) Load Condition	11-103
11-62	Fuselage Point Design Environment, Strength Design - Task IIB, Mach 1.25 Negative Maneuver Condition	11-104
11-63	Fuselage Point Design Environment, Strength Design - Task IIB, Mach 1.25 (V_D) Load Condition	11-105
11-64	Fuselage Point Design Environment, Strength Design - Task IIB, Mach 1.25 (V_D) Descent Condition	11-106
11-65	Fuselage Point Design Environment, Strength Design - Task IIB, Mach 2.7 Start-of-Cruise Condition	11-107
11-66	Fuselage Point Design Environment, Final Design - Task IIB, Start-of-Cruise Condition	11-108

LIST OF TABLES (Cont)

<u>Table</u>		<u>Page</u>
11-67	Fuselage Point Design Environment, Final Design - Task IIB, Start-of-Cruise Condition	11-109
11-68	Fuselage Point Design Environment, Final Design - Task IIB, Start-of-Cruise Condition	11-110
11-69	Fuselage Point Design Environment, Final Design - Task IIB, Dynamic Landing Condition	11-111



LIST OF SYMBOLS

BL	Butt line
FS	Fuselage station
g	Gravitational acceleration
h	Average fuel height
M	Moment; Mach number
N_x, N_y, N_{xy}	Inplane forces (lb./in.) associated with the x-y plane
n_x, n_y, n_z	Load factors in x-, y-, and z-directions
P	Pressure
T	Temperature
V_A, V_C, V_D, V_S	Design maneuvering speed, design cruise speed, design dive speed, and design stall speed
V_e	Equivalent airspeed
W	Weight
x, y, z	Cartesian coordinates
$\epsilon_x, \epsilon_y, \gamma$	Extensional strains and shear strain in xy coordinate system
ρ	Density
$\sigma_x, \sigma_y, \tau_{xy}$	Extensional stresses and shear stress in xy coordinate system

PRECEDING PAGE BLANK NOT FILMED

1

2

3

SECTION 11

POINT DESIGN ENVIRONMENT

INTRODUCTION

The environment imposed on the supersonic cruise aircraft during its flight schedule was defined and used as the basis for evaluating the structural concepts. The procedure used for specifying the load-temperature environment was as follows:

- (1) Specific regions of the wing and fuselage were selected to use as point design regions for conducting the detail structural analysis.
- (2) Load intensities and thermal strains (if applicable) were defined for each region using the results of the NASTRAN internal loads solution.
- (3) Normal loads acting on these regions were specified, considering both the aerodynamic pressure and/or fuel inertia heads.
- (4) Average component temperatures and gradients associated with the structure were compiled using the results of the aerodynamic-heating analysis, and
- (5) The results of the above analyses were combined to specify the complete load-temperature environment at each of the point design regions.

The point design environments resulting from using the above procedure are described in the following text for the Task I, Task IIA, and Task IIB investigations.

AIRPLANE DESIGN ENVIRONMENT - TASK I

The wing and fuselage point design environments were defined for the structural analyses conducted in support of the Task I analytical studies.

The basis for establishing the wing point design environment was the internal forces/stresses obtained from NASTRAN redundant-analysis solutions. These solutions were obtained using finite element models which incorporated stiffnesses representative of each of the three general types of wing load carrying structures: chordwise, spanwise, and monocoque which are described in Section 2, Structural Design Concepts. Wing point design environments were defined for each type of primary load carrying structure.

In addition to the internal loads derived using the NASTRAN system, the design environment included aerodynamic pressures, fuel tank pressures, and temperature gradients. The internal loads (air and thermal) and temperature gradients varied with each of the three structural arrangement; whereas, the aerodynamic and fuel tank pressures were assumed invariant.

As described in Section 9 Structural Analysis Models, a coarse model was used to represent the fuselage in the Task I structural analysis; hence, the same basis used for establishing the wing environment could not be employed in specifying the fuselage point design environment. In place of the NASTRAN solutions, the body shear and bending moment diagrams specified in references 1 and 2 were used in the definition of the Task I fuselage point design environment.

The following text contains a general discussion of the point design regions and a detailed description of the wing and fuselage point design environments. The wing environment is presented in its entirety prior to a description of the fuselage point design environment.

Point Design Regions

Representative structure was specified at selected wing and fuselage regions. These regions, hereafter referred to as point design regions, were used as the basis for determining the load-temperature environment.

Wing Point Design Regions - The location of wing point design regions are shown in Figure 11-1 and include the six regions which are displayed on the wing planform of the structural model. Point design regions are identified by the corresponding NASTRAN panel element numbers. Representative structure is specified at each of these locations and includes a definition of the upper and lower surface panels, typical rib and spar structure, and the associated non-optimum factors. These regions were selected as representative of wing critical design regions. A description of these regions is as follows:

- Forward wing box - Point design region 40322 is located forward of the main landing gear in a fuel tank region. This area is characterized as basically transmitting pressure loads with low load intensities with respect to wing bending loads.
- Aft box region - Point design regions 40236, 40536, and 41036 are located in the wing aft box with 40236 and 40536 located in fuel tanks and 41036 in a dry bay region. In general, these areas represent regions of high spanwise load intensities and variable chordwise load intensities due to wing bending. The chordwise load intensities in region 40236 reflect the influence of fuselage body bending, while those in region 41036 indicating the effect of the wing tip load redirection.
- Wing tip region - Dry bay regions 41316 and 41348 are located approximately at the root and mid-span of the wing tip. High load intensities are indicative of the aeroelastic effect on this flexible region.

Fuselage Point Design Regions - Four point design regions were selected as representative of the actual fuselage design. These regions are shown in Figure 11-2 and are located at fuselage stations 750, 2000, 2500, and 3000. Conventional structure composed of skin/stringer panels and sheet metal frames was selected for these regions. The panel concept were varied to reflect the specific design being evaluated. These regions were selected as typical of the critical design regions on the fuselage and, in general, are classified as follows:

- Fuselage Forebody (FS 750) - Generally characterized as fatigue designed structure with low load intensities due to fuselage bending.
- Fuselage Centerbody (FS 2000 and 2500) - Wing/fuselage regions subjected to maximum body bending and wing spanwise loads.
- Fuselage Aftbody (FS 3000) - High body bending and torsion loads with regions subjected to a high acoustic environment.

Fuselage point design regions located at FS 2000 and FS 2500 are coincidental with the wing forward box and aft box point design regions.

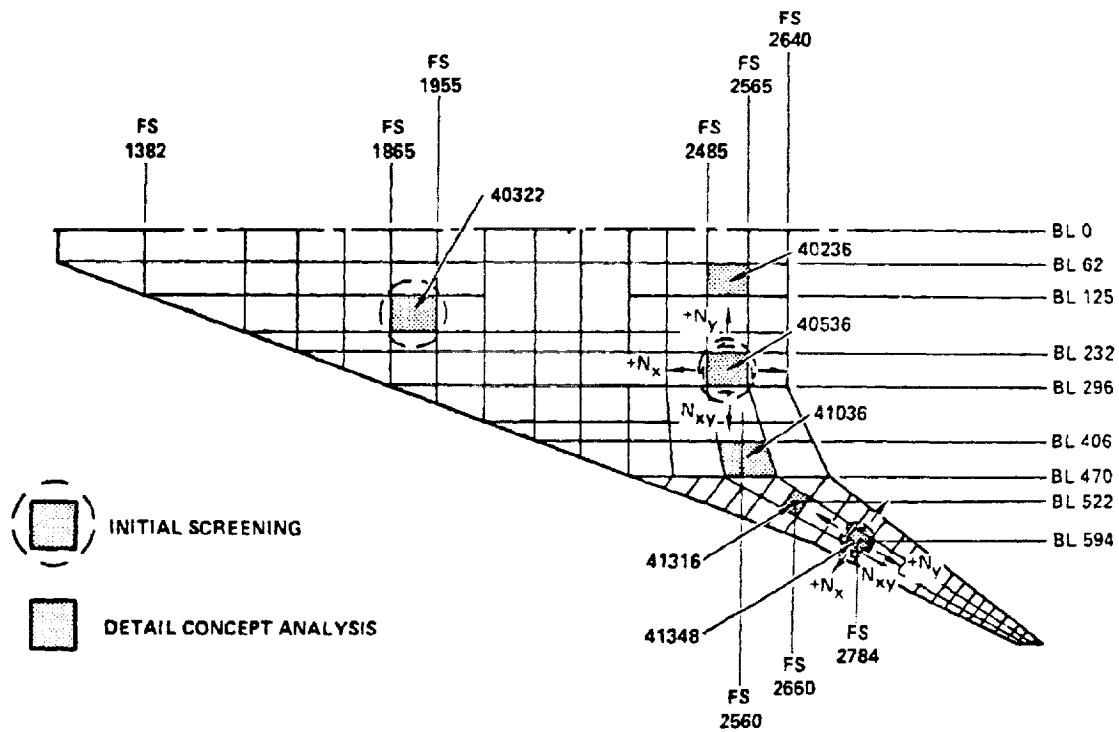


FIGURE 11-1. DEFINITION OF WING POINT DESIGN REGIONS

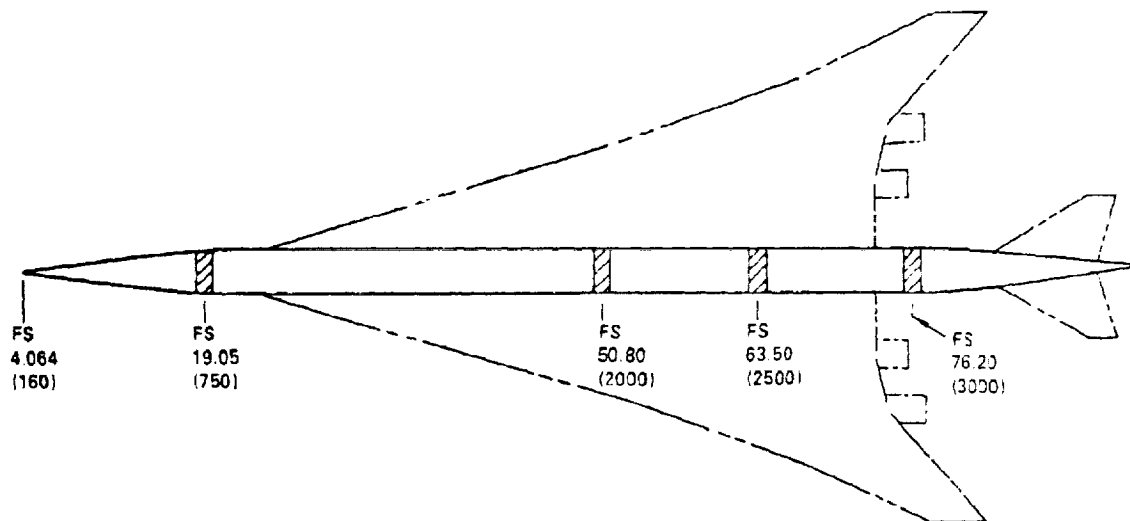


FIGURE 11-2. DEFINITION OF FUSELAGE POINT DESIGN REGIONS - TASK I

Wing Design Load Conditions - Task I

A comprehensive list of design conditions was investigated during the Task I effort. A detailed description of these conditions is contained in Section 5, Structural Design Loads.

The critical Task I load conditions were screened by conducting a NASTRAN redundant-analysis solution using the chordwise model flexibilities and its related aeroelastic loads, reviewing the magnitude of the resultant load intensities, and selecting the critical design conditions. These conditions are shown on Table 11-1, and encompass the 2.5-g symmetric flight conditions for Mach numbers of 0.40, 0.90, and 1.25. In addition, both the airloads and corresponding temperatures are included for the start-of-cruise and mid-cruise conditions. The weight, Mach number, altitude, load factor, and velocity are also indicated for each of these critical load conditions.

The point design load-temperature environment was defined for these critical design conditions for each of the Task I models i.e., chordwise, spanwise, and monocoque.

Wing Aerodynamic Pressures - Task I

Surface pressure data were calculated using the NASA - Ames pressure distribution (Woodward) program. Pressure distributions were determined at Mach numbers of 0.40, 0.90, 1.25, and 2.7. Unfortunately, the integrated force data was considerably lower than available wind tunnel measured force data. As a result, the Woodward pressures were used to define matching functions which, when applied to the net pressure coefficients from the loads determination, provided the compatible loading on each surface.

Ultimate pressure loadings for the entire wing were developed for the critical design load conditions. The grid system, which is a subset of the Structural Influence Coefficients (SIC) grid, is shown in Figure 11-3. The upper and lower surface pressures for the 2.5-g symmetric maneuver condition at Mach 1.25 are

TABLE 11-1. CRITICAL LOAD CONDITIONS - TASK I

NASTRAN COND. NO.	AIRPLANE		MACH NUMBER	ALTITUDE		LOAD FACTOR n_z	VELOCITY		COMMENT
	MASS 10^{-3} kg	WEIGHT 10^{-3} lb		10^{-3} km	10^{-3} ft		km/h	keas	
1	TEMPERATURE CONDITIONS								M2.7, MID-CRUISE
2									M2.7, START-OF-CRUISE
9	338	745	0.40	SL	SL	2.5	482	260	SYMM. FLT., STEADY MAN. @ MO.40
12	318	700	0.90	9.1	30.0	2.5	602	325	SYMM. FLT., STEADY MAN. @ MO.90 (V_C)
15	313	690	1.25	11.6	38.2	2.5	689	372	SYMM. FLT., STEADY MAN. @ M1.25 (V_C)
20	299	660	2.70	18.7	61.5	2.5	852	460	SYMM. FLT., STEADY MAN. @ M2.7 (V_C) START-OF-CRUISE
22	249	550	2.70	19.5	64.0	2.5	803	433.6	SYMM. FLT., STEADY MAN. @M2.7 (V_C) MID-CRUISE
31	313	690	1.25	16.0	52.4	2.5	491	265	SYMM. FLT., STEADY MAN. @ M1.25 (V_S)

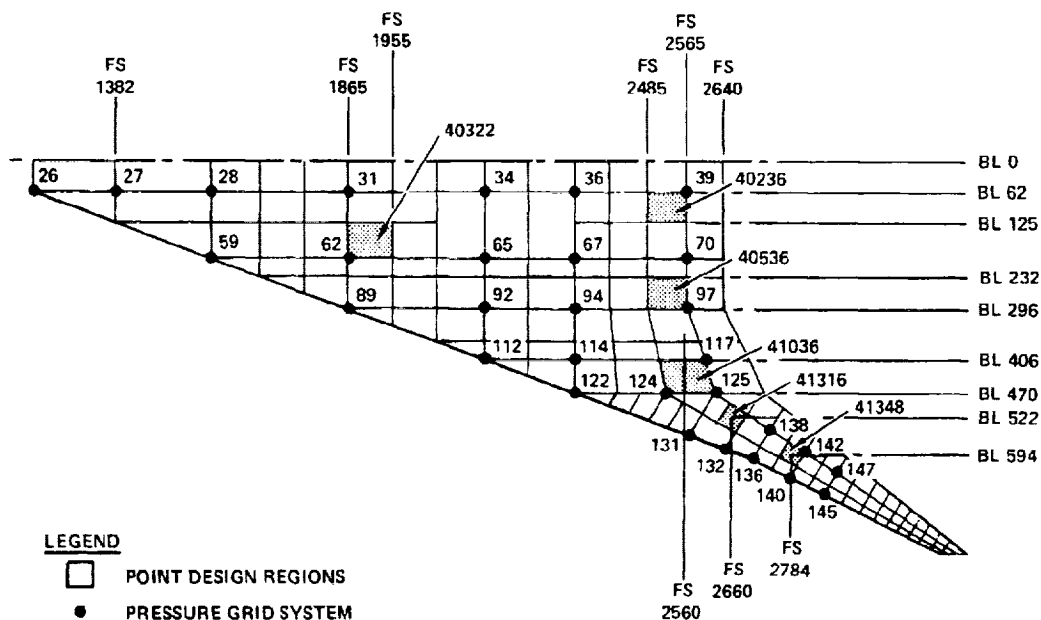


FIGURE 11-3. AERODYNAMIC PRESSURE GRID

shown in Table 11-2. The corresponding point design pressure for the Mach 1.25 condition and five additional conditions are shown in Table 11-3. This table contains the upper and lower surface pressure for these six critical flight conditions which were discussed in the previous section.

Wing Fuel Tank Pressures - Task I

The fuel tank pressures for the applicable point design regions were calculated for the critical design load conditions.

A schematic of the fuel tanks, with the "wet bay" point design regions noted is shown in Figure 11-4. The applicable point design regions are 40322, 40236, and 40536.

Average fuel heights were calculated for the critical design conditions and are shown in Table 11-4.

The horizontal (n_x) and vertical (n_z) load factors for the critical load conditions are displayed in Table 11-5, with the sign convention indicated in the accompanying footnotes. These load factors were assumed to be applied uniformly on the fuel mass defined by the point design region.

For the fuel tank pressure calculations the limit fuel pressure was defined as the sum of the fuel head multiplied by the accelerations for the particular condition. Conservatively, an additional ± 3.0 psig was added to account for the maximum tolerances of the relief valves. The limit pressure and corresponding ultimate pressure (1.5 times limit) are given by:

$$p(\text{limit}) = \rho h n \pm 3.0$$

where ρ and h are the fuel density and average fuel height respectively and n is the applicable load factor.

TABLE 11-2. WING PRESSURE LOADINGS - TASK I
COND. (31) SYMMETRIC FLIGHT AT M1.25

GRID ID.			(1) (2) LIMIT PRESSURE, PSI		GRID ID.			(1) (2) LIMIT PRESSURE, PSI	
NO.	X (IN.)	Y (IN.)	UPPER SURFACE	LOWER SURFACE	NO.	X (IN.)	Y (IN.)	UPPER SURFACE	LOWER SURFACE
26	1210	62.0	-3.51	-0.33	97	2565	296.0	-0.85	-0.17
27	1382	62.0	1.87	0.29	112	2145	406.0	-5.35	-0.00
28	1580	62.0	-0.80	-0.20	114	2330	406.0	-1.23	0.11
31	1865	62.0	-0.96	-0.44	117	2603	406.0	-0.89	0.03
34	2145	62.0	-2.61	-1.42	122	2330	470.0	-5.48	1.09
36	2330	62.0	-1.70	-0.72	124	2520	470.0	-0.72	1.06
39	2565	62.0	-2.30	-0.94	125	2625	470.0	-0.94	0.07
59	1580	196.0	-2.40	0.96	131	2562	554.0	-7.99	-0.57
62	1865	196.0	-0.98	0.04	132	2645	585.0	-13.34	-0.60
65	2145	196.0	-0.26	-0.05	136	2696	603.0	-5.19	0.14
67	2330	196.0	-1.33	-0.38	138	2742	543.0	-0.22	0.00
70	2565	196.0	-1.45	-0.47	140	2772	640.0	-13.52	3.02
89	1865	296.0	-1.01	0.14	142	2812	558.0	-1.48	-0.07
92	2145	296.0	-1.26	0.02	145	2849	676.0	-5.54	0.68
94	2330	296.0	-0.93	-0.10	147	2882	634.0	-1.97	0.08

(1) FOR ULTIMATE PRESSURE, MULTIPLY BY 1.5

(2) SIGN CONVENTION: + p = RAM, - p = SUCTION

TABLE 11-3. WING AERODYNAMIC PRESSURE LOADINGS, POINT DESIGN REGIONS - TASK I

ULTIMATE PRESSURE, kPa

WING LOCATION	POINT DESIGN REGION	COND. 9 M = 0.4		COND. 12 M = 0.9		COND. 15 M = 1.25		COND. 20 M = 2.7*		COND. 22 M = 2.7**		COND. 31 M = 1.25	
		UPPER	LOWER	UPPER	LOWER	UPPER	LOWER	UPPER	LOWER	UPPER	LOWER	UPPER	LOWER
FORWARD BOX	40322	-6.27	1.65	-9.65	-2.07	-10.27	0.41	-11.51	-1.17	-9.31	-0.96	-10.14	0.41
	40236	-6.55	-2.00	-6.83	-3.03	-22.96	-9.03	-11.72	-5.10	-8.82	-3.72	-20.89	-8.27
AFT BOX	40536	-3.65	2.28	-9.31	-3.38	-7.38	-1.45	-10.14	-2.48	-8.14	-2.07	-8.76	-1.79
	41036	-6.96	6.34	-14.48	-2.48	-8.27	0.76	-8.62	2.62	-7.17	2.28	-8.76	0.76
TIP	41316	-23.93	-0.21	-46.54	-25.92	-31.02	-1.86	-11.38	6.90	-9.79	6.34	34.34	-1.79
	41348	-32.89	-0.96	-25.37	-2.07	-30.06	4.55	-8.89	7.17	-7.31	5.92	-34.96	6.62

ULTIMATE PRESSURE, psi

WING LOCATION	POINT DESIGN REGION	COND. 9 M = 0.4		COND. 12 M = 0.9		COND. 15 M = 1.25		COND. 20 M = 2.7*		COND. 22 M = 2.7**		COND. 31 M = 1.25	
		UPPER	LOWER	UPPER	LOWER	UPPER	LOWER	UPPER	LOWER	UPPER	LOWER	UPPER	LOWER
FORWARD BOX	40322	-0.91	0.24	-1.40	-0.30	-1.49	0.06	-1.67	-0.17	-1.35	-0.14	-1.47	0.06
	40236	-0.95	-0.29	-0.99	-0.44	-3.33	-1.31	-1.70	-0.74	-1.28	-0.54	-3.03	-1.20
AFT BOX	40536	-0.53	-0.33	-1.35	-0.49	-1.07	-0.21	-1.47	-0.36	-1.18	-0.30	-1.27	-0.26
	41036	-1.01	-0.92	-2.10	-0.36	-1.20	0.11	-1.25	0.38	-1.04	0.33	-1.27	0.11
TIP	41316	-3.47	-0.03	-6.75	-3.76	-4.50	-0.27	-1.65	1.00	-1.42	0.92	4.98	-0.26
	41348	-4.77	-0.14	-3.68	-0.30	-4.36	0.66	-1.29	1.04	-1.06	0.86	-5.07	0.96

NOTES:

*Start of Cruise

**Mid Cruise

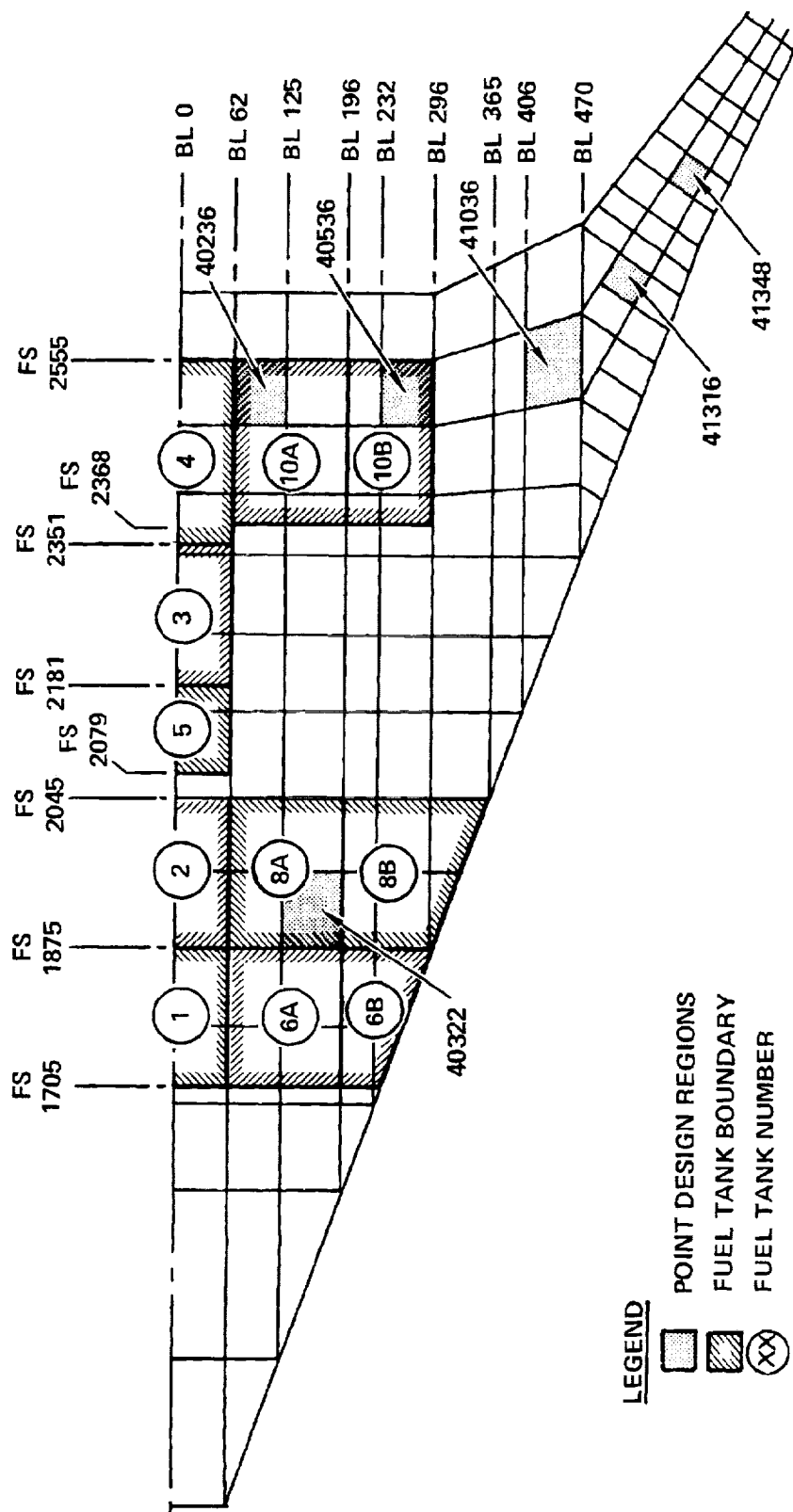


FIGURE 11-4. FUEL TANK LOCATIONS - TASK I

TABLE 11-4. SUMMARY OF FUEL HEIGHTS - TASK I

POINT DESIGN REGION	40236	40536	40322
TANK NO.	10A	10B	8A
COND.	FUEL HEIGHT (IN.)		
⑨	34.0	26.5	41.0
⑫	34.0	26.5	41.0
⑮	34.0	26.5	41.0
⑳	34.0	26.5	41.0
㉒	21.0	2.0	21.5
㉓	34.0	26.5	41.0

TABLE 11-5. SUMMARY OF LOAD FACTORS - TASK I

POINT DESIGN REGION	40236		40536		40322	
	LOAD FACTORS (LIMIT) (1)					
COND.	n_x	n_z	n_x	n_z	n_x	n_z
⑨	0.08	-2.73	0.08	-2.73	0.08	-2.50
	-0.11	0.77	-0.11	0.77	-0.11	1.13
⑫	0.08	-2.73	0.08	-2.73	0.08	-2.50
	-0.11	0.77	-0.11	0.77	-0.11	1.13
⑮	0.08	-2.76	0.08	-2.76	0.08	-2.50
	-0.15	0.74	-0.15	0.74	-0.15	1.15
⑳	0	-2.50	0	-2.50	0	-2.66
		1.28		1.28		0.84
㉒	0	-2.50	0	-2.50	0	-2.66
		1.28		1.28		0.84
㉓	0.08	-2.76	0.08	-2.76	0.08	-2.50
	-0.15	0.74	-0.15	0.74	-0.15	1.15

(1) SIGN CONVENTION:

+ n_x = AFTWARD+ n_z = UPWARD

A summary of the fuel tank pressure calculations are shown in Table 11-6. The component and combined limit pressures are indicated as well as the resulting ultimate values for each of the critical design conditions.

Wing Internal Loads - Task I

The wing internal loads, displacements, and structural influence coefficients for the Task I structural arrangements were determined using the NASTRAN redundant-structure analysis solutions. These solutions were performed using each of the three Task I structural models (i.e., Chordwise, Spanwise, and Monocoque) and included the thermal stresses for two temperature conditions, start-of-cruise and mid-cruise. A detail description of the Task I models and the results of the NASTRAN solution are covered in Section 9. This section presents the wing internal loads for the critical design conditions, the average thermal strains for the hot conditions, and for completeness, a brief review of the temperature gradients.

Internal Loads-Airloads - The wing ultimate loads for Condition 31, the most critical Task I flight condition (2.5-g symmetric maneuver at Mach 1.25), are presented in Figures 11-5, 11-6, and 11-7 for each of the Task I models. These running loads are displayed on the wing planform of the structural model and represent the inplane load state (N_x, N_y and N_{xy}) for the majority of the upper surface panels. Based on the modeling technique, model symmetry about the x-y plane, the wing lower surface inplane loads have the same magnitude as the displayed upper surface loads except all signs are of opposite values. The inplane loads for the point design regions are noted.

A summary of the load intensities at the point design regions are shown in Table 11-7. These tables list the loads from each structural model for comparison purposes.

Internal Loads - Thermal - The NASTRAN solution determined the thermal stresses and thermo-elastic deflections due to the thermal expansion of the axial elements. Figures 11-8 through 11-10 show the wing load intensities resulting from this NASTRAN solution for the start-of-cruise temperature condition. These figures

TABLE 11-6. FUEL TANK PRESSURES - TASK I

POINT DESIGN REGION		40236				40536				40322			
TANK NO.		10A				10B				8A			
PRESSURE (psi)		LIMIT - p			ULT COMB - p	LIMIT - p			ULT COMB - p	LIMIT - p			ULT COMB - p
COND.	SURF.	FUEL HEAD	VALVE	COMB		FUEL HEAD	VALVE	COMB		FUEL HEAD	VALVE	COMB	
9	UPPER	0.92	3.00	3.92	5.88	0.75	3.00	3.75	5.63	1.49	3.00	4.49	6.74
	LOWER	2.87	3.00	5.87	8.81	2.27	3.00	5.27	7.91	2.97	3.00	5.97	8.96
12	UPPER	0.92	3.00	3.92	5.88	0.75	3.00	3.75	5.63	1.49	3.00	4.49	6.74
	LOWER	2.87	3.00	5.87	8.81	2.27	3.00	5.27	7.91	2.97	3.00	5.97	8.96
15	UPPER	0.95	3.00	3.95	5.93	0.78	3.00	3.78	5.67	1.57	3.00	4.57	6.86
	LOWER	2.96	3.00	5.96	8.94	2.35	3.00	5.35	8.02	3.00	3.00	6.00	9.00
20	UPPER	1.28	3.00	4.28	6.42	1.00	3.00	4.00	6.00	1.00	3.00	4.00	6.00
	LOWER	2.23	3.00	5.23	7.84	1.74	3.00	4.74	7.11	3.20	3.00	6.20	9.30
22	UPPER	0.79	3.00	3.79	5.68	0.08	3.00	3.08	4.62	0.53	3.00	3.53	5.30
	LOWER	1.38	3.00	4.38	6.57	0.13	3.00	3.13	4.70	1.68	3.00	4.68	7.02
31	UPPER	0.95	3.00	3.95	5.93	0.78	3.00	3.78	5.67	1.57	3.00	4.57	6.86
	LOWER	2.96	3.00	5.96	8.94	2.35	3.00	5.35	8.03	3.00	3.00	6.00	9.00

SIGN CONVENTION: -p = SUCTION +p = RAM

POINT DESIGN REGION		40236					40536					40322				
TANK NO.		10A					10B					8A				
PRESSURE (kPa)		LIMIT - p			ULT COMB - p	LIMIT - p			ULT COMB - p	LIMIT - p			ULT COMB - p			
COND.	SURF.	FUEL HEAD	VALVE	COMB		FUEL HEAD	VALVE	COMB		FUEL HEAD	VALVE	COMB				
9	UPPER	6.34	20.68	27.02	40.54	5.17	20.68	25.85	38.82	10.27	20.68	30.95	46.47			
	LOWER	19.79	20.68	40.47	60.74	15.65	20.68	36.33	54.54	20.48	20.68	41.16	61.78			
12	UPPER	6.34	20.68	27.02	40.54	5.17	20.68	25.85	38.82	10.27	20.68	30.95	46.47			
	LOWER	19.79	20.68	40.47	60.74	15.65	20.68	36.33	54.54	20.48	20.68	41.16	61.78			
15	UPPER	6.54	20.68	27.22	40.88	5.38	20.68	26.06	39.09	10.82	20.68	31.51	47.30			
	LOWER	20.41	20.68	41.09	61.64	16.20	20.68	36.88	55.30	20.68	20.68	41.37	62.05			
20	UPPER	8.82	20.68	29.50	44.26	6.89	20.68	27.57	41.37	6.89	20.68	27.58	41.37			
	LOWER	15.38	20.68	36.06	54.05	12.00	20.68	32.68	49.02	22.06	20.68	42.75	64.12			
22	UPPER	5.44	20.68	26.13	39.16	0.55	20.68	21.23	31.85	3.65	20.68	24.34	36.54			
	LOWER	9.51	20.68	30.20	45.30	0.90	20.68	21.58	32.40	11.58	20.68	32.27	48.40			
31	UPPER	6.55	20.68	27.23	40.88	5.38	20.68	26.06	39.09	10.82	20.68	31.51	47.30			
	LOWER	20.41	20.68	40.09	61.64	16.20	20.68	36.88	55.30	20.68	20.68	41.37	62.05			

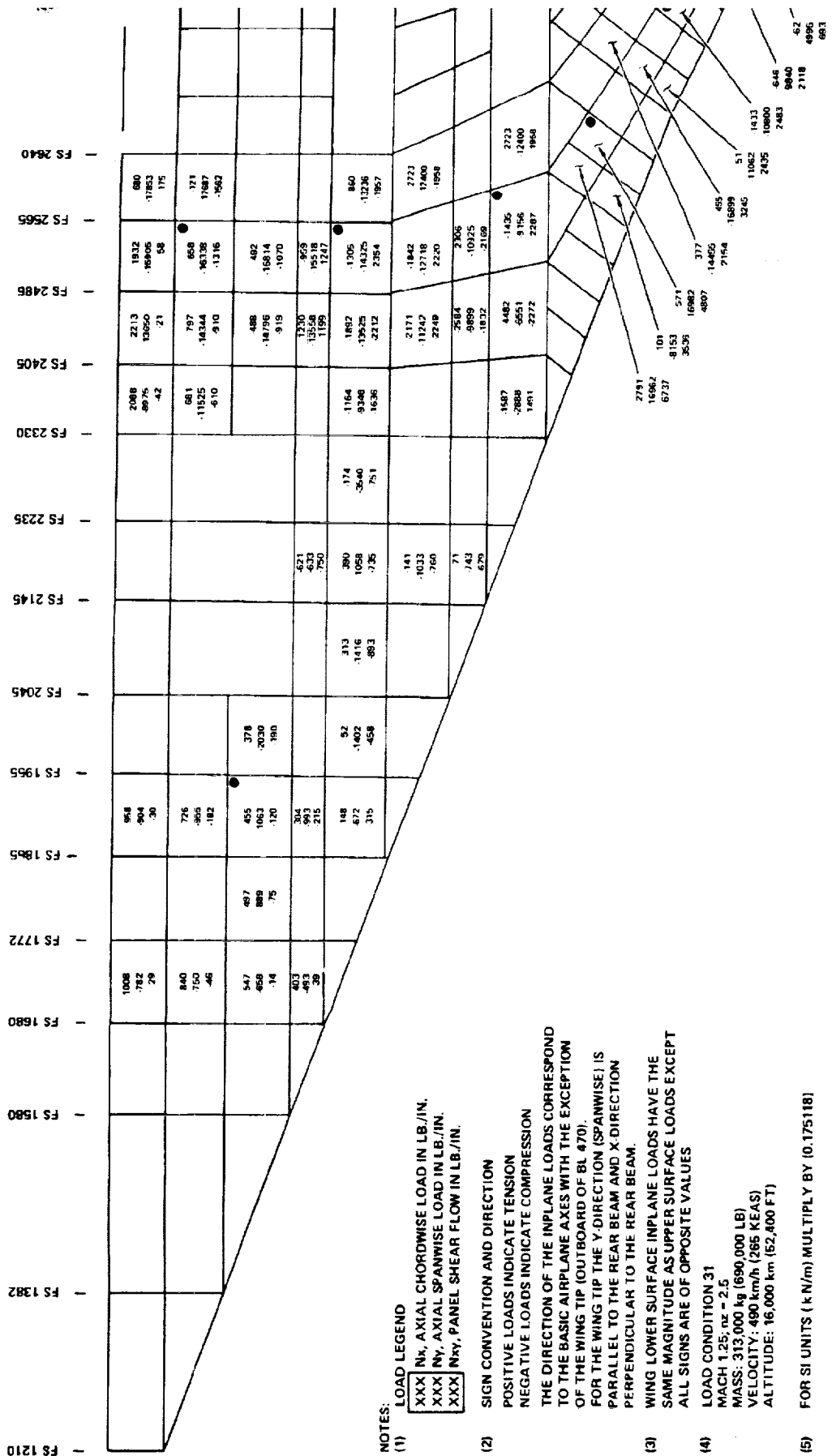
SIGN CONVENTION: -p = SUCTION +p = RAM

ORIGINAL PAGE IS
OF POOR QUALITY

1

2

3



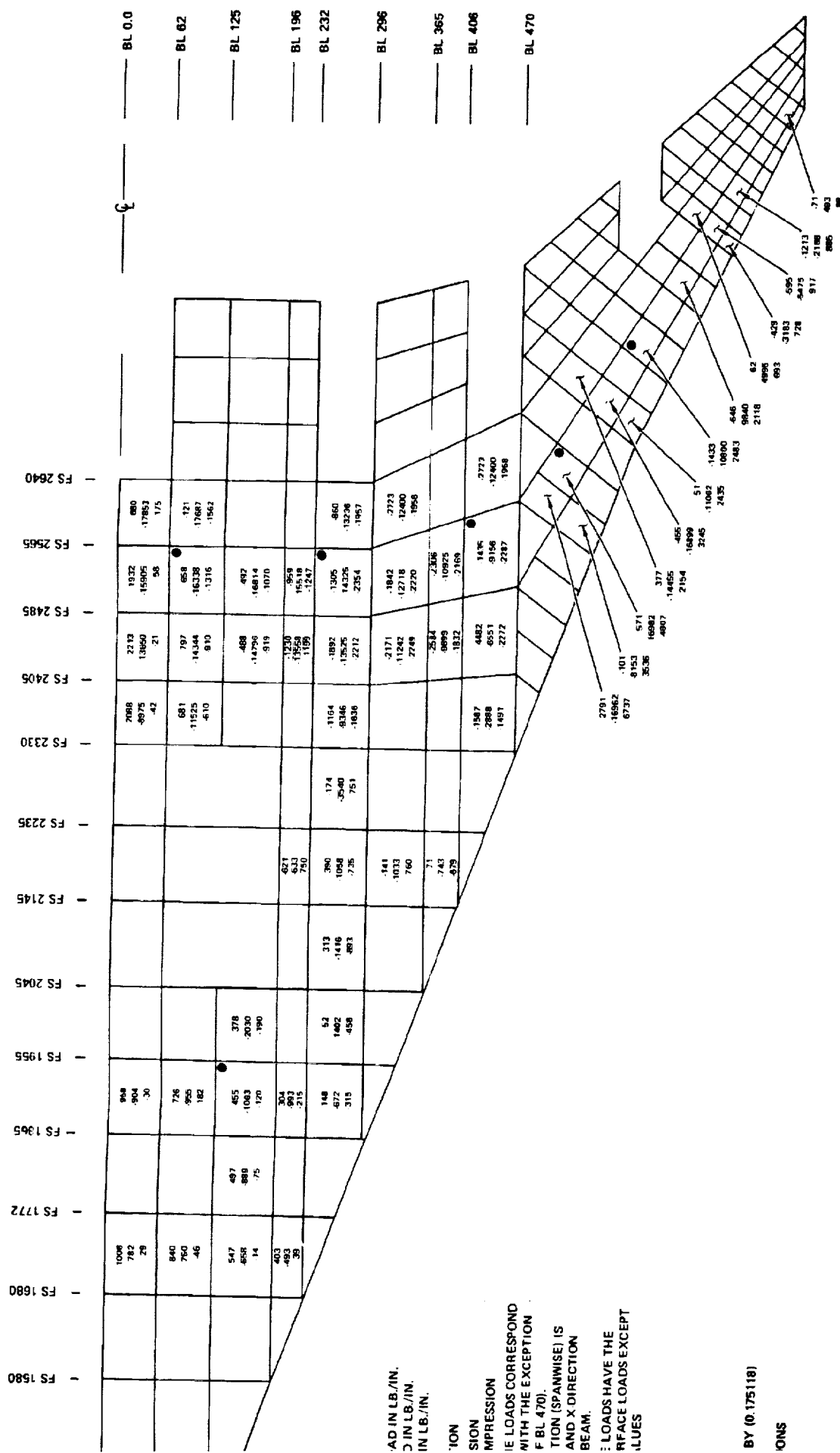
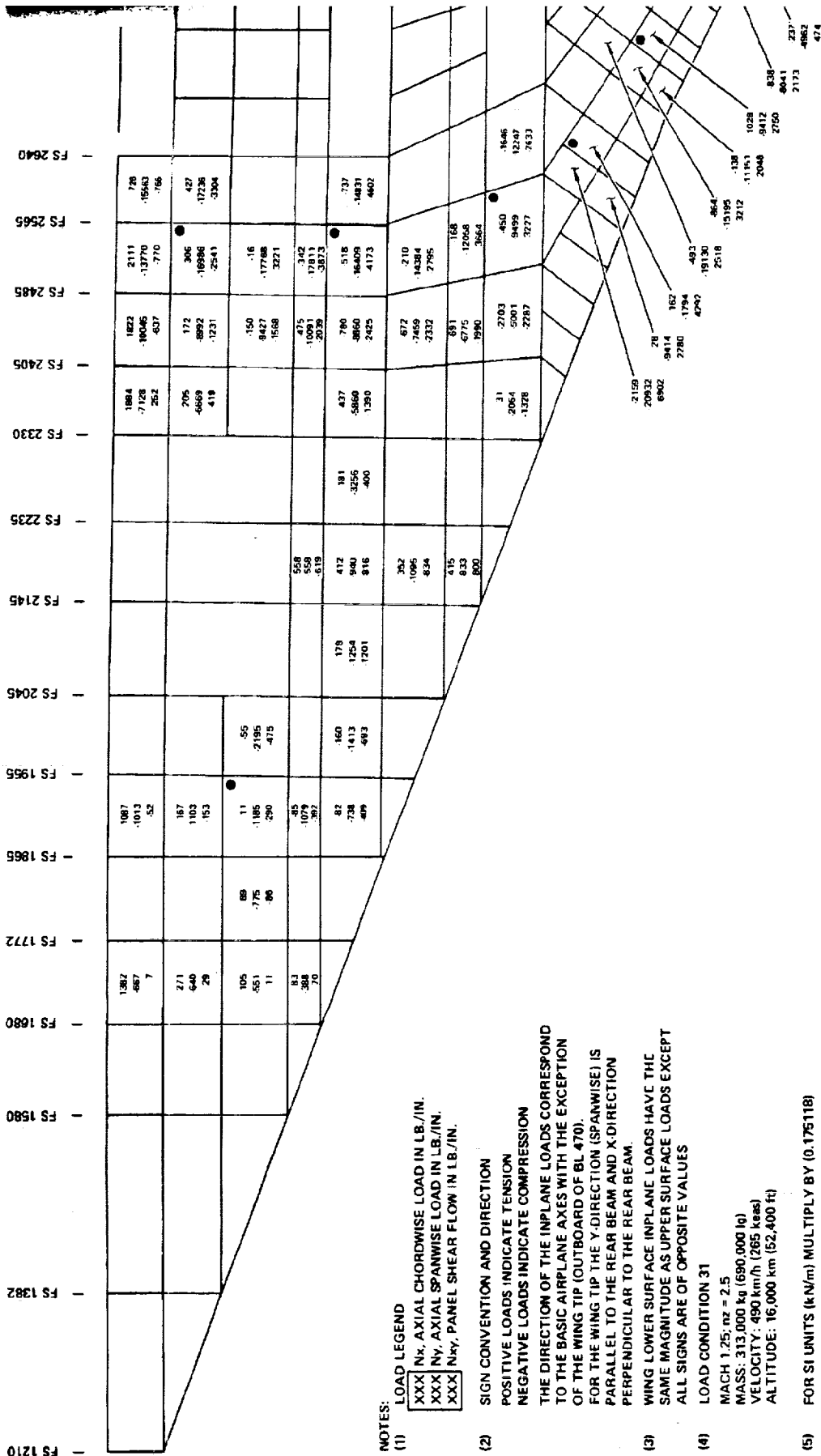


FIGURE 11-5. WING UPPER SURFACE LOAD INTENSITIES, CHORDWISE ARRANGEMENT

11-17
MULTIPOINT FRAME

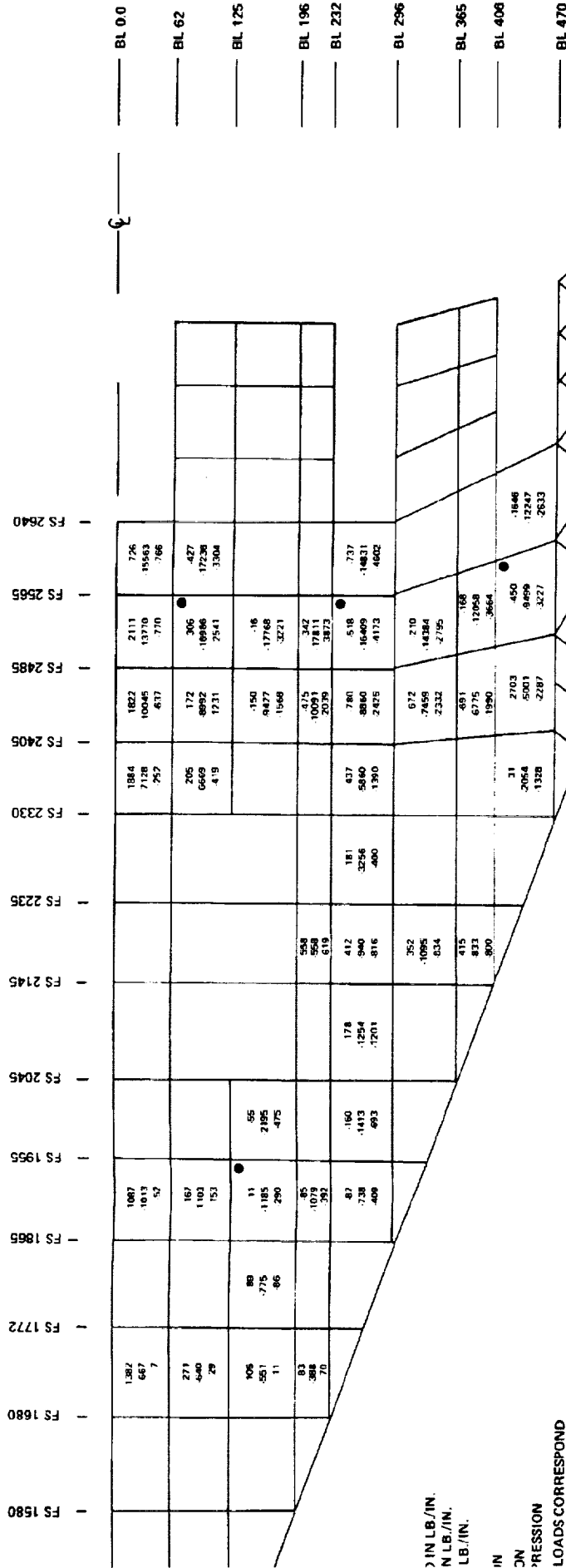
FOLDOUT FRAME 2



PRECEDING PAGE BLANK NOT FILMED

FOLDOUT FRAME 1

FOLDOUT FRAME 2



IN LB./IN.
N LB./IN.
LB./IN.

IN
ON

PRESSION
LOADS CORRESPOND
TO THE EXCEPTION
BL 470.

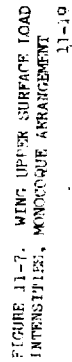
ON (SPANWISE) IS
VD X-DIRECTION

LOADS HAVE THE
FACE LOADS EXCEPT
UES

(0.175118)

ONS

FIGURE 11-6. WING UPPER SURFACE LOAD
INTENSITIES, SPANWISE ARRANGEMENT



07-17

TABLE 11-7. WING UPPER SURFACE LOAD INTENSITIES - ALL MODELS,
MACH 1.25 LOAD CONDITION

PANEL IDENTIFICATION		*LOAD INTENSITY (ULTIMATE), LBS/IN			
REGION	NUMBER	DIRECTION	STRUCTURAL ARRANGEMENT		
			CHORDWISE	SPANWISE	MONOCOQUE
WING FORWARD	40322	NX	455	11	51
		NY	-1,063	-1,185	-529
		NXY	120	290	191
WING AFT BOX	40236	NX	658	306	-1,193
		NY	-16,338	-16,986	-11,638
		NXY	1,316	2,541	2,099
	40536	NX	-1,305	-518	-3,171
		NY	-14,325	-16,409	-11,424
		NXY	2,354	4,173	4,647
	41036	NX	-1,435	-450	-2,219
		NY	-9,156	-9,499	6,423
		NXY	2,237	3,227	3,209
WING TIP	41316	NX	571	162	-1,587
		NY	-16,982	-17,948	-12,183
		NXY	4,807	4,292	3,310
	41348	NX	-1,433	-1,028	-1,190
		NY	-10,800	9,412	-7,263
		NXY	2,483	2,750	3,285

*CONDITION 31: MACH 1.25 $n_z = 2.5$, $W = 690,000$ LB., $V_e = 265$ KEAS

PANEL IDENTIFICATION		*LOAD INTENSITY (ULTIMATE), kN/m			
REGION	NUMBER	DIRECTION	STRUCTURAL ARRANGEMENT		
			CHORDWISE	SPANWISE	MONOCOQUE
WING FORWARD	40322	NX	80	2	9
		NY	186	-208	-93
		NXY	21	51	33
WING AFT BOX	40236	NX	115	54	-209
		NY	-2,861	-2,975	-2,038
		NXY	230	445	368
	40536	NX	-228	-91	-555
		NY	-2,508	-2,874	-2,000
		NXY	412	731	814
	41036	NX	-251	-79	-389
		NY	-1,603	-1,663	-1,125
		NXY	392	565	562
WING TIP	41316	NX	100	28	-278
		NY	-2,974	-3,143	-2,133
		NXY	842	752	580
	41348	NX	-251	-180	-209
		NY	-1,891	-1,648	-1,272
		NXY	435	482	575

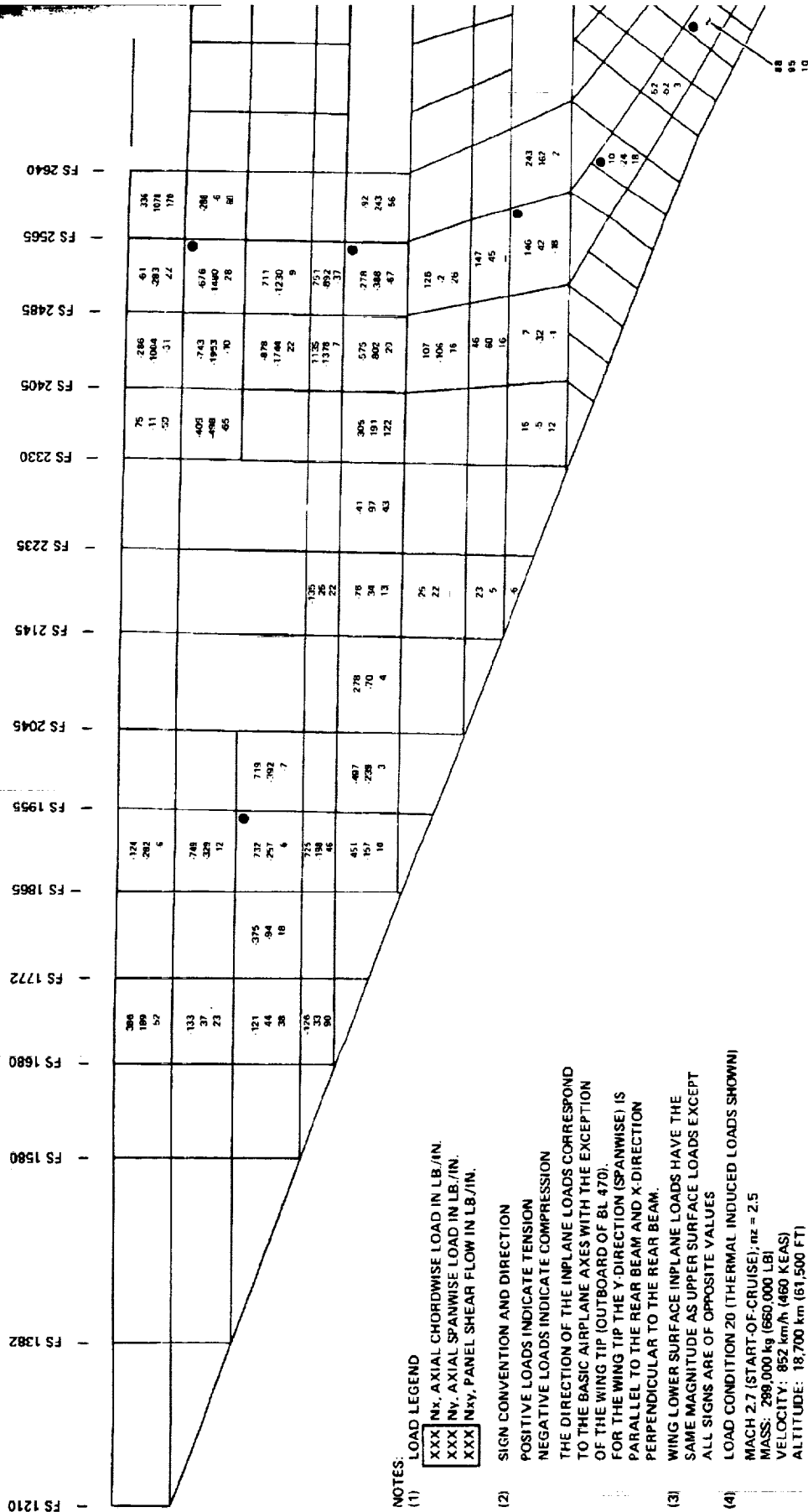
*CONDITION 31: MACH 1.25, $n_z = 2.5$, $M = 313,000$ kg, $V = 490$ km/h

PRECEDING PAGE BLANK NOT FILMED

1

2

3



NOTES:

(1) LOAD LEGEND

XXX Nx, AXIAL CHORDWISE LOAD IN LB./IN.
 XXX Nv, AXIAL SPANWISE LOAD IN LB./IN.
 XXX Nxy, PANEL SHEAR FLOW IN LB./IN.

(2) SIGN CONVENTION AND DIRECTION

POSITIVE LOADS INDICATE TENSION
 NEGATIVE LOADS INDICATE COMPRESSION
 THE DIRECTION OF THE INPLANE LOADS CORRESPOND TO THE BASIC AIRPLANE AXES WITH THE EXCEPTION OF THE WING TIP (OUTBOARD OF BL 470).
 FOR THE WING TIP THE Y-DIRECTION (SPANWISE) IS PARALLEL TO THE REAR BEAM AND X-DIRECTION PERPENDICULAR TO THE REAR BEAM.

(3) WING LOWER SURFACE INPLANE LOADS HAVE THE SAME MAGNITUDE AS UPPER SURFACE LOADS EXCEPT ALL SIGNS ARE OF OPPOSITE VALUES

(4) LOAD CONDITION 20 (THERMAL INDUCED LOADS SHOWN)

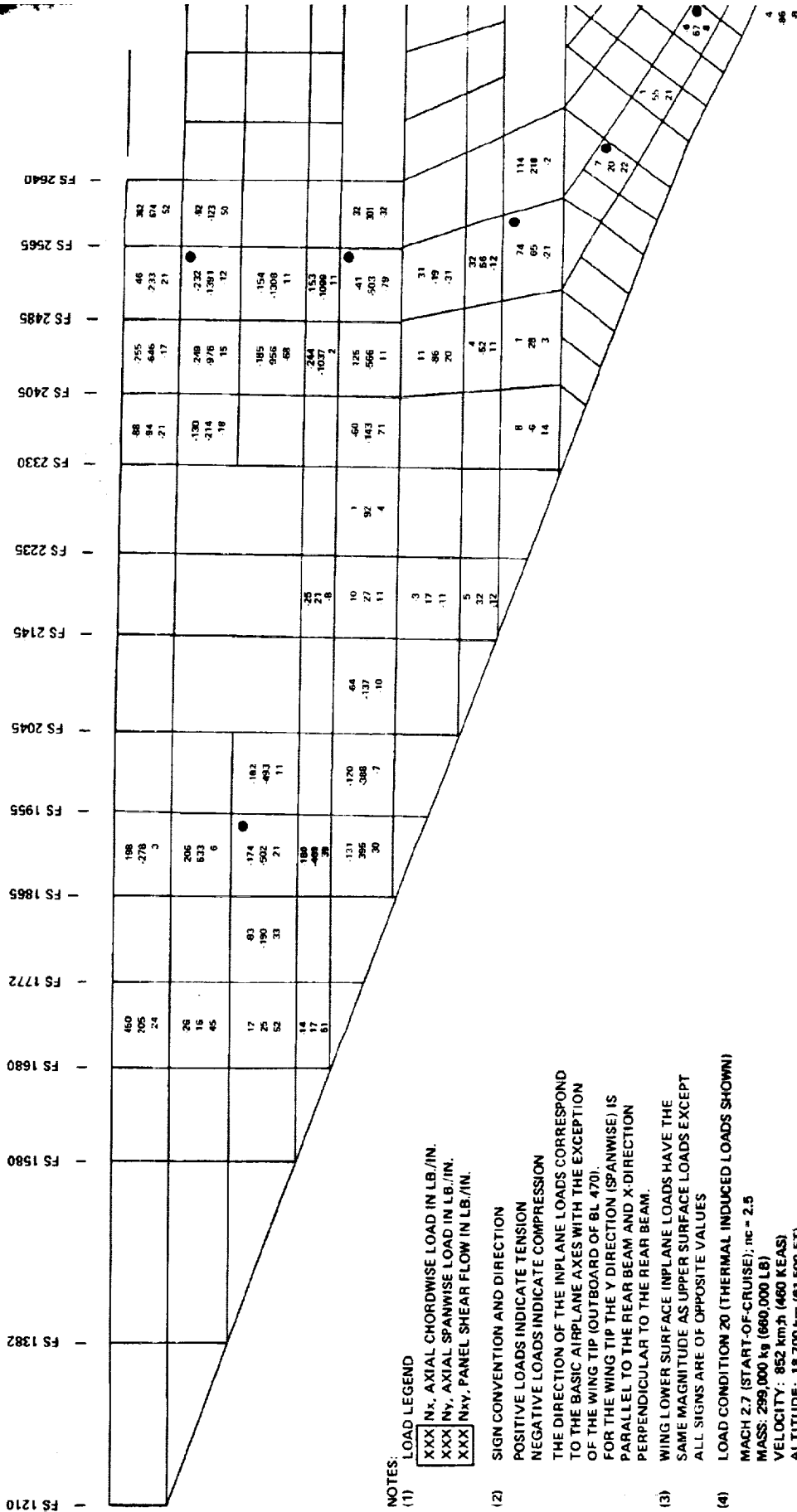
MACH 2.7 (START-OF-CRUISE); $n_z = 2.5$
 MASS: 289,000 kg (660,000 LBI)
 VELOCITY: 852 km/h (460 KEAS)
 ALTITUDE: 18,700 km (61,500 FT)

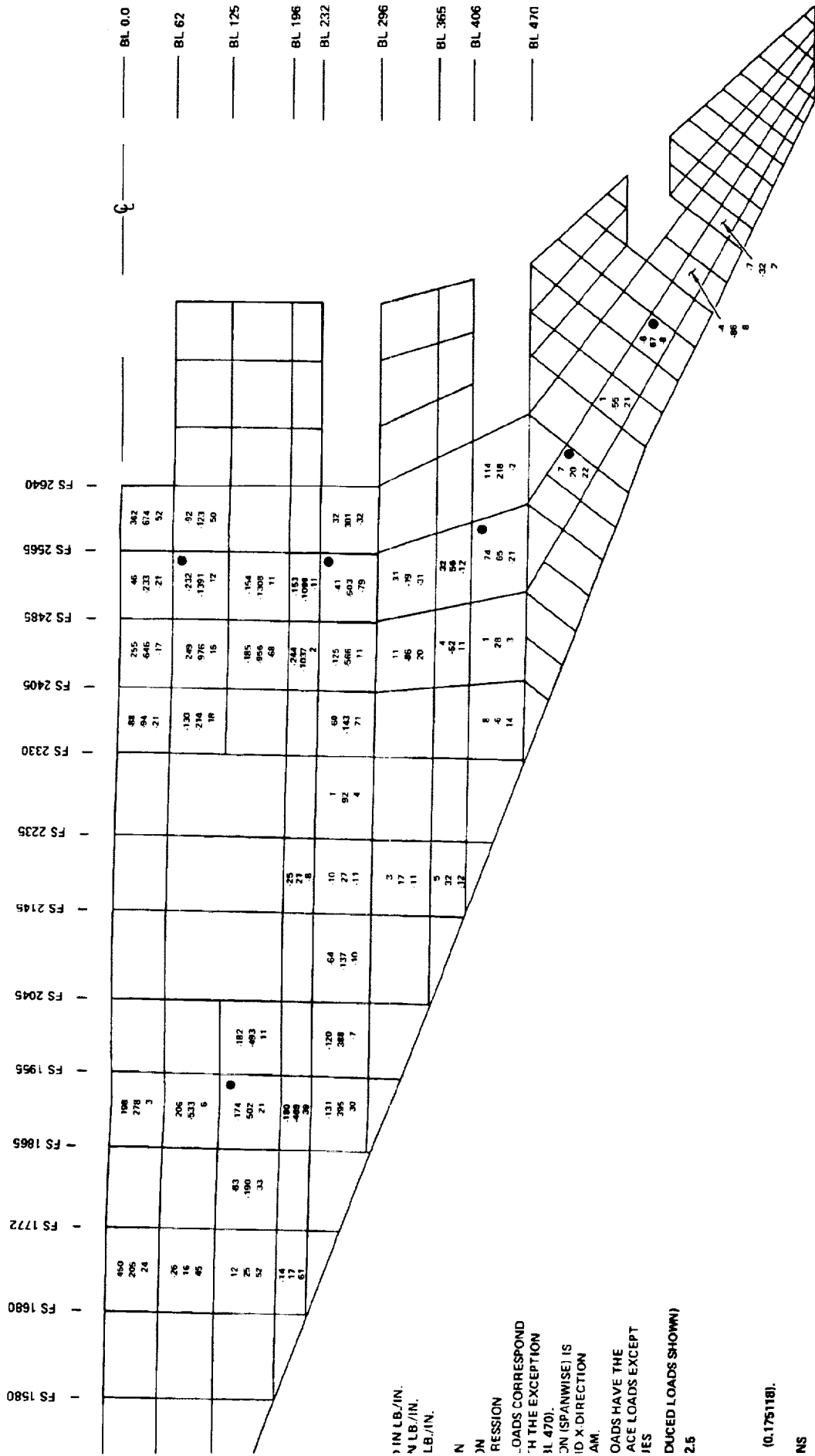
(5) FOR SI UNITS (k N/m) MULTIPLY BY (0.175118)

(6) ● DENOTES POINT DESIGN REGIONS

PRECEDING PAGE BLANK NOT FILMED
 FOLDOUT FRAME/

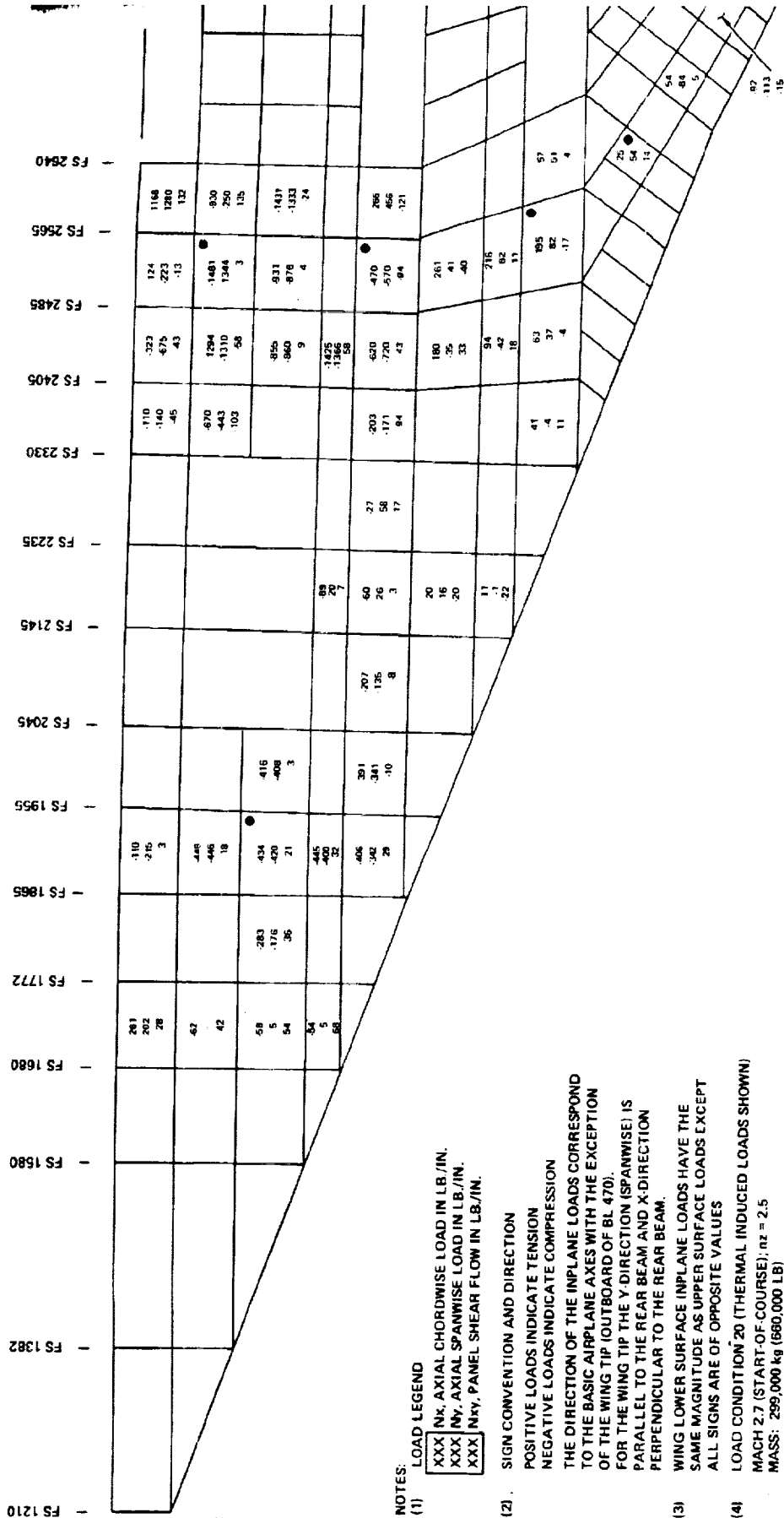
FOLDOUT FRAME 2





(0.175118).

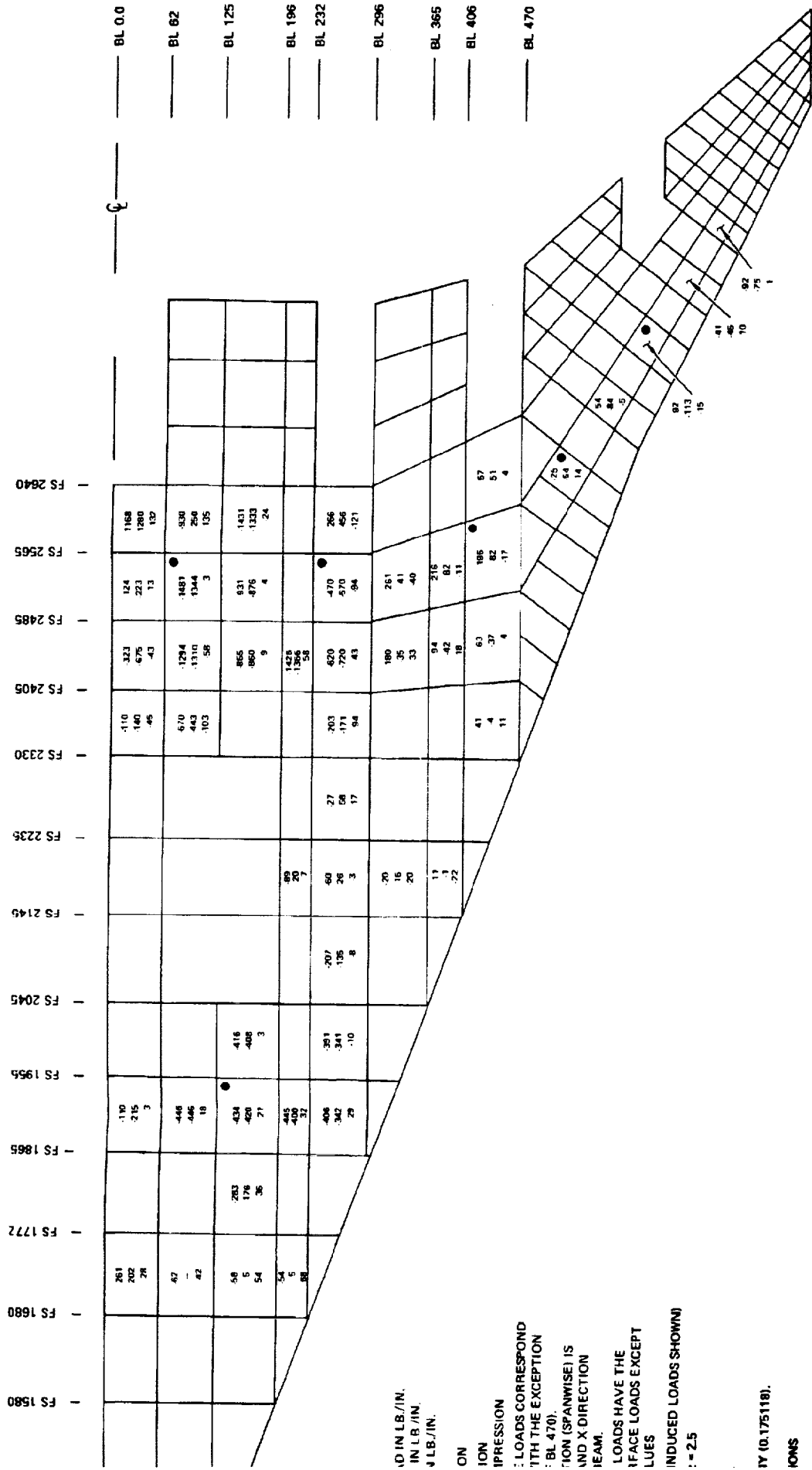
NS



PRECEDING PAGE BLANK NOT FILMED

FOLDOUT FRAME /

Full frame



10 IN LB./IN.
 IN LB./IN.
 1 LB./IN.
 ON
 ION
 IPRESSION
 : LOADS CORRESPOND
 TTH THE EXCEPTION
 : BL 470).
 ION (SPANWISE) IS
 AND X DIRECTION
 IEAM.
 LOADS HAVE THE
 IFACE LOADS EXCEPT
 LUES
 (INDUCED LOADS SHOWN)
 : = 2.5
 IY (0.175118).
 IONS

FIGURE 11-10. WING THERMALLY INDUCED LOAD INTENSITIES, INBOARD ARRANGEMENT

FULLOUT FRAMES 11-27

contain the thermally induced inplane loads for the wing upper surface for each of the Task I models, with the point design regions noted.

The NASTRAN thermal stresses are converted to strains for input to the structural analysis computer programs. The stresses and equivalent strains are shown in Table 11-8 for each structural arrangement for the two temperature conditions investigated.

In addition to the thermally induced inplane loads, the average temperature and thermal gradient within an element are required to complete the definition of the point design environment. Time-temperature histories were calculated for representative structure at the point design regions; see Section 6 (Structural Temperatures) for a detail description of this analysis. For the sake of completeness, a typical example of the temperature data is shown in Table 11-9. This data is for the Chordwise arrangement surface panels and indicates the component temperatures, average temperature, and the temperature gradients for the critical Task I load conditions.

For this example, only point design regions 40236, 40536, and 40322 are shown; the temperatures for all point design regions are included in the following wing point design environment summary tables.

Wing Point Design Environment - Task I

The basis for the detail structural evaluation of the Task I concept is the point design environment; this environment was defined as comprehensively as feasible to provide credence to the selection of the best structural arrangement.

The wing point design environment was defined for each wing structural arrangement for the Task I critical design load conditions. The chordwise arrangement wing point design environments are presented in Tables 11-10 through 11-15, Spanwise arrangement environments in Tables 11-16 through 11-21, and the point design environments for the Monocoque arrangement in Tables 11-22 through 11-27.

PRECEDING PAGE BLANK NOT FILMED

TABLE 11-8. SUMMARY OF WING THERMAL STRESSES AND STRAINS - TASK I

CHORDWISE STIFFENED ARRANGEMENT

WING LOCATION	POINT DESIGN REGION	CONDITION 20 START OF CRUISE						CONDITION 22 MID CRUISE					
		STRESSES (psi)			STRAINS $\times 10^{-6}$			STRESSES (psi)			STRAINS $\times 10^{-6}$		
		σ_x	σ_y	τ_{xy}	ϵ_x	ϵ_y	γ	σ_x	σ_y	τ_{xy}	ϵ_x	ϵ_y	γ
FORWARD BOX	40322	-9,606	-11,420	-77	-632	-751	-14	-10,032	-11,133	138	-660	-732	25
AFT BOX	40236	-3,439	-2,443	2,324	-226	-161	426	-11,269	-8,866	244	-741	-583	45
	40536	-489	-1,115	-1,223	-32	-73	224	-2,776	-2,897	-1,388	-183	-191	-255
	41036	1,422	235	-91	94	15	-17	1,427	-528	-359	94	-35	-66
TIP	41316	162	288	521	10	19	93	-49	-205	176	-3	-14	32
	41348	0.6	13	-4	0	1	1	534	-667	-123	-35	-44	-22

SPANWISE STIFFENED ARRANGEMENT

FORWARD BOX	40322	-6,760	-5,262	219	-445	-346	40	-12,160	-9,290	740	-800	-611	136
AFT BOX	40236	3,883	3,125	212	255	206	39	13,656	9,275	151	898	610	-28
	40536	1,898	907	743	125	-60	136	-2,282	-3,103	-946	-151	-204	-174
	41036	3,068	493	-296	202	32	-54	2,107	544	-333	-139	36	-61
TIP	41316	1,350	128	655	89	8	120	546	-129	261	36	-8	48
	41348	230	96	28	15	6	5	-401	-674	-159	23	-44	-29

MONOCOQUE ARRANGEMENT

FORWARD BOX	40322	-7,072	-6,539	315	-455	-430	58	-14,465	14,020	699	-952	-922	128
AFT BOX	40236	-10,010	-9,965	338	-659	-656	76	1,082	-1,940	35	71	-128	6
	40536	-1,376	1,964	626	-91	129	-115	-3,616	-4,390	721	-238	-289	-132
	41036	10	126	-77	1	8	14	2,055	864	176	136	57	-32
TIP	41316	100	229	382	7	15	70	-189	-408	103	-12	-27	19
	41348	5	-4.4	-0.7	0.3	-0.3	-0.1	782	-967	-128	-51	-54	23

NOTE: STRESSES ARE ULTIMATE AVERAGE STRESSES.
STRAINS ARE IN/IN

CHORDWISE STIFFENED ARRANGEMENT

WING LOCATION	POINT DESIGN REGION	CONDITION 20 START OF CRUISE						CONDITION 22 MID CRUISE					
		STRESSES (kPa)			STRAINS $\times 10^{-6}$			STRESSES (kPa)			STRAINS $\times 10^{-6}$		
		σ_x	σ_y	τ_{xy}	ϵ_x	ϵ_y	γ	σ_x	σ_y	τ_{xy}	ϵ_x	ϵ_y	γ
FORWARD BOX	40322	-66,231	-78,738	-531	-632	-751	-14	69,168	-76,759	951	-660	-732	25
AFT BOX	40236	-23,711	-16,844	16,023	-226	-161	426	-77,697	-61,129	1,682	-741	-583	45
	40536	-3,372	-7,688	-8,432	-32	-73	224	-19,140	-19,974	-9,570	-183	-191	-255
	41036	9,604	1,620	-627	94	15	-17	9,839	-3,640	-2,475	94	-35	-66
TIP	41316	1,117	1,986	3,592	10	19	93	-338	-1,413	1,213	-3	14	32
	41348	4	90	-28	0	1	1	-3,682	-4,599	-848	-35	-44	-22

SPANWISE STIFFENED ARRANGEMENT

FORWARD BOX	40322	-46,608	-36,280	1,510	-445	-346	40	-83,840	-64,052	5,102	-800	-611	136
AFT BOX	40236	-26,772	-21,546	1,462	-255	-206	39	94,155	-63,949	-1,041	-898	-610	28
	40536	13,086	-6,254	-5,123	125	-60	-136	-15,803	-21,394	-6,522	-151	-204	-174
	41036	21,153	3,399	-2,041	202	32	-54	14,527	3,751	-2,296	-139	36	-61
TIP	41316	9,308	882	4,516	89	8	-120	3,764	-889	1,800	36	-8	48
	41348	1,586	662	193	15	6	5	-2,765	-4,647	-1,096	23	-44	-29

MONOCOQUE ARRANGEMENT

FORWARD BOX	40322	-48,760	-45,085	2,172	-465	-430	58	-99,733	-96,664	4,819	-952	-922	128
AFT BOX	40236	-69,016	68,706	2,330	-659	-656	76	7,460	-13,376	241	71	-128	6
	40536	-9,487	13,541	-4,316	91	129	115	24,931	30,268	-4,971	-238	-289	-132
	41036	69	869	531	1	8	14	14,169	5,957	1,213	135	57	-32
TIP	41316	689	1,579	2,634	7	15	70	-1,303	-2,813	710	-12	-27	19
	41348	34	-30	-5	0.3	-0.3	-0.1	-5,392	-6,667	-882	51	54	23

NOTE: STRESSES ARE ULTIMATE AVERAGE STRESSES.
STRAINS ARE m/m

TABLE 11-9. WING SURFACE PANEL TEMPERATURES, CHORDWISE ARRANGEMENT - TASK I

POINT DESIGN REGION			40236					40536					40322				
			TEMPERATURES (F)					TEMPERATURES (F)					TEMPERATURES (F)				
COND.	TIME (MIN)	SURF	T _O	T _i	T _{AVG}	ΔT	T _O	T _i	T _{AVG}	ΔT	T _O	T _i	T _{AVG}	ΔT			
9	10.0	UPPER LOWER	90 86	73 70	82 78	-17 -16	91 86	73 70	81 78	-18 -16	91 88	75 70	84 79	-17 -18			
12	21.0	UPPER LOWER	38 39	66 70	52 54	29 32	38 38	66 70	52 54	29 32	34 33	64 70	50 52	30 37			
15	24.0	UPPER LOWER	58 60	67 70	62 65	9 10	60 61	67 70	64 65	8 10	64 64	64 70	64 67	1 6			
20	36.0	UPPER LOWER	306 275	111 76	204 176	-195 -199	311 283	112 77	212 180	-199 -206	338 334	140 75	239 204	-198 -259			
22	61.0	UPPER LOWER	319 279	125 87	222 183	-194 -192	336 288	242 93	289 191	-94 -195	349 337	220 82	284 210	-129 -255			
31	30.0	UPPER LOWER	198 195	88 72	143 134	-110 -123	203 199	88 73	146 136	-115 -127	224 228	101 72	164 150	-123 -156			

TEMPERATURE LEGEND

T_o = EXPOSED SURFACE TEMPERATURE

T_i = INTERIOR SURFACE TEMPERATURE

T_{AVG} = (T_o + T_i)/2

+ ΔT = T_i > T_o

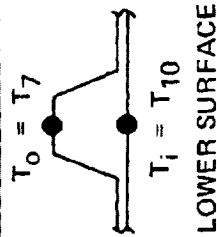
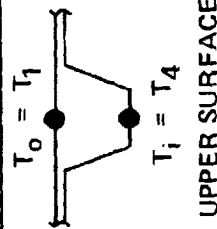


TABLE 11-10. WING POINT DESIGN ENVIRONMENT, CHORDWISE ARRANGEMENT - TASK I,
MACH 0.40 LOAD CONDITION

MASS 338×10^3 KG

CONNECTION (2) TAIL: $W_{10} = 20.1$; $W_{20} = 6.40$; $W_{30} = 2.5$

ULTIMATE DESIGN LOADS	ITEM	UNITS	POINT DESIGN REGION											
			40236		41036		41316		40536		41348		40322	
			UPPER SURFACE	LOWER SURFACE	UPPER SURFACE	LOWER SURFACE	UPPER SURFACE	LOWER SURFACE	UPPER SURFACE	LOWER SURFACE	UPPER SURFACE	LOWER SURFACE	UPPER SURFACE	LOWER SURFACE
AIR LOADS	Nx	KN/m	70	-70	-103	103	107	-157	6	-277	144	-145	9	-4
	Ny	KN/m	-2408	2408	-1400	1400	-2637	2637	-277	277	-159	159	-233	233
	Nzy	KN/m	122	-122	316	-316	746	-746	395	-395	335	-335	45	-45
	Ex	m/m	0	0	0	0	0	0	0	0	0	0	0	0
THERMAL STRAIN	Ey	m/m	0	0	0	0	0	0	0	0	0	0	0	0
	Ezy	m/m	0	0	0	0	0	0	0	0	0	0	0	0
PRESSURE	AERO	KPa	-5.55	-2.00	-6.96	6.34	-33.92	-0.21	-3.65	0.28	-3.52	-0.96	-6.27	1.65
	FUEL	KPa	-40.54	-50.74	0	0	0	0	-35.82	-51.54	0	0	-46.47	-61.73
	NET	KPa	-47.09	-52.74	-6.96	6.34	-33.92	-0.21	-41.47	-51.82	-0.96	-0.96	-52.74	-63.10
TEMPERATURE	TAV	°K	321	292	295	326	305	324	303	299	314	304	31	292
	ΔT	°K	-9	-9	-2	-2	-3	-3	-10	-9	-4	-4	-9	-10

WEIGHT - 746 X 10³ LB

ULTIMATE DESIGN LOADS	ITEM	UNITS	POINT DESIGN REGION											
			40236		41036		41316		40536		41348		40322	
			UPPER SURFACE	LOWER SURFACE	UPPER SURFACE	LOWER SURFACE	UPPER SURFACE	LOWER SURFACE	UPPER SURFACE	LOWER SURFACE	UPPER SURFACE	LOWER SURFACE	UPPER SURFACE	LOWER SURFACE
AIR LOADS	Nx	LB/IN	402	-402	-599	599	955	-955	33	-33	544	-544	76	-76
	Ny	LB/IN	-13,754	13,754	-7,995	7,995	-15,059	15,059	-13,003	13,003	-9,048	9,048	-1,333	1,333
	Nzy	LB/IN	634	-634	1,506	-1,506	3,261	-3,261	1,624	-1,624	1,215	-1,215	157	-157
	Ex	IN/IN	0	0	0	0	0	0	0	0	0	0	0	0
THERMAL STRAIN	Ey	IN/IN	0	0	0	0	0	0	0	0	0	0	0	0
	Ezy	IN/IN	0	0	0	0	0	0	0	0	0	0	0	0
PRESSURE	AERO	PSI	-0.79	-0.29	-1.01	0.97	-3.47	-0.03	-0.53	0.33	-4.77	-0.14	-0.91	0.24
	FUEL	PSI	-5.36	-5.21	0	0	0	0	-5.03	-5.01	0	0	-4.74	-4.96
	NET	PSI	-6.33	-5.12	-1.01	0.97	-3.47	-0.03	-6.16	-5.03	-4.77	-0.14	-5.64	-5.72
TEMPERATURE	TAV	°F	82	78	59	87	59	87	81	75	83	77	74	79
	ΔT	°F	-17	-16	-4	-3	-5	-3	-14	-10	-7	-4	-17	-13

NOTES: (1) A 1.25 FACTOR HAS BEEN APPLIED TO THE THERMAL STRAIN WHEN THE SIGN IS SAME AS THE AIRLOAD

SIGN, OTHERWISE NO FACTOR APPLIED.

(2) PRESSURE SIGN CONVENTION: NEGATIVE = SUCTION

TABLE 11-11. WING POINT DESIGN ENVIRONMENT, CHORDWISE ARRANGEMENT - TASK I,
MACH 0.90 LOAD CONDITION

MASS - 318 X 10³ KG

CONVENTION (1) : MACH NO. = 0.90; $n_z = 2.5$

ULTIMATE DESIGN LOADS	ITEM	UNITS	POINT DESIGN REGION											
			40236			41036			41316			40536		
			UPPER SURFACE	LOWER SURFACE		UPPER SURFACE	LOWER SURFACE		UPPER SURFACE	LOWER SURFACE		UPPER SURFACE	LOWER SURFACE	
AIR LOADS	Nx	KN/M	33	-33		-46	46		123	-123		15	-15	
	Ny	KN/M	-1804	1804		-1150	1150		-2241	2241		-1863	1863	
	Nzy	KN/M	73	-73		240	-240		510	-510		196	-196	
THERMAL STRAIN	Cx	M/M	0	0		0	0		0	0		0	0	
	Cy	M/M	0	0		0	0		0	0		0	0	
	Czy	M/M	0	0		0	0		0	0		0	0	
PRESSURE	AERO	KPA	-6.89	-3.03		-14.46	-2.46		-26.74	-29.92		-9.31	-3.34	
	FUEL	KPA	-40.54	-60.74		0	0		0	0		-54.82	-54.54	
	NET	KPA	-47.36	-63.77		-14.46	-2.46		-26.74	-29.92		-9.31	-3.34	
TEMPERATURE	TAV	°K	884	884		272	272		280	280		284	284	
	ΔT	°K	36	13		1	8		8	9		26	29	

WEIGHT - 700 X 10³ LB.

ULTIMATE DESIGN LOADS	ITEM	UNITS	POINT DESIGN REGION											
			40236			41036			41316			40536		
			UPPER SURFACE	LOWER SURFACE		UPPER SURFACE	LOWER SURFACE		UPPER SURFACE	LOWER SURFACE		UPPER SURFACE	LOWER SURFACE	
AIR LOADS	Nx	LB/IN	158	-134		-272	272		701	-701		85	-85	
	Ny	LB/IN	-10,814	10,814		-6,270	6,270		-11,700	11,700		-12,640	12,640	
	Nzy	LB/IN	418	-425		1,364	-1,364		3,440	-3,440		1,113	-1,113	
THERMAL STRAIN	Cx	IN/IN	0	0		0	0		0	0		0	0	
	Cy	IN/IN	0	0		0	0		0	0		0	0	
	Czy	IN/IN	0	0		0	0		0	0		0	0	
PRESSURE	AERO	PSI	-0.92	-0.44		-2.10	-0.36		-0.75	-1.76		-1.35	-0.43	
	FUEL	PSI	-5.84	-8.68		0	0		0	0		-8.63	-8.40	
	NET	PSI	-6.77	-9.12		-2.10	-0.36		-0.75	-1.76		-1.35	-0.43	
TEMPERATURE	TAV	°F	52	34		43	41		40	43		36	34	
	ΔT	°F	22	30		14	15		14	17		22	30	

NOTES: (1) A 1.25 FACTOR HAS BEEN APPLIED TO THE THERMAL STRAIN WHEN THE SIGN IS SAME AS THE AIRLOAD
SIGN, OTHERWISE NO FACTOR APPLIED.
(2) PRESSURE SIGN CONVENTION: NEGATIVE = SUCTION

ORIGINAL PAGE IS
OF POOR QUALITY

TABLE 11-12. WING POINT DESIGN ENVIRONMENT, CHORDWISE ARRANGEMENT - TASK I,
MACH 1.25 LOAD CONDITION

MASS: $313 \times 10^3 \text{ Kg}$ CONDITION (5): 136 H PC., 1.25; η_c 2.5

ULTIMATE DESIGN LOADS	ITEM	UNITS	POINT DESIGN REGION											
			40236		41036		41316		40536		41348		40322	
			UPPER SURFACE	LOWER SURFACE	UPPER SURFACE	LOWER SURFACE	UPPER SURFACE	LOWER SURFACE	UPPER SURFACE	LOWER SURFACE	UPPER SURFACE	LOWER SURFACE	UPPER SURFACE	LOWER SURFACE
AIR LOADS	Nx	kN/m	72	-25	-59	51	2	-2	-71	71	-62	62	57	-37
	Ny	kN/m	-50.13	50.13	-1076	1076	-6136	6136	-2067	2067	-1375	1375	-143	143
	Nxy	kN/m	430	130	272	272	547	547	762	762	336	336	28	28
	Ex	m/m	0	0	0	0	0	0	0	0	0	0	0	0
THERMAL STRAIN	Ey	m/m	0	0	0	0	0	0	0	0	0	0	0	0
	Exy	m/m	0	0	0	0	0	0	0	0	0	0	0	0
PRESSURE	AERO	KPa	-262.4	-262.4	-67.57	67.57	-31.62	31.62	-11.56	11.56	-40.36	40.36	-10.27	10.27
	FUEL	KPa	-100.85	-100.85	0	0	0	0	-24.63	24.63	0	0	-47.30	47.30
	NET	KPa	-13.84	-13.84	-67.57	67.57	-31.62	31.62	-4.17	4.17	-39.36	39.36	-57.57	57.57
TEMPERATURE	TAV	°K	290	291	294	293	293	293	294	294	296	296	292	292
	ΔT	°K	0	0	-1	1	0	0	1	1	2	2	1	1

WEIGHT: $690 \times 10^3 \text{ LB}$

ULTIMATE DESIGN LOADS	ITEM	UNITS	POINT DESIGN REGION											
			40236		41036		41316		40536		41348		40322	
			UPPER SURFACE	LOWER SURFACE	UPPER SURFACE	LOWER SURFACE	UPPER SURFACE	LOWER SURFACE	UPPER SURFACE	LOWER SURFACE	UPPER SURFACE	LOWER SURFACE	UPPER SURFACE	LOWER SURFACE
AIR LOADS	Nx	LB/IN	1.30	-1.30	-33	33	553	-553	-4.3	4.3	-1189	1189	224	-224
	Ny	LB/IN	-10.63	10.63	-27.7	27.7	-17.63	17.63	-11.840	11.840	-7.951	7.951	-2.100	2.100
	Nxy	LB/IN	7.25	7.25	1.956	1.956	3.941	3.941	1.462	1.462	1.461	1.461	1.62	1.62
	Ex	IN/IN	0	0	0	0	0	0	0	0	0	0	0	0
THERMAL STRAIN	Ey	IN/IN	0	0	0	0	0	0	0	0	0	0	0	0
	Exy	IN/IN	0	0	0	0	0	0	0	0	0	0	0	0
PRESSURE	AERO	PSI	-3.83	-3.83	-1.70	1.70	-4.79	4.79	-0.81	0.81	-4.36	4.36	-1.19	1.19
	FUEL	PSI	-14.03	-14.03	0	0	0	0	-3.57	3.57	0	0	-4.56	4.56
	NET	PSI	-1.20	-1.20	-1.70	1.70	-4.79	4.79	-4.38	4.38	-4.36	4.36	-5.75	5.75
TEMPERATURE	TAV	°F	53	55	58	56	56	56	57	57	55	55	54	54
	ΔT	°F	0	0	-13	13	11	11	1	1	-13	13	1	1

NOTES (1) A 1.25 FACTOR HAS BEEN APPLIED TO THE THERMAL STRAIN WHEN THE SIGN IS SAME AS THE AIRLOAD

SIGN OTHERWISE NO FACTOR APPLIED.

(2) PRESSURE SIGN CONVENTION NEGATIVE = SUCTION

TABLE 11-13. WING POINT DESIGN ENVIRONMENT, CHORDWISE ARRANGEMENT - TASK I,
START-OF-CRUISE CONDITION

CONDITION (1) (START OF CRUISE): WING NO. 2000

MASS = 298 x 10³ kg

ULTIMATE DESIGN LOADS	ITEM	UNITS	POINT DESIGN REGION									
			40236		41036		41316		40536		41348	
			UPPER SURFACE	LOWER SURFACE	UPPER SURFACE	LOWER SURFACE	UPPER SURFACE	LOWER SURFACE	UPPER SURFACE	LOWER SURFACE	UPPER SURFACE	LOWER SURFACE
AIR LOADS	Nx	KN/m	-4	4	-107	107	124	-114	0	0	4	-4
	Ny	KN/m	-1591	1591	-336	336	-336	336	-1305	1305	-374	374
	Nxy	KN/m	-105	105	-234	234	34	-34	-608	608	234	-234
THERMAL STRAIN	Ex	m/m	-230 x 10 ⁻⁶	230 x 10 ⁻⁶	-94 x 10 ⁻⁶	94 x 10 ⁻⁶	13 x 10 ⁻⁶	-13 x 10 ⁻⁶	40 x 10 ⁻⁶	-40 x 10 ⁻⁶	0	0
	Ey	m/m	-201 x 10 ⁻⁶	201 x 10 ⁻⁶	-15 x 10 ⁻⁶	15 x 10 ⁻⁶	-19 x 10 ⁻⁶	19 x 10 ⁻⁶	-31 x 10 ⁻⁶	31 x 10 ⁻⁶	-1 x 10 ⁻⁶	1 x 10 ⁻⁶
	Exy	m/m	-126 x 10 ⁻⁶	126 x 10 ⁻⁶	-71 x 10 ⁻⁶	71 x 10 ⁻⁶	116 x 10 ⁻⁶	-116 x 10 ⁻⁶	-59 x 10 ⁻⁶	59 x 10 ⁻⁶	1.25 x 10 ⁻⁶	-1.25 x 10 ⁻⁶
PRESSURE	AERO	MPa	-11.72	5.10	-8.56	8.56	-11.28	11.28	-10.13	10.13	-1.59	1.59
	FUEL	MPa	-14.26	-54.05	0	0	0	0	-42.37	42.37	0	0
	NET	MPa	-55.48	-59.15	-8.56	8.56	-11.28	11.28	-51.50	51.50	-41.37	41.37
TEMPERATURE	TAV	°K	369	363	333	434	440	440	35	35	441	441
	ΔT	°K	-106	-111	-60	-61	-66	-66	-111	-114	-79	-79
											-115	-115

WEIGHT = 680 x 10³ LB

CONDITION (2) (END OF CRUISE): WING NO. 2000

MASS = 298 x 10³ kg

ULTIMATE DESIGN LOADS	ITEM	UNITS	POINT DESIGN REGION									
			40236		41036		41316		40536		41348	
			UPPER SURFACE	LOWER SURFACE	UPPER SURFACE	LOWER SURFACE	UPPER SURFACE	LOWER SURFACE	UPPER SURFACE	LOWER SURFACE	UPPER SURFACE	LOWER SURFACE
AIR LOADS	Nx	LB/IN	-2.0	2.0	-4.4	4.4	-10.0	10.0	0	0	-1.3	1.3
	Ny	LB/IN	-159.1	159.1	-33.6	33.6	-33.6	33.6	-130.5	130.5	-37.4	37.4
	Nxy	LB/IN	-10.5	10.5	-23.4	23.4	3.4	-3.4	-60.8	60.8	23.4	-23.4
THERMAL STRAIN	Ex	IN/IN	-230 x 10 ⁻⁶	230 x 10 ⁻⁶	-94 x 10 ⁻⁶	94 x 10 ⁻⁶	13 x 10 ⁻⁶	-13 x 10 ⁻⁶	40 x 10 ⁻⁶	-40 x 10 ⁻⁶	0	0
	Ey	IN/IN	-201 x 10 ⁻⁶	201 x 10 ⁻⁶	-15 x 10 ⁻⁶	15 x 10 ⁻⁶	-19 x 10 ⁻⁶	19 x 10 ⁻⁶	-31 x 10 ⁻⁶	31 x 10 ⁻⁶	-1 x 10 ⁻⁶	1 x 10 ⁻⁶
	Exy	IN/IN	-126 x 10 ⁻⁶	126 x 10 ⁻⁶	-71 x 10 ⁻⁶	71 x 10 ⁻⁶	116 x 10 ⁻⁶	-116 x 10 ⁻⁶	-59 x 10 ⁻⁶	59 x 10 ⁻⁶	1.25 x 10 ⁻⁶	-1.25 x 10 ⁻⁶
PRESSURE	AERO	PSI	-11.72	5.10	-8.56	8.56	-11.28	11.28	-10.13	10.13	-1.59	1.59
	FUEL	PSI	-14.26	-54.05	0	0	0	0	-42.37	42.37	0	0
	NET	PSI	-55.48	-59.15	-8.56	8.56	-11.28	11.28	-51.50	51.50	-41.37	41.37
TEMPERATURE	TAV	°F	364	363	333	434	440	440	35	35	441	441
	ΔT	°F	-103	-111	-60	-61	-66	-66	-111	-114	-79	-79
											-115	-115

NOTES: (1) A 1.25 FACTOR HAS BEEN APPLIED TO THE THERMAL STRAIN WHEN THE SIGN IS SAME AS THE AIRLOAD

SIGN, OTHERWISE NO FACTOR APPLIED

(2) PRESSURE SIGN CONVENTION: NEGATIVE = SUCTION

ORIGINAL PAGE IS
OF POOR QUALITY

IN ENVIRONMENT, CHORDWISE ARRANGEMENT - TASK I,
MID-CRUISE CONDITION

[illegible]

WEIGHT = 550 X 10³ LB

ULTIMATE DESIGN LOADS	ITEM	UNITS	POINT DESIGN REGION											
			40236		41036		41316		40536		41348		40322	
			UPPER SURFACE	LOWER SURFACE	UPPER SURFACE	LOWER SURFACE	UPPER SURFACE	LOWER SURFACE	UPPER SURFACE	LOWER SURFACE	UPPER SURFACE	LOWER SURFACE	UPPER SURFACE	LOWER SURFACE
AIR LOADS	Nx	LB/IN	7.25	-7.03	-6.63	-6.3	-6.7	-6.6	-1.3	1.3	1.3	3.9	-2.9	
	Ny	LB/IN	-5.23	5.23	-5.42	-5.42	-5.33	-5.33	-7.04	7.04	5.019	-7.7	7.7	
	Nxy	LB/IN	941	-941	-3.85	-3.85	1.43	-1.43	-1.06	1.06	-9.3	-9.3	-9.3	
THERMAL STRAIN	Ex	IN/IN	-24. x 10 ⁻⁶	24. x 10 ⁻⁶	24. x 10 ⁻⁶	-24. x 10 ⁻⁶	-3.8 x 10 ⁻⁶	3.8 x 10 ⁻⁶	29. x 10 ⁻⁶	-29. x 10 ⁻⁶	-24. x 10 ⁻⁶	-24. x 10 ⁻⁶	24. x 10 ⁻⁶	
	Ey	IN/IN	22. x 10 ⁻⁶	-22. x 10 ⁻⁶	44. x 10 ⁻⁶	-44. x 10 ⁻⁶	1.7 x 10 ⁻⁶	-1.7 x 10 ⁻⁶	2.8 x 10 ⁻⁶	-2.8 x 10 ⁻⁶	2.8 x 10 ⁻⁶	-2.8 x 10 ⁻⁶	2.8 x 10 ⁻⁶	
	Exy	IN/IN	3. x 10 ⁻⁶	-3. x 10 ⁻⁶	-5.3 x 10 ⁻⁶	5.3 x 10 ⁻⁶	-4.6 x 10 ⁻⁶	4.6 x 10 ⁻⁶	-4.1 x 10 ⁻⁶	4.1 x 10 ⁻⁶	-2.7 x 10 ⁻⁶	2.7 x 10 ⁻⁶	-2.7 x 10 ⁻⁶	
PRESSURE	AERO	PSI	-1.69	-56.24	-52.24	5.23	-2.47	2.47	-1.53	1.53	-2.47	-1.53	1.53	
	FUEL	PSI	-3.68	-9.57	3	3	3	3	-4.3	-4.3	-4.3	-4.3	-4.3	
	NET	PSI	-3.68	-9.57	-1.04	1.04	-1.45	1.45	-2.47	2.47	-2.47	-2.47	-2.47	
TEMPERATURE	TAV	°F	222	386	386	384	341	341	295	295	331	285	230	
	ΔT	°F	-134	-156	1	3	1	4	-34	-34	-34	-34	-34	

NOTES: (1) A 1.25 FACTOR HAS BEEN APPLIED TO THE THERMAL STRAIN WHEN THE SIGN IS SAME AS THE AIRLOAD SIGN, OTHERWISE NO FACTOR APPLIED.

(2) PRESSURE SIGN CONVENTION: NEGATIVE = SUCTION

(2) PRESSURE SIGN CONVENTION: NEGATIVE = SUCTION

TABLE 11-15. WING POINT DESIGN ENVIRONMENT, CHORDWISE ARRANGEMENT - TASK I,
MACH 1.25 (V_g) LOAD CONDITION

MASS 313 X 10³ Kg

CONDITION (1): MACH NO. = 1.25; P₂ 2.5

ULTIMATE DESIGN LOADS	ITEM	UNITS	POINT DESIGN REGION									
			40236		41036		41316		40536		41348	
			UPPER SURFACE	LOWER SURFACE	UPPER SURFACE	LOWER SURFACE	UPPER SURFACE	LOWER SURFACE	UPPER SURFACE	LOWER SURFACE	UPPER SURFACE	LOWER SURFACE
AIR LOADS	Nx	KN/m	115	-115	-291	291	100	-100	-208	208	-451	451
	Ny	KN/m	-284	284	-1203	1203	-2774	2774	-2538	2538	-1591	1591
	Nxy	KN/m	240	-240	392	-392	942	-942	412	-412	435	-435
	Cx	m/m	0	0	0	0	0	0	0	0	0	0
THERMAL STRAIN	Cy	m/m	0	0	0	0	0	0	0	0	0	0
	Cxy	m/m	0	0	0	0	0	0	0	0	0	0
	AERO	MPa	-20.89	-8.97	-5.76	0.76	-34.33	-1.74	-6.76	-1.74	-34.33	-1.74
	FUEL	MPa	-40.88	-61.64	0	0	0	0	-34.04	-55.36	0	0
PRESSURE	NET	KPa	-61.77	-12.91	-8.76	1.76	-34.33	-1.74	-17.75	-57.15	-34.36	6.62
	TAV	°K	335	330	365	323	371	364	337	331	346	370
	ΔT	°K	-61	-68	-65	-67	-66	-68	-74	-71	-43	-39
TEMPERATURE												

WEIGHT = 690 X 10³ LB

ULTIMATE DESIGN LOADS	ITEM	UNITS	POINT DESIGN REGION									
			40236		41036		41316		40536		41348	
			UPPER SURFACE	LOWER SURFACE	UPPER SURFACE	LOWER SURFACE	UPPER SURFACE	LOWER SURFACE	UPPER SURFACE	LOWER SURFACE	UPPER SURFACE	LOWER SURFACE
AIR LOADS	Nx	LB/IN	152	-152	-1135	1135	402	-402	-1340	1340	-1453	1453
	Ny	LB/IN	-209,338	209,338	-24,136	24,136	-26,888	26,888	-24,375	24,375	-159,300	159,300
	Nxy	LB/IN	1,316	-1,316	2,937	-2,937	1,457	-1,457	6,334	-6,334	1,453	-1,453
	Cx	IN/IN	0	0	0	0	0	0	0	0	0	0
THERMAL STRAIN	Cy	IN/IN	0	0	0	0	0	0	0	0	0	0
	Cxy	IN/IN	0	0	0	0	0	0	0	0	0	0
	AERO	PSI	-3.04	-1.27	-0.11	0.11	-4.23	-0.11	-1.27	-0.11	-4.23	-0.11
	FUEL	PSI	-6.13	-9.74	0	0	0	0	-3.67	-5.63	0	0
PRESSURE	NET	PSI	-9.86	-10.14	-1.27	1.11	-4.23	-0.11	-2.44	-4.63	-4.23	0.86
	TAV	°F	183	134	184	154	174	174	147	134	154	150
	ΔT	°F	-110	-123	-45	-49	-46	-47	-113	-107	-39	-173
TEMPERATURE												

NOTES: (1) A 1.25 FACTOR HAS BEEN APPLIED TO THE THERMAL STRAIN WHEN THE SIGN IS SAME AS THE AIRLOAD
SIGN, OTHERWISE NO FACTOR APPLIED.

(2) PRESSURE SIGN CONVENTION: NEGATIVE = SUCTION

ORIGINAL PAGE IS
OF POOR QUALITY

TABLE 11-16. WING POINT DESIGN ENVIRONMENT, SPANWISE ARRANGEMENT - TASK I,
MACH 0.40 LOAD CONDITION

MASS: 3.28×10^3 kg

REF: 11-16-10, 0.40: 0.40

ULTIMATE DESIGN LOADS	ITEM	UNITS	POINT DESIGN REGION									
			40236		41036		41316		40536		41348	
			UPPER SURFACE	LOWER SURFACE	UPPER SURFACE	LOWER SURFACE	UPPER SURFACE	LOWER SURFACE	UPPER SURFACE	LOWER SURFACE	UPPER SURFACE	LOWER SURFACE
AIR LOADS	Nx	kN/m	4.1	-1.1	-1.4	1.1	-	-	-	-	-	-
	Ny	kN/m	-2.37	0.50	-1.45	1.15	-1.4	0.5	-1.4	0.5	-1.4	0.5
	Nxz	kN/m	0.04	0.01	0.01	0.01	0.01	0.01	0.01	0.01	0.01	0.01
THERMAL STRAIN	Ex	m/m	0	0	0	0	0	0	0	0	0	0
	Ey	m/m	0	0	0	0	0	0	0	0	0	0
	Exy	m/m	0	0	0	0	0	0	0	0	0	0
PRESSURE	AERO	kPa	-6.55	-1.79	-1.79	0.74	-3.37	0.74	-1.79	0.74	-1.79	0.74
	FUEL	kPa	-40.54	-0.14	0	0	-3.37	0	-1.79	0	-1.79	0
	NET	kPa	-47.09	-1.93	-1.79	0.74	-3.37	0.74	-1.79	0.74	-1.79	0.74
TEMPERATURE	TAV	°K	280	280	280	280	280	280	280	280	280	280
	ΔT	°K	-11	-2	-2	-2	-2	-2	-2	-2	-2	-2

WEIGHT = 7.45×10^3 LB

ULTIMATE DESIGN LOADS	ITEM	UNITS	POINT DESIGN REGION									
			40236		41036		41316		40536		41348	
			UPPER SURFACE	LOWER SURFACE	UPPER SURFACE	LOWER SURFACE	UPPER SURFACE	LOWER SURFACE	UPPER SURFACE	LOWER SURFACE	UPPER SURFACE	LOWER SURFACE
AIR LOADS	Nx	LB/IN	0.34	-0.30	-0.4	0.3	0.3	-0.3	-0.3	0.3	-0.3	0.3
	Ny	LB/IN	-1.03	0.22	-0.52	0.22	-1.03	0.22	-1.03	0.22	-1.03	0.22
	Nxz	LB/IN	0.06	0.01	0.01	0.01	0.01	0.01	0.01	0.01	0.01	0.01
THERMAL STRAIN	Ex	IN/IN	0	0	0	0	0	0	0	0	0	0
	Ey	IN/IN	0	0	0	0	0	0	0	0	0	0
	Exy	IN/IN	0	0	0	0	0	0	0	0	0	0
PRESSURE	AERO	PSI	-0.95	-0.22	-1.01	0.22	-0.95	0.22	-0.22	0.22	-0.22	0.22
	FUEL	PSI	-5.88	-0.02	0	0	-0.95	0	-0.22	0	-0.22	0
	NET	PSI	-6.83	-0.24	-1.01	0.22	-0.95	0.22	-0.22	0.22	-0.22	0.22
TEMPERATURE	TAV	°F	528	528	528	528	528	528	528	528	528	528
	ΔT	°F	-20	-4	-4	-4	-4	-4	-4	-4	-4	-4

NOTES: (1) A 1.25 FACTOR HAS BEEN APPLIED TO THE THERMAL STRAIN WHEN THE SIGN IS SAME AS THE AIRLOAD

SIGN: OTHERWISE NO FACTOR APPLIED

(2) PRESSURE SIGN CONVENTION: NEGATIVE - SUCTION

TABLE 11-17. WING POINT DESIGN ENVIRONMENT, SPANWISE ARRANGEMENT - TASK I,
MACH 0.90 LOAD CONDITIONS

MASS 318×10^3 LB

SOLUTION 11; $\eta_1 = 0.90$; $\eta_2 = 2.5$

ULTIMATE DESIGN LOADS	ITEM	UNITS	POINT DESIGN REGION											
			40236			41036			41316			40536		
			UPPER SURFACE	LOWER SURFACE		UPPER SURFACE	LOWER SURFACE		UPPER SURFACE	LOWER SURFACE		UPPER SURFACE	LOWER SURFACE	
AIR LOADS	N_x	KN/M	-1	-1		-1	-1		5	5		-3	-3	
	N_y	KN/M	-1.33	1.12		-1.04	1.04		-1.97	1.97		-0.15	0.15	
	N_{xy}	KN/M	0	0		0	0		0	0		0	0	
THERMAL STRAIN	ϵ_x	M/M	0	0		0	0		0	0		0	0	
	ϵ_y	M/M	0	0		0	0		0	0		0	0	
	ϵ_{xy}	M/M	0	0		0	0		0	0		0	0	
PRESSURE	AERO	KPa	-0.87	-3.02		-14.45	-14.45		-4.74	-4.74		-9.31	-9.31	
	FUEL	KPa	-40.56	-60.34		0	0		0	0		0	0	
	NET	KPa	-47.36	-63.37		-24.49	-24.49		-4.74	-4.74		-9.31	-9.31	
TEMPERATURE	T_{AV}	°K	285	285		285	285		285	285		285	285	
	ΔT	°K	28	28		1	1		1	1		1	1	

WEIGHT = 700×10^3 LB.

ULTIMATE DESIGN LOADS	ITEM	UNITS	POINT DESIGN REGION											
			40236			41036			41316			40536		
			UPPER SURFACE	LOWER SURFACE		UPPER SURFACE	LOWER SURFACE		UPPER SURFACE	LOWER SURFACE		UPPER SURFACE	LOWER SURFACE	
AIR LOADS	N_x	LB/IN	120	-100		-3	3		-27	-27		3	3	
	N_y	LB/IN	-12.23	12.23		-0.79	0.79		-1.54	1.54		-1.31	1.31	
	N_{xy}	LB/IN	1.11	1.12		0	0		3.41	3.41		0	0	
THERMAL STRAIN	ϵ_x	IN/IN	0	0		0	0		0	0		0	0	
	ϵ_y	IN/IN	0	0		0	0		0	0		0	0	
	ϵ_{xy}	IN/IN	0	0		0	0		0	0		0	0	
PRESSURE	AERO	PSI	-0.99	-14.4		-1.03	-14.4		-1.5	-1.5		-1.35	-1.35	
	FUEL	PSI	-5.96	-5.96		0	0		0	0		0	0	
	NET	PSI	-6.95	-11.92		-1.03	-14.4		-1.5	-1.5		-1.35	-1.35	
TEMPERATURE	T_{AV}	°F	53	53		53	53		53	53		53	53	
	ΔT	°F	33	33		33	33		33	33		33	33	

NOTES (1) A 1.25 FACTOR HAS BEEN APPLIED TO THE THERMAL STRAIN WHEN THE SIGN IS SAME AS THE AIRLOAD SIGN, OTHERWISE NO FACTOR APPLIED.

(2) PRESSURE SIGN CONVENTION: NEGATIVE = SUCTION

TABLE 11-18. WING POINT DESIGN ENVIRONMENT, SPANWISE ARRANGEMENT - TASK I,
MACH 1.25 LOAD CONDITION

MASS 313×10^3 kg

COEFFICIENT (5) MACH NO. 1.25 q_c 2.5

ULTIMATE DESIGN LOADS	ITEM	UNITS	POINT DESIGN REGION											
			40236			41036			41316			40236		
			UPPER SURFACE	LOWER SURFACE	40236	UPPER SURFACE	LOWER SURFACE	41036	UPPER SURFACE	LOWER SURFACE	41316	UPPER SURFACE	LOWER SURFACE	40236
AIR LOADS	Nx	kN/m	43	-43	-21	21	-21	21	-23.71	23.71	-23.71	23.71	23.71	11
	Ny	kN/m	-2405	2405	-1364	1364	-1364	1364	-23.71	23.71	-23.71	23.71	23.71	-202
	Nzy	kN/m	289	-289	412	-412	412	-412	412	-412	412	-412	412	45
THERMAL STRAIN	Ex	m/m	0	0	0	0	0	0	0	0	0	0	0	0
	Ey	m/m	0	0	0	0	0	0	0	0	0	0	0	0
	Ezy	m/m	0	0	0	0	0	0	0	0	0	0	0	0
PRESSURE	AH0	kPa	-22.96	-9.03	-8.77	0.76	-31.02	-1.86	-31.02	-1.86	-31.02	-1.86	-31.02	0.41
	FUEL	kPa	-40.58	-61.64	0	0	0	0	0	0	0	0	0	-62.05
	NET	kPa	-13.34	-70.67	-8.27	0.76	-31.02	-1.86	-31.02	-1.86	-31.02	-1.86	-31.02	-61.64
TEMPERATURE	TAV	°K	290	291	287	285	288	287	288	287	288	287	288	293
	ΔT	°K	7	7	-3	-1	1	1	1	1	1	1	1	3

WEIGHT = 680×10^3 LB

ULTIMATE DESIGN LOADS	ITEM	UNITS	POINT DESIGN REGION											
			40236			41036			41316			40236		
			UPPER SURFACE	LOWER SURFACE	40236	UPPER SURFACE	LOWER SURFACE	41036	UPPER SURFACE	LOWER SURFACE	41316	UPPER SURFACE	LOWER SURFACE	40236
AIR LOADS	Nx	LB/IN	246	-246	-123	123	-123	123	-13.54	13.54	-13.54	13.54	13.54	11
	Ny	LB/IN	-13.735	13.735	-7.79	7.79	-7.79	7.79	-13.54	13.54	-13.54	13.54	13.54	-1.152
	Nzy	LB/IN	1.649	-1.649	2.355	-2.355	2.355	-2.355	2.355	-2.355	2.355	-2.355	2.355	0.73
THERMAL STRAIN	Ex	IN/IN	0	0	0	0	0	0	0	0	0	0	0	0
	Ey	IN/IN	0	0	0	0	0	0	0	0	0	0	0	0
	Ezy	IN/IN	0	0	0	0	0	0	0	0	0	0	0	0
PRESSURE	AERO	PSI	-3.33	-1.31	-1.70	0.11	-0.77	-1.07	-0.77	-1.07	-0.77	-1.07	-1.07	0.26
	FUEL	PSI	-5.93	-8.94	0	0	0	0	0	0	0	0	0	-9.00
	NET	PSI	-9.26	-10.25	-1.70	0.11	-0.77	-1.07	-0.77	-1.07	-0.77	-1.07	-1.07	-8.74
TEMPERATURE	TAV	°F	53	64	57	54	56	53	54	53	54	53	54	57
	ΔT	°F	13	13	-6	-6	6	6	6	6	6	6	6	6

NOTES (1) A 1.25 FACTOR HAS BEEN APPLIED TO THE THERMAL STRAIN WHEN THE SIGN IS SAME AS THE AIRLOAD
SIGN, OTHERWISE NO FACTOR APPLIED.
(2) PRESSURE SIGN CONVENTION NEGATIVE = SUCTION

TABLE 11-19. WING POINT DESIGN ENVIRONMENT, SPANWISE ARRANGEMENT - TASK I,
START-OF-CRUISE CONDITION

MASS = 209 X 10³ Kg

CONVENTION: (20) (START-OF-CRUISE), VAS 100, 2-7, F₂ = 2.5

ULTIMATE DESIGN LOADS	ITEM	UNITS	POINT DESIGN REGION											
			40236			41036			41316			40536		
			UPPER SURFACE	LOWER SURFACE		UPPER SURFACE	LOWER SURFACE		UPPER SURFACE	LOWER SURFACE		UPPER SURFACE	LOWER SURFACE	
AIR LOADS	N _x	kN/m	5	-5		-12	12		4	-4		40	-33	
	N _y	kN/m	-1771	1771		-533	533		-1739	1739		-854	854	
	N _{xy}	kN/m	-214	214		-308	308		310	-310		335	-136	
THERMAL STRAIN	E _x	m/m	-255 X 10 ⁻⁶	255 X 10 ⁻⁶		-202 X 10 ⁻⁶	202 X 10 ⁻⁶		89 X 10 ⁻⁶	-89 X 10 ⁻⁶		-125 X 10 ⁻⁶	15 X 10 ⁻⁶	
	E _y	m/m	-258 X 10 ⁻⁶	258 X 10 ⁻⁶		-42 X 10 ⁻⁶	42 X 10 ⁻⁶		3 X 10 ⁻⁶	-3 X 10 ⁻⁶		75 X 10 ⁻⁶	-6 X 10 ⁻⁶	
	E _{xy}	m/m	39 X 10 ⁻⁶	-39 X 10 ⁻⁶		-63 X 10 ⁻⁶	63 X 10 ⁻⁶		150 X 10 ⁻⁶	-150 X 10 ⁻⁶		170 X 10 ⁻⁶	-6 X 10 ⁻⁶	
PRESSURE	AERO	KPa	-11.72	5.10		-8.62	2.62		-11.38	6.39		-10.12	5.39	
	FUEL	KPa	-14.26	-54.02		0	0		0	0		-19.02	0	
	NET	KPa	-55.98	59.15		-3.60	2.62		-11.38	6.39		-51.50	5.39	
TEMPERATURE	TAV	°K	369	369		423	430		414	370		363	431	
	ΔT	°K	-133	-127		-61	-54		-14	-80		-129	-66	

WEIGHT = 680 X 10³ LB

ULTIMATE DESIGN LOADS	ITEM	UNITS	POINT DESIGN REGION											
			40236			41036			41316			40536		
			UPPER SURFACE	LOWER SURFACE		UPPER SURFACE	LOWER SURFACE		UPPER SURFACE	LOWER SURFACE		UPPER SURFACE	LOWER SURFACE	
AIR LOADS	N _x	LB/IN	39	-39		-541	541		271	-271		226	-190	
	N _y	LB/IN	-10,112	10,112		-5,043	5,043		-10,593	10,593		-4,379	4,379	
	N _{xy}	LB/IN	-1,224	1,224		-1,748	1,748		1,768	-1,768		173	-778	
THERMAL STRAIN	E _x	IN/IN	-255 X 10 ⁻⁶	255 X 10 ⁻⁶		-212 X 10 ⁻⁶	212 X 10 ⁻⁶		89 X 10 ⁻⁶	-89 X 10 ⁻⁶		-125 X 10 ⁻⁶	15 X 10 ⁻⁶	
	E _y	IN/IN	-258 X 10 ⁻⁶	258 X 10 ⁻⁶		-33 X 10 ⁻⁶	33 X 10 ⁻⁶		8 X 10 ⁻⁶	-8 X 10 ⁻⁶		75 X 10 ⁻⁶	-6 X 10 ⁻⁶	
	E _{xy}	IN/IN	39 X 10 ⁻⁶	-39 X 10 ⁻⁶		-63 X 10 ⁻⁶	63 X 10 ⁻⁶		150 X 10 ⁻⁶	-150 X 10 ⁻⁶		170 X 10 ⁻⁶	-6 X 10 ⁻⁶	
PRESSURE	AERO	PSI	-1.70	0.74		-1.25	0.39		-1.65	0.92		-1.47	0.77	
	FUEL	PSI	-6.42	-74.24		0	0		0	0		-7.11	0	
	NET	PSI	-8.12	74.99		-1.25	0.39		-1.65	0.92		-7.40	0.77	
TEMPERATURE	TAV	°F	264	269		301	315		296	296		193	329	
	ΔT	°F	-239	-228		-110	-97		-134	-124		-132	-85	

NOTES: (1) A 1.25 FACTOR HAS BEEN APPLIED TO THE THERMAL STRAIN WHEN THE SIGN IS SAME AS THE AIRLOAD
SIGN, OTHERWISE NO FACTOR APPLIED.

(2) PRESSURE SIGN CONVENTION: NEGATIVE = SUCTION

ORIGINAL PAGE IS
OF POOR QUALITY

TABLE 11-20. WING POINT DESIGN ENVIRONMENT, SPANWISE ARRANGEMENT - TASK I,
MID-CRUISE CONDITION

MASS - 240 x 10³ KG

POINT DESIGN REGION

ULTIMATE DESIGN LOADS	ITEM	UNITS	POINT DESIGN REGION											
			40236			41036			41316			40536		
AIR LOADS	Nx	KN/M	UPPER SURFACE	LOWER SURFACE		UPPER SURFACE	LOWER SURFACE		UPPER SURFACE	LOWER SURFACE		UPPER SURFACE	LOWER SURFACE	
			29	-59		-27	64		1639	1039		14	14	
			-1535	1535		-764	764		-1639	1039		-14	14	
THERMAL STRAIN	Ny	KN/M												
PRESSURE	Nz	MPa												
TEMPERATURE	Tx	°K												

WEIGHT - 550 x 10³ LB

POINT DESIGN REGION

ULTIMATE DESIGN LOADS	ITEM	UNITS	POINT DESIGN REGION											
			40236			41036			41316			40536		
AIR LOADS	Nx	LB/IN	UPPER SURFACE	LOWER SURFACE		UPPER SURFACE	LOWER SURFACE		UPPER SURFACE	LOWER SURFACE		UPPER SURFACE	LOWER SURFACE	
			167	-167		-172	152		226	226		102	102	
			-8766	8766		-1735	1365		-9359	9359		-8308	8308	
THERMAL STRAIN	Ny	IN/IN												
PRESSURE	Nz	PSI												
TEMPERATURE	Tx	°F												

NOTES (1) A 1.25 FACTOR HAS BEEN APPLIED TO THE THERMAL STRAIN WHEN THE SIGN IS SAME AS THE AIRLOAD SIGN, OTHERWISE NO FACTOR APPLIED.
(2) PRESSURE SIGN CONVENTION: NEGATIVE - SUCTION

TABLE 11-21. WING POINT DESIGN ENVIRONMENT, SPANWISE ARRANGEMENT - TASK I,
MACH 1.25 (V_g) CONDITION

MASS - 313×10^3 kg

CONDITION (1); MACH NO. = 1.25; $n_z = 2.5$

ULTIMATE DESIGN LOADS	ITEM	UNITS	POINT DESIGN REGION											
			40336			41348			40322			40236		
			UPPER SURFACE	LOWER SURFACE	41348 UPPER SURFACE	41348 LOWER SURFACE	UPPER SURFACE	LOWER SURFACE	UPPER SURFACE	LOWER SURFACE	UPPER SURFACE	UPPER SURFACE	LOWER SURFACE	41316 UPPER SURFACE
AIR LOADS	Nx	KN/m	-91	91	-130	130	2	-2	54	-54	79	28	-38	
	Ny	KN/m	-2874	2874	-1548	1548	-203	203	-275	275	-1663	-3143	3143	
	Nxy	KN/m ²	731	731	382	482	51	51	445	445	565	752	752	
THERMAL STRAIN	Cx	m/m	0	0	0	0	0	0	0	0	0	0	0	
	Cy	m/m	0	0	0	0	0	0	0	0	0	0	0	
	Cxy	m/m	0	0	0	0	0	0	0	0	0	0	0	
PRESSURE	AERO	MPa	-20.89	-8.27	-9.76	0.76	-31.33	-2.79	-8.76	-1.79	-34.96	6.62	-10.13	0.41
	FUEL	MPa	-40.88	-61.64	0	0	0	0	-39.39	-55.36	0	0	-47.30	-62.05
	NET	MPa	-51.77	-69.91	-8.76	0.76	-31.33	-1.79	-47.85	-57.15	-34.96	6.62	-57.43	-62.46
TEMPERATURE	TAV	°K	334	334	354	352	342	340	333	333	350	344	344	345
	ΔT	°K	-74	-77	-62	-57	-79	-88	-72	-75	-50	-63	-63	-70

WEIGHT - 600 X 10³ LB

ULTIMATE DESIGN LOADS	ITEM	UNITS	POINT DESIGN REGION											
			40336			41348			40322			40236		
			UPPER SURFACE	LOWER SURFACE	41348 UPPER SURFACE	41348 LOWER SURFACE	UPPER SURFACE	LOWER SURFACE	UPPER SURFACE	LOWER SURFACE	UPPER SURFACE	UPPER SURFACE	LOWER SURFACE	41316 UPPER SURFACE
AIR LOADS	Nx	LB/IN	-51.9	51.9	-1.028	1.028	11	-11	3.76	-3.76	4.90	162	-162	
	Ny	LB/IN	-15,409	15,409	-9,412	9,412	-1,185	1,185	-16,946	16,946	-9,499	-17,948	17,948	
	Nxy	LB/IN	4,173	4,173	2,750	2,750	290	290	2,541	2,541	3,227	4,292	4,292	
THERMAL STRAIN	Cx	IN/IN	0	0	0	0	0	0	0	0	0	0	0	
	Cy	IN/IN	0	0	0	0	0	0	0	0	0	0	0	
	Cxy	IN/IN	0	0	0	0	0	0	0	0	0	0	0	
PRESSURE	AERO	PSI	-1.27	-0.26	-5.07	0.96	-1.47	0.06	-3.03	-1.20	-1.27	0.11	4.96	-0.26
	FUEL	PSI	-5.67	-8.03	0	0	-6.36	-9.00	-5.93	-3.94	0	0	0	
	NET	PSI	-6.94	-8.29	-5.07	0.96	-3.33	-8.94	-8.96	-10.11	-1.27	0.11	4.98	-0.26
TEMPERATURE	TAV	°F	142	142	177	187	156	152	139	139	171	180	160	162
	ΔT	°F	-133	-139	-111	-102	-143	-159	-130	-136	-108	-106	-114	-126

NOTES: (1) A 1.25 FACTOR HAS BEEN APPLIED TO THE THERMAL STRAIN WHEN THE SIGN IS SAME AS THE AIRLOAD
SIGN, OTHERWISE NO FACTOR APPLIED.
(2) PRESSURE SIGN CONVENTION: NEGATIVE = SUCTION

ORIGINAL PAGE 1
OF FOUR QUALITY

TABLE 11-22. WING POINT DESIGN ENVIRONMENT, MONOCOQUE ARRANGEMENT - TASK I
MACH 0.40 LOAD CONDITION

C 8.111 ON (9) MACH 0.40 MACH 0.40 MACH 0.40

MASS - 300 x 10³ Kg

ULTIMATE DESIGN LOADS	ITEM	UNITS	POINT DESIGN REGION											
			40236				41036				41316			
			UPPER SURFACE	LOWER SURFACE	UPPER SURFACE	LOWER SURFACE	UPPER SURFACE	LOWER SURFACE	UPPER SURFACE	LOWER SURFACE	UPPER SURFACE	LOWER SURFACE	UPPER SURFACE	LOWER SURFACE
AIR LOADS	Nx	KN/m	-175	175	-243	243	-324	324	-324	324	-324	324	-324	324
	Ny	KN/m	-1724	1724	-284	284	-1223	1223	-1223	1223	-1223	1223	-1223	1223
	Nzy	KN/m	-504	504	-433	433	-504	504	-504	504	-504	504	-504	504
THERMAL STRAIN	Ex	mm/m	0	0	0	0	0	0	0	0	0	0	0	0
	Ey	mm/m	0	0	0	0	0	0	0	0	0	0	0	0
	Ezy	mm/m	0	0	0	0	0	0	0	0	0	0	0	0
PRESSURE	AERO	KPa	-1155	-2000	-1155	-1155	-1155	-1155	-1155	-1155	-1155	-1155	-1155	-1155
	FUEL	KPa	-40.54	-0.74	0	0	0	0	0	0	0	0	0	0
	NET	KPa	-1195	-2074	-1155	-1155	-1155	-1155	-1155	-1155	-1155	-1155	-1155	-1155
TEMPERATURE	TAV	°K	311	509	335	335	334	334	334	334	334	334	334	334
	ΔT	°K	-11	-9	-2	-3	-5	-5	-5	-5	-5	-5	-5	-5

WEIGHT - 745 x 10³ LB

ULTIMATE DESIGN LOADS	ITEM	UNITS	POINT DESIGN REGION											
			40236				41036				41316			
			UPPER SURFACE	LOWER SURFACE	UPPER SURFACE	LOWER SURFACE	UPPER SURFACE	LOWER SURFACE	UPPER SURFACE	LOWER SURFACE	UPPER SURFACE	LOWER SURFACE	UPPER SURFACE	LOWER SURFACE
AIR LOADS	Nx	LB/IN	-1318	1318	-1813	1813	-2534	2534	-2534	2534	-2534	2534	-2534	2534
	Ny	LB/IN	-9523	9523	-2147	2147	-10395	10395	-10395	10395	-10395	10395	-10395	10395
	Nzy	LB/IN	-1177	1177	-952	952	-1074	1074	-1074	1074	-1074	1074	-1074	1074
THERMAL STRAIN	Ex	IN/IN	0	0	0	0	0	0	0	0	0	0	0	0
	Ey	IN/IN	0	0	0	0	0	0	0	0	0	0	0	0
	Ezy	IN/IN	0	0	0	0	0	0	0	0	0	0	0	0
PRESSURE	AERO	PSI	-165	-292	-165	-165	-165	-165	-165	-165	-165	-165	-165	-165
	FUEL	PSI	-5.83	-0.11	0	0	0	0	0	0	0	0	0	0
	NET	PSI	-165	-292	-165	-165	-165	-165	-165	-165	-165	-165	-165	-165
TEMPERATURE	TAV	°F	599	779	623	623	622	622	622	622	622	622	622	622
	ΔT	°F	-19	-16	-3	-3	-9	-9	-9	-9	-9	-9	-9	-9

NOTES: (1) A 1.25 FACTOR HAS BEEN APPLIED TO THE THERMAL STRAIN WHEN THE SIGN IS SAME AS THE AIRLOAD SIGN, OTHERWISE NO FACTOR APPLIED.

(2) PRESSURE SIGN CONVENTION: NEGATIVE = SUCTION

TABLE 11-23. WING POINT DESIGN ENVIRONMENT, MONOCOQUE ARRANGEMENT - TASK I,
MACH 0.90 LOAD CONDITION

MASS - 318 x 10³ Kg

CONDITION 12 : MACH NO. = 0.90; ρ_c = 2.5

ULTIMATE DESIGN LOADS	ITEM	UNITS	POINT DESIGN REGION											
			40236			41036			41316			40536		
			UPPER SURFACE	LOWER SURFACE	UPPER SURFACE	UPPER SURFACE	LOWER SURFACE	UPPER SURFACE	UPPER SURFACE	LOWER SURFACE	UPPER SURFACE	UPPER SURFACE	LOWER SURFACE	UPPER SURFACE
AIR LOADS	Nx	kN/m	-160	150	-200	-200	150	-150	-150	150	-150	-150	150	-150
	Ny	kN/m	-1519	1419	-200	-200	150	-150	-150	150	-150	-150	150	-150
	Nzy	kN/m	145	145	341	341	401	401	443	443	443	443	373	373
THERMAL STRAIN	Ex	m/m	0	0	0	0	0	0	0	0	0	0	0	0
	Ey	m/m	0	0	0	0	0	0	0	0	0	0	0	0
	Ezy	m/m	0	0	0	0	0	0	0	0	0	0	0	0
PRESSURE	AERO	MPa	-5.30	-3.03	-14.45	-14.45	-3.03	-3.03	-3.03	-3.03	-3.03	-3.03	-3.03	-3.03
	FUEL	MPa	-10.54	-10.74	1	1	1	1	1	1	1	1	1	1
	NET	MPa	-14.36	-14.48	-14.48	-14.48	-14.48	-14.48	-14.48	-14.48	-14.48	-14.48	-14.48	-14.48
TEMPERATURE	TAV	°K	284	279	279	279	284	284	284	284	284	284	284	284
	ΔT	°K	19	19	19	19	13	13	13	13	13	13	13	13

WEIGHT - 700 x 10³ LB

ULTIMATE DESIGN LOADS	ITEM	UNITS	POINT DESIGN REGION											
			40236			41036			41316			40536		
			UPPER SURFACE	LOWER SURFACE	UPPER SURFACE	UPPER SURFACE	LOWER SURFACE	UPPER SURFACE	UPPER SURFACE	LOWER SURFACE	UPPER SURFACE	UPPER SURFACE	LOWER SURFACE	UPPER SURFACE
AIR LOADS	Nx	LB/IN	-205	205	-205	-205	205	-205	-205	205	-205	-205	205	-205
	Ny	LB/IN	-2100	2100	-2100	-2100	2100	-2100	-2100	2100	-2100	-2100	2100	-2100
	Nzy	LB/IN	208	208	208	208	208	208	208	208	208	208	208	208
THERMAL STRAIN	Ex	IN/IN	0	0	0	0	0	0	0	0	0	0	0	0
	Ey	IN/IN	0	0	0	0	0	0	0	0	0	0	0	0
	Ezy	IN/IN	0	0	0	0	0	0	0	0	0	0	0	0
PRESSURE	AERO	PSI	-1.99	-1.44	-1.99	-1.99	-1.44	-1.44	-1.44	-1.44	-1.44	-1.44	-1.44	-1.44
	FUEL	PSI	-5.83	-4.21	0	0	0	0	0	0	0	0	0	0
	NET	PSI	-7.197	-2.95	-2.95	-2.95	-2.95	-2.95	-2.95	-2.95	-2.95	-2.95	-2.95	-2.95
TEMPERATURE	TAV	°F	50	40	40	40	50	50	50	50	50	50	50	50
	ΔT	°F	32	34	34	34	14	14	14	14	14	14	14	14

NOTES (1) A 1.25 FACTOR HAS BEEN APPLIED TO THE THERMAL STRAIN WHEN THE SIGN IS SAME AS THE AIRLOAD
SIGN, OTHERWISE NO FACTOR APPLIED
(2) PRESSURE SIGN CONVENTION NEGATIVE = SUCTION

ORIGINAL PAGE IS
OF POOR QUALITY

TABLE 11-24. WING POINT DESIGN ENVIRONMENT, MONOCOQUE ARRANGEMENT - TASK I,
MACH 1.25 LOAD CONDITION

MASS 319×10^3 KG

REFLECTOR (15) EACH NO. 1.05; η_1 2.5

ULTIMATE DESIGN LOADS	ITEM	UNITS	POINT DESIGN REGION											
			40236			41036			41316			40536		
			UPPER SURFACE	LOWER SURFACE		UPPER SURFACE	LOWER SURFACE		UPPER SURFACE	LOWER SURFACE		UPPER SURFACE	LOWER SURFACE	
AIR LOADS	Nx	kN/m	-173	173	-233	-233	233	-233	-233	233	-233	-233	233	-233
	Ny	kN/m	-1449	1449	-918	-918	918	-918	-918	918	-918	-918	918	-918
	Nxy	kN/m	243	243	243	243	243	243	243	243	243	243	243	243
THERMAL STRAIN	Ex	m/m	0	0	0	0	0	0	0	0	0	0	0	0
	Ey	m/m	0	0	0	0	0	0	0	0	0	0	0	0
	Exy	m/m	0	0	0	0	0	0	0	0	0	0	0	0
PRESSURE	AERO	kPa	-22.46	-22.46	-22.46	-22.46	-22.46	-22.46	-22.46	-22.46	-22.46	-22.46	-22.46	-22.46
	FUEL	kPa	-45.93	-45.93	-45.93	-45.93	-45.93	-45.93	-45.93	-45.93	-45.93	-45.93	-45.93	-45.93
	NET	kPa	-63.40	-63.40	-63.40	-63.40	-63.40	-63.40	-63.40	-63.40	-63.40	-63.40	-63.40	-63.40
TEMPERATURE	TAV	°K	291	291	291	291	291	291	291	291	291	291	291	291
	ΔT	°K	5	5	5	5	5	5	5	5	5	5	5	5

WEIGHT - 690 X 10³ LB

ULTIMATE DESIGN LOADS	ITEM	UNITS	POINT DESIGN REGION											
			40236			41036			41316			40536		
			UPPER SURFACE	LOWER SURFACE		UPPER SURFACE	LOWER SURFACE		UPPER SURFACE	LOWER SURFACE		UPPER SURFACE	LOWER SURFACE	
AIR LOADS	Nx	LB/IN	-973	973	-1133	-1133	1133	-1133	-1133	1133	-1133	-1133	1133	-1133
	Ny	LB/IN	-3917	3917	-2416	-2416	2416	-2416	-2416	2416	-2416	-2416	2416	-2416
	Nxy	LB/IN	1411	1411	1411	1411	1411	1411	1411	1411	1411	1411	1411	1411
THERMAL STRAIN	Ex	IN/IN	0	0	0	0	0	0	0	0	0	0	0	0
	Ey	IN/IN	0	0	0	0	0	0	0	0	0	0	0	0
	Exy	IN/IN	0	0	0	0	0	0	0	0	0	0	0	0
PRESSURE	AERO	PSI	-3.23	-3.23	-3.23	-3.23	-3.23	-3.23	-3.23	-3.23	-3.23	-3.23	-3.23	-3.23
	FUEL	PSI	-6.93	-6.93	-6.93	-6.93	-6.93	-6.93	-6.93	-6.93	-6.93	-6.93	-6.93	-6.93
	NET	PSI	-9.96	-9.96	-9.96	-9.96	-9.96	-9.96	-9.96	-9.96	-9.96	-9.96	-9.96	-9.96
TEMPERATURE	TAV	°F	291	291	291	291	291	291	291	291	291	291	291	291
	ΔT	°F	5	5	5	5	5	5	5	5	5	5	5	5

NOTES (1) A 1.25 FACTOR HAS BEEN APPLIED TO THE THERMAL STRAIN WHEN THE SIGN IS SAME AS THE AIRLOAD
SIGN OTHERWISE NO FACTOR APPLIED

(2) PRESSURE SIGN CONVENTION: NEGATIVE = SUCTION

TABLE 11-25. WING POINT DESIGN ENVIRONMENT, MONOCOQUE ARRANGEMENT - TASK I,
START-OF-CRUISE CONDITION

SECTION 11-25. WING POINT DESIGN ENVIRONMENT, MONOCOQUE ARRANGEMENT - TASK I, START-OF-CRUISE CONDITION

MASS $289 \times 10^3 \text{ kg}$

ULTIMATE DESIGN LOADS	ITEM	UNITS	POINT DESIGN REGION									
			40236		41036		41316		40536		41348	
			UPPER SURFACE	LOWER SURFACE	UPPER SURFACE	LOWER SURFACE	UPPER SURFACE	LOWER SURFACE	UPPER SURFACE	LOWER SURFACE	UPPER SURFACE	LOWER SURFACE
AIR LOADS	Nx	kN/m	-202	202	-253	253	-131	131	-23	23	-3	3
	Ny	kN/m	-1253	1253	-1253	1253	-1384	1384	-1253	1253	-1253	1253
	Nxz	kN/m	-1253	1253	-1253	1253	-1384	1384	-1253	1253	-1253	1253
THERMAL STRAIN	Ex	m/m	-594 x 10 ⁻⁶	594 x 10 ⁻⁶	-1.3 x 10 ⁻⁶	1.3 x 10 ⁻⁶	-1.3 x 10 ⁻⁶	1.3 x 10 ⁻⁶	-1.3 x 10 ⁻⁶	1.3 x 10 ⁻⁶	-1.3 x 10 ⁻⁶	1.3 x 10 ⁻⁶
	Ey	m/m	-822 x 10 ⁻⁶	822 x 10 ⁻⁶	-8 x 10 ⁻⁶	8 x 10 ⁻⁶	-15 x 10 ⁻⁶	15 x 10 ⁻⁶	-15 x 10 ⁻⁶	15 x 10 ⁻⁶	-15 x 10 ⁻⁶	15 x 10 ⁻⁶
	Exy	m/m	-76 x 10 ⁻⁶	76 x 10 ⁻⁶	-15 x 10 ⁻⁶	15 x 10 ⁻⁶	-15 x 10 ⁻⁶	15 x 10 ⁻⁶	-15 x 10 ⁻⁶	15 x 10 ⁻⁶	-15 x 10 ⁻⁶	15 x 10 ⁻⁶
PRESSURE	AERO	MPa	-11.2	11.2	-2.2	2.2	-11.2	11.2	-2.2	2.2	-2.2	2.2
	FUEL	MPa	-44.7	44.7	-5.2	5.2	-44.7	44.7	-5.2	5.2	-5.2	5.2
	NET	MPa	-55.9	55.9	-7.4	7.4	-55.9	55.9	-7.4	7.4	-7.4	7.4
TEMPERATURE	TAV	°K	373	373	402	402	373	373	373	373	373	373
	ΔT	°K	-10	10	-2	2	-10	10	-2	2	-2	2

WEIGHT = $660 \times 10^3 \text{ lb}$

ULTIMATE DESIGN LOADS	ITEM	UNITS	POINT DESIGN REGION									
			40236		41036		41316		40536		41348	
			UPPER SURFACE	LOWER SURFACE	UPPER SURFACE	LOWER SURFACE	UPPER SURFACE	LOWER SURFACE	UPPER SURFACE	LOWER SURFACE	UPPER SURFACE	LOWER SURFACE
AIR LOADS	Nx	LB/IN	-1144	1144	-1253	1253	-131	131	-23	23	-3	3
	Ny	LB/IN	-1153	1153	-1253	1253	-1384	1384	-1253	1253	-1253	1253
	Nxz	LB/IN	-1153	1153	-1253	1253	-1384	1384	-1253	1253	-1253	1253
THERMAL STRAIN	Ex	IN/IN	-594 x 10 ⁻⁶	594 x 10 ⁻⁶	-1.3 x 10 ⁻⁶	1.3 x 10 ⁻⁶	-1.3 x 10 ⁻⁶	1.3 x 10 ⁻⁶	-1.3 x 10 ⁻⁶	1.3 x 10 ⁻⁶	-1.3 x 10 ⁻⁶	1.3 x 10 ⁻⁶
	Ey	IN/IN	-822 x 10 ⁻⁶	822 x 10 ⁻⁶	-8 x 10 ⁻⁶	8 x 10 ⁻⁶	-15 x 10 ⁻⁶	15 x 10 ⁻⁶	-15 x 10 ⁻⁶	15 x 10 ⁻⁶	-15 x 10 ⁻⁶	15 x 10 ⁻⁶
	Exy	IN/IN	-76 x 10 ⁻⁶	76 x 10 ⁻⁶	-15 x 10 ⁻⁶	15 x 10 ⁻⁶	-15 x 10 ⁻⁶	15 x 10 ⁻⁶	-15 x 10 ⁻⁶	15 x 10 ⁻⁶	-15 x 10 ⁻⁶	15 x 10 ⁻⁶
PRESSURE	AERO	PSI	-16.2	16.2	-3.2	3.2	-16.2	16.2	-3.2	3.2	-3.2	3.2
	FUEL	PSI	-64.7	64.7	-7.4	7.4	-64.7	64.7	-7.4	7.4	-7.4	7.4
	NET	PSI	-80.9	80.9	-10.6	10.6	-80.9	80.9	-10.6	10.6	-10.6	10.6
TEMPERATURE	TAV	°F	373	373	402	402	373	373	373	373	373	373
	ΔT	°F	-18	18	-4	4	-18	18	-4	4	-4	4

NOTES: (1) A 1.25 FACTOR HAS BEEN APPLIED TO THE THERMAL STRAIN WHEN THE SIGN IS SAME AS THE AIRLOAD SIGN, OTHERWISE NO FACTOR APPLIED.

(2) PRESSURE SIGN CONVENTION: NEGATIVE = SUCTION

ORIGINAL PAGE IS
OF POOR QUALITY

TABLE 11-26. WING POINT DESIGN ENVIRONMENT, MONOCOQUE ARRANGEMENT - TANK I,
MID-CRUISE CONDITION

MASS: 249×10^3 Kg

ULTIMATE DESIGN LOADS	ITEM	UNITS	POINT DESIGN REGION											
			40236		41036		41316		40536		41348		40322	
AIR LOADS	ITEM	UNITS	UPPER SURFACE	LOWER SURFACE	UPPER SURFACE	LOWER SURFACE	UPPER SURFACE	LOWER SURFACE	UPPER SURFACE	LOWER SURFACE	UPPER SURFACE	LOWER SURFACE	UPPER SURFACE	LOWER SURFACE
			Nx	-1.36	-1.36	-1.36	-1.36	-1.36	-1.36	-1.36	-1.36	-1.36	-1.36	-1.36
THERMAL STRAIN	ITEM	UNITS	Ny	-1.062	-1.062	-1.062	-1.062	-1.062	-1.062	-1.062	-1.062	-1.062	-1.062	-1.062
			Nxy	-1.51	-1.51	-1.51	-1.51	-1.51	-1.51	-1.51	-1.51	-1.51	-1.51	-1.51
PRESSURE	ITEM	UNITS	Ex	1×10^{-4}	1.49×10^{-4}	1.49×10^{-4}	1.49×10^{-4}	1.49×10^{-4}	1.49×10^{-4}	1.49×10^{-4}	1.49×10^{-4}	1.49×10^{-4}	1.49×10^{-4}	1.49×10^{-4}
			Ey	1.49×10^{-4}	1.49×10^{-4}	1.49×10^{-4}	1.49×10^{-4}	1.49×10^{-4}	1.49×10^{-4}	1.49×10^{-4}	1.49×10^{-4}	1.49×10^{-4}	1.49×10^{-4}	1.49×10^{-4}
TEMPERATURE	ITEM	UNITS	Exy	1.49×10^{-4}	1.49×10^{-4}	1.49×10^{-4}	1.49×10^{-4}	1.49×10^{-4}	1.49×10^{-4}	1.49×10^{-4}	1.49×10^{-4}	1.49×10^{-4}	1.49×10^{-4}	1.49×10^{-4}
			AERO	-39.16	-39.16	-39.16	-39.16	-39.16	-39.16	-39.16	-39.16	-39.16	-39.16	-39.16
	ITEM	UNITS	FUEL	-45.36	-45.36	-45.36	-45.36	-45.36	-45.36	-45.36	-45.36	-45.36	-45.36	-45.36
			NET	-45.36	-45.36	-45.36	-45.36	-45.36	-45.36	-45.36	-45.36	-45.36	-45.36	-45.36
	ITEM	UNITS	TAV	3.59	3.59	3.59	3.59	3.59	3.59	3.59	3.59	3.59	3.59	3.59
			ΔT	-1.56	-1.56	-1.56	-1.56	-1.56	-1.56	-1.56	-1.56	-1.56	-1.56	-1.56

WEIGHT: 560×10^3 LB

ULTIMATE DESIGN LOADS	ITEM	UNITS	POINT DESIGN REGION											
			40236		41036		41316		40536		41348		40322	
AIR LOADS	ITEM	UNITS	UPPER SURFACE	LOWER SURFACE	UPPER SURFACE	LOWER SURFACE	UPPER SURFACE	LOWER SURFACE	UPPER SURFACE	LOWER SURFACE	UPPER SURFACE	LOWER SURFACE	UPPER SURFACE	LOWER SURFACE
			Nx	-1.06	-1.06	-1.06	-1.06	-1.06	-1.06	-1.06	-1.06	-1.06	-1.06	-1.06
THERMAL STRAIN	ITEM	UNITS	Ny	-1.064	-1.064	-1.064	-1.064	-1.064	-1.064	-1.064	-1.064	-1.064	-1.064	-1.064
			Nxy	-1.51	-1.51	-1.51	-1.51	-1.51	-1.51	-1.51	-1.51	-1.51	-1.51	-1.51
PRESSURE	ITEM	UNITS	Ex	1×10^{-4}	1.49×10^{-4}	1.49×10^{-4}	1.49×10^{-4}	1.49×10^{-4}	1.49×10^{-4}	1.49×10^{-4}	1.49×10^{-4}	1.49×10^{-4}	1.49×10^{-4}	1.49×10^{-4}
			Ey	1.49×10^{-4}	1.49×10^{-4}	1.49×10^{-4}	1.49×10^{-4}	1.49×10^{-4}	1.49×10^{-4}	1.49×10^{-4}	1.49×10^{-4}	1.49×10^{-4}	1.49×10^{-4}	1.49×10^{-4}
TEMPERATURE	ITEM	UNITS	Exy	1.49×10^{-4}	1.49×10^{-4}	1.49×10^{-4}	1.49×10^{-4}	1.49×10^{-4}	1.49×10^{-4}	1.49×10^{-4}	1.49×10^{-4}	1.49×10^{-4}	1.49×10^{-4}	1.49×10^{-4}
			AERO	-39.16	-39.16	-39.16	-39.16	-39.16	-39.16	-39.16	-39.16	-39.16	-39.16	-39.16
	ITEM	UNITS	FUEL	-45.36	-45.36	-45.36	-45.36	-45.36	-45.36	-45.36	-45.36	-45.36	-45.36	-45.36
			NET	-45.36	-45.36	-45.36	-45.36	-45.36	-45.36	-45.36	-45.36	-45.36	-45.36	-45.36
	ITEM	UNITS	TAV	3.59	3.59	3.59	3.59	3.59	3.59	3.59	3.59	3.59	3.59	3.59
			ΔT	-1.56	-1.56	-1.56	-1.56	-1.56	-1.56	-1.56	-1.56	-1.56	-1.56	-1.56

NOTES: (1) A126 FACTOR HAS BEEN APPLIED TO THE THERMAL STRAIN WHEN THE SIGN IS SAME AS THE AIRLOAD

SIGN: OTHERWISE NO FACTOR APPLIED

(2) PRESSURE SIGN CONVENTION: NEGATIVE = SUCTION

TABLE 11-27. WING POINT DESIGN ENVIRONMENT, MONOCOQUE ARRANGEMENT - TASK I,
MACH 1.25 (V_g) CONDITION

MASS - 213 X 10³ Kg

ULTIMATE DESIGN LOADS	ITEM	UNITS	POINT DESIGN REGION											
			40236		51036		41316		40536		41348		40322	
AIR LOADS	N _x	KN/m	UPPER SURFACE	LOWER SURFACE	UPPER SURFACE	LOWER SURFACE	UPPER SURFACE	LOWER SURFACE	UPPER SURFACE	LOWER SURFACE	UPPER SURFACE	LOWER SURFACE	UPPER SURFACE	LOWER SURFACE
			-209	202	-399	339	-278	278	-555	555	-130	201	9	-9
THERMAL STRAIN	N _y	KN/m	-2038	2038	-1145	1145	-1133	1133	-1060	1060	-1270	1272	-93	93
			368	368	542	542	850	850	914	914	555	555	33	33
PRESSURE	C _x	m/m	0	0	0	0	0	0	0	0	0	0	0	0
			0	0	0	0	0	0	0	0	0	0	0	0
TEMPERATURE	C _y	m/m	0	0	0	0	0	0	0	0	0	0	0	0
			0	0	0	0	0	0	0	0	0	0	0	0
	AERO	MPa	-0.06	-0.06	-0.06	0.06	-0.33	-0.33	-0.76	-0.76	-0.96	-0.96	-1.13	-1.13
			-0.06	-0.06	0	0	0	0	-0.09	-0.09	0	0	-0.30	-0.30
	NET	MPa	-0.06	-0.06	-0.06	0.06	-0.33	-0.33	-0.76	-0.76	-0.96	-0.96	-1.13	-1.13
			-0.06	-0.06	-0.06	0.06	-0.33	-0.33	-0.76	-0.76	-0.96	-0.96	-1.13	-1.13
	TAV	°K	336	337	341	341	354	354	361	361	371	371	389	389
			-77	-77	-77	-77	-54	-54	-54	-54	-54	-54	-54	-54

WEIGHT - 690 X 10³ LB

ULTIMATE DESIGN LOADS	ITEM	UNITS	POINT DESIGN REGION											
			40236		41036		41316		40536		41348		40322	
AIR LOADS	N _x	LB/IN	UPPER SURFACE	LOWER SURFACE	UPPER SURFACE	LOWER SURFACE	UPPER SURFACE	LOWER SURFACE	UPPER SURFACE	LOWER SURFACE	UPPER SURFACE	LOWER SURFACE	UPPER SURFACE	LOWER SURFACE
			-1123	1123	-114	114	-16	16	-311	311	-1130	1190	51	-51
THERMAL STRAIN	N _y	LB/IN	-1123	1123	-114	114	-16	16	-311	311	-1130	1190	-59	59
			1099	1099	309	309	3310	3310	344	344	346	346	191	191
PRESSURE	C _x	IN/IN	0	0	0	0	0	0	0	0	0	0	0	0
			0	0	0	0	0	0	0	0	0	0	0	0
TEMPERATURE	C _y	IN/IN	0	0	0	0	0	0	0	0	0	0	0	0
			0	0	0	0	0	0	0	0	0	0	0	0
	AERO	PSI	-3.03	-3.03	-1.27	0.11	-4.94	-4.94	-1.17	-1.17	-5.07	-0.96	-1.47	-1.47
			-5.23	-5.23	0	0	0	0	-5.43	-5.43	0	0	-0.96	-0.96
	NET	PSI	-3.03	-3.03	-1.27	0.11	-4.94	-4.94	-1.17	-1.17	-5.07	-0.96	-1.47	-1.47
			-3.03	-3.03	-1.27	0.11	-4.94	-4.94	-1.17	-1.17	-5.07	-0.96	-1.47	-1.47
	TAV	°F	146	147	204	204	313	313	344	344	346	346	191	191
			-129	-129	-129	-129	-77	-77	-141	-141	-109	-109	-109	-109

NOTES (1) A 1.25 FACTOR HAS BEEN APPLIED TO THE THERMAL STRAIN WHEN THE SIGN IS SAME AS THE AIRLOAD
SIGN, OTHERWISE NO FACTOR APPLIED
(2) PRESSURE SIGN CONVENTION: NEGATIVE = SUCTION

ORIGINAL PAGE IS
OF POOR QUALITY

General Fuselage Environment - Task I

The fuselage point design environment was specified for each stage of the structural investigations conducted during the Task I analytical studies. Specifically for the fuselage, the two stages of analysis included:

- Initial Screening - A preliminary parametric frame spacing study to ascertain the spacing associated with minimum weight design; then using this spacing to perform a structural analysis to screen the fuselage panel candidates and to determine the most promising concept(s) for the next stage of analysis.
- Detail Concept Analysis - A detail analysis of the surviving concept(s) from the initial screening analysis.

The details included in the definition of each of the point design environments progressed with the stage of design under consideration.

For the initial screening analyses only inplane loads (N_x and N_{xy}) due to vertical shear and body bending were considered in the analysis of the shell with no attempt to include the effect of pressure or temperature. In line with this philosophy, the frame were subjected to a very rudimentary analysis based on the theory derived by Shanley in Reference 3.

In support of the Detail Concept Analysis, a more detail point design environment was specified and included not only the inplane loads but also included the effects of pressure and temperature.

Fuselage Cabin Pressure - Task I

As previously discussed only the point design environment defined for the detail concept analysis included normal pressure; conservatively, only the internal cabin pressure was considered for this analysis.

The two critical flight conditions investigated during the detail concept analyses were the start-of-cruise condition and a Mach 1.2 transonic climb condition.

The cabin pressures and associated flight parameters for these conditions are shown in Table 11-28.

Fuselage Internal Loads - Task I

The basis for the Task I internal loads was existing body shear and bending moment diagrams as specified in References 1 and 2. These diagrams are presented in Figures 11-11 and 11-12 and were used with the exception of the specified 3-g taxi condition which was considered too stringent and arbitrarily reduced to the lower values noted by dashed lines. The sign convention for those ultimate shears and bending moments are displayed on the ordinate of these diagrams.

Internal Loads - Airloads - Internal loads were defined for each stage of the Task I analyses. The stresses and associated inplane loads were derived using theoretical bending (MQ/I) and shear (VQ/I) distributions.

For the structural analyses conducted during the initial screening, panel load intensities were calculated and are presented in Tables 11-29 and 11-30. The first table reflects the load intensities used for the parametric frame spacing study and the later table presents those loads employed for the structural screening of the fuselage panel candidates. All loads indicated on both tables are ultimate values and reflect the section properties associated with the stage of the design under consideration. The fuselage panel load intensities used for the Task I detail concepts analysis are displayed in Table 11-31.

Internal Loads - Thermal - As previously mentioned in the general fuselage environment discussion, only the analysis conducted during the detail concept analysis contained the effects of pressure and temperature. Table 11-32 contains the temperature gradients and average temperature of the skin panels for the two flight conditions considered. Temperature values are shown for skin panels located at the top, side, and bottom of the fuselage cross section at each of the point design regions. The corresponding values for the fuselage frames are shown in Section 6, Table 6-4.

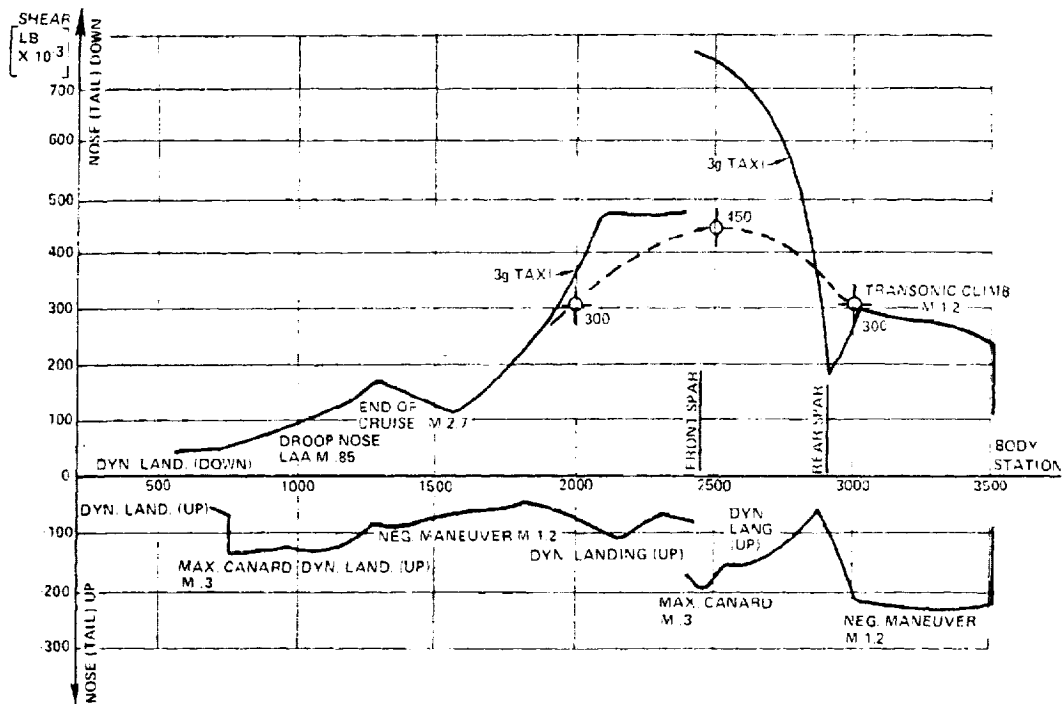


FIGURE 11-11. FUSELAGE SHEAR DIAGRAM - TASK I

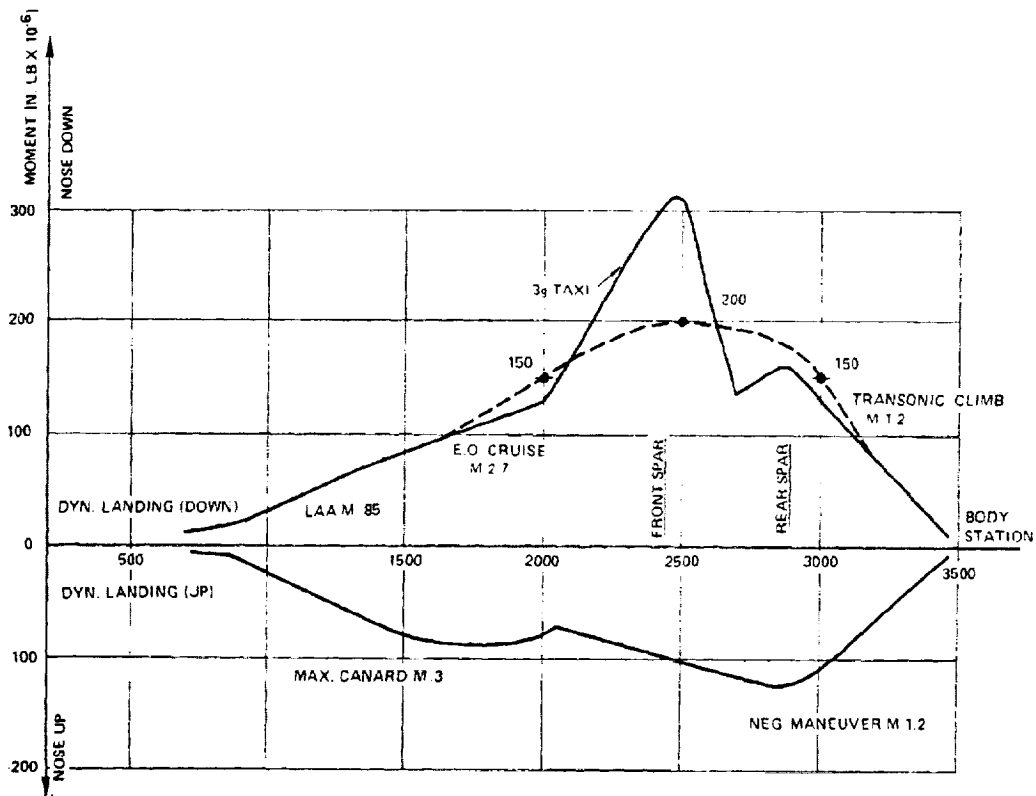


FIGURE 11-12. FUSELAGE BENDING MOMENT DIAGRAM - TASK I

ORIGINAL PAGE IS
OF POOR QUALITY

TABLE 11-28. FUSELAGE CABIN PRESSURE - TASK I

CONDITION	WT. X 10 ⁻³ LBS	MACH NO.	LOAD FACTOR n_z	V_e K _{eas}	ALT. X 10 ⁻³ FT.	CABIN ⁽¹⁾ PRESSURE (PSI)
START-OF-CRUISE	660	2.7	2.5	460	61.5	17.55
TRANSONIC CLIMB AT M1.2	690	1.2	2.5	372	38.2	17.55

1. ULTIMATE $p = 1.5 \times \text{LIMIT } p$ TABLE 11-29. FUSELAGE PANEL LOAD INTENSITIES,
PARAMETRIC FRAME SPACING STUDY - TASK I

LOCATION	FUSELAGE PANEL LOAD INTENSITIES (ULT.), LB/IN			
	DIRECTION	FS 2000	FS 2500	FS 3000
UPPER PANEL	N_x	13200	17600	13200
	N_{xy}	170	255	170
SIDE PANEL	N_x	0	0	0
	N_{xy}	1400	2100	1400
LOWER PANEL	N_x	-13200	-17600	-13200
	N_{xy}	170	255	170

TABLE 11-30. FUSELAGE PANEL LOAD INTENSITIES,
CONCEPT SCREENING STUDY - TASK I

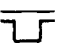


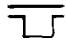
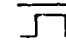
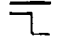
LOCATION	FUSELAGE PANEL LOAD INTENSITIES (ULT.), LB/IN						
	DIRECTION	FS 2000, FS 3000			FS 2500		
							
UPPER PANEL	N _x	11600	11700	11600	15700	14600	15690
	N _{xy}	412	417	413	629	597	629
SIDE PANEL	N _x	377	406	300	422	545	416
	N _{xy}	1361	1357	1330	2025	2000	1998
LOWER PANEL	N _x	-11700	-11650	-12000	-16100	-16800	15900
	N _{xy}	415	412	426	645	670	633

TABLE 11-31. FUSELAGE PANEL LOAD INTENSITIES,
DETAILED CONCEPT ANALYSIS - TASK I

LOCATION	FUSELAGE PANEL LOAD INTENSITIES (ULT.), LB/IN.				
	DIRECTION	FS 750	FS 2000	FS 2500	FS 3000
UPPER PANEL	N _x	1580	11630	15730	11630
	N _{xy}	50	412	629	412
SIDE PANEL	N _x	1580	1230	1230	1230
	N _{xy}	50	1360	2025	1360
LOWER PANEL	N _x	-1580	—	—	-11670
	N _{xy}	50	—	—	415

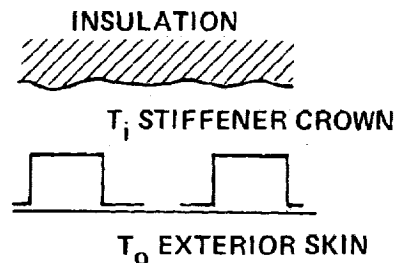
- (1) ULTIMATE LOAD = 1.5 X LIMIT LOADS
(2) CRITICAL DESIGN CONDITION: START-OF-CRUISE

TABLE 11-32. TEMPERATURE AND GRADIENTS FOR FUSELAGE
SKIN PANELS - TASK I

NOTES:

1. BASED ON HOT DAY (STD+8K)
4200 n.mi. FLIGHT PROFILE.
2. HAT-STIFFENED PANELS,
EXCEPT ZEE-STIFFENED
AT FS 750.
3. 'TOP', 'BOTTOM' AT G;
'SIDE' AT 90° OR ABOVE
WING.

PANEL SCHEMATIC



TEMPERATURES IN F

LOCATION	FLIGHT CONDITION			
	START OF CRUISE		MACH 1.2 DESCENT	
	$T_i - T_o$	T_{AVG}	$T_i - T_o$	T_{AVG}
<u>TOP</u>				
FS 750	-105	342	+111	114
2000	-175	295	+171	144
2500	-186	281	+181	156
3000	-174	292	+170	145
<u>SIDE</u>				
FS 750	-106	332	+109	108
2000	-157	324	+156	129
2500	-171	311	+170	139
3000	-147	301	+142	122
<u>BOTTOM</u>				
FS 750	-106	333	+109	109
3000	-177	278	+171	141

Fuselage Point Design Environment - Task I

The fuselage point design environments for the initial screening investigation include only the inplane loads due to vertical shear and body bending loads and were previously presented in Tables 11-29 and 11-30.

The more detail point design environment used in the detail concept analyses is shown in Table 11-33 for the most critical Task I load condition, i.e., start-of-cruise condition. This table included the inplane loads, normal pressures, panel temperature gradients, and average panel temperature for the four point design regions. The stated inplane loads and normal pressures are ultimate values.

AIRPLANE DESIGN ENVIRONMENT - TASK IIA

The Task IIA configuration change investigation was a study to define the effects of airplane configuration and mass properties changes on the flutter characteristics of the Task II airplane configuration. To attain this objective an abbreviated design cycle was conducted using the Task I chordwise structural model with the aforementioned configuration and mass revisions. In support of the strength analysis conducted during this investigation, the wing point design environment was defined for the flutter critical flight condition (Mach 0.9). The fuselage point design environment was not specified for this investigation since the flight condition under consideration was non-critical for the fuselage structure.

The critical flight conditions were the symmetric flight conditions at Mach 0.9, V_C and V_A . Static aeroelastic loads were calculated for these conditions with the following load factors: positive 1-g, 2.5-g steady maneuver, 2.5-g transient maneuver, and a negative 1-g.

Since the wing configuration change occurred outboard of the wing fin, approximately butt line 600, negligible effect on the inboard aerodynamic pressures can be expected. The Task I aerodynamic pressure defined for the wing point design regions are applicable for the Task IIA investigation, Condition 12 on Table 11-3.

TABLE 11-33. FUSELAGE POINT DESIGN ENVIRONMENT, DETAILED CONCEPT
ANALYSIS - TASK I, START-OF-CRUISE CONDITION

START OF CRUISE; MACH NO. 2.7; $N_z = 2.5$													
ITEM	UNITS	FS 750			FS 2000			FS 2500			FS 3000		
		UPPER PANEL	SIDE PANEL	LOWER PANEL	UPPER PANEL	SIDE PANEL	LOWER PANEL	UPPER PANEL	SIDE PANEL	LOWER PANEL	UPPER PANEL	SIDE PANEL	LOWER PANEL
N_x	LB/IN	1580	200	-1580	11630	1230	-	15730	1230	-	11630	1230	-11670
N_{xy}	LB/IN	50	250	50	412	1360	-	629	2025	-	412	1360	415
INTERNAL PRESSURE	PSI	17.55	17.55	17.55	17.55	17.55	-	17.55	17.55	-	17.55	17.55	17.55
T_{AVG}	°F	342	332	333	295	324	-	281	311	-	292	301	278
ΔT	°F	-105	-106	-106	-175	-157	-	-186	-171	-	-174	-147	-177

In addition, the Task I fuel tank pressures defined in Table 11-6 for flight condition 12 are appropriate.

The NASTRAN redundant analysis solution provided internal forces and stresses for the Mach 0.9 flight condition. The wing surface load intensities for this condition are shown in Table 11-34. For comparison purposes the load intensities for the Task I and Task IIB models are included. No temperature conditions were considered for the Task IIA internal load runs.

The wing point design environment for the 2.5-g symmetric flight-steady maneuver condition at Mach 0.90 (V_C) is shown in Table 11-35. This environment was used to conduct a simplified weight comparison study at several point design regions, see Section 12 for the results of this analysis.

AIRPLANE DESIGN ENVIRONMENT - TASK IIB

The Task IIB Detail Engineering Studies were conducted by exercising the design cycle twice; first, for a baseline strength design airplane and then performing an iteration on that design to incorporate the stiffness requirement dictated by the flutter optimization study. The wing and fuselage point design environments were defined in support of the stress analysis associated with each of the above design cycles.

The location of the point design regions (wing and fuselage) were approximately the same as those specified for the Task I and Task IIA efforts. The wing regions are shown in Figure 11-1 and the regions for Task IIB fuselage, which was modeled in more detail than the earlier versions, are presented in Figure 11-13. The structural definition of the Task IIB point design regions is different from those specified for the earlier tasks; i.e., the most promising Task I arrangement (chordwise/monocoque hybrid design) was utilized for the Task IIB investigation. A description of this arrangement is presented in Figure 11-14.

TABLE 11-34. WING SURFACE LOAD INTENSITIES - TASK IIA,
MACH 0.90 LOAD CONDITION

PANEL IDENTIFICATION		*LOAD INTENSITY (ULTIMATE), LBS/IN.									
		REGION	NUMBER	DIRECTION	TASK I			IIA	TASK II-B		
					CHORDWISE	SPANWISE	MONOCOQUE		CHORDWISE	HYBRID (STRENGTH)	HYBRID (FINAL)
WING-FORWARD	40322	Nx Ny Nxy	- 10 - 1145 201	- 148 - 1155 275	- 199 - 595 211	- 819 - 1120 143	- 122 - 1109 112	- 219 - 1049 75			
WING-AFT BOX	40236	Nx Ny Nxy	188 -10846 418	122 -12181 1181	- 925 -8102 858	- 377 -11474 436	179 -12779 271	15 -14311 272			
	40536	Nx Ny Nxy	85 -10680 1118	- 132 -12318 2288	-1483 -8763 2521	- 471 -11207 1409	- 458 -12680 1068	- 315 -14410 1159			
	41036	Nx Ny Nxy	- 274 - 6570 1369	- 36 - 6876 2027	-1094 -4544 1949	- 567 - 7040 1581	- 1052 - 3522 1583	- 1562 - 4725 1773			
WING-TIP	41316	Nx Ny Nxy	701 -11655 3492	298 -12546 3240	- 932 -8268 2528	592 -12145 3773	- 1226 - 9504 3686	- 1478 -10106 3730			
	41348	Nx Ny Nxy	- 719 - 6293 1535	- 574 - 5886 1797	- 605 -4731 2132	- 1068 - 6402 1990	- 877 - 5148 2290	- 856 - 6598 2608			

*LOAD CONDITIONS:

TASK I CONDITION 12: MACH 0.90, $n_z = 2.5$, $W = 700,000$ LB, $V_e = 325$ KEAS
 TASK IIA CONDITION 9: MACH 0.90, $n_z = 2.5$, $W = 700,000$ LB, $V_e = 325$ KEAS
 TASK IIB CONDITION 8: MACH 0.90, $n_z = 2.5$, $W = 700,000$ LB, $V_e = 325$ KEAS

TABLE 11-35. WING POINT DESIGN ENVIRONMENT, CHORDWISE ARRANGEMENT - TASK IIA,
MACH 0.90 LOAD CONDITION

CONDITION 9 SYMMETRICAL FLIGHT, STEADY MANEUVER AT MACH 0.90 (V_D)

ULTIMATE DESIGN LOADS	ITEM	UNITS	POINT DESIGN REGION											
			40322		41316		41348		40236		40536		41036	
			UPPER SURFACE	LOWER SURFACE	UPPER SURFACE	LOWER SURFACE	UPPER SURFACE	LOWER SURFACE	UPPER SURFACE	LOWER SURFACE	UPPER SURFACE	LOWER SURFACE	UPPER SURFACE	LOWER SURFACE
AIR LOADS	N _x	LB/IN	-819	819	592	592	-1068	1068	-377	377	-471	471	-567	567
	N _y	LB/IN	-1120	1120	-12145	12145	-6402	6402	-11474	11474	-11207	11207	-7040	7040
	N _z	LB/IN	143	143	3773	3773	1990	1990	436	436	1409	1409	1581	1581
THERMAL STRAIN	ε _x	IN/IN	-	-	-	-	-	-	-	-	-	-	-	-
	ε _y	IN/IN	-	-	-	-	-	-	-	-	-	-	-	-
	ε _{xy}	IN/IN	-	-	-	-	-	-	-	-	-	-	-	-
PRESSURE	AERO	PSI	-1.40	-0.30	-6.75	-3.76	-3.86	-0.30	-0.99	-0.44	-1.35	-0.49	-2.10	0.36
	FUEL	PSI	-6.74	8.96	-	-	-	-	-5.88	8.81	-5.63	-7.91	-	-
	NET	PSI	-8.14	-9.26	-6.75	-3.76	-3.86	0.30	-6.87	-9.25	-6.98	-8.40	-2.10	-0.36
TEMPERATURE	T _{AV}	°F	50	52	45	43	46	41	52	54	52	54	43	41
	ΔT	°F	30	37	14	17	25	18	29	32	29	32	14	15

NOTES: (1) A 1.25 FACTOR HAS BEEN APPLIED TO THE THERMAL STRAIN WHEN THE SIGN IS SAME AS THE AIRLOAD

SIGN, OTHERWISE NO FACTOR APPLIED.

(2) PRESSURE SIGN CONVENTION: NEGATIVE - SUCTION

ORIGINAL PAGE IS
OF POOR QUALITY

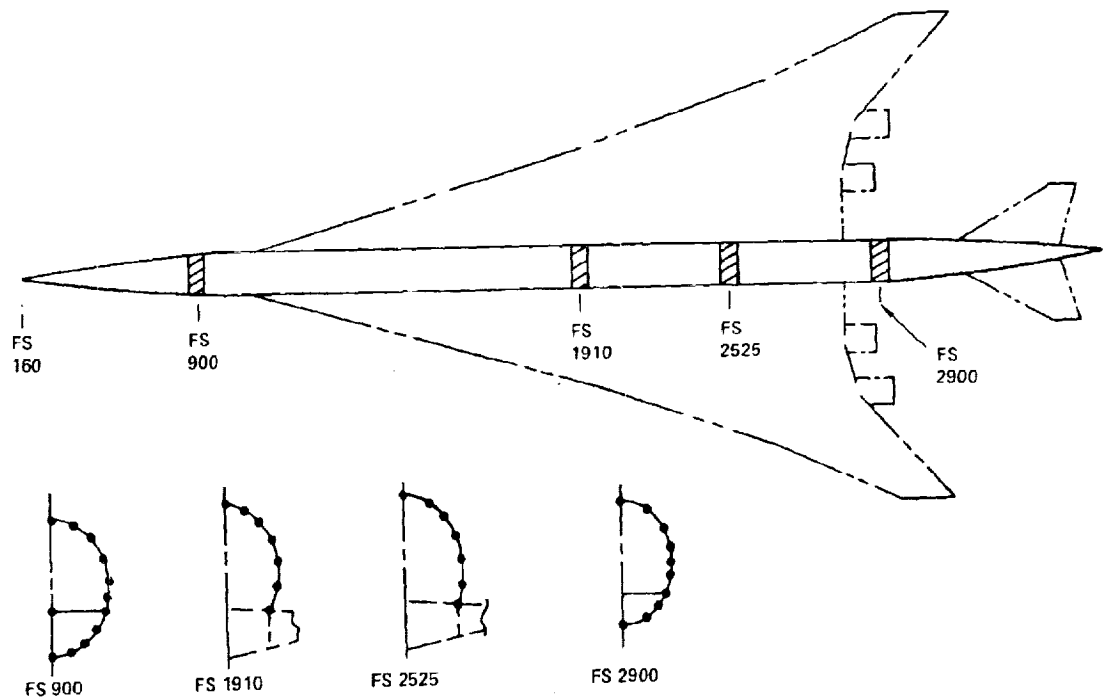


FIGURE 11-13. DEFINITION OF FUSELAGE POINT DESIGN REGIONS - TASK IIB

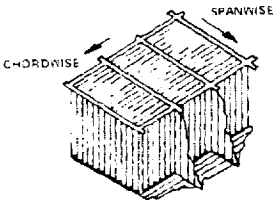

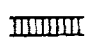
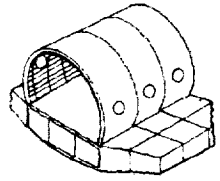



STRUCTURAL APPROACH	STRUCTURAL ARRANGEMENTS
	TASK IIB
<p>WING</p> 	<p><u>WING</u></p> <ul style="list-style-type: none"> BASIC WING SURFACE PANELS CHORDWISE STIFFENED -  WING TIP PANELS MONOCOQUE ALUM. BRAZED HONEYCOMB  SUBSTRUCTURE METALLIC RIB CAPS SUBMERGED SPAR CAPS - B/P REINFORCED (AFT BOX REGION) TRUSS AND CIRCULAR-ARC WEBS MAT'L - Ti6Al-4V ANN.
<p>FUSELAGE</p> 	<p><u>FUSELAGE</u></p> <ul style="list-style-type: none"> SHELL (SKIN/STRINGER) HAT-STIFFENED CONCEPT (MIDBODY AND AFT BODY)  ZEE-STIFFENED CONCEPT (FOREBODY) MAT'L - Ti6Al-4V ANN.  FRAMES FLOATING FRAMES Ti6Al-4V ANN. 

FIGURE 11-14. STRUCTURAL ARRANGEMENT - TASK IIB

Design Load Conditions - Task IIB

A summary of the number and type of load conditions investigated for each of the Task IIB designs is shown in Table 11-36. A total of nineteen conditions were included in the strength design analysis. The strength/stiffness design cycle incorporated additional gust and landing conditions for a total of twenty-five conditions. From a review of the NASTRAN internal loads runs the critical load conditions were defined for each design. These critical conditions are listed in Table 11-37 for the strength design. The corresponding conditions for the strength/stiffness design are contained in Table 11-38.

Wing Aerodynamic Pressures - Task IIB

The Task IIB airplane configuration was identical to that studied in the Task IIA configuration change investigation. The wing tip configuration change had negligible effect on the aerodynamic pressures distribution inboard of wing fin (BL 600) and those pressures specified for the Task I configuration, Table 11-3, are also applicable to this configuration. The Task I point design pressures are repeated in Table 11-39 with the equivalent Task IIB flight condition numbers.

Fuel Tank Pressures - Task IIB

In addition to the wing tip revision incorporated on the Task II airplane configuration, the location of the fuel tanks and the fuel usage schedules were modified to provide an aftward shift in the center of gravity. This modification required a reanalysis of the fuel tank pressures.

A schematic of the Task IIB fuel tank boundaries are shown in Figure 11-15, the fuel heights for the "wet bay" regions are presented in Table 11-40. The longitudinal (n_x) and vertical (n_z) load factors for the critical Task II conditions are summarized in Table 11-41.

A summary of the fuel tank pressures for point design regions 40236, 40536 and 40322 are contained in Table 11-42. This table presents the fuel inertia head and

TABLE 11-36. SUMMARY OF LOAD CONDITIONS - TASK IIB

TASK/MODEL	NUMBER/TYPE CONDITIONS					
	SYMM. FLT. COND.			GUST CONDS.	ROLL CONDS.	LANDING CONDS.
	ASCENT TO CRUISE	CRUISE CONDS.	DESCENT FROM CRUISE			
TASK IIB (3 D MODEL)						
• HYBRID (STRENGTH)	13	4	2	—	—	—
• HYBRID (STRENGTH/STIFF.)	13	4	2	2	—	4

TABLE 11-37. CRITICAL LOAD CONDITIONS, STRENGTH DESIGN - TASK 12B

NASTRAN COND. NO.	WEIGHT $\times 10^{-3}$ LB.	MACH NO.	ALTITUDE $\times 10^{-3}$ FT	LOAD FACTOR (N_z)	V_e (KEAS)	COMMENT
1						M2.7, START OF CRUISE
2						M2.7, MID-CRUISE
3						M1.25 DESCENT
4	745	0.40	SL	2.5	284.6	SYMM. FLT., STEADY MAN. AT M0.40 (V_S)
6	700	0.90	36.0	2.5	282.4	SYMM. FLT., STEADY MAN. AT M0.90 (V_S)
8	700	0.90	30.0	2.5	325.0	SYMM. FLT., STEADY MAN. AT M0.90 (V_C)
12	690	1.25	48.0	2.5	294.3	SYMM. FLT., STEADY MAN. AT M1.25 (V_S)
14	690	1.25	48.0	-1.0	294.3	-1.0G SYMM. FLT., STEADY MAN. AT M1.25 (V_S)
15	690	1.25	38.2	2.5	372.0	SYMM. FLT., STEADY MAN. AT M1.25 (V_C)
17	445	1.25	34.0	2.5	420.0	SYMM. FLT., STEADY MAN. AT M1.25 (V_D), DESCENT
19	660	2.70	61.5	2.5	460.0	SYMM. FLT., STEADY MAN. AT M2.7 (V_C), START OF CRUISE
21	550	2.70	64.0	1.0	433.6	SYMM. FLT., STEADY MAN. AT M2.7 (V_C), MID-CRUISE

TABLE 11-38. CRITICAL LOAD CONDITIONS, STRENGTH/STIFFNESS DESIGN - TASK IIB

NASTRAN COND. NO.	WEIGHT (1000 LB)	MACH NO.	ALTITUDE (1000 FT)	LOAD FACTOR	AIRSPEED (KNOTS)	REMARKS
1						M2.7, START OF CRUISE
2						M2.7, MID-CRUISE
3						M1.25 DESCENT
TEMPERATURE CONDITIONS						
4, 5	745	0.40	0.0	2.5	264.6	STRENGTH DESIGN
6, 7	700	0.90	36.0	2.5	282.4	STRENGTH DESIGN
8, 9	700	0.90	30.0	2.5	325.0	STRENGTH DESIGN
10, 11	700	0.90	22.0	2.5	390.0	STRENGTH DESIGN
12, 13	690	1.25	48.0	2.5	294.3	STRENGTH DESIGN
14	690	1.25	48.0	-1.0	294.3	NEGATIVE FLIGHT
15, 16	690	1.25	38.2	2.5	372.0	STRENGTH DESIGN
17, 18	445	1.25	34.0	2.5	420.0	DESCENT - THERMAL
19, 20	660	2.70	61.5	2.5	460.0	START OF CRUISE
21, 22	550	2.70	64.0	1.0, 2.5	433.6	MID CRUISE
23, 24	700	0.90	30.0	-	325.0	PSUEDO - GUST (POSITIVE AND NEGATIVE)
25 - 28	430	-	0.0	-	100.0	DYNAMIC LANDING CONDITIONS

TABLE 11-39. WING PRESSURE LOADINGS, POINT DESIGN REGIONS - TASK 113

ULTIMATE PRESSURE, kPa

WING LOCATION	POINT DESIGN REGION	COND. 4 M = 0.4		COND. 8 M = 0.9		COND. 15 M = 1.25		COND. 20 M = 2.7*		COND. 22 M = 2.7**		COND. 12 M = 1.25	
		UPPER	LOWER	UPPER	LOWER	UPPER	LOWER	UPPER	LOWER	UPPER	LOWER	UPPER	LOWER
FORWARD BOX	40322	-6.27	1.65	-9.65	-2.07	-10.27	0.41	-11.51	-1.17	-9.31	-0.96	-10.14	0.41
AFT BOX	40236	-6.55	-2.00	-6.83	-3.03	-22.96	-9.03	-11.72	-5.10	-8.82	-3.72	-20.89	-8.27
	40536	-3.65	2.28	-9.31	-3.38	-7.38	-1.45	-10.14	-2.48	-8.14	-2.07	-8.76	-1.79
	41036	-6.96	6.34	-14.48	-2.48	-8.27	0.76	-8.62	2.62	-7.17	2.28	-8.76	0.76
TIP	41316	-23.93	-0.21	-46.54	-25.92	-31.02	-1.86	-11.38	6.90	-9.79	6.34	34.34	-1.79
	41348	-32.89	-0.96	-25.37	-2.07	-30.06	4.55	-8.89	7.17	-7.31	5.92	-34.96	6.62

ULTIMATE PRESSURE, psi

WING LOCATION	POINT DESIGN REGION	COND. 4 M = 0.4		COND. 8 M = 0.9		COND. 15 M = 1.25		COND. 20 M = 2.7*		COND. 22 M = 2.7**		COND. 12 M = 1.25	
		UPPER	LOWER	UPPER	LOWER	UPPER	LOWER	UPPER	LOWER	UPPER	LOWER	UPPER	LOWER
FORWARD BOX	40322	-0.91	0.24	-1.40	-0.30	-1.49	0.06	-1.67	-0.17	-1.35	-0.14	-1.47	0.06
AFT BOX	40236	-0.95	-0.29	-0.99	-0.44	-3.33	-1.31	-1.70	-0.74	-1.28	-0.54	-3.03	-1.20
	40536	-0.53	-0.33	-1.35	-0.49	-1.07	-0.21	-1.47	-0.36	-1.18	-0.30	-1.27	-0.26
	41036	-1.01	-0.92	-2.10	-0.36	-1.20	0.11	-1.25	0.38	-1.04	0.33	-1.27	0.11
TIP	41316	-3.47	-0.03	-6.75	-3.76	-4.50	-0.27	-1.65	1.00	-1.42	0.92	4.98	-0.26
	41348	-4.77	-0.14	-3.68	-0.30	-4.36	0.66	-1.29	1.04	-1.06	0.86	-5.07	0.96

NOTES:

*Start of Cruise

**Mid Cruise

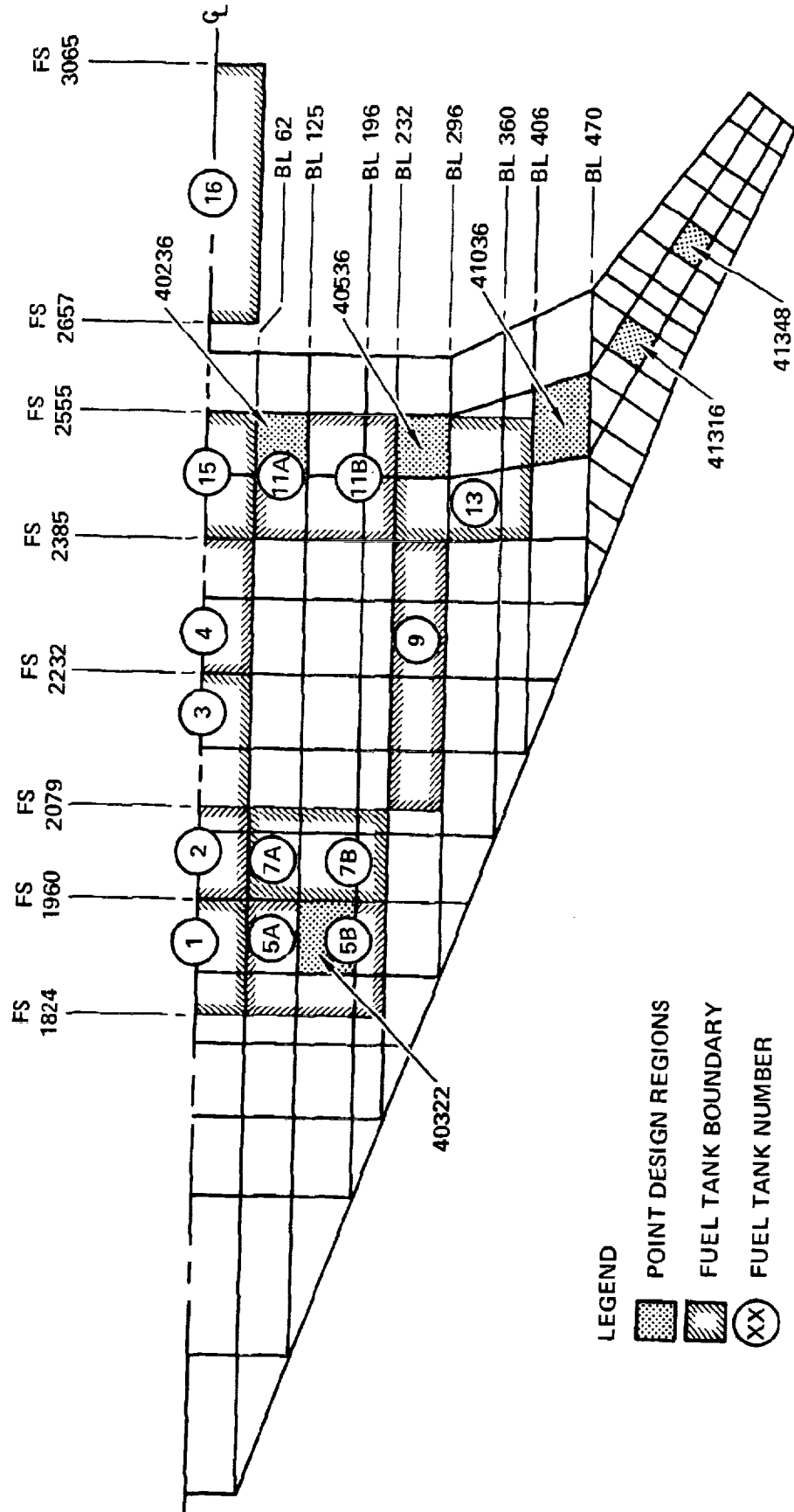


FIGURE 11-15. FUEL TANK LOCATIONS - TASK IIB

TABLE 11-40. SUMMARY OF FUEL HEIGHTS - TASK IIB

POINT DESIGN REGION	40236	40536	40322
TANK NO.	11A	13	5B
COND.	FUEL HEIGHT (IN.)		
(4)	38.5	24.5	35.5
(6)	38.5	—	35.5
(8)	38.5	—	35.5
(12)	38.5	—	35.5
(14)	38.5	—	35.5
(15)	38.5	—	35.5
(17)	—	—	—
(19)	38.5	—	35.5
(21)	—	—	12.0

TABLE 11-41. SUMMARY OF LOAD FACTORS - TASK IIB

POINT DESIGN REGION	40236		40536		40322	
	LOAD FACTORS (LIMIT)					
COND.	n_x	n_z	n_x	n_z	n_x	n_z
(4)	-0.46	2.52	-0.46	2.52	-0.46	2.50
(6)	-0.37	2.68	-0.37	2.68	-0.37	2.50
(8)	-0.27	2.62	-0.27	2.62	-0.27	2.50
(12)	-0.31	2.56	-0.31	2.56	-0.31	2.51
(15)	-0.17	2.75	-0.17	2.75	-0.17	2.51
(17)	0.02	2.75	0.02	2.75	0.02	2.51
(19)	-0.14	2.51	-0.14	2.51	-0.14	2.50
(21)	-0.14	2.50	-0.14	2.50	-0.14	2.50

1. SIGN CONVENTION

+ n_x = AFTWARD+ n_z = UPWARD

TABLE 11-42. FUEL TANK PRESSURES - TASK IIB

POINT DESIGN REGION		40236				40536				40322			
TANK NO		11A				13				5B			
PRESSURE (psi)		LIMIT p ⁽¹⁾				LIMIT p ⁽¹⁾				LIMIT p ⁽¹⁾			
COND.	SURF.	FUEL HEAD	VALVE	COMB	(1)(2) ULT. COMB p	FUEL HEAD	VALVE	COMB	(1)(2) ULT. COMB p	FUEL HEAD	VALVE	COMB	(1)(2) ULT. COMB p
④	UPPER LOWER	0.57 3.41	3.00 3.00	3.57 6.41	5.36 9.62	0.57 2.37	3.00 3.00	3.57 5.37	5.36 8.05	0.46 3.06	3.00 3.00	3.46 6.06	5.19 9.09
⑥	UPPER LOWER	0.46 3.28	3.00 3.00	3.46 6.28	5.19 9.42	— —	3.00 3.00	3.00 3.00	4.50 4.50	1.04 2.97	3.00 3.00	4.04 5.97	5.06 8.96
⑧	UPPER LOWER	0.34 3.16	3.00 3.00	3.34 6.16	5.01 9.24	— —	3.00 3.00	3.00 3.00	4.50 4.50	0.27 2.80	3.00 3.00	3.27 5.80	4.91 8.70
⑫	UPPER LOWER	0.39 3.21	3.00 3.00	3.39 6.21	5.08 9.31	— —	3.00 3.00	3.00 3.00	4.50 4.50	0.31 2.93	3.00 3.00	3.31 5.93	4.97 8.89
⑮	UPPER LOWER	0.21 3.03	3.00 3.00	3.21 6.03	4.82 9.05	— —	3.00 3.00	3.00 3.00	4.50 4.50	0.17 2.79	3.00 3.00	3.17 5.79	4.76 8.68
⑰	UPPER LOWER	0.03 0.03	3.00 3.00	3.03 3.03	4.54 4.54	— —	3.00 3.00	3.00 3.00	4.50 4.50	— —	3.00 3.00	3.00 3.00	4.50 4.50
⑳	UPPER LOWER	0.17 2.99	3.00 3.00	3.17 5.99	4.76 8.99	— —	3.00 3.00	3.00 3.00	4.50 4.50	0.14 2.74	3.00 3.00	3.14 5.74	4.71 8.61
㉔	UPPER LOWER	— —	3.00 3.00	3.00 3.00	4.50 4.50	— —	3.00 3.00	3.00 3.00	4.50 4.50	— 1.02	3.00 3.00	3.00 4.02	4.50 6.03

(1) ALL PRESSURES ARE SUCTION (-p)

(2) ULTIMATE PRESSURE = 1.5 LIMIT PRESSURE

valve pressure components as well as the combined pressures for the critical Task II conditions. In addition, the ultimate values (1.5 times limit) of the combined pressure are specified.

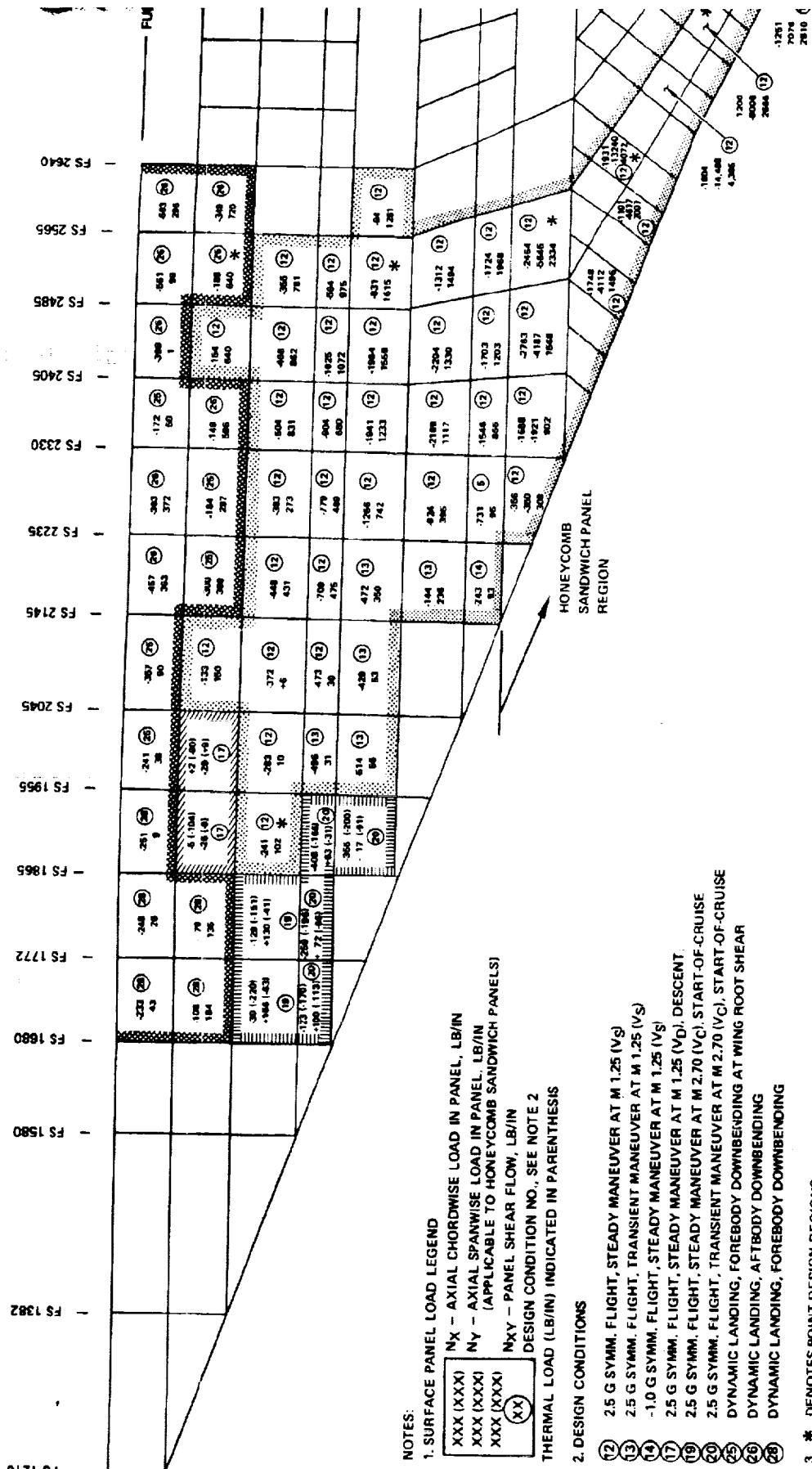
Wing Internal Loads - Task IIB

The internal loads for the Task II designs were determined using the NASTRAN redundant-structure analysis solution. Finite element models (3-D) were used with the specific flexibilities of the design being considered, i.e., strength and strength/stiffness designs. A detailed description of the Task IIB models is contained in Section 9.

Internal Loads - Airloads - Representative wing upper surface and lower surface loads are presented in Figures 11-16 and 11-17 for the Task IIB final design. These loads are displayed on the wing planform of the structural model and reflect the maximum upper surface chordwise compression and lower surface chordwise tension conditions. All inplane load intensities (N_x , N_y , and N_{xy}) presented are ultimate values with the applicable thermal induced loads indicated in parenthesis. See Section 9 for a more comprehensive listing of wing load intensities.

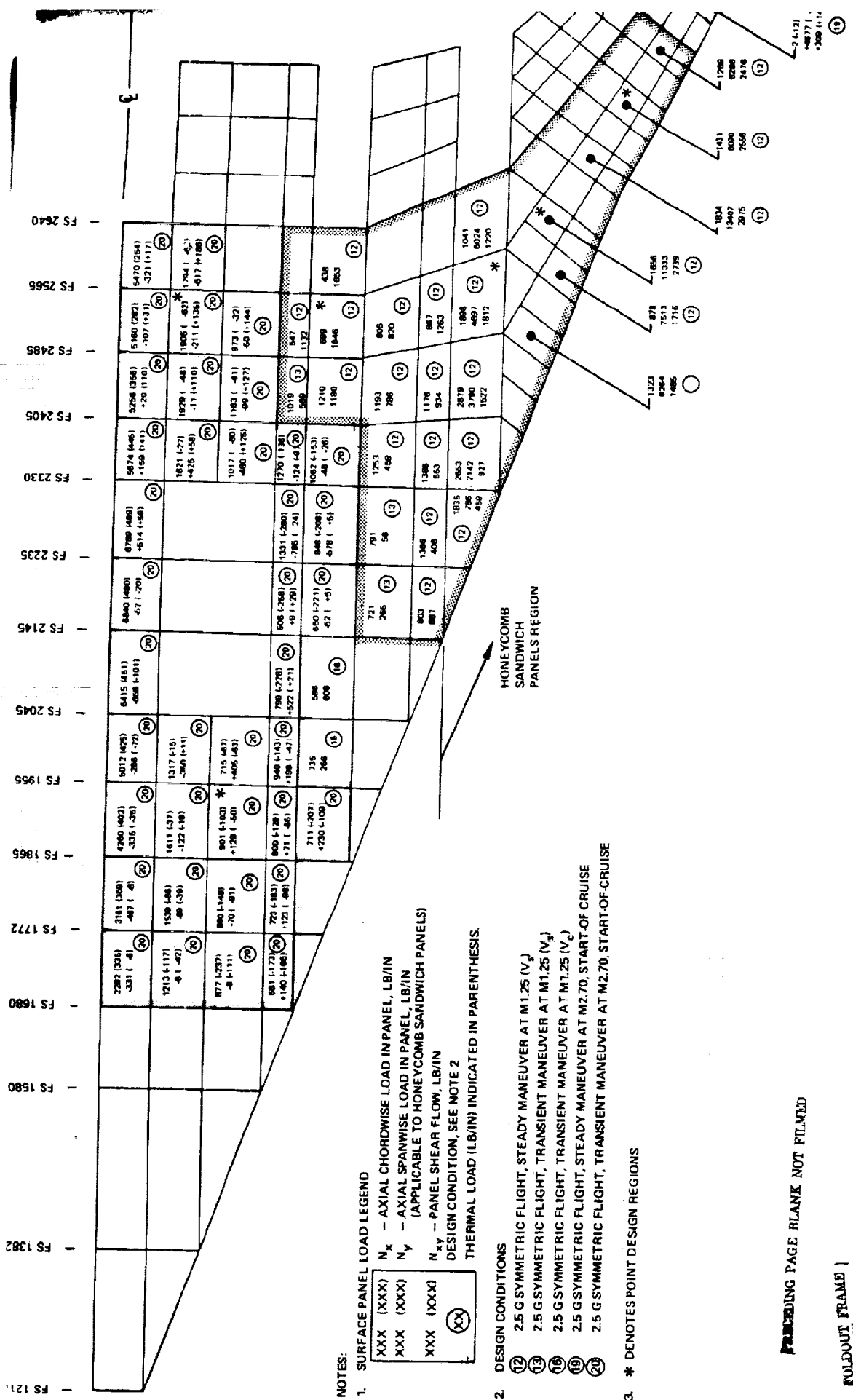
A comparison of the wing surface load intensities between the strength and final designs is shown in Table 11-43. These loads intensities correspond to a 2.5-g symmetric maneuver conditions at Mach 1.25.

Internal Loads - Thermal - The NASTRAN solution contained the thermal loads for the three critical temperature conditions: start-of-cruise, mid-cruise, and a Mach 1.25 descent condition. The corresponding upper and lower surface thermal stresses and corresponding strains for these conditions are shown in Table 11-44 and 11-45. These values are ultimate values which are used in the detail stress analysis of the structural components. In addition to stresses (strains) due to the thermal expansion of the model elements, the local temperature gradients and average temperatures are calculated and included in the point design environment. Complete temperature histories were developed for the wing structure at selective design point to furnish this data. Section 6 contains a detail description of methods used in obtaining these temperatures.



FOLDOUT FRAME /

WING BODY PANEL 2



NOTES:

1. SURFACE PANEL LOAD LEGEND

XXX (XXX)	N_x - AXIAL CHORDWISE LOAD IN PANEL, LB/IN
XXX (XXX)	N_y - AXIAL SPANWISE LOAD IN PANEL, LB/IN
XXX (XXX)	(APPLICABLE TO HONEYCOMB SANDWICH PANELS)
XXX (XXX)	N_{xy} - PANEL SHEAR FLOW, LB/IN
XXX (XXX)	DESIGN CONDITION, SEE NOTE 2
XXX (XXX)	THERMAL LOAD (LB/IN) INDICATED IN PARENTHESIS.

2. DESIGN CONDITIONS

- 12 2.5 G SYMMETRIC FLIGHT, STEADY MANEUVER AT M1.25 (V_s)
- 13 2.5 G SYMMETRIC FLIGHT, TRANSIENT MANEUVER AT M1.25 (V_s)
- 16 2.5 G SYMMETRIC FLIGHT, TRANSIENT MANEUVER AT M1.25 (V_s)
- 19 2.5 G SYMMETRIC FLIGHT, STEADY MANEUVER AT M2.70, START-OF-CRUISE
- 20 2.5 G SYMMETRIC FLIGHT, TRANSIENT MANEUVER AT M2.70, START-OF-CRUISE

3. * DENOTES POINT DESIGN REGIONS

PRECEDING PAGE BLANK NOT FILMED

FOLDOUT FRAME

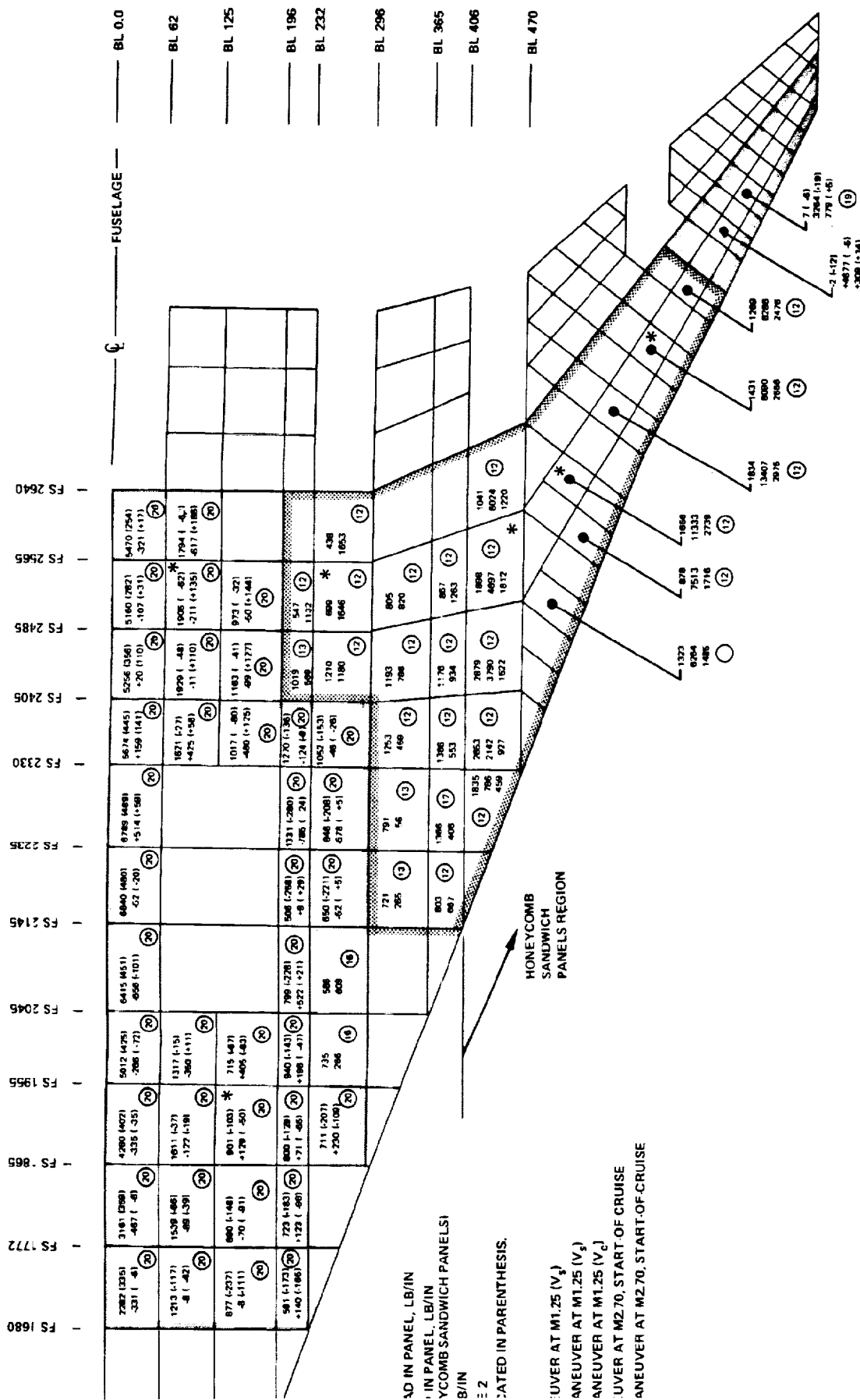


FIGURE 11-17. WING LOWER SURFACE MAXIMUM CHORDWISE TENSION LOADS, FINAL DESIGN - TASK ITR

TABLE 11-43. COMPARISON OF WING SURFACE LOAD INTENSITIES - TASK IIB,
MACH 1.25 LOAD CONDITION

PANEL IDENTIFICATION		*LOAD INTENSITY (ULTIMATE), LBS/IN.				
		DIRECTION	HYBRID (STRENGTH)		HYBRID (FINAL)	
			UPPER	LOWER	UPPER	LOWER
WING- FORWARD	40322	Nx	-151	597	-242	434
		Ny	-1106	1400	-1032	1425
		Nxy	130	215	102	166
WING- AFT BOX	40236	Nx	-67	246	-183	62
		Ny	-14650	15196	-16456	16622
		Nxy	453	367	491	781
	40536	Nx	-1073	1099	-831	699
		Ny	-14303	14014	-16372	15508
		Nxy	1495	1599	1615	1646
	41036	Nx	-1812	1297	-2464	1898
		Ny	-4220	3588	-5645	4697
		Nxy	2106	1909	1915	1812
WING TIP	41316	Nx	-1638	1405	-1931	1656
		Ny	-12407	11188	-13240	11333
		Nxy	4009	2990	4072	2739
	41348	Nx	-1207	1379	-1200	1431
		Ny	-6897	6657	-9006	8090
		Nxy	2284	2281	2666	2556

*LOAD CONDITIONS:

TASK II-B CONDITION 12: MACH 1.25, $n_z = 2.5$, $W = 690,000$ LB, $V_e = 294$ KEAS

PRECEDING PAGE BLANK NOT FILMED

TABLE 11-11. SUMMARY OF WING UPPER SURFACE THERMAL STRESSES
AND STRAINS, TASK IIB

CONDITION (19), (20) START OF CRUISE							
WING LOCATION	POINT DESIGN REGION	STRESSES (psi) ⁽¹⁾			STRAINS x 10 ⁻⁶ (IN/IN) ⁽¹⁾		
		σ_x	σ_y	τ	ϵ_x	ϵ_y	γ
FORWARD BOX	40322	-3503	2290	-1039	-220	144	-179
AFT BOX	40236	55	1292	3412	4	47	588
	40536	-802	1076	1519	-51	39	262
	41036	12058	1612	2174	793	106	375
WING TIP	41316	-2234	-3611	-1344	-150	-242	-236
	41348	-716	-1425	-648	-48	-96	-114
CONDITION (21), (22) MID-CRUISE							
FORWARD BOX	40322	-2522	7140	-438	-159	449	-75
AFT BOX	40236	1396	1322	2875	88	48	496
	40536	-348	1121	1981	-22	41	342
	41036	-2036	-5646	321	-134	-372	55
WING TIP	41316	-446	-586	-76	-30	-39	-13
	41348	-691	-1916	-822	-46	-129	-144
CONDITION (17), (18) MACH 1.25 DESCENT							
FORWARD BOX	40322	-285	-224	408	-18	-14	70
AFT BOX	40236	-1371	185	-750	-86	7	-129
	40536	156	152	-31	10	6	-5
	41036	-13044	-6715	-2499	-858	-442	-431
WING TIP	41316	1286	2811	1025	86	189	180
	41348	70	-472	-350	5	-32	-61

ULTIMATE STRESS (STRAIN) = 1.25 x LIMIT STRESS (STRAIN)

TABLE 11-45. SUMMARY OF WING LOWER SURFACE THERMAL STRESSES AND STRAINS, TASK IIB

CONDITION (19), (20) START OF CRUISE							
WING LOCATION	POINT DESIGN REGION	STRESSES (psi)			STRAINS $\times 10^{-6}$ (IN/IN)		
		σ_x	σ_y	τ	ϵ_x	ϵ_y	γ
FORWARD BOX	140322	-3151	3698	-1965	-198	232	-330
AFT BOX	140236	-1418	1035	3950	-89	36	664
	140536	-902	1615	3710	-57	56	624
	141036	13912	3800	3224	892	244	542
WING TIP	141316	-3071	-2526	-2373	-206	-170	-416
	141348	-218	39	136	-15	3	24
CONDITION (21), (22) MID-CRUISE							
FORWARD BOX	140322	-2171	10046	-2138	-136	632	-359
AFT BOX	140236	-3310	2162	6254	-208	75	1051
	140536	-115	2248	5723	-7	78	962
	141036	519	-4745	1608	33	-304	270
WING TIP	141316	-646	275	-278	-43	19	-49
	141348	162	525	289	11	35	51
CONDITION (17), (18) MACH 1.25 DESCENT							
FORWARD BOX	140322	711	-164	-249	45	-10	-42
AFT BOX	140236	-574	221	366	-36	7	62
	140536	820	540	699	52	19	112
	141036	-12949	-6946	-2336	-830	-445	-393
WING TIP	141316	2144	4682	1700	144	314	298
	141348	424	1049	182	28	70	32

ULTIMATE STRESS (STRAIN) = 1.25 x LIMIT STRESS (STRAIN)

Table 11-46 presents temperatures for the six point design regions for the following five flight conditions:

- Mach 0.90 climb
- Mach 1.25 climb
- Mach 1.25 descent
- Mach 2.7 start of cruise
- Mach 2.7 mid-cruise

Temperatures for the nominal Mach 2.7 conditions are obtained from analysis at the Mach 2.62, hot day (standard +8K) cruise profile. Subscripted temperatures in the table are defined as follows:

- T_1 upper surface panel outer skin
- T_4 upper surface panel inner skin
- T_7 lower surface panel inner skin
- T_{10} lower surface panel outer skin

Wing Point Design Environment - Task IIB

The wing point design load/temperature environment for the strength and final design airplanes were defined for their critical load conditions, see Tables 11-37 and 11-38. The definition of the wing surface environment included: inplane load intensities, inplane thermal strains, normal pressures, and the average structural temperature and gradient.

Table 11-47 through 11-51 contain the wing point design environment for the strength design airplane. The corresponding environment for the final design (strength/stiffness) airplane are presented in Tables 11-52 through 11-56.

TABLE 11-46. TEMPERATURES AND GRADIENTS FOR WING STRUCTURE - TASK IIB

POINT DESIGN REGION	UPPER SURFACE PANEL					LOWER SURFACE PANEL					WFR	UPPER CAP		LOWER CAP		FUEL		
	T ₁ (F)	T ₂ (F)	T ₃ (F)	T ₄ (F)	T ₅ (F)	T ₁ (F)	T ₂ (F)	T ₃ (F)	T ₄ (F)	T ₅ (F)		T _B (F)	T _R (F)	T _B (F)	T _R (F)	ZF (INCH)	TF (F)	
MACH 0.9 (CLIMB)																		
40322	32	69	47	+ 37		70	29	52	+ 41		70		69	37	70	55	35.30	70
40236	32	69	47	+ 37		70	29	53	+ 40		70		65	37	70	56	38.60	70
40536	33	64	45	+ 30		66	29	45	+ 36		68		66	38	70	38	0	
41036	35	62	48	+ 27		49	34	41	+ 15		68		70	55	68	50		
41316	35	62	48	+ 27		49	34	41	+ 15		68		70	70	70	70		
41348	34	54	44	+ 20		39	31	33	+ 8		67		70	70	70	70		
MACH 1.25 (CLIMB)																		
40322	61	70	63	+ 8		70	58	65	+ 11		70		66	54	70	65	35.30	70
40236	60	69	62	+ 9		70	56	64	+ 14		70		65	52	70	65	38.60	70
40536	58	57	57	- 1		56	56	56	0		63		65	51	69	49	0	
41036	56	52	54	- 3		41	50	46	- 10		62		67	60	66	55		
41316	56	52	54	- 3		41	50	46	- 10		61		65	65	65	65		
41348	57	46	52	- 11		42	51	49	- 9		59		65	65	65	65		
MACH 1.25 (DESCENT)																		
40322	86	260	163	+ 174		261	84	154	+ 177		305		307	103	314	101	0	
40236	86	240	153	+ 154		248	84	154	+ 104		292		345	110	348	106	0	
40536	88	243	148	+ 155		239	84	150	+ 155		289		338	113	342	106	0	
41036	94	214	152	+ 120		141	95	117	+ 46		286		310	150	315	130		
41316	94	214	152	+ 120		141	95	117	+ 46		276		200	200	165	165		
41348	91	162	127	+ 72		111	87	92	+ 24		261		175	175	140	140		
MACH 2.7 (START OF CRUISE)																		
40322	362	81	246	- 281		77	367	203	- 290		74		124	329	73	164	35.30	74
40236	353	83	243	- 270		76	348	185	- 272		73		81	313	72	148	38.60	73
40536	355	219	298	- 136		225	367	303	- 142		164		90	314	90	332	0	
41036	361	265	315	- 96		321	357	340	- 36		173		150	290	140	310		
41316	361	265	315	- 96		321	357	340	- 36		182		265	265	290	290		
41348	380	320	350	- 60		349	373	367	- 24		208		300	300	320	320		
MACH 2.7 (MID-CRUISE)																		
40322	356	203	281	- 154		108	357	215	- 249		155		191	344	99	173	15.47	106
40236	361	302	332	- 59		300	361	333	- 61		276		210	340	155	337	0	
40536	367	359	364	- 8		360	370	365	- 10		353		325	360	315	362	0	
41036	382	382	382	0		382	382	382	0		380		365	365	355	365		
41316	386	384	385	- 2		384	385	385	- 1		380		375	375	375	375		
41348	397	396	396	- 1		388	388	388	0		392		385	385	375	375		

ORIGINAL PAGE 11
OF FOUR QUALITY

TABLE 11-47. WING POINT DESIGN ENVIRONMENT, STRENGTH DESIGN - TASK IIB,
MACH 0.40 AND 0.90 (V_g) LOAD CONDITIONS

CONDITION 4 WEIGHT = 745,000 LB., MACH 0.40, H = SEA LEVEL, V_g = 264.8 KEAS

ULTIMATE DESIGN LOADS	ITEM	UNITS	POINT DESIGN REGION											
			40236		40536		41036		40322		41316		41348	
AIR LOADS	N_x	LB/IN	UPPER SURFACE	LOWER SURFACE	UPPER SURFACE	LOWER SURFACE	UPPER SURFACE	LOWER SURFACE	UPPER SURFACE	LOWER SURFACE	UPPER SURFACE	LOWER SURFACE	UPPER SURFACE	LOWER SURFACE
	N_y	LB/IN	-13.3	-14.1	-13.5	-14.0	-13.5	-14.0	-13.5	-14.0	-13.5	-14.0	-13.5	-14.0
	N_{xy}	LB/IN	-1.5	-1.5	-1.5	-1.5	-1.5	-1.5	-1.5	-1.5	-1.5	-1.5	-1.5	-1.5
THERMAL STRAIN	ϵ_x	IN/IN	0	0	0	0	0	0	0	0	0	0	0	0
	ϵ_y	IN/IN	0	0	0	0	0	0	0	0	0	0	0	0
	ϵ_{xy}	IN/IN	0	0	0	0	0	0	0	0	0	0	0	0
PRESSURE	AERO	PSI	-0.95	-0.95	-0.95	-0.95	-0.95	-0.95	-0.95	-0.95	-0.95	-0.95	-0.95	-0.95
	FUEL	PSI	5.3	5.3	5.3	5.3	5.3	5.3	5.3	5.3	5.3	5.3	5.3	5.3
	NET	PSI	5.3	5.3	5.3	5.3	5.3	5.3	5.3	5.3	5.3	5.3	5.3	5.3
TEMPERATURE	TAV	°F	0	0	0	0	0	0	0	0	0	0	0	0
	ΔT	°F	0	0	0	0	0	0	0	0	0	0	0	0

CONDITION 6 WEIGHT = 700,000 LB. MACH 0.90, H = 30,000 FT, V_g = 282 KEAS

ULTIMATE DESIGN LOADS	ITEM	UNITS	POINT DESIGN REGION											
			40236		40536		41036		40322		41316		41348	
AIR LOADS	N_x	LB/IN	34	34	34	34	34	34	34	34	34	34	34	34
	N_y	LB/IN	-13.3	-14.1	-13.5	-14.0	-13.5	-14.0	-13.5	-14.0	-13.5	-14.0	-13.5	-14.0
	N_{xy}	LB/IN	33	33	33	33	33	33	33	33	33	33	33	33
THERMAL STRAIN	ϵ_x	IN/IN	0	0	0	0	0	0	0	0	0	0	0	0
	ϵ_y	IN/IN	0	0	0	0	0	0	0	0	0	0	0	0
	ϵ_{xy}	IN/IN	0	0	0	0	0	0	0	0	0	0	0	0
PRESSURE	AERO	PSI	-0.95	-0.95	-0.95	-0.95	-0.95	-0.95	-0.95	-0.95	-0.95	-0.95	-0.95	-0.95
	FUEL	PSI	5.3	5.3	5.3	5.3	5.3	5.3	5.3	5.3	5.3	5.3	5.3	5.3
	NET	PSI	5.3	5.3	5.3	5.3	5.3	5.3	5.3	5.3	5.3	5.3	5.3	5.3
TEMPERATURE	TAV	°F	0	0	0	0	0	0	0	0	0	0	0	0
	ΔT	°F	0	0	0	0	0	0	0	0	0	0	0	0

NOTES 1) A 1.25 FACTOR HAS BEEN APPLIED TO THE THERMAL STRAIN WHEN THE SIGN IS SAME AS THE AIRLOAD

SIGN, OTHERWISE NO FACTOR APPLIED.

2) PRESSURE SIGN CONVENTION: NEGATIVE = SUCTION

TABLE 11-18. WING POINT DESIGN ENVIRONMENT, STRENGTH DESIGN - TASK IIB,
MACH 0.90 (V_0) AND 1.25 (V_0) LOAD CONDITIONS

CONDITION 8 WEIGHT = 700,000 LB., MACH 0.90, h = 30,000 FT., $V_0 = 325$ kts

ULTIMATE DESIGN LOADS	ITEM	UNITS	POINT DESIGN REGION											
			40236			40536			41036			40322		
			UPPER SURFACE	LOWER SURFACE		UPPER SURFACE	LOWER SURFACE		UPPER SURFACE	LOWER SURFACE		UPPER SURFACE	LOWER SURFACE	
AIR LOADS	Nx	LB/IN	-179	-50		-455	-1,359		-21,859	-1,100		-2,100	-1,004	
	Ny	LB/IN	-12,779	-13,557		-12,000	-11,771		-3,529	-3,074		-1,119	-1,350	
	Nz	LB/IN	-571	-30		-1,183	-1,156		-1,583	-1,550		-111	-933	
THERMAL STRAIN	Ex	IN/IN				0	0		0	0		0	0	
	Ey	IN/IN				0	0		0	0		0	0	
	Exy	IN/IN				0	0		0	0		0	0	
PRESSURE	AERO	PSI	-0.94	-0.44		-1.39	-1.00		-1.10	-0.30		-1.00	-0.30	
	FUEL	PSI	-3.01	-0.24		-4.50	-4.50		0	0		-4.91	-4.90	
	NET	PSI	-3.95	-0.68		-5.89	-5.50		-2.12	-0.30		-5.91	-5.20	
TEMPERATURE	TAV	°F	57	53		59	55		14	11		58	41	
	ΔT	°F	+37	+40		+30	+30		+0	+1		+30	+20	

CONDITION 17 WEIGHT = 680,000 LB., MACH 1.25, h = 40,000 FT., $V_0 = 294$ kts

ULTIMATE DESIGN LOADS	ITEM	UNITS	POINT DESIGN REGION											
			40236			40536			41036			40322		
			UPPER SURFACE	LOWER SURFACE		UPPER SURFACE	LOWER SURFACE		UPPER SURFACE	LOWER SURFACE		UPPER SURFACE	LOWER SURFACE	
AIR LOADS	Nx	LB/IN	-67	-20		-1,100	-4,100		-1,100	-1,100		-1,100	-1,100	
	Ny	LB/IN	-14,750	-15,170		-15,330	-15,100		-4,000	-4,000		-1,100	-1,100	
	Nz	LB/IN	-453	-30		-1,400	-1,300		-2,100	-1,100		-1,100	-1,100	
THERMAL STRAIN	Ex	IN/IN				0	0		0	0		0	0	
	Ey	IN/IN				0	0		0	0		0	0	
	Exy	IN/IN				0	0		0	0		0	0	
PRESSURE	AERO	PSI	-3.03	-3.00		-1.00	-1.00		-1.00	-1.00		-1.00	-1.00	
	FUEL	PSI	-5.00	-0.31		-4.50	-4.50		-4.50	-4.50		-4.50	-4.50	
	NET	PSI	-4.11	-0.61		-5.50	-5.50		-5.50	-5.50		-5.50	-5.50	
TEMPERATURE	TAV	°F												
	ΔT	°F												

NOTES: (1) A 1.25 FACTOR HAS BEEN APPLIED TO THE THERMAL STRAIN WHEN THE SIGN IS SAME AS THE AIRLOAD
SIGN OTHERWISE NO FACTOR APPLIED
(2) PRESSURE SIGN CONVENTION: NEGATIVE = SUCTION

TABLE 11-49. WING POINT DESIGN ENVIRONMENT, STRENGTH DESIGN - TASK IIB, MACH 1.25 (V_0),
 $n_z = -1.0-g$ AND MACH 1.25 (V_0) LOAD CONDITIONS

CONDITION (14) WEIGHT - 690,000 LB., MACH 1.25, $h = 48,800$ FT., $V_0 = 294$ KNOTS

ULTIMATE DESIGN LOADS	ITEM	UNITS	POINT DESIGN REGION											
			40236		40536		41036		40322		41316		41348	
			UPPER SURFACE	LOWER SURFACE	UPPER SURFACE	LOWER SURFACE	UPPER SURFACE	LOWER SURFACE	UPPER SURFACE	LOWER SURFACE	UPPER SURFACE	LOWER SURFACE	UPPER SURFACE	LOWER SURFACE
AIR LOADS	N_x	LB/IN	4.5	1.145	-1.36	-1.5	-1.5	-1.5	3	3	-1.5	-1.5	-1.5	-1.5
	N_y	LB/IN	-1.1	-0.3	-0.5	-0.5	-1.3	-1.3	41	41	-1.0	-1.0	-3.70	-3.55
	N_{xy}	LB/IN	1.2	1.1	-1.1	-1.05	-1.3	-1.3	3	3	-1.34	-1.31	-2.29	-2.29
THERMAL STRAIN	ϵ_x	IN/IN												
	ϵ_y	IN/IN												
	ϵ_{xy}	IN/IN												
PRESSURE	AERO	PSI	1.02	1.0	1.0	1.0	1.0	1.0	1.0	1.0	1.0	1.0	1.0	1.0
	FUEL	PSI												
	NET	PSI	1.0	1.0	1.0	1.0	1.0	1.0	1.0	1.0	1.0	1.0	1.0	1.0
TEMPERATURE	T_{AV}	$^{\circ}F$												
	ΔT	$^{\circ}F$												

CONDITION (15) WEIGHT - 690,000 LB., MACH 1.25, $h = 38,200$ FT., $V_0 = 372$ KNOTS

ULTIMATE DESIGN LOADS	ITEM	UNITS	POINT DESIGN REGION											
			40236		40536		41036		40322		41316		41348	
			UPPER SURFACE	LOWER SURFACE	UPPER SURFACE	LOWER SURFACE	UPPER SURFACE	LOWER SURFACE	UPPER SURFACE	LOWER SURFACE	UPPER SURFACE	LOWER SURFACE	UPPER SURFACE	LOWER SURFACE
AIR LOADS	N_x	LB/IN	3	1.1	-1.4	-1.3	-1.4	-1.4	5	5	-1.36	-1.3	-1.3	-1.3
	N_y	LB/IN	-1.1	-0.3	-0.5	-0.5	-1.3	-1.3	-1.1	-1.1	-1.41	-1.4	-5.30	-5.15
	N_{xy}	LB/IN	1.2	1.1	-1.1	-1.05	-1.3	-1.3	1.1	1.1	3.3	3.3	4.11	4.1
THERMAL STRAIN	ϵ_x	IN/IN												
	ϵ_y	IN/IN												
	ϵ_{xy}	IN/IN												
PRESSURE	AERO	PSI	3.22	1.0	1.0	1.0	1.0	1.0	1.0	1.0	1.0	1.0	1.0	1.0
	FUEL	PSI												
	NET	PSI	1.0	1.0	1.0	1.0	1.0	1.0	1.0	1.0	1.0	1.0	1.0	1.0
TEMPERATURE	T_{AV}	$^{\circ}F$												
	ΔT	$^{\circ}F$												

NOTES (1) A 1.25 FACTOR HAS BEEN APPLIED TO THE THERMAL STRAIN WHEN THE SIGN IS SAME AS THE AIRLOAD SIGN, OTHERWISE NO FACTOR APPLIED
 (2) PRESSURE SIGN CONVENTION: NEGATIVE = SUCTION

TABLE 11-50. WING POINT DESIGN ENVIRONMENT, STRENGTH DESIGN - TASK IIB, MACH 1.25 (V_D)
DESCENT AND MACH 2.7 (START-OF-CRUISE) LOAD CONDITIONS

CONDITION (17) WEIGHT = 445,000 LB, MACH 1.25, h = 34,000 FT., V = 420 kts

ULTIMATE DESIGN LOADS	ITEM	UNITS	POINT DESIGN REGION											
			40236			40536			41036			40322		
			UPPER SURFACE	LOWER SURFACE		UPPER SURFACE	LOWER SURFACE		UPPER SURFACE	LOWER SURFACE		UPPER SURFACE	LOWER SURFACE	
AIR LOADS	N _x	LB/IN	- 44	- 34.5		- 1.1	- 51.3		- 1.73	- 17.4		- 34	- 1.4	
	N _y	LB/IN	- 1,008	- 1,512		- 1,177	- 1,119		- 1,119	- 1,119		- 1,119	- 1,119	
	N _z	LB/IN	- 559	- 94		- 59	- 40.5		- 37.4	- 59.7		- 34	- 1.4	
THERMAL STRAIN	C _x X 10 ⁶	IN/IN	- 7.1	- 64.5		- 12.2	- 43.3		- 71.4	- 49.7		- 11.5	- 14.7	
	C _y X 10 ⁶	IN/IN	- 1.1	- 5.7		- 1.3	- 7.0		- 531.3	- 421.3		- 1.1	- 5.5	
	C _z X 10 ⁶	IN/IN	- 103.1	- 55.1		- 1.1	- 113.0		- 10.1	- 38.4		- 10.1	- 17.1	
PRESSURE	AERO	PSI	- 1.29	- 4.9		- 1.5	- 1.1		- 1.5	- 1.5		- 1.5	- 1.5	
	FUEL	PSI	- 4.54	- 5.26		- 4.6	- 4.6		- 4.6	- 4.6		- 4.6	- 4.6	
	NET	PSI	- 3.25	- 0.36		- 3.1	- 5.7		- 3.1	- 6.1		- 3.1	- 6.1	
TEMPERATURE	T _{AV}	°F	131	184		145	176		111	136		117	127	
	ΔT	°F	- 2.3	- 1.4		- 1.5	- 1.5		- 1.5	- 1.5		- 1.5	- 1.5	

CONDITION (18) WEIGHT = 660,000 LB, MACH 2.7, START OF CRUISE, h = 61,500 FT., V = 460 kts

ULTIMATE DESIGN LOADS	ITEM	UNITS	POINT DESIGN REGION											
			40236			40536			41036			40322		
			UPPER SURFACE	LOWER SURFACE		UPPER SURFACE	LOWER SURFACE		UPPER SURFACE	LOWER SURFACE		UPPER SURFACE	LOWER SURFACE	
AIR LOADS	N _x	LB/IN	- 131	- 13,077		- 1	- 3.7		- 1.1	- 3.7		- 1	- 1.1	
	N _y	LB/IN	- 1,736	- 1,736		- 1,736	- 1,736		- 1,736	- 1,736		- 1,736	- 1,736	
	N _z	LB/IN	- 291	- 553		- 14	- 3.3		- 56	- 3		- 1.4	- 1.3	
THERMAL STRAIN	C _x X 10 ⁶	IN/IN	- 3.29	- 34.5		- 57.4	- 37.3		- 11.4	- 11.4		- 11.4	- 11.4	
	C _y X 10 ⁶	IN/IN	- 1.1	- 5.7		- 1.3	- 7.0		- 1.3	- 1.3		- 1.3	- 1.3	
	C _z X 10 ⁶	IN/IN	- 103.1	- 55.1		- 1.1	- 113.0		- 10.1	- 38.4		- 10.1	- 17.1	
PRESSURE	AERO	PSI	- 1.29	- 4.9		- 1.5	- 1.1		- 1.5	- 1.5		- 1.5	- 1.5	
	FUEL	PSI	- 4.54	- 5.26		- 4.6	- 4.6		- 4.6	- 4.6		- 4.6	- 4.6	
	NET	PSI	- 3.25	- 0.36		- 3.1	- 5.7		- 3.1	- 6.1		- 3.1	- 6.1	
TEMPERATURE	T _{AV}	°F	131	184		145	176		111	136		117	127	
	ΔT	°F	- 2.3	- 1.4		- 1.5	- 1.5		- 1.5	- 1.5		- 1.5	- 1.5	

NOTES (1) A 1.25 FACTOR HAS BEEN APPLIED TO THE THERMAL STRAIN WHEN THE SIGN IS SAME AS THE AIRLOAD
SIGN OTHERWISE NO FACTOR APPLIED
(2) PRESSURE SIGN CONVENTION: NEGATIVE = SUCTION

ORIGINAL PAGE IS
OF POOR QUALITY

TABLE 11-51. WING POINT DESIGN ENVIRONMENT, STRENGTH DESIGN - TASK IIB,
MACH 2.7 (MID-CRUISE) LOAD CONDITION

CONDITION (2) WEIGHT = 550,000 LB. MACH 2.7 (MID-CRUISE). h = 84,000 FT. $V_p = 434$ KNOTS. $\sigma_p = 1.0$

ULTIMATE DESIGN LOADS	ITEM	UNITS	POINT DESIGN REGION											
			40236		40536		41036		40322		41316		41348	
			UPPER SURFACE	LOWER SURFACE	UPPER SURFACE	LOWER SURFACE	UPPER SURFACE	LOWER SURFACE	UPPER SURFACE	LOWER SURFACE	UPPER SURFACE	LOWER SURFACE	UPPER SURFACE	LOWER SURFACE
AIR LOADS	Nx	LB/IN	-1.036	-1.036	-1.036	-1.036	-1.036	-1.036	-1.036	-1.036	-1.036	-1.036	-1.036	-1.036
	Ny	LB/IN	-1.036	-1.036	-1.036	-1.036	-1.036	-1.036	-1.036	-1.036	-1.036	-1.036	-1.036	-1.036
	Nz	LB/IN	-1.036	-1.036	-1.036	-1.036	-1.036	-1.036	-1.036	-1.036	-1.036	-1.036	-1.036	-1.036
THERMAL STRAIN	EXX X 10 ⁻⁶	IN/IN	-1.440	-1.440	-1.440	-1.440	-1.440	-1.440	-1.440	-1.440	-1.440	-1.440	-1.440	-1.440
	EYX X 10 ⁻⁶	IN/IN	-1.440	-1.440	-1.440	-1.440	-1.440	-1.440	-1.440	-1.440	-1.440	-1.440	-1.440	-1.440
	EXY X 10 ⁻⁶	IN/IN	-1.440	-1.440	-1.440	-1.440	-1.440	-1.440	-1.440	-1.440	-1.440	-1.440	-1.440	-1.440
PRESSURE	AERO	PSI	-1.20	-1.20	-1.20	-1.20	-1.20	-1.20	-1.20	-1.20	-1.20	-1.20	-1.20	-1.20
	FUEL	PSI	-1.20	-1.20	-1.20	-1.20	-1.20	-1.20	-1.20	-1.20	-1.20	-1.20	-1.20	-1.20
	NFT	PSI	-1.20	-1.20	-1.20	-1.20	-1.20	-1.20	-1.20	-1.20	-1.20	-1.20	-1.20	-1.20
TEMPERATURE	TAV	°F	334	334	334	334	334	334	334	334	334	334	334	334
	DT	°F	-50	-50	-50	-50	-50	-50	-50	-50	-50	-50	-50	-50

ORIGINAL PAGE IS
OF POOR QUALITY

TABLE 11-52. WING POINT DESIGN ENVIRONMENT, FINAL DESIGN - TASK IIB,
MACH 0.40 AND 0.90 (V_8) LOAD CONDITIONS

CONDITION 4 SYMMETRICAL FLIGHT, STEADY MANEUVER AT MACH 0.40 (V_8), $n_z = 2.5$

ULTIMATE DESIGN LOADS	ITEM	UNITS	POINT DESIGN REGION											
			40322			41316			41348			40236		
			UPPER SURFACE	LOWER SURFACE	UPPER SURFACE	UPPER SURFACE	LOWER SURFACE	UPPER SURFACE	UPPER SURFACE	LOWER SURFACE	UPPER SURFACE	UPPER SURFACE	LOWER SURFACE	UPPER SURFACE
AIR LOADS	N_x	LB/IN	-1.99	-4.76	-1.35	-1.11	-1.11	-3.71	-1.11	-1.11	-5.94	-5.94	-3.15	-1.35
	N_y	LB/IN	-1.100	-1.405	-1.105	-1.11	-1.11	-1.10	-1.11	-1.11	-1.10	-1.10	-1.10	-1.10
	N_{xy}	LB/IN	2.04	-4.5	-3.42	-3.42	-3.42	-3.42	-3.42	-3.42	-3.42	-3.42	-3.42	-3.42
THERMAL STRAIN	ϵ_x	IN/IN	0	0	0	0	0	0	0	0	0	0	0	0
	ϵ_y	IN/IN	0	0	0	0	0	0	0	0	0	0	0	0
	ϵ_{xy}	IN/IN	0	0	0	0	0	0	0	0	0	0	0	0
PRESSURE	AERO	PSI	-2.21	-3.4	-3.4	-3.4	-3.4	-3.4	-3.4	-3.4	-3.4	-3.4	-3.4	-3.4
	FUEL	PSI	-5.19	-9.09	-9.09	-9.09	-9.09	-9.09	-9.09	-9.09	-9.09	-9.09	-9.09	-9.09
	NFT	PSI	-6.10	-9.95	-9.95	-9.95	-9.95	-9.95	-9.95	-9.95	-9.95	-9.95	-9.95	-9.95
TEMPERATURE	TAV	°F	37	37	37	37	37	37	37	37	37	37	37	37
	ΔT	°F	0	0	0	0	0	0	0	0	0	0	0	0

CONDITION 6 SYMMETRICAL FLIGHT, STEADY MANEUVER AT MACH 0.90 (V_8), $n_z = 2.5$

ULTIMATE DESIGN LOADS	ITEM	UNITS	POINT DESIGN REGION											
			40322			41316			41348			40236		
			UPPER SURFACE	LOWER SURFACE	UPPER SURFACE	UPPER SURFACE	LOWER SURFACE	UPPER SURFACE	UPPER SURFACE	LOWER SURFACE	UPPER SURFACE	UPPER SURFACE	LOWER SURFACE	UPPER SURFACE
AIR LOADS	N_x	LB/IN	-1.99	-4.76	-1.35	-1.11	-1.11	-3.71	-1.11	-1.11	-5.94	-5.94	-3.15	-1.35
	N_y	LB/IN	-1.100	-1.405	-1.105	-1.11	-1.11	-1.10	-1.11	-1.11	-1.10	-1.10	-1.10	-1.10
	N_{xy}	LB/IN	2.04	-4.5	-3.42	-3.42	-3.42	-3.42	-3.42	-3.42	-3.42	-3.42	-3.42	-3.42
THERMAL STRAIN	ϵ_x	IN/IN	0	0	0	0	0	0	0	0	0	0	0	0
	ϵ_y	IN/IN	0	0	0	0	0	0	0	0	0	0	0	0
	ϵ_{xy}	IN/IN	0	0	0	0	0	0	0	0	0	0	0	0
PRESSURE	AERO	PSI	-2.21	-3.4	-3.4	-3.4	-3.4	-3.4	-3.4	-3.4	-3.4	-3.4	-3.4	-3.4
	FUEL	PSI	-5.19	-9.09	-9.09	-9.09	-9.09	-9.09	-9.09	-9.09	-9.09	-9.09	-9.09	-9.09
	NET	PSI	-6.10	-9.95	-9.95	-9.95	-9.95	-9.95	-9.95	-9.95	-9.95	-9.95	-9.95	-9.95
TEMPERATURE	TAV	°F	37	37	37	37	37	37	37	37	37	37	37	37
	ΔT	°F	0	0	0	0	0	0	0	0	0	0	0	0

NOTES (1) A 1.25 FACTOR HAS BEEN APPLIED TO THE THERMAL STRAIN WHEN THE SIGN IS SAME AS THE AIRLOAD
SIGN, OTHERWISE NO FACTOR APPLIED.

(2) PRESSURE SIGN CONVENTION - NEGATIVE - SUCTION

ORIGINAL PAGE IS
OF POOR QUALITY

TABLE 11-53. WING POINT DESIGN ENVIRONMENT, FINAL DESIGN - TASK IID,
MACH 0.90 (V_0) AND 1.25 (V_0) LOAD CONDITIONS

CONDITION 8 SYMMETRICAL FLIGHT, STEADY MANEUVER AT MACH 0.90 (V_0), $n_z = 2.5$

ULTIMATE DESIGN LOADS	ITEM	UNITS	POINT DESIGN REGION											
			40322			41316			41348			40236		
			UPPER SURFACE	LOWER SURFACE		UPPER SURFACE	LOWER SURFACE		UPPER SURFACE	LOWER SURFACE		UPPER SURFACE	LOWER SURFACE	
AIR LOADS	N_x	LB/IN	-1.0	1.0		-1.0	1.0		-1.0	1.0		-1.0	1.0	
	N_y	LB/IN	-1.042	1.042		-1.042	1.042		-1.042	1.042		-1.042	1.042	
	N_{xy}	LB/IN	0.5	1.0		0.5	1.0		0.5	1.0		0.5	1.0	
THERMAL STRAIN	ϵ_x	IN/IN	0	0		0	0		0	0		0	0	
	ϵ_y	IN/IN	0	0		0	0		0	0		0	0	
	ϵ_{xy}	IN/IN	0	0		0	0		0	0		0	0	
PRESSURE	AERO	PSI	-1.14	1.30		-1.14	1.30		-1.14	1.30		-1.14	1.30	
	FUEL	PSI	-2.01	2.01		-2.01	2.01		-2.01	2.01		-2.01	2.01	
	NET	PSI	-1.31	0.00		-1.31	0.00		-1.31	0.00		-1.31	0.00	
TEMPERATURE	T_{AV}	$^{\circ}F$	37	25		37	25		37	25		37	25	
	ΔT	$^{\circ}F$	3	41		3	41		3	41		3	41	

CONDITION 12 SYMMETRICAL FLIGHT, STEADY MANEUVER AT MACH 1.25 (V_0), $n_z = 2.5$

ULTIMATE DESIGN LOADS	ITEM	UNITS	POINT DESIGN REGION											
			40322			41316			41348			40236		
			UPPER SURFACE	LOWER SURFACE		UPPER SURFACE	LOWER SURFACE		UPPER SURFACE	LOWER SURFACE		UPPER SURFACE	LOWER SURFACE	
AIR LOADS	N_x	LB/IN	-1.0	1.0		-1.0	1.0		-1.0	1.0		-1.0	1.0	
	N_y	LB/IN	-1.042	1.042		-1.042	1.042		-1.042	1.042		-1.042	1.042	
	N_{xy}	LB/IN	0.5	1.0		0.5	1.0		0.5	1.0		0.5	1.0	
THERMAL STRAIN	ϵ_x	IN/IN	0	0		0	0		0	0		0	0	
	ϵ_y	IN/IN	0	0		0	0		0	0		0	0	
	ϵ_{xy}	IN/IN	0	0		0	0		0	0		0	0	
PRESSURE	AERO	PSI	-1.14	1.30		-1.14	1.30		-1.14	1.30		-1.14	1.30	
	FUEL	PSI	-2.01	2.01		-2.01	2.01		-2.01	2.01		-2.01	2.01	
	NET	PSI	-1.31	0.00		-1.31	0.00		-1.31	0.00		-1.31	0.00	
TEMPERATURE	T_{AV}	$^{\circ}F$	37	25		37	25		37	25		37	25	
	ΔT	$^{\circ}F$	3	41		3	41		3	41		3	41	

NOTES (1) A 1.25 FACTOR HAS BEEN APPLIED TO THE THERMAL STRAIN WHEN THE SIGN IS SAME AS THE AIRLOAD

SIGN OTHERWISE NO FACTOR APPLIED

(2) PRESSURE SIGN CONVENTION: NEGATIVE = SUCTION

TABLE 11-54. WING POINT DESIGN ENVIRONMENT, FINAL DESIGN - TASK IIB, MACH 1.25 (V_g),
 $n_z = -1.0-g$ AND MACH 1.25 (V_g) LOAD CONDITIONS

CONDITION 14 SYMMETRICAL FLIGHT, STEADY MANEUVER AT MACH 1.25 IV, $n_z = 1.0$

ULTIMATE DESIGN LOADS	ITEM	UNITS	POINT DESIGN REGION											
			40322		41316		41348		40236		40536		41036	
AIR LOADS	N_x	LB/IN	UPPER SURFACE	LOWER SURFACE	UPPER SURFACE	LOWER SURFACE	UPPER SURFACE	LOWER SURFACE	UPPER SURFACE	LOWER SURFACE	UPPER SURFACE	LOWER SURFACE	UPPER SURFACE	LOWER SURFACE
	N_y	LB/IN	4.03	-0.06	5.52	-0.33	3.45	-3.94	1.79	-1.13	1.40	-1.13	1.40	-1.13
	N_{xy}	LB/IN	4.7	0.2	1.79	1.37	1.29	-1.13	4.25	3.4	4.0	3.91	4.47	3.95
THERMAL STRAIN	ϵ_x	IN/IN	0	0	0	0	0	0	0	0	0	0	0	0
	ϵ_y	IN/IN	0	0	0	0	0	0	0	0	0	0	0	0
	ϵ_{xy}	IN/IN	0	0	0	0	0	0	0	0	0	0	0	0
PRESSURE	AERO	PSI	0.59	-0.74	0.7	0.23	0.46	-0.35	1.23	0.87	0.51	-0.15	0.51	-0.04
	FUEL	PSI	0	0	0	0	0	0	0	0	0	0	0	0
	NET	PSI	0.59	-0.74	0.7	0.23	0.46	-0.35	1.23	0.87	0.51	-0.15	0.51	-0.04
TEMPERATURE	T_{AV}	$^{\circ}F$	5	-1.4	0.0	0.0	4.2	3.3	1.21	0.40	0.51	-0.13	0.51	-0.11
	ΔT	$^{\circ}F$	0	0	0	0	0	0	0	0	0	0	0	0

CONDITION 15 SYMMETRICAL FLIGHT, STEADY MANEUVER AT MACH 1.25 IV, $n_z = 2.5$

ULTIMATE DESIGN LOADS	ITEM	UNITS	POINT DESIGN REGION											
			40322		41316		41348		40236		40536		41036	
AIR LOADS	N_x	LB/IN	UPPER SURFACE	LOWER SURFACE	UPPER SURFACE	LOWER SURFACE	UPPER SURFACE	LOWER SURFACE	UPPER SURFACE	LOWER SURFACE	UPPER SURFACE	LOWER SURFACE	UPPER SURFACE	LOWER SURFACE
	N_y	LB/IN	11.79	0.0	11.19	0.02	7.02	-7.14	1.74	-1.37	1.40	-1.37	1.40	-1.37
	N_{xy}	LB/IN	10.5	1.1	3.52	0.53	0.15	-0.22	3.9	3.0	4.47	3.91	4.47	3.95
THERMAL STRAIN	ϵ_x	IN/IN	0	0	0	0	0	0	0	0	0	0	0	0
	ϵ_y	IN/IN	0	0	0	0	0	0	0	0	0	0	0	0
	ϵ_{xy}	IN/IN	0	0	0	0	0	0	0	0	0	0	0	0
PRESSURE	AERO	PSI	1.13	0.0	0.0	0.0	0.0	0.0	3.23	1.31	1.07	0.0	1.07	0.0
	FUEL	PSI	0	0	0	0	0	0	0	0	0	0	0	0
	NET	PSI	1.13	0.0	0.0	0.0	0.0	0.0	3.23	1.31	1.07	0.0	1.07	0.0
TEMPERATURE	T_{AV}	$^{\circ}F$	1.25	-1.4	0.0	0.0	0.0	0.0	1.13	0.0	0.0	0.0	0.0	0.0
	ΔT	$^{\circ}F$	0	0	0	0	0	0	0	0	0	0	0	0

NOTES: (1) A 1.25 FACTOR HAS BEEN APPLIED TO THE THERMAL STRAIN WHEN THE SIGN IS SAME AS THE AIRLOAD SIGN, OTHERWISE NO FACTOR APPLIED.
 (2) PRESSURE SIGN CONVENTION: NEGATIVE = SUCTION

ORIGINAL PAGE 13
 OF POOR QUALITY

TABLE 11-55. WING POINT DESIGN ENVIRONMENT, FINAL DESIGN - TASK IIB, MACH 1.25 (V_D) DESCENT AND MACH 2.7 START-OF-CRUISE LOAD CONDITIONS

CONDITION (17) SYMMETRICAL FLIGHT, STEADY MANEUVER AT MACH 1.25 (V_D), DESCENT, $n_y = 2.5$

ULTIMATE DESIGN LOADS	ITEM	UNITS	POINT DESIGN REGION											
			40322			41316			41348			40236		
AIR LOADS	N _x	LB/IN	UPPER SURFACE	LOWER SURFACE	UNITS	UPPER SURFACE	LOWER SURFACE	UNITS	UPPER SURFACE	LOWER SURFACE	UNITS	UPPER SURFACE	LOWER SURFACE	UNITS
			-35	-154		-935	-475		-564	-4,321		-779	-53	
THERMAL STRAIN	N _y	LB/IN	-659	-491		-4,354	-4,354		-4,787	-4,321		-7,739	-4,321	
			-46	-7		-5,093	-4,354		-11,188	-1,114		-395	-575	
PRESSURE	N _z	IN/IN	-17.9	-35.8		-69.1	-243.9		-3.3	-134.5		-9.9	-41.3	
			-14.1	-5.2		-15.9	-314.6		-31.4	-70.1		-4.1	-1.1	
TEMPERATURE	CY X 10 ⁻⁶	IN/IN	-56.6	-33.4		-146.7	-37		-25.1	-25.6		-62.5	-115.1	
			-0.97	-0.86		-3.71	-0.13		-2.55	-1.3		-0.01	-0.1	
PRESSURE	FUEL	PSI	-4.50	-4.50		-4.50	-4.50		-4.50	-4.50		-4.50	-4.50	
			-5.47	-4.40		-4.40	-4.40		-4.40	-4.40		-4.40	-4.40	
TEMPERATURE	NET	°F	163	159		152	147		107	96		154	150	
			-174	-177		-120	-121		-7	-4		-255	-155	

CONDITION (20) SYMMETRICAL FLIGHT, TRANSIENT MANEUVER AT MACH 2.7 (V_D), START OF CRUISE, $n_y = 2.5$

ULTIMATE DESIGN LOADS	ITEM	UNITS	POINT DESIGN REGION											
			40322			41316			41348			40236		
AIR LOADS	N _x	LB/IN	-212	-96.1		-931	-4,354		-1	-137		-179	-1,075	
			-354	-17.2		-2,243	-4,354		-5,240	-5,240		-2,489	-1,075	
THERMAL STRAIN	N _y	LB/IN	-93	-139		-1,694	-1,694		-264	-1.3		-435	-1,075	
			-220.2	-57.7		-142.3	-1,694		-37.4	-11		-56.5	-1,075	
PRESSURE	CY X 10 ⁻⁶	IN/IN	-115.2	-23.5		-242.4	-135.6		-15.4	-1.3		-31.3	-50.1	
			-143.3	-66.6		-172.6	-414.1		-8.2	-19.4		-294.5	-623.5	
TEMPERATURE	AERO	PSI	-1.67	-0.17		-1.5	-1.5		-1.0	-1.3		-1.49	-1.49	
			-4.71	-4.71		-4.71	-4.71		-4.71	-4.71		-4.50	-4.50	
TEMPERATURE	NET	°F	-6.38	-7.5		-1.5	-1.5		-1.7	-1.4		-5.97	-4.50	
			146	103		31.5	34		35	43		94	393	
TEMPERATURE	ΔT	°F	-231	-28		-9	-3		-10	-4		-13	-149	

NOTES: (1) A 1.25 FACTOR HAS BEEN APPLIED TO THE THERMAL STRAIN WHEN THE SIGN IS SAME AS THE AIRLOAD

SIGN, OTHERWISE NO FACTOR APPLIED

(2) PRESSURE SIGN CONVENTION: NEGATIVE = SUCTION

ORIGINAL PAGE IS
OF POOR QUALITY

TABLE 11-56. WING POINT DESIGN ENVIRONMENT, FINAL DESIGN - TASK IIB,
MACH 2.7 MID-CRUISE LOAD CONDITIONS

ULTIMATE DESIGN LOADS	ITEM	UNITS	POINT DESIGN REGION											
			40222			41316			41348			40236		
			UPPER SURFACE	LOWER SURFACE		UPPER SURFACE	LOWER SURFACE		UPPER SURFACE	LOWER SURFACE		UPPER SURFACE	LOWER SURFACE	
AIR LOADS	N _a	LB/IN	-111	-575		-111	-575		-111	-575		-111	-575	
	N _y	LB/IN	-190	-146		-190	-146		-190	-146		-190	-146	
	N _{ay}	LB/IN	-91	-1,372		-91	-1,372		-91	-1,372		-91	-1,372	
THERMAL STRAIN	C ₁ X 10 ⁻⁶	IN/IN	-154.4	-139.0		-154.4	-139.0		-154.4	-139.0		-154.4	-139.0	
	C ₂ X 10 ⁻⁶	IN/IN	359.2	31.9		359.2	31.9		359.2	31.9		359.2	31.9	
	C ₄ X 10 ⁻⁶	IN/IN	-65.3	-17.3		-65.3	-17.3		-65.3	-17.3		-65.3	-17.3	
PRESSURE	AERO	PSI	-1.35	-0.24		-1.35	-0.24		-1.35	-0.24		-1.35	-0.24	
	FUEL	PSI	-4.58	-0.03		-4.58	-0.03		-4.58	-0.03		-4.58	-0.03	
	NET	PSI	-3.85	-0.17		-3.85	-0.17		-3.85	-0.17		-3.85	-0.17	
TEMPERATURE	T _{AV}	°F	-281	245		-281	245		-281	245		-281	245	
	ΔT	°F	-154	-109		-154	-109		-154	-109		-154	-109	

NOTES: (1) A 1.25 FACTOR HAS BEEN APPLIED TO THE THERMAL STRAIN WHEN THE SIGN IS SAME AS THE AIRLOAD
SIGN, OTHERWISE NO FACTOR APPLIED.
(2) PRESSURE SIGN CONVENTION: NEGATIVE = SUCTION

ORIGINAL PAGE IS
OF FOUR QUALITY

Fuselage Cabin Pressure - Task IIB

Design pressures for the Supersonic Cruise Aircraft are based on providing a 6000 ft. cabin altitude at a flight altitude of 70,000 feet. These conditions produce a normal differential pressure of 11.2 psi, i.e., nominal cabin pressure combined with ambient pressure.

Maximum design differential pressure includes a tolerance which accounts for variations in static reference, regulator valve tolerance, and relief valve tolerances. A graphic display of these tolerances are illustrated in Section 4, Figure 4-10.

An envelope of differential pressure values used to determine loads on the pressurized cabin is shown in Figure 11-18.

See the structural Design Criteria Section, Section 4, for a more detailed description of the criteria for applying these pressures in the structural design analyses.

The ultimate cabin pressures (1.50 times limit) for the critical flight conditions are contained in Table 11-57. This table includes a list of flight conditions as identified by the NASTRAN condition numbers and the associated flight parameters for these conditions.

Fuselage Internal Loads - Task IIB

The fuselage air and thermal loads were defined using the 3-D structural model which included a detail fuselage model. For the Task IIB redundant - structure analyses two design cycles were conducted; strength design and strength/stiffness design. The fuselage flexibilities were held constant for these two design iterations. The load intensities (airload and thermal) are discussed in the following text.

Internal Loads - Airloads - Ultimate internal loads for the primary structure of the fuselage were defined for each of the design cycles included in the Task IIB investigation.

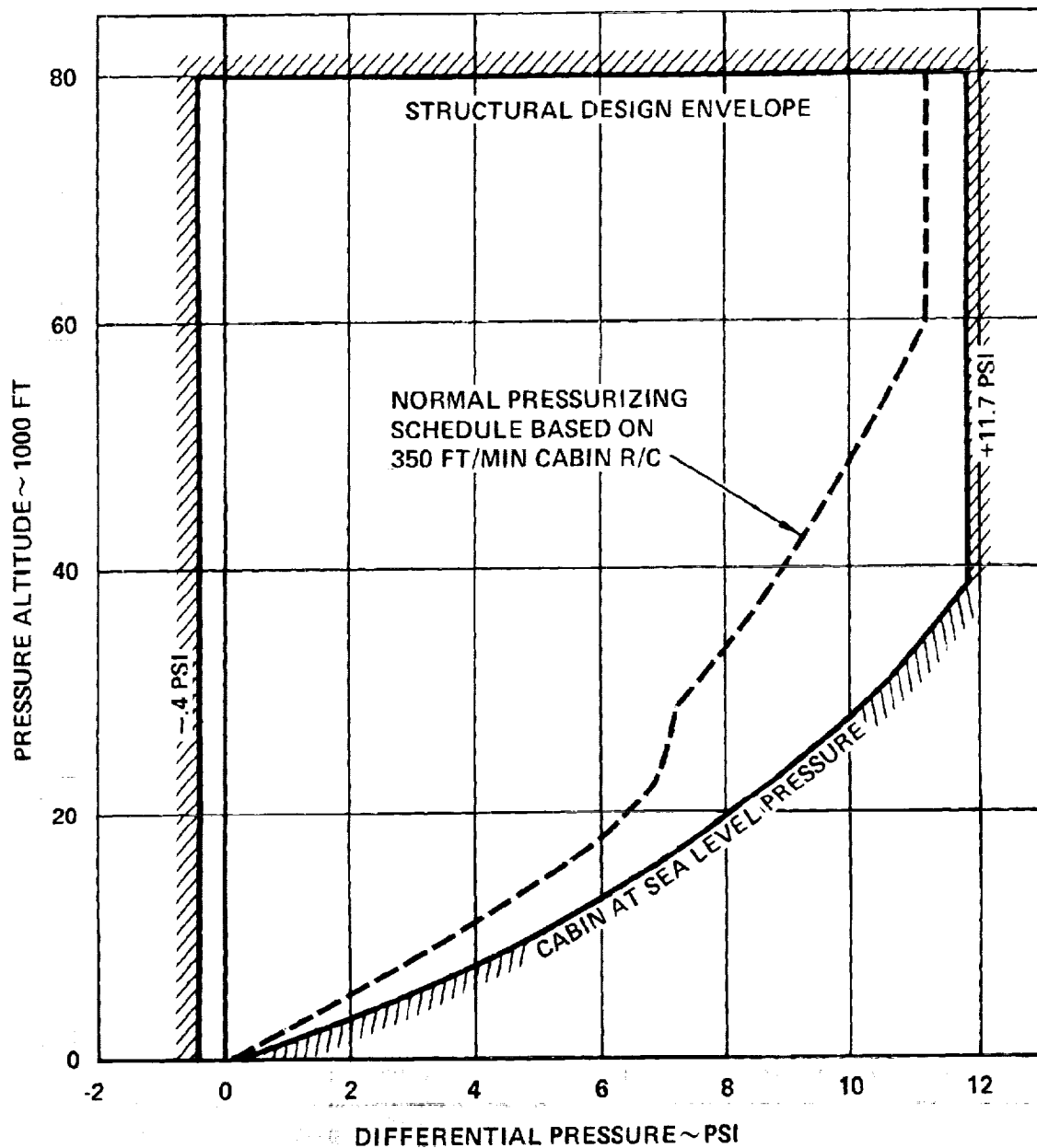


FIGURE 11-18. CABIN PRESSURE STRUCTURAL DESIGN ENVELOPE

TABLE 11-57. FUSELAGE CABIN PRESSURE - TASK IIB

NASTRAN COND. NO.	WEIGHT $\times 10^{-3}$ LB	MACH NO.	LOAD FACTOR (n_z)	V_e (KEAS)	ALT. $\times 10^{-3}$ FT	CABIN PRESSURE ULT. (psi)
(6)	700	0.90	2.5	282.4	36.0	16.95
(12)	690	1.25	2.5	294.3	48.0	17.55
(14)	690	1.25	-1.0	294.3	48.0	17.55
(16)	690	1.25	2.5	372.0	38.2	17.55
(18)	445	1.25	2.5	420.0	34.0	16.50
(20)	660	2.70	2.5	460.0	61.5	17.55
(22)	550	2.70	1.0	433.6	64.0	17.55
(24)	700	0.90	2.5	282.4	30.0	15.30
(25) - (28)	430	—	1.0	100.0	S.L.	0

TABLE 11-58. COMPARISON OF FUSELAGE PANEL LOAD INTENSITIES -
TASK IIB, MACH 1.25 LOAD CONDITION

LOCATION	(1) FUSELAGE PANEL LOAD INTENSITIES (ULT.), LB/IN.								
	DIRECTION	STRENGTH DESIGN				STRENGTH/STIFFNESS			
		FS 900	FS 1910	FS 2525	FS 2900	FS 900	FS 1910	FS 2900	FS 2900
UPPER PANEL	N_x	473	-3867	-1002	-635	497	-3078	772	909
	N_{xy}	33	158	166	67	29	103	178	81
SIDE PANEL	N_x	-121	270	61	82	-156	-4	-107	-257
	N_{xy}	158	594	1127	257	169	452	1218	394
LOWER PANEL	N_x	LDG GEAR WELL	WING	WING	1070 8	LDG GEAR WELL	WING	WING	-728 75
	N_{xy}								

(1) LOAD CONDITION—CONDITION 12 : MACH 1.25, $N_z = 2.5$, $W = 690,000$ LB., $V_e = 294$ KEAS

The internal forces/stresses were determined using the NASTRAN solution and converted to load intensities by the auxiliary running loads program. A comparison of the point design load intensities for the strength and strength/stiffness designs are shown in Table 11-58. These loads reflect the load state of the "extreme fiber" upper and lower centerline panels and the high-shear side panel for the 2.5-g symmetric maneuver condition at Mach 1.25.

Representative load intensities for the final strength/stiffness design are presented in Figure 11-19 and 11-20. These loads are ultimate loads and represent the maximum compression and tension condition respectively.

Internal Loads - Thermal - Three critical temperature conditions were included in the NASTRAN solution: start-of-cruise, mid-cruise, and a Mach 1.25 descent condition. See Tables 11-37 and 11-38 for a description of the flight parameters and the identifying NASTRAN condition numbers.

The load intensities for the critical hot conditions are indicated in parenthesis on the aforementioned Figures 11-19 and 11-20. The start-of-cruise condition, Condition 23, was the predominant hot condition.

In addition to the above thermal stresses, the local temperature gradients and average temperatures were calculated for inclusion in the fuselage point design environment.

Section 6 contains a detail description of the results of the Task IIB thermal analysis. For the sake of completeness, fuselage skin panel gradients and average temperatures are shown on Table 11-59 for the four point design regions at various circumferential locations. In addition to the three conditions included in the NASTRAN solution, the temperatures for a Mach 1.25 climb condition are shown. As can be seen from a review of this table, the temperatures associated with this condition are negligible and were not included in the NASTRAN solution.

1

2

3

1

2

3

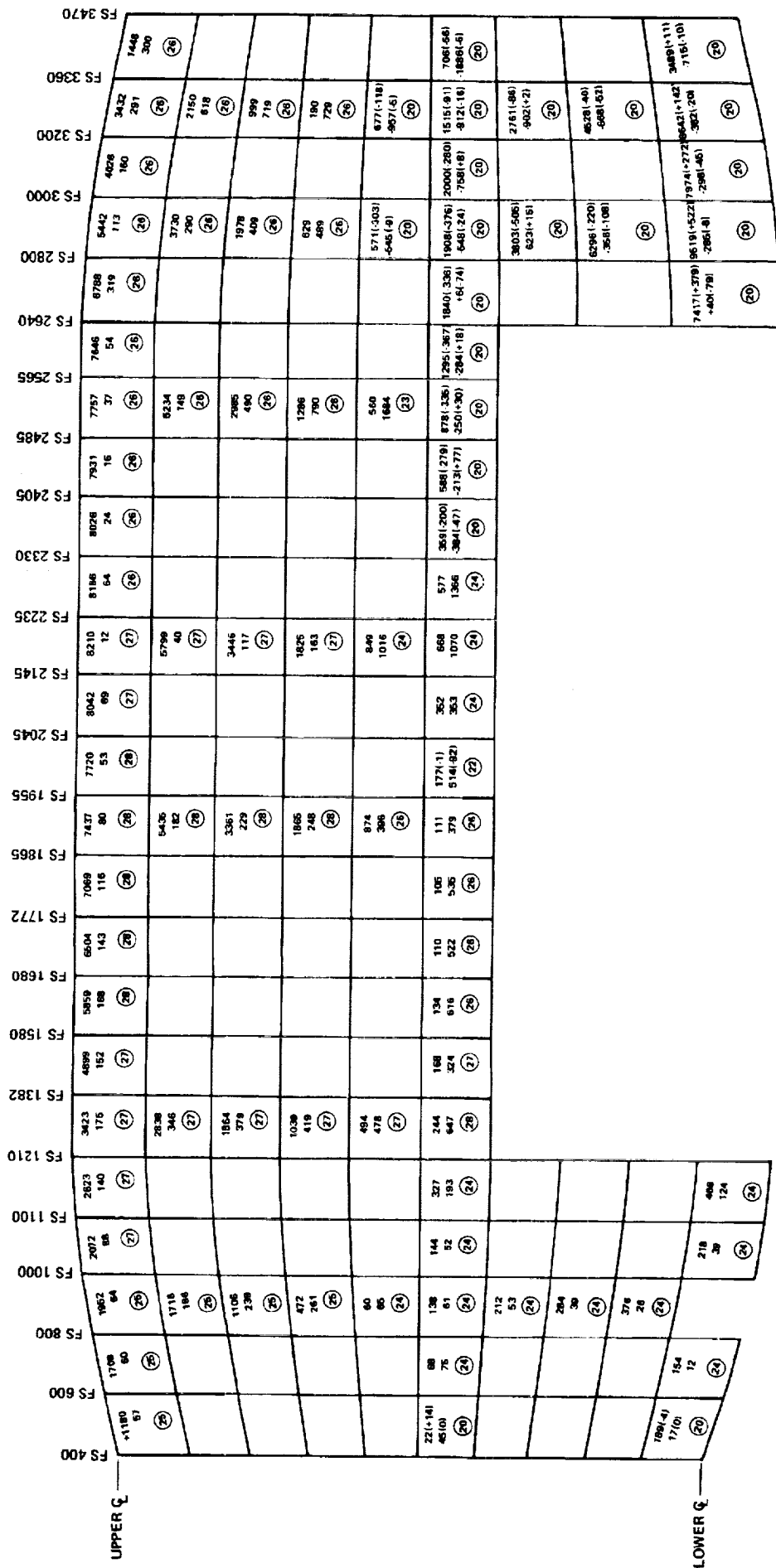


FIGURE 11-20. FOLDOUT FRAME 2

PRELIMINARY PANEL MAXIMUM TENSION LOADS, TABLE 11P FURTHER DESIGN

NOTES:

(1) PANEL LOAD LEGEND

XXX(XXX) Nx, PANEL AXIAL LOAD, LB/IN.

XXX(XXX) Nxy, PANEL SHEAR FLOW, LB/IN.

XX CONDITION NUMBER, SEE NOTE 2.

THERMAL LOAD (LB/IN.) INDICATED IN PARENTHESIS

R C E D I N G P A G E B L A N K N O T F I L M E D

FOLDOUT FRAME 1

(2) DESIGN CONDITIONS

(20) 2.5G SYMM. FLIGHT, TRANS. MANEUVER @ START OF CRUISE M2.7

(22) 2.5G SYMM. FLIGHT, STEADY MANEUVER @ MID-CRUISE M2.7

(24) STATIC GUST (NEGATIVE), M0.90 (Vc) CLIMB

(26) DYNAMIC LANDING, FOREBODY DOWN BENDING & WING ROOT SHEAR

(26) DYNAMIC LANDING, AFTBODY DOWN BENDING

(27) DYNAMIC LANDING, FOREBODY DOWN BENDING

(28) DYNAMIC LANDING, FOREBODY DOWN BENDING

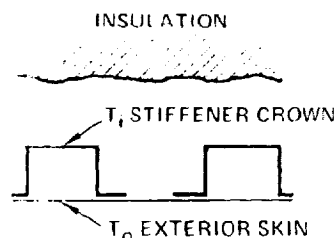


TABLE 11-59. FUSELAGE SKIN PANELS MAXIMUM THERMAL GRADIENTS AND TEMPERATURES, TASK IIF

NOTES:

1. BASED ON HOT DAY (STD+8K)
4200 n mi FLIGHT PROFILE.
2. HAT STIFFENED PANELS.
EXCEPT ZEE STIFFENED
AT FS 750.
3. 'TOP', 'BOTTOM' AT 0°;
'SIDE' AT 90° OR ABOVE WING.

PANEL SCHEMATIC



TEMPERATURES IN F

LOCATION	FLIGHT CONDITION							
	MACH 1.2 CLIMB		START OF CRUISE		MID TO END OF CRUISE		MACH 1.2 DESCENT	
	$T_i - T_o$	T_{AVG}	$T_i - T_o$	T_{AVG}	$T_i - T_o$	T_{AVG}	$T_i - T_o$	T_{AVG}
<u>TOP</u>								
FS 750	+ 9	55	-105	342	-11	380	+111	114
2000	+23	53	-175	295	-11	374	+171	144
2500	+24	54	-186	281	-11	372	+181	156
3000	+23	53	-174	292	-11	371	+170	145
<u>SIDE</u>								
FS 750	+12	49	-106	332	-11	369	+109	108
2000	+21	50	-157	324	-11	394	+156	129
2500	+22	50	-171	311	-11	393	+170	139
3000	+23	47	-147	301	-11	358	+142	122
<u>BOTTOM</u>								
FS 750	+12	50	-106	333	-11	370	+109	109
3000	+28	47	-177	278	-10	360	+171	141

TEMPERATURES IN K

LOCATION	FLIGHT CONDITION							
	MACH 1.2 CLIMB		START OF CRUISE		MID TO END OF CRUISE		MACH 1.2 DESCENT	
	$T_i - T_o$	T_{AVG}	$T_i - T_o$	T_{AVG}	$T_i - T_o$	T_{AVG}	$T_i - T_o$	T_{AVG}
<u>TOP</u>								
FS 750	+6	296	-74	336	-103	409	-31	368
2000	+3	296	-41	319	- 89	409	-42	385
2500	+3	296	-35	316	- 82	408	-40	390
3000	+3	296	-41	319	- 89	408	-42	384
<u>SIDE</u>								
FS 750	+8	295	-70	333	- 99	405	-29	364
2000	+4	296	-50	323	- 95	417	-37	388
2500	+4	296	-42	319	- 88	417	-36	393
3000	+5	295	-44	319	- 84	403	-34	376
<u>BOTTOM</u>								
FS 750	+7	295	-70	333	-100	405	-29	364
3000	+4	296	-35	315	- 86	403	-42	381

Fuselage Point Design Environment - Task IIB

The fuselage point design load/temperature environments for the strength and final (strength/stiffness) design airplanes were defined for their critical load conditions. The point design environment was defined at each point design location (FS 900, FS 1910, FS 2525, and FS 2900) for various circumferential locations around the shell. The specific panel load/temperature environment corresponds to the panel locations used on the 3-D structural model. Figure 11-21 illustrates the NASTRAN panel identification system. The fuselage point design environments for the strength design airplane are shown in Tables 11-60 through 11-65. These point design environments encompass six design load conditions.

The corresponding point design environments for the final design are contained in Tables 11-66 through 11-69 for the following design conditions.

- Start-of-Cruise, Mach 2.7
- Mid-cruise, Mach 2.7
- Static Gust at Mach 0.90
- Dynamic Landing Conditions (4)

ORIGINAL PAGE IS
OF POOR QUALITY

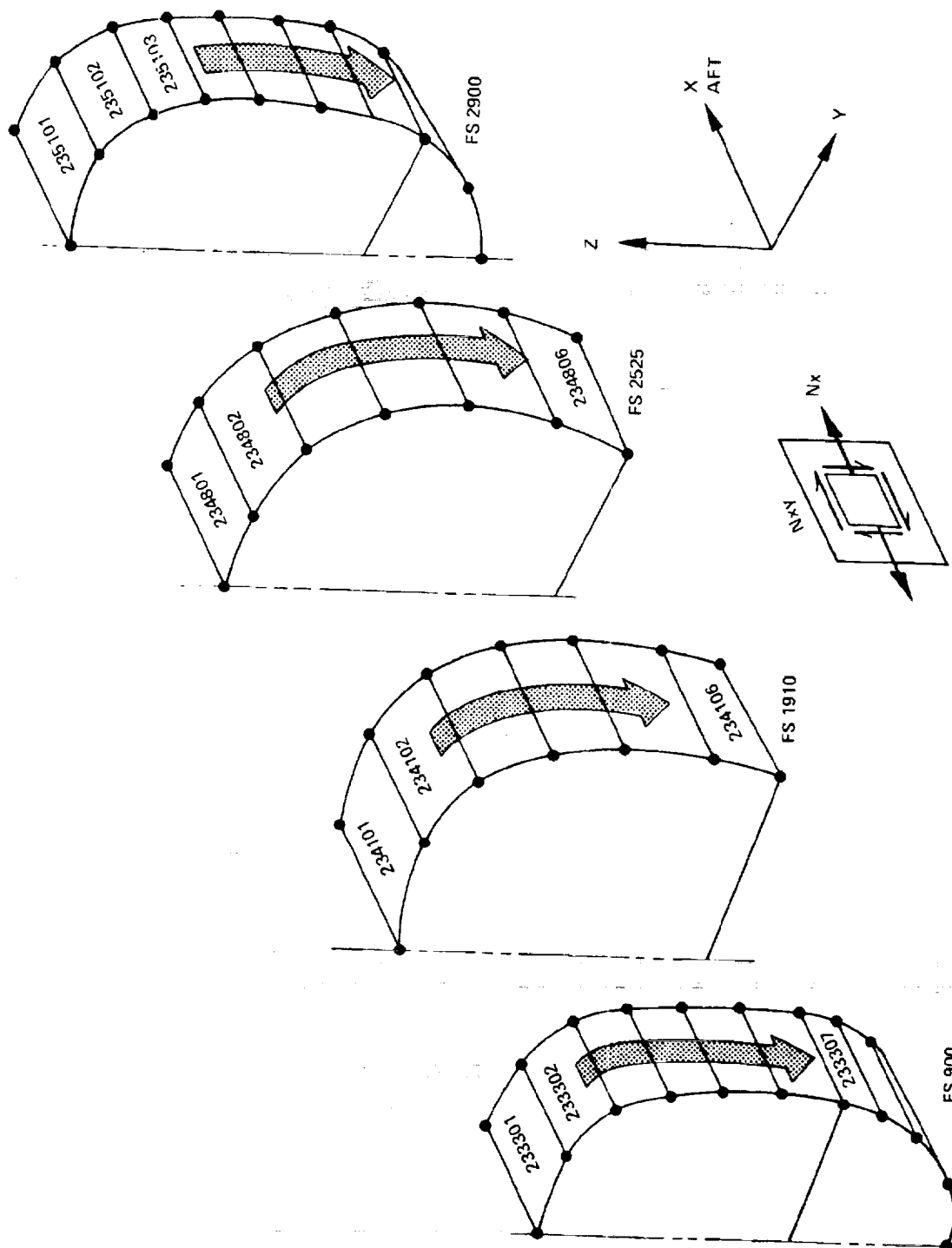


FIGURE 11-21. FUSELAGE PANEL IDENTIFICATION SYSTEM, TASK IIB

TABLE 11-60. FUSELAGE POINT DESIGN ENVIRONMENT, STRENGTH DESIGN - TASK IIB,
MACH 0.90 (V_S) LOAD CONDITION

CONDITION 6 SYMMETRIC MANEUVER AT MACH 0.90 (V_S). WEIGHT = 700,000 LB. $n_z = 2.5$

ITEM	UNITS	POINT DESIGN REGION (23XXXXX)														
		3301	3302	3303	3304	3305	3306	3307	3308	3309	4101	4102	4103	4104	4105	4106
N _X	LB/IN	+374	+296	+180	+65	-50	-102	-188	-302	-383	3600	-2792	-1802	965	330	+254
N _{XY}	LB/IN	-25	51	-64	-74	-73	-60	-73	-46	-29	+159	+467	+624	+653	+629	+605
AERO PRESS.	PSI	-	-	-	-	-	-	-	-	-	-	-	-	-	-	-
INTERNAL PRESS.	PSI	16.95	16.95	16.95	16.95	16.95	16.95	16.95	16.95	16.95	16.95	16.95	16.95	16.95	16.95	16.95
NET PRESS.	PSI	16.95	16.95	16.95	16.95	16.95	16.95	16.95	16.95	16.95	16.95	16.95	16.95	16.95	16.95	16.95
T _{AVG}	OF	RT	RT	RT	RT	RT	RT	RT	RT	RT	RT	RT	RT	RT	RT	RT

ITEM	UNITS	POINT DESIGN REGION (23XXXXX)														
		4801	4802	4803	4804	4805	4806	5101	5102	5103	5104	5105	5106	5107	5108	5109
N _X	LB/IN	1642	-504	+222	+414	+381	+266	-1483	-1208	-749	-290	+66	+309	+658	+1213	+1992
N _{XY}	LB/IN	-126	-317	-483	-637	-736	-822	+62	+99	+93	+92	+113	+144	+73	+52	-32
AERO PRESS.	PSI	-	-	-	-	-	-	-	-	-	-	-	-	-	-	-
INTERNAL PRESS.	PSI	16.95	16.95	16.95	16.95	16.95	16.95	16.95	16.95	16.95	16.95	16.95	16.95	16.95	16.95	16.95
NET PRESS.	PSI	16.95	16.95	16.95	16.95	16.95	16.95	16.95	16.95	16.95	16.95	16.95	16.95	16.95	16.95	16.95
T _{AVG.}	OF	RT	RT	RT	RT	RT	RT	RT	RT	RT	RT	RT	RT	RT	RT	RT

NOTE: REFER TO FIGURE 11-21 FOR FUSELAGE STATION (FS) AND CIRCUMFERENTIAL LOCATION

ORIGINAL PAGE IS
OF POOR QUALITY

TABLE 11-61. FUSELAGE POINT DESIGN ENVIRONMENT, STRENGTH DESIGN - TASK IIB,
MACH 1.25 (V_0) LOAD CONDITION

CONDITION 12 SYMMETRIC MANEUVER AT MACH 1.25 (V_0). WEIGHT = 680,000 LB. $n_z = 2.5$

ITEM	UNITS	POINT DESIGN REGION (23XXXX)														
		3301	3302	3303	3304	3305	3306	3307	3308	3309	4101	4102	4103	4104	4105	4106
NX	LB/IN	+473	+401	-262	+106	-60	-121	-247	-409	514	3867	-2979	-1916	-1028	-352	+270
NXY	LB/IN	-33	-91	-141	-172	-177	-158	-182	-129	-95	+158	+462	+616	+644	-619	+594
AERO PRESS.	PSI	-	-	-	-	-	-	-	-	-	-	-	-	-	-	-
INTERNAL PRESS.	PSI	17.55	17.55	17.55	17.55	17.55	17.55	17.55	17.55	17.55	17.55	17.55	17.55	17.55	17.55	17.55
NET PRESS.	PSI	17.55	17.55	17.55	17.55	17.55	17.55	17.55	17.55	17.55	17.55	17.55	17.55	17.55	17.55	17.55
T AVG.	OF	RT	RT	RT	RT	RT	RT	RT	RT	RT	RT	RT	RT	RT	RT	RT

ITEM	UNITS	POINT DESIGN REGION (23XXXX)														
		4801	4802	4803	4804	4805	4806	5101	5102	5103	5104	5105	5106	5107	5108	5109
NX	LB/IN	-1002	54	-481	-489	-306	+61	-635	-646	-471	216	-1	+82	+234	+591	+1070
NXY	LB/IN	-166	-446	-708	-931	-1053	-1127	+67	+136	-160	-178	-212	+257	+159	+95	+8
AERO PRESS.	PSI	-	-	-	-	-	-	-	-	-	-	-	-	-	-	-
INTERNAL PRESS.	PSI	17.55	17.55	17.55	17.55	17.55	17.55	17.55	17.55	17.55	17.55	17.55	17.55	17.55	17.55	17.55
NET PRESS.	PSI	17.55	17.55	17.55	17.55	17.55	17.55	17.55	17.55	17.55	17.55	17.55	17.55	17.55	17.55	17.55
T AVG.	OF	RT	RT	RT	RT	RT	RT	RT	RT	RT	RT	RT	RT	RT	RT	RT

ORIGINAL PAGE IS
OF POOR QUALITY

TABLE 11-62. FUSELAGE POINT DESIGN ENVIRONMENT, STRENGTH DESIGN - TACK IIR,
MACH 1.25 NEGATIVE MANEUVER CONDITION

CONDITION 14 NEGATIVE MANEUVER AT MACH 1.25 (V_g), WEIGHT = 690,000 LB., n_y = 2.5

ITEM	UNITS	POINT DESIGN REGION (23XXXXX)														
		3301	3302	3303	3304	3305	3306	3307	3308	3309	4101	4102	4103	4104	4105	4106
N _X	LB/IN	-120	-101	-69	-32	+9	+24	+56	+105	+139	-457	-213	-33	+38	+49	+29
N _{XY}	LB/IN	+14	+39	+62	+74	+76	+71	+76	+62	+43	+33	-26	+3	-6	-7	-14
AERO PRESS.	PSI	-	-	-	-	-	-	-	-	-	-	-	-	-	-	-
INTERNAL PRESS.	PSI	17.55	17.55	17.55	17.55	17.55	17.55	17.55	17.55	17.55	17.55	17.55	17.55	17.55	17.55	17.55
NET PRESS.	PSI	17.55	17.55	17.55	17.55	17.55	17.55	17.55	17.55	17.55	17.55	17.55	17.55	17.55	17.55	17.55
T _{AVG.}	OF	RT	RT	RT	RT	RT	RT	RT	RT	RT	RT	RT	RT	RT	RT	RT

ITEM	UNITS	POINT DESIGN REGION (23XXXX)														
		4801	4802	4803	4804	4805	4806	5101	5102	5103	5104	5105	5106	5107	5108	5109
N _X	LB/IN	4938	3632	-2264	938	+99	+1071	4610	2962	-1415	-344	+392	+1133	+2192	+3404	+4938
N _{XY}	LB/IN	+189	+466	+705	-900	+990	+1022	-94	-274	397	-474	-516	-560	-526	-263	-171
AERO PRESS.	PSI	-	-	-	-	-	-	-	-	-	-	-	-	-	-	-
INTERNAL PRESS.	PSI	17.55	17.55	17.55	17.55	17.55	17.55	17.55	17.55	17.55	17.55	17.55	17.55	17.55	17.55	17.55
NET PRESS.	PSI	17.55	17.55	17.55	17.55	17.55	17.55	17.55	17.55	17.55	17.55	17.55	17.55	17.55	17.55	17.55
TAVG.	OF	RT	RT	RT	RT	RT	RT	RT	RT	RT	RT	RT	RT	RT	RT	RT

TABLE 11-63. FUSELAGE POINT DESIGN ENVIRONMENT, STRENGTH DESIGN - TASK IIB,
MACH 1.25 (V_D) LOAD CONDITION

CONDITION (16) SYMMETRIC MANEUVER AT MACH 1.25 (V_C) WEIGHT - 690,000 LB. $n_z = 2.5$

ITEM	UNITS	POINT DESIGN REGION (23XXXX1)														
		3301	3302	3303	3304	3305	3306	3307	3308	3309	4101	4102	4103	4104	4105	4106
NX	LB/IN	+286	+262	+184	+75	-56	-87	-183	-299	-318	-7747	-5631	3367	-1669	-481	+541
NY	LB/IN	-17	-55	-93	-120	-123	-102	-126	-73	-48	+347	+887	+1134	+1184	+1147	+1091
AERO PRESS.	PSI	-	-	-	-	-	-	-	-	-	-	-	-	-	-	-
INTERNAL PRESS.	PSI	17.55	17.55	17.55	17.55	17.55	17.55	17.55	17.55	17.55	17.55	17.55	17.55	17.55	17.55	17.55
NET PRESS.	PSI	17.55	17.55	17.55	17.55	17.55	17.55	17.55	17.55	17.55	17.55	17.55	17.55	17.55	17.55	17.55
T AVG.	°F	RT	RT	RT	RT	RT	RT	RT	RT	RT	RT	RT	RT	RT	RT	RT

ITEM	UNITS	POINT DESIGN REGION (23XXXXX)														
		4801	4802	4803	4804	4805	4806	5101	5102	5103	5104	5105	5106	5107	5108	5109
N _X	LB/IN	-10823	-6787	-3367	-940	+626	+1989	-9228	-6323	-3289	-965	+696	+2110	+4236	+7028	+10550
N _{XY}	LB/IN	+35	-14	-119	-218	-292	-356	-70	-265	-423	-513	-517	504	-650	-293	-280
AERO PRESS.	PSI	-	-	-	-	-	-	-	-	-	-	-	-	-	-	-
INTERNAL PRESS.	PSI	17.55	17.55	17.55	17.55	17.55	17.55	17.55	17.55	17.55	17.55	17.55	17.55	17.55	17.55	17.55
NET PRESS.	PSI	17.55	17.55	17.55	17.55	17.55	17.55	17.55	17.55	17.55	17.55	17.55	17.55	17.55	17.55	17.55
T AVG.	°F	RT	RT	RT	RT	RT	RT	RT	RT	RT	RT	RT	RT	RT	RT	RT

ORIGINAL PAGE IS
OF POOR QUALITY

TABLE 11-64. FUSELAGE POINT DESIGN ENVIRONMENT, STRENGTH DESIGN - TASK IIB,
MACH 1.25 (V_D) DESCENT CONDITION

CONDITION 18 SYMMETRIC MANEUVER AT MACH 1.25 (DESCENT - V_D) WEIGHT = 445,000 LB. $n_z = 2.5$

ITEM	UNITS	POINT DESIGN REGIONS (23XXXXX)														
		3301	3302	3303	3304	3305	3306	3307	3308	3309	4101	4102	4103	4104	4105	4106
N _X	LB/IN	+452	-369	+230	+87	-52	-111	-218	356	-475	-1778	-1193	-633	-259	-14	+200
N _{XY}	LB/IN	-28	-68	-98	-118	-121	-108	-128	-92	74	+155	+379	+467	+475	+451	+427
N _{X, TH}	LB/IN	-6	-	+2	+2	+4	+11	+15	+13	-3	-34	+26	+72	+112	+151	128
N _{XY, TH}	LB/IN	+2	+2	-1	-1	-	+1	-	-2	-3	-3	-10	-15	-18	-19	-16
AERO PRESS.	PSI	-	-	-	-	-	-	-	-	-	-	-	-	-	-	-
INTERNAL PRESS.	PSI	16.50	16.50	16.50	16.50	16.50	16.50	16.50	16.50	16.50	16.50	16.50	16.50	16.50	16.50	16.50
NET PRESS.	PSI	16.50	16.50	16.50	16.50	16.50	16.50	16.50	16.50	16.50	16.50	16.50	16.50	16.50	16.50	16.50
T _{AVG.}	OF	+114	+113	+111	+110	+108	+108	+108	+108	+109	+144	-141	+138	+135	+132	+129
ΔT	OF	+111	+111	+110	+110	+109	+109	+109	+109	+109	+171	-168	+165	+162	+159	+156

ITEM	UNITS	POINT DESIGN REGIONS (23XXXXX)														
		3801	4802	4803	4804	4805	4806	5101	5102	5103	5104	5105	5106	5107	5108	5109
N _X	LB/IN	-4665	2900	-1410	-364	+306	-908	-4576	-3104	1583	437	+371	-1079	+2116	+3454	+5158
N _{XY}	LB/IN	+64	+173	+315	+448	+510	+532	-16	-117	-214	269	279	282	-332	-153	-135
N _{X, TH}	LB/IN	94	2	+81	+163	+305	21	86	+7	+65	+104	+170	+138	+19	-54	68
N _{XY, TH}	LB/IN	+5	+14	+26	+30	+18	-8	-5	-14	-13	-1	+11	+21	+24	+2	22
AERO PRESS.	PSI	-	-	-	-	-	-	-	-	-	-	-	-	-	-	-
INTERNAL PRESS.	PSI	16.50	16.50	16.50	16.50	16.50	16.50	16.50	16.50	16.50	16.50	16.50	16.50	16.50	16.50	16.50
NET PRESS.	PSI	16.50	16.50	16.50	16.50	16.50	16.50	16.50	16.50	16.50	16.50	16.50	16.50	16.50	16.50	16.50
TAVG.	OF	156	152	148	145	142	139	145	139	133	127	122	125	130	135	141
ΔT	OF	+181	+179	+177	+175	+172	-170	-170	+162	+154	+146	+142	+145	+155	+163	+171

TABLE 11-65. FUSELAGE POINT DESIGN ENVIRONMENT, STRENGTH DESIGN - TASK 11B,
MACH 2.7 START-OF-CRUISE CONDITION

CONDITION (20) SYMMETRIC MANEUVER AT MACH 2.70 (START-OF-CRUISE), WEIGHT = 660,000 LB., $n_z = 2.5$

ITEM	UNITS	POINT DESIGN REGIONS (23XXXXX)														
		3301	3302	3303	3304	3305	3306	3307	3308	3309	4101	4102	4103	4104	4105	4106
N _X	LB/IN	-56	-37	-8	5	-37	-2	-13	-30	+72	-8618	-6284	-3779	-1885	-550	+611
N _{XY}	LB/IN	-	-7	-27	-44	-45	-27	-44	7	+8	+358	-890	+1110	+1136	+1088	+1025
N _{X, TH}	LB/IN	-22	-9	+12	+25	+26	+29	+16	+1	-11	+165	-11	-255	-498	-738	-23
N _{X, TH}	LB/IN	-	+4	-7	-4	+1	-	-9	7	-10	-13	-32	-40	-42	-37	-27
AERO PRESS.	PSI	-	-	-	-	-	-	-	-	-	-	-	-	-	-	-
INTERNAL PRESS.	PSI	17.55	17.55	17.55	17.55	17.55	17.55	17.55	17.55	17.55	17.55	17.55	17.55	17.55	17.55	17.55
NET PRESS.	PSI	17.55	17.55	17.55	17.55	17.55	17.55	17.55	17.55	17.55	17.55	17.55	17.55	17.55	17.55	17.55
T AVG.	OF	342	339	336	334	332	333	333	333	333	295	300	305	312	320	324
ΔT	OF	-105	-105	-106	-106	-106	-106	-106	-106	-106	-175	-170	-166	-162	-159	-157

ITEM	UNITS	POINT DESIGN REGIONS (23XXXXX)															
		4801	4802	4803	4804	4805	4806	5101	5102	5103	5104	5105	5106	5107	5108	5109	
N _X	LB/IN	-12413	-7932	-4066	-1222	-664	+2319	-10441	-7108	-3674	-1071	+785	+2403	+4822	+7934	+11862	
N _{XY}	LB/IN	-67	-67	+6	-59	-120	-187	-110	-368	-564	-676	-695	-697	-827	-387	-338	
N _{X, TH}	LB/IN	+329	+57	301	-646	-785	-272	+177	-37	-124	-261	301	375	501	220	+518	
N _{X, TH}	LB/IN	+5	+14	+26	+24	+14	-10	+10	-21	+17	+7	-8	-22	-16	-99	-8	
AERO PRESS.	PSI	-	-	-	-	-	-	-	-	-	-	-	-	-	-	-	
INTERNAL PRESS.	PSI	17.55	17.55	17.55	17.55	17.55	17.55	17.55	17.55	17.55	17.55	17.55	17.55	17.55	17.55	17.55	
NET PRESS.	PSI	17.55	17.55	17.55	17.55	17.55	17.55	17.55	17.55	17.55	17.55	17.55	17.55	17.55	17.55	17.55	
T AVG.	°F	281	287	293	300	307	311	292	295	298	300	301	295	288	283	278	
ΔT	°F	-186	-183	180	-177	173	-171	-174	-165	-156	-149	-147	-150	-157	-167	-177	

ORIGINAL PAGE IS
OF POOR QUALITY

TABLE 11-66. FUSELAGE POINT DESIGN ENVIRONMENT, FINAL DESIGN - TASK IIB,
START-OF-CRUISE CONDITION

CONDITION (20) SYMMETRIC FLIGHT - TRANSIENT MANEUVER AT MACH 2.7 (VC). START-OF-CRUISE, $n_z = 2.5$

ITEM	UNITS	POINT DESIGN REGIONS (23 XXXX)														
		3301	3302	3303	3304	3305	3306	3307	3308	3309	4101	4102	4103	4104	4105	4106
NX	lb/in.	-22	-14	-15	-21	-33	-29	-35	-16	+58	-7084	-5433	-3569	-2045	929	+56
NXY	lb/in.	+2	-12	-34	-45	-47	-41	-38	-14	-4	+243	+621	+788	+819	+797	+773
NX,TH	lb/in.	-21	-8	+12	+24	+26	+23	+9	-1	10	+218	+13	-264	-528	-782	-68
NXY,TH	lb/in.	0	+4	+6	+4	0	-3	-8	-6	-10	-17	-42	-53	-54	-47	-36
AERO PRESS	psi	-	-	-	-	-	-	-	-	-	-	-	-	-	-	-
INTERNAL PRESS	psi	17.55	17.55	17.55	17.55	17.55	17.55	17.55	17.55	17.55	17.55	17.55	17.55	17.55	17.55	17.55
NET PRESS	psi	17.55	17.55	17.55	17.55	17.55	17.55	17.55	17.55	17.55	17.55	17.55	17.55	17.55	17.55	17.55
TAVG	F	342	339	336	334	332	333	333	333	333	295	300	305	312	320	324
ΔT	F	-105	-105	-106	-106	-106	-106	-106	-106	-106	-175	-170	-166	-162	-159	-157

ITEM	UNITS	POINT DESIGN REGIONS (23 XXXX)														
		4801	4802	4803	4804	4805	4806	5101	5102	5103	5104	5105	5106	5107	5108	5109
NX	lb/in.	-9188	-5988	-3261	-1335	-1295	+878	-8226	-5701	-3030	946	+571	+1908	+3803	+6296	+9519
NXY	lb/in.	+78	+91	-3	-112	-188	-250	-45	-225	-401	-517	-545	-548	-623	-356	-285
NX,TH	lb/in.	+379	+70	-324	-692	-1042	-335	+180	+36	-128	-265	-303	-376	-505	-220	+522
NXY,TH	lb/in.	+4	+14	+30	+51	+56	+30	+12	+22	+18	+7	9	-24	+15	-108	-8
AERO PRESS	psi	-	-	-	-	-	-	-	-	-	-	-	-	-	-	-
INTERNAL PRESS	psi	17.55	17.55	17.55	17.55	17.55	17.55	17.55	17.55	17.55	17.55	17.55	17.55	17.55	17.55	17.55
NET PRESS	psi	17.55	17.55	17.55	17.55	17.55	17.55	17.55	17.55	17.55	17.55	17.55	17.55	17.55	17.55	17.55
TAVG	F	281	287	293	300	307	311	292	295	298	300	301	295	288	283	278
ΔT	F	-186	-183	-180	-177	-173	-171	-174	-165	-156	-149	-147	-150	-157	-167	-177

NOTE: REFER TO FIGURE 11-21 FOR FUSELAGE STATION (F.S.) AND CIRCUMFERENTIAL LOCATION

TABLE 11-67. FUSELAGE POINT DESIGN ENVIRONMENT, FINAL DESIGN - TASK IIB,
START-OF-CRUISE CONDITION

CONDITION 22 SYMMETRIC FLIGHT - STEADY MANEUVER AT MACH 2.7 (V_C), MID-CRUISE, M₂ = 2.5

ITEM	UNITS	POINT DESIGN REGIONS (23 XXXX)														
		3301	3302	3303	3304	3305	3306	3307	3308	3309	4101	4102	4103	4104	4105	4106
N _X	lb/in.	+170	+143	+82	+22	-34	-67	-113	-146	-160	-4352	-3307	-2134	-1206	-531	+71
N _{XY}	lb/in.	-8	-32	-53	-63	-65	-60	60	-38	28	+186	+468	+584	+597	+574	+553
N _{X,TH}	lb/in.	-22	-4	+20	+31	+22	+23	+21	+4	-19	+165	-39	-326	-610	-904	+50
N _{XY,TH}	lb/in.	+3	+6	+6	+2	0	0	-8	-11	-10	-21	-45	-54	-66	-71	-73
AERO PRESS	psi	-	-	-	-	-	-	-	-	-	-	-	-	-	-	-
INTERNAL PRESS	psi	17.55	17.55	17.55	17.55	17.55	17.55	17.55	17.55	17.55	17.55	17.55	17.55	17.55	17.55	17.55
NET PRESS	psi	17.55	17.55	17.55	17.55	17.55	17.55	17.55	17.55	17.55	17.55	17.55	17.55	17.55	17.55	17.55
TAVG	F	380	378	375	370	369	370	370	370	370	374	378	382	386	390	394
ΔT	F	-11	-11	11	-11	-11	-11	-11	-11	-11	-11	-11	-11	-11	-11	-11

ITEM	UNITS	POINT DESIGN REGIONS (23 XXXX)														
		4801	4802	4803	4804	4805	4806	5101	5102	5103	5104	5105	5106	5107	5108	5109
N _X	lb/in.	-6642	-4208	-2195	-823	+4	+684	-6501	4531	-2419	-760	+446	+1509	+3011	+4999	+7549
N _{XY}	lb/in.	+87	+159	+165	+148	+122	+91	-7	-133	-272	-363	-385	-390	-453	-261	-206
N _{X,TH}	lb/in.	+371	+72	-326	-705	-853	-257	+174	+60	-80	-221	-282	-441	-693	-336	+631
N _{XY,TH}	lb/in.	+1	+14	+52	+101	+134	+164	+12	+15	+8	+4	+5	+13	+1	66	31
AERO PRESS	psi	-	-	-	-	-	-	-	-	-	-	-	-	-	-	-
INTERNAL PRESS	psi	17.55	17.55	17.55	17.55	17.55	17.55	17.55	17.55	17.55	17.55	17.55	17.55	17.55	17.55	17.55
NET PRESS	psi	17.55	17.55	17.55	17.55	17.55	17.55	17.55	17.55	17.55	17.55	17.55	17.55	17.55	17.55	17.55
TAVG	F	372	376	380	385	390	393	371	368	365	361	358	358	360	260	360
ΔT	F	-11	-11	-11	-11	-11	-11	-11	-11	-11	-11	-11	-11	-10	-10	-10

NOTE: REFER TO FIGURE 11-21 FOR FUSELAGE STATION (F.S.) AND CIRCUMFERENTIAL LOCATION

TABLE 11-68. FUSELAGE POINT DESIGN ENVIRONMENT, FINAL DESIGN - TASK IIB,
START-OF-CRUISE CONDITION

CONDITION (25) THROUGH (28) DYNAMIC LANDING

CONDITION NO.	POINT DESIGN REGIONS (23 XXXX)																
	ITEM	UNITS	3301	3302	3303	3304	3305	3306	3307	3308	3309	4101	4102	4103	4104	4105	4106
(25)	NX	lb/in.	+1952	+1716	+1106	+472	-79	-523	-1012	-1528	-2233	+3723	+2649	+1568	+816	+344	-29
	NXY	lb/in.	-64	-186	-239	-261	-274	-274	-293	-238	-214	-144	-338	-443	-493	-508	-505
(26)	NX	lb/in.	+1678	+1363	+810	+306	-104	-422	-777	-1178	-1784	+6981	+5129	+3205	+1810	+874	+111
	NXY	lb/in.	-88	-213	-271	-293	-302	-302	-316	-276	-247	-126	-278	-347	-382	-396	-379
(27)	NX	lb/in.	+1668	+1294	+724	+242	-132	-412	-728	-1096	-1687	+7252	+5154	+3080	+1672	+785	+101
	NXY	lb/in.	-104	-241	-309	-334	-343	-341	-355	-316	-284	-111	-257	-336	-380	-398	-383
(28)	NX	lb/in.	+1077	+789	+412	+120	-94	-252	-428	-652	-1040	+7437	+5435	+3361	+1865	+867	+34
	NXY	lb/in.	-82	-176	-222	-239	-243	-243	-250	-230	-205	-80	-182	-229	-248	-255	-247

11-110

CONDITION NO.	POINT DESIGN REGIONS (23 XXXX)																
	ITEM	UNITS	4801	4802	4803	4804	4805	4806	5101	5102	5103	5104	5105	5106	5107	5108	5109
(25)	NX	lb/in.	+4665	+3103	+1714	+709	+100	-367	+2385	+1609	+851	+278	-150	-545	-1118	-1814	-2721
	NXY	lb/in.	+39	+267	+565	+799	+912	+979	+98	+194	+239	+275	+289	+290	+291	+158	+121
(26)	NX	lb/in.	+7757	+5234	+2985	+1286	+187	-694	+5442	+3730	+1978	+629	-357	-1234	-2511	-4156	-6275
	NXY	lb/in.	-37	+149	+490	+790	+957	+1050	+113	+290	+409	+489	+510	+512	+554	+322	+234
(27)	NX	lb/in.	+6754	+4542	+2577	+1122	+201	-528	+3646	+2476	+1310	+418	-241	-817	-1675	-2765	-4190
	NXY	lb/in.	+57	+375	+796	+1135	+1310	+1402	+134	+289	+370	+426	+438	+431	+458	+264	+196
(28)	NX	lb/in.	+4982	+3264	+1788	+765	+162	-299	+2207	+1534	+845	+296	-122	-465	-1004	-1712	-2609
	NXY	lb/in.	+122	+472	+875	+1191	+1346	+1422	+97	+187	+225	+256	+257	+242	+282	+156	+121

(25) DYNAMIC LANDING, FOREBODY DOWN BENDING AND WING ROOT SHEAR

(26) DYNAMIC LANDING, AFTBODY DOWN BENDING

(27) DYNAMIC LANDING, FOREBODY DOWN BENDING

(28) DYNAMIC LANDING, FOREBODY DOWN BENDING

NOTE: REFER TO FIGURE 11-21 FOR FUSELAGE STATION (FS) AND CIRCUMFERENTIAL LOCATION

TABLE 11-69. FUSELAGE POINT DESIGN ENVIRONMENT, FINAL DESIGN - TASK IIB,
DYNAMIC LANDING CONDITION

CONDITION (24) STATIC GUST (NEGATIVE) AT MACH 0.90 (V _C)																
ITEM	UNITS	POINT DESIGN REGIONS (23 XXXX)														
		3301	3302	3303	3304	3305	3306	3307	3308	3309	4101	4102	4103	4104	4105	4106
NX	lb/in.	-413	-306	-153	-31	+60	+138	+212	+284	+376	+2843	+2499	+1862	+1173	+578	-12
NXY	lb/in.	+27	+59	+67	+67	+65	+61	+53	+39	+26	83	325	-465	-490	-474	-474
NX,TH	lb/in.	-	-	-	-	-	-	-	-	-	-	-	-	-	-	-
NXY,TH	lb/in.	-	-	-	-	-	-	-	-	-	-	-	-	-	-	-
AERO PRESS	psi	-	-	-	-	-	-	-	-	-	-	-	-	-	-	-
INTERNAL PRESS	psi	15.3	15.3	15.3	15.3	15.3	15.3	15.3	15.3	15.3	15.3	15.3	15.3	15.3	15.3	15.3
NET PRESS	psi	15.3	15.3	15.3	15.3	15.3	15.3	15.3	15.3	15.3	15.3	15.3	15.3	15.3	15.3	15.3
TAVG	oF	-	-	-	-	-	-	-	-	-	-	-	-	-	-	-
ΔT	oF	-	-	-	-	-	-	-	-	-	-	-	-	-	-	-

		POINT DESIGN REGIONS (23 XXXX)														
ITEM	UNITS	4801	4802	4803	4804	4805	4806	5101	5102	5103	5104	5105	5106	5107	5108	5109
NX	lb/in.	-3881	-3363	-2530	-1431	511	+404	-3685	-2210	-967	-200	+306	+914	+1771	+2658	+3742
NXY	lb/in.	+300	+772	+1178	+1503	+1684	+1831	-146	-374	-515	-610	-684	-761	-671	-395	-195
NX,TH	lb/in.	-	-	-	-	-	-	-	-	-	-	-	-	-	-	-
NXY,TH	lb/in.	-	-	-	-	-	-	-	-	-	-	-	-	-	-	-
AERO PRESS	psi	-	-	-	-	-	-	-	-	-	-	-	-	-	-	-
INTERNAL PRESS	psi	15.3	15.3	15.3	15.3	15.3	15.3	15.3	15.3	15.3	15.3	15.3	15.3	15.3	15.3	15.3
NET PRESS	psi	15.3	15.3	15.3	15.3	15.3	15.3	15.3	15.3	15.3	15.3	15.3	15.3	15.3	15.3	15.3
TAVG	oF	-	-	-	-	-	-	-	-	-	-	-	-	-	-	-
ΔT	oF	-	-	-	-	-	-	-	-	-	-	-	-	-	-	-

NOTE: REFER TO FIGURE 11-21 FOR FUSELAGE STATION (F.S.) AND CIRCUMFERENTIAL LOCATION

ORIGINAL PAGE IS
OF POOR QUALITY

1

2

3

REFERENCES

1. Lockheed-California Company, Supersonic Transport Development Program, Phase III Proposal, Volume II-C Airframe Design, FA-SS-66-7, September 1966
2. The Boeing Company, Mach 2.7 Fixed Wing SST Model 969-336C (SCAT-15F), D6A 11666-1, 1969
3. Shanley, F. R., Weight-Strength Analysis of Aircraft Structures, Dover Publications, Inc., 1960.

PRECEDING PAGE BLANK NOT FILMED

1

2

3